Allosteric Regulation of MDM2 protein

Bartosz Wawrzynów

This thesis has been submitted for the degree of Doctor of Philosophy (Ph.D)

University of Edinburgh
2010

To my Mother

Acknowledgements

Professor Kathryn Ball took on a Herculean task when she accepted me as a PhD student in her lab, for this I will be forever grateful. In my numerous moments of doubt and frustration she never stopped believing in me and always found something positive in my results. Additionally I owe Professor Ted Hupp many thanks for his guidance and remarkable support throughout the whole project endlessly providing myriad ideas that motivated me to explore new pathways of knowledge. Many thanks go to Emma and Vikram for being such good friends for all these years and sharing moments inside and outside science. Thanks also to a great lab of friends whose support was invaluable Jenny, Jen, Lisa, Sarah, Magda, Euan, Angeli, Craig, Yao, Nicky, Erin, Hannan, Susanne, Jew-Kwang, as well as past members Ben, David, Ashley, Maura, Lindsay, Miriam. I am also very grateful to Shirley and Jade for their great technical support. Last but not least I would like to thank Andrea, for being a fantastic friend and always taking care of administrative problems and bureaucratic red tape with a smile on her face. When it comes to actual text formatting and printout of this monstrous document Craig Nicol has been a saviour and a mentor, for which I am very thankful.

Declaration

I hereby declare that I am the author of this thesis and that I performed all the work described herein, except where specifically stated. All sources of information have been acknowledged by means of reference.

Bartosz Wawrzynów 6/01/10

Abstract

The diverse functions of the MDM2 oncoprotein in growth control and tumourigenesis are managed through coordinated regulation of its discrete domains induced by both extrinsic and intrinsic stimuli. A picture of MDM2 is immerging where structurally discrete but interdependent functional domains are linked through changes in conformation. However compelling insights into how this process is carried out have been hindered by inadequate information on the structure and conformation of the full-length protein.
The data presented indicates that the C-terminal RING domain of MDM2, primarily responsible of the E3 ubiquitin ligase activity of the protein, has other intriguing functions. The binding of ATP within the RING domain, triggers conformational changes of MDM2 and its main interaction partner – p53. This in effect promotes efficient binding of the p53 tumour suppressor to specific DNA promoter sequences. Moreover, results presented in this thesis demonstrate a novel role for the RING domain of MDM2 in determining the conformation and activity of its N-terminal hydrophobic cleft, the key target of anticancer drugs designed to activate the function of p53 tumour suppressor protein. Specific modulations within the RING domain, affecting Zinc coordination are synonymous with increased binding affinity of the hydrophobic pocket to the transactivation domain of p53 resulting in a gain of MDM2 transrepressor function thus leading to a decrease in p53-dependant gene expression. ThermoFluor measurements and size exclusion chromatography show that changes in the RING motif lack an effect on the overall integrity of the MDM2 protein. The intrinsic fluorescence measurements manifest that these changes generate long range conformational transitions that are transmitted through the core/central acidic domain of MDM2 resulting in allosteric regulation of the N-terminal hydrophobic pocket. Such RING generated conformational changes result in the relaxation of the hydrophobic pocket. Additionally, it is shown that the cooperation between the RING and the hydrophobic cleft in MDM2 has implications in the efficiency of binding of anticancer drugs such as Nutlin by MDM2. Cooperation between the RING and hydrophobic domain of MDM2 to regulate function demonstrates an allosteric relationship and highlights the need to study MDM2 in a native conformation. In essence the presented data demonstrates that the complex relationship between different domains of MDM2 can impact on the efficacy of anticancer drugs directed towards its hydrophobic pocket.

Aims

- Gain insight into the allosteric regulation of MDM2 protein.

- Focus on a key functional domain of MDM2 - the C-terminal RING domain, as a potential regulator of structure and function, of the whole protein.

- Illustrate intrinsic chaperone function of MDM2 on its main interacting partner, the p53 tumour suppressor.

Abbreviations

17-AAG	17-Allylaminogeldanamycin (17[Allylamino]17demethoxygeldanamycin)
a.a	amino acids
Ab	Antibody
Aha1	Activator of Hsp90 ATPase 1
AIF	apoptosis inducing factor
Akt	alias of protein kinase B (PKB)
ANF	anterior neural folds
AP-1	activator protein 1
Apaf-1	apoptosis protease-activating factor 1
APC	adenomatous polyposis coli
APS	ammonium persulfate
AR	androgen receptor
ARF	alias for cyclin-dependent kinase inhibitor CKDN
ASOs	anti-sense oligonucleotides
Asp	Asparagine amino acid
ATCC	American tissue culture collection
ATM	ataxia telengiectasia
ATN	adenine nucleotide translocator
ATR	ataxia telengiectasia and Rad3 related
ATRIP	ATR interacting protein
AU/a.u.	Arbitrary Units
Bad	Bcl2-associated agonist of cell death
Bag1	Bcl2 associated athanogene 1
BAI1	brain-specific angiogenesis inhibitor 1
BAIAP3	BAI1-associated protein 3
Bak	Bcl2-antagonist/killer 1
BAT3	HLA-B associated transcript 3
Bax	Bcl2-associated X protein
Bcl-2	B-cell lymphoma 2
BCMP11	Breast cancer membrane protein 11
Bid	BH3 interacting domain death agonist
Bim	Bcl2-like 11 apoptosis facilitator
Bip	alias of hspA5
bp	base pair
BRCA1	breast cancer 1, early onset
BSA	Bovine Serum Albumin
C/EBP	CCAAT/ enhancer binding protein
CAK	cyclin-activating kinase
Caspase	cysteine asaprtate protease
CBP	CREB binding protein
CDH6	cadherin 6
CDK 4/6	cyclin-dependent kinase 4/6
CDKN 1/2A	cyclin-dependent kinase inhibitor 1/2A
cDNA	complimentary DNA
Ced-3	cell death abnormality family member
CFTR	Cystic Fibrosis Transmembrane conductance Regulator
CHIP	Carboxyl terminus of Hsp70Interacting Protein
ChIP	Chromatin immunoprecipitation
Chk1/2	checkpoint homolog
CHUK	conserved helix-loop-helix ubiquitous kinase
CK	Creatine Kinase

CKAP2	cytoskeleton-associated protein 2
CKII	Casein Kinase II
CMV	Cytomegalovirus
Cop-1	caspase-1 dominant-negative inhibitor pseudo-ICE
CP	Phosphocreatine
CPT	Camptothecin
CRUK	Cancer Research United Kingdom
CSS	charcoal stripped serum
CyP40	Cyclophilin 40
Cys	cysteine
Da	daltons
Dabco	1,4-Diazabicyclo[2.2.2]octane solution
DAG1	alpha dystroglycan
DAPK	death-associated protein kinase
DBD	DNA-binding domain
DCA	deoxycholic acid
DDR	DNA damage response pathway
DISC	death-inducing signalling complex
DLG1	discs, large homolog 1
DMSO	dimethyl sulphoxide
DNA-PK	DNA-dependent protein kinase
DR3/4/5	death receptor 3/4/5
Drp	dynamin-related protein
dsb	double strand break
dsRNA	double-stranded RNA
DTT	Dithiothreitol solution
E. coli	*Escherichia coli*
E2F	E2F transcription factor
ECACC	European collection of cell cultures
ECL	enhanced chemiluminescence
EDTA	ethylene diamine tetra acetic acid
EDTA	Ethylenediaminetetraacetic acid
EGF	epidermal growth factor
EGFR	epidermal growth factor receptor
EMSA	Electrophoretic Mobility Shift Assay
ER	estrogen receptor
ER	Endoplasmatic Reticulum
ERBB2	v-erb2 erythroblastic leukemia viral oncogene homolog 2
ERK	alias of MAPK1
ERp	endoplasmic reticulum resident proteins
ERR	oestrogen receptor-related receptor
EST	expressed sequence tag
FADD	FAS-associated death domain
FAS	TNF receptor superfamily, member
FBS	Fetal Bovine Serum
FCS	foetal calf serum
FISH	fluorescent in situ hybridization
FOXA	forkhead box protein
FP	fluorescent protein
FRET	fluorescence resonance energy transfer
GA	Geldanamycin
GADD54	growth arrest and DNA-damage-inducible
GAPDH	Glyceraldehyde Phosphate Dehydrogenase
GFP	Green Fluoresent Protein
GI	gastro-intestinal
GIT1	G protein-coupled receptor kinase interactor 1
Gob-4	alias of AGR-2
GPCR	G-protein-coupled receptor

GPCRs	G-protein-coupled receptors
GR	glucocorticoid receptor
GRH	gonadotrophin releasing hormone
GRK	G-protein-coupled receptor kinase
GRKs	G-protein-coupled receptor kinases
GSTM4	glutathione S-transferase M4
GTFIIH	general transcription factor IIH, polypeptide 4
HCC	hepatocellular carcinoma
hCG	human choriogonadotropin
HDAC	histone deacetylase
Hdj	Human DnaJ homolog
HERC2	hect domain and RLD2
HIC-1	hypermethylated in cancer 1
HIF-1	hypoxia inducing factor 1
HIP1R	huntingtin interacting protein 1 related
Hop	Hsp orgainizing protein
HRP	horseradish peroxidase
HSP/Hsp	Heat Shock Protein
hTERT	human Telomarase Reverse Transriptase
HUWE1	HECT, UBA and WWE domain containing 1
IGF-1	insulin growth factor-1
IGF-1R	insulin growth factor-1 receptor
IH	immunohistochemistry
IkB	alias of CHUK
IKK	IκB kinase kinase
IL-1	interleukin-1
IPTG	Isopropylβ-D-1thiogalactopyranosidine
IR	ionising radiation
IXL1	alias of MED29
JNK	alias for MAPK8
LC3	alias of MAP1LC3A
LRBA	LPS-responsive vesicle trafficking, beach and anchor containing
MAP	multiple antigenic peptides
MAPK	mitogen-activating protein kinase 1
MAST1	microtubule associated serine/threonine kinase 1
Mdm	mitochondrial distribution and morphology protein
Mdm2	mouse double minute 2
MDM2	Mouse Double Minute 2 Homolog
MED29	mediator complex subunit 29
MEF	mouse embryonic fibloblast
mRNA	messenger RNA
MS	mass spectrometry
mtDNA	mitochondrial DNA
MTs	microtubules
MTT	methylthiazoletetrazolium
Mutant	a protein variant changed by a mutation in the DNA encoding it (e.g. mutant p53)
MYBBP1A	v-myb myeloblastosis viral oncogene homolog
MYBBP1A	MYB binding protein
NB	neuroblastoma
NCBI	National Centre for Biotechnology Information
NEAA	non-essential amino acids
NES	nuclear export signal/sequence
NF-κB	nuclear factor kappa B
NLS	nuclear localization signal/sequence
NuMA	nuclear protein associated with the mitotic apparatus
$P14^{ARF}$	alias for CDKN2A
P53AIP1	P53 regulated Apoptosis Inducing Protein 1
PAGE	Polyacrylamide Gel Electrophoresis

PARG1	PTPL1-associated RhoGAP 1
PBS	Phosphate Buffered Saline
PBS-T	phosphate buffered saline tween
PCNA	proliferating cell nuclear antigen
PCR	polymerase chain reaction
PDI	protein disulfide isomerase
PF	parafolmadehyde
PI3K	phosphatidyl inositol 3 kinase
PIG8	P53 Induced Gene 8
PIKK	phosphoinositide-3-kinase-related kinase
Pirh-2	alias fof RCHY1
PKC	protein kinase C
PM	plasma membrane
PMSF	Phenylmethylsulfonyl Fluoride
PPM1D	protein phosphatase 1D magnesium-dependent, delta isoform
pRB	Retinoblastoma protein
PS	phospatidylserine
PSME1	proteasome (prosome, macropain) activator subunit 1 (PA28 alpha)
PT	PostTranslational
PTEN	phosphatase and tensin homolog
Puma	Bcl2 binding component 3
PUMA	P53 Upregulated Modulator of Apoptosis
qRT-PCR	quantitative real-time PCR
R.L.U	Relative Light Units
Rad	Radicicol
Rb	retinoblastoma
RCHY1	ring finger and CHY zinc finger domain containing 1
RGB	red green blue
RING	Really Interesting New Gene
RIP140	nuclear receptor interacting protein 140
RNA	ribonucleic acid
ROI	reactive oxygen intermediate
ROS	reactive oxygen species
RPMI	Roswell Park Memorial Institute (medium)
RT	Room Temperature
RU	relative units
S. cerevisiae	*Saccharomyces cerevisisae*
SDS	Sodium Dodecyl Sulfate
SELEX	Systematic Evolution of Ligands by EXponential enrichment
Ser	serine amino acid
SHR	Steroid Hormone Receptor
shRNA	short hairpin RNA
Siah-1	seven in absentia homolog 1
siRNA	small interfering RNA
SPTBN1	spectrin, beta, non-erythrocytic 1
ssDNA	single strand DNA
STAT	signal transducers and activators of transcription
TBP	TATA-binding protein
TCA	trichloracetic acid
TFIIH	alias of GTFIIH
TGF	transforming growth factor
TLN1	talin 1
TNF	tumour necrosis factor
TNFR	TNF receptor
TNFRSF10B	Tumor Necrosis Factor Receptor Superfamily, member 10B
TRAIL	TNF-related apoptosis-inducing ligand
TRAPP	transport protein particle
tRNA	transfer RNA

Trx	thioredoxin
UPR	unfolded protein response
US	United States
UV	ultra-violet
v/v	volume/volume
VDAC	voltage-dependent anion channel
VEGF	vascular endothelial growth factor
VTCs	vesiculotubular clusters
w/v	weight/volume
WAF1	alias of CDKN1
Wip-1	alias for PPMID
WT/wt	Wild-type
WWC1	WW and C2 domain containing 1
Y2H	Yeast-two-hybrid

Table of Contents

List of figures

Chapter 1

Introduction

Contents

1.1 Carcinogenesis

The experimental observations of cancers and cancer cells developed during the second half of the nineteenth and the first half of the twentieth century, indicated that tumours were nothing more than normal cell populations which had become rogue. Moreover, many tumours seemed to be composed of descendants of a single cell that had crossed the line from a physiologically normal state to malignancy and proceeded to spawn myriad offspring constituting neoplastic masses.

The fundamental abnormality resulting in the development of cancer is the continual unregulated proliferation of cancer cells. Rather than responding appropriately to the signals that control normal cell behaviour, these cells grow and divide in a dynamic manner, forming tumour foci. Tumours can be either benign (localized, non-invasive) or malignant (invasive, metastatic), invading normal tissues and organs and eventually spreading throughout the body. The metastases spawned by malignant tumours are responsible for almost all deaths from cancer. The generalized loss of growth control facilitated by genome instability of these cells is exhibited in the net result of accumulated abnormalities in multiple cell regulatory systems and is reflected in several aspects of cell behaviour that distinguish cancer cells form their untransformed counterparts.

Cancer can result from abnormal proliferation of virtually all cell types in the human body, hence there are more than a hundred distinct types of cancer, which vary considerably in rate of development, behaviour and response to treatment. Most common human cancers are of epithelial origin – the carcinomas. These can be classified into two categories; squamous cell carcinomas arise from epithelia that form protective cell layers, while adenocarcinomas arise from secretory epithelia.

1.2 Tumour suppressors and oncogenes

Cancers result from alternations in critical regulatory genes that control cell proliferation, differentiation and survival. Studies of tumour viruses revealed that specific genes (called oncogenes) are capable of inducing cell transformation, thereby providing the first insights into the molecular basis of cancer. In other words an oncogene is a gene that, when mutated or expressed at high levels, helps turn a normal cell into a cancer cell. The inability to find tumour viruses in the majority of human cancers (80%) during the Nixon anti-cancers campaign left the research field with one major theory of how most human cancers arise (mid 1970s); namely that carcinogens act as mutagens and function by mutating vital, endogenous to the human genome, growth-controlling proto-oncogenes into oncogenes. This hypothesis fuelled by an avalanche of scientific data provided a simple and powerful explanation of how the proliferation of cells is driven. The proteins encoded by the proto-oncogenes participate in various ways in receiving and processing growth-stimulatory signals that originate in the extracellular environment. When these genes suffer mutation, the flow of the signal becomes deregulated. Instead of emitting them in carefully controlled bursts, the oncoproteins release a steady stream of growth-stimulating signals, resulting in the unrelenting proliferation associated with cancer cells.

When one applies logic to a functioning control signalling system, the conclusion can be drawn that process promoting components must be counterbalanced by others that oppose this process. Biological systems, which by far are the most complex signalling arrays known to man, seem to follow this logic as well. The tumour suppressor genes constitute a large group of genes that specify protein products mediating diverse cell-physiologic functions. These proteins operate in all parts of the cell, and there is only one shared attribute that allows their inclusion in this gene grouping; in one way or another each one of these genes functions to reduce the likelihood that clinically detectable tumour will appear in one of the body's tissues.

1.3 The p53 tumour suppressor protein

The year 2009 celebrates the 30th anniversary of the discovery of p53. The p53 protein was initially discovered as a protein interacting with the oncogenic T antigen from SV40 virus (DeLeo et al., 1979; Kress et al., 1979; Lane and Crawford, 1979; Linzer and Levine, 1979; Linzer et al., 1979; Melero et al., 1979).
Since then three decades of intense investigation have produced a progressively sharper image of why the p53 tumour suppressor protein is so important for cancer protection. Upon the infliction of almost any cellular stress this normally short-lived protein accumulates and gains full competence in transcriptional activation. The p53 transcriptional programme includes the activation of a number of cell cycle inhibitors leading to temporary growth arrest and pro-apoptotic proteins, which results in apoptosis or irreversible proliferate arrest, the later is also known as senescence.

In essence the p53 tumour suppressor protein is a transcription factor, which regulates cellular response to stress, abnormal cell proliferation and DNA damage (Fuster et al., 2007; Romer et al., 2006; Sharpless and DePinho, 2002; Vogelstein et al., 2000). Over 50% of human tumours possess mutated *TP53* (Hollstein et al., 1999), moreover the inactivation of p53 function leads to cellular transformation (Hollstein et al., 1991; Levine et al., 1991). Interestingly, oncogenic mutations of *TP53* are localized mostly in the DNA Binding Domain (DBD, p53 residues 102-292) (Petitjean et al., 2007) of p53. This domain is responsible for physical contact with specific DNA sequences that reside in promoters of p53 controlled genes and obey the rules of the specific consensus sequence (el-Deiry et al., 1992). The DBD can be rendered incapable of binding to such sequences by distinct mechanisms. Some changes caused by *TP53* mutations are known to cause a destabilization of its structure (class II or "structural" mutants, some of which affect the binding of the zinc atom, important for the DNA binding domain structure) while others directly disrupt its DNA contact (class I or "contact" mutants) (Bullock et al., 2000; Cho et al., 1994) (Figure 1.1). The N-terminal part of the p53 protein is divided into two transcription-inducing regions within distinct target gene specificity (residues 1-40 and 41-63) (Venot et al., 1999) and the proline rich region (residues 64-97). These

domains are responsible for recruitment of cell's transcriptional machinery elements to p53 responsive promoters, activation or suppression of which plays the most prominent role in p53-dependent anti-tumour response (Laptenko et al., 2006). The N-terminal p53 domain is also a site of extensive, regulatory post-translational modifications as well as binding of p53 modulating molecules, such as MDM2 or viral proteins (May and May, 1999). The C-terminal part of p53 contains two other domains. The physiologically relevant form of p53, efficiently binding specific DNA sequences, is a tetramer (McLure and Lee, 1998). The oligomerization domain (residues 323-356), which is relatively well structured, is responsible for tetramerization of p53. The extreme C-terminal domain (res. 363-393) is important for regulation of p53 activity, by being modified with phosphate and acetyl groups as well as possessing its own, unspecific DNA binding activity. Most of the data gathered so far suggests that this domain inhibits the specific p53 DNA-binding activity, and its post-translational modifications or short-DNA contacts play an important, although not exclusive, role in activation of otherwise latent p53 molecules (Laptenko et al., 2006). Interestingly, the functional importance of N- and C-terminal p53 domains is not mirrored by the number of human tumour mutations detected in *TP53* gene regions encoding those domains (BOX 1) (Petitjean et al., 2007). Recently a provocative hypothesis has been suggested that mutational changes in the DBD – much more frequent in tumours than in any other p53 region – are not only inactivating p53 and acting in the dominant negative manner on wt p53 monomer/dimer molecules, but additionally allow to obtain new, oncogenic target gene and interaction specificities by a gain-of-function mechanism (Strano et al., 2007). Moreover, p53 may also be rendered inactive by other cellular events, such as the sequestration of wild-type p53 in the cytoplasm, due to the increased nuclear export (Stommel et al., 1999a; Stommel et al., 1999b), association of p53 with cytoplasmic proteins (Wadhwa et al., 2002) or degradation induced by ubiquitination mediated by the MDM2 E3 ubiquitin ligase (Moll and Petrenko, 2003).

Numerous superlatives such as "Guardian of the genome", "Cellular Gatekeeper" and "Policeman of the oncogenes" (Efeyan and Serrano, 2007) are attributed to p53 for its role in the suppression of human tumour development. Nevertheless from a biophysical point of view the p53 protein is mostly known for its thermodynamic

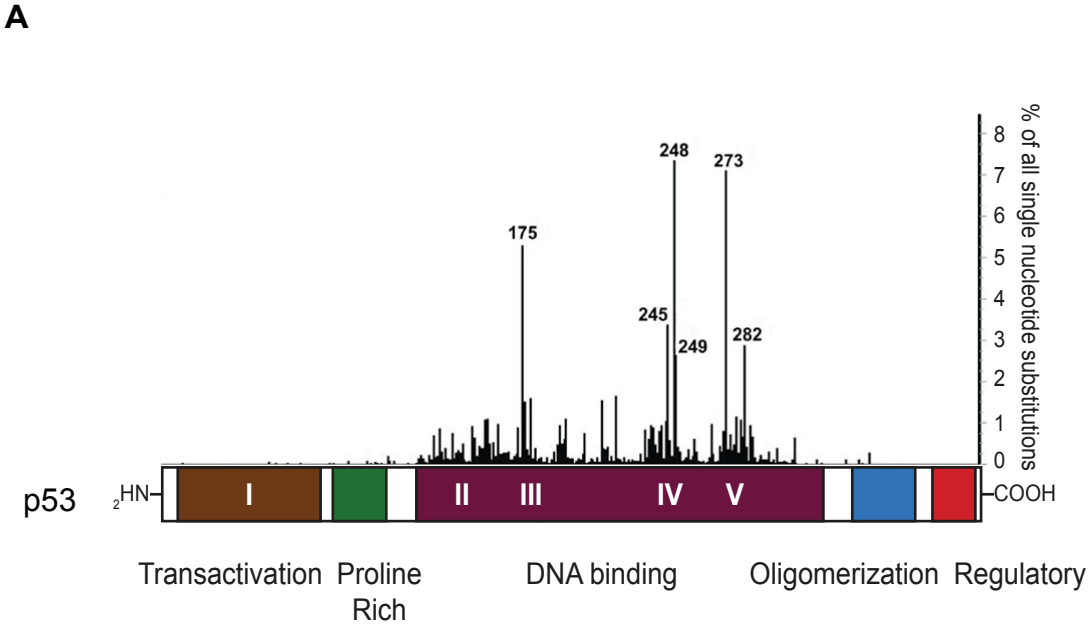

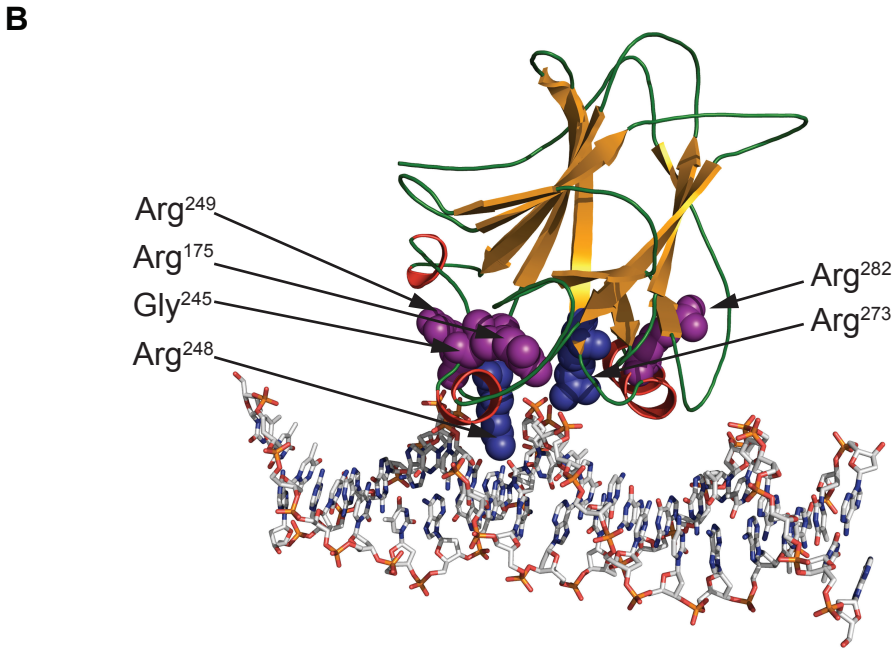

Figure 1.1 Domain localization of p53 mutations in human tumours

(**A**) Diagram representing the distribution and frequency of single nucleotide substitutions in *TP53* gene codons found in human cancers (according to November 2007 and 2008 edition of IACR *TP53* mutation database http://www-p53.iacr.fr) fitted against p53 protein domains. Vertical bars indicate the percentage of all 20828 single nucleotide substitutions in the database. Codons (corresponding to amino acid position within the protein primary structure) most frequently changed are additionally numbered. Roman numerals in the p53 domain organisation diagram represent evolutionary conserved motifs.
(**B**) The structure of the DNA binding domain (DBD) of p53 bound to target DNA sequence; (PDB id: 1TSR - Cho et al., 1994) p53 residues 96-289 shown as a ribbon model with secondary structure specific colours. Additionally six marked residues (presented as spheres) correspond to the most frequently changed in human tumours (see panel **A**). Ariginines 248,273 coloured in blue are responsible for direct contact of the DBD with the DNA, while amino acid residues coloured in purple are important for stabilization of the DBD structure conformation, which allows binding to tumour-suppresive p53 target gene promoters.

instability (Bell et al., 2002; Canadillas et al., 2006) and being largely unstructured (Bell et al., 2002). Around the physiological temperature range of a human body (35°C – 42°C), even the most structured part of purified wild-type p53 - the DBD - unfolds, adopts an inactive misfolded conformation and aggregates at a relatively high rate (Butler and Loh, 2006; Hansen et al., 1996; Muller et al., 2004). Whether this feature of the protein is directly required for p53's role as an important control node in the network of a cellular reaction to stress, remains an open question. Nevertheless this intrinsic p53 instability is evolutionary conserved (Canadillas et al., 2006; Veprintsev et al., 2006).

The wild-type native form of p53, in spite of its relative instability under physiological conditions, has sufficient affinity for specific DNA sequences that reside in p53 controlled gene promoters (Dearth et al., 2007). In the reaction to stresses, such as ionizing radiation, UV and hypoxia, misregulated intracellular-signalling caused by oncogenes, p53 is activated, stabilized and imported into the nucleus, where it promotes or represses transcription of genes whose products induce cell cycle arrest, DNA repair or apoptosis (Figure 1.2) (Balint and Vousden, 2001). Under stress conditions the half-life of the p53 protein is extended due to reduced degradation. Under non-stress conditions, the level of p53 in the cells is mainly regulated at the post-translational level by MDM2 (Haupt et al., 1997; Honda et al., 1997; Kubbutat et al., 1997; Li et al., 2003), additionally recent data suggest that this focal regulator of p53 also has a controlling effect on the translation of the tumour suppressor (Candeias et al., 2008b). In recent years the direct role of p53 post-translational modifications in the p53 activation has been the subject of much debate, since several studies questioned the essential role of phosphorylation (Ashcroft et al., 1999; Ashcroft and Vousden, 1999; Blattner et al., 1999) or acetylation (Krummel et al., 2005) in p53 stabilization and induction. At the same time the more subtle role for p53 acetylation has been discovered, governing the long unknown mechanism of decision-making between p53-dependent cell-cycle arrest and apoptosis (Sykes et al., 2006; Tang et al., 2006). Other p53 regulatory mechanisms involve its interaction and competition with paralogues – p63 and p73 (Li and Jin, 2007), as well as with recently discovered protein products of alternative translation initiation and splicing of *p53* mRNA (Bourdon et al., 2005; Yin et al., 2002).

As being the most frequently tumour-associated molecule in humans, p53 is an obvious target of potential anti-cancer therapies. Since in most tumours wt p53 is altered by mutations or otherwise inactivated, strategies based on overproduction of wt p53 have had a limited efficiency (Roth et al., 1996). A potentially more effective p53-related anti-cancer therapy requires methods that would attempt to inhibit gain-of-function and dominant-negative properties of oncogenic p53 variants (often referred to as "mutant p53" for short), and even more importantly, the reconstitution of wild-type structure and function to inactivated p53 (Selivanova and Wiman, 2007). However, it is also apparent that in healthy cells there must be a set of mechanisms that keep wild-type p53 in a state required for activation of its target genes. These mechanisms have to deal with conformation and stability maintenance of the p53 DNA binding domain structure, prone to unfolding even at 37°C.

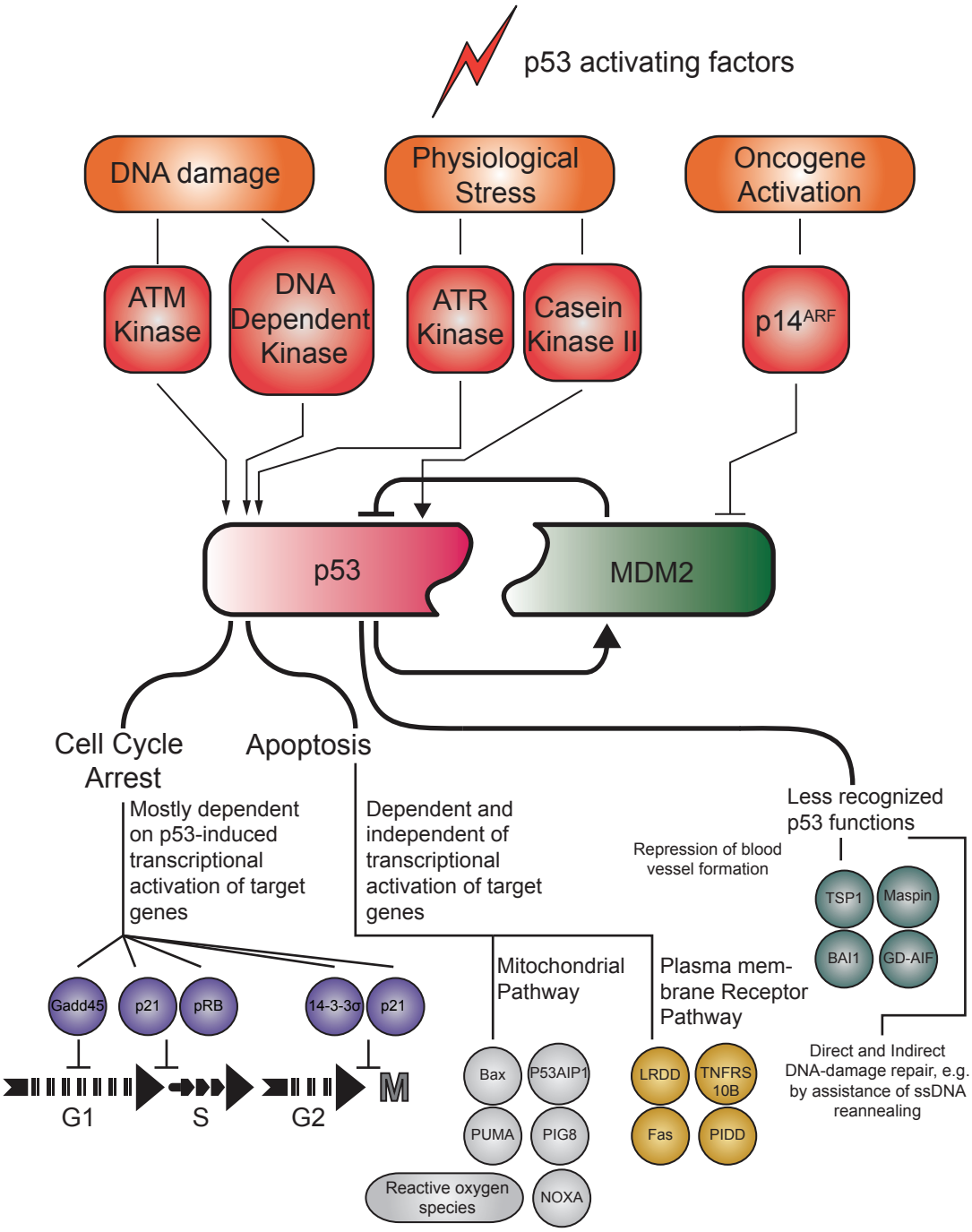

Figure 1.2 The p53 network

The p53 tumour suppressor protein is an important node in the vast cellular network response to genome damage and other forms of stress. A simplified view of known components is presented above. Stress induction upon the cell is the first stage of p53 activation, which leads to increased p53 stability and affinity towards target gene promoters. Target gene expression regulated by p53 most of all to cell cycle arrest and/or apoptosis. Each process is controlled by protein products of several p53 induced genes, which modulate the progression of a given process (examples listed). The p53 protein is also suggested to undertake transcription-independent actions to accomplish tasks such as DNA repair or inhibition of angiogenesis and apoptosis. A principal feedback loop between MDM2 and p53 restrains this network thus supervising the accuracy and timing of the p53 response. The localization of p53 in the centre of this key cellular signalling network has its advantages and disadvantageous. While its existence facilitates the coordination of the multiplex stress response process, it also exposes the cell to the danger of being unable to perform this process if the central network node is deactivated.

1.4 MDM2 - MOUSE DOUBLE MINUTE 2 HOMOLOG

It is well established that under numerous forms of cellular stress, activation of the p53 pathway leads to a protective outcome ensuring tissue integrity. Nevertheless, cellular proliferation and differentiation is indispensable for tissues to maintain their proper structure and function. It follows that in the absence of stress signals, there is a requirement to keep p53 under tight control.

Around a decade after the discovery of the *TP53* gene and the tumour suppressor protein it encodes, another crucial discovery was made. That was the discovery of MDM2 one of the numerous target genes activated by p53. However, unlike other p53 target gene products, the MDM2 protein does not act downstream of p53 to mediate the biological effects of this tumour suppressor. Rather it interacts with p53 itself and regulates its function in a number of ways. At the present time the scientific community considers MDM2 as the major cellular antagonist of p53.

1.4.1 Identification of the MDM2 protein and its Biological Function

The murine double minute 2 (*mdm2)*[1] (Fakharzadeh et al., 1991) was originally identified as one of three genes (*mdm1, 2,* and *3)* which were overexpressed greater than 50-fold by amplification in the spontaneously transformed mouse cell line BALB/c (3T3-DM). The *mdm2* genes were located on small, acentromeric extrachromosomal nuclear bodies, called double minutes, which were retained, by the cells only if they provided a growth advantage. A cDNA library was constructed using RNA from these cells and cDNA clones were isolated representing sequences that are amplified and overexpressed in these 3T3-DM cells. From the results of Northern- and Southern-blot analyses, it was concluded that these cDNAs represented two distinct genes, which were designated *mdm-1* and *mdm-2*. Using

[1] The abbreviations used throughout this thesis are *MDM2*, human gene and oncogene, MDM2, human protein and isoform; *mdm2*, mouse gene; Mdm2, mouse protein.

DNAs from a panel of Chinese hamster-mouse somatic cell hybrids together with in situ hybridization protocols for gene mapping studies, it was found that these DM-associated, amplified DNA sequences originate from mouse chromosome 10, region C1-C3. Sequences homologous to *mdm-1* and *mdm-2* are present in the genomes of several species examined, including that of man (Cahilly-Snyder et al., 1987).

The gene product of the *mdm2* gene was later shown to be responsible for transformation of NIH3T3 and Rat2 cells when overexpressed (Cahilly-Snyder et al., 1987; Fakharzadeh et al., 1991). In summary, the data presented in these two initial publications supports the conclusion that *mdm2* represents an evolutionarily conserved gene with tumourigenic potential and a predicted role in mechanisms of cellular growth control.

1.4.1.1 MDM2 and tumourigenesis

Not long after the identification of the *mdm2* gene, the reason for its transformation potential was discovered. The protein product of this gene was shown to be a cellular phosphoprotein, with an apparent molecular mass of 90 kDa (Mdm2), which forms a tight complex with the tumour suppressor p53 and inhibits p53-mediated transactivation (Momand et al., 1992).

At the same time, *MDM2* gene amplification was observed in human sarcomas that retained wild-type p53. To determine whether the MDM2 protein plays a role in human cancer, Oliner and colleagues have cloned the human orthologueue of the *mdm2* gene and showed that the recombinant derived human MDM2 protein binds p53 *in vitro* (Oliner et al., 1992). Moreover, they mapped the *MDM2* gene to chromosome 12q13-14 (later the exact position of the gene was shown to be at 12q14.3-q15 distal to CDK4 and flanked by Genethon microsatellites D12S80 and D12S83 (Mitchell et al., 1995)). Strikingly this position appeared to be altered in many sarcomas (Mandahl et al., 1989; Meltzer et al., 1991; Turc-Carel et al., 1986) with the *MDM2* gene amplified in over a third of 47 sarcomas, including common bone and soft tissue forms. Amplification of the *MDM2* gene is also present in

oesophageal carcinomas (Shibagaki et al., 1995), gliomas, anaplastic astrocytomas (Reifenberger et al., 1993; Reifenberger et al., 1994), and neuroblastomas (Corvi et al., 1995). Interestingly, up regulation of the MDM2 protein in cancer cells can also be achieved through enhanced translation of mRNA, independent of gene amplification (Landers et al., 1997; Landers et al., 1994). More recent data have shown that a naturally occurring polymorphism (SNP309) within the *MDM2* promoter leads to an increase in *MDM2* mRNA and protein in human populations (Bond et al., 2004).

In essence, amplification of the *MDM2* gene is observed in a variety of human tumours. At least 5-10% of all human tumours possess inappropriate MDM2 overexpression, due to either gene amplification or transcriptional and post-transcriptional mechanisms (Daujat et al., 2001b; Juven-Gershon and Oren, 1999; Momand et al., 2000).

These pioneering studies were the cornerstone of the hypothesis that overexpression of MDM2 was another mechanism by which the cell could inactivate p53 in the process of transformation. Whereas this hypothesis is clearly valid, transformation is more complex. Some tumours contain both high levels of MDM2 and mutations in the *p53* gene. The reasons for disrupting two components of the same pathway are unclear but suggest that MDM2 may have other growth-promoting functions.

1.4.2 Gene Structure and Function

Both the *mdm2* gene and its human orthologueue *MDM2* consist of 12 exons that can generate many protein isoforms. Interestingly over 40 different splice variants of *MDM2* transcripts have been identified both in tumours and normal tissues in mice and humans alike (for review see (Bartel et al., 2002)). In humans, *MDM2-A* and *MDM2-2B* are the major splice variants that delete exons 4-9 and 4-11, respectively. Neither of these two end protein products contain the p53-binding motif (Figure 1.3).

MDM2-2B also known as MDM2-ALT1, interacts with full length MDM2 and sequesters it into the cytoplasm (Evans et al., 2001).

The human gene, similar to the murine orthologueue, contains two different promoter regions, the second of which is responsive to p53. These two promoters in end generate two proteins, the full-length p90 (of apparent molecular mass 90 kDa estimated by SDS PAGE) and a shorter p76 (of apparent molecular mass 76 kDa) at an internal ATG (Olson et al., 1993; Perry et al., 1993; Saucedo et al., 1999). The p76 isoform is missing part of the p53-binding domain (Figure 1.3) and it can act as a dominant negative inhibitor of the full length MDM2 protein.

1.4.3 Protein Structure

The human full length MDM2 protein is a 491-amino acid long polypeptide (Figure 1.3 Panel B). This multi-domain protein comprises of; i) a hydrophobic cleft at its N-terminus, ii) a central acid domain and, iii) a C-terminal RING finger domain.

As the ability of MDM2 to inactivate p53 relies on a direct physical interaction between the two proteins, this is carried out through the NH_2 terminal 100 amino acids of the MDM2 protein with an alpha helix present in the NH_2 transactivation domain of p53 (Kussie et al., 1996a). Conformation and hydrophobicity appear to be two critical requirements for this key interaction to occur. Other motifs include a nuclear localization signal and a nuclear export signal. These signals are believed to shuttle the protein back and forth between the cytoplasm and the nucleus, thus providing yet another means by which p53 activity is tightly regulated (Freedman and Levine, 1998; Roth et al., 1998). The authors postulate that mutation of the nuclear export signal (NES) in MDM2 abolishes its ability to shuttle p53 to the cytoplasm for degradation. Similarly, blocking CRM-1 mediated nuclear export of NES-containing proteins with leptomycin B leads to nuclear accumulation and increased steady-state levels of p53 and MDM2 (Freedman and Levine, 1998; Stommel et al., 1999a). Therefore these findings suggest that, whether p53 shuttles out of the nucleus autonomously (Tao and Levine, 1999a; Zhang and Xiong, 2001) or in an MDM2-mediated fashion (Boyd et al., 2000; Geyer et al., 2000; Stommel et al., 1999a), nuclear export appears to be key for MDM2 mediated p53 regulation.

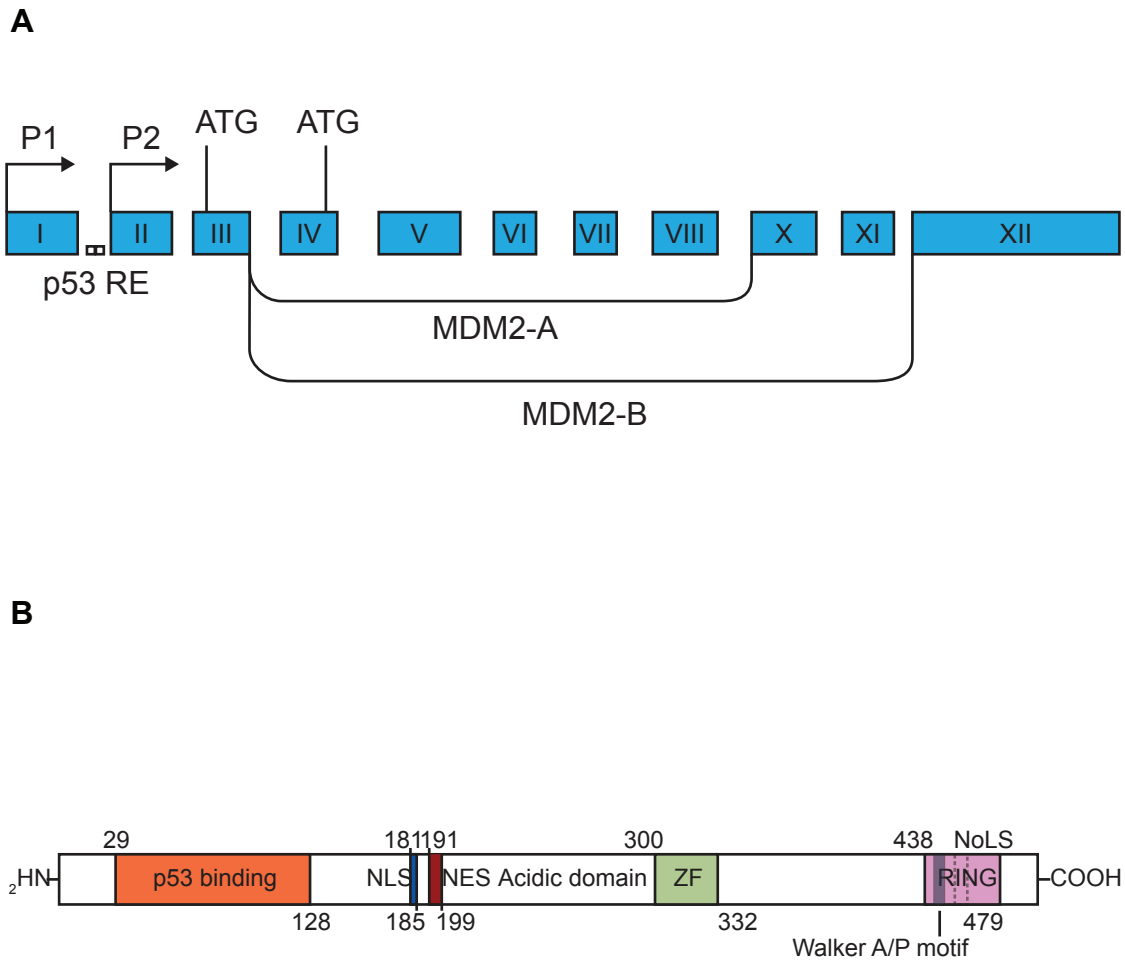

Figure 1.3 Structure of the *MDM2* gene and protein

(**A**) The *MDM2* gene consists of 12 exons and two p53 responsive elements (p53 RE) in intron I. Two promoters are highlighted by arrows. Full-length MDM2 (p90 - migrating on an SDS PAGE as a 90kDa species) is translated from the first start codon ATG in eon III and the short form, p76 is translated from the second ATG in exon IV. Two major aternative splice variants in the human genes MDM2-A and MDM2-B are shown these have exons IV-IX and IV-XI deleted respecitevely.

(**B**) Primary structure of the full length human MDM2 491 amino acid isoform (p90). p53 binding - primary ineraction site with p53 protein, NLS- Nuclear localization signal, NES- Nuclear export signal, NoLS- Nucleolar localization signal ZN - Zinc finger domain, RING- ring-finger domain. The numbers above the diagrams denote amino acid numbers and roman numerals are exon numbers.

The central acidic domain of MDM2 is necessary for interaction with ribosomal proteins L5 (Dai et al., 2006; Marechal et al., 1994), L11 (Lohrum et al., 2003; Zhang et al., 2003) and L23 (Dai et al., 2004) (Jin et al., 2004) and with p300/CBp (CREB-binding protein). Recently this domain was found to contribute to the MDM:p53 interaction by constituting a secondary interaction site with the tumour suppressor, highlighting an allosteric mode interaction between the two proteins (Shimizu et al., 2002; Wallace et al., 2006). Downstream of the acidic domain is a zinc finger domain (a conserved interaction module that binds DNA, RNA, proteins or small molecules) a site of cancer associated missense mutations leading to limited interaction with the mentioned L5 and L11 proteins, retention of the mutated protein in the nucleus and decreased regulatory potential on p53 (Lindstrom et al., 2007). The RING domain is at the C-terminus of the MDM2 polypeptide. The RING finger domain is a subtype of zinc-finger domain found in a numerous mammalian proteins (more than 300-RING finger genes have been identified in the human genome). The true potential of the RING finger motif was realised around ten years ago. Before that no specific function had been ascribed to the RING finger beyond a role in dimerization of several proteins. In was not until 1999/2000 (ten years post the discovery of MDM2) that numerous reports from laboratories studying diverse biological processes have led to the realization that RING finger proteins play a critical role in the ubiquitin mediated proteasome degradation pathway by facilitating the transfer of ubiquitin both to heterologous substrates as well as to the RING finger proteins themselves. Eukaryotic proteins can be differentially modified through attachment to various small molecules and proteins. One such modification is conjugation to ubiquitin, which controls a broad range of physiological processes (Hochstrasser, 2009). These include the regulations of interaction of a given protein with other macromolecules, for example binding to the proteasome or recruitment to chromatin. The RING domain present in MDM2 renders it biochemically active as an E3 ubiquitin ligase (Fang et al., 2000), is a site of nucleotide binding by the protein (Poyurovsky et al., 2003) and mediates MDM2 interaction with RNA (Candeias et al., 2008a; Elenbaas et al., 1996; Naski et al., 2009).

1.4.4 p53-dependent functions of MDM2

1.4.4.1 Mouse Model

The importance of Mdm2 and p53 was elucidated through elegant mouse genetics (Jones et al., 1995; Montes de Oca Luna et al., 1995). Mice lacking the *mdm2* gene are early embryonic lethal and die before implantation. The phenotype is completely rescued by concomitant deletion of *p53,* strongly suggesting an important genetic dependence between these two genes in murine development. It is thought that the lethality of *mdm2* knockout is caused by inappropriate p53-dependent apoptosis due to the hypoxic embryonic environment. Therefore, in order for p53 to accumulate and become highly active in response to stress, the autoregulatory loop must be interrupted so that p53 can escape Mdm2 regulation. Nevertheless one must remember that despite the fact that mouse gene knockout technology is a powerful tool in regards to gene crosstalk/interdependence, at the same time it might provide an over simplistic model, as no dosage dependent interactions of protein complexes can be studied.

In regards to Mdm2 and the physiological consequences of its down regulation in mice, intriguing results were obtained a few years post the *mdm2* knockout studies (Mendrysa et al., 2003; Mendrysa et al., 2006; Mendrysa and Perry, 2000). By crossing animals containing either wild-type, hypomorhic or null *mdm2* alleles a set of lines expressing a range of Mdm2 protein levels was generated. These mice expressing sub-physiological levels of Mdm2 were later crossed with mice that carried a mutated APC allele (these animals are predisposed to developing intestinal adenomas). The results showed that even a subtle (~20%) decrease of Mdm2 levels led to a significant reduction in intestinal adenoma formation, while further down-regulation of Mdm2 (to ~30% of wild type) reduced the number of such tumours by a factor of >16 (Mendrysa et al., 2003). The observed anti-tumour response mediated by heightened p53 activity did not coincide with an overall increase in p53 protein levels, leading the authors to conclude that in normal tissues, Mdm2 primarily regulates the activity of p53 and may have only minimal effects on p53

protein stability. Further speculation was made that the two canonical activities towards p53 - repression and degradation (detailed below) are independently regulated both in a tissue specific manner as well as following stress response.

To conclude these findings, one may state that small amounts of Mdm2 are sufficient for maintenance of overall p53 levels and moreover lead to increased p53 response, while only a near or complete loss of Mdm2 would result in overall accumulation of the p53 protein and consequently lead to extensive cell death and embryonic lethality in the organism.

1.4.4.2 Transrepression of p53 transcriptional activity

MDM2 mediated regulation of p53 is carried out on several levels. Despite their complexity and divergence i.e. trafficking out of the nucleus, control of binding to chromatin, post-translational modifications with mono- and polyubiquitin (Brooks and Gu, 2006; Pickart, 2004), all of them rely of the fact that these two proteins directly interact and form a complex. Initially the interaction was shown to result in the inhibition of p53-mediated transcriptional activity (Chen et al., 1995; Momand et al., 1992; Oliner et al., 1993). MDM2 within its N-terminus possesses a structural motif that can house p53's transcriptional activation domain (TAD), via induced fit and hydrophobic interactions. This results in MDM2 mediated concealment of the p53 TAD from critical transcription initiation proteins; consequently leading to an transcriptionally inactive p53-MDM2 complex (Chen et al., 1993; Lin et al., 1994; Oliner et al., 1993; Picksley et al., 1994). Moreover, MDM2 has been shown to inhibit p53-mediated transcription not only masking its TAD, but also through a direct repressor effect on basal transcription from p53-responsive promoters (Leng et al., 1995; Thut et al., 1997). Domain mapping of MDM2 had shown that residues 50-222 bind to the 34K subunit of TFIIE (member of the general transcription machinery) independent of p53. Other studies have mapped the interaction of MDM2 with general transcription factor TFIID, $TAF_{II}250$/CCG1 and TBP through RING finger and acidic domains respectively (Leveillard and Wasylyk, 1997). Recent studies have shown that MDM2 induces monoubiquitination of histones surrounding

the p53-response elements resulting in transcriptional repression (Minsky and Oren, 2004).

In essence one may conclude that these combined activities of MDM2 assure efficient inactivation of p53-dependent transcription by MDM2.

1.4.4.3 The ubiquitin/proteasome pathway of protein degradation

The abundance of many cellular proteins must be tightly controlled in response to a variety of physiological signals. This is done by two highly controlled processes; protein synthesis and protein degradation. The foundations of the ubiquitin/proteasome pathway started to emerge in the early 1980s (Ciechanover et al., 1980; Hershko et al., 1980; Hershko et al., 1983), with experimental data aimed at understanding why intracellular proteolysis measured as the release of amino acids from intact cells, requires metabolic energy (Simpson, 1953). At present the bulk of scientific data gathered since these early experiments supports the notion that the ubiquitin/proteasome pathway is the principal mechanism for turnover of normal short-lived proteins in mammalian cells. A protein substrate intended for proteolytic degradation needs to be targeted. This usually requires the covalent attachment of a ubiquitin polymer, containing at least four tandemly conjugated ubiquitin moieties (Ciechanover et al., 2000; Thrower et al., 2000) onto the protein destined for degradation. One ubiquitin molecule is initially linked via its C-terminal glycine to the ε-amino side chain of a lysine present in the target protein; a second ubiquitin molecule is then linked to Lys^{48} of the first ubiquitin, and the process is repeated a number of times. This multi-step mechanism involves a sequential cascade of activating (E1), conjugating (E2) and ligase (E3) enzymes. The E1 enzyme activates ubiquitin in an ATP dependent manner to synthesize ubiquitin C-terminal adenylate, which then serves as an enzyme bound substrate for the formation of an E1-ubiquitin thiol ester (Hershko et al., 1982; Hershko et al., 1983)(Figure 1.4). The ubiquitin molecule is then transferred to a ubiquitin conjugating enzyme (E2) through a thiol ester bond. An ubiquitin-protein ligase (E3) specifically attaches ubiquitin to the target protein. The presence of multiple substrate-linked ubiquitins recruits

transporter proteins shuttling the tagged protein moiety to the 26S proteasome This is a 2.5 MDa complex that in an ATP dependent manner unfolds the substrate polypeptide chain translocates it into an interior chamber where peptide bond hydrolysis occurs to produce small peptides (Baumeister et al., 1998). Ubiquitin is spared from degradation through its release from the substrate by deubiquitinating enzymes (Hershko et al., 1980). Thus, there are two independent reasons why ATP is required for intracellular proteolysis; to activate the ubiquitin C terminus in preparation for conjugation and to support the proteasome's substrate unfolding and translocation activities (Figure 1.4) (Pickart, 2001).

To date only a few E1 enzymes have been identified to be encoded by the human genome. Interestingly humans have more than 30 different E2s. As E3 ligases are primarily responsible for substrate recognition their numbers are the highest (exact number not known in the region 500-1000 (Hicke et al., 2005).

E3 ubiquitin ligases from a mechanistic standpoint, can be categorized into two groups (Figure 1.5); those that utilize a covalent mechanism – HECT domain E3s (ubiquitin is covalently bound to a E3 before being transferred to the target protein) and those that do not bind ubiquitin directly but rather form a scaffold for specific transfer of ubiquitin from an E2 to the target protein - (RING, U-box, PHD, F-box domain E3s). The representatives of the latter group can be single multi-domain polypeptides (CHIP, MDM2) or large multiprotein complexes (SCF, ECV, Cul4) in which each subunit is a member of a distinct protein family and each bearing a different function in the assembled complex (SKP1-CUL1-F-box composing the SCF complex) (Nakayama and Nakayama, 2006).

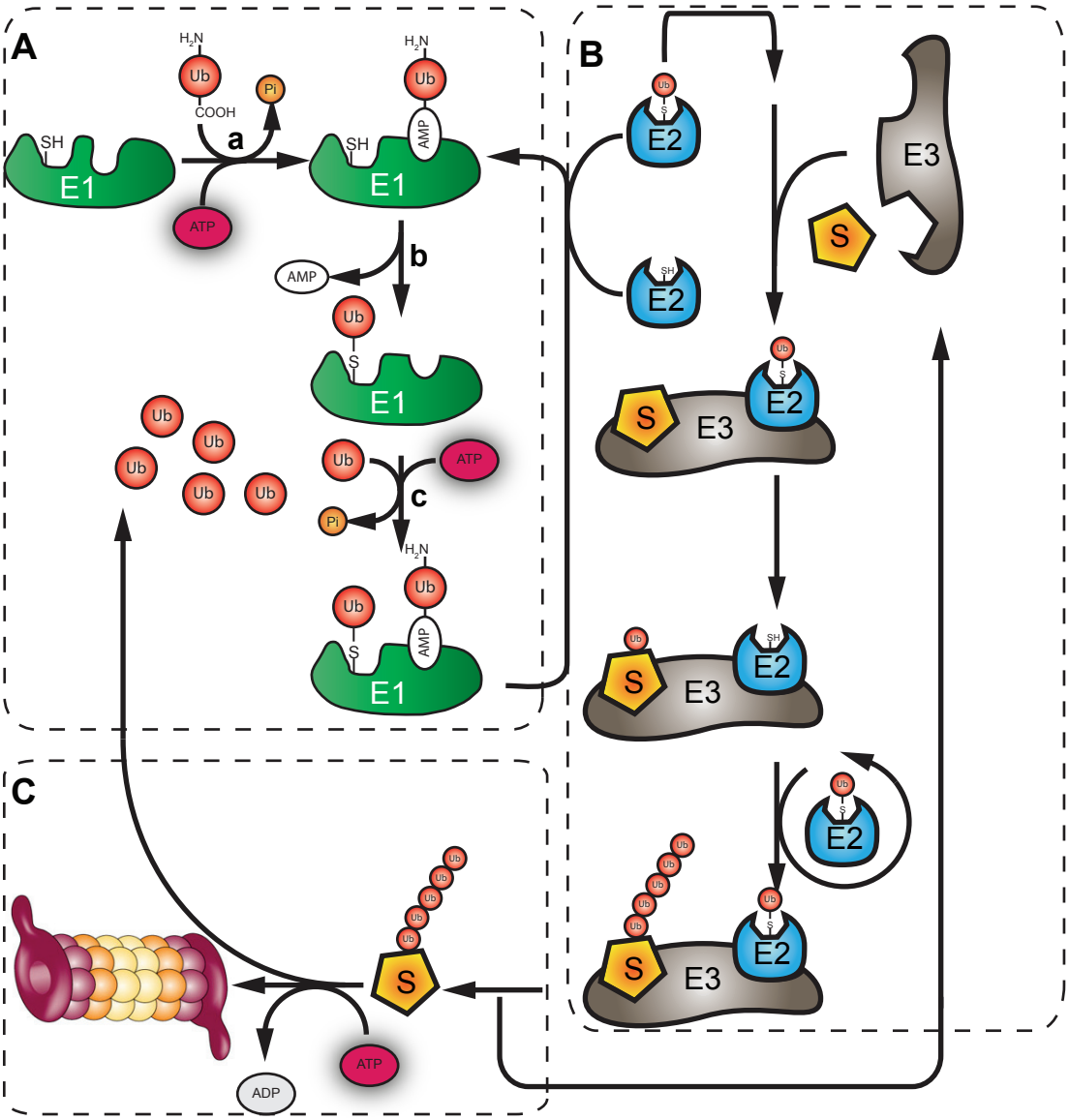

Figure 1.4 Overview of the ubiquitin proteasome system

Protein degradation through the Ubiquitin Proteasome System (UPS) is a highly regulated process involving several consecutive steps.

(**A**) The first step in the cascade is the activation of ubiquitin (Ub) by an ubiquitin-activating enzyme (E1). This step of the ubiquitination cascade requires ATP binding to the ATP-binding cleft of E1. This process can be subdivided into three major sub-steps: (**a**) ubiquitin adenylate formation (**b**) rapid cis transfer of the E1-bound ubiquitin molecule from AMP to active site cysteine in E1 (**c**) second round of adenylate formation to yield a fully loaded enzyme.
(**B**) The ubiquitination conjugation cascade. The ubiquitin conjugating enzyme (E2) is recruited to the E1 which is followed by transfer of the activated ubiquitin from the active cysteine of E1 to the catalytic cysteine in E2. The next step of efficient transfer of ubiquitin molecules to specific lysines of the substrate protein (S) is carried out by a class of enzymes called ubiquitin ligases (E3). These generally provide a scaffold for the formation of a S~E3~E2-Cys-Ub complex.
(**C**) The 'marked for death' polyubiquitinated substrate is released from the E3. The modified substrate is shuttled to the proteasome, where in an ATP dependent manner the polyubiquitin tagged protein is unfolded, the ubiquitin chains are recycled through proteasome associated ubiquitin hydrolases. The unfolded polypeptide is threaded into the proteasome chamber, where protease active sites are located.
(Adapted from Nalepa et al., 2006 and Pickart 2004)

1.4.4.4 Polyubiquitin chains are diverse

It should be kept in mind that protein ubiquitination is not exclusively synonymous with protein degradation. Protein ubiquitination has over the past years emerged as complex network matched in intricacy by the eukaryotic kinome (Adhikari and Chen, 2009). Indeed, proteins devoted to ubiquitin conjugation, deconjugation and recognition constitute one of the largest families in the proteome. Thus this post-translationalmodification is involved in a broad spectrum of cellular processes (Pickart, 2001). Monoubiquitination has been implicated in a number of degradation-independent processes, including endocytosis, virus budding and transcriptional silencing via attachment of ubiquitin moiety to histones leading to chromatin remodelling (Ciechanover and Brundin, 2003; Fingerman and Briggs, 2004; Sun and Allis, 2002).

The enzymes involved in the covalent conjugation of ubiquitin to specific protein substrates also promote the formation of long polyubiquitin chains through lysine residues in ubiquitin. Pioneering studies using yeast genetics showed that Lys^{48}-linked polyubiquitin chains are the principal targeting signal for proteasomal degradation (Chen et al., 1996; Spence et al., 1995). Unconventional ubiquitin chains (through the other remaining lysines within ubiquitin; Lys^{11}, Lys^{27}, Lys^{29}, Lys^{33}) attached to proteins, although much more scare, could target proteasomal degradation *in vivo* (Jin et al., 2008).

Moreover, the role of Lys^{63}-linked polyubiquitin chains in DNA repair and stress response, has been proposed (Pickart, 2000; Spence et al., 1995). Further studies demonstrated the role of Lys^{63}-polyubiquitin chains in kinase activation and vesicle trafficking within the cell (Chen et al., 1996; Deng et al., 2000).

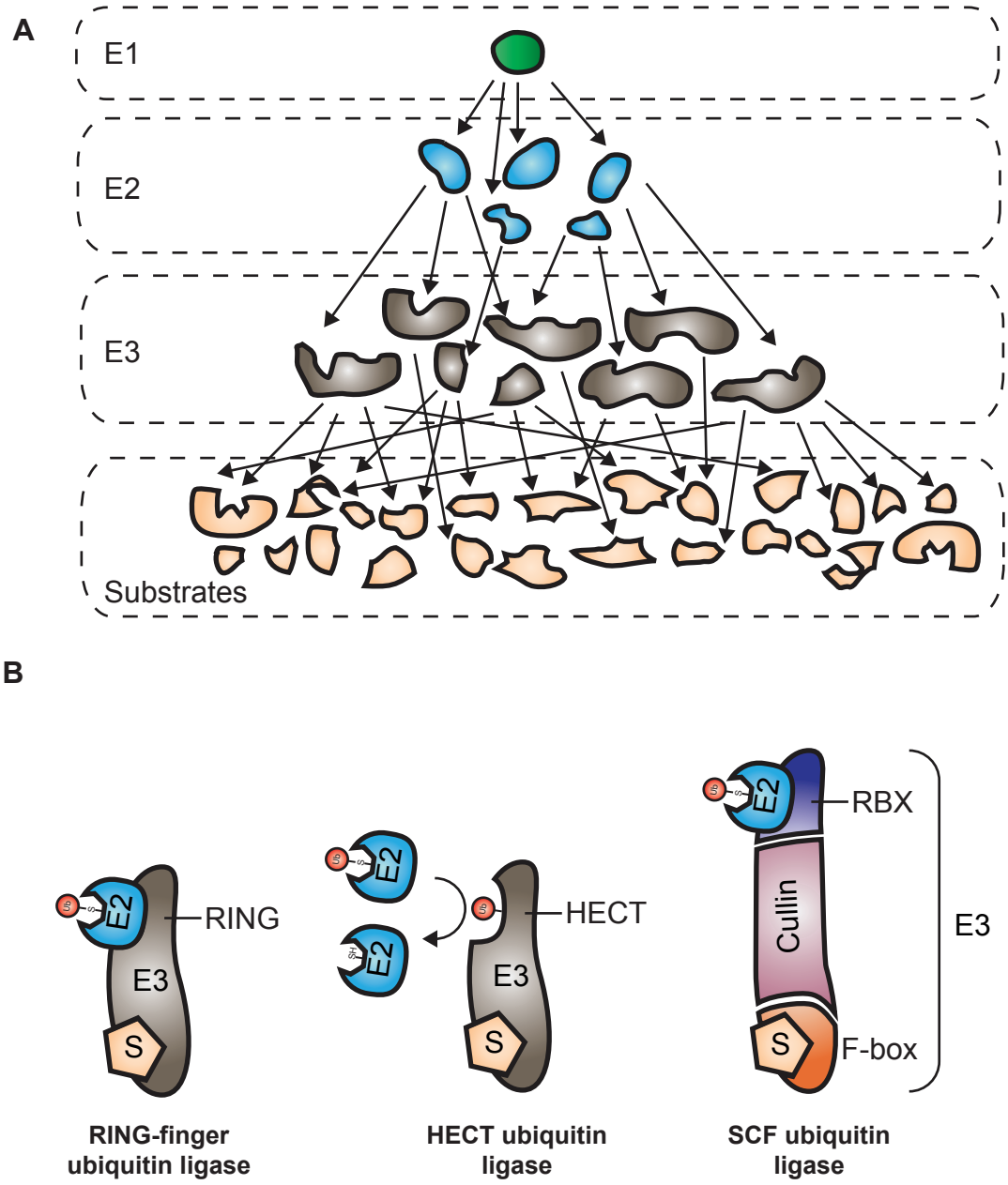

Figure 1.5 The ubiquitin proteasome pathway

(**A**) The ubiquitin cascade is pyramidal in design. A single E1 activating enzyme transfers ubiquitin to roughly three dozen E2s, which function together with several hundred different E3 ubiquitin ligases to ubiquitinate thousands of protein substrates.

(**B**) Several classes of ubiquitin ligases are known so far. Single RING E3 ligases bear all the necessary domains for their activity within one polypeptide stretch. HECT E3 ubiquitin ligases which in contrast to the others form a covalent bond with ubiquitin during polyubiquitination of their target proteins. Multi-subunit RING-finger E3 ubiquitin ligases here are exemplified by the SCF complex. This multiprotein E3 ligase consists of a scaffolding cullin molecule, a RING-finger-containing subunit (RBX1 or RBX2), which functions as a docking site for E2 enzymes, and a substrate specificity module - F-box, which binds substrates.

1.4.4.5 MDM2 is a RING finger E3-Ubiquitin Ligase

Originally identified as a transrepressor of p53 mediated transcription, MDM2 was subsequently shown to control the steady state levels of p53 in unstressed cells by acting as a RING finger domain E3-ubiquitin ligase (Fang et al., 2000; Honda and Yasuda, 2000), which results in the polyubiquitination of p53 and subsequent 26S proteasomal degradation. Additionally, MDM2 has been shown to control its own abundance and activity within the cell via auto ubiquitination (Fang et al., 2000; Honda and Yasuda, 2000). This process as well as the E3 ubiquitin ligase activity on target proteins other than MDM2 is believed to be regulated by the quaternary structure of the active E3 complex and may involve interactions with the paralogue of MDM2 – MDM4 (MOUSE DOUBLE MINUTE 4 HOMOLOG) (Jackson and Berberich, 2000) (Stad et al., 2001) (Gu et al., 2002; Iwakuma and Lozano, 2003).

The enzymatic process of covalent ubiquitin attachment by the E3 ligase onto an amino group within a lysine residue cannot be explained by a simple enzyme substrate complex kinetics. Upon complex formation of MDM2 with p53, several conformational shifts occur within the intradomains for both of the proteins, providing a basis for allosteric crosstalk of p53 binding sites within MDM2 (Wallace et al., 2006). Despite the discovery of several other p53 specific E3 ubiquitin ligases such as Pirh2, COP-1 and CHIP, Arf-BP1 (Brooks and Gu, 2006), to date MDM2 is still believed to be the principal physiological antagonist of p53, acting to curb the pool of active p53 transcription factor in unstressed cells.

MDM2 was also found to differentially catalyze mono-ubiquitination and poly-ubiquitination of p53 in a dosage-dependent manner (Li et al., 2003). Mono-ubiquitination is believed to be predominant in the presence of low levels of MDM2, whereas high levels promote poly-ubiquitination and nuclear degradation of p53. Moreover, mono-ubiquitinated p53 protein was shown to localize within the

cytoplasm and it has been suggested that mono-ubiquitination of p53 modulates the tetramerization of the transcription factor, unmasking the nuclear export signal (Stommel et al., 1999a). This data tempted the scientific field to hypothesize that these distinct post-translational modes of action of MDM2 on p53 are exploited under different physiological conditions. For example, MDM2-mediated poly-ubiquitination and nuclear degradation may play a critical role in suppressing p53 function during the later stages of the DNA damage response or rather when MDM2 is malignantly overexpressed (Shirangi et al., 2002; Xirodimas et al., 2001b). On the other hand, MDM2-mediated mono-ubiquitination and subsequent cytoplasmic translocation of p53 may represent an important means of p53 regulation in unstressed cells, where MDM2 is maintained at low levels. Despite the logical grounds for this hypothesis there are still a few avenues, which are vexing. Namely, what happens to the mono-ubiquitinated p53 moiety in the cytoplasm? Does it undergo further poly-ubiquitination and proteasome mediated degradation by a novel E3 or E4 (p300) enzyme complex, or rather does it surpass degradation by being retained at low levels in an inactive oligomeric complex in association with abundant molecular chaperones (King et al., 2001; Zylicz et al., 2001; Zylicz and Wawrzynow, 2001)? As ubiquitination like all other post-translational modifications is reversible, this p53 state upon a signalling shift in the cell could be reactivated via an appropriate deubiquitinating enzyme (Brooks et al., 2007a; Brooks et al., 2007b). Moreover, movement of p53 into the cytoplasm may be important for transcriptional-independent functions of p53 such as the interaction with mitochondrial proteins in the apoptosis response (Chipuk and Green, 2004; Chipuk et al., 2004; Marchenko et al., 2007; Mihara et al., 2003).

1.4.4.6 Involvement in translational control

The MDM2 oncoprotein has a direct effect on the abundance of the p53 protein in the cell. MDM2 has been shown not only to control the cellular levels of p53 through ubiquitination but also has been shown to induce and repress its synthesis. MDM2 induces translation of the p53 mRNA from two alternative initiation sites, giving rise

to full-length p53 and another protein with a relative molecular mass of approximately 47 kDa. This translation induction requires MDM2 to interact directly with the nascent p53 polypeptide (Yin et al., 2003). Moreover this MDM2 mediated induction of p53 synthesis is not due to an increase in *p53* mRNA levels, yet as the authors propose through increased *p53* mRNA translation efficiency. This is shown by elegant experiments indicating that MDM2 is recruited to active polyribosomes by the nascent p53 N-termini, resulting in cis regulation of p53 mRNA translation. In other words for MDM2 to induce efficient p53 translation it has to interact with p53 while it is still on the ribosome.

Interestingly, the *p53* mRNA region encoding the MDM2-binding site interacts directly with the RING motif of MDM2. This complex renders the MDM2 oncoprotein transiently impaired as an E3 ubiquitin ligase and results in the promotion of *p53* mRNA translation (Candeias et al., 2008b; Naski et al., 2009).

The RNA binding and the E3 ubiquitin ligase domain of MDM2 overlap, indicating that the two functions of MDM2 to control p53 abundance have evolved in parallel. Based on this the role of MDM2 as a positive regulator of p53 activity is starting to emerge. Another recent study shows MDM2 as an inhibitor of p53 translation (Ofir-Rosenfeld et al., 2008). The authors report that MDM2 decreases p53 translational levels by binding, via the acidic domain, and subsequently catalyzing polyubiquitination of L26 ribosomal protein. This protein has been shown to bind *p53* mRNA and augment its translation.

This apparent contradiction of MDM2 action on p53 translation can be understood when one considers the mechanism in more depth. First of all one is dealing with two different types of regulation. In the case where MDM2 binds to *p53* mRNA we are dealing with a direct (in *cis*) positive mode of action. In the later case the control is indirect as MDM2 limits the pool of a positive effector catalyzing p53 translation.

Moreover different domains within MDM2 govern these interactions. The direct binding of *p53* mRNA is facilitated by the RING domain, whereas L26 binding by MDM2 is carried out by the acidic domain. Furthermore, as the authors discuss, the level of L26 ubiquitination appears to impact only a minor, presumably functionally distinct, subpopulation of L26.

Numerous interactions of MDM2 through the acidic domain with ribosomal proteins have been reported. The oncoprotein interacts with the components of the large ribosomal subunit - L5 protein (Dai and Lu, 2004; Marechal et al., 1994) as well as with several other ribosomal proteins like L11, L23, S7 (Jin et al., 2004; Lindstrom et al., 2007; Lohrum et al., 2003; Zhang et al., 2003). For these cases, such binding, is thought to sequester MDM2 and inhibit p53 protein polyubiquitination resulting in the increase of transcriptionally active p53 pool (Dai and Lu, 2004).

All these recent discoveries highlight additional points of MDM2 mediated regulation of p53, showing the involvement of MDM2 not only in the degradation of the tumour suppressor but also in its synthesis.

1.4.4.7 Feedback loops

A variety of studies have identified numerous positive and negative loops in the p53 pathway (Harris and Levine, 2005). Each of these loops bases on a circuit of components composed of proteins whose activities or rates of synthesis are influenced by the activation of p53, and this in turn results in the alteration of p53 activity in the cell.

Those that involve MDM2 in them will be discussed below:

One of the foremost-characterized target genes of p53 is the *MDM2* gene. It binds to two adjacent p53-responsive elements located at an intronic, highly conserved p53 - dependent promoter (P2) within the *MDM2* gene (Zauberman et al., 1995a), and promotes the initiation of transcription. The resulting MDM2 protein possesses E3 ubiquitin ligase activity towards p53, resulting in targeting it for proteasomal degradation [for review see (Michael and Oren, 2003)], yet at the same time has a positive effect on p53 translation efficiency (Candeias et al., 2008b; Naski et al., 2009). In such circumstances MDM2 and p53 are linked through an autoregulatory feedback loop in which p53 induces *MDM2* transcription and MDM2 in the end targets p53 for degradation (review by Michael and Oren, 2002). Several

mechanisms are in place to modulate the p53-MDM2 pathway during times of cellular stress. Under these conditions p53 synthesis is increased, and MDM2–dependent degradation of p53 is inhibited. These mechanisms include p14 ARF binding to MDM2 (Kamijo et al., 1998; Pomerantz et al., 1998b).

1.4.4.7.1 p14 ARF

The p14 ARF (also referred to as p14/19 ARF) protein binds to MDM2 and inhibits its ubiquitin ligase activity increasing the levels of p53 protein in the cell (Honda and Yasuda, 1999). The transcription of the *p14 ARF* gene is positively regulated by E2F-1 (Zhu et al., 1999) and beta-catenin (Damalas et al., 2001) and negatively regulated by p53. The active p53 protein positively regulates the transcription of ubiquitin ligase Siah-1 (Fiucci et al., 2004), which in turn acts to degrade beta-catenin protein (Iwai et al., 2004). Beta-catenin levels can positively regulate p14ARF, which in turn is a suppressor of MDM2 leading to higher levels of p53. Siah-1 thus connects the Wnt-beta-catenin-APC pathway to the p53 pathway.

1.4.4.7.2 Retinoblastoma protein

The Retinoblastoma protein (Rb) is found in a complex with MDM2 and p53 in cells, resulting in high p53 activity and enhanced apoptotic function (Xiao et al., 1995). High levels of active E2F-1 not bound to Rb switch the p53 response from G1 arrest to apoptosis. Both Rb and MDM2 are phosphorylated and inhibited by the CDK2/CycE complex. When p53 is activated, it stimulates the synthesis of the $p21^{CIP1/WAF1}$ protein, inhibitor of CDK2/CycE activity. This in turn acts on the Rb/MDM2 complex that promotes p53 activity and apoptosis.

Upon DNA damage both MDM2 and p53 are modified by the ATM protein kinase (Chang et al., 2008; Chehab et al., 1999; Craig et al., 1999; Maya et al., 2001; Shieh et al., 1997). This leads to subsequent binding of the p300 co-activator and further acetylation of p53 in its C-terminal region (Shimizu and Hupp, 2003). This results in

the increase of the steady-state level of the p53 and consequential surge in the expression of more than a hundred p53 target genes, including those involved in cell cycle arrest, senescence and apoptosis (Michael and Oren, 2002).

1.4.4.7.3 CyclinG/PP2A complex

Another p53 responsive gene is *cyclin G.* It is transcribed to high levels upon p53 activation in various cell lines (Bates et al., 1996; Okamoto and Beach, 1994; Yardley et al., 1998; Zauberman et al., 1995b). The Cyclin G protein forms a complex with PP2A phosphatase, rendering it active and mediating dephosphorylation of MDM2 (Okamoto et al., 2002). Phosphorylation of MDM2 by Cdk2/CycA (Zhang and Prives, 2001) inhibits its activity, thus the PPA/CycG phosphatase complex acts oppositely, which in the end leads to a decrease of p53 activity. This loop acts both on the basal level of p53, and on higher levels activated upon stress induction (Okamoto et al., 2002).

1.4.4.7.4 Ubiquitin Ligases

Apart from MDM2 several other E3 ubiquitin ligases have been identified; COP1 , Pirh2, CHIP, ARF-BP1. These, apart from CHIP and ARF-BP1, similarly to MDM2 form an autoregulatory loop resulting in lower p53 activity (Dornan et al., 2004a; Dornan et al., 2004b; Leng et al., 2003). The genes encoding these proteins are transcriptionally activated by p53.

1.4.5 p53-independent functions of MDM2

For a tumour to overexpress MDM2 and inactivate p53 would seem redundant, unless MDM2 has other functions. The MDM2 oncoprotein also possesses numerous

p53-independent activities, which contribute to the development of tumours where MDM2 is overexpressed.

1.4.5.1 Evidence in tumours and cell lines

MDM2 overexpression occurs mostly by gene amplification possibly caused by polymorphism at the *mdm2* promoter sequence (Bond et al., 2004) for review see also (Daujat et al., 2001a; Ganguli and Wasylyk, 2003; Zhang et al., 2005b). Human cancers with non-functional p53 and amplification of *MDM2* have poor prognosis (Cordon-Cardo et al., 1994; Dworakowska et al., 2004). MDM2 also confers a growth advantage to cells without p53 and pRb, overcoming G1-cell cycle arrest induced by p107 (Dubs-Poterszman et al., 1995).

Transgenic mice with a wild-type MDM2 gene are predisposed to spontaneous tumour formation in a *p53 -/-* background, and have a high incidence of lymphoma and sarcoma (Jones et al., 1998). More than forty MDM2 isoforms have been detected in human cancers (Bartel et al., 2004). Interestingly, splice variants lacking the p53-binding domain were identified in human and murine tumours and subsequently shown to promote transformation *in vitro* and tumour development *in vivo* (Harris, 2005). Furthermore synonymous mutants were shown to be associated with high-grade and late-stage human cancer (Liang et al., 2004; Steinman et al., 2004).

1.4.5.2 p53-independent activation of MDM2 expression

To add to the complexity of MDM2 regulation, it must be stated that its gene expression is regulated by additional mechanisms independent of p53. *MDM2* expression profile during development has been shown to be independent of p53 in different organs (Leveillard et al., 1998). *MDM2* expression increases following FGF-2 treatment in cells (Bates et al., 1998). The *MDM2* promoter has been shown to be a target of the MAPK kinase pathway, thus upregulation of Ras during normal

cell signalling or through mutation can induce increase of MDM2 functions (Ries et al., 2000).

1.4.5.3 MDM2 Interactome

Although the published data indicates that elevated levels of MDM2 contribute to tumour development independently of p53, the biochemical mechanism of oncogenic activity of MDM2 remains elusive. Indeed, though MDM2 interacts with proteins fulfilling a variety of cellular functions (p300, pRb, Numb, MTBP, DNA polymerase ε, PML, Tip60, YY1, IGF-IR, GR/ER, AR, HIF-1, p73, NF-κB, PSP-95, ARF, E2F1, TBP, TAFII250, Sp1, ribosomal proteins, TSG 101, Ras-GAP binding proteins, $p21^{CIP1/WAF1}$), the biological significance of these multiple interactions remains to be explained. It should be stressed that not all MDM2 interacting proteins are targeted for proteasome-dependent degradation, hence not all involvement of MDM2 protein can be explained by its E3 ubiquitin ligase activity.

It is not the intention to directly elaborate on each and everyone member of the above-listed MDM2 protein interactors, though it is informative when one sub-categorizes this group into sets of proteins involved in major cellular pathways; cell cycle (Rb, E2F1/DP1, $p21^{CIP1/WAF1}$, PML, MTBP, TGF-β1), differentiation (Numb), DNA synthesis (DNA Polymerase ε), ribosome biosynthesis (L5, L11, L23 ribosomal proteins, 5SrRNA), transcription (TBP, $TAF_{II}250$, p300, NFκB).

Of note is the fact that not all of the MDM2 interactions mentioned fall in the tumourigenesis promoting category. The physical interaction between human DNA polymerase ε is of particular interest. Initially established by a yeast two hybrid screen has been confirmed by *in vitro* binding of the proteins isolated either from *E.coli* or insect cells and co-immunoprecipitation from cell culture (Vlatkovic et al., 2000). Further analysis mapped the interaction motif within MDM2 to the N-terminal 166 amino acids, in addition to binding this region is essential for induced activation of DNA polymerase ε. The proposed roles of this enzyme include DNA repair, recombination, replication, damage sensing and chromatin remodelling. In

response to DNA damage, MDM2 may mediate a beneficial process that allows the polymerase to associate with repair/recombination proteins.

Additionally a link between MDM2 and cyclin A, a regulator of cell cycle, has been reported. This particular cyclin is important for a cell to enter S phase. MDM2 was shown to regulate the expression of cyclin A, indirectly through interaction with component of the general transcription factor family. MDM2 binds $TAF_{II}250$ through its C-terminal RING domain. Basal levels of MDM2 activate *cyclin A* transcription, whereas high levels of MDM2 inhibit the process (Leveillard and Wasylyk, 1997).

1.4.5.4 MDM2 mediated ubiquitination of other proteins

Although the enzymatic E3 ubiquitin ligase activity of MDM2 is considered primarily in terms of p53, it can also catalyse the addition of ubiquitin moieties to other proteins. Growing evidence indicates that a subpool of proteins within the MDM2 interactome can be regulated by its ligase activity.

1.4.5.4.1 β-arrestins

G-protein-coupled receptors (GPCRs) constitute a vast family of signalling molecules. They are shown to have fundamental roles in regulation of a variety of cellular functions including, cell growth, differentiation and metabolism. This is due to their signalling transduction potential from myriad extracellular signalling mediators (hormones, neurotransmitters, chemokines, environmental stimuli etc.) to intracellular effector pathways. A key feature that occurs upon the activation of these receptors is the negative feedback loop activation that prevents potentially harmful effects resulting from persistent activation of signal pathways. This regulatory loop is maintained by G-protein-coupled receptor kinases (GRKs), which upon agonist binding to the receptor, mediate phosphorylation of the intracellular fragment of the

receptor. This is followed by translocation to the cell membrane of β-arrestins – negative-regulators of GPCRs. Two known paralogues namely, β-arrestin 1 and 2 were shown to bind to the phosphorylated agonist bound GPCR and facilitate uncoupling and internalisation of the receptor in effect leading to desensitization of the cell to a given signal (Ma and Pei, 2007).

MDM2 is known to participate in this regulatory negative feedback loop, moreover its E3 ubiquitin ligase activity is key. The ligase binds to β-arrestins and catalyzes their ubiquitination, which leads to receptor internalization (Shenoy et al., 2001). For the ubiquitination reaction to occur two points need to be met, agonist occupancy on the GPCR and GRK-mediated phosphorylation of his receptor, ensuring β-arrestin displacement to the vicinity of the receptor. The region within MDM2 mediating physical interaction with β-arrestin was roughly mapped to amino acids 161-321 (Shenoy et al., 2001), which in part encompasses the acid domain of MDM2. MDM2-catalysed ubiquitination of β-arrestin is required for the internalization of the GPCR. Moreover, the receptor itself was shown to be polyubiquitinated, which can be mediated by MDM2, though the oncoprotein is not essential, as other E3 ligases can catalyse this reaction (Shenoy and Lefkowitz, 2003). Ubiquitination of β-arrestin and of the receptor appears to serve different functions in regulating the life cycle of the receptor. β-arrestin ubiquitination is required for receptor internalization, whereas direct receptor ubiquitination leads to proteasomal degradation (Shenoy et al., 2001; Strous and Schantl, 2001).

The β-arrestin mediated recruitment of MDM2 to the proximity of the receptor complex has additional features worth mentioning. First, a G-protein-coupled receptor kinase, namely GRK2 was found, through a series of elegant experiments, as an additional target of MDM2 E3 ligase activity (Salcedo et al., 2006). Secondly, these series of events dramatically affects subcellular localization of MDM2. The E3 ligase in resting cells is distributed primarily in the nucleus, where it carries out transcriptional regulation of p53. Upon ligand induced activation of the GPCR, the formation of the cytoplasmic complex is stimulated which contains MDM2, β-arrestin, and the receptor, thus MDM2 for some time is retained in distinct

compartment than the p53 transcription factor. Hence this flux may directly stimulate p53 transcriptional activity (Ma and Pei, 2007).

1.4.5.4.2 FOXO4

The Forkhead box O (FOXO) class of transcription factors are involved in the regulation of several cellular responses including cell cycle progression and apoptosis. These proteins additionally act as transcription factors and affectors of ageing in model organisms (van der Horst and Burgering, 2007; Wolff and Dillin, 2006; Wolff et al., 2006).

Additionally FOXOs and p53 are remarkably similar within their spectrum of regulatory proteins (van der Horst and Burgering, 2007). Hence, it may come to no surprise that MDM2 was found be an active E3 ubiquitin ligase towards FOXO4 (Brenkman et al., 2008). The ligase was shown to catalyse monoubiquitination of FOXO4 induced by hydrogen peroxide treatment. Increase in proteasomal degradation of the targeted protein post modification was not observed, in contrast the attachment of monoubiquitin to the target protein, as mentioned earlier is thought to be linked to regulated compartmental trafficking within the cell.

1.4.5.5 Genome instability affected by MDM2

Maintenance of genome integrity and stability is paramount in maintaining myriad pathways that cooperate to ensure that the genome remains intact and mutations are not passed on to daughter cells.

Data supports the notion that MDM2 is a prominent node regulating genome stability ultimately leading to cellular transformation [for comprehensive reviews see (Bouska and Eischen, 2009a, b)]. Overexpression of human MDM2 in murine fibroblasts led to centrosome amplification, which resulted in chromosome instability (Carroll et al., 1999). Subsequently transgenic Mdm2 expression in mammary epithelial cells caused polyploidy in mice independent of the status of p53 (Lundgren et al., 1997).

Cell culture based studies indicate that *MDM2* overexpression drives cell-cycle progression and increases the percentage of cells entering S-phase (Bond et al., 2005; Lundgren et al., 1997; Sdek et al., 2005). This in part is due to p53 inhibition. Nevertheless p53 independent activities of MDM2 should be acknowledged as well, namely MDM2 mediated disruption of the Rb-E2F1 control axis (Sdek et al., 2004).

The MDM2 oncoprotein also regulates proteins involved in DNA repair and cell cycle control. Therefore MDM2-overexpressing cells are doubly disadvantaged because they would have less time to repair their DNA rendering the process less efficient, making accumulation of mutations even more likely.

Nevertheless MDM2's oncogenic potential was contradicted by several experimental findings; G1 cell cycle arrest induced by MDM2 driven cyclin A depletion (Zhou et al., 2005) is of note. Furthermore, MDM2 mediated activation of DNA polymerase ε is also in direct contradiction of the dogma.

$p21^{CIP1/WAF1}$ (a cyclin-dependent kinase inhibitor blocking G1/S phase transition) is another provoking example. The classical studies have clearly shown that MDM2 negatively regulates the levels of *p21* expression through a p53 dependent pathway. Moreover, evidence has also emerged that MDM2 regulates p21 expression independently of p53. MDM2 can directly bind p21 leading to p21-C8 proteasome subunit association and a subsequent decrease in p21 protein levels (Jin et al., 2003; Zhang et al., 2004b). Despite this *p21* transcription driven by a p53 paralogue – p63 was considerably enhanced by MDM2 in Saos2 tumour cells (Calabro et al., 2002). Another p53 paralogue – p73 that is capable of inducing transcription of many p53 responsive genes, was shown to be stabilized by MDM2 (Ongkeko et al., 1999).

MDM2 activity has also been shown to correlate directly to the induction of apoptosis in a cell and context specific manner. MDM2 overexpression in medullary thyroid carcinoma cells, lacking functional p53, induced an increase in E2F-1 expression. E2F-1 dependent transcriptional activity sensitized the cells to gamma-radiation induced apoptosis (Dilla et al., 2002). Cancers can evade treatment-induced apoptosis by upregulating NFκB, a heterodimeric anti-apoptotic transcription factor.

In rhabdamyosarcoma cell line in which the NFκB pathway is constitutively active alongside with mutant p53 expression, MDM2 overexpression led to suppression of cell growth and increased apoptosis (Cheney et al., 2008).

1.4.6 Regulation of MDM2 protein activity

Post-translational modification of eukaryotic proteins governs their functional output in the cellular environment or in the extracellular matrix.

Post-translational mechanisms acting on the MDM2 protein not only regulate its intrinsic enzymatic activity in response to cellular stresses, but also govern its subcellular localization, differentiate between substrate-ubiquitination and auto-ubiquitination, and last but not least integrate the stress response with mechanisms mediating cell survival.

1.4.6.1 Interacting proteins

Numerous protein interactors other than p53, exert a regulatory effect on MDM2, both in light of the p53-MDM2 autoregulatory feedback loop, and its p53-independent activities.

1.4.6.1.1 Nucleophosmin

Nucleophosmin (NPM) is a nucleolar phosphoprotein that acts as a molecular chaperone for ribosome assembly and protein transport, shuttling between the nucleolus and cytoplasm also being essential for centrosome duplication (Okuda et al., 2000). It has been reported that MDM2 binds to NPM in a p53-independent manner, both *in vitro* and in cell culture (Kurki et al., 2004). The NPM binding region was mapped to the p53 binding domain and the RING-finger domain of MDM2. Upon UV stress an increase of the MDM2-NPM complex is observed mediating p53 sumoylation and leading to the stabilization of the tumour suppressor

(Kurki et al., 2004). Moreover MDM2 overexpression was shown to be induced by NPM in a *p53 -/-* background (Saos cells). As described earlier within this particular cellular context MDM2 was shown to upregulate the transcriptional activity of p63, yielding an increase in p21 levels (Calabro et al., 2002). Although the exact mechanism of NPM activity on MDM2 is yet to be elucidated, given the data published up to date, NPM might be considered as a molecular switch controlling MDM2 activity.

1.4.6.1.2 Merlin

Merlin is one of the numerous proteins involved in control of cell growth and differentiation (Morrison et al., 2001). Its tumour suppressor function has been implicated by studies in the mouse model. Germ line heterozygous *nf2* (gene encoding Merlin) mutant mice develop a variety of aggressive malignancies with metastatic properties (Kim et al., 2004). Merlin, by direct interaction with MDM2 induces auto-ubiquitination and degradation of the latter. This in effect augments cellular death induced by doxorubicin in lung cancer cells with wild-type p53.

1.4.6.1.3 p300

The p300 protein and its homologue CREB-binding protein (CBP) were shown to co-activate p53 in response to DNA damage via acetylation (Grossman, 2001). MDM2 was shown to interact with the p300 transcriptional co-activator (Ito et al., 2001; Jin et al., 2002; Kobet et al., 2000; Wang et al., 2004). The result of this interaction is quite complex. It involves the effects of p300 on p53 and MDM2 protein turnover and MDM2 synthesis. It was shown that p300 is required by p53 to induce the transcription of the *MDM2* gene. Moreover, inhibition of p300 results in p53 stabilization and apoptosis (Thomas and White, 1998). In agreement with this observation it was subsequently shown that CBP/p300 and MDM2 play a synergistic role in the regulation of p53 stability. In unstressed cells, CBP/p300, p53 and MDM2 form a ternary complex that mediates p53 turnover (Grossman et al., 1998). Interestingly, further data postulate that p300 is the major enzyme catalyzing p53

poly-ubiquitination, whereas MDM2 mediates only multiple mono-ubiquitin attachment to p53 (Grossman et al., 2003).

Under stress conditions, such as DNA damage, the following model is proposed. The p53 protein becomes stabilized and activated by phosphorylation at multiple sites, leading to a dramatic decrease in MDM2 affinity for the tumour suppressor. Enhanced recruitment of CBP/p300 to p53 follows, leading to acetylation within the C-terminal regulatory domain of p53 (Appella and Anderson, 2001) (Bode and Dong, 2004; Dornan et al., 2003; Xu, 2003). Site-specific phosphorylation of p53 and MDM2 alike determine the preferential binding of the coactivator complex by the tumour suppressor while at the same time impairing the MDM2-p53 interaction (Shimizu and Hupp, 2003).

1.4.6.1.4 ARF

The *INK4a-ARF* locus (*CDKN2A* in humans) encodes two intimately linked but distinct tumour-suppressor proteins, $p16^{INK4a}$ and $p14^{ARF}$ ($p19^{ARF}$ in mouse) that indirectly govern the activities of retinoblastoma protein (RB) and the p53 transcription factor [for a thorough review see (Sherr, 2006)].

The $p14^{ARF}$ protein from now on referred to as ARF is believed to be prominent player in tumour surveillance as it was shown to protect p53 from MDM2 mediated degradation (Chin et al., 1998; Kamijo et al., 1998; Pomerantz et al., 1998a; Saporita et al., 2007; Zhang et al., 1998). As a result of this antagonizing effect of ARF on MDM2, the p53 transcription factor is stabilized and its activity is increased. ARF induced p53 stabilization is though to be mediated by sequestration of MDM2 into the nucleolus, thus due to distinct compartment localization, the interaction between the tumour suppressor and the E3 ubiquitin ligase will not occur (Pomerantz et al., 1998a; Tao and Levine, 1999b).

1.4.6.1.5 MDM4

MDM4 (also referred to as MDMX) was identified in 1996 as a p53-binding protein, which is structurally and functionally related to MDM2 (Shvarts et al., 1996a)

This MDM2 paralogue contains an N-terminal p53 binding domain, a central Zinc-finger motif and a RING-finger motif located in the C-terminus. Nevertheless unlike MDM2, MDM4 is not an active E3 ubiquitin ligase for p53.

Its role as another critical regulator of p53 emerged with studies on MMD4 knockout mice displaying embryonic lethality that was prevented with parallel *p53* gene deletion (Finch et al., 2002; Migliorini et al., 2002). Intriguingly, MDM2 and MDM4 are non-redundant, mutually dependent regulators of p53, as each regulator is normally unable to compensate for the loss of the other.

Similar to MDM2, MDM4 can bind to the transactivation domain of p53, thus limiting its transcriptional activity by restricting access to essential transcription co-activators, and presumably basal transcription machinery (Marine and Jochemsen, 2005).

Structural studies are beginning to unravel the MDM2-MDM4-p53 regulation mechanism. MDM4 has been shown to heterodimerize with MDM2 via the RING domain present in both of the proteins and a crystal structure of such a complex has recently been solved (Linke et al., 2008). The authors propose that MDM4 regulates p53 abundance by modulating the levels and activity of MDM2. Dimerization, mediated by the conserved C-terminal RING domains of both MDM2 and MDM4, is critical to this activity. Numerous reports indicate that MDM4 regulates MDM2 activity on p53 in cell based models, although initially contradictive, a consensus is starting to emerge showing that the MDM2:MDM4 protein abundance ratio is key in the decision fork leading to p53 stabilization or degradation and/or MDM2 turnover. (Gu et al., 2002; Kawai et al., 2007; Okamoto et al., 2005; Stad et al., 2001).

1.4.6.1.6 Protein Kinases

A number of stress response and cell cycle regulatory kinases have been shown to interact and phosphorylate several sites within MDM2 in a cellular context. The general outcome of these modifications is the destabilization of the p53-MDM2 interaction. Further details on the known phosphorylation sites and the mediating kinases will be discussed in the phosphorylation subsection.

1.4.6.2 Ubiquitination

MDM2 protein is an active E3 ubiquitin ligase mediating the transfer of ubiquitin to substrates such as p53 tumour and others such as NUMB, IRF-2, beta arrestin (Juven-Gershon et al., 1998; Pettersson et al., 2009; Shenoy et al., 2001). Moreover MDM2 is able to catalyze auto-ubiquitination, thus regulating its own abundance in the cell (Fang et al., 2000; Honda et al., 1997).

It is worth to note that while sites of ubiquitination have been clearly mapped to a cluster of lysine residues in the C-terminal regulatory domain of p53 (Rodriguez et al., 2000) and the DNA binding domain as well (Chan et al., 2006), the identities of the auto-ubiquitination sites in MDM2 have so far been only proposed to lie within the α-helix of the ββαβ super-secondary structure fold of the C-terminal RING domain of MDM2 (Linke et al., 2008).

Specificity in the transfer of ubiquitin to p53 and MDM2 itself is thought to be dictated by the RING domain, as the substitution of this domain with a heterologous RING finger permits auto-ubiquitination but abolishes ubiquitination of p53 (Fang et al., 2000). The balance between auto- and substrate-ubiquitination of MDM2 is modulated physiologically by post-translational modifications, including sumoylation, phosphorylation and acetylation.

1.4.6.3 Sumoylation

Reversible modification of a number of proteins involved in gene expression by a small ubiquitin-like modifier, SUMO, has profound effects on the activity of the protein. This modification has been shown to affect protein stability/turnover, localization, protein-protein interaction and DNA binding potential. The addition of SUMO to lysyl ε-amino groups in target proteins occurs through an enzyme cascade, analogous to that of the ubiquitination machinery.

The site of SUMO modification has been mapped in MDM2 to lie within the stretch of amino acid residues 134-212, this region contain the Lys^{182} as well as $Lys^{136,146,185}$ (Miyauchi et al., 2002; Xirodimas et al., 2002).

There are at least two models elucidating MDM2 sumoylation. One proposes the SUMO moiety is attached to MDM2 as it enters the nucleus, because RanBP2 is a part of the nuclear pore, and further sumoylated by PIAS proteins within the nucleus itself (Miyauchi et al., 2002). The second model postulates that conjugation of SUMO to MDM2 is promoted by ARF (Xirodimas et al., 2002). This is of particular interest as it diminishes MDM2 mediated degradation of p53 and is consistent with the notion that SUMO and ubiquitin modifications may be mutually exclusive and/or antagonistic (Meek and Knippschild, 2003). This suggests that SUMO modification of MDM2 can differentially modulate the outcome of MDM2 E3 ubiquitin ligase activity in a manner that favours p53 accumulation. This is a stress responsive switch, as UV irradiation has been shown to decrease the interaction between MDM2 and Ubc9 (SUMO E3 ligase), resulting in the loss of MDM2 sumoylation (Buschmann et al., 2001).

1.4.6.4 Phosphorylation

If one considers the primary structure of MDM2 in terms of amino acid residue abundance, almost 20% of the total amino acids building MDM2 are either serine or

threonine residues. Two major clusters of phosphorylation sites have been mapped and are located at the N-terminal and the central acidic domains of MDM2.

1.4.6.4.1 DNA-PK

The DNA-activated protein kinase (DNA-PK) is a member of the phosphatidyloinositol 3-kinase (PI3-K) family, which includes ATM (ataxia telangiectasia-mutated) and ATR (ATM and Rad3-related) protein kinases. DNA-PK, ATM, and ATR share many substrates and are each targeted toward a SQ core motif in the target protein.

Of eight potential DNA-PK targets in MDM2, Ser^{17} site is of particular interest. This site has been shown to be phosphorylated *in vitro* (Mayo et al., 1997b) and although this phosphorylation site in physiological (*in vivo*) context has yet to be confirmed, the significance of it on p53 MDM2 interaction/complex formation is prominent. This is due to the proximity of the serine to the ordered hydrophobic cleft of MDM2 (amino acids 25-109) which accommodates the BOXI (part of the transactivation domain) domain of p53. It has been reported the residues (16-24) preceding the hydrophobic pocket of MDM2 form a flexible lid /pseudo substrate motif (McCoy et al., 2003). This labile polypeptide, due to its location, has great potential for intramolecularly controlling MDM2 affinity towards p53 by selectively blocking or enhancing the access to the hydrophobic pocket of MDM2, which constitutes the major p53 interaction site. Furthermore, it can be deduced from the information given above, Ser^{17} lies within this region and is part of a consensus DNA-PK, ATM site (SQ motif). In vitro phosphorylation of this site has been shown to diminish the p53-MDM2 complex (Mayo et al., 1997a).

1.4.6.4.2 ATM

MDM2 was shown to be rapidly phosphorylated in an ATM–dependent manner in response to specific DNA-damaging agents (Khosravi et al., 1999). Subsequent studies indicated that ATM phosphorylates MDM2 on Ser^{395} *in vitro* and in cell culture based assays (Maya et al., 2001). The phosphorylated form of MDM2 was

shown to decrease control activity over p53 indicating a reduction of the affinity towards the interacting partner.

1.4.6.4.3 PI3-K/Akt Pathway

In response to the activation of lipid PI3-K kinase with its appropriate second messenger phospatydyloinositol(3,4,5)-triphosphate (PIP_3), by upstream growth factor and cytokine binding to plasma membrane receptors, the down stream effect ensues which involves the activation of Akt kinase by phosphorylation. Once activated this kinase is released from the cytoplasmic envelope and is free to interact with potential targets, one of which is MDM2. The Akt phospho-acceptor sites in MDM2 have been mapped to Ser^{166} and Ser^{186}, these two amino acids lie in close proximity of the NES and NLS and evidence suggests that phosphorylation of these residues by Akt stimulates entry of MDM2 into the nucleus (Mayo and Donner, 2001; Zhou et al., 2001). Moreover, MDM2 phosphorylated at $Ser^{166,186}$ was shown to have decreased binding to its negative regulator ARF (Blattner et al., 2002). In addition, the modulation of MDM2 by the PI3-K/Akt pathway by Insulin growth factor 1 receptor stimulation (member of the G protein coupled receptors, described previously in this introduction) alters G protein receptor kinase 2 (GRK2) degradation and augments the cellular levels of the kinase, putting forward a new mechanism for controlling GRK2 activity (Salcedo et al., 2006).

1.4.6.4.4 c-Abl Tyrosine Kinase

The *ABL* proto-oncogene encodes a protein tyrosine kinase, capable of shuttling between the cytoplasm and nucleus. The cytoplasmic c-Abl is involved in mediating the response to growth and survival signals, whereas nuclear c-Abl plays a pivotal role in mediating apoptosis.

MDM2 was shown to associate with c-Abl both *in vitro* and in the nuclei of cultured cells leading to the phosphorylation of MDM2 at multiple sites (Goldberg et al., 2002). Of these the key phosphorylation site was identified to be Tyr^{394}. Upon phosphorylation of MDM2 by c-Abl, the activity of the former to down-regulate p53

has been shown to decrease dramatically, keeping in line with the model that this modification contributes to the promotion of p53 induced apoptosis.

1.4.6.4.5 CDK2-cyclinA

The role of MDM2 in cell cycle regulation is at multiple levels. Taking aside the p53 dependent actions and direct, p53 independent, interaction with $p21^{WAF1/CIP1}$. MDM2 protein was shown to regulate the levels of cyclin A protein. The latter in complex with CDK2 (Cyclin dependent kinase), phosphorylates MDM2 at Thr^{216} (Zhang and Prives, 2001) in effect leading to a decrease in the MMD2-p53 interaction and an increase of association of ARF to MDM2.

1.4.6.4.6 CK2

The CK2 protein kinase phosphorylates MDM2 at Ser^{269} and although this modification occurs physiologically. Its direct effect, apart from a minor increase in MDM2 mediated p53 turnover, is yet to be discovered (Dumaz et al., 2001; Gotz et al., 1999; Guerra et al., 1997).

1.4.6.4.7 Multisite phosphorylation of the acidic domain

The acidic domain of MDM2 is centrally located in the primary structure of the protein and contains several structural elements that contribute to the interaction with p300, ARF, Rb, some ribosomal proteins. A cluster of phosphorylation sites has been shown to reside within the acidic domain (Ser 240-262) (Blattner et al., 2002; Hay and Meek, 2000). The published data suggest that that this cluster of residues is normally phosphorylated in the cell under non-stress conditions, nevertheless the kinases involved in this process still remain to be identified. Functionally, however, based on site directed mutagenesis studies, this modified cluster may significantly contribute to MDM2 mediated turnover of p53.

As in the case of many post-translational modifications, phosphorylation is a reversible process. Dephosphorylation of the acidic domain in agreement with other sites is thought to play a role in the network of events mediating stress responses and

p53 induction. It was shown that key phospho-serine residues in the acidic domain are dephosphorylated in response to ionizing radiation in a manner that clearly precedes p53 accumulation (Blattner et al., 2002).

1.4.6.5 Acetylation

MDM2 was reported to be a target for acetylation (Wang et al., 2004). MDM2 is acetylated *in vitro* and in tissue based experiments by CREB-binding protein (CBP) and to a lesser extent by p300. Acetylation occurs primarily within the RING domain of the protein, moreover the native fold of this structural motif is key for this post-translational modification to occur. Furthermore the authors have shown that the acetylation-mimicking mutant of MDM2 ($Lys^{466/467Glu}$) is impaired to promote p53 ubiquitination as well as auto-ubiquitination (Wang et al., 2004).

Acetylation of the p53 transcription factor generally regarded as important component of the activation cascade of the protein in response to various stress stimuli. Thus, regulated acetyltransferase activity may contribute to the p53 response through a dual mechanism, involving simultaneous activation of p53 and inactivation of its regulator MDM2.

1.4.7 Intrinsic chaperone activity of MDM2

If one considers the plethora of research data published in regards to MDM2 there are several findings that indicate MDM2 as having similar activity to those described for molecular chaperones. Namely, binding to nascent polypeptide chain (Yin *et al,* 2002), activation of transcription factors E2F1, p63 (Martin *et al,* 1995; Calabro *et al*, 2002), protection and activation of DNA polymerases (Asahara *et al*, 2003), involvement in ribosome assembly (Marechal *et al*, 1994), (Hartl and Hayer-Hartl, 2002).

Molecular chaperones are defined as a vast class of structurally unrelated proteins that assist in correct non-covalent assembly of other polypeptide-containing

structures, but which are not components of these assembled structures when they are performing their normal biological functions (review Ellis, 1993). Through controlled binding and release cycles, chaperones facilitate the correct fate of polypeptides bearing non-native conformation. Recently it was shown that the Hsp90 molecular chaperone, in an ATP-dependent reaction, retains p53 in a conformation that allows binding to a specific promoter sequence (Walerych et al., 2004).

Given that MDM2 protein can bind ATP, interact with the Hsp90 chaperone, has a significant role in the activation of transcription factors, protection and activation of DNA polymerases, involvement in ribosome assembly and nascent p53 protein biosynthesis, the experimental data in this thesis shows MDM2 protein to possess an intrinsic molecular chaperone activity.

1.5 Targeting the MDM2-p53 interaction for cancer therapy

The p53 protein is a stress responsive transcription factor that is intimately involved in myriad surveillance networks that monitor genome status, dynamically respond to variation in gene expression and changes in the extracellular matrix composition. These are in place to govern cellular function and integrity, moreover preventing the cell from neoplastic transformation. The importance of the p53 node in these networks is highlighted by the fact that it is either mutated or inactivated roughly half of human tumours. For those human cancers that retain wild-type p53, its activity is disabled by alternative mechanisms, in part mediated by MDM2 overproduction.

Given the fact that MDM2 is considered to be the chief negative regulator of p53, several therapeutic strategies aimed at liberating the tumour suppressor from MDM2 are analysed, all in principle focus on restoring p53 activity, which in effect is expected to limit tumourigenesis.

1.5.1 Proof of principle

The data provided by mouse knockout and knockdown models have clearly shown the genetic interdependence of p53 and MDM2. Basing on the on the fact that decreased sub-physiological levels of the MDM2 protein in a p53 wild-type background are beneficial for the organism to resist tumour formation. Early studies through the use of biological reagents have validated MDM2 as a potential drug target (Bottger et al., 1997b; Picksley et al., 1994; Wasylyk et al., 1999). Transient RNA interference gene knockdown techniques utilized a decrease of MDM2 abundance in the cell, thus facilitating pronounced p53 activation leading to growth arrest and/or apoptosis (Tortora et al., 2000; Zhang et al., 2005a). Moreover, microinjection of MDM2 specific antibodies as well as introduction of scaffold attached competitive peptides, disrupted the p53:MDM2 protein interaction, ensuing an increase of the p53 tumour suppressor response. These biological reagents provided proof of concept for the activation of p53 by targeting MDM2.

1.5.2 Inhibition of MDM2 E3 ligase activity

Biochemically, the MDM2 protein should be regarded as an enzyme. By providing a discrete platform for the interaction of the target protein – p53 with the E2 conjugating enzyme, it increases the rate at which the ubiquitin transfer reaction reaches equilibrium. This is a simplified view, nevertheless it does provide grounds to consider this RING finger E3 ubiquitin ligase as a drug discovery target. In theory there are two potential approaches to block MDM2s E3 ubiquitin ligase activity. One is to develop molecules that disrupt the interaction between the RING finger and the E2 protein. The other is to disrupt the interaction between the ubiquitination substrate-p53 and the substrate interaction domain on the E3-MDM2. These two approaches differ greatly by the specificity of action - the first one, aims at extinguishing MDM2 E3 ligase activity irrespective of the ubiquitination substrate, whereas the later focuses purely on the MDM2:p53 primary interaction site.

Small molecule inhibitors of E3 enzymes are still in the preliminary stage, to date only a few compounds have been reported to decrease MDM2s E3 ubiquitin ligase activity. Through *in vitro* based enzyme chemical screening assays, three inhibitors were identified belonging to chemically distinct classes (benzosulfonamides, ureas, imidazolones) , each with the potency in the micromolar range (Lai et al., 2002). These three compounds were synonymous in selective inhibition of MDM2 E3 ligase activity, with little or no effect on other enzymes of the ubiquitination cascade. The mode of action of these three compounds is mutually exclusive indicating a common site of interaction within MDM2, which still remains to be identified. Moreover they showed a non-competitive profile with respect to the major substrate – p53. Surprisingly these molecules did not inhibit MDM2 mediated auto-ubiquitination.

Another class of small molecules (HLI98) was reported to inhibit the E3 ubiquitin ligase activity of MDM2 (IC_{50} 20-50 μM range) leading to p53 dependent activation of transcription in cell models (Yang et al., 2005). Nevertheless the authors underline the preliminary nature of their findings, as cellular induced toxicity was observed and also unspecific inhibitory effects on structurally and mechanistically unrelated E3 ubiquitin ligases (HECT domain E3s) was acknowledged. Further, optimization of these inhibitors to increase their potency and selectivity is required to assess the potential of this p53-activating strategy.

1.5.3 Blocking the interaction between p53 and MDM2

1.5.3.1 Competitive inhibitors targeted to bind MDM2

MDM2 is unable to downregulate p53 if prevented from interacting with it. For a small molecule to function effectively as an inhibitor of protein-protein interaction it must fulfil two interdependent key requirements: affinity and specificity (Vassilev, 2004). From a structural standpoint the primary p53-binding interface in MDM2 looks inviting for experimental drug design. This is due to the existence of a well-defined open p53-binding pocket on the MDM2 polypeptide into which exogenous

low molecular weight compounds could preferentially bind, therefore diminishing the physiological p53:MDM2 interaction. Whether these potential drugs act simply as competitive inhibitor and/or have a diminishing effect on the ubiquitination state of p53, is open for discussion. This is due to the allosteric mechanism by which MDM2 catalyzes ubiquitination of p53 and shall be discussed in further detail in appropriate parts of this thesis.

The set of inhibitors falling within this category, both small molecule and peptide based, have been steadily increasing for almost a decade now. Early members of this group represented diverse chemotypes and although shown satisfactory inhibition of tumour cell proliferation *in vitro*, they failed (with a few exceptions) to reproduce satisfactory potency *in vivo* (for review see (Dudkina and Lindsley, 2007).

Through extensive biochemical fine mapping, of the primary interaction site comprising the N-terminal amphipatic peptide fragment of p53 and the N terminus of MDM2, a potent 12 amino acid peptide inhibitor (later in this thesis described in more detailed and referred to as the 12.1 peptide) was discovered (Bottger et al., 1996). The offspring of this discovery were peptide antagonists shown to posses binding affinities over 1700-fold greater than the protoplast (Garcia-Echeverria et al., 2000).

Historically, members of the first set of small non-peptidic molecular p53:MDM2 inhibitors were the 4-phenyl-piperazine derivatives. These molecules were developed based on the class of peptide inhibitors described above. The architectural scaffold for their design, capitalized on the biochemical and crystallographic data regarding the mode of binding between MDM2 and p53. With the aid of structure based design and computational chemistry the following classes of molecules were proposed:

- **α-helicetical mimetics** (Chen et al., 2005b; Kutzki et al., 2002; Orner et al., 2001; Orner et al., 2002)
- **Norcamphane derivatives** (Zhao et al., 2002)
- **Chalone derivatives** (Stoll et al., 2001; Stoll et al., 2000)
- **Bisarylsulfonomides** (Vassilev, 2005; Zheleva et al., 2003)

- **Isoindolinone scaffold derivatives** (Hardcastle et al., 2005; Hardcastle et al., 2006)
- **Benzodiazepinediones** (Raboisson et al., 2005) (Parks et al., 2005; Zhang et al., 2004a)
- **Quilinol Derivatives** (Lu et al., 2006)
- **Spiro-oxindoles** (Ding et al., 2005; Ding et al., 2006)
- **Cis-imidazolines (Nutlins)** (Ambrosini et al., 2007; Vassilev, 2004, 2005, 2007; Vassilev et al., 2004)

The list above should be considered as representative, as it is not exhaustive. Nor should all of the list components be considered as potential drug leads. The point to acknowledge is the fact that all of these compounds exploded onto the scientific field in less than a decade post the year 2000. This is extremely encouraging as this pyramid of compounds shows increasing levels of potency. This is achieved through the increase in p53 ligand spatial mimicry, binding affinity – decrease of IC_{50} (the last four underlined classes of molecules representing IC_{50} in the nM range), specificity/selectivity and most important bioavailability.

1.5.3.2 Compounds binding to p53 and reactivating its function

A forced chemical induced activation of the p53 tumour suppressor may offer a therapeutic benefit for tumourigenesis decrease in the patient. Given that this protein is retained in the patient in a genetically non-mutated state, this in principle could be achieved through the mentioned above classes of anti-MDM2 compounds.

RITA (reactivation of p53 and induction of tumour cell apoptosis) is small molecule compound (2,5-bis-(5-hydroxymethyl-2thienyl)furan) initially discovered in the National Cancer Institute Anticancer Drug Screen (Issaeva et al., 2004). RITA is structurally and functionally unrelated to the previously described classes of compounds, as it does not seem to bind MDM2. Instead it is believed to bind the N terminus of p53 and prevents the recognition of p53 by MDM2 (Issaeva et al., 2004),

although no structural data depicting this is available at the moment. Interestingly, RITA seems to prevent p53 from interacting with other regulatory proteins such as PARC and p300 (Grinkevich et al., 2009; Issaeva et al., 2004). The RITA -stabilized p53 is transcriptionally active as it can promote transcription of downstream effector genes (Issaeva et al., 2004), moreover it slows down the growth of human tumour xenogrfts in mice in a dose dependent manner, although the oral bioavailability of this compound still remains to be confirmed.

The pharmacological rescue of p53 transcription factor function up to this point relied on one key point that the reader should be reminded of. The protein in question needed to be in a wild-type/non mutated form.

PRIMA-1 (p53 reactivation and induction of massive apoptosis) this is another prominent small molecule compound (2,2-bis-(hydroxymethyl)-1-azabicyclo[2,2,2]octan-3-one) discovered through screening of chemical libraries in cell based assays (Bykov et al., 2002b).

This compound and its methylated version PRIMA-1^{MET} were shown to effectively induce p53 downstream transcription targets in human cancer cells. Systematic administration of PRIMA-1 and PRIMA-1^{MET} inhibits human xenograft tumour growth in mice (Bykov et al., 2002a) (Bykov and Wiman, 2003; Foster et al., 1999). Elegant *in vitro* studies have shown that PRIMA-1 can preserve the physiological transcriptionally active conformation of the tumour suppressor under stress conditions. Moreover, PRIMA-1 restores mutant p53 function. Transcription dependent and independent induction of apoptosis facilitated by mutant p53 (H175R) in combination with drug treatment was shown (Bykov et al., 2002b; Chipuk et al., 2003; Zache et al., 2008). The molecular mechanism by which PRIMA-1 exerts it function on p53 was recently published (Lambert et al., 2009). The authors demonstrated that PRIMA-1 within the cell is converted to reactive products that can modify thiol groups, namely the cysteine residues in the core domain of p53. These residues represent a nucleophile profile and thus can be alkylated by the drug in question. The presented results indicate that covalent modification of one or several

cysteine residues in the core domain of the transcription factor is responsible for restoring the wild-type p53 conformation.

1.5.4 Drug leads applied in synergy

Given the plethora of potential drug leads aimed at restoring p53 function, one question is in need of answering, that is whether combinatorial use of the pharmacophores will show a synergistic antitumour effect. The grounds for such studies seem logical, as the molecules have been shown to attack different facets of the MDM2-p53 recognition process (for review see (Nalepa et al., 2006)). Surprisingly however, very little work has been done in this field. Although PRIMA-1 was tested in combination with commonly used anticancer drugs showing promising results. Namely, combined treatment with cisplatin (DNA alkylator) PRIMA-1^{MET} resulted in synergistic induction of tumour cell apoptosis and inhibition of human tumour xenografts in mice (Bykov et al., 2005). No studies yet have been performed to consider the recently identified broad panel (Nutlins, spiro-oxindoles, RITA, PRIMA-1) of possible pharmacological synergism between each other and/or possibly with more robust methods such as radiotherapy.

Chapter 2

Materials and Methods

Contents

2.1 General Reagents

Chemicals and reagents were supplied by Sigma unless stated otherwise. Tissue culture reagents including Dulbecco/Vogt modified Eagle's minimal essential medium (DMEM), Roswell Park Memorial Institute medium (RPMI 1640), McCoy's 5A medium, penicillin/streptomycin solution, trypsin- EDTA free solution and Lipofectamine™2000 were supplied by Invitrogen unless otherwise stated, while fetal bovine serum (FBS) was supplied by Autogen Bioclear.

2.2 General Lab Equipment

Fluroskan (Ascent FL), PowerwaveXS™ microplate reader (Bio-Tek), were used to read 96-well plates. DNA concentrations were measured using a NanoDrop® spectrophotometer. SDS PAGE was carried out using Biorad Protean II mini-gel system. X-ray films were developed using a Mediphot 937 developer. Sorvall RC-5C plus and Eppendorf 5415R were used for all centrifugations.

2.3 Cell Culture

2.3.1 Cell lines and Media

Cells were incubated at the recommended temperature and humidity (see table below) in incubators supplied by Hera. The following table lists the various cell lines used, their origin, optimum growth conditions and culture media.

Cell Line	Origin	Growth Conditions	Culture media	Media supplements
H1299	Human (lung – metastatic site lymph node), non-small cell lung carcinoma	5% CO_2 37ºC	RPMI-1640	10% (v/v) FBS 1% (v/v) P/S
HCT-116wt	Human (colon) colorectal carcinoma	5% CO_2 37ºC	McCoy's 5A	10% (v/v) FBS 1% (v/v) P/S
A375	Human (skin) malignant melanoma	10% CO_2 37ºC	DMEM	10% (v/v) FBS 1% (v/v) P/S
MEF DKO	Mouse Embryonic Fibroblasts *p53 -/- mdm2 -/-*	10% CO_2 37ºC	DMEM	10% (v/v) FBS 1% (v/v) P/S
MCF7	Human breast carcinoma	10% CO_2 37ºC	DMEM	10% (v/v) FBS 1% (v/v) P/S
A549	Human lung carcinoma	10% CO_2 37ºC	DMEM	10% (v/v) FBS 1% (v/v) P/S

Table 2.1 Cell lines used.

Abbreviation key: RPMI – Roswell Park Memorial Institute
DMEM – Dulbecco's Minimal Essential Medium
FBS – Fetal Bovine Serum
P/S – Penicillin/Streptomycin

2.3.2 Subculturing, storage and recovery of cells

Freezing media

50 % (v/v) Fetal bovine serum

10 % (v/v) DMSO

40 % (v/v) Tissue culture media (depending on cell line)

Cells were subcultured 2-3 times per week in 10 cm diameter culture dishes in sterile conditions and split to a maximal dilution of 1/10. The media was discarded and the cells were washed with sterile phosphate buffered saline (PBS). 1x Trypsin-EDTA solution (0.5 ml/ 10 cm diameter culture dishes) was added and the cells were placed in the incubator until the cells started to detach from the culture dish. The cells were taken up into media (9.5 ml/ 10 cm diameter culture dishes) and then split 1:10 into new culture dishes with fresh media (10 ml/ 10 cm diameter culture dishes).

Cells were kept in liquid nitrogen for long-term storage. To prepare cells for storage a 10 cm diameter culture dish with confluent cells was trypsinised and the cells collected by centrifugation (1000 rpm, 5 min, 4 ºC). The cell pellet was gently resuspended in 4 ml freezing media and transferred to cryotubes (Nunc) at 1 ml/ tube. The cells were frozen down slowly in Nalgene™ Cryo 1 ºC freezing containers and then transferred to liquid nitrogen.

To recover the cells the tubes were thawed quickly at 37 ºC and the cells transferred to a culture dish containing fresh media. The media was changed the following day and the cells were left to grow until they were confluent before being subcultured for the first time

2.3.3 Transient transfections

Cells were seeded out onto 6-, 24well plates or 10 cm^2 plates 24 h prior to transfection with/without antibiotics and grown to 80-90 % confluency. The cells were transfected with plasmid DNA using Lipofectmine™ 2000 (Invitrogen) according to manufacturer's handbook. DNA was trasfected at a ratio of 1:1 using

Lipofectamine^{TM} 2000. Cells were then incubated at 37°C overnight before they were harvested or subjected to chemical treatment or stress.

2.4 Microbiological Techniques

All microbiological techniques were carried out under aseptic conditions. Standard code of practice in line with health and safety regulation was employed.

2.4.1 *Escherichia Coli* - bacterial Strains

DH5α — *[F^- (ϕ80dΔ(lacZ)M15) recA1 endA1 gyrA96 thi-1 hsdR17(r_k^- m_k^-) supE44 relA1 deoR Δ(lacZYA-argF)U169]*

BL21 (DE3) — *[F^- ompT hsdS (rB^- mB^-) dcm^+ gal I (DE3) endA The]*

BL21 (DE3) CodonPlus – RP (Stratagene) — *F^- ompT hsdS (rB^- mB^-) dcm^+ gal I (DE3) endA Hte [argU proL Cam^r]*

BL21 Rozetta —(Stratagene) *[F^- ompT hsdS(rB^- mB^-) dcm+ Tet^r gal ë(DE3) endA metA::Tn5(kanr)Hte [argU proL Cam^r]]*

BL21 pLys — (Stratagene) *[F^- ompT hsdS(rB^- mB^-) dcm+ Tet^r gal ë(DE3) endA Hte [pLysS Cam^r]]*

BL21 Ril — (Stratagene) *[F^- ompT hsdS(rB^- mB^-) dcm+ Tet^r gal endA Hte [argU ileY leuW Cam^r]]*

2.4.2 Growing bacterial cultures

Luria-Bertani (LB) broth

1 % (w/v) Tryptone
0.5 % (w/v) Yeast extract
1 % (w/v) NaCl
Sterilised by autoclaving at 121 °C for 20 min

Selective antibiotics used
Ampicillin (Sigma) at 100 μg/ml
Kanamycin at 100 μg/ml
Tetracyclin at 100 μg/ml

5 ml LB media (containing a selective antibiotic if required) was inoculated with a colony of bacteria from a stock plate or from a glycerol stock and incubated for several hours overnight at 37 °C (225 rpm). This starter culture was then transferred to 200 ml LB media (containing antibiotics if appropriate) and incubated under the same conditions overnight. Culture flask capacities were at least 5x the volume of the culture being grown to allow for aeration.

2.4.3 Glycerol stocks

Glycerol stocks of bacterial cells were prepared by adding 0.15 ml of sterile glycerol to 0.85 ml of liquid bacterial culture in a cryovial (Nunc) and snap frozen. The cells were stored at –70 °C.

2.4.4 Agar bacterial culture dishes

LB agar
1 % (w/v) Tryptone
0.5 % (w/v) Yeast extract
1 % (w/v) NaCl
1.5 % (w/v) Agar, granulated
Sterilised by autoclaving at 121 °C for 20 min.

LB agar was liquefied by means of heat provided by microwave oven. When the agar was hand warm (at body temperature) it was poured into 90 mm diameter Petri dishes (Sterilin) and left to cool. If antibiotic selection was required, the antibiotic was added to the agar immediately before pouring. The culture dishes were stored at 4 °C for no longer than one month. Prior to use the plates were dried at 37 °C for 1 h.

2.4.5 Preparation of competent cells

Heat shock method

Transforming buffer 1 (TFBI)	**Transforming buffer 2 (TFBII)**
30 mM Potassium acetate	10 mM MOPS
100 mM RbCl	75 mM $CaCl_2$
10 mM $CaCl_2$	10 mM $RbCl_2$
50 mM $MnCl_2$	15 % (v/v) Glycerol
15 % (v/v) Glycerol	Adjust to pH 6.5 with KOH and sterilise by filtration.
Adjust to pH 5.8 with acetic acid and sterilise by filtration.	

A starter culture of *E.coli* DH5α cells was set up by transferring a colony of bacteria from a stock-plate to 2 ml of LB in a 15 ml sterile tube. The culture was incubated overnight at 37 °C and with agitation. This culture was diluted 1/100 in 200 ml of LB and incubated at 37 °C at 225 rpm until the OD_{600nm} lay within 0.3-0.5. The cells were collected by centrifugation (10 min, 8000 rpm, 4 °C) and resuspended in ice-cold 80 ml of TFBI buffer at 2/5 of the original 200 ml culture volume. After 10 min of incubation on ice the cells were again centrifuged (5 min, 2500 rpm, 4 °C) and gently resuspended in 8 ml of TFBII buffer at 1/25 of the original 200 ml culture volume. The cells were incubated on ice for 15 min and 200 µl aliquots were added

to pre-chilled microcentrifuge tubes. The aliquots were snap frozen on dry ice and stored at –70 °C.

2.4.6 Transformation of bacteria

2.4.6.1 Heat shock method

100 µl of *E.coli* DH5α competent cells were defrosted on ice and mixed with 0.1-0.5 µg of plasmid DNA. The cells were incubated on ice for 30 min and heat-shocked at 42°C for 1 min. Following another 5 min incubation on ice, 1 ml LB media was added and the culture was incubated at 37 °C at 225 rpm for 30 min in a 15 ml sterile tube. Cells were then plated onto LB agar bacterial culture dishes containing selective antibiotic where appropriate and incubated overnight at 37 °C.

2.5 Molecular Biology Methods

2.5.1 Plasmid DNA

Amplification of plasmid DNA – A single colony of bacteria containing the plasmid required was used to inoculate a starter culture of 5 ml of LB containing selective antibiotic and incubated at 37 °C at 225 rpm for 4-8 h in a 50 ml sterile tube. The starter culture was then transferred to a larger 100 ml liquid bacterial culture and incubated overnight at 37 °C at 225 rpm in a 500 ml flask.

Purification of plasmid DNA – Cells from the culture grown for amplification of plasmid DNA were collected by centrifugation at 6000 rpm for 20 min at 4 °C. Plasmid DNA was isolated using Qiagen Maxi™ and Mini™ prep kits according to manufacturer's instructions. The DNA was resuspended in nuclease-free dH_2O and stored at -20 °C.

Quantification of plasmid DNA – The concentration of plasmid DNA was determined by spectrophotometry at 260 nm using the PowerwaveXS™ Microplate Spectrophotometer (Bio-Tek). Plasmid DNA was diluted 1/100 and 100 µl volumes were added to wells of a 96-well UV-Star™ Plate (Greiner), using 100 µl dH_2O as a blank control. 50 µg/ml DNA gives an OD_{260nm} of 1 A thus DNA concentrations could be calculated. The plate reader software (KCJunior™) was adjusted for a 1 cm light pathlength.

2.5.2 SDS-PAGE

2.5.2.1 Preparation of cell lysates

Cell lysis

0.1 % or 1 % Triton X-100 lysis buffer
50 mM HEPES pH 7.6
0.1 mM EDTA
150 mM NaCl
1x protease inhibitor mix*
0.1 % or 1 % (v/v) Triton X-100
10 mM NaF
Stored at -20 ºC in aliquots.
2 mM DTT (add prior to use)

Urea lysis (Denaturing) buffer
7 M Urea
0.1 M DTT
0.05 % (v/v) Triton X-100
25 mM NaCl
25 mM HEPES pH 7.6
Buffer prepared just prior to use.

NP40 Lysis Buffer
1% NP40
25 mM HEPES-KOH, pH 7.6
0.4 M NaCl
5 mM DTT
120 nM okadaic acid
1x Protease Inhibitor mix*

***10x Protease inhibitor mix**
10 µg/ml Leupeptin

SDS sample buffer (SB)
5 % (w/v) SDS

4 µg/ml Aprotinin
2 µg/ml Pepstatin
1.2 mM Benzamidine
10 µg/ml Soya bean trypsin inhibitor
400 µg/ml Pefabloc
1 mM EDTA
Stored at -20 ºC in aliquots.

25 % (v/v) Glycerol
125 mM Tris pH 6.8
0.02 % (w/v) Bromophenol blue
DTT (1 M) added to buffer (1 DTT : 4 SB) prior to use

Cells were washed with cold PBS, scraped with 150 µl of PBS into microcentrifuge tubes and then centrifuged at 5000 rpm for 5 min at 4 ºC. The supernatant was removed and cell lysis buffer was added in excess of the cell pellet (50-100 µl per well in a 6-well plate). The cells were resuspended by pipeting the cell lysis buffer up and down several times. Samples were then incubated on ice for 20 min. The cell lysate was centrifuged at 13000 rpm for 2 min and the supernatant was recovered. The cell pellet was recovered and lysed further by resuspending it in 200 µl of SDS sample buffer and heated at 95 ºC for 5 min. Samples were then sonicated (Soniprep150^{TM}, MSE) twice for 10 sec (Level 2-3), snap-frozen in liquid nitrogen and stored at -70 ºC.

2.5.2.2 Protein precipitation

Trichloroacetic acid (TCA) was used to precipitate protein and concentrate protein samples using the following method. 2 % deoxycholate (DOC) was added to the samples to a final concentration of 0.02 % and incubated at room temperature for 15 min. 24 % TCA was added to a final concentration of 8 % and incubated on ice for 1 hr. The precipitated proteins were pelleted by centrifugation at 13,000 *g* for 10 min at 4 ^{o}C. The supernatant was removed and the pellet washed with 200 µl ice cold acetone to remove residual TCA. The protein pellet was air dried for 1 – 2 min

before resuspending in either urea lysis buffer or 4 x SDS sample buffer (4 % SDS, 250 mM Tris-HCl pH 6.8, 10 mM EDTA, 0.2 M DTT, 1% Bromophenol blue).

2.5.2.3 Protein quantification

Protein concentrations were determined using the BCA™ Assay kit (Pierce, Perbio Science) in a 96-well plate measuring absorbance at 562 nm with the PowerwaveXS™ Microplate Spectrophotometer (Bio-Tek). Read-outs were converted to concentrations using the standard curve generated from the BSA standards and adjusted by the dilution factor.

Protein concentration of individual samples was also carried out by means of Bradford Assay supplied from BioRad. The assay was carried out according to the instruction manual supplied by the manufacturer. Bovine serum albumin (BSA) was used as the protein standard in order to plot the standard curve. The reaction was carried out on 96 well microtitre plates. The absorbance for the protein-dye complexes was measured at λ= 595nm by means of KC-Junior microplate reader.

2.5.3 **Preparation of gels and separation of proteins by SDS-PAGE**

Running buffer
192 mM Glycine
25 mM Tris
0.1 % (w/v) SDS

Separating gel – 10% (per 5 ml)
30 % Acrylamide mix* 1.7 ml
1.5 M Tris (pH 8.8) 1.3 ml
10 % SDS 0.05 ml
10 % Ammonium peroxidisulphate 0.05 ml
TEMED (Sigma) 0.002 ml
dH_2O 1.9 ml

Separating gel – 15 % (per 5 ml)
30 % Acrylamide mix* 2.5 ml
1.5 M Tris (pH 8.8) 1.3 ml
10 % SDS 0.05 ml

Stacking gel – 5 % (per 1 ml)
30 % Acrylamide mix* 0.17 ml
1.5 M Tris (pH 6.8) 0.13 ml
10 % SDS 0.01 ml

10 % Ammonium peroxidisulphate 0.05 ml	10 % Ammonium peroxidisulphate 0.01 ml
TEMED (Sigma) 0.002 ml	TEMED (Sigma) 0.001 ml
dH_2O 1.1 ml	dH_2O 0.68 ml

* Acrylamide mix (National Diagnostics; Ultrapure Protogel) consists of 30 % (w/v) acrylamide and 0.8 % (w/v) bis-acrylamide.

SDS-polyacrylamide gels at acrylamide concentrations of 8%, 10 % or 15 % were prepared [described by Laemlli *et al* (1970)] using a MiniProtean3^{TM} (Bio-Rad) blot. The separating gel was left to polymerise and overlaid with water to straighten the top of the gel. The water was then removed and the stacking gel with a polyacrylamide concentration of 5 % was added together with a 10- or 15-well comb, which was also left to polymerise. The combs were removed and the wells were washed out with Running buffer.

SDS sample buffer was added to the cell lysates containing between 25-50 µg of protein in a ratio of 1:1 (v/v) and samples were heated at 95 ºC for 5 min prior to loading. 5 µl of pre-stained protein standards (Bio-Rad) were loaded in the first well as size markers. Proteins were separated by electrophoresis in Running buffer at 100-170 V until the Bromophenol blue dye front reached the bottom of the gel.

2.5.4 Detection of fractionated protein

Gels were removed from the glass plates and the stacking gel was discarded.

Coomassie brilliant blue staining

Destain 1	**Coomassie brilliant blue stain**
50 % (v/v) Methanol	50 % (v/v) Methanol
10 % (v/v) Acetic acid	10 % (v/v) Acetic acid
	0.2 % (w/v) Coomassie Blue R-250

Destain 2

7.5 % (v/v) Methanol

10 % (v/v) Acetic acid

Gels were transferred to a dish containing Destain 1 for >5 min and then placed into another dish containing Coomassie Blue Stain. The duration of the staining

procedure depended on the strength of the staining required (5 min to 12 h) and in some cases the stain was preheated to 45 ºC to increase staining even further. Gels were then placed in a dish containing Destain 2. A folded tissue was used to absorb excess dye and Destain 2 was renewed as needed. Destaining was performed until the bands became visible and the background staining was removed. Gels were air-dried in between DryEase MiniCellophane™ sheets (Invitrogen) in a DryEase GelDrying™ system (Invitrogen).

2.5.5 Immunoblotting

10x PBS (Phosphate-Buffered Saline)
1.37 M NaCl
0.1 M Na_2HPO4
0.027 M KCl
0.018 M KH_2PO_4
Adjust pH to 7.4 with HCl

PBS+Tween (PBST)
1x PBS + 0.1 % (v/v) Tween 20

ECL Solution 1
100 mM Tris pH 8.5
2.5 mM Luminol stock
0.4 mM p-Coumaric acid

ECL Solution 2
100 mM Tris pH 8.5
0.02 % (v/v) H_2O_2
Solutions stored at 4 ºC in the dark.

Transfer buffer
192 mM Glycine
25 mM Tris
20 % (v/v) Methanol

The separated proteins were transferred electrophoretically to PROTRAN™ nitrocellulose transfer membranes (Schleicher & Schuell Biosciences) in tanks with agitated Transfer buffer and an ice block to control the temperature. Electroblotting was carried out at constant 100 V for 1 h or at constant 20 mA overnight. After transfer of proteins the membranes were washed in PBST and stained with black ink

(Pelikan) diluted in PBST (1/100) for 10-15 min. Membranes were washed again in PBST to remove the excess stain and non-specific antibody binding was blocked by a 1 h incubation in buffer A - PBST + 5 % (w/v) dried skimmed milk (PBST5M; Marvel) + 0.5% (w/v) BSA. The membranes were then incubated with the primary antibody in buffer A for 1 h at RT (or overnight at 4 ºC). Following 5x 5 min washes in PBST, the appropriate secondary antibody (conjugated to horse radish peroxidase; DAKO) diluted 1/1000 – 1/2000 in buffer A, was added to the membrane and incubated for 1 h at RT. Membranes were again washed for 5x 5 min with PBST and specific bands were detected by enhanced chemiluminescence (ECL). Membranes were overlaid with ECL solution 1 and 2 (mixed 1:1) for 1 min, blotted dry and exposed to Hyperfilm^{TM} ECL (Amersham Biosciences), which was then developed.

2.5.6 Antibodies

2.5.6.1 Primary antibodies

Target	kDa	Clonality	Supplier	Dilution
β - actin	42	Mouse Monoclonal	Abcam	1:5000
GAPDH	35	Mouse Monoclonal	Santa Cruz	1:10000
IRF-1 (C-20)	48	Mouse Monoclonal	BD	1:1000
MDM2 (2A9)	90	Mouse Monoclonal	Moravian Biotechnology	1:1000
MDM2 (2A10)	90	Mouse Monoclonal	Moravian Biotechnology	1:2000
MDM2 (4B2)	90	Mouse Monoclonal	Moravian Biotechnology	1:1000
MDM2 (3G5)	90	Mouse Monoclonal	Moravian Biotechnology	1:1000
MDM2 (SMP 14)	90	Mouse Monoclonal	Moravian Biotechnology	1:1000
BAX	21	Mouse Monoclonal		1:1000
p21 (Ab-1)	21	Mouse Monoclonal	Oncogene	1:1000
p53 (DO1)	53	Mouse Monoclonal	Moravian Biotechnology	1:5000
p53 (DO12)	53	Mouse Monoclonal	Moravian Biotechnology	1:1000
p53 (CM-1)	53	Rabbit Polyclonal	Moravian Biotechnology	1:1000

Table 2.2 List of primary antibodies used in this study.

2.5.6.2 Secondary antibodies

Secondary antibodies were sourced from DAKO and HRP-conjugated forms of Rabbit α-Mouse IgG; Swine α-Rabbit IgG; Rabbit α-goat IgG; Rabbit α-sheep IgG were used.

2.5.7 Stripping Membranes

Stripping buffer

50 mM Tris pH 6.8

2 % (w/v) SDS

100 mM β-mercaptoethanol

Antibodies bound to membranes were removed by stripping when the blots needed to be re-probed. The stripping buffer was heated to 50 ºC in a water bath and added to the membrane. The blot was kept at 50 ºC in the water bath for 15-30 min with occasional agitation. The membrane was rinsed multiple times with PBS and was then immunoblotted as described above.

2.6 Clonning and Site Directed Mutagenesis (SDM)

2.6.1 Polymerases

Hot-start Taq polymerase amplification

PCR Master mix/reaction	**Cycling conditions**
1xPCR buffer (Qiagen)	Taq activation:95°C for 15min,
1mM dNTPs (Promega)	Denaturation:95°C for 30sec,
0.1μM forward and reverse primers	Annealing: 53.6°C for 30sec,
1μg DNA template	Elongation:72°C for 1min
HotstarTaqTM DNA polymerase 5units/reaction (Qiagen)	Cycle to step 2 x30 times,
ddH2O up to a final volume of 50 μl	72°C x 5min.
	4 °C for t∞

In order to ensure maximum yield of amplification for each product, different annealing times, varying from 50-70°C, along with elongation times between 30sec-3min, were tried. 100ng of DNA template were used as initial concentration.

2.6.2 PFU polymerase reaction

PFU® Turbo amplification was used instead of Taq polymerase for site directed mutagenesis because of its high thermostability and 3' to 5' exonuclease proof-reading activity that enables the polymerase to correct nucleotide-misincorporation errors. This means that *Pfu* DNA polymerase-generated PCR fragments will have fewer errors than *Taq*-generated PCR inserts. All reactions performed in a DNA Engine DyadTM machine.

PCR Master mix/reaction	**Cycling conditions**
1x cloned PFU® buffer (Stratagene)	Taq activation:95°C for 15min,
1mM dNTPs (Promega)	Denaturation:95°C for 30sec,
0.5mM MgCl2 (Qiagen)	Annealing: 53.6°C for 30sec,
0.1μM forward and reverse primers	Elongation:72°C for 1min
5% (v/v) DMSO	Cycle to step 2 x30 times,
1μg DNA template	72°C x 5min.
PFU® Turbo DNA polymerase 2.5 units/reaction (Stratagene)	4 °C for t∞
ddH2O up to a final volume of 50 μl	

2.6.3 Agarose gel electrophoresis

50x TAE (Tris-Acetate EDTA)	**6x DNA loading buffer**
2M Tris pH 6.8,	0.25% Bromophenol blue (w/v)
0.1M Na2EDTA.2H2O	0.25% Xylene cyanol (w/v)
4% Acetic acid (v/v)	15% Ficoll 400 (w/v)
Adjust pH to 8.5	

TAE buffer was diluted (50x) to 1x and 1% (w/v) ultrapure agarose was added. The

solution was heated in a microwave oven until the agarose is completely dissolved and left to cool down to handwarm under the hood. Ethidium Bromide EtBr was added to a final concentration of 5% (w/v). The solution was then poured into a horizontal electrophoresis gel tray with a 10-well or bigger comb inserter and left to solidify. When solid, the agarose gel was submerged in a horizontal electrophoresis tank filled in 1xTAE buffer. DNA loading buffer (6x) was added to the samples (3µl of site-directed mutagenesis DNA or 10µl of PCR amplified DNA) to 1x and then loaded onto the gel. 1kb DNA ladder was also loaded at 5µl volume. Electrophoresis at 100V at room temperature followed till adequate separation was achieved and then the bands were visualized by UV light using a CHEMI Genius2 BioImaging SystemTM (Syngene) and the GenesnapTM tool with an ethidium bromide filter and transilluminator. The images were captured with a Sony UP-D895MD.

For cloning the DNA was extracted from the gel using a DNA gel purification kit from Qiagen.

2.6.4 Restriction enzyme digestion and Ligation of DNA in the appropriate vector

Restriction enzyme digestion of the vector and the DNA-insert is required after PCR amplification. The restriction endonucleases recognize specific sequences to digest. As far as the insert is concerned the adequate restriction enzymes were chosen according to the Multiple Cloning Site (MCS) of the vector to be inserted in. Restriction digests were performed to manufacturers protocol (New England Bio-labs).

Ligation reaction	**Formula for the vector:insert ratio**
1x Ligation Buffer (10x Promega) 10-100ng vector DNA xng insert 10units of T_4 ligase (10u/µl , Promega) ddH_2O up to 10µl	µg of vector x size of insert (Kb) x ratio insert size pf vector (Kb) vector

After digestion the vector plasmid and the DNA-insert were ready to be ligated. The above reaction was incubated at 4 °C in Eppendorf tubes, overnight. For each ligation different ratios insert:vector were applied each time, varying between 3:1 and 10:1, according to the size of the insert when compared to the vector.

2.6.5 Site-directed mutagenesis and Cloning

2.6.5.1 Primer design

Cloning primers were designed with a length of around 20-30 bp spaced over the beginning or end of the MDM2 open reading frame with restriction sites or a homologous recombination site incorporated into them.
Oligonucleotides were purchased from Sigma-Aldrich, de-salt purified for cloning and were reconstituted in nuclease-free ddH_2O.

Name	**Restriction Site and vector**	**Primer Sequence**
Full length MDM2 Forward	Nco1 pENTR11	$^{5'}$GACCATGTGCAATACCAACATGT C$^{3'}$

Full length MDM2 Reverse	Xho1 pENTR11	5'GCCTCGAGCTAGGGGAAATAAG TTAG3'

Table 2.3 Cloning Primers.

2.6.5.2 Site-directed mutagenesis

Primers containing the desired mutations were designed according to the quidelines in the QuikChange™ Site-Directed Mutagenesis Kit Manual (Stratagene). Oligonucleotides were purchased from Sigma-Aldrich de-salt purified and were reconstituted in nuclease-free ddH_2O. Site-directed mutagenesis was carried using the QuikChange™ Site-Directed Mutagenesis Kit (Stratagene) was applied according to manufacturer's instructions. After mutant strand synthesis reaction, 1 µl of DpnI restriction enzyme (10U/µl) was added to the amplification reaction and mixed. The reaction mixture was centrifuged for 1 minutes and incubated at 37°C for up to 4 hours to digest the parental (non-mutated) dsDNA. After incubation, 2 µl of DpnI-treated DNA was used to transform 25 µl of *E.coli* DH5α competent cells using heat-shock method.

Name	**Amino acid mutation**	**Primer sequence**
Mdm2K454A forward	Lysine 454 to Alanine	5'GCATTGTCCATGGCGCAACAGGACATC3'
MDM2 K454A reverse	Lysine 454 to Alanine	5'GATGTCCTGTTGCGCCATGGACAATGC 3'
MDM2 C464A forward	Cysteine 464 to Alanine	5'GGACATCTTATGGCCTGCTTTACAGCGGCAAAGAA GCTAAAGAAAAGG 3'
MDM2 C464A reverse	Cysteine 464 to Alanine	5'CCTTTTCTTTAGCTTCTTTGCCGCTGTAAAGCAGG CCATAAGATGTCC 3'

MDM2 forward	C478S	Cysteine 478 to Serine	5'GGAATAAGCCCTGCCCAGTAAGCAGACAACCAATTCAAATGATTGTG 3'
MDM2 reverse	C478S	Cysteine 478 to Serine	5'CACAATCATTTGAATTGGTTGTCTGCTTACTGGGCAGGGCTTATTCC 3'
MDM2 forward	C438A	Cysteine 438 to Alanine	5'CTTAATGCCATTGAACCTGCCGTGATTTGTCAAGG 3'
MDM2 reverse	C438A	Cysteine 438 to Alanine	5'CCTTGACAAATCACGGCAGGTTCAATGGCATTAAG 3'
MDM2 forward	C461S	Cysteine 461 to Serine	5'CAGGACATCTTATGGCCAGCTTTACATGTG 3'
MDM2 reverse	C461S	Cysteine 461 to Serine	5'CACATGTAAAGCTGGCCATAAGATGTCCTG 3'
MDM2 forward	G448S	Glycine 448 to Serine	5'CGACCTAAAAATAGCTGCATTGTCCATGGC 3'
MDM2 reverse	G448S	Glycine 448 to Serine	5'GCCATGGACAATGCAGCTATTTTTAGGTCG 3'
MDM2 forward	I440A	Isoleucine 440 to Alanine	5'GCCATTGAACCTTGTGTGGCTTGTCAAGGTCG3'
MDM2 reverse	I440A	Isoleucine 440 to Alanine	5'CGACCTTGACAAGCCACACAAGGTTCAATGGC 3'

MDM2 forward	I482A	Isoleucine 482 to Alanine	$^{5'}$GCCCTGCCCAGTATGTAGACAACCAGCCCAAATG ATTGTGCTAAC$^{3'}$
MDM2 reverse	I482	Isoleucine 482 to Alanine	$^{5'}$GTTAGCACAATCATTTGGGCTGGTTGTCTACATAC TGGGCAGGGC$^{3'}$

Table 2.4 Site Directed Mutagenesis Primers

2.6.6 Sequence analysis of plasmid DNA

All sequence analysis was performed by the Sequencing Unit at the MRC Human Genetics Unit, Edinburgh. The sequencing reactionset up to final volume of 10µl containing 2 µl of BigDye® Terminator 3.1 (Applied Biosystems), 3.2 pmol of primer, 1x BigDye Sequencing buffer (Applied Biosystems), 150 ng of DNA template and nuclease-free ddH_2O was assembled. The sequencing reaction was thermal-cycled using cycling parameters according to the manufacturer's instructions.

The sequenced DNA was then precipitated by mixing the reaction with 30 µl of 100 % (v/v) ethanol and 2.5 µl of 125 mM EDTA. Following vortexing, the reaction was incubated at room temperature for 15 minutes. After centrifuging at 13000 rpm for 20 minutes, the solution was removed and precipitated DNA was microcentrifuged for 20 seconds. Residual ethanol was removed before 30 µl of 70 % (v/v) ethanol was added to the precipitated DNA and centrifuged at 13000 rpm for 5 minutes. The ethanol was removed before the precipitated DNA was microcentrifuged for 20 seconds. Residual ethanol was removed and the precipitated DNA was left to air-dry before sequence-analysed.

2.7 Protein Purification

2.7.1 His-purification

Cultures were grown and induced with 0.5mM IPTG for 3 hours at 20 °C. After induction the cells were pelleted and resuspended in 10ml of lysis buffer (20mM Tris pH8, 150mM NaCl, 0.1% NP-40, 10% glycerol, 10mM $MgCl_2$), sonicated and spun down. The supernatant was added to 250ul of Ni-NTA agarose beads (Qiagen) washed in PBS, and incubated for 1 hour at 4^{o}C. Supernatant was removed, leaving enough to transfer beads to a small column and washed 6x with lysis buffer + 40mM imidazole. Protein was then eluted in 14 fractions of 0.5 ml using lysis buffer plus 250mM imidazole. All fractions were run out on an 18% gel. Peak fractions were then pooled and loaded onto an equilibrated fast flow Q-column (GE Healthcare) and eluted off with a high salt concentration.

2.7.2 Native protein Purification. Isolation of MDM2 species form *E.coli*

Wild-type human MDM2 was overexpressed in *E.coli* BL-21 RIL DE3 strain at 20 ºC for 3 hours after induction with 0.5 mM IPTG. Cells were harvested by centrifugation at 8 000 g for 10 min and snap frozen in liquid nitrogen. The bacterial pellet was lysed in buffer A: (100 mM Tris-HCl pH 8.0, 200 mM KCl, 10% glycerol, 1 mM PMSF, 5 mM Mg $(CH_3COO)_2$, 5 mM DTT, 1 mM benzamidine, protease inhibitor cocktail EDTA free (Roche), 1 tablet per 50 ml of buffer A) containing 1 mg/ml lysozyme for 1.5 hours at 4ºC with frequent stirring followed by 2 minutes at 37ºC and an additional 15 minutes at 4ºC. Afterwards the suspension was centrifuged at 100 000 g for 1 hour at 4°C. Under these lysis conditions most of the desired protein was insoluble and localized within the pellet after centrifugation. Extraction of the MDM2 protein from the cell pellet was carried out overnight at 4ºC with constant shaking. The following extraction buffer (B) was used: 25 mM Tris-HCl pH 7.6, 1.2 M KCl, 5 mM $Mg(CH_3COO)_2$, 1% Triton X-100, 5 mM DTT, 10% sucrose, 1 mM PMSF, 1 mM benzamidine, protease inhibitor tablets. Following centrifugation (100 000g for 1 hour at 4°C) the supernatant was collected, dialysed

into buffer (C): 25 mM HEPES-KOH pH 7.3, 1 M $(NH_4)_2SO_4$, 1 M KCl, 5% glycerol, 2 mM DTT, 1 mM PMSF. Following two hour dialysis the sample was loaded onto a Butyl-Sepharose column (Amersham) equilibrated with the same buffer. The protein, which bound to the column, was eluted using a linear gradient of decreasing ionic strength and increasing glycerol concentration. The fractions containing MDM2 protein were pooled and loaded onto a Q-Sepharose column equilibrated with buffer (D): 25 mM HEPES pH 7.6, 50 mM KCl, 10% glycerol, 2 mM DTT, 1 mM PMSF. The flow through from the column was immediately loaded onto a SP-Sepharose column equilibrated with buffer D. The bound proteins were eluted by means of a linear salt gradient (from 50 mM to 800 mM KCl in buffer D). Fractions containing MDM2 protein were pooled, frozen in liquid nitrogen and kept at -80 ºC for further experiments.

An analogous method was used to isolate $MDM2^{K454A}$, $MDM2^{C464A}$, $MDM2^{C478S}$, $MDM2^{I440A}$ from *E.coli*.

Human recombinant p53 was purified essentially as described by (Nichols and Matthews, 2002).

2.8 Assays

2.8.1 p53 DNA binding assay

The DNA binding activity of p53 was quantified by EMSA (Electrophoretic Mobility Shift Assay; gel-shift). Indicated amount of human recombinant p53 was diluted in the final volume of 5 µl or 7 µl of EMSA buffer: 25 mM Hepes pH 7.5, 5% glycerol, 100 mM KCl, 10mM MgCl2, and 3 mM DTT. Samples were supplemented optionally with constant increasing amounts of MDM2 and/or BSA and ATP (for exact amounts used see Figure descriptions). Such samples were then incubated at 4 ºC to 50ºC for the indicated time in a thermocycler. The activation step followed that included addition of 15 µl or 13 µl mix containing: 1x EMSA buffer, 0.2 MDPM of ^{32}P labeled specific DNA sequence (below), 1 µg of unspecific 44-bp dsDNA (sequence below, usage based on (Anderson et al., 1997)) and 100ng of the antibody

pAb421 (Ab-1; Oncogene). 20 µl samples with the specific DNA were afterwards incubated for 5 min at room temperature (RT), loaded onto a 4% native polyacrylamide TB gel and electrophoresed at 15mA for 2h at 4°C. Gels were dried and exposed to the phosphoimager screen and scanned by STORM phosphoimager (Amersham).

For p53 activated by CKII, the activation mix was made, containing per every 4 µl of volume: 50ng p53, 7U of CKII (Calbiochem), 0.3 U of creatine kinase, 150mM of phosphocreatine (ATP regeneration system; Roche), 5 mM of ATP and 1x EMSA buffer. CKII activation was done for 30 min at 25ºC and then each 4 µl of CKII activation reaction was supplemented separately with Hsp90/BSA in 1xEMSA buffer up to 5 µl. Afterwards, 1h incubation step either at 4ºC or 37^{o}C was performed, followed by addition of 15µl DNA mix without the antibody. Electrophoresis was performed as described above.

For testing the unspecific p53-DNA binding activity, 0.2 MDPM of unspecific, radiolabeled 44-bp dsDNA (below) was used per 1 sample instead of labeled promoter-derived sequence in the activation step. The remaining part of the experiment was performed as mentioned before for specific DNA but no additional unlabeled DNA, antibody or CKII was used in this case.

DNA sequences used in EMSA (annealed from complementary ssDNA to form dsDNA):

CON (artificial p53-binding "consensus") sequence:

5'-AGCTTAGACATGCCTAGACATGCCTA-3'

WAF1 promoter derived sequence:

5'-TGGCCATCAGGAACATGTCCCAACATGTTGAGCTCTGGCA-3',

MDM2 promoter derived sequence:

5'-

GAGCTGGTCAAGTTCAGACACGTTCCGAAACTGCAGTAAAAGGAGTTAA

GTCC

TGACTTGTCT CCAGC-3'

BAX promoter derived sequence:

5'-GATCTCACAAGTTAGAGACAAGCCTGGGCGTGGGCTATATTGTCGA-3'
Unspecific, 44-bp DNA:
5'-GCTTCGAGATGTTCCGAGAGGCGAATGAGGCCTTGGAACTCAAG-3',
Sequences were annealed to form double stranded DNA in a thermocycler using following program: 5min 94ºC, 5min 50ºC, 4ºC. Presence of the dsDNA was tested with a 16% polyacrylamide TB gel electrophoresis. Sequences used in the EMSA assay were labeled with the T4 Polynucleotide Kinase (PNK; Fermentas) as described in the producer's manual. 2-week long series of experiments was performed using DNA radioactivity determined at this point. This allowed the same amounts of specific DNA per reaction but caused differences in overall intensity of results, as radioactivity of sequences decreased due to the isotope half-life. Image Quant TL software (Amersham) was used to adjust intensities of obtained images to a comparable background to signal ratio.
In most described experiments the pAb421 antibody was used to activate p53 for specific DNA-binding, despite without it p53 clearly binds the promoter-derived DNA specifically in the presence of short, unspecific dsDNA included as a competitor in the activation mix. This is in agreement with earlier reports (Anderson et al., 1997). However, in the presence of pAb421 the binding is increased and bands more suitable for quantitative analysis, while overall result outcome remains unchanged (data not shown).

2.8.2 Enzyme Linked Immunosorbent Assay (ELISA)

A 96-well microtiter plate (Corning Inc.) was coated with purified p53 (50ng per well) diluted in 0.1 M Na_2HCO_3, pH 8.6-9.2, and incubated overnight at 4 °C. An analogous approach was undertaken when the experiment required an anchoring anitobody to be coatedonto wells. Each well was washed 6x with PBS containing 0.1% Tween 20 (PBS-T) followed by incubation for 1 h at room temperature with gentle agitation in PBS-T supplemented with 3% bovine serum albumin. The wells were washed 6x with PBS-T prior to incubation with appropriate amounts of purified $MDM2^{WT}$ and the desired mutants diluted in PBS-T 3% bovine serum albumin for 1

h at room temperature. For competition ELISA's a fixed concentration of 100ng MDM2 was used with a titration of appropriate inhibitor added at the same time. After 1 h incubation the plate was washed again 6x with PBS-T and incubated with MDM2 specific abtibody 2A10 (1:1000 in PBS-T 3% BSA) for 1 h at room temperature. For peptide ELISA's plate was coated with streptavidin overnight, washed 6x with PBS-T and biotinylated peptides were added for 1 hour followed by addition of MDM2. Following a further 6x washes with PBS-T wells were incubated with secondary rabbit anti mouse horseradish peroxidase antibodies followed by further washing and ECL. The results were quantified using Fluoroskan Ascent FL equipment (Labsystems) and analyzed with Ascent Software version 2.4.1 (Labsystems).

Peptides BOXIa, BOXIb, BOXVa, and BOXVb were from Chiron Mimetopes and Nutlin3a from Alexis Biochemicals

BOXIa	Biotin-SGSGPPLSQETFSDLWKLLP
BOXIb (12.1peptide)	Biotin-SGSGMPRFMDYWEGLN
BOXVa	Biotin-SGSGRNSFEVRVCACPGRD
BOXVb (RB-1 peptide)	Biotin-SGSGDQIMMCSMYGICKVKNIDLK

2.8.3 **In Vitro Ubiquitination Assay**

Human recombinant p53 (100ng) purified from *E.coli* was incubated in a 20 µl reaction volume containing 1x ubiquitination buffer (UB): 50 mM Tris pH 7.6, 100 mM KCl, 10 mM $MgCl_2$, 2 mM DTT, 0.07 units of creatine kinase, 10 mM creatine phosphate, 5 mM ATP, 6 µg ubiquitin (human recombinant purified from *E. coli* or from Boston Biochem.), 50 nM E1 ubiquitin activating enzyme (rabbit/human recombinant), 1.5 µM E2 conjugating enzyme - UbcH5a (mouse/human recombinant), 3-150 nM E3- human recombinant $MDM2^{WT}$, $MDM2^{K454A}$, $MDM2^{C464A}$ or $MDM2^{C478S}$, . The reactions were incubated at 30ºC-37ºC for 10 min-2 hours. Afterwards they were terminated with SDS-sample buffer with

Dithiotreitol (DTT) and the reaction products were fractioned by SDS-PAGE (8-10%). Transfer to a nitrocellulose/PVDF film followed and standard immunoblot blot detection was carried out using anti p53 DO-1 antibody.

Master Mix:

366µl H_2O

10µl 1M HEPES (pH8)

2.4µl 1M $MgCl_2$

2µl 10% Triton X-100

0.2µl 1M DTT

6µl 0.2M ATP

0.4µl 1M Benzamidine

3.2µl 10mg/ml Ubiquitin

2.8.4 In vivo ubiquitination assay

H1299 cells were seeded onto 6 well plates. When the cells reached 80-90% confluency they were transfected by means of lipofectamine™ 2000 reagent with the total amount of DNA for all wells kept constant at 4 µg. These 4 µg consisted of 1 µg of pCNA3.1 p53 wt, 0.5-2 µg pcDNA3.1 MDM2 wt or the K454A , C464A, C478S mutants along with 0.5 µg of pCMV His-Ub plasmid. The DNA mixtures, with appropriate controls were made up accordingly for each well to be transfected with the addition of pCDNA3.1 empty vector the make up the 4µg were necessary.
The proteasome inhibitor MG132 (CalBiochem) was added to final concentration of 10 µM per well for four hours prior to harvesting.
Twenty four hours post transfection, the cells were washed twice in ice-cold PBS before being scraped and collected in 1 ml of ice-cold PBS. At this step the cells were divided into two fractions: 200 µl fraction which was to be directly lysed in NP-40 lysis buffer and assayed via western blot (transfection control) 800 µl fraction which was to be used in the ubiquitination assay.

Both fractions were centrifuged at 5000rpm 4ºC for 5min and snap frozen in liquid nitrogen.

Stock solutions used in the procedure described below

Buffer A

6 M Guanidium-HCl

94.7 mM Na_2HPO_4

5.3 mM NaH_2PO_4

10 mM Tris-HCl, pH8.0

10 mM β-mercaptoethanol

(Buffer made up to desired volume pH adjusted to pH8.0)

Lysis Buffer

Buffer A supplemented with 5 mM Imidazole

Buffer B

8 M Urea

94.7 mM Na_2HPO_4

5.3 mM NaH_2PO_4

10 mM β-mercaptoethanol

(Buffer made up to desired volume pH adjusted to pH8.0)

Buffer C

8 M Urea

22.5 mM Na_2HPO_4

77.5 mM NaH_2PO_4

10 mM Tris-HCl pH8.0

10 mM β-mercaptoethanol

(Buffer made up to desired volume pH adjusted to pH6.3)

Buffer D

Buffer C supplemented with 0.2% Triton X-100

Buffer E

Buffer C supplemented with 0.1% Triton X-100

Elution Buffer

0.2 M Imidazole

5% SDS

150 mM Tris-HCl pH 6.8

10% Glycerol

0.7 M β-mercaptoethanol

The thawed pellet (800µl) was lysed in 1 ml of freshly prepared lysis buffer by pipetting up and down using fine tip liquid pipette. The lysate was transferred to 15 ml falcon tube containing additional 4 ml of lysis buffer and 75 µl of Ni^{2+}-NTA agarose beads (Qiagen). The falcon tubes were placed on a rotating table for 4 hours or O/N at 4ºC.

The beads were collected by centrifugation at 2000 rpm for 4 minutes and the supernatant was carefully removed or aspirated off. The beads were washed with 750µl of Buffer A and transferred to eppendorf tubes. The beads were washed with 750 µl of each of the Buffers B-E for 15 minutes at room temperature on a rotating table. After each wash a 4min centrifugation step at 2000 rpm followed.

Following this the beads were incubated with 75 µl of Elution Buffer for 30 minutes at room temperature on a rotating table. The beads were collected by centrifugation at 13000 rpm for 5 minutes and the supernatant was mixed with equal volume of 2x sample buffer, 40 µl of each sample were loaded on 4-12% Novex gel for analysis by western blot.

2.8.5 Dual Luciferase Reporter Assay

The term 'dual reporter' refers to the simultaneous expression and measurement of two individual reporter enzymes within a single system. Typically, the 'experimental' reporter is correlated with the effect of the specific experimental conditions, while the activity of the co-transfected 'control' reporter provides an internal control that serves as a baseline response. Normalizing the activity of the experimental reporter to the activity of the internal control minimizes experimental variability caused by differences in cell viability or transfection efficiency, thus greatly improving the accuracy of the assay.

H1299 cells were seeded onto 24 well plates. Upon reaching 80-90% confluency the cells were transfected by means of lipofectamine™ 2000 reagent with the total amount of DNA for all wells kept constant at 0.8 µg.

In all experiments focusing on transcriptional potential of desired proteins an optimised ratio between the 'experimental' reporter and the 'control' reporter has been set up in order to minimize unspecific *in trans* effects between promoters of cotransfected plasmids.

In experiments which focused on p53-dependent transcriptional activity constant (30ng) pGL4.10[*luc2*] bearing a 44base stretch of the *p21* promoter ('experimental' reporter) was mixed with 70ng of the phRL-CMV ('control' reporter). To this mixture 150ng of the pCNA3.1 p53wt, 75-550ng pcDNA3.1 MDM2 wt or the previously mentioned single amino acid mutants were added. The DNA mixtures, with appropriate controls were made up accordingly for each well to be transfected with the addition of pCNA3.1 empty vector the make up the 0.8µg total DNA were necessary.

Twenty four hours post transfection, the cells were washed once in ice-cold PBS and passively lysed with 1x Passive Lysis Buffer (supplied with the Dual-Luciferase® Reporter Assay System from Promega) Afterwards the Dual-Luciferase® assay was performed in accordance with the protocol provided by the manufacturer. The assay was carried out on 96 well black polypropylene plates and the luminescent signals were measured with the Thermo Scientific Fluoroskan Ascent Multimode Reader.

For further immunoblot analysis the lysates were precipitated with Trichloroacetic acid (TCA) with Deoxycholate (DOC). Briefly DOC was added to the lysates final concentration of 0.02% v/v and incubated at room temperature for 15 minutes. Afterwards TCA was added to final concentration of 6% v/v and the samples were incubated at 4ºC for 1hour. The samples were spun down and the pellets were washed with ice-cold acetone and centrifuged once again. The air dried pellet was resuspended in an appropriate volume of 1x SDS PAGE sample buffer.

2.8.6 Monitoring p53 conformation in cells

Human lung carcinoma H1299 cells were grown at 37 °C in RPMI with 10% (v/v) fetal bovine serum, 5% CO_2. Cells were gently lysed on ice in Nonidet P-40 buffer (25 mM Hepes pH 7.5, 0.1% (v/v) Nonidet P-40, 150 mM KCl, 5mM DTT, 50 mM NaF, protease inhibitor mixture by Roche Applied Science (1 tablet was added per 10 ml of lysis buffer)). The protein concentration of the cell lysates was quantified using the Bio-Rad Bradford assay kit. To estimate the amount of correctly folded p53 in H1299 $p53_{-/-}$ cell lines transfected with appropriate plasmids (pCDNA3.1 (EV)-mock, pCDNA3.1/p53wt, pCDNA3.1/MDM2wt, pCDNA3.1/ MDM2K454A, pCDNA3.1/MDM2C464A, and pCDNA3.1/MDM2C478S in appropriate combinations), the ratio between the level of p53 captured by pAb1620 and DO-1 was calculated.

The ELISA procedure was carried out as follows: the wells were coated with wt-p53 conformation-specific pAb1620 monoclonal antibody or DO-1 (both mouse origin, Moravian Biotechnology) at 200 ng per well in 100 mM carbonate buffer, pH 9.0, at 4 °C for 16 h. The wells were blocked for 1 h at 17 °Cwith blocking buffer (4 mg/ml BSA in phosphate-buffered saline). This was followed by titration of increasing amounts of appropriate cell lysate diluted with the reaction buffer (25 mM HEPES, pH 7.3, 150 mM KCl, 5 mM DTT, 10% glycerol, 0.1% Triton X-100, 4 mg/ml BSA, protease inhibitor mixture). The reaction was performed for 1 h at 17 °C. Detection of p53 protein was carried out using the FL-393 antibody (rabbit origin, Santa Cruz Biotechnology) for1hat 17 °C. This was followed by the addition of anti-rabbit IgG-

horseradish peroxidase secondary antibodies (Santa Cruz Biotechnology). Analysis of bound antibodies was performed by colorimetric detection with the TMB peroxidase kit (Bio-Rad) followed by quenching the reaction with 1 M H_2SO_4 and by absorbance measurements at 450 nm. The results obtained were plotted as a function of absorbance with respect to the amount of protein in question. For each particular case within the linear range the first derivative was calculated. The final values presented on the graph in Figure 3.12 represent the normalization fractions obtained by division of pAb1620 derivative values *versus* DO-1 derivative values. The data represent the mean from five independent experiments with a standard deviation.

2.8.7 Immunoprecipitation protocol

Lysis Buffer

50mM HEPES pH 7.2

150mM NaCl

0.5%Tween20

Protease Inhibitor mix (10x)

Cell pellets were resuspended in 200ml of ice cold lysis buffer mixed well and incubated on ice for 15 minutes. Cell debris was spun down at 10000 rpm for 20 minutes at 4^{o}C. Lysate was pre-cleared with 100µl of Sephadex CL-4B beads (Sigma-Aldrich). Beads were washed 3x in cold lysis buffer. The beads were added to the cell lysate in a 1.7ml eppendorf tube and incubated for 40 minutes at 4^{o}C with rotation. The beads were spun down at 5000 rpm and supernatant transferred to a new eppendorf tube and protein concentration was calculated by Bradford method.

2µg of specific antibody (DO-1 for p53) was added to lysate (200-800 µg) and incubated for 2 hrs at 4°C with rotation. 15µl of protein G beads (GE healthcare) were added to eppendorf tube and left to incubate for an hour. The beads were spun down at 5000rpm at 4°C for 2 minutes. Beads were washed 4x with ice cold PBS.

The antibody-antigen complex was removed by the addition of 50µl of sample buffer followed by incubation at 95°C for 5 minutes. Beads were spun at 10000 rpm for 5 minutes and sample buffer removed. 10µl of elution was resolved on a 10% gel.

2.8.8 Pulse-Labelling Assay for Measuring Protein Synthesis

H1299 cells were seeded onto a 6 well plate, upon reaching 80-90% confluency, they were transiently transfected with plasmids encoding for p53 and MDM2. Twenty four hours post transfection the cells were washed twice with PBS. ^{35}S-methionine labelling was carried out by culturing the cells in methionine-free medium containing 2% dialysed fetal calf serum (FCS) for 1 hour (22 µM, Merck Biosciences). Easytag Express Protein Labelling Mix (^{35}S, 90 µCi; PerkinElmer) was added for 20 min or 60min in the presence of proteasome inhibitor MG132. Afterwards the p53 protein was immunoprecipitated using CM-1 antibody (a gift from B. Vojtesek, Masaryk Memorial Cancer Institute, Brno, Czech Republic) and separated by SDS–PAGE.

2.8.9 Tryptic digestion

Wt or mutant MDM2 protein (1 µg) plus trypsin (10 ng) was incubated at 30°C in 50 mM ammonium bicarbonate buffer for up to 30 min. Aliquots were removed and the

reaction stopped by the addition of SDS sample buffer and heating at 80^{o}C for 4 min. The samples were analysed by on 4-12% gradient gels (invitrogen) and immunoblot.

2.8.10 Intrinsic fluorescence assay

Fluorescence emission spectra were recorded with the use of the SPEX FLUOROMAX-3 (Jobin Yvon Horiba) spectrofluorometer. The bandwidths for excitation and emission were set at 5nm. An excitation wavelength of 295nm was used. Fluorescence spectra were recorded from 320 to 450 nm in 0.5 nm steps, with an integration time of 1 s. Each obtained spectrum is the average of three emission scans minus the average of three blank (buffer) scans. All of the experiments were carried out at 4 °C in buffer containing: 25 mM Hepes (pH 7.5), 50 mM KCl, 5% (v/v) glycerol, 10μM $ZnSO_4$ and 2mM DTT. $MDM2^{WT}$ **,** $MDM2^{C464A}$ **,** $MDM2^{C478S}$ used in this assay were initially preincubated on ice for 5 minutes at final concentration raging from 20nM to 1μM (V_{total}=0.5 ml).

2.8.11 Thermal denaturation assay

To monitor protein unfolding, the fluorescent dye Sypro orange was used. Sypro orange is an environmentally sensitive dye. The unfolding process exposes the hydrophobic region of proteins and results in a large increase in fluorescence, which is used to monitor the protein-unfolding transition. The thermal shift assay was conducted in the iCycler iQ Real Time Detection System (Bio-Rad, Hercules,CA), originally designed for PCR. The system contains a heating/cooling device for accurate temperature

control and a charge-coupled device (CCD) detector for simultaneous imaging of the fluorescence changes in the wells of the microplate. Solutions of 50 µl per well were aliquated to 96 well iCycler iQ PCR plate. They consisted of 0.5-1µM MDM2, 25mM Hepes pH 7.6, 100mM NaCl, 2mM DTT, 4mM $MgSO_4$, 10x conc. Sypro orange dye and +/- 5mM ATP.

The plate was heated from 20 to 95 °C with a heating rate of 0.5 °C/min.

The fluorescence intensity was measured with Ex/Em:490/530 nm.

Chapter 3

Structure-function analysis of the MDM2 RING finger

Contents

3.1 Introduction

3.1.1 The structure of MDM2 C2H2C4 RING

In terms of how an E3 Ubiquitin Ligase mediates transfer of ubiquitin to the target protein two prominent classes can be distinguished. Historically the first E3 ubiquitin ligases to be discovered were the HECT domain E3s. Protein members of this group form a covalent intermediate with ubiquitin before transferring it to the target protein. The second group comprises of enzymes that, instead of binding directly to ubiquitin, rather bring the ubiquitin-bound E2 conjugating enzyme into close proximity to the acceptor lysine residue on the target protein and allosterically enhance the transfer reaction. This class comprises of RING (**R**eally **I**nteresting **N**ew **G**ene), U-box and PHD domain E3s. Members of both of these classes have been found to target the p53 tumour suppressor. It was found that p53 forms a complex with the HECT containing papilomavirus E6 protein and the cellular E6-AP (E6 Associated Protein 1) (Scheffner et al., 1993) as well as the ARF-BP1 (ARF-binding protein 1) (Chen et al., 2005a). From the second group Pirh2 (Leng et al., 2003), COP1 (Dornan et al., 2004a), TOPORS (Rajendra et al., 2004), CHIP (Esser et al., 2005b) and the main focus of this thesis MDM2 (Haupt et al., 1997; Honda et al., 1997; Kubbutat et al., 1997) have been shown to bind and catalyse ubiquitination of p53.

The MDM2 protein is by far the most studied p53-specific ubiquitin protein ligase. The full-length form (predominant isoform) of MDM2 is 491 amino acid residues long (Figure 3.1 Panel A), building a multidomain protein that contains several regions of high evolutionary conservation. Of these the last 60 amino acids residues are of particular interest in this chapter. These are critical for MDM2 to retain its E3 ubiquitin ligase activity and were initially identified as the RING domain, based on protein sequence alignment (Boddy et al., 1994) (Figure 3.1 Panel A). Two zinc ions are essential for the proper folding and function of the MDM2 RING domain, eight

amino acids, six cysteine and two histidine residues coordinate the ion binding (Kostic et al., 2006; Linke et al., 2008) (Figure 3.1 panel B).

Proteins bearing the RING domain portray a unique key amino acid residue sequence arrangement of eight strictly conserved metal binding residues, with the accepted consensus sequence; C-X_2-C-$X_{(9-39)}$-C-X-H/C-$X_{(2-3)}$-C/H-X_2-C-$X_{(4-48)}$-C-X_2-Cn (Freemont et al., 1991; Lovering et al., 1993). However the conservation of active residue spacing in MDM2 RING is different. The two zinc-binding sites are called C4 and H2C2 respectively (Figure 3.1 panel B). The C4 coordination site as the name suggests comprises of four cysteine residues; Cys^{438}, Cys^{441}, Cys^{461}, Cys^{464}. The second zinc binding site, H2C2, is built up of; His^{452}, His^{457}, Cys^{475}, Cys^{478}. The characteristic "cross-brace" topology of the afore mentioned zinc coordinating ligands is illustrated schematically on Figure 3.1 panel C and is equivalent with what is observed in other RING/U-box bearing proteins. Moreover, the super-secondary structure ββαβ fold of the MDM2 RING (Figure 3.1 panel D) is also compatible with other members of the RING domain family. The MDM2 RING shows asymmetrical surface charge distribution (Figure 3.1 panel E) the bulk of the positive charge is located on one side of the domain, primarily due to the presence of solvent-exposed basic residues located in the α-helix building the ββαβ domain fold.

When comparing the available structures of the MDM2 RING monomer from RSCB Protein Data Bank (http://www.rcsb.org/pdb/) (Figure 3.1 Panel F) one can see a high similarity of the structures with the least variable regions including zinc binding site I (C4) and the following α-helix, while the placement of the β-sheet and the second (C2H2) zinc-binding site exhibits more divergence. The first CXXC zinc-binding pair Cys^{438}, Cys^{441} stabilizes the N-terminal region of the RING (C4) subunit, a stretch of seven residues bearing irregular structure follows leading to β-strand 1 (Figure 3.2 Panel A and B). At the end of β1 His^{452} is present and is involved in zinc-binding by the second subunit (H2C2). This is followed by a short loop (Gly^{453}-Lys^{454}) leading into β2, which ends with His^{457}. Two histidine side-chains extend from the ends of the antiparallel β-strands to form one side of the second (H2C2) zinc-binding site.

Several RING/U-box domains are found to form homo- or heterodimers, furthermore specific dimer organization is proposed to be an important regulating step in

activating E3 ubiquitin ligase activity of these domains (Vander Kooi et al., 2006). Structurally BRCA1/BARD1(Brzovic et al., 2001) and Ring1b/Bmi1(Buchwald et al., 2006) have been shown to form heterodimers and Pirp19 and CHIP form homodimers (Vander Kooi et al., 2006) (Xu et al., 2006). MDM2 RING domain similarly was shown to structurally homo- (Figure 3.2 panel C) and heterodimerize with itself and its paralogue MDMX (MDM4) respectively (Kostic et al., 2006; Linke et al., 2008). The hydrophobic patch of each MDM2 RING monomer is the region employed primarily in formation of dimer interface, resulting in burial of a large hydrophobic region that would be solvent exposed in a monomeric state (Figure 3.2 panel D). Despite the converging crystallographic and biochemical results highlighting the ability of the MDM2 monomer to homo- and heterooligomerize with its paralogue MDMX, no studies have clearly shown whether this is the case for the full length form of the proteins. All the available data are based on purified RING subdomains of MDM2 and MDMX, and though informative, do not shed light on how this process is controlled and affected by remaining prominent subunits of the proteins. Moreover, no structural information is available on how the remaining protein backbone of MDM2, excluding the RING motif, behaves upon dimerization.

3.2 Experimental Results

3.2.1 Point Mutations within Key Residues building the MDM2 RING domain

The C-terminal RING Domain of MDM2 is critical for its activity, each RING monomer shows a ββαβ fold, a small hydrophobic core and coordinates two Zn^{2+} ions which are essential for maintaining the native domain structure resulting in an active phenotype of the enzyme. Zinc binding is carried out by a set of eight amino acid residues; four cysteines and two histidines and two cysteines respectively.

In order to study the RING domain in the context of full-length MDM2 a series of RING finger domain mutant constructs was generated. Two of these, Cys^{464A}

($MDM2^{C464A}$) and Cys^{478S} ($MDM2^{C478S}$), introduced single point mutations into two independent Zn^{2+} coordination sites within the C2H2C4 Zinc coordinating structure (Kostic et al., 2006) and a third, Lys^{454A} ($MDM2^{K454A}$), is a RING domain residue which is not required for Zinc coordination but is essential for MDM2 to bind ATP (Poyurovsky et al., 2003; Wawrzynow et al., 2007a).

The Cys^{464A} mutation (Figure 3.3 Panel A) is located within the first zinc-binding site of the monomer and is one of the first to be identified as disruptive to the E3 ubiquitin ligase potential of MDM2. This mutation, which alters the structurally critical zinc coordinating cysteine has been show to abolish MDM2's enzymatic activity without affecting MDM2-p53 binding (Geyer et al., 2000). Mutating the last cysteine within the C4 coordination site proves to have its advantages, despite the fact that one looses a Zn^{2+} coordinating residue its location within the α-helix of the RING, (Figure 3.3 Panel B) implicates that the mutant is predicted to globally have a similar conformational status as its wild type counterpart. Moreover, the mutation has little or no effect on the local chemical exposure to the solvent (Figure 3.3 compare panel C and D).

The Cys^{478S} mutation (Figure 3.4 Panel A) is located within the second zinc-binding site of the monomer. This mutation also alters the structurally critical zinc coordinating cysteine and furthermore diminishes the interaction of MDM2 with its paralogue MDMX (Sharp et al., 1999). This also is the last cysteine within the H2C2 coordination site. The mutation is located within an irregular structured loop region of the MDM2 RING, thus its effect on the global fold of the domain is predicted to be minimal (Figure 3.4 panel B). The chemical nature of the mutation from cysteine to serine is also quite valuable here in contrast to the previous Cys^{464A}, as here a sulphydryl proton donor group is replaced with a hydroxyl one. Furthermore the Cys^{478S} in contrast to the Cys^{464A}, has a prominent effect on the local chemical exposure to solvent (Figure 3.4 compare panel C and D).

A Walker A or P loop motif is localized within the RING MDM2 domain (Figure 3.5 panel A). This is a common feature of ATP/GTP binding proteins (Walker et al., 1982). The P loop consensus sequence (GXXXXGK(T/S)) in MDM2 consists of **G(448)**CIVH**GKT(455)**. It is highly conserved in all vertebrate MDM2 orthologues and is also present in the MDMX paralogue. It must be stressed that among other

RING/U-box E3 ubiquitin ligase proteins, MDM2 and its paralogue MDMX are unique for possessing this motif. Published data highlights that MDM2 preferentially binds ATP over GTP with a K_D =13.5 μM (Poyurovsky et al., 2003). Additionally no ATPase activity of MDM2 has been detected (Poyurovsky et al., 2003). Mutation of the *mdm2* ORF in the Lys^{454A} position inhibits ATP binding by the protein but does not interfere with its E3 ubiquitin ligase activity (Poyurovsky et al., 2003).

The crucial amino acids Gly^{453}, Lys^{454}, Thr^{454} of the P Walker motif are located in the loop between β1 strand and β2 strand of the RING domain (Figure 3.5 panel A). During structural and functional studies of the MDM2 RING domain it has been shown that Thr^{455} although not involved directly in zinc binding plays an important role in maintaining the structural and functional integrity of MDM2 (Kostic et al., 2006; Lovering et al., 1993; Poyurovsky et al., 2003). The Thr^{455} is located at the monomer subunit interface and has contacts with several residues on the opposite monomer. For this reason Lys^{454A} was mutated for the experiments in this thesis, nevertheless by comparing panel D and E of Figure 3.5 one can predict that mutation of Lys^{454} has a greater effect on the local structure and chemical exposure to the solvent, than the previously described mutations.

3.2.2 MDM2 E3 Ubiquitin Ligase Activity in Cell Culture

All of the above mutations were introduced into full-length MDM2 encoding plasmids and were transfected into two distinct cell lines in order to assay for E3 ubiquitin ligase activity, by means of a well characterized His-tagged ubiquitin pulldown assay (Xirodimas et al., 2001a). This cell-culture assay system originally developed in 1994 (Treier et al., 1994) is very efficient for investigating MDM2-mediated ubiquitination of p53 within a specific cell-culture background. By means of transient tranfection, a construct expressing modified – His_6-tagged version of ubiquitin is introduced to a given cell line. Thus a protein undergoing ubiquitination is likely to be tagged with this exogenous ubiquitin protein moiety, rendering it possible to extract it from the cell lysate by means of His - Ni^{2+} affinity chromatography.

Human lung carcinoma H1299 *p53*-/- cells (Wang et al., 1998), which express limited amounts of endogenous MDM2 (Figure 3.6) were cotransfected with a combination of plasmids encoding His_6-ubiquitin, wild-type p53 and wild-type or $MDM2^{C464A}$, $MDM2^{C478S}$, $MDM2^{K454A}$ and $MDM2^{K454A/C478S}$ double mutant respectively. Two reasons support the use of this cell line for the assay. Firstly, it is very easily transfected, thus allowing straightforward detection of proteins linked to ubiquitin. Secondly, as stated above it is deficient for p53 expression, hence resulting in low levels of endogenous MDM2.

In order to further enhance the total pool of ubiquitinated proteins within the cell prior to lysis, the cell culture was treated for several hours with a proteasome inhbitor MG132. This was followed by protein extraction under denaturating conditions (6M guanidium-HCl) in order to prevent deubiquitination of protein-ubiquitin conjugates as well as curb any non-covalent protein-protein interactions. Following protein extraction under denaturating conditions, His_6-ubiquitinated proteins were isolated from the total pool by using Ni^{2+} - agarose beads. Eluates were separated by means of SDS-PAGE, and further analysed by immunoblotting.

The results presented in Figure 3.6 show a high specificity of p53 ubiquitination dependent on MDM2 transfection (compare lines 3 and 5 Panel A and B Figure 3.6). The tumour suppressor is di-, tri-, tetra-, penta-ubiquitinated in a dose dependant fashion by MDM2. As this assay is more qualitative than quantitative it is difficult to establish whether $MDM2^{K454A}$ is more or less active as a ubiquitin ligase than $MDM2^{WT}$ (Figure 3.6 compare panels A and B), nevertheless the mutant shows considerable ligase activity which is consistent with published data (Poyurovsky et al., 2003). Surprisingly, p53 was also ubiquitinated when mutants within key cysteine residues of the MDM2 RING, $MDM2^{C464A}$ and $MDM2^{C478S}$ were transfected (Figure 3.6 panel C). This seams contradictory to previous published experiments, where these mutants are clearly described as being E3 ubiquitin ligase 'dead' (Geyer et al., 2000). However, as the H1299 cell line used in this experiment harbours, although at low levels, endogenous MDM2 and MDMX, the observed phenomenon can be explained as such. When the physiological level of MDM2 is increased by transient transfection one observes an increase in the ubiquitination ladder of p53. This may be due to the generation of heterogeneous complexes between endogenous

and trasfected MDM2 mutant proteins. The p53 tumour suppressor shows increase in ubiquitination which is dose dependent on the amount of $MDM2^{C464A}$ and $MDM2^{C478S}$ expressed in the cell (Figure 3.6 Panel C). Thus, the increasing protein pool of exogenous MDM2 mutant proteins may recruit endogenous MDM2 leading to formation of an active complex and visible ubiquitination of the target protein.

To test this hypothesis a different cell line was used, namely Mouse Embryonic Fibroblast, which were *p53 -/-* , *mdm2 -/-* (MEF DKO), in this case the cell environment is deprived of endogenous MDM2 hence p53 ubiquitination should only rely on the amount of MDM2 introduced by transient transfection. This is indeed the case; p53 is ubiquitinated only in the presence of $MDM2^{WT}$ and $MDM2^{K454A}$ mutant (Figure 3.7 Panel A and C) and no visible ubiquitination was detected in the presence of $MDM2^{C464A}$ and $MDM2^{C478S}$. This assay clearly shows dependence on the genotype of the cell line used. The synergy of the two performed experiments hints that MDM2 in cells functions as an E3 ubiquitin ligase not in a monomeric state. Indeed the Cys^{464A} and Cys^{478S} mutations render the protein inert in terms of enzymatic activity yet still make it possible for interaction with the WT counterpart.

3.2.3 Chaperone Activity of MDM2

The p53 protein is widely recognized for its critical role in suppression of tumour development. Nevertheless when one considers its biophysical properties it is an adequate representative of a thermodynamically instable protein (Canadillas et al., 2006) with numerous vast unstructured motifs (Bell et al., 2002). Given the physiological temperature that the human body maintains, even the most structured part of purified p53 protein – the DNA binding domain adopts inactive misfolded conformations and aggregates at relatively high rates (Butler and Loh, 2006; Canadillas et al., 2006; Hansen and Braithwaite, 1996; Muller et al., 2004).

It has been shown that the Hsp90 molecular chaperone, in an ATP-dependent reaction, retains p53 in a conformation that allows binding to a specific promoter sequence at physiological temperature (Muller et al., 2004; Walerych et al., 2004). The authors have investigated this specific protein:DNA interaction by means of

numerous techniques, one of which is the Electrophoretic Mobility Gel Shift Assay (EMSA). This technique also known as bandshift, gelshift or gel retardation assay, serves to analyse the interactions of proteins with DNA. This method is based on the fact that unbound DNA in a non-denaturated gel exhibits a higher electrophoretical mobility than protein-bound DNA. The protein-bound DNA is denoted as "gel-shifted" in respect to unbound DNA.

The EMSA based experiments described in this section stem from the outline described in Figure 3.8 panel A. Briefly, a sample containing p53 alone or with other proteins is subjected to a pre-incubation step performed at different temperatures, afterwards its potency for binding a specific promoter DNA sequence is investigated. As shown by previously published data, p53 incubated at 17°C *in vitro* binds specifically to p53-responisve promoter sequences after activation by C-terminal specific p53 antibody or phosphorylation by CK2 kinase (Hupp et al., 1995) (Walerych et al., 2004) and lanes 1,2 in Figure 3.8 panel B. The same reaction performed under more physiological temperatures, i.e. 37°C, does not lead to the formation of a p53-consensus site DNA complex (Figure 3.8 panel B, lane 6). As published before, at 37°C p53 loses its correct fold which is required for efficient specific binding of p53 to the promoter sequence (Walerych et al., 2004). However, the ability of p53 to bind to a promoter sequence at 37°C is maintained in the presence of the Hsp90 molecular chaperone and ATP, both *in vivo* and *in vitro* (Muller et al., 2004; Walerych et al., 2004; Wawrzynow et al., 2007a). In the current study when Hsp90 molecular chaperone was substituted with MDM2 protein in this reaction efficient binding of p53 to the promoter sequence was observed (compare lanes 1-6 with 8-13 Figure 3.8 panel B). Moreover, Hsp90 and MDM2 work synergistically (Wawrzynow et al., 2007a). The MDM2-dependent binding of p53 to the promoter sequence is limited to the physiological temperature of 37°C (Figure 3.8 panel B), hinting that under heat shock conditions other chaperones could also be involved in these reactions. The presence of MDM2 does not supershift the p53-promoter DNA complex (Figures 3.8 and 3.9 Panel B), suggesting that MDM2 is only transiently required for p53 to adopt a DNA binding-competent conformation. To test this hypothesis monoclonal antibodies were used that interfered with p53-MDM2 complex formation; 2A10 binds to two epitopes within MDM2 (postioned

respectively at aa 255-265 and 384-400) and 4B2 antibody recognizing the epitope in the N-terminus of MDM2. The presence of these antibodies during the preincubation of MDM2 with p53 at 37°C severely, in the case of 2A10, and partially, in the case of 4B2, reduced the ability of p53 to bind to the promoter sequence (Figure 3.9 Panel B lanes 5 and 6). Interestingly, the addition of the same antibodies after the preincubation of MDM2 with p53 at 37°C had no inhibitory effect on p53 binding to the promoter sequence (Figure 3.9 Panel B lanes 9 and 10), suggesting that at this stage MDM2 is no longer in the complex with p53. Moreover, the monoclonal MDM2- specific antibodies 4B2 or 2A10 do not change the mobility of p53-DNA complex which further supports the absence of MDM2 in the p53-DNA complex (Figure 3.9, lane 9 and 10). However, if such a reaction is conducted at 4°C, the monoclonal antibody supershifts the p53-DNA complex (Figure 3.9, lane 14), suggesting that recycling of MDM2 from the p53 complex is caused by the diffusion accelerated by temperature. The data presented suggest that the presence of MDM2 is required only when p53 is preincubated at 37°C and that the p53-MDM2 complex dissociates after conversion of latent p53 to a transcriptionally active p53. In a control experiment (Figure 3.9 Panel B lane 12), we found that the addition of the p53-specific DO-1 antibody before and after preincubation of p53 at 37°C leads to antibody-induced supershift, indicating that p53 is present in the complex with the promoter DNA sequence. In addition, by means of ELISA it has been shown that, DO-1 does not interfere with MDM2-p53 complex formation (Wawrzynow et al., 2007a).

In the absence of ATP, MDM2 interacts with p53 independent of p53 conformation, namely, a correct fold *i.e.* native-like or mutant-like fold. This situation changes however in the presence of ATP. The nucleotide does not significantly influence the affinity of MDM2 for p53 with the correct wild type conformation but has an effect when the wild-type conformation of p53 is abrogated (Wawrzynow et al., 2007a). The presence of ATP in this scenario leads to a reduction in the affinity of MDM2 for p53. The $MDM2^{K454A}$ purified mutant tightly binds p53 regardless of the presence of ATP or the conformational status of p53. These experiments suggest that binding of ATP by MDM2 triggers the release of MDM2 from the MDM2-p53

complex only when p53 is not in a wild-type conformation. The $MDM2^{K454A}$ protein, which still possesses E3 ubiquitin ligase activity on a level comparable with wild-type MDM2 (Figures 3.6 and 3.7), is not able to rescue p53 binding to the promoter sequence at 37°C (Figure 3.10). Because the $MDM2^{K454A}$ mutation is within the RING finger domain, one cannot exclude the possibility that this mutation not only affects the ability of MDM2 to bind ATP but in addition has other effect(s) on the overall conformation of the RING finger domain. However, two experimental facts strongly suggest that this is not the case. First, the $MDM2^{K454A}$ mutant protein possesses E3 ubiquitin ligase activity similar to MDM2 wt protein both in cell culture and *in vitro*. In fact kinetic studies show that $MDM2^{K454A}$ is slightly more enzymatically active than $MDM2^{WT}$ (Poyurovsky et al., 2003) (and data presented in Chapter 4 of this thesis). Secondly the point mutants Cys^{464A} and Cys^{478S} in the zinc binding motif that are completely inactive in the p53 ubiquitination reaction *in vitro* (Chapter 4) yet still efficiently bind ATP (Chapter 4) and are able to partially rescue p53 binding to the promoter DNA sequence at 37°C (Figure 3.11).

3.2.4 MDM2 induces proper folding of p53 in cells

To test the influence of MDM2 assisted p53 folding within the cell, an immunochemical-based assay was used that measures the affinity of conformation-specific antibodies for p53 (Gannon et al., 1990; Shimizu et al., 2006). H1299 *p53-/-* cells were cotransfected with a combination of plasmids encoding wild-type p53 and wild-type or mutant proteins, $MDM2^{K454A}$, $MDM2^{C464A}$, and $MDM2^{C478S}$. After gentle cell lysis, the ratio of p53 correctly folded in a wild-type conformation (ELISA test with pAb1620) to total p53 (ELISA test with DO-1) in cell lysate was measured (Figure 3.12 Panel A and B). Following normalization to the total amount of p53 in cells the data shows that transfection of H1299 cells with p53 alone gives less than 40% of wild-type conformation (Figure 3.12 Panel C). It is highly probable that in this case the correct folding of p53 is stimulated by the presence of other molecular chaperones, like the abundant Hsp90. Cotransfection of p53 with $MDM2^{WT}$ substantially stimulates the folding of p53. More than 70% of p53 was found in a wild-type conformation. Cotransfection of p53 with the $MDM2^{C478S}$ or

$MDM2^{C464A}$ mutants caused an even higher level of pAb1620 positive p53 species than was seen with $MDM2^{WT}$. It must be stressed that in the case when $MDM2^{WT}$ is used, we are dealing with at least three effects; that is, an increase of the degradation of p53, an increase of the chaperone-like activity of MDM2, and folding of p53 catalyzed by other chaperones like Hsp90. Cotransfection of cells with p53 and mutant $MDM2^{K454A}$ substantially reduces the amount of p53 found in wild-type conformation (Figure 3.12 panel C), indicating that the observed effect of MDM2 on p53 folding requires ATP and is most likely due to molecular chaperone activity of MDM2.

3.2.5 Translation of p53 is assisted by MDM2 in an ATP dependent manner

The abundance of a given protein in a cell can summarized into the following equation:

Protein Abundance = Protein Synthesis – Protein Degradation.

Theoretically if one were to apply this simplified equation to the abundance of the p53 tumour suppressor protein and neglected the input of stress induced signalling (caused by DNA Damage, UV radiation, activation of oncogenes etc) leading to a dramatic increase of p53 synthesis and a prominent decrease of its degradation, then one would surely consider the role of MDM2 oncoprotein as an advantageous coefficient of protein degradation.

Nevertheless, the aim of the previous sections was to portray to the reader that despite its E3 ubiquitin ligase activity MDM2 has other functions. It acts as a molecular chaperone, both in an *in vitro* controlled experiment [the EMSA experiments described in this chapter and supplementary data (Wawrzynow et al., 2007b)], as well as in cells where it favours the adoption of p53 wt conformation (Figure 3.12).

The involvement of MDM2 in p53 folding is also supported by other *in vivo* findings where increased levels of MDM2, in the presence of protease inhibitors, increase the level of *p53* expression, whereas mRNA levels remained unchanged (Yin et al., 2002). Moreover, $MDM2^{C464A}$ had a comparable effect to its WT counterpart,

meaning that the capacity of MDM2 to regulate p53 mRNA translation is independent of its E3-ubiquitin ligase activity. As it has been shown, ^{35}S-Met pulse-labelled H1299 cells cotransfected with p53 and MDM2^{WT} led to an increase in the amount of soluble ^{35}S-Met p53 immunoprecipitated with DO-1 (Figure 3.13). Interestingly, when MDM2^{WT} was substituted by MDM2^{K454A} such an increase in the amount of soluble ^{35}S-Met p53 was not observed (Figure 3.13 Panel B). One interpretation of this cell based assay could be that MDM2 not only increases translation of p53 protein (as suggested by Yin *et al*, 2002) but also, using its chaperone-like activity, maintains proper folding of the p53 polypeptide. In the absence of active molecular chaperones, incorrectly folded p53 protein could aggregate and be sequestered in various cell structures. It has been shown before that molecular chaperones can not only protect proteins from aggregation but also dissociate already existing protein aggregates (Parsell et al., 1994; Skowyra et al., 1990; Ziemienowicz et al., 1993; Ziemienowicz et al., 1995).

3.2.6 C2H2C4 MDM2 mutant proteins have a gain of transrepressor activity

It has recently been shown that the E3-ubiquitin ligase activity of MDM2 requires interactions at both the hydrophobic pocket and the acid domain (Wallace et al., 2006). These interactions are linked by an allosteric mechanism, where initial binding of p53 at the hydrophobic pocket of MDM2 favours recognition of a p53 ubiquitination signal from its core DNA binding domain (BOX-V). These findings prompted one to question whether similar mechanisms linked other MDM2 domains and how cooperation between domains impacted on the protein's multi-functional nature. The RING finger domain of MDM2 is required for both its E3 ubiquitin ligase and ATP-dependent chaperone activities through binding to an E2-ubiquitin conjugating enzyme and to ATP, respectively (Linke et al., 2008; Wawrzynow et al., 2007a). However, whether conformational changes in the RING domain are transmitted to other MDM2 functional domains affecting their activity, remains unclear.

Although the introduction of the Cys mutations is sufficient to inactivate MDM2 as an E3-ubiquitin ligase they do not affect the overall integrity of the C-terminus as the Cys^{464A} and Cys^{478S} MDM2 mutants retain the ability to bind ATP, whilst ATP-binding activity is lost in the Lys^{454A} mutant (Wawrzynow et al., 2007a) (Figure 3.11 and Figure 4. Chapter 4). Thus, mutation of Cys residues in the RING appears to specifically inactivate RING function during ligation of ubiquitin to target substrates whilst leaving other RING domain functions intact.

The MDM2 RING finger domain mutants presented in this chapter were tested in a p53-dependent transcription assay in order to determine if inactivation of either its E3-ubiquitin ligase or ATP-binding activities affected the potential of MDM2 to repress p53–dependent transcription. The ability of p53 to activate transcription was determined using the p53 responsive region of the *WAF1/p21*-promoter and an *in silico* designed p53 binding consensus promoter (cons-promoter) to drive luciferase expression (Figure 3.14). When p53 was transfected into H1299 cells (*p53-/-*) along with the p21-luciferase reporter and cons-luciferase reporter a p53 specific activation of the promoter was detected, co-expression of $MDM2^{WT}$ in a dose-dependent manner manner led to a progressive decrease in reporter activity indicative of transrepression, with an $I_{0.5}$ in the region of 300 ng of MDM2 plasmid (150 ng of p53 plasmid; Figure 3.14 Panel A). All the RING mutants were expressed to a similar level and were able to inhibit p53-dependent transcription, however, both the Cys mutants displayed a gain of transrepressor function with an $I_{0.5}$ of < 75 ng for $MDM2^{C464A}$ and <150 ng for $MDM2^{C478S}$. In contrast, mutation of Lys^{454A} did not enhance the repressor activity of MDM2 and like the wild-type protein this mutant had an $I_{0.5}$ of around 300 ng. Similarly, whilst a titration of p53 could overcome transrepression imposed by a fixed amount of wild-type MDM2 and the Lys^{454A} mutant, there was a significant reduction in the ability of p53 to overcome the effects of the Cys^{464A} and Cys^{478S} mutants (Figure 3.15). This data further supports the fact that MDM2 E3-ubiquitin ligase activity can be fully uncoupled from its ability to repress p53 transcription and second, it provides evidence that the RING domain can modulate the activity of MDM2 as a transrepressor of p53-dependent transcription.

Together the data presented above suggest that mutation of residues within the RING finger domain that directly affect MDM2 E3-ligase activity facilitate transrepression

of p53 transcriptional activity. In contrast, mutation of the ATP binding site in MDM2 (Lys^{454A}) had no effect on transrepression of p53.

A control experiment (Figure 3.16) where p53 was replaced with a mutant $p53^{F19A}$ protein sheds further light on the complex interaction of MDM2 with p53. The Phe^{19A} mutant of p53 is transcriptionally active yet is refractory to MDM2 mediated ubiquitination and binding. Early crystallographic data that elucidated the biochemical basis of MDM2-mediated inhibition of p53 function showed that the amino terminal domain of MDM2 forms a deep hydrophobic cleft in which a fragment of the amino terminal transactivation domain (BOX-I) of p53 binds, thereby becoming concealed from the transcriptional machinery (Kussie et al., 1996a). The interacting domains show a tight key-lock configuration. The hydrophobic side of the amphipathic p53 α-helix (BOX-I), which is formed by amino acids 19-26 (of which Phe^{19} , Trp^{23} and Leu^{26} are the most crucial due to the fact that they make contact), fits deeply into the hydrophobic groove of MDM2. Accordingly the p53 binding mutants (of which Phe^{19A} is a member) are resistant to degradation by MDM2, as the E3-ligase activity of the protein cannot be allosterically triggered by $p53^{F19A}$.

Co-expression of $MDM2^{WT}$ in the $p53^{F19A}$ background did not lead to a progressive decrease in reporter activity (Figure 3.16). Moreover co-expression of all the mentioned RING mutants similarly had no effect. This data suggests that the canonical interaction of the transactivation domain with the hydrophobic pocket in MDM2 is necessary for proper transrepression of p53 by the latter. Furthermore the Cys^{464} and Cys^{478} MDM2 mutants which showed a gain of function as inhibitors of p53 dependent transcription require the mentioned native interaction to have their effect.

Eight amino acid residues build the C2H2C4 the two zinc coordination sites within the RING domain of MDM2. The proper folding of this domain is zinc-dependent and a native fold is required for proper E3-ubiquitin ligase activity. Disruption of any of the six cysteines and two histidines hinders the proper coordination of zinc by the MDM2 protein. Two of these mutations, namely $MDM2^{C464A}$ and $MDM2^{C478S}$, showed a gain of function phenotype in the p53-dependant transcription assays. Thus

one was led to ask whether these mutations are unique or whether disruption of any of the eight critical amino acids will give a similar effect.

The Cys^{438} residue builds the first C4 Zn^{2+} coordination site alongside with Cys^{441} it stabilizes the N-terminal region of the subunit (Kostic et al., 2006) and furthermore is located within a loop region (Figure 3.2 panel A) in contrast to Cys^{464} which is located roughly in the middle of the α-helix. For these reasons the Cys^{438} residue was chosen for site directed mutagenesis to Ala. The second vexing issue was the chemical nature of the mutation. The Cys^{478} residue located within the second zinc binding region (H2C2) was mutated to serine although it also had an apparent gain of transrepressor activity; this was not as prominent as the Cys^{464A} mutation in MDM2. At this time the question asked was, whether a substitution of cysteine residue to serine residue within the first zinc binding site will have a similar effect to the one of the studied mutants. In other words whether a less destructive mutation of cysteine to serine (substitution of the sulphydryl group with a hydroxyl one within the side chain of the amino acid) would render a similar phenotype as the cysteine to alanine substitution. As expected the new mutated proteins $MDM2^{C438A}$ and $MDM2^{C461S}$ displayed comparable inhibitory potential (Figure 3.17 Panel B) as the studied Cys^{464} and Cys^{478} mutants.

3.2.7 Endogenous downstream targets of p53 are affected by $MDM2^{C464A}$ and $MDM2^{C478S}$ mutants

The Dual Luciferase Reporter Assay is a powerful tool when looking at the control of transcriptional activity of a given protein. First of all due to the design of the assay one looks at the final normalized readout from limited pool of cells which underwent transient transfection, which usually is roughly 40% of total cells. Secondly, the results obtained represent the picture within the cell when it comes to initiation of transcription regulation. Thirdly they are quantitative and the effects observed are dependent on dose of the inhibitor or activator.

Nevertheless, one can consider this as a partly artificial system where the cell acts as a reaction vessel, with the amount of transfected proteins being far from

physiological levels. Taking this into consideration the observed inhibitory potential of the Cys^{464} and Cys^{478} mutants seen using the luciferase reporter was assayed in a more physiological environment where endogenous wild type p53 was present and its potential to activate a downstream response could be checked at the protein level. In order to do this an independent human cancer cell line was chosen; the human breast carcinoma MCF7 cell line (details on http://www.sanger.ac.uk/genetics/CGP/CellLines/). It was transiently transfected with increasing amounts of $MDM2^{WT}$ and the two Cys mutants (Figure 3.18). The E3 dead phenotype of the Cys^{464} and Cys^{478} mutants towards p53 is in accordance with the accumulation of endogenous p53 (Figure 3.18 Panel A). Despite this visible accumulation of p53 a significant increase in the amounts of the Cyclin-dependent kinase inhibitor 1A – p21 ($WAF1^{Cip1}$) nor the Bcl-2–associated X (BAX) protein was not observed (BAX is a well characterised target for p53 (Miyashita and Reed, 1995)). On the contrary, levels of p21 and BAX decrease depending on the amount of $MDM2^{C464A}$ or $MDM2^{C478S}$. Moreover Figure 3.18 Panel B shows that BAX protein levels are unaffected by the expression of wt MDM2 at the concentrations used in the experiment (Figure 3.18 Panel B ; lanes 2-4), however under the same conditions the $MDM2^{C464A}$ mutant suppressed BAX protein expression even at the lowest amount used (lanes 8-10), and consistent with the reporter assays, the $MDM2^{C478S}$ mutant had intermediate activity as it suppressed BAX protein expression when present at the highest amount (lane 7).

3.2.8 Functional implications of the RING domain in MDM2

RING domains have two roles in a protein. Firstly, they act as E3 ubiquitin ligases. Secondly, they provide a scaffold for protein-protein interactions. The number of RING domains implicated in ubiquitination is exponentially increasing. MDM2 is a RING-dependant E3 well known for its ability to regulate p53 protein degradation.
Considering structural data one can conclude that several regions of RING domains have been implicated as important in E2 recognition and binding (Kostic et al., 2006). These regions include two zinc-binding loops, between the first and second Zn^{2+} -binding residues, and some residues in the α-helix building the ββαβ fold of the

MDM2 RING. This data was obtained by superimposing known crystallized RING/U-box domains with interacting E2 ubiquitin conjugating enzymes (BRCA1/UbcH5c and c-Cbl/UbcH7 complex (Brzovic et al., 2001; Katoh and Katoh, 2003)) onto the MDM2 model. Although the exact number of potential interacting residues varies dependent on the template used, a minimal interacting consensus can be made. A substitution of Ile^{440} with Ala was chosen to investigate the effect of the mutation on the activity of the MDM2 protein (Figure 3.19). The $MDM2^{I440A}$ mutant displays a lack of E3 ubiquitin ligase activity in a cell based ubiquitination assay (Figure 3.19 Panel B) and *in vitro* (Petterson, S., et al unpublished results) thus being consistent with the role for this residue at the MDM2-UbcH5 interface. Moreover, its ability to transrepress p53 induced transcription is comparable to that seen for the $MDM2^{C464A}$, $MDM2^{C478S}$ mutants. Hence the gain of transrepressor function of MDM2 protein is linked with the E3-ubiquitin ligase activity of the polypeptide. Once the latter is inactivated, either by disruption of the RING tertiary organization or mutations within the interface involved in E2-conjugating enzyme interaction, such MDM2 mutant protein adopts an altered global conformation rendering it a better repressor of transcription that its WT counterpart.

The involvement of nucleotide binding at this stage in this process is unclear. Disruption of the Walker P motif topologically located within the RING domain of MDM2 does not disrupt the E3-ligase activity *in vitro* and in cell culture based experiments, moreover no gain of transrepressor function of p53 transcription is seen for the $MDM2^{K454A}$ (which, as shown in the later parts of this thesis, has a low affinity for nucleotide binding in contrast to the wild type form)

Together the data presented above suggest that mutation of residues within the RING finger domain that directly affect MDM2 E3-ligase activity facilitate transrepression of p53 transcriptional activity. In contrast, loss of MDM2 molecular chaperone activity in the ATP binding mutant (Lys^{454A}) had no effect on transrepression of p53. Further, the data demonstrate that MDM2 E3-ligase activity can be completely uncoupled from its ability to repress p53 transcription.

3.2.9 RNA binding does not induce a gain of transrepression function of MDM2

The MDM2 oncoprotein possesses several other activities, which seem independent of its E3-ubiquitin ligase activity. MDM2 was proposed to catalyze ribosomal assembly (Marechal et al., 1994), it forms a protein complex *in vivo* with the L5 ribosomal protein, moreover it is found to associate with 5S rRNA (Elenbaas et al., 1996). Truncation mutants demonstrate that amino acids 425-491 are necessary and sufficient for RNA binding (Lai et al., 1998). Specific RNA binding was shown to occur through the RING finger domain of MDM2 and does not seem to occur in a zinc-dependent manner (Elenbaas et al., 1996; Lai et al., 1998). Moreover this interaction can be abolished by a single point mutation of Gly^{448} (Gly^{446} in mouse Mdm2) to serine. To test whether RNA binding, or in fact the lack of it, has control of MDM2 transrepression on p53 induced transcription, a Dual Luciferase Transcription Assay was performed (Figure 3.20 panel B) in which the transrepressor potential of the $MDM2^{G448S}$ mutant protein was compared to $MDM2^{K454A}$ (deficient in ATP binding) $MDM2^{C464A}$ (inactive as an E3-ligase) and $MDM2^{WT}$. The data shows that the $MDM2^{G448S}$ mutant does not exhibit a gain of transrepressor function compared to $MDM2^{C464A}$. That being said, the $MDM2^{G448S}$ behaves more comparably to wt MDM2. This data sheds further light on the intricate organization of the MDM2 RING domain and mutations created within this domain are not all synonymous in their outcome. Only key amino acids, involved in either stabilization of the tertiary fold of the domain or involved in E2-RING interaction, when mutated render a gain of function, increased transrepressor phenotype.

3.2.10 Gross deletions and extreme C-terminal truncation mutations within the RING domain of MDM2 have opposing effects on transrepression of p53

The structural integrity of the MDM2 RING domain is required for E3-ubiquitin ligase activity of the protein and also is a site for homo and hetero-oligomerization. Mutations within the key residues that coordinate zinc binding abolish enzymatic

activity of the protein, yet are stimulatory for transrepression measured by transcription based assays. Despite no established ATPase activity the RING is also a site for nucleotide binding, which acts as a positive switch for the molecular chaperone properties of the protein, yet has no effect on its E3 activity. The domain is also necessary for RNA binding yet this interaction was shown to be zinc independent. Considering all of the above, a protein bearing this domain will display multifunctional properties. The question at hand is how will the MDM2 protein behave when it is lacking the RING domain? Surely E3 ubiquitin ligase activity will be abolished, yet this gross mutation still makes it possible for MDM2 to interact with p53 via the N-terminal hydrophobic pocket. As presented in Figure 3.21 Panel A, MDM2 lacking the RING is efficient at decreasing p53 mediated transcription, so efficient in fact that its $I_{0.5}$ is consistent with the gain of function mutations at Cys^{464} and Cys^{478} in MDM2. On the protein level (Figure 3.21 Panel B) the decrease of p53 activated endogenous downstream targets such as p21 and BAX are also visible, though in this case the Cys mutants of MDM2 downregulate the expression of p21 and BAX more effectively than the gross ΔRING MDM2 mutation (Panel B Figure 3.21, compare lanes 7-10 with 15-18).

Recent data (Poyurovsky et al., 2007; Uldrijan et al., 2007) illuminate the importance of the extreme C-terminal 'tail' residues in maintaining efficient MDM2 E3-ubiquitin ligase activity. Loss of ubiquitin ligase function for these mutants correlated with the predicted failure of MDM2 to oligomerize with itself or with the paralogue MDMX. To test the effect of such mutations on MDM2 mediated transrepression of p53 transcriptional activity a series of nonsense mutations were generated (Figure 3.22 Panel A), resulting in the formation of four species of truncated forms of MDM2 protein, lengthwise different by 3 amino acids each.

The $MDM2^{Q480STOP}$ nonsense mutation renders the protein inert in controlling p53 activity (Figure 3.22 Panel B), yet the $MDM2^{Q483STOP}$, $MDM2^{V486STOP}$ and $MDM2^{V489STOP}$ nonsense mutants are active. This result demonstrates, that nine C-terminal amino acid residues are dispensable for efficient repression of p53 driven transcription. Both the $MDM2^{Q480STOP}$ and $MDM2^{Q483STOP}$ mutants have been shown to be inactive as E3-ubiquitin ligases for p53 *in vitro* and in cell culture (Uldrijan et al., 2007). Co-immunoprecipation experiments showed that $MDM2^{Q483STOP}$ interacts

well with p53, yet no such data was shown for $MDM2^{Q480STOP}$. How can one explain such a dramatic difference in transrepression between nonsense mutants $MDM2^{Q480STOP}$ and $MDM2^{Q483STOP}$? One hint may be to consider the predicted space fill model with electrostatic potential distribution of the mutant monomers (Figure 3.23). Although each mutant subunit is highly positively charged and the majority of that charge is located on one side of the molecule, a clear difference of negative charge distribution is visible when comparing the two mutants. Moreover a cavity is predicted to form for the $MDM2^{Q480STOP}$ mutant. As mentioned both of these C-terminal truncations are inactive as E3 ubiquitin ligases, and the $MDM2^{Q483STOP}$ mutant has an $I_{0.5}$ comparable to $MDM2^{C464A}$ (Figure 3.22 Panel B). This led to the assumption that $MDM2^{Q483STOP}$ resembles a similar gain of transrepressor function, to that of the mutants in key zinc binding cysteine residues. The nature of the mutant renders it inactive as an E3 ubiquitin ligase (Uldrijan et al., 2007) yet most probably considering its predicted structure it is still able to oligomerize.

3.3 Discussion

3.3.1 Alternative variants of MDM2 oncoprotein retain the RING domain

The importance of MDM2 in the regulation of p53 protein stability and function has been illustrated in many systems. The RING domain is located within the C-terminus of the protein and contributes to numerous activities of the protein outlined in this chapter. To date, several reports have noted that human tumours can express alternatively and aberrantly spliced MDM2 variants (among the 40 identified in total) not found in normal tissue (for review see (Bartel et al., 2002).

Paradoxically these mutants have the canonical N-terminal p53 binding domain truncated or deleted along with other central regions, yet still retain the RING domain. Interestingly these variants have been shown to be as oncogenic as the full length isoform of MDM2 (Fridman et al., 2003).

Although the molecular basis for their oncogenic activity is not obvious from known structure-function relationships, it appears independent from physical association with p53, highlighting the p53 independent role of MDM2 in tumour development (Sigalas et al., 1996).

It is important to note that alternatively and aberrantly spliced variants *MDM2* mRNAs are usually found together with full-length *MDM2* transcripts. Although from the pool of variant transcripts not all of them are translated into proteins, to date at least several have been shown to interact with full-length MDM2 (Bartel et al., 2002; Evans et al., 2001; Fridman et al., 2003) and sequester it in the cytoplasm. As the site for MDM2 homo- and hetero-dimerization is mapped to the RING domain of the monomer, this presents the domain in a new light as a necessary component contributing to the oncogenic potential of MDM2.

The RING domain is primarily a scaffold for protein-protein interactions and is a key determinant of MDM2 E3-ubiquitin ligase activity. The Walker P motif located within the RING renders the protein capable of binding ATP. Additionally the RING finger has been implicated to be, at least in part, the site for RNA interaction (Bartel et al., 2002; Lai et al., 1998). Other activities ascribed to the RING include nucleolar

localization (Lohrum et al., 2000; Poyurovsky et al., 2003) and histone ubiquitination (Minsky and Oren, 2004). All of the above modulate the end activity of the protein complex. Additionally key point mutations within this domain may specifically hinder one activity whilst others are retained.

3.3.2 Regulatory effects of nucleotide binding by MDM2

The results highlighting nucleotide bound MDM2 activity presented in this chapter suggest one possible scenario; upon MDM2:p53 complex formation, p53 protein undergoes partial unfolding (MacPherson et al., 2004; Yu et al., 2006). During stress conditions, e.g. UV radiation, p53 undergoes phosphorylation by CK2 (MacPherson et al., 2004), MDM2 dissociates from partially unfolded p53, thus allowing p53 to spontaneously fold. Such repeated binding, unfolding, dissociation and folding reaction could lead p53 to reach a conformation of higher affinity towards its promoter sequence. Published cell culture based data strongly supports the idea of MDM2 dissociation following activation of p53. Using chromatin immunoprecipitation, White and colleagues (White et al., 2006) have shown that MDM2 localizes with latent p53 on the chromatin near *P21(WAF1)* and *MDM2* genes before but not after DNA damage. A transient complex of p53 with MDM2- and the Hsp90-molecular chaperone may be important for the decision to activate or degrade p53, by employing a series of post-translational modifications, like phosphorylation, acetylation, ubiquitination, sumoylation, neddylation and others. The situation where eukaryotic molecular chaperones are involved in folding and degradation of proteins is similar to prokaryotic Hsp100/Clp family members, where the ATPase subunit of appropriate protease at the same time is a molecular chaperone, and the specificity factor for the protein substrate's degradation (Parsell et al., 1994; Wawrzynow et al., 1995a; Wawrzynow et al., 1995b; Wickner et al., 1994). It is highly probable that in eukaryotes the quality-control process starts upstream of the 19S proteasome subunit, namely when the E3 ubiquitin ligase demonstrates its activity and the decision to repair or degrade the protein substrate occurs. This apparent contradictory mode of MDM2 as a component of the degradation machinery (E3 ubiquitin ligase activity) and as molecular chaperone-like

activity resembles a dual-function of CHIP, a co-chaperone/ubiquitin ligase that also is p53 specific and targets a broad range of chaperone substrates for proteasomal degradation (Hohfeld et al., 2001) (Rosser et al., 2007). In addition to the fact that MDM2 can assist in correct non-covalent assembly of the p53-promoter complex, where MDM2 is not a component of this assembled structure, MDM2 fulfils other molecular chaperone criteria. The purified MDM2 protein, in an ATP-independent reaction, can function like the Hsp90 chaperone in protecting citrate synthase and firefly luciferase from aggregation [(Wawrzynow et al., 2007a) Supplementary data].

3.3.3 Activities of MDM2 on p53 can be uncoupled

Recent genetic studies strongly postulate that the primary physiological role of MDM2 in the regulation of p53 protein levels is brought about through E3-ligase mediated ubiquitination (Itahana et al., 2007; Toledo and Wahl, 2006). These experiments were largely carried out in MEFs and developing mouse embryo's where MDM2 activity has been lost, or reduced, and is therefore rate limiting. However, this situation is unlikely to reflect the environment encountered in most tumour cells. In fact current estimates suggest that MDM2 levels are elevated in ~10% of all human tumours (Toledo and Wahl, 2006) due for example to enhanced translation or transcription in addition to amplification of the MDM2 gene (Ganguli and Wasylyk, 2003). In contrast to the studies in non-transformed mouse cell models mentioned above, work in tumour cells endogenously over-expressing MDM2 protein suggests that its ability to act as a transrepressor contributes significantly to the impaired p53-response seen in these cells. Thus, in cells which are homozygous for a polymorphism (SNP309) that enhances SP1-dependent *MDM2* transcription the MDM2 protein is found in association with p53 resulting in transcriptionally inactive complexes (Arva et al., 2005; Bond et al., 2004). Depletion of MDM2 by siRNA in these cells results in activation of p53-dependent transcription in the absence of increase p53 protein levels supporting the idea that, at least in some tumour cells, MDM2 acts predominantly as a transrepressor of p53 function (Arva et al., 2005). Furthermore, it has been demonstrated that tumour cells which do not have increased

MDM2 levels also operate an MDM2-dependent mechanism for controlling p53 transcription in the absence of changes in p53 protein levels (White et al., 2006). Thus, the data presented in this chapter showing that C2H2C4 RING mutants that lose E3-ubiquitin ligase activity preferentially bind to p53 inhibiting its transactivation activity may be pertinent to the physiological environment of a tumour cell where MDM2 is controlling p53 activity primarily through transrepression.

MDMX (also referred to as MDM4) a paralogue of MDM2 has recently emerged as another critical negative regulator of p53. MDM2 and MDMX share close similarity to two vital conserved domains: an N-terminal p53 binding domain and a C-terminal RING domain (Shvarts et al., 1996b). These two proteins can form a complex through their C-terminal domains, and although quite similar MDMX does not posses an intrinsic E3 ubiquitin ligase activity ((Stad et al., 2001; Tanimura et al., 1999). On the other hand, genetic studies show that deletion of the *MDMX* gene leads to p53-dependent lethality during early embryogenesis, as is the case for *mdm2* deletion (Migliorini et al., 2002; Parant et al., 2001). MDMX is believed to control p53 abundance in the cell indirectly by modulating the levels and activity of MDM2 (Gu et al., 2002; Linares and Scheffner, 2003; Sharp et al., 1999). The conserved C-terminal RING domains in both MDM2 and MDMX allow homo- and hetero-dimerization between the mentioned proteins and this is seen as a critical for the mentioned E3 ubiquitin ligase activity of MDM2 (Tanimura et al., 1999). While MDM2 RING forms dimers quite readily (Kostic et al., 2006), heterodimers are believed to form preferentially resulting in reduced auto-ubiquitination of MDM2 and increased p53 ubiquitination (Kawai et al., 2007; Linares and Scheffner, 2003; Sharp et al., 1999). Recent crystallographic data supports the notion (Linke et al., 2008) and states that the structure of the MDM2/MDMX heterodimer is required to ubiquitinate in trans. MDMX therefore is believed to stabilize MDM2 and keep 53 levels and activity low in healthy cells.

Although the data presented in this chapter does not directly undermine these findings, another possibility may be considered. It is true that the MDM2/MDMX interaction ensures a low activity of p53 under non stress conditions. Yet in a tumour system the MDM2/MDM2 interaction may be preferential. The MDM2 Cys^{464} and

Cys^{478} mutants are inactive as E3 ligases *in vitro* (Chapter 4) yet in cell culture are inactive only in *mdm2 -/-* background. Human lung carcinoma, H1299 cells which possess endogenous levels of MDM2 although in low amounts, used as experimental background show that p53 can be ubiquitinated in a dose dependent manner by the mentioned RING mutants. This implies a homodimeric complex formation in terms of protein MDM2/MDM2 and at the same time heterodimeric in terms of state $MDM2^{WT}/MDM2^{C464A}$. This hypothesis is further supported by the emerging picture for MDM2 RING with E2 ubiquitin conjugating enzyme interaction, where one subunit of the RING dimer interacts with E2 whereas the other subunit remains uninvolved in E2 binding (Kostic et al., 2006). Moreover, the RING dimer interface is independent of the E2 binding surface. Based on this, one cannot rule out the possibility in which $MDM2^{C464A}$ or $MDM2^{C478S}$ interact with $MDM2^{WT,}$ where the latter provides the scaffold for E2 binding and the mutants interact with the p53 polypeptide chain.

The findings presented in this chapter give an introduction to the hypothesis, which is expanded on accordingly, that MDM2 RING E3 ligase activity in tumour environment is not the only biochemical activity required to suppress p53 activity.
Later chapters of this thesis provide further investigation elucidating the reason why the key mutations within the RING presented, namely Cys^{464} and Cys^{478} give rise to a gain of transrepressor function and may be seen as oncogenic. These mutations are considered in the background of the full length protein, a more logical and informative approach than considering the sub-domain alone.

3.4 Figures

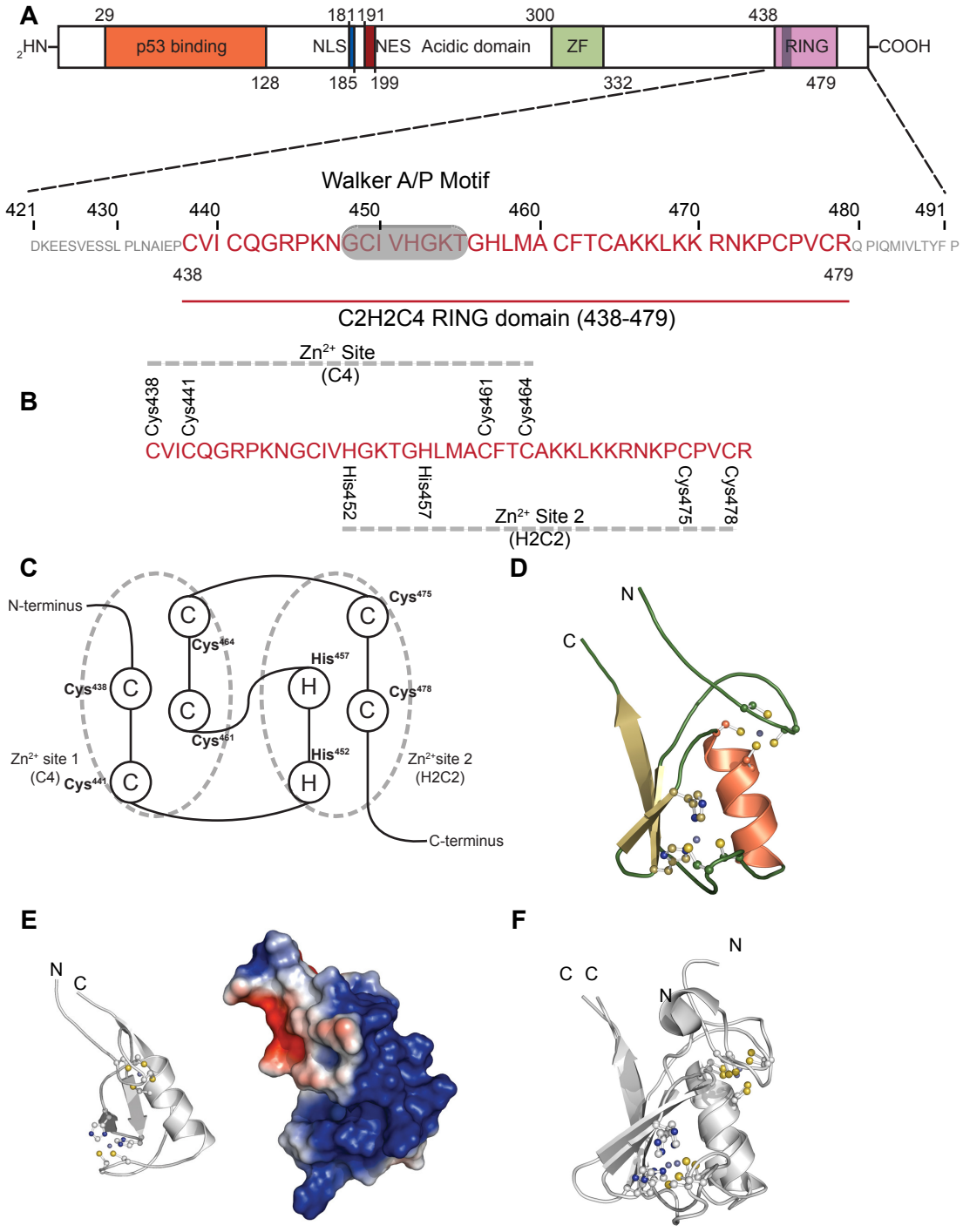

Figure 3.1 Topology and structure of the MDM2 C2H2C4 RING domain.

(**A**) Primary structure of the full length human MDM2 491aa isoform. The C2H2C4 RING domain spans from amino acid 438 to 479 is highlighted in red. The Walker P Motif located within the RING domain which utilizes nucleotide binding by the protein is highlighted in grey.
(**B**) The MDM2 C2H2C4 RING domain with the highlighted amino acids providing the scaffold for two zinc-binding sites.
(**C**) Zinc coordination scheme of human MDM2 RING highlighting the cross brace configuration of the amino acids involved in coordinating two zinc atoms.
(**D**) A super-secondary structure ββαβ fold in ribbon representation of a single subunit of human MDM2 RING (aa 429-491), with Zn^{2+} coordinating side chain highlighted.
(**E**) Surface mapped electrostatic potential of MDM2 RING monomer. Red and blue regions represent localization of negative and positive charges respectively.
(**F**) Structural alignment of the MDM2 RING subunits (Kostic et al., 2006 and Linke et al., 2008).
This figure was prepared using PyMOL [http://www.pymol.sourceforge.net/] and structural data from Kostic et al., 2006 andLinke et al., 2008 (file 2HDP,2VJE respectively RCSB PDB).

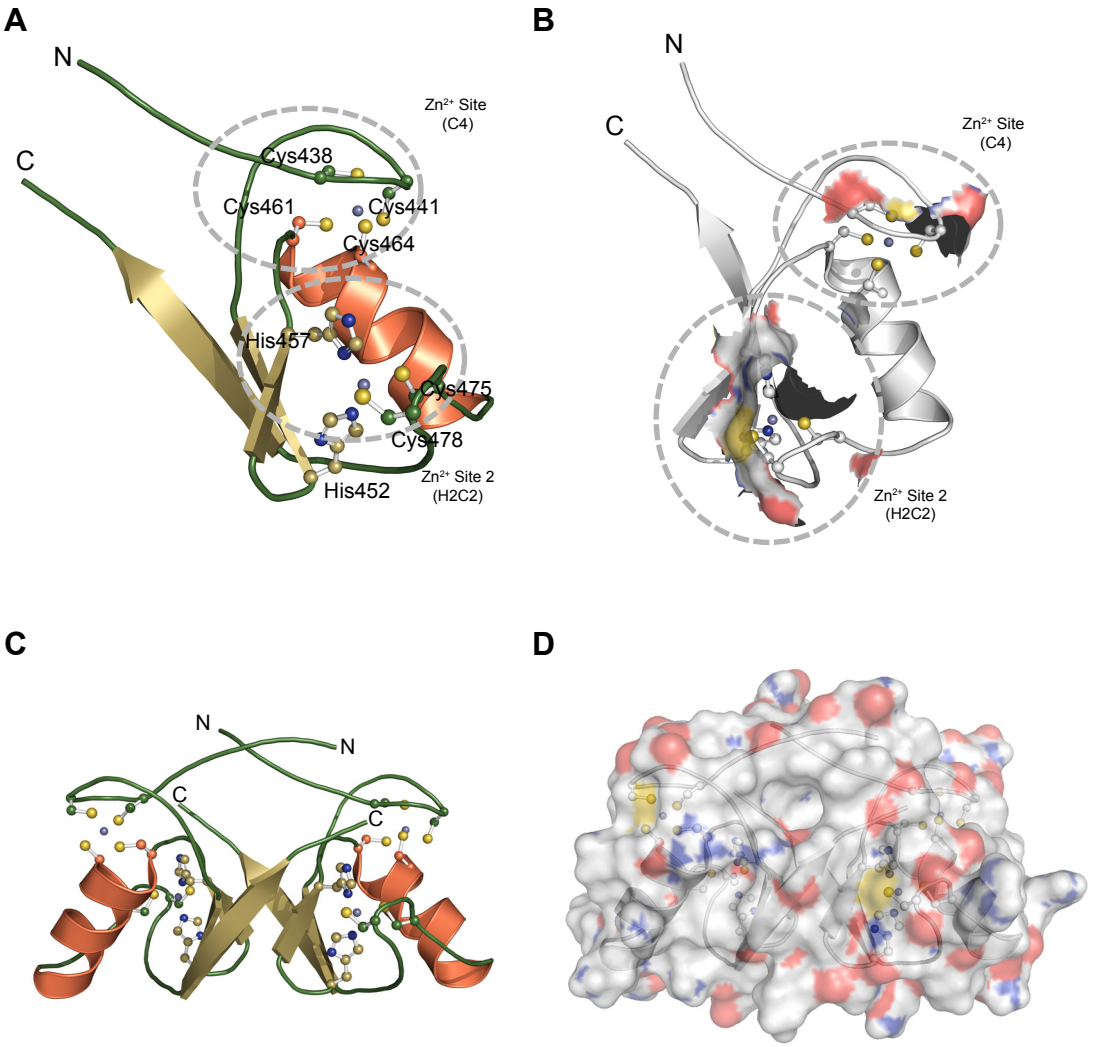

Figure 3.2 Structure of MDM2 C2H2C4 RING as a monomer and homodimer.

(**A**) Super-secondary structure ββαβ fold in ribbon representation of a single subunit of human MDM2 (aa 429-491), showing the distribution of regular secondary structure elements and the location of two Zn^{2+}-binding sites highlighted by dashed lines. The MDM2 C2H2C4 RING is an essential domain for ubiquitination of p53. The first zinc-binding site (C4) is formed by Cys438, Cys441, Cys461 and Cys464; the key players in the second zinc binding site (H2C2) are His452, His457, Cys457, Cys478. The side chains of the zinc ligands are shown. Zinc ions are shown as grey spheres.
(**B**) Analogous to (**A**) additionally highlighting the input of Zn^{2+} binding sites to the architecture and chemical composition of the space fill model. (Carbon-white, oxygen-red, nitrogen-blue, sulphur-yellow)
(**C**) Homodimer comprising of two C2H2C4 RING subunits.
(**D**) Space fill model of the C2H2C4 MDM2 homodimer.

This figure was prepared using PyMOL and structural data from Kostic et al., 2006 and Linke et al., 2008 (file 2HDP,2VJE respectively RCSB PDB).

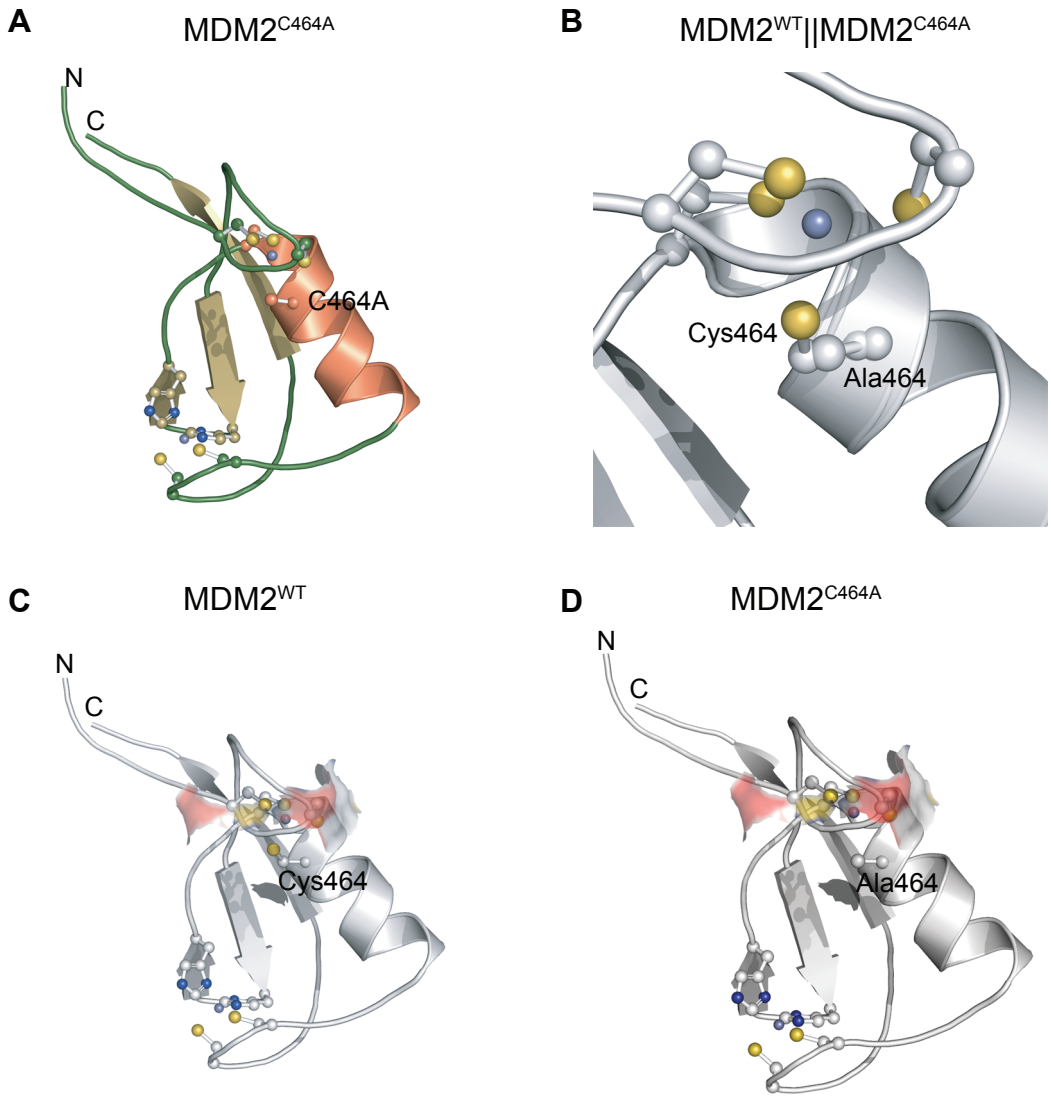

Figure 3.3 MDM2^{C464A} single amino acid mutation within the C4 Zn^{2+} binding site.

(**A**) Ribbon representation of the MDM2 RING C464A mutant. Carbon atoms of highlighted residues (in stick representation) coloured according to the secondary structure they build. Nitrogen atoms highlighted in blue and sulphur atoms in yellow.
(**B**) Structural alignment of MDM2 RING C464A mutant to WT. Zn^{2+} ions represented as grey spheres, carbon atoms in white and sulphur atoms in yellow.
(**C**) Space fill model of the C4 Zn^{2+} coordination site within MDM2^{WT}. Oxygen in red, carbon in white, nitrogen in blue and sulphur in yellow.
(**D**) Space fill model of the C4 Zn^{2+} coordination site within MDM2^{C464A} mutant; analogous colour representation as in (**C**).

This figure was prepared using PyMOL and structural data from Kostic et al., 2006 and Linke et al., 2008 (file 2HDP,2VJE respectively RCSB PDB).

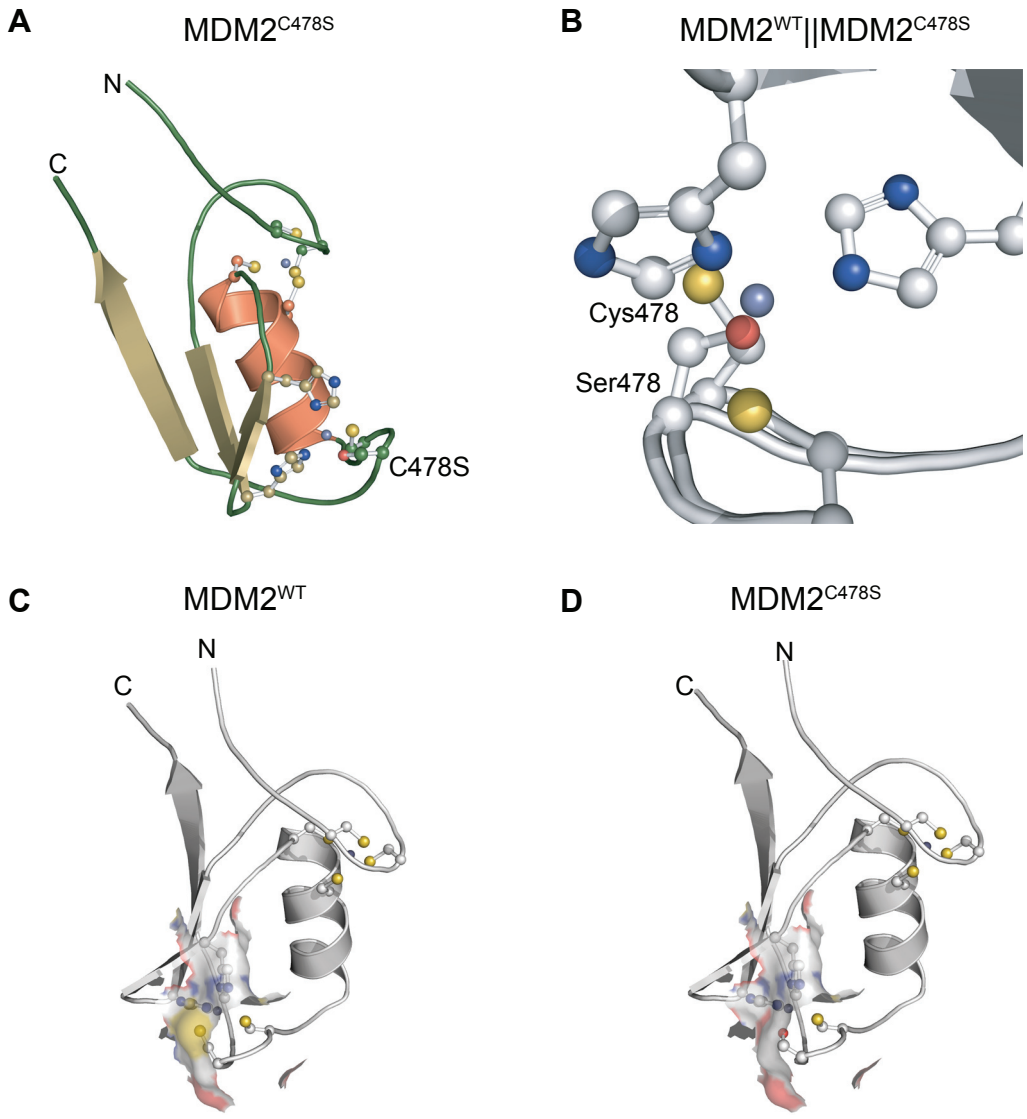

Figure 3.4 MDM2^{C478S} single amino acid mutation within the H2C2 Zn^{2+} binding site.

(A) Ribbon representation of the MDM2 RING C478S mutant. Carbon atoms of highlighted residues (in stick representation) coloured according to the secondary structure they build. Nitrogen atoms highlighted in blue and sulphur atoms in yellow, oxygen atoms in red.
(B) Structural alignment of MDM2 RING C478S mutant to WT. Zn^{2+} represented as grey spheres, carbon atoms in white and sulphur atoms in yellow, oxygen atoms in red.
(C) Space fill model of the H2C2 Zn^{2+} coordination site within MDM2^{WT}. Oxygen atoms highlighted in red, carbon in white, nitrogen in blue and sulphur in yellow.
(D) Space fill model of the H2C2 Zn^{2+} coordination site within MDM2^{C478S} mutant; analogous colour representation as in (C).
This figure was prepared using PyMOL and structural data from Kostic et al., 2006 andLinke et al., 2008 (file 2HDP,2VJE respectively RCSB PDB).

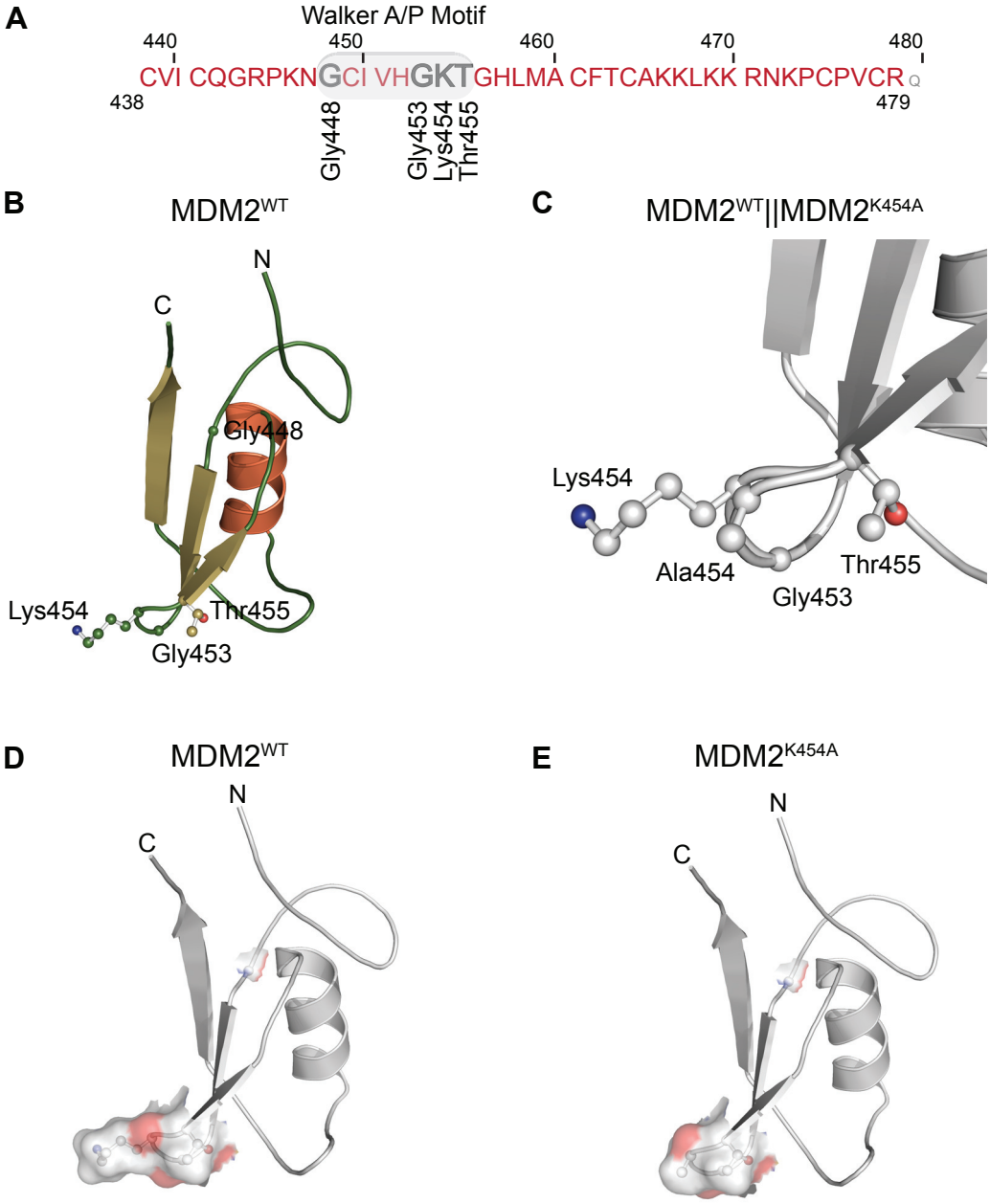

Figure 3.5 MDM2^{K454A} single amino acid mutation within the P Walker ATP binding site.

(**A**) Topological localization of the Walker P motif within the C2H2C4 RING domain of MDM2. MDM2 RING domain shown in red, Walker motif highlighted in grey. Amino acids building the GxxxxGK(T/S) consensus are outlined respectively.
(**B**) Ribbon representation of the MDM2 Walker P motif mutant. Carbon atoms of highlighted residues (in stick representation) coloured according to the secondary structure they build. Nitrogen atoms highlighted in blue and sulphur atoms in yellow, oxygen atoms in red. Amino acids building the motif outlined respectively.
(**C**) Structural alignment of MDM2 Walker K454A mutant to WT. Carbon atoms in white, nitrogen in blue and oxygen atoms in red.
(**D**) Space fill model of the Walker P motif ATP binding site within MDM2^{WT}. Oxygen atoms highlighted in red, carbon in white, nitrogen in blue.
(**E**) Space fill model of the Walker P motif ATP binding site within MDM2^{K454A} mutant; analogous colour representation as in (**C**).

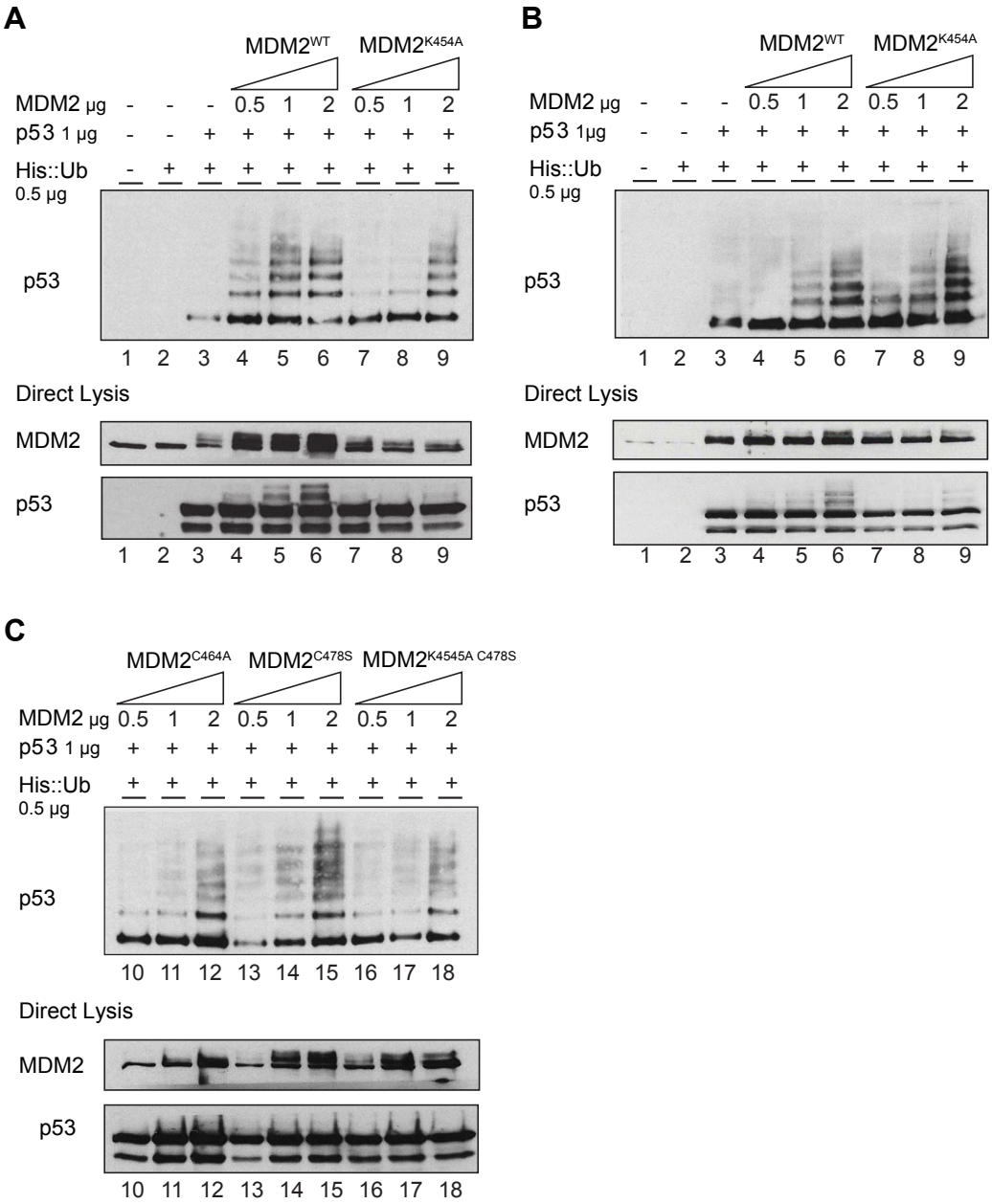

Figure 3.6 In vivo ubiquitination of p53 by MDM2 in H1299 cell line.

H1299 cell line was transfected with the appropriate plasmids and amounts as depicted above. Four hours prior to lysis the cells were treated with 10 µM proteasome inhibitor MG132. 24 hours post transfection the cells were lysed and His::ubiquitinated proteins were isolated by His::Ni^{2+} affinity pulldown method.
Panels **A, B, C** Immunoblot of p53 from p53-/- H1299 transfected with p53 and MDM2 (wt and mutant constructs as indicated) plus His-Ub. His-conjugated proteins were isolated using nickel –agarose and analysed on a 4-12% gradient gel. p53 was detected using DO-1. Top illustrations for all the panels represent western blots with pulled down His Ub proteins probed with p53 specific antibody (DO-1).The data are representative of 2 independent experiments. Middle and bottom illustrations for all panels represent direct lysis blots of H1299 cell extracts transfected with appropriate plasmids.

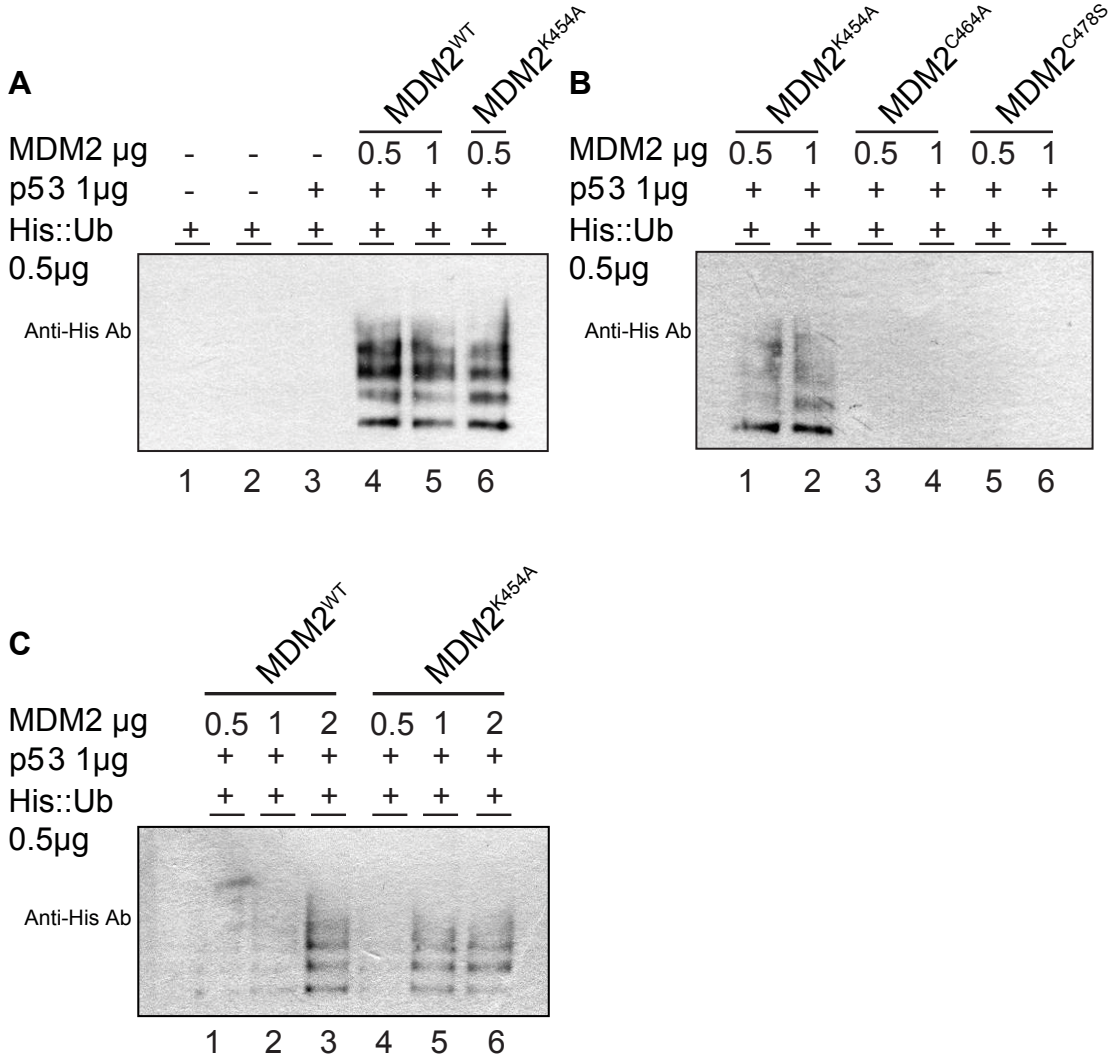

Figure 3.7 In vivo ubiquitination of p53 by MDM2 in MEF *p53 -/- mdm2 -/-* cell line.

MEF *p53 -/- mdm2 -/-* cell line was transfected with the appropriate plasmids and amounts as depicted above. Four hours prior to lysis the cells were treated with 10 µM proteasome inhibitor MG132. 24 hours post transfection the cells were lysed and His::Ubiquitinated proteins were isolated.
Panels **A, B, C** Immunoblot of p53 from *p53-/- mdm2-/-* MEFs transfected with p53 (150 ng) and MDM2 (wt and mutant constructs as indicated) plus His-Ub. His-conjugated proteins were isolated using nickel –agarose and analysed on a 4-12% gradient gel. p53 was detected using DO-1. The data are representative of 2 independent experiments.

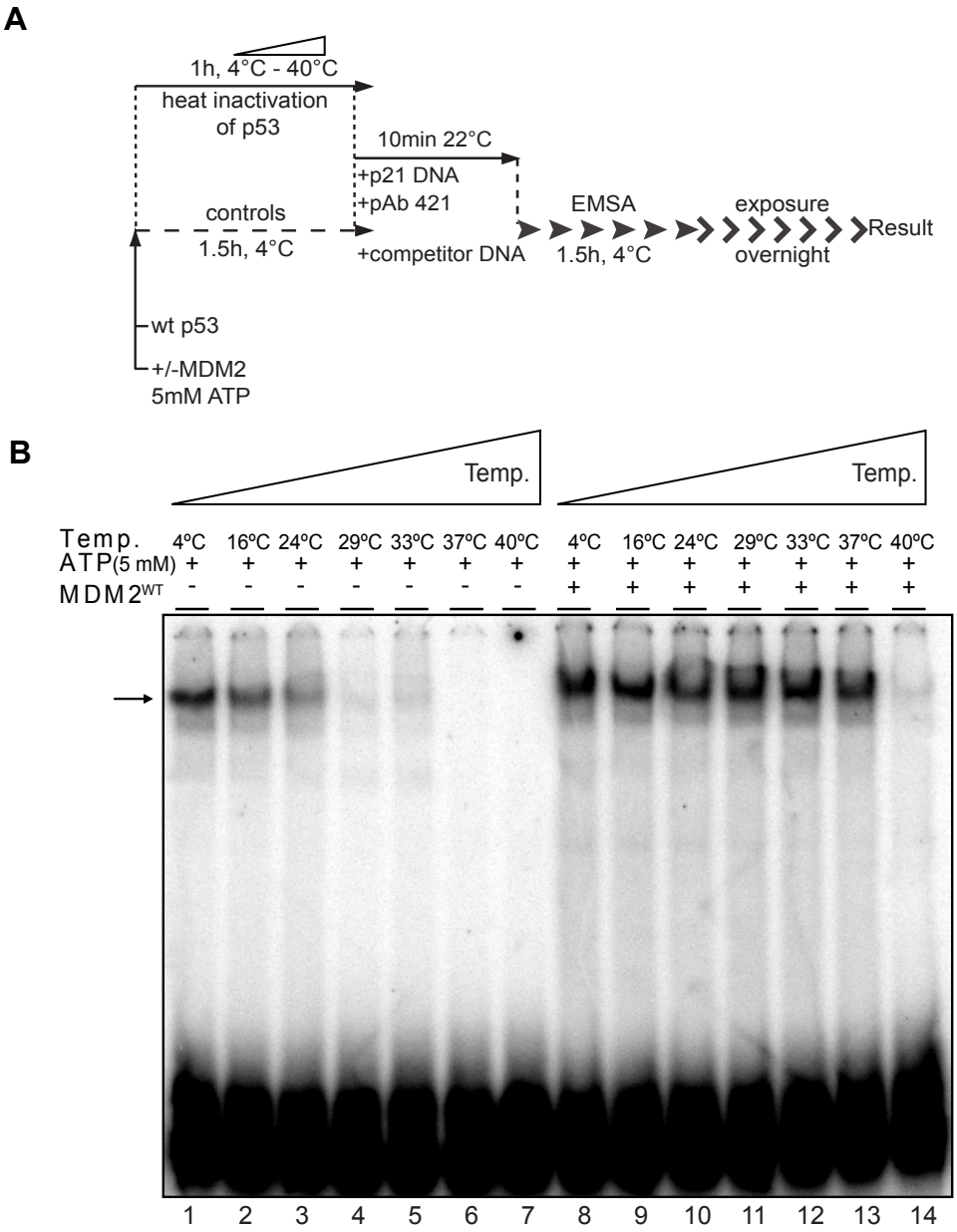

Figure 3.8 p53 binding to a $p21^{WAF1}$ promoter derived sequence is temperature dependent, in the presence and absence of MDM2.

(**A**) Schematic view of p53 EMSA following temperature gradient incubation. The p53 tumour suppressor was subjected to a temperature gradient in the presence or absence of MDM2 protein for 1 hour, after which the protein mixture was preincubated with specific radiolabelled $p21^{WAF1}$ sequence, short nonspecific double-stranded competitor DNA and an activating antibody (Ig 421). The separation of the protein:DNA complexes followed in an non-denaturating 4% acrylamide gel electrophoresis. The final result was obtained by overnight exposition of the dried gel onto a phosphor-imager screen.
(**B**) Human recombinant MDM2 restores p53 specific DNA binding activity, after 1h inactivation in a temperature gradient (4-40°C). In all the lanes where MDM2 was added to p53, a constant 1:10 mass ratio of p53:MDM2 was used. At a 1:10 protein mass ratio, 0.05 µg of p53 was used (58.1 nM of the monomer) and 0.5µg of MDM2 protein (0.45 µM of the monomer). In order to rule out unspecific protection/chaperone effects all reactions were supplemented with 1 µg/µl BSA. The arrow indicates the specific position of the p53 tetramer:p21 promoter sequence complex as shown by (Walerych et al., 2004).

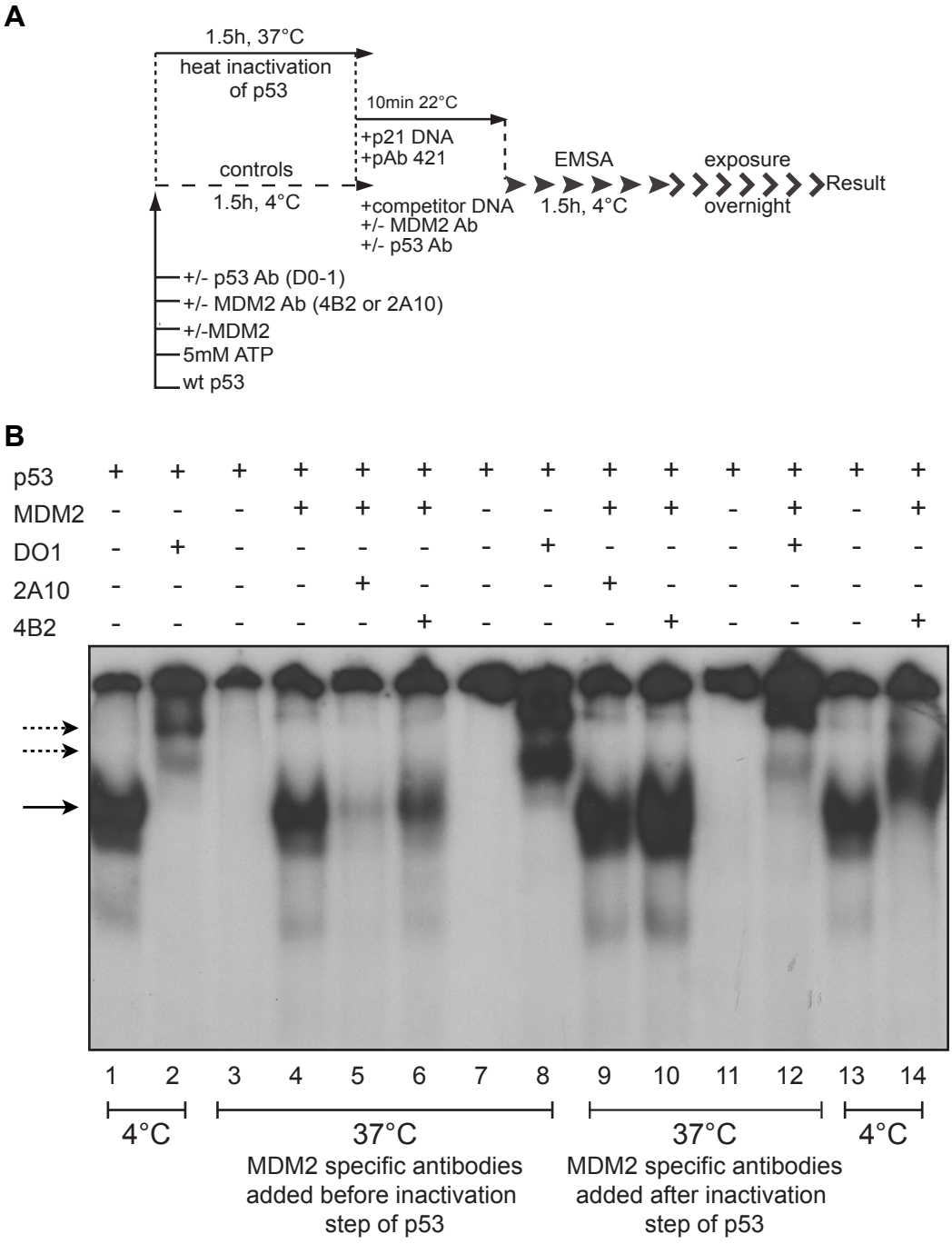

Figure 3.9 Correct non-covalent assembly of the p53 promoter complex is facilitated by transient interaction with MDM2.

(**A**) Schematic represenation of the p53 EMSA assay with indication of points when the specific competitor antibodies were added.
(**B**) MDM2 specific antibodies can competetively inhibit MDM2 p53 interaction during the crucial heat denaturation step of p53. The specific p53 antibody (DO-1) and MDM2 antibodies (2A-10 or 4B-2) were added during and after the incubation of p53 with MDM2 and ATP at 37°C, as visible above.

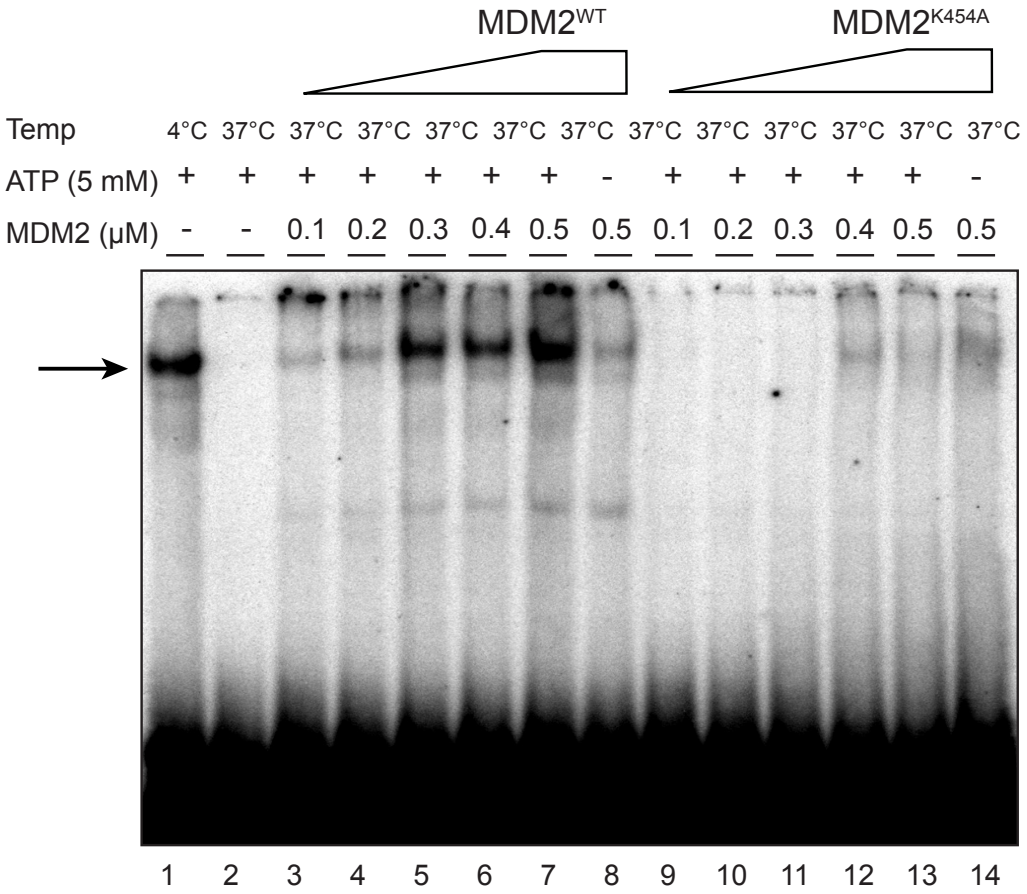

Figure 3.10 MDM2^{K454A} the ATP-binding mutant of MDM2 is defective in promoting p53 binding to the p21^{WAF1} promoter sequence.

The retention of DNA binding conformation for p53 incubated at 37°C is mediated by the presence of MDM2, moreover this reaction is ATP dependent. The MDM2^{K454A} mutant was unable to maintain p53 binding to the p21 promoter sequence at restrictive temperature in comparison to MDM2^{WT}. As indicated above, comparable amounts of the two proteins were used in the EMSA assay.

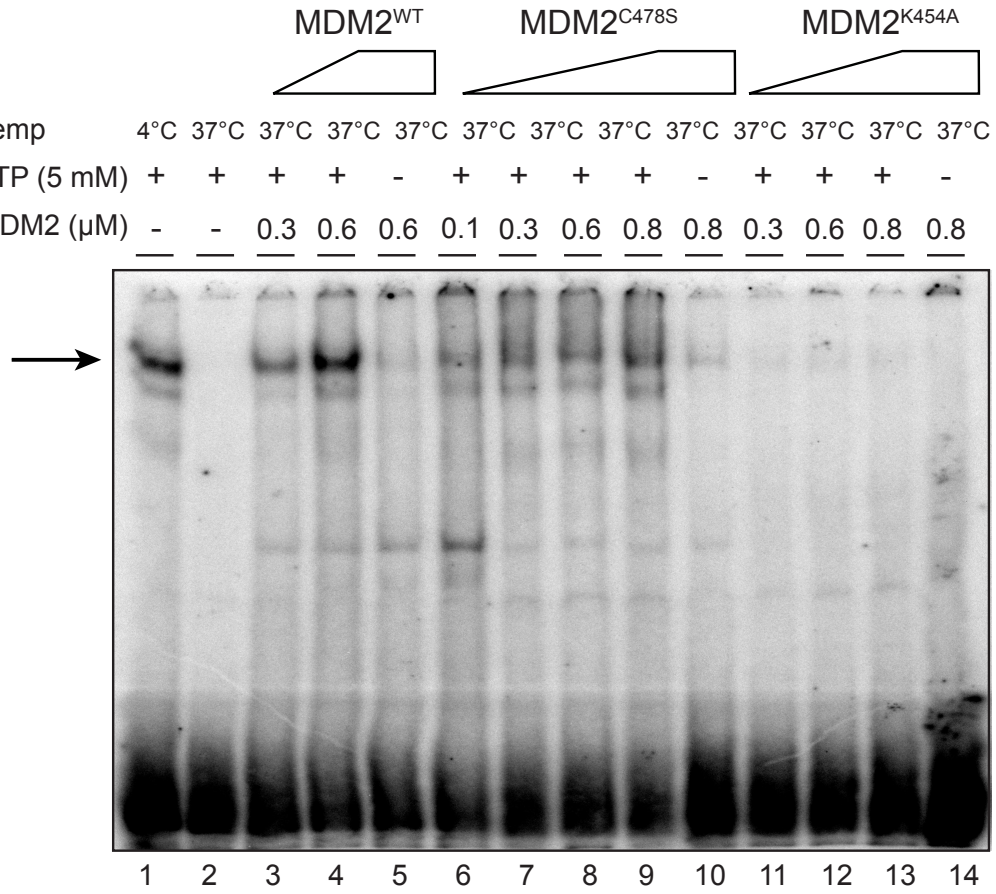

Figure 3.11 MDM2^{K454A} the ATP-binding mutant of MDM2 is defective in folding p53 protein whereas MDM2^{C478S} the E3 Ubiquitin ligase 'dead' mutant is not.

The retention of DNA binding conformation for p53 incubated at 37°C is mediated by the presence of MDM2, moreover this reaction is ATP dependent. Mutation within the Walker P motif responsible for ATP binding by MDM2 renders the protein inactive in folding the p53, when the latter is incubated at non-permissive temperature. Mutations within the H2C2 Zn^{2+} coordination site within the RING motif of MDM2 has little inhibitory effect on MDM2 mediated folding of p53 at 37°C.

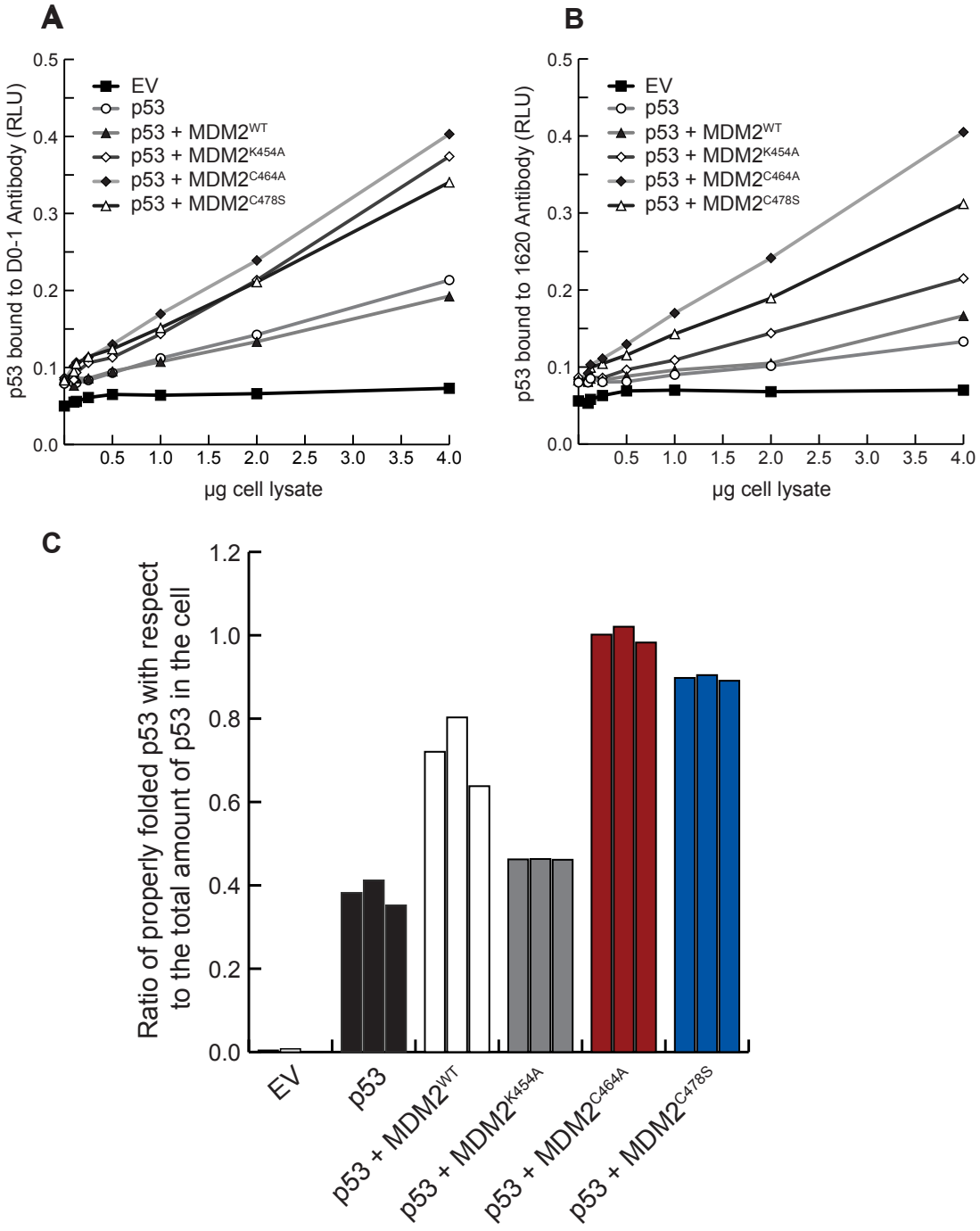

Figure 3.12 MDM2 assisted folding of p53 in cells.

In order to measure the involvement of MDM2 oncoprotein in the folding process of p53 polypeptide H1299 p53-/- cell line was transfected with empty vector, p53 (0.5 µg) alone, and combinations of p53 (0.5 µg) with $MDM2^{WT}$ (1 µg), $MDM2^{K454A}$ (1 µg), $MDM2^{C464A}$ (1 µg), $MDM2^{C478S}$(1 µg), respectively.
(**A**) and (**B**) After cell lysis and the ELISA experiments, described in detail in the Material and Methods section, were carried out. The ratio of p53 with a wild-type conformation (pAb 1620 reactive) with respect to the total amount of p53 (DO-1 reactive) in the cell was calculated.
(**C**) $MDM2^{WT}$ transfection stimulates the proper folding of p53. The ATP-binding mutant of MDM2 (K454A) has no effect on p53 protein folding. In contrast the E3 ubiquitin ligase mutants of MDM2 (C464A, C478S which retain chaperone activity) stimulate the folding of p53 protein to an even greater extent than $MDM2^{WT}$.

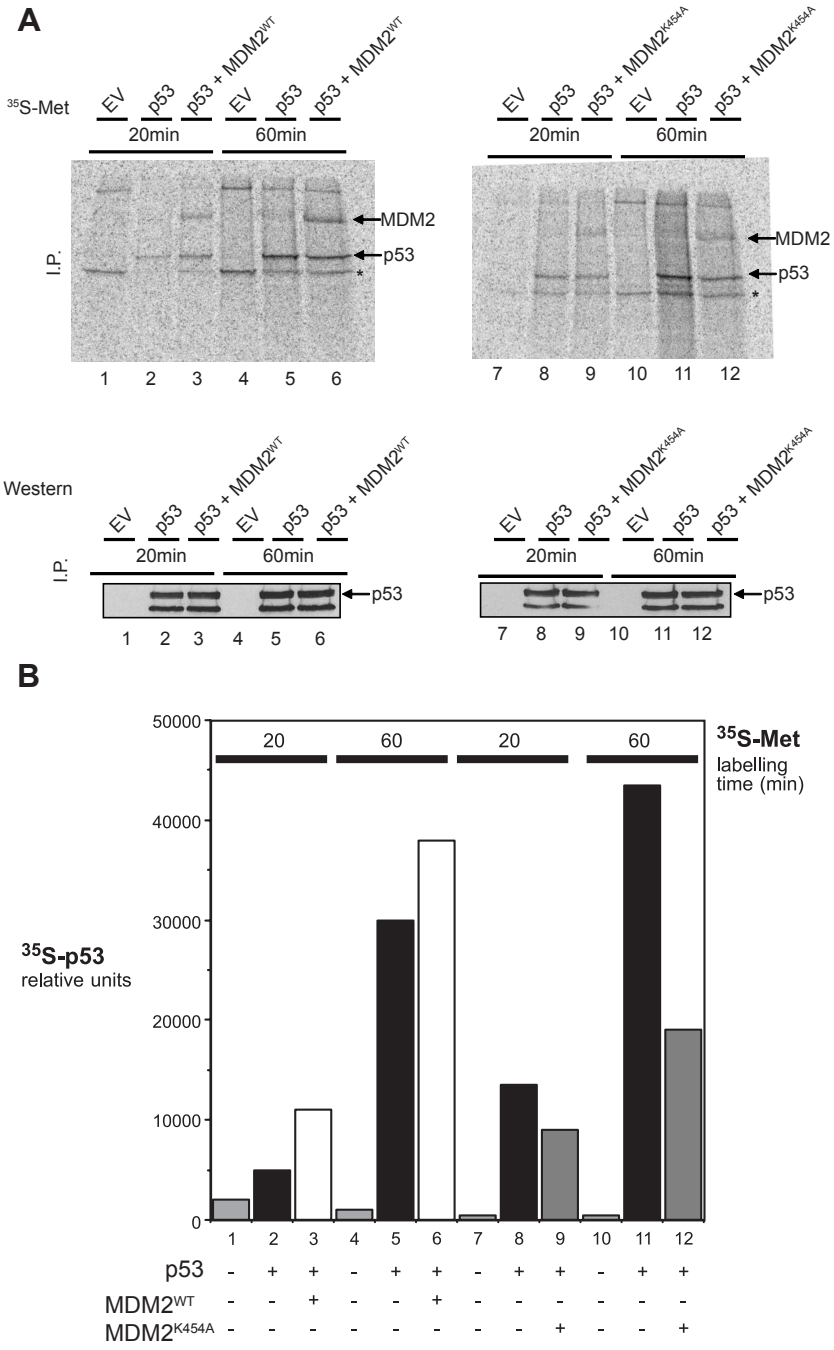

Figure 3.13 MDM2 is involved in the induction of p53 translation.

MDM2 interacts directly with the nascent p53 polypeptide during translation. H1299 cell line was transfected with empty vector, p53 (0.5µg) alone, and combinations of p53 (0.5 µg) with $MDM2^{WT}$ (1 µg), $MDM2^{K454A}$ (1 µg). Afterwards ^{35}S-Methionine pulse labelling was carried out for 20 or 60 minutes. Following cell lysis the amount of soluble ^{35}S-p53 present was detected using immunoprecipitation, SDS-electrophoresis, autoradiography and densitometry of autoradiograms with appropriate background correction. The total amounts of p53 folding immunoprecipitation were verified by means of western blot analysis.

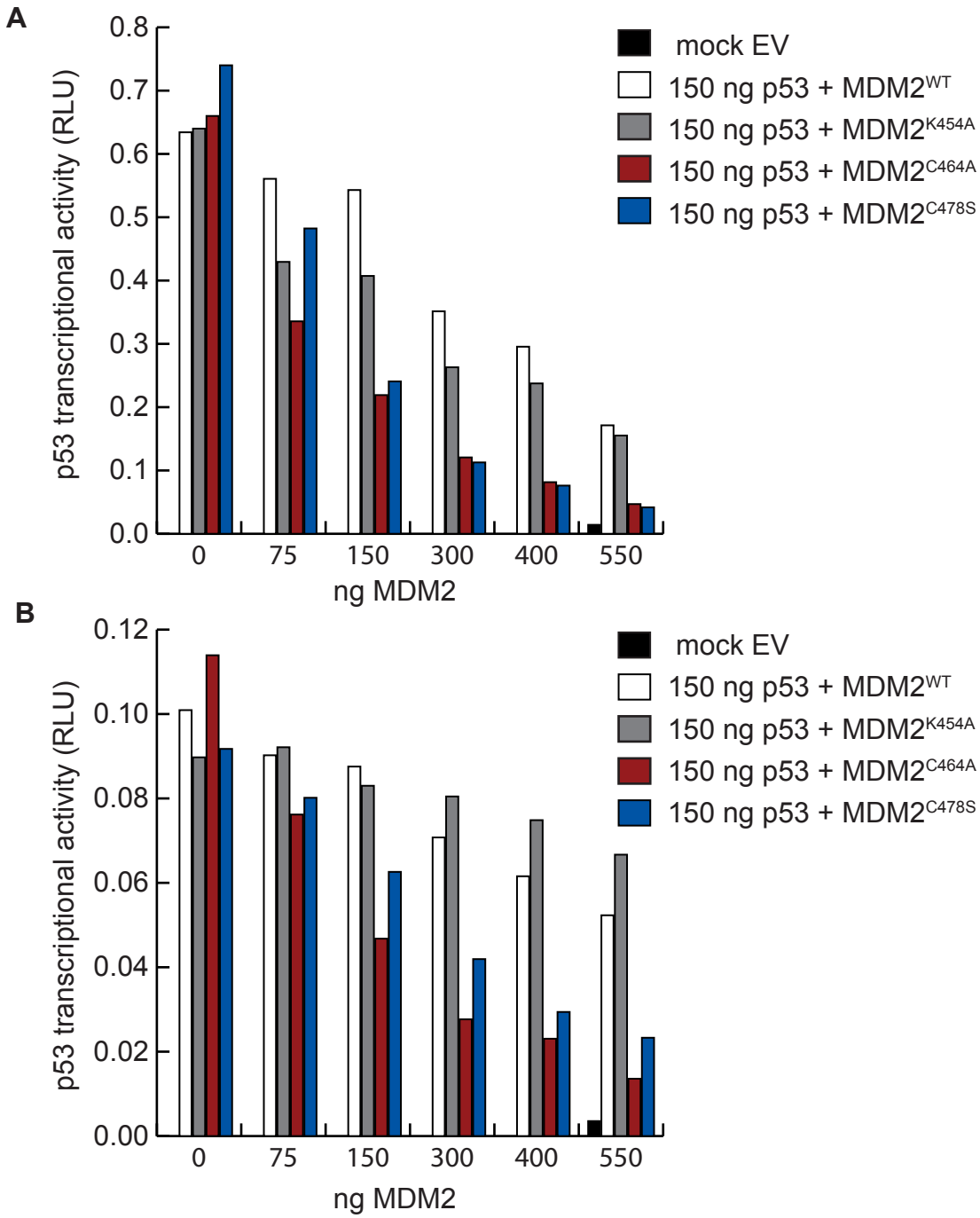

Figure 3.14 Dose dependent MDM2 repression of p53 transcriptional activity

H1299 cell line was transfected with the appropriate amounts of plasmids as indicated on the graphs. Twenty four hours post transfection the Dual Luciferase Assay was performed.
(**A**) MDM2 effect of p53 dependent transcription was performed using the p21::luc construct.
(**B**) MDM2 effect of p53 dependent transcription was performed using the p53 consensus::luc construct. Each of the bars represents a mean from three independent experiments.

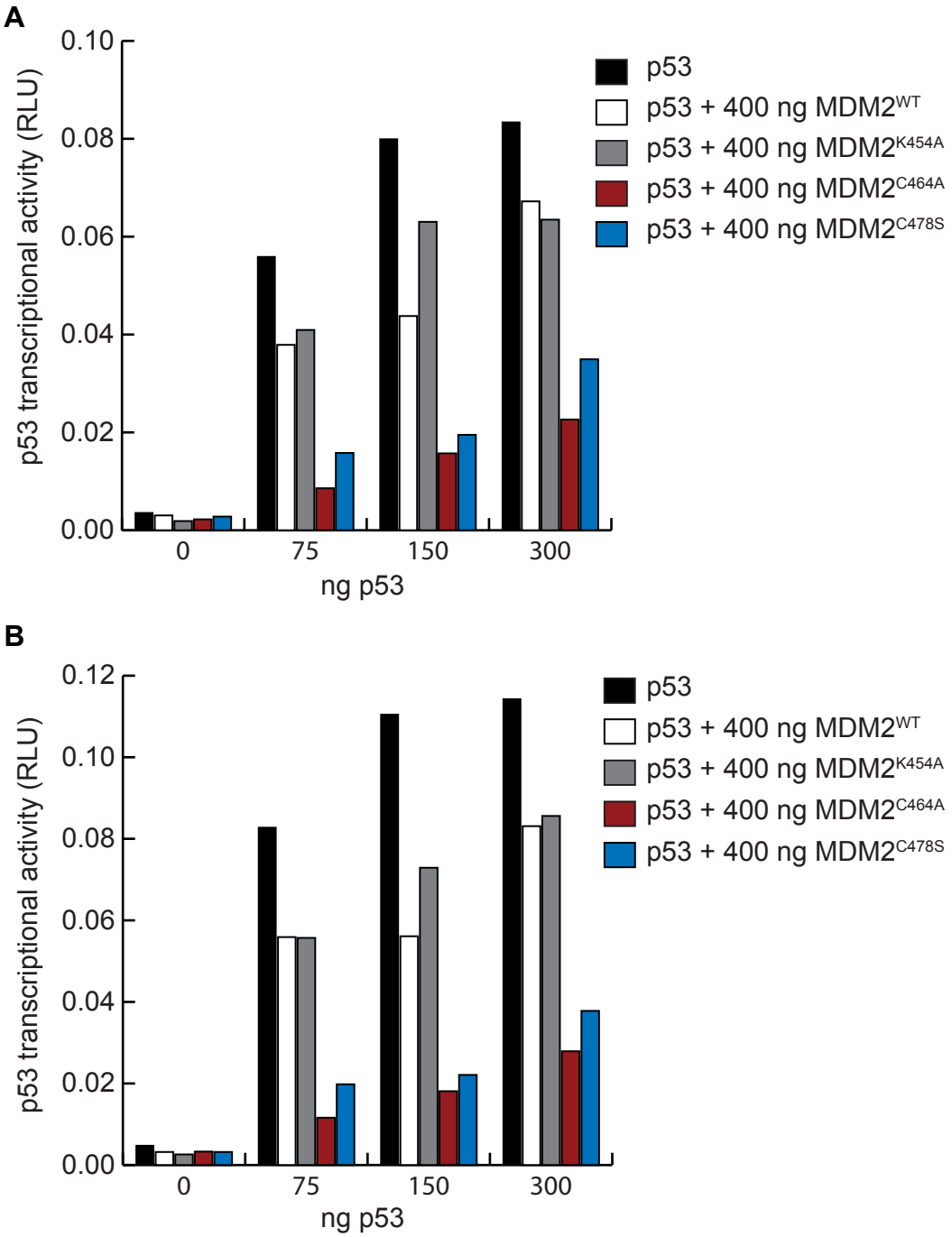

Figure 3.15 Increasing p53 transfection to overcome MDM2 transrepression.

H1299 cell line was transfected with the appropriate amounts of plasmids as indicated on the graphs. This is an inverse experiment to Figure 3.14, where constant levels of appropriate plasmids encoding MDM2 were co-transfected with increasing levels of the p53 encoding plasmid.
Twenty four hours post transfection the Dual Luciferase Assay was performed.
(**A**) MDM2 effect of p53 dependent transcription was performed using the p21::luc construct.
(**B**) MDM2 effect of p53 dependent transcription was performed using the p53 consensus::luc construct. Each of the bars represents a mean from three independent experiments.

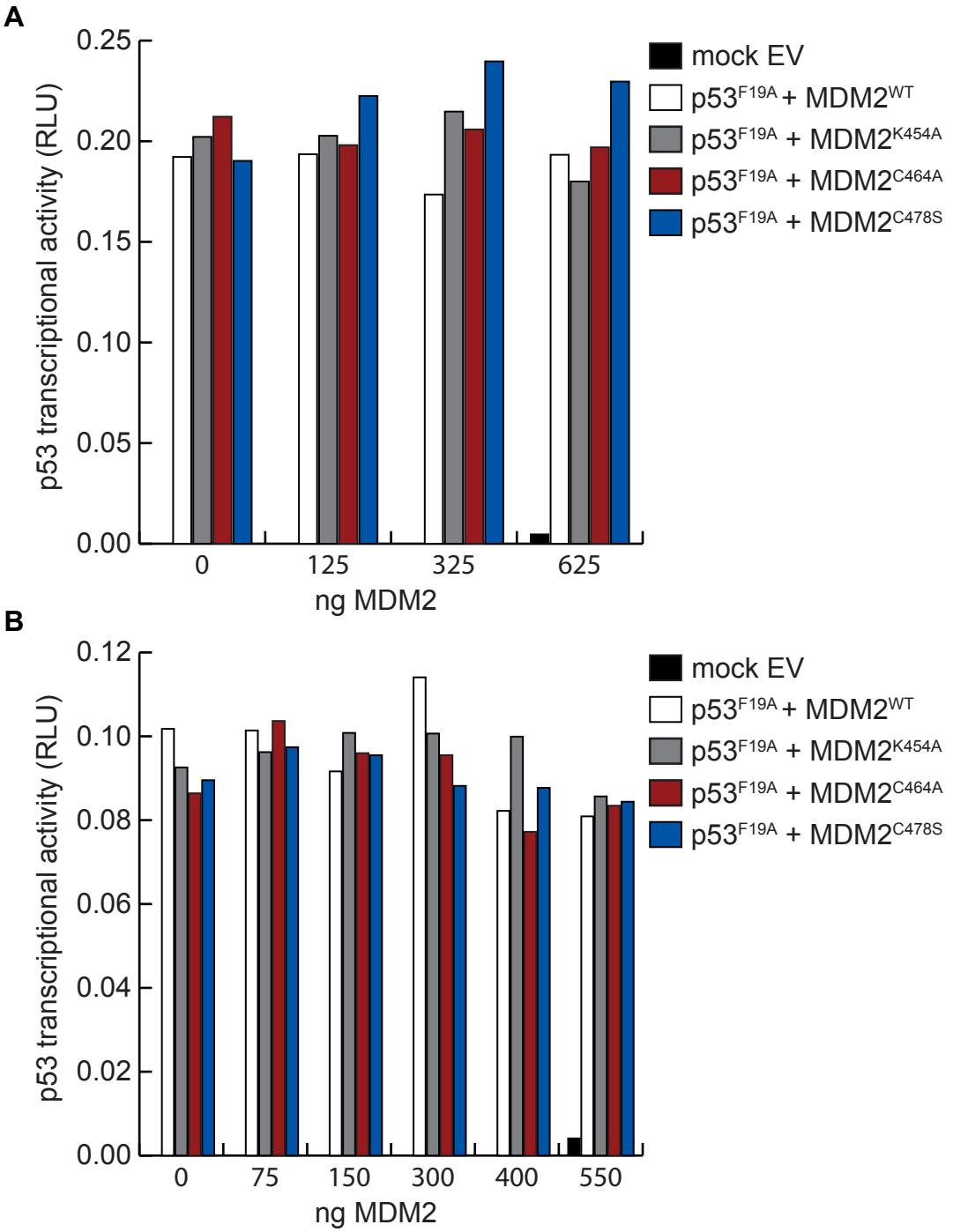

Figure 3.16 MDM2 mediated transrepression on $p53^{F19A}$ transcriptional activity

H1299 cell line was transfected with the appropriate amounts of plasmids as indicated on the graphs.Twenty four hours post transfection the Dual Luciferase Assay was performed. (**A**) MDM2 effect of p53 dependent transcription was performed using the p21::luc construct. (**B**) MDM2 effect of p53 dependent transcription was performed using the p53 consensus::luc construct. Each of the bars represents a mean from three independent experiments.

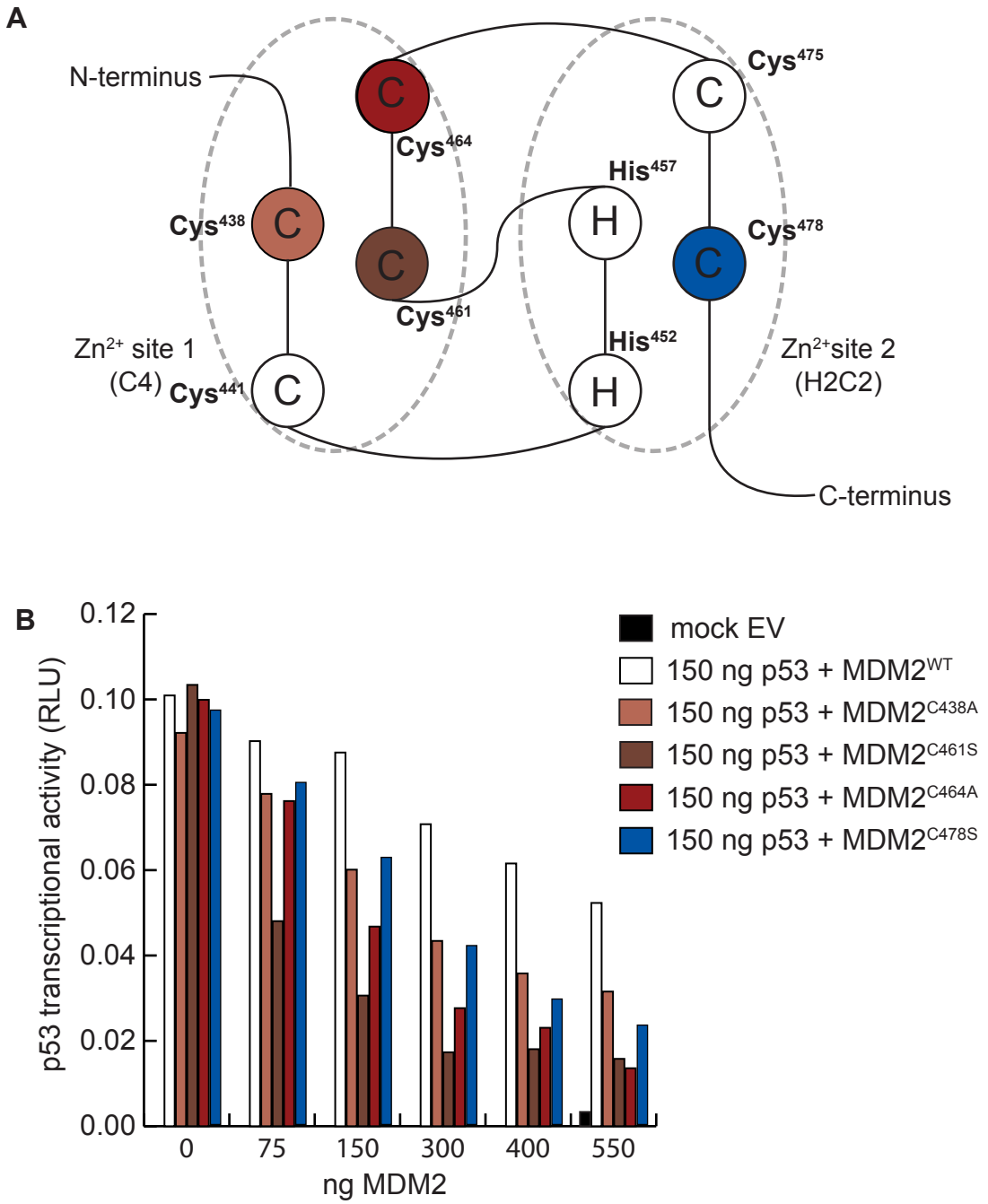

Figure 3.17 Dose dependent MDM2 repression on p53 transcriptional activity

Mutations in other key residues building up the two Zn^{2+} coordination sites within the C2H2C4 RING motif in MDM2, show similar phenotype as the studied $MDM2^{C464A}$, $MDM2^{C478S}$ mutants. (**A**) Zinc coordination scheme of human MDM2 highlighting the cross brace configuration of the amino acids involved in coordinating two zinc ions. The key residues which were mutated are highlighted in colours.
(**B**) MDM2 effect of p53 dependent transcription was performed using the p21::luc construct. H1299 cell line was transfected with the appropriate amounts of plasmids as indicated on the graphs. Twenty four hours post transfection the Dual Luciferase Assay was performed. Each of the bars represents a mean from three independent experiments.

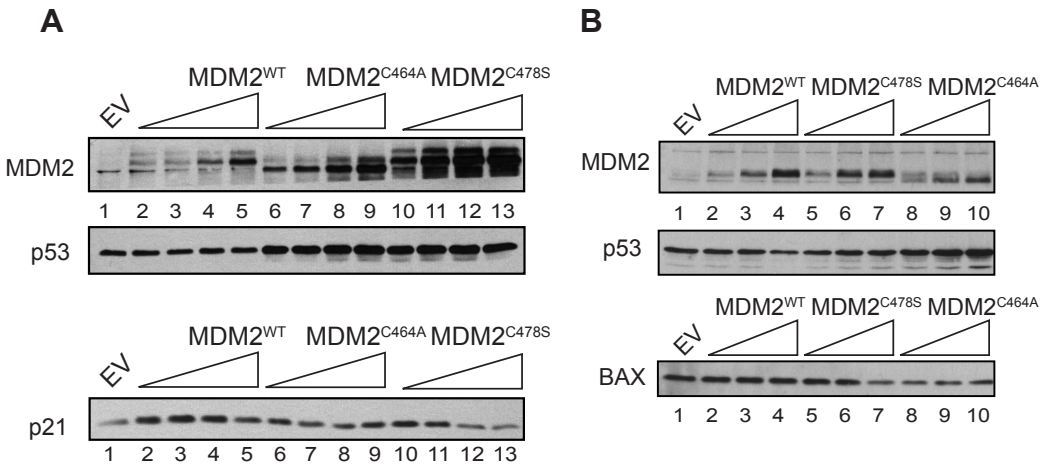

Figure 3.18 MDM2 mediated transreppression on endogenous downstream transcription targets of p53.

MCF7 cell line used in this experiment harbour endogenous WT p53. The cells were only transfected with the plasmids encoding for $MDM2^{WT}$, $MDM2^{C464A}$, $MDM2^{C478S}$, (0-4µg) respectively as depicted above. This was done in order to compare the effect of the mentioned mutants of MDM2 on levels and transcriptional activity of endogenous p53. Total DNA amount was normalized using empty vector control.
(**A**) (**B**) MCF7 cell line was transfected with appropriate amounts of plasmids.Twenty four hours post transfection, cells were lysed and the resulting lysate was analysed by western blotting for the presence of the proteins highlighted above.
Antibodies used for detection MDM2-2A10, p53-DO-1, BAX-mAb anti BAX, p21-Ab1.

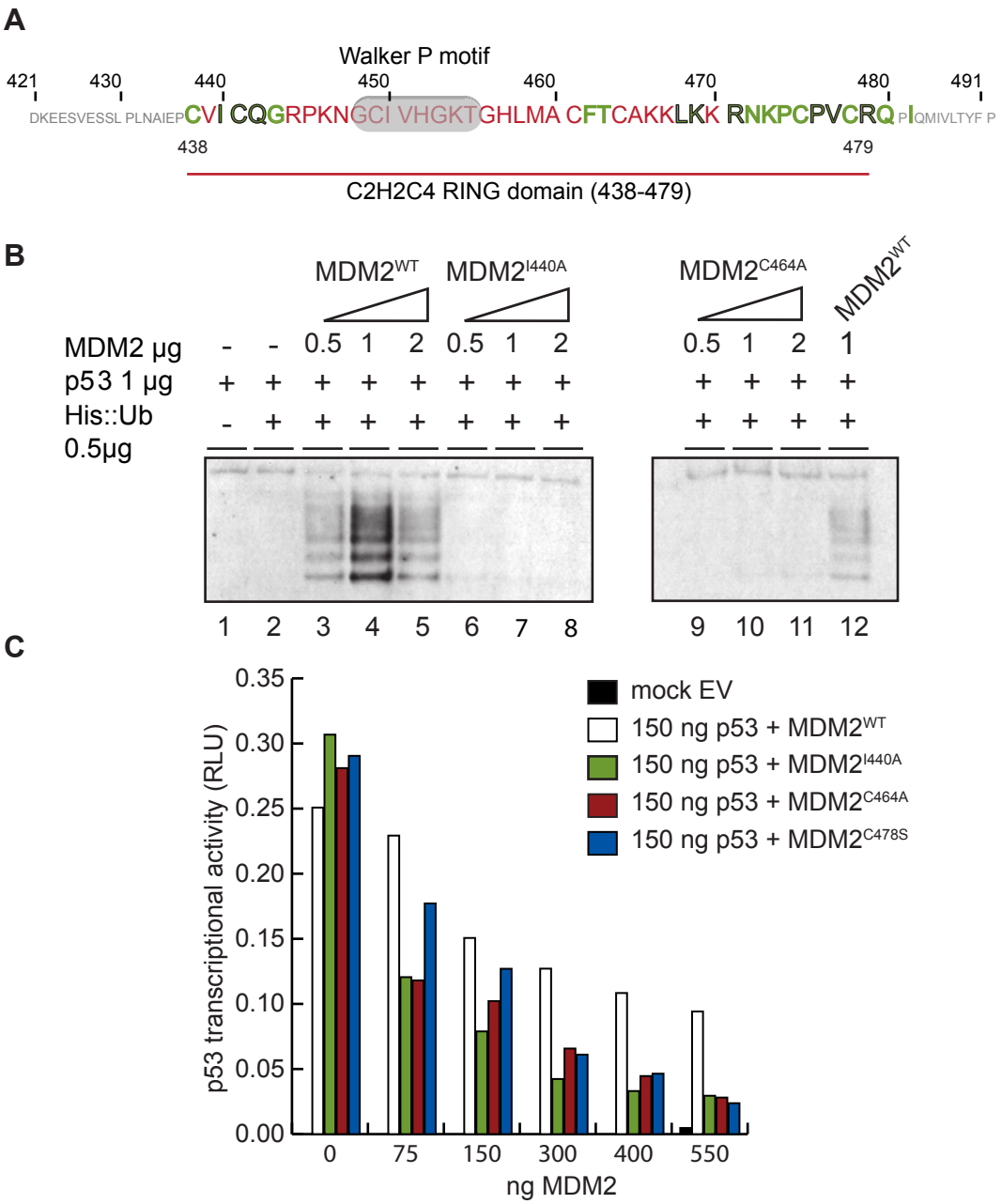

Figure 3.19 Mutation of a key residue required for interaction with E2 conjugating enzyme shows a similar gain of transrepressor function as the MDM2^{C464A}, MDM2^{C478S} mutants.

(**A**) Schematic representation of residues (highlighted in green) within MDM2 predicted to be important for E2 conjugating enzyme UbcH5 family binding (BRCA1/UbcH5c used a modelling template), whereas the residues highlighted in green with dark outline were predicted to be binding based on c-Cbl/UbcH7 used as a template.
(**B**) Cell based ubiquitination assay to check for E3 Ubiquitin ligase activity of the MDM2^{I440}. The cells were transfected with appropriate amounts of plasmids as shown in the figure above. Following lysis and isolation of the His-Ub protein pool, western blot analysis was performed, probed with p53 specific antibody (DO-1).
(**C**) MDM2 effect of p53 dependent transcription was performed using the p21::luc construct. H1299 cell line was transfected with the appropriate amounts of plasmids as indicated on the graphs. Twenty four hours post transfection the Dual Luciferase Assay was performed. Each of the bars represents a mean from three independent experiments.

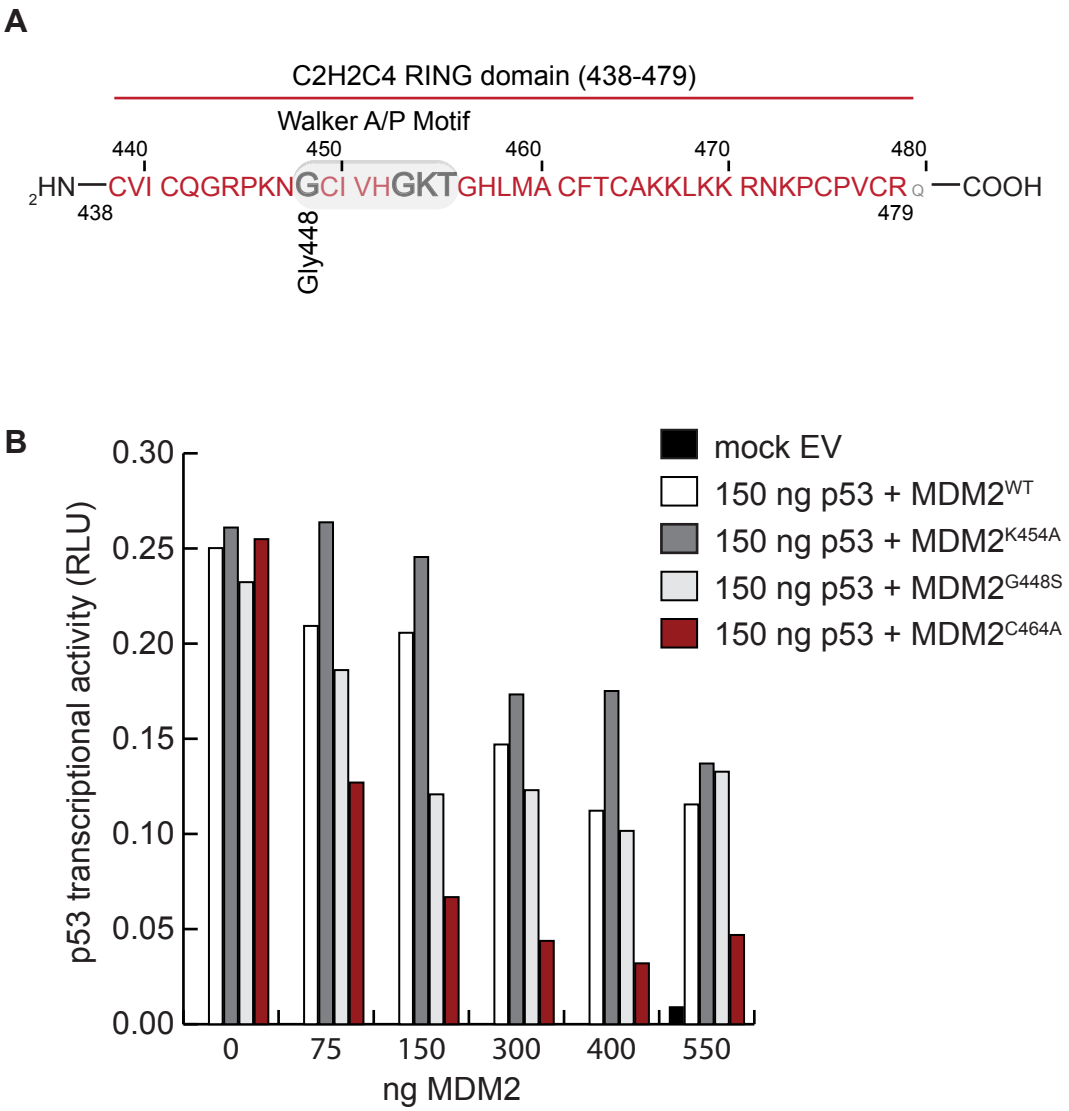

Figure 3.20 The potential of the MDM2^{G448S} mutant in transrepressing p53 mediated transcription.

The G448S point mutation in MDM2 RING finger completely abolishes specific RNA binding by the oncoprotein.
(**A**) Schematic representation of residue (highlighted in black) within MDM2 predicted to be imperative for specific RNA binding.
(**B**) MDM2 effect of p53 dependent transcription was performed using the p21::luc construct. H1299 cell line was transfected with the appropriate amounts of plasmids as indicated on the graphs. Twenty four hours post transfection the Dual Luciferase Assay was performed. For accuracy Each of the bars represents a mean from three independent experiments.

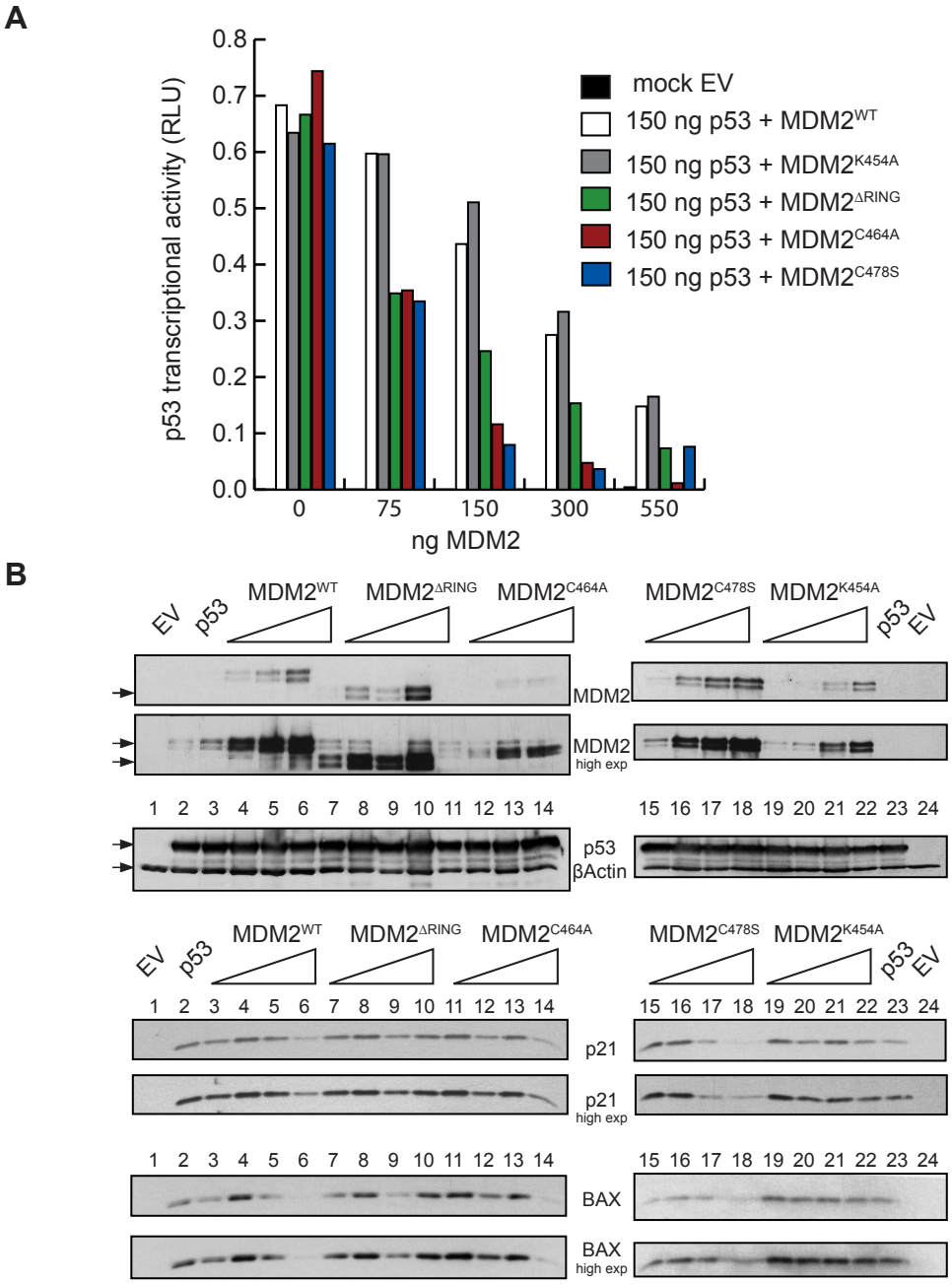

Figure 3.21 The involvement of the C2H2C4 RING in MDM2 mediated transrepression on p53.

Deletion of the RING domain for MDM2 enhances the transrepression potential of the protein.
(**A**) MDM2 effect of p53 dependent transcription was performed using the p21::luc construct. H1299 cell line was transfected with the appropriate amounts of plasmids as indicated on the graphs. Twenty four hours post transfection the Dual Luciferase Assay was performed. Each of the bars represents a mean from three independent experiments.
(**B**) The lysates from the Dual Luciferace Assay were TCA/DOC precipitated and analysed by means of Western blotting in order to assess transfection efficiency and the effect of the transfected MDM2 on downstream endogenous transcription targets of p53.

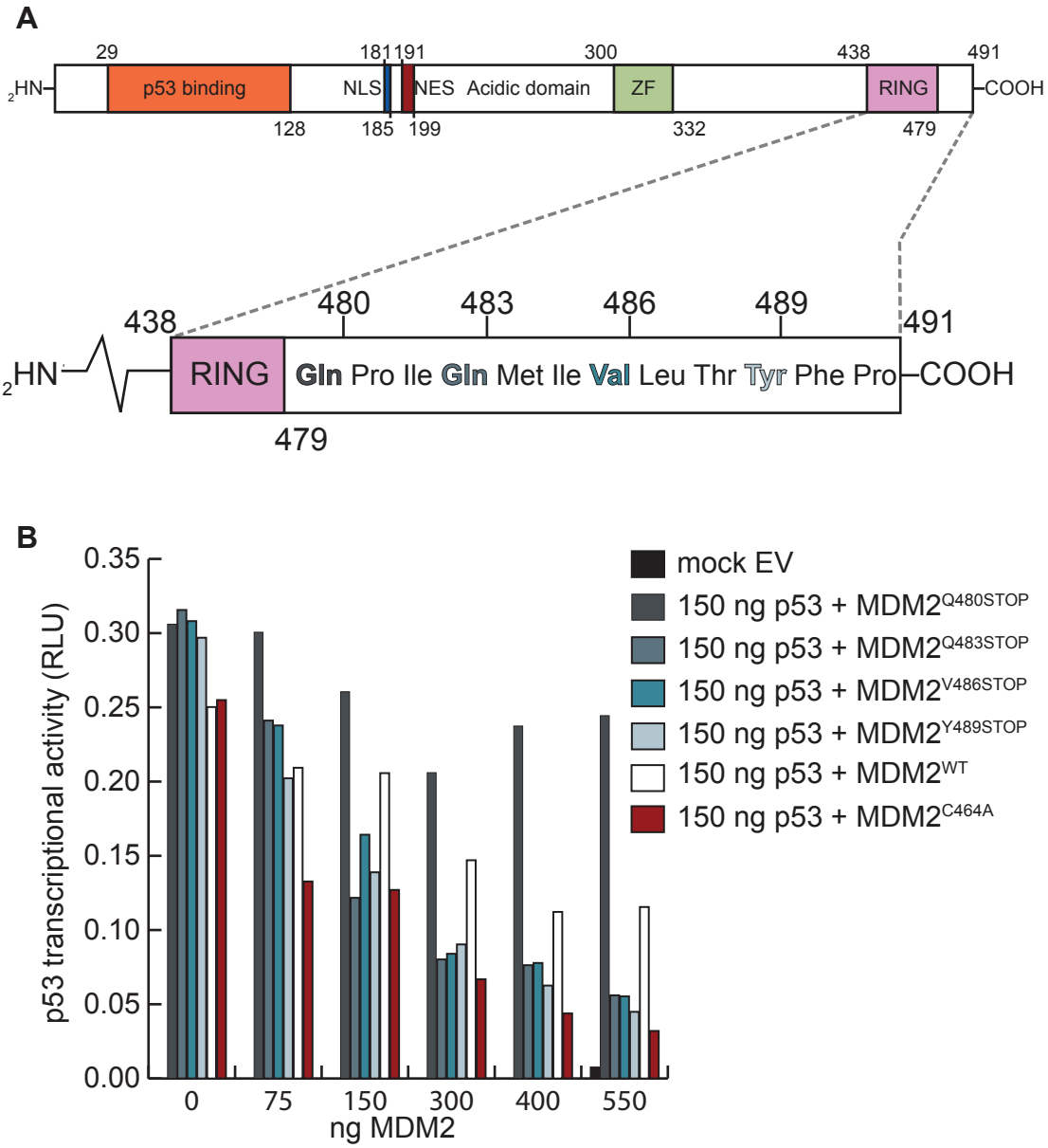

Figure 3.22 The involvement of the last 12 C-terminal aminoacids of MDM2 in transrepression of p53 transcriptional activity.

(**A**) Topological graphic representation of the C-terminus of MDM2. The codons encoding amino acids highlighted in colour were mutated to nonsense mutations, resulting in premature stop in translation, yielding a truncated protein.
(**B**) MDM2 effect of p53 dependent transcription was performed using the p21::luc construct. H1299 cell line was transfected with the appropriate amounts of plasmids as indicated on the graphs. Twenty four hours post transfection the Dual Luciferase Assay was performed. Each of the bars represents a mean from three independent experiments.

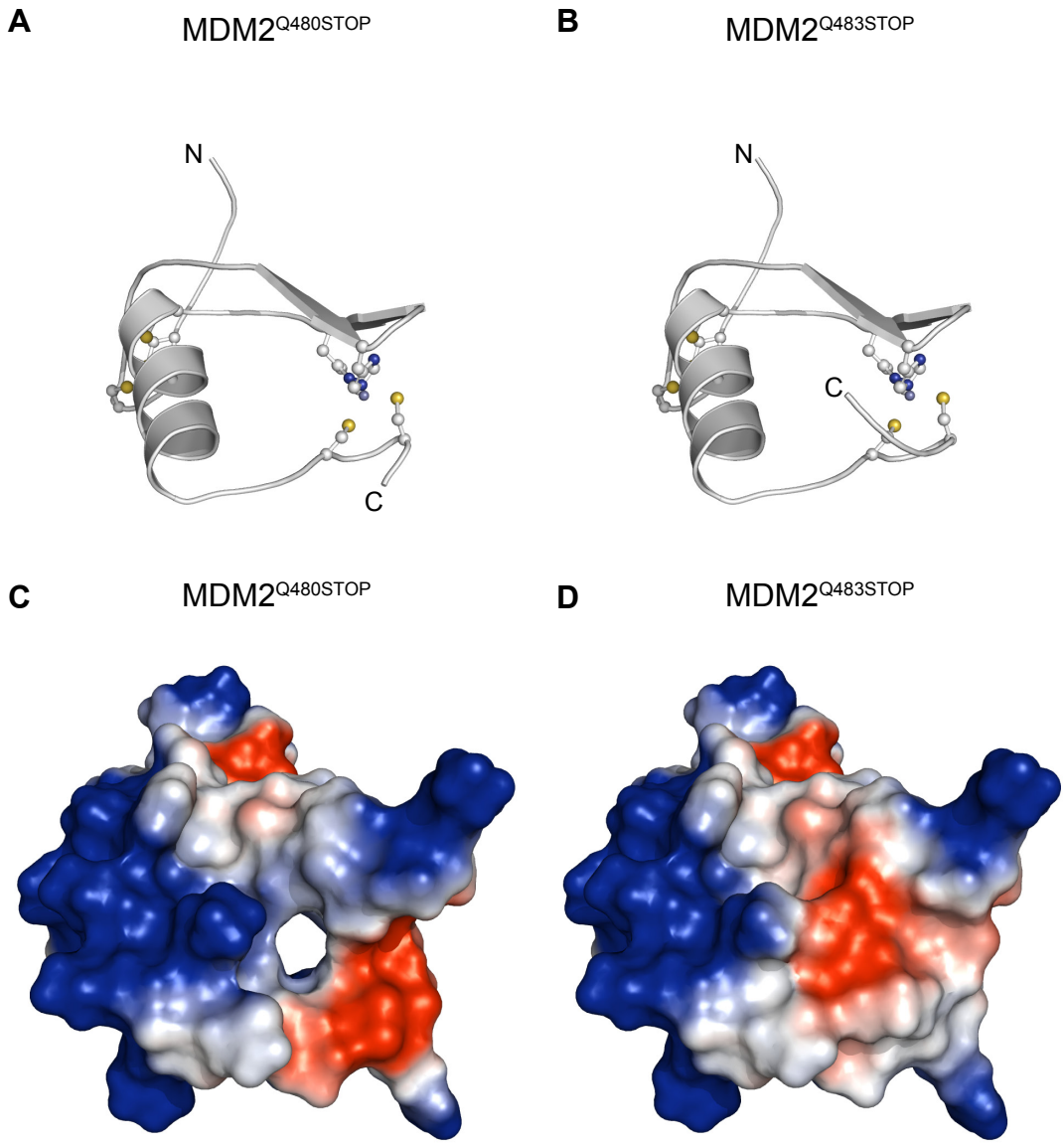

Figure 3.23 Structure comparison of MDM2^{Q480STOP} to MDM2^{Q483STOP}

(**A**) Space fill model of MDM2^{Q480STOP} RING. Carbon atoms building the structure are highlighted in white, oxygen in red, nitrogen in blue and sulphur in yellow.
(**B**) Space fill model of MDM2^{Q483STOP} RING. Carbon atoms building the structure are highlighted in white, oxygen in red, nitrogen in blue and sulphur in yellow.
(**C**) Surface mapped electrostatic potential of MDM2^{Q480STOP} RING monomer. Red and blue regions represent localization of negative and positive charges respectively.
(**D**) Surface mapped electrostatic potential of MDM2^{Q483STOP} RING monomer. Red and blue regions represent localization of negative and positive charges respectively.
Please note, the difference in negative charge localization and cavity formation for the MDM2^{Q480STOP} mutant.

This figure was prepared using PyMOL [http://www.pymol.sourceforge.net/] and structural data from Kostic et al., 2006 andLinke et al., 2008 (file 2HDP,2VJE respectively RCSB PDB).

Chapter 4

RING – dependent allosteric regulation of the MDM2 hydrophobic pocket

Contents

4.1 Molecular basis for p53:MDM2 structure complex formation and inhibition

Gain of transrepressor-function activity driven by key Cys mutations within the C2H2C4 RING domain of MDM2 on p53 observed earlier, shall be further investigated in this chapter. This gain of function of MDM2 to transrepress p53-dependent transcription is seen when Zinc coordinating residues are mutated, whereas mutation of a residue within the RING required for ATP binding has no effect on MDM2 mediated transrepression. To aim at elucidating this phenomenon on the molecular level one must consider the process of MDM2::p53 complex formation.

Protein-protein interactions are ubiquitous in biological systems. They are key in all physiological processes occurring within living organisms such as cell growth, division and differentiation, intracellular signalling and apoptosis (Fotouhi and Graves, 2005; Fry and Vassilev, 2005). Although cell based assays are the standard benchmark for investigating protein-protein interactions and, given an appropriate assay is used, they provide powerful insights into transcriptional, translational, degradation rates and interacting partners of molecules of interest. The cell system may be too robust when considering intricate affinity of the proteins in question, especially when allosteric transition, and conformation modulation occurs upon complex formation. The (classical school of thought) canonical theory regarding protein-protein interactions claims that they occur over a relatively large surface area, on average approximately 800±200Å^2 of protein surface is buried on each side of the interface [for full review see (Lo Conte et al., 1999)]. Nevertheless, further studies have shown that the surface contact area can be divided into subsets, which contribute to high-affinity binding, also known as the "hot spot" (Clackson and Wells, 1995). Such hot spots of binding free energy are a common feature of protein complexes. Residues building these subsets are clustered together and are surrounded by energetically minor residues that serve to occlude bulk solvent (Bogan and Thorn, 1998). Several studies have reported phage-display selection of small peptides that bind to protein hormones or receptors (DeLano et al., 2000; Sidhu et al., 2003).

Interestingly these randomly selected peptides bind at protein hot-spots, even though they were not selected for protein-protein inhibition. This suggests that protein hot-spots located at the protein-complex interface appear to be preferred owing to their intrinsic conformational and chemical properties. Thus, in many cases protein-protein recognition sites may be concentrated in a few key anchor residues bearing a characteristic conformational state. Basing on this, a concept of "protein-surface mimetics" was proposed describing the compounds (peptide analogs as well as other small molecules) that retain the essential functionalities and a particular three-dimensional arrangement complimentary to the protein surface.

Considering the MDM2::p53 complex a wealth of biochemical (Bottger et al., 1997a), crystallographic (Kussie et al., 1996a) and genetic (Oliner et al., 1993) studies have provided extensive information on the primary interaction site of the two proteins in question. The secondary interaction site though discovered almost ten years later (Shimizu et al., 2002; Yu et al., 2006) is increasingly studied on as a determinant of MDM2 mediated p53 ubiquitination (Kawai et al., 2003; Wallace et al., 2006).

The primary interaction site has been mapped to the N-terminus of p53 tumour suppressor. One region within the transactivation domain is highly conserved among diverse mammalian species (Liu et al., 2001). This region termed BOX-I (Figure 4.1 Panel B), spans residues 13 to 26 of the polypeptide chain of p53. Interestingly this region is also conserved in two other p53 paralogues, p63 and p73 (Kaghad et al., 1997; Yang et al., 1998). Several amino acid residues within the BOX-I region are essential for the interaction of p53 with MDM2. These key residues are Phe^{19}, Trp^{23}, Leu^{26} (Figure 4.1 Panel B marked in red). The resolution of the X-ray structure of the MDM2 region bound to BOX-I region of p53 (Kussie et al., 1996b) (Figure 4.2 Panel B) revealed key features about the nature of interaction between these two proteins. The primary p53-binding region of MDM2 is roughly 25 Å long and 10 Å wide and is constituted by two pairs of α-helices, related by an approximate dyad axis of symmetry. The two repeats come together via their hydrophobic faces forming a profound groove or cleft at their interface. This deep hydrophobic cavity is the primary site within MDM2 where p53 binds. The stabilization of the MDM2-p53

complex is mainly produced by anchoring of two aromatic residues and one aliphatic of p53 (Phe^{19}, Trp^{23}, Leu^{26}) to this hydrophobic cleft. Thus, the interface relies on the steric complementarity between the MDM2 cleft and the hydrophobic face of the p53 region and the p53-MDM2 binding apparently involves only weak interactions that rely mostly on hydrophobicity. Interestingly the BOX-I peptide of p53, representing the primary interaction site to MDM2, on its own is unstructured in solution, according to NMR data (Botuyan et al., 1997; Dawson et al., 2003; Lee et al., 2000) and it adopts an amphipathic α-helical conformation as it comes in contact with the N-terminus of MDM2 (Figure 4.2 Panel B).

The secondary interaction site that is contiguous with the S9-S10 linker motif located within the DNA binding region (BOX-V) (Figure 4.1 Panel B) of p53 interacts with the acid domain of MDM2. It was initially discovered by phage peptide display and characterized (Shimizu et al., 2002; Yu et al., 2006). Despite the fact that binding of the BOX-V region of p53 to the acid domain of MDM2 has a low affinity, it is key in determining the rate of p53 ubiquitination as it comprises part of the p53 ubiquitination signal (Wallace et al., 2006).

MDM2 is unable to downregulate p53 if prevented from interacting with it (Vassilev, 2007). Therefore, inhibition of MDM2-p53 complex formation is a very desirable strategy for p53 activation and stabilization. As stated before, the p53-MDM2 primary interaction site is limited to a few amino acid residues critical for successful interaction of the two proteins. This small number of hydrophobic groups buried in a deep cleft represents a relatively good example of protein-protein interactions that is a prime candidate for inhibition by small, drug-like ligands (Uhrinova et al., 2005). It is beyond the scope of this chapter to fully elucidate on the numerous groups (Details of which are provided in the Introduction chapter of this thesis) of competitive inhibitors of p53-MDM2 complex formation, thus focus will be drawn to one inhibitor used extensively in this chapter as a tool, namely Nutlin-3 (Figure 4.2 Panel A). Nutlins (a series of cis-imidazoline analogues) were discovered by means of high throughput screening of a diverse set of chemical compounds that could inhibit p53-MDM2 binding (Vassilev et al., 2004). The inhibitory potential of these compounds is due to structural mimic of the three key amino acids of p53 BOX-I

region. The imidazoline scaffold of Nutlin-3 replaces the helical backbone of the BOX-I peptide and is able to direct in a fairly rigid fashion (Figure 4.2 Panel C) the projection of three groups into the pockets within MDM2 normally occupied by Phe^{19}, Trp^{23}, and Leu^{26} of p53. The two haloaryl groups (chlorophenyl groups for Nutlin-3) overlap the position of Leu^{26} and Trp^{23}, and the position of Phe^{19} is filled by the iso-propoxy group (Figure 4.2 panel C-F). Nutlins have demonstrated activity against p53-MDM2 complex formation with the median inhibitory concentration (IC_{50}) in the range of 100-300 nM. Remarkably, a 150-200 fold difference in inhibitory potential was observed between enantiomers of Nutlin-3 (Vassilev et al., 2004). Due to their chemical nature, Nutlins were found to have good cell permeability, leading to activation of p53 target genes in cell based assays (Tovar et al., 2006). In *vivo* experiments with SJSA-1 osteosarcoma xenografts in nude mice showed that Nutlin-3 was orally bioavailable, achieving steady-state plasma levels of 3.5 μM following 200 mg/kg bid dosing regimen and leading to 90% inhibition of tumour growth. The compound was well tolerated during a 20-day study at this dose. In line with this, Nultin-3 was found to stabilize p53 and induce cell cycle arrest and apoptosis in Hodgkin lymphoma (Drakos et al., 2007). These studies provided the first *in vivo* proof-of concept that activation of wild-type p53 by pharmalogical inhibitors of the p53-MDM2 interaction is feasible and might be exploited for cancer therapy (Vassilev,2007).

4.2 Experimental results

4.2.1 The MDM2 hydrophobic pocket but not the acid domain is required for efficient transrepression of p53

As discussed in the introduction to this chapter, in order for p53 to be regulated by MDM2, the latter must bind to the tumour suppressor. Previous studies have suggested that the hydrophobic pocket of MDM2 is critical for its transrepressor activity (Lin et al., 1994; Liu et al., 2001) however these studies were carried out before the complexity of the interaction between MDM2 and p53 was fully illuminated. As the acid domain of MDM2 is now known to bind to the BOX-V domain of p53 (Wallace et al., 2006; Yu et al., 2006) constituting a secondary interaction site of the complex, MDM2 deletion mutants were used to determine which interactions were salient for MDM2 mediated transrepression. To investigate the influence of MDM2 domain structure on p53 transrepression, two discrete domain deletion mutants of MDM2 were used, where one or other of the two known p53 interacting domains had been deleted (Figure 4.3 Panel A; $MDM2^{\Delta N}$ and $MDM2^{\Delta Ac}$). $MDM2^{\Delta N}$ prevents the interaction between the transactivation domain of p53 (BOX-I) and the hydrophobic pocket in the N-terminus of MDM2 (Kussie et al., 1996b) whereas the $MDM2^{\Delta Ac}$ precludes binding of the core domain of p53 (BOX-V) and the acid domain of MDM2 that is essential for MDM2 mediated ubiquitination of p53 (Wallace et al., 2006).

When the deletion mutants were analysed in the p53-reporter assay (Figure 4.3 panel B) loss of the hydrophobic pocket essentially inactivated MDM2 as a transrepressor of p53-mediated transcription, whereas deletion of the acid domain did not have a major impact on this activity of MDM2. This data suggest that the interaction between the acid domain of MDM2 and the BOX-V region of the p53 core domain is subsidiary for MDM2 mediated transrepression, whereas binding of the hydrophobic pocket to the BOX-I transactivation domain of p53 is absolutely required, as the ΔN mutant is essentially dead in this assay.

Together with the results presented in the previous chapter one can draw a conclusion that the RING domain mutants that lose the ability to ubiquitinate p53 but gain p53 repressor activity do so, most likely, through modulation of the MDM2-hydrophobic pocket: p53-BOX-I interaction.

4.2.2 Isolation of human recombinant MDM2

The cell based experiments described in Chapter 3 and above show that; the C2H2C4 RING mutants have a gain of transrepressor activity, and that the hydrophobic pocket, but not the acid domain, is essential for MDM2 repressor activity respectively. These results suggested that the affinity of the hydrophobic pocket for the BOX-I domain of p53 might be sufficient to dictate the potency of MDM2 as a transrepressor and may also determine the efficacy of hydrophobic pocket binding drugs such as Nutlin-3.

In order to confirm this hypothesis an *in vitro* approach was taken up to further study the association of full length p53 with full length MDM2 and a lateral investigation of p53 peptide aptamer interactions with MDM2 was carried out.

For this approach to be fruitful, one requires for the two proteins in question to be purified to high homogeneity. Human recombinant p53 tumour suppressor protein was isolated from a prokaryotic expression system and provided, as a kind gift to the author, by Prof. Alicja Zylicz at the International Institute of Molecular and Cell Biology in Warsaw, Poland, with whom close collaboration is being upheld.

The MDM2 oncoprotein although extensively studied due to its prominent negative regulator of p53 status (at the time of writing this thesis over 3500 publications recorded at NCBI http://www.pubmed.gov) the data regarding the biochemical nature of the full length protein is quite limited.

Due to the extensively time consuming task of producing an optimized, reproducible MDM2 isolation protocol, which in the end provided satisfactory amounts of the protein, a brief description of the method shall be provided in this result chapter.

Human recombinant MDM2 protein and all the described mutant forms were isolated from a prokaryotic expression system using the following method (Figure 4.4).

Plasmid encoding human MDM2 cDNA (Midgley et al., 2000) was introduced into *E.coli* BL21 (DE3) RiL strain. In must be stressed that the open reading frame of the *mdm2* gene introduced to the vector did not contain any regions encoding for C, or N-terminal tags, which could partially simplify the isolation procedure though at the end could prove artifactual as the intention is to study the full-length species with its N-terminus and the C-terminus in native surroundings. An overnight culture with antibiotic selection was diluted to a final volume of 10 litres. At the moment when the suspension reached $OD_{\lambda=600nm}$ - 0,4, the temperature that the culture was kept at was decreased from 30 °C to 18°C and induction followed with IPTG added at final concentration of 0.5 mM. After 3 hours post induction the bacterial pellet was collected be means of centrifugation. Delicate lysozyme/detergent lysis was performed on the pellet followed by brief heat shock and genomic DNA shattering. Centrifugation of the solution followed. Under these conditions a bulk of the desired protein was insoluble and localized within the pellet fraction, which falls in line with previously published procedures (Midgley et al., 2000). Delicate extraction with the use of an ionic detergent and high salt concentration carried out overnight with constant rotation proved fruitful in transferring a large portion of the MDM2 protein to soluble state. This fraction was shortly dialysed to reduce detergent concentration, yet retaining high anti-chaotropic salt concentration. After dialysis the sample was loaded onto a hydrophobic interaction chromatography (HIC) adsorbent. Protein binding to HIC adsorbents is promoted by moderately high concentrations of anti-chaotropic salts, which also have a stabilizing influence on protein structure. Elution was achieved by a linear decrease in the concentration of salt in the adsorption buffer. The collected fractions containing MDM2 protein were pooled and loaded onto anion exchange chromatography adsorbent, the proteins passive to this adsorbent including MDM2 passed directly into the flow through and were immediately loaded onto a cation exchange chromatography adsorbent. Fractions containing MDM2 were eluted from the adsorbent collected by means of increasing ionic strength. The identical procedure, including same competent bacterial strain batch and adsorbents was used in order to isolate the Cys^{464}, Cys^{478} and Lys^{454} MDM2 mutants. Alongside the mentioned mutations several others were introduced

into the human MDM2 ORF and the resulting mutant proteins were isolated, though shown (Figure 4.5 panel A) it is beyond the scope of this chapter to describe them in more detail.

Human $MDM2^{WT}$, $MDM2^{K454A}$, $MDM2^{C464A}$, and $MDM2^{478S}$ are presented in the first four lanes from the left on a Coomasie Blue stained gel (Figure 4.4 Panel A). Despite the apparent difference in concentration and thus purity the main band for all the MDM2 protein species migrates in a denaturating gel at a molecular mass representative of 90-100 kDa protein. This does seem controversial as the predicted molecular mass for human MDM2 is 55 kDa, similar results strengthened with immunoblotting were reported and discussed (Shimizu et al., 2002) indicating that despite denaturating conditions the MDM2 moiety may adopt a higher quatenerary structure. This indeed was investigated in the following chapter and shall be discussed in more detail there. As, despite all efforts, the isolated MDM2 proteins were heterogenic in purity. The protein concentrations were normalised and the quantitation was confirmed using an Enzyme Linked Immunosorbent Assay (ELISA) assay (Figure 4.5 Panel B). This simple procedure utilizing specific antigen (in this case MDM2 protein) antibody recognition is more advantageous than classical Bradford based concentration assay, as it confirms that the purified species is in fact MDM2 and the concentration values of the proteins tested is more accurate as the background is non reactive with the antibody.

4.2.3 Initial characterization of the isolated MDM2

In order for the isolated MDM2 species to be of any use in further experiments, one must show that they retain specific activity *in vitro.* As MDM2 is the main antagonist of p53 and a clear physical interaction of these two proteins occurs, this property should be verified initially.

A quick and efficient method at investigating protein-protein interactions is a modified version of the Enzyme Linked Immunosorbent Assay. The noteworthy features of this method are that the relatively small amounts of biological material (10-150 ng) used, produce reproducible and statistically significant results.

The results showing specific binding of MDM2 to p53 and vice versa are presented in Figure 4.6 indicating a specific, dose-dependant complex formation. In this case a two-site (two-stage) capture ELISA was performed. This variation of the method relies on the fact that a specific antibody can be attached to microtiter wells (for Panel A anti p53 DO-1 antibody was attached, Panel B anti MDM2 2A10 antibody was attached) and serve a ligand specific anchor, binding the epitope, in this case the desired protein. Thus either a fixed amount of p53 (Figure 4.6 Panel A) or MDM2 (Panel B) is exposed to the reaction buffer containing increasing amounts the complementary binding partner. For both of the presented Panels in Figure 4.6, Albumin isolated from Bovine Serum was used as the inert, non-specific binding partner.

The C-terminal RING domain of MDM2 ensues the protein to posses at least two distinguishable properties. The Walker P motif situated within the RING is the site of nucleotide binding (ATP preferentially) by the protein, additionally 8 other amino acids, 6 cysteines and 4 histidines provide a scaffold for zinc binding resulting in E3-ubiquitin ligase activity of the MDM2. As presented in Chapter 3 these two properties by means of single amino acid substitutions can be abolished independently. Thus it is vital to verify if this is the case for the purified proteins. The Lys^{454} mutation to Ala in MDM2 was reported (Poyurovsky et al., 2003) to successfully lower the affinity for ATP. It must be noted that these results were obtained by investigating the GST-RING domain purified on its own and no data was established for the whole protein. Figure 4.7 represents data showing ATP binding preference for $MDM2^{WT}$, $MDM2^{K454A}$, $MDM2^{C464A}$, $MDM2^{C478S}$ proteins. In this experiment α-^{32}P ATP was used in order to rule out the possibility that binding reflected activity of a contaminating prokaryotic kinase. Two methods were used to assay for ATP binding by MDM2 (Figure 4.7). One relies on the fact that nucleotides that interact with the protein can be crosslinked to the later by means of UV pulse λ=254 nm (310 $\mu W/cm^2$). These complexes were precipitated from solution by means of TCA/DOC, extensively washed and resolved via SDS-PAGE (Figure 4.7 Panel A). The second method exploits the binding properties of proteins to nitrocellulose, whereas unbound nucleotide molecules pass freely through the pores,

bound ones are retained with the protein at the surface of the filter/membrane. Thus, the amount of radiolabelled ATP bound to protein can be assayed quantitavely with a scintillation counter (Figure 4.7 Panel B). The normalized values of ATP bound to MDM2 clearly indicate at least a 2-fold decrease in binding for the Lys^{454} mutant in comparison to its wt counterpart. Moreover mutations within the key Cys residues have no inhibitory effect on nucleotide association; in fact the $MDM2^{C478S}$ shows a slight increase in affinity for the nucleotide in comparison to the wt form. This result demonstrates the requirement of an intact P Walker motif for optimal nucleotide binding and strongly supports the notion that the two mentioned activities within the RING can be uncoupled.

Next a purified assay system (Wallace et al., 2006) was used to check for the E3 ubiquitin ligase activity of the purified MDM2 proteins. The reaction mixture consisted of human E1 ubiquitin activating enzyme, E2 ubiquitin conjugating enzyme, free ubiquitin and a target protein – human recombinant p53. The presence of the nucleotide in this mixture is required for E1 activity as ubiquitin conjugation is an energy dependant process. The only variable for the reactions presented in Figure 4.8 was the absence or presence (in an increasing manner) of $MDM2^{WT}$ and the 3 investigated mutants. The results concur with the data presented in Chapter 3 (cell based ubiquitination assay done in MEFs) where the wt protein and the ATP mutant ($MDM2^{K454A}$) are active in acting as an E3-ligase for p53 and neither the Cys^{464A} nor the Cys^{478S} mutant were able to mediate ubiquitination of p53 (Figure 4.8 Panel B). In this case a non crucial mutation Lys^{4545A} in regards to zinc coordination did not manifest its handicap in the above assay. Thus basing the above results combined with complimentary data from Chapter 3 one can postulate that the lack/decrease of ATP binding by MDM2 is not directly involved in modulating its ubiquitin ligase activity. Moreover, the $MDM2^{K4545A}$ mutant when compared to its wt counterpart when added to the reaction mixture at the lowest amount, exhibits better potential to attach ubiquitin adducts to p53. This observation is supported by (Poyurovsky et al., 2003) where on a per mole basis the analogous mutant displayed significantly greater ability to ubiquitinate p53 (approximately 3-fold more) than did wild-type MDM2. Additionally the degree of repressing p53 transcriptional activity of the Lys^{4545A}

mutants was comparable to the wild-type protein, which is also coherent with the observations in cell based assays presented in Chapter 3.

4.2.4 MDM2 Cys RING finger mutant proteins bind with a higher affinity to the transactivation domain of p53

The mutations within the P Walker motif of MDM2 hinder its ATP binding potential yet do not display any decrease in ubiquitin ligase activity, moreover they do not modulate the ability of MDM2 to interact with p53 as shown by (Wawrzynow et al., 2007a) and (Poyurovsky et al., 2003). The ability of the remaining mutant proteins ($MDM2^{C464A}$ and $MDM2^{C478S}$) to bind to full-length purified p53 was determined (Figure 4.9). In this assay a constant amount of full-length untagged p53, purified form *E.coli*, was captured onto microtiter wells and incubated with a titration of wt or mutant MDM2 protein. Following extensive washing bound MDM2 was detected using a monoclonal antibody (2A10). This showed that both of the MDM2 C2H2C4 mutant proteins bound with a higher affinity to full-length p53 than did wt MDM2, however, consistent with its lower $I_{0.5}$ in the transrepressor assays (Chapter 3), the Cys^{464A} mutant bound better to p53 than the Cys^{478S} mutant protein.

Although the interaction between the acid domain of MDM2 and the BOX-V domain of p53 is not essential for MDM2 mediated transrepression (Figure 4.3) it is likely to play a role in binding of MDM2 to full-length p53 protein (Wallace et al., 2006) Binding to the isolated BOX-I domain was therefore investigated to determine whether the increase in affinity of the Cys^{464A} and Cys^{478S} mutants for full-length p53 reflected a change in affinity for the p53 BOX-I domain. Binding of wt and the C2H2C4 mutant MDM2 proteins to a peptide based on the BOX-I domain of p53, or to an optimised hydrophobic pocket binding peptide, 12.1 (Bottger et al., 1996), was determined (Figure 4.10 Panel A and B). Biotinylated BOX-I domain or 12.1 peptide were immobilised on streptavidin coated wells and incubated with a titration of wt MDM2 or the two C2H2C4 mutant proteins. Consistent with the data presented, above showing that the mutants bind better to full-length p53, both the Cys^{464A} and Cys^{478S} proteins bound with a higher affinity to BOX-I and 12.1 than wt

MDM2 protein. Mirroring its decreased $I_{0.5}$ for transrepression seen in Chapter 3 and increased affinity for full-length p53 the Cys^{464A} mutant consistently bound better to BOX-I or the BOX-I mimetic than the Cys^{478} mutant protein (Figure 4.10 A, B). Of note is the fact that the BOX-I mimetic the 12.1 peptide, shows 2-fold increase in affinity towards MDM2 than its protoplast.

The data presented in Figure 4.10 Panel A, B suggests that the increased transrepressor activity of the MDM2 C2H2C4 RING mutants is dictated by an increase in the affinity of their hydrophobic pockets for the BOX-I transactivation domain of p53. Nevertheless, the data presented in the following Panels (C and D) of the Figure 4.10 indicate that the two Cys mutants of MDM2 further show a dramatic increase in affinity towards the secondary interaction site between MDM2 and p53. Biotinylated BOX-V domain peptide (representative of the secondary interaction site within p53) or Rb-1 [a fragment located within the C-terminus of the Rb protein, shown to interact and inhibit E3 ubiquitin ligase activity of MDM2 (Wallace et al., 2006)] peptide were immobilised on streptavidin coated wells and incubated with a titration of wt MDM2 or the two C2H2C4 mutant proteins. It must be stressed that the interaction between MDM2 and p53 is a multi step process, and the resulting complex is not simply a result of additive interactions of MDM2 towards the BOX-I and BOX-V domain. Exposure of the secondary interaction site (BOX-V within p53) is dependent on the initial binding of BOX-I of p53 by MDM2. A conformational change follows within both of the proteins (Schon et al., 2002; Schon et al., 2004; Wallace et al., 2006) yielding an exposed BOX-V region. Although this exposed fragment of the p53 protein has a much lower affinity towards MDM2 (Figure 4.10 Panel C, D) it is crucial for efficient ubiquitination of p53 by the oncoprotein studied. Considering this, one can hypothesize that the discussed Cys mutations within the RING may have a long range effect on the global conformation of the protein. This can be achieved through two possible mechanisms. Firstly, the increased affinity towards the BOX-I peptide by the Cys^{464} and Cys^{478} indicates a gain in conformational affinity of their hydrophobic cavity towards p53, this more efficient binding may allosterically induce both of the proteins in question to interact better through the secondary interaction site. Moreover, the specific Cys mutations within

the RING of MDM2 may 'transmit' their effect on the hydrophobic pocket *in cis* through the central region of MDM2 encompassing the acid domain which forms the molecular basis within MDM2 for interacting with p53 (Shimizu et al., 2002). Deciphering between these two exciting possibilities shall be further solely investigated in the following chapter of this thesis.

4.2.5 The MDM2 RING mutant proteins differ in their sensitivity to the hydrophobic pocket binding drug, Nutlin-3

The atomic level of understanding of MDM2-p53 interaction through X-ray crystallography (Kussie et al., 1996b) provided strong information for structure mimic design of small-molecule antagonists of this interaction (Fry et al., 2005), such as Nutlin-3. This cis-imidazoline analogue competitively binds to the hydrophobic cleft of MDM2 preventing it from intact with the transactivation domain of p53, thus relieving the latter for its prominent tumour suppressor activity (Tovar et al., 2006; Vassilev, 2005, 2007; Vassilev et al., 2006).

The ability of Nutlin-3 to inhibit the MDM2-p53 complex formation was checked initially by means of an ELISA based assay (Figure 4.11). Panel A represents the results obtained from an assay, where a constant amount of full-length untagged p53, purified from *E.coli*, was captured onto microtiter wells, increasing amounts of MDM2 were initially preincubated with DMSO (carrier), or fixed amounts of Nutlin-3 (2.5-10 μM) then added onto the wells. After extensive washes the MDM2 bound to p53 was detected with 2A10 antibody. Panel B represents an assay where a fixed amount of MDM2 was preincubated with increasing amounts of Nutlin-3, after which the protein was added onto wells bearing the coated p53. The $I_{0.5}$ =1.25 μM for Nutlin-3 calculated is consistent with published data (Vassilev, 2004).

The above results indicate that in a dose dependant manner Nutlin-3 inhibits the purified MDM2 protein from binding to p53.

Based on the above, the ability of Nutlin-3 to compete with BOX-I for binding to $MDM2^{WT}$ and $MDM2^{C464A}$, $MDM2^{C478S}$ was investigated (Figure 4.12). In this assay equal amounts of biotinylated BOX-I peptide were captured onto streptavidin coated

microtitre wells and incubated with a fixed amount of wt or mutant MDM2 in the presence of increasing Nutlin-3 concentrations. The result of this assay demonstrated an apparent difference in the ability of the RING mutants to bind Nutlin-3, suggesting that mutations within the C2H2C4 structure have a direct influence on Nutlin-3 binding that is not mediated by other cellular proteins. Thus, Nutlin-3 is a weak inhibitor of BOX-I binding to the Cys^{464A} mutant, relative to wild-type MDM2 protein, with an $I_{0.5}$ 4-fold greater than for wt MDM2. This suggests that the Cys^{464A} protein has a lower affinity for Nutlin-3 than the wild-type protein and binds with a higher affinity to BOX-I resulting in preferential BOX-I binding. Conversely the Cys^{478S} mutant appears to bind Nutlin-3 with a higher affinity than the Cys^{464A} and wt proteins. Thus, in this case Nutlin-3 competes more easily with BOX-I for binding to the hydrophobic pocket. In order to determine if the differences observed in Nutlin-3 binding are reflected in the ability of Nutlin-3 to disrupt the interaction between full-length p53 and MDM2 the following experiment was performed. Full-length p53 was coated onto the microtiter well and incubated with a titration of MDM2 in the presence of various fixed concentrations of Nutlin-3 (Figure 4.13; 2.5, 5 and 10 μM). Again there was a clear difference in Nutlin-3-dependent disruption of full-length p53 binding to the MDM2 proteins, with the p53:Cys^{478S} mutant complex showing increase Nutlin-3 sensitivity compared to Cys^{464A}. Once more this suggests that the Cys^{478S} mutant has a higher affinity for Nutlin-3 than does the Cys^{464A} protein. Panel D (Figure 4.13) indicates the rate of p53:MDM2 complex disruption, with respect to Nutlin-3 concentration, present in the system, from it a clear decreased sensitivity to the drug for the Cys^{464} mutant is visible.

4.2.6 RING mutation affect the efficacy of Nutlin-3 as an inhibitor of MDM2-mediated repression of p53

The data presented above strongly favours the notion that the affinity of MDM2 hydrophobic pocket towards p53, is dependant on the zinc binding state of the C-terminal RING domain. Furthermore, the C2H2C4 RING mutants have a gain of transrepressor activity when compared to the wt protein (Chapter 3). To further

investigate the link between hydrophobic pocket binding and RING domain function. Nutlin-3 was used in cell based assays as due to its chemical nature it is perfectly cell permeable (Vassilev, 2004; Vassilev et al., 2004).

It has been previously suggested that Nutlin-3 most likely functions as an anticancer agent by affecting the ability of MDM2 to act as a transrepressor of p53 transcription rather than as an inhibitor of MDM2-dependent p53 ubiquitination. This hypothesis was based on the published results (Wallace et al., 2006) and is further supported by the data presented in Figure 4.14, clearly indicating that Nutlin-3 is not able to inhibit the ubiquitination of p53 *in vitro* using purified proteins (Panel A) and that the addition of Nutlin-3 to A375 cells (harbouring *p53 WT/WT* gene) does not decrease the number of modified p53 forms detected (Panel B). In fact one observes that an increase in p53 modification is proportionate to increases in total p53 protein levels and to the activation of p53, as assessed by an increase in p21 protein levels. Together these results suggest that modification of existing or newly synthesised p53 protein continues in the presence of Nutlin-3.

If the above hypothesis is correct one would predict that Nutlin-3 binding to MDM2 would be sufficient to relieve transrepression imposed by both wt and E3-inactive MDM2 protein. Using the p53-reporter assay (introduced in Chapter 3) the ability of Nutlin-3 to reverse transrepression imposed by a fixed amount of wt MDM2 was shown (Figure 4.15). Nutlin-3 had a striking effect on the transrepressor activity of the Cys^{478S} protein with p53 activity recovering to near the level seen in the absence of MDM2. This result lends strong support to the idea that Nutlin-3-dependent inhibition of MDM2 as a transrepressor occurs independently of MDM2 E3-ligase function and that this could be sufficient to explain the activating effect of Nutlin-3 on p53.

Interestingly, although Nutlin-3 was active against the Cys^{478S} MDM2 mutant protein it had only weak activity against the Cys^{464A} protein and even at 14 μM Nutlin-3 did not inhibit this mutant. To confirm this result a different cell based transcriptional assay system was employed. It investigated the ability of Nutlin-3 to overcome wt and mutant MDM2 imposed transrepression of p53, this time using endogenous p21, a downstream target of transcriptionally active p53, as a readout (Figure 4.16). An

amount of transfected MDM2 wt and mutant constructs was chosen that gave maximal repression of endogenous p21 protein expression in H1299 cells, Nutlin-3 was then added to the cells in a dose-dependent manner and the effect on p21 levels was determined. Quantitation of the data generated by in Figure 4.16 Panel B shows that Nutlin-3 can relieve transrepression imposed by both the wt and Cys^{478S} mutant forms of MDM2 at the lowest concentration used (1.5 μM). However at 1.5 μM, Nutlin-3 had no measurable effect on the levels of p21 protein in the presence of $MDM2^{C464A}$, in fact it required 7 μM Nutlin-3 to relieve transrepression by the $MDM2^{C464A}$ on p21 protein expression. This observation, strengthened by *in vitro* results, shows that the differential effect of Nutlin-3 is dependent on the status of the C2H2C4 RING structure, and suggests that the introduction of mutations that directly impact on RING structure can differentially impact on the affinity or availability of MDM2's hydrophobic pocket for p53 BOX-I binding.

In conclusion, although both the Cys^{464A} and Cys^{478S} proteins bind with a higher affinity to hydrophobic pocket interacting ligands than the wt protein, resulting in a gain of transrepressor activity they do so differentially. Thus, whereas the Cys^{478S} protein binds preferentially to Nutlin-3, the Cys^{464A} protein binds with a higher affinity to BOX-I resulting in differential Nutlin-3 sensitivity in the cell. Therefore, mutations within the C2H2C4 RING differentially affect the affinity of the hydrophobic pocket for distinct interacting ligands.

4.3 Discussion

Studies addressing how MDM2 structure supports its functional diversity have begun to provide insight into the protein's conformational flexibility. Thus, a picture is emerging of interdependent functional domains linked through changes in conformation, emphasising the need to study the domain structure of MDM2 within the context of the whole protein. Key point mutations within the RING finger are fruitful in bestowing data demonstrating a cross-talk between the C-terminus and interactions taking place at the N-terminal hydrophobic pocket of MDM2. Therefore

they provide a good starting point for investigating this matter further. A link between the hydrophobic pocket of MDM2 and its acid domain has been previously described (Wallace et al., 2006). There a model was presented, where occupation of the hydrophobic pocket promoted conformational changes in MDM2, that favoured acid domain binding to ubiquitination signal in the core DNA binding domain of p53. This allosteric mechanism promotes MDM2 function as an E3-ubiquitin ligase by stabilizing a low affinity interaction between the BOX-V domain of p53 and the acid domain of MDM2. The data presented in this chapter, and the previous chapter as well, adds to this model for the regulation of one domain of MDM2 through modulation of a second by demonstrating that the RING finger domain, and more specifically residues required to form the C2H2C4 RING structure, can allosterically modulate hydrophobic pocket interactions. In this case the result is an increase in the affinity of the hydrophobic pocket which produces a gain in transrepressor function in cells. Interestingly, mutation of Cys^{464} and Cys^{478} residues are not equivalent in terms of their effect on the hydrophobic pocket. Thus, although both mutants display increased binding to the BOX-I domain of p53, the Cys^{478S} mutant binds Nutlin-3 in preference to BOX-I, whereas the Cys^{464A} protein preferentially binds to BOX-I.

Structural and computational analysis of the MDM2 hydrophobic pocket interaction with p53 has revealed that this domain has a high degree of plasticity and has suggested that the shape of the binding cleft can change significantly (Espinoza-Fonseca and Garcia-Machorro, 2008; Espinoza-Fonseca and Trujillo-Ferrara, 2006a, b). A mechanism has been proposed where binding to the BOX-I domain of p53 requires a progressive opening up of the binding cleft to reveal a hydrophobic interface. The binding of p53 then proceeds through an intermediate complex where the cleft gradually adopts a more open conformation eventually accommodating Thr^{18}-Asp^{29} of BOX-I. Based on this type of study it has been hypothesised that the cleft has enough plasticity to allow a range of low-energy states rather than a single 'open' or 'closed' conformation. As a result the pocket can accommodate a range of peptides and small molecules that might not have any obvious structural similarity (Bowman et al., 2007; Espinoza-Fonseca and Garcia-Machorro, 2008; Espinoza-Fonseca and Trujillo-Ferrara, 2006a, b; Stoll et al., 2001; Vassilev et al., 2004). It is

likely therefore, that the differential binding preferences of the two Cys mutants are a result of different degrees of cleft accessibility.

4.4 Figures

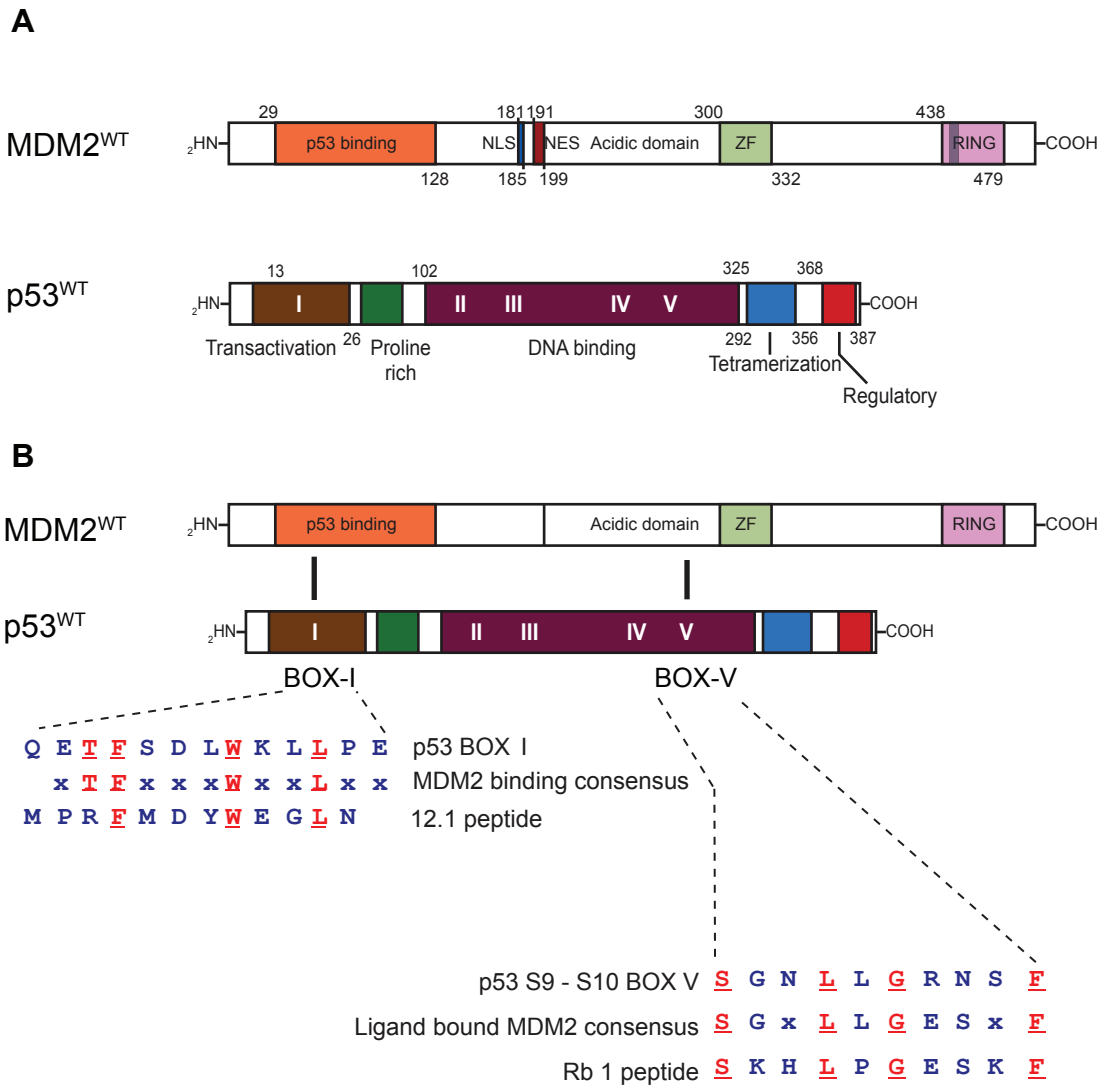

Figure 4.1 Characterization of the MDM2-p53 interaction

(**A**) Multidomain organization of MDM2 and p53. The location of highly conserved domains (I-V) within p53 is indicated in white roman numerals.
(**B**) Topological representation of the two defined interaction sites, building the MDM2::p53 complex. The primary structure of BOX-I and BOX-V is shown below. The crucial amino acids for the binding are outlined in red. Amino acids within the consesus marked as x are free for divergence. Peptide 12.1 presented as identified by Bottger et al., 1996. The Rb 1 peptide as shown above is located within the C-terminal primary structure of the Rb protein.

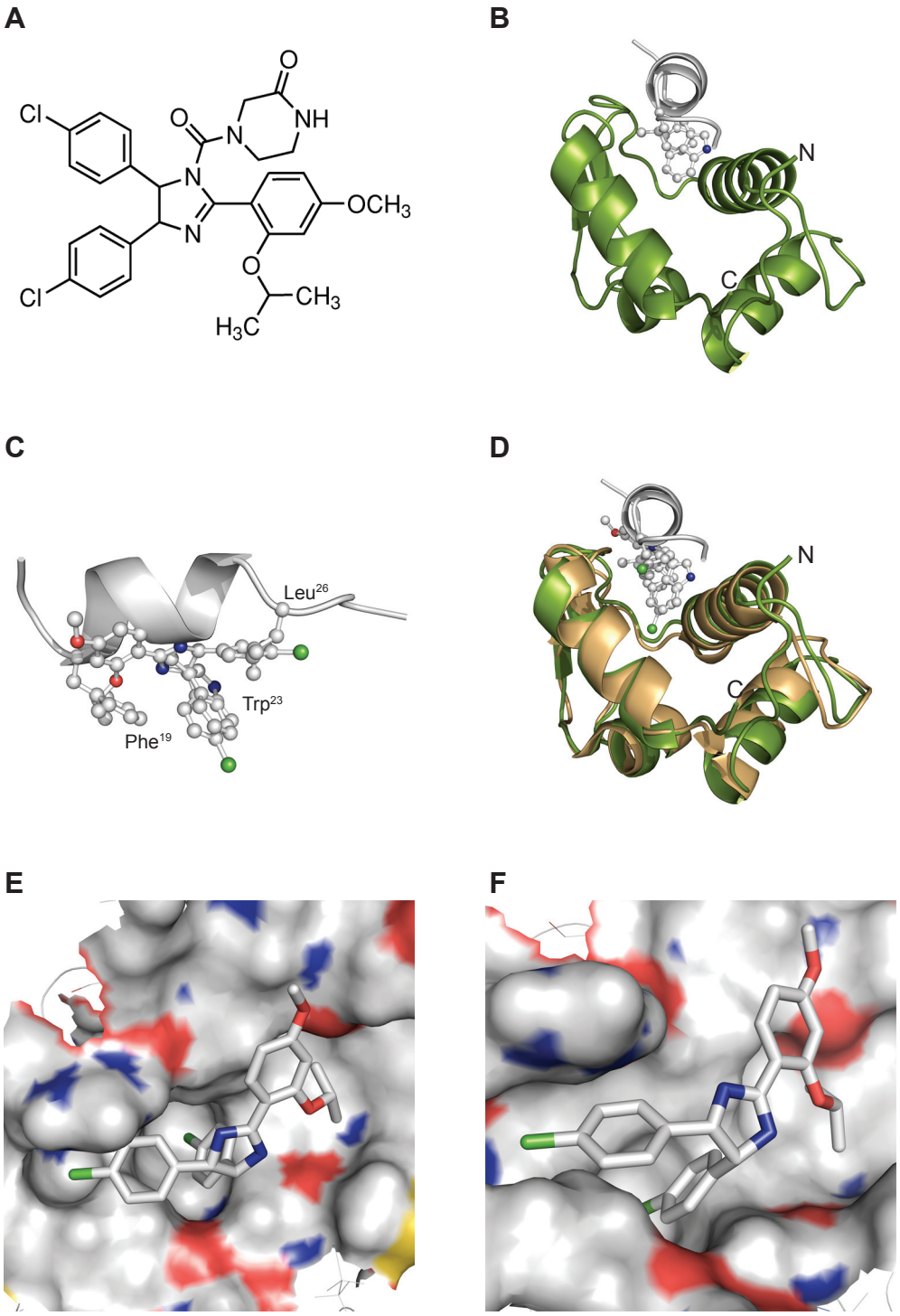

Figure 4.2 Nutlin-3 structure and mode of binding to MDM2

(**A**) Chemical structure of Nutlin-3 ($C_{30}H_{30}Cl_2N_4O_4$)* (B) Structural representation of the BOX-I peptide of p53 bound to the N-terminal binding site of MDM2 (C) Structural alignment of p53 BOX-I (critical amino acids Phe^{19}, Trp^{23}, Leu^{26} side-chains outlined in ball and stick representation) with Nutlin-3 (carbon atoms represented in white, nitrogen in blue, oxygen in red and chlorine in green). (D) Structural alignment of solved structures showing MDM2 bound to BOX-I domain (in green), and MDM2 bound to Nutlin-3 (in gold). (E), (F) Space fill model of the MDM2 N-terminal hydrophobic pocket bound to Nutlin-3 inhibitor (the inhibitor molecule represented in stick model). Colour scheme analogous to (C).

*(±)-4-[4,5-Bis(4-chlorophenyl)-2-(2-isopropoxy-4-methoxy-phenyl)-4,5-dihydro-imidazole-1-carbonyl]-piperazin-2-one

This figure was prepared using PyMOL [Warren L. DeLano "The PyMOL Molecular Graphics System." DeLano Scientific LLC, San Carlos, CA, USA. http://www.pymol.org] and structural data from Kussie et al., 1996 and Fry et al., 2004 (file 1YCR, 1TTV respectively RCSB PDB).

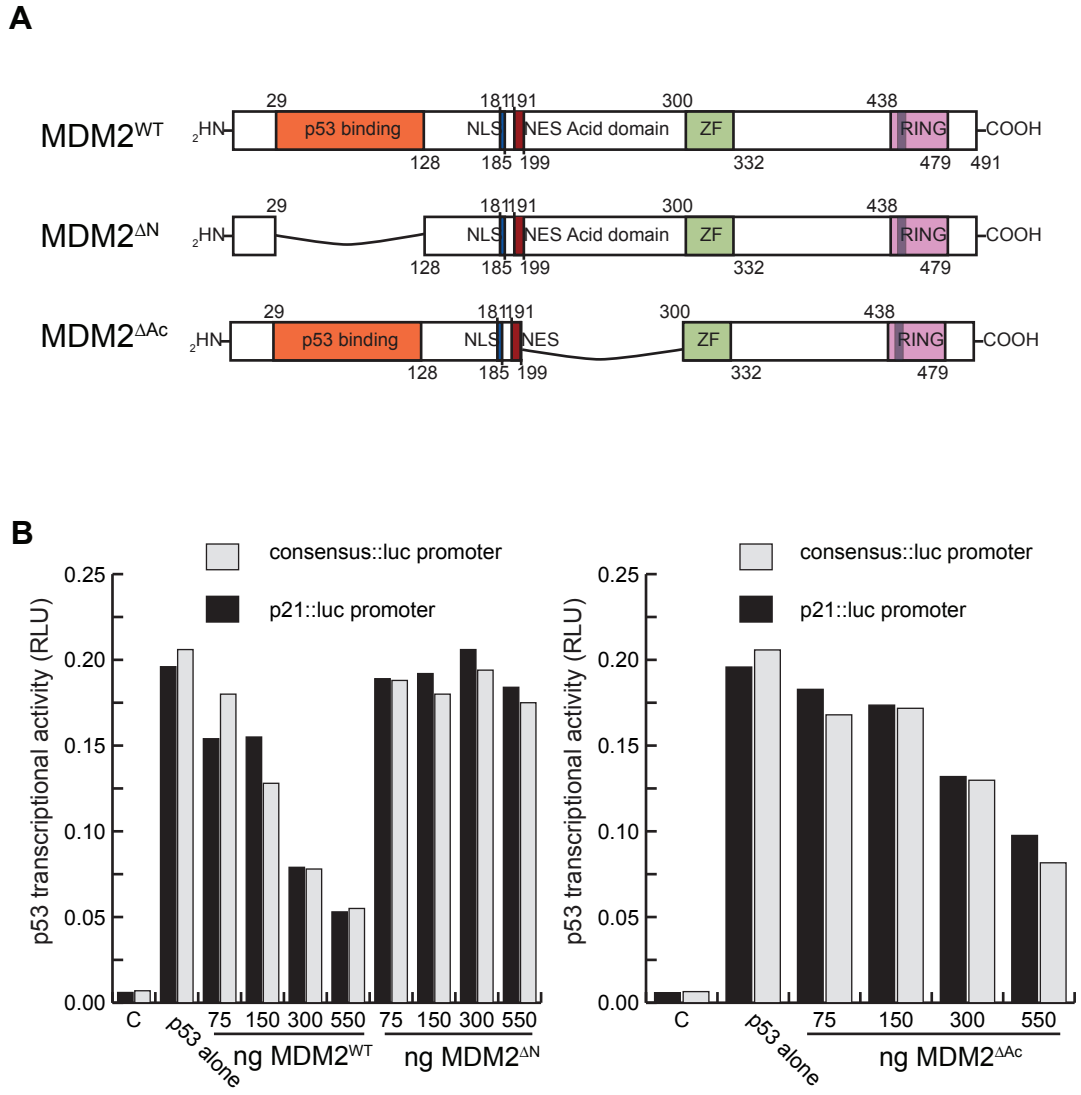

Figure 4.3 The hydrophobic pocket of MDM2 is essential for transrepression of p53

(**A**) A schematic representation showing MDM2 deletion constructs. MDM2$^{\Delta N}$ is missing the MDM2 hydrophobic pocket which binds the BOX-I domain of p53 and MDM2$^{\Delta Ac}$ does not have the acid domain which binds the BOX-V domain of p53.
(**B**) H1299 cells were transfected with p53 alone (150 ng) or with a titration (75, 150, 300, 550 ng) of MDM2^{WT}, MDM2$^{\Delta N}$ or MDM2$^{\Delta Ac}$ plus the reporter plasmids. Total DNA was normalised using the vector control. Post transfection (24 h) the Dual Luciferase Assay was performed. The results are normalised by expressing p21 or consenus-Luciferase/Renilla activity in relative light units (RLU), c is the vector only control.

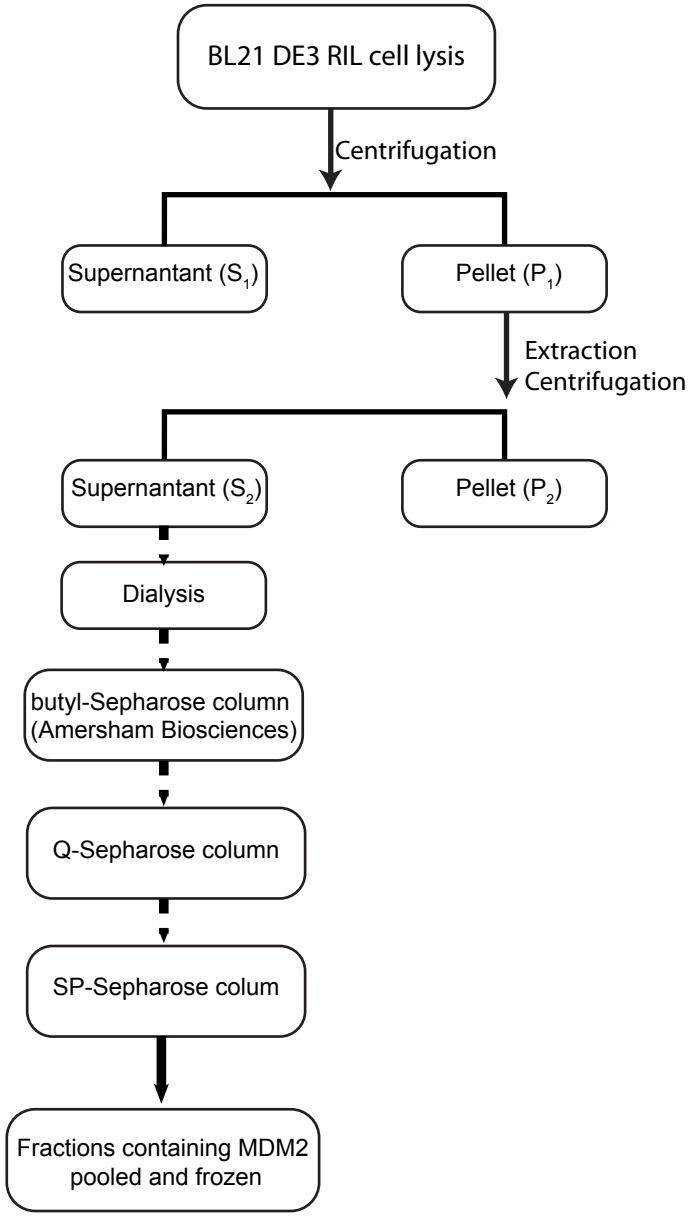

Figure 4.4 Purification scheme for isolating full length MDM2 from a prokaryotic expression system

Expression and Purification of Recombinant Protein—Human MDM2 wt was overexpressed in E. coli BL-21 RIL DE3 strain at 20 °C for 3 h after induction with 0.5 mM IPTG. Cells were harvested by centrifugation at 8000×g for 10 min and frozen in liquid nitrogen. Bacteria pellet was lysed for 1.5 h at 4 °C with frequent stirring followed by 2 min at 37 °C and an additional 15 min at 4 °C. Afterward the suspension was centrifuged at 100,000×g for 1 h at 4 °C. Under these lysis conditions most of the desired protein was insoluble and localized within the pellet after centrifugation. Extraction of the MDM2 protein from the cell pellet was carried out overnight at 4 °C with constant shaking. After centrifugation (100,000×g for 1 h at 4 °C) the supernatant was collected and dialysed After 2 h dialysis the sample was loaded onto a butyl-Sepharose column (Amersham Biosciences). The protein that bound to the column was eluted via gradient of decreasing ionic strength and increasing glycerol concentration. The fractions containing MDM2 protein were pooled and loaded onto a Q-Sepharose column. The flow-through from the column was immediately loaded onto a SP-Sepharose column equilibrated with an analogous buffer as the Q-Sepharose. The bound proteins to the SP-column were eluted by means of ionic strength gradient. Fractions containing MDM2 protein were pooled, frozen in liquid nitrogen and stored at -80°C for further experiments.

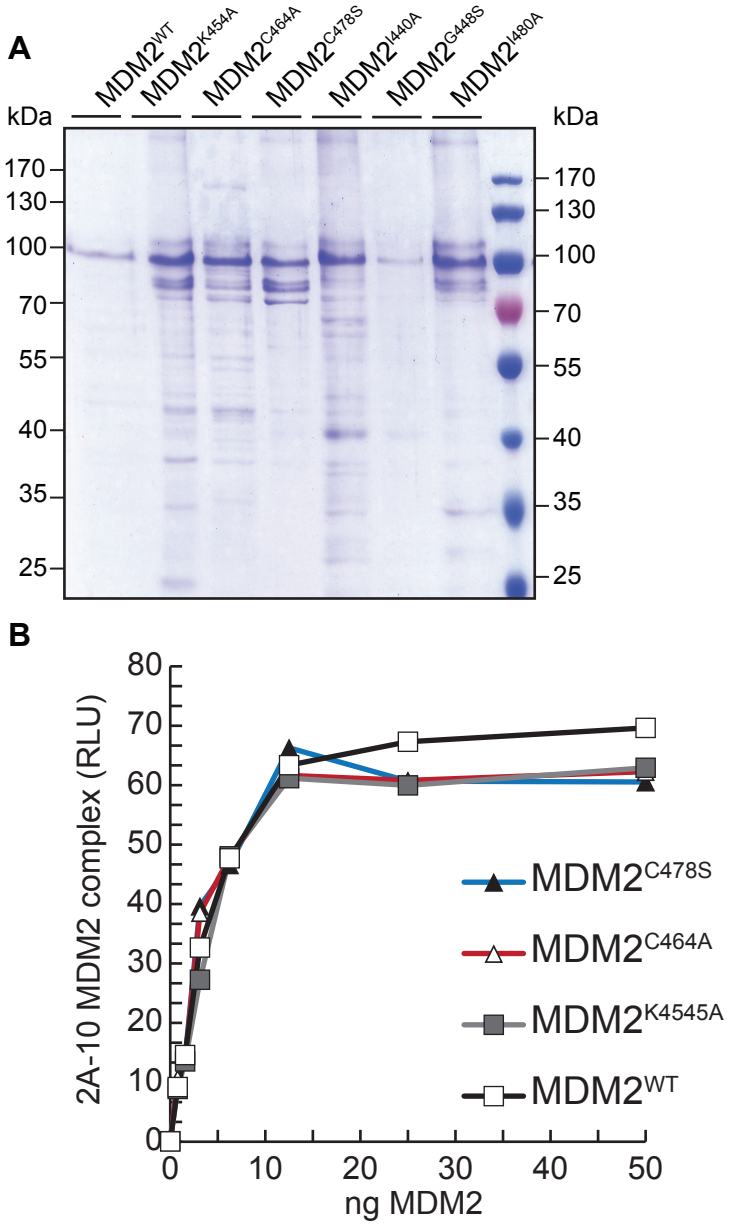

Figure 4.5 Purification of human MDM2 protein

Full-length untagged human MDM2 protein and six single point mutants were purified from bacterial expression system using the procedure described in the previous figure.
(**A**) Coomasie Blue stained gels after SDS-PAGE representing the results from purification procedure, where $MDM2^{WT}$ and all the listed mutants were purified analogously. 10 µl of each sample premixed with 1X SDS Sample Buffer was loaded.
(**B**) Amount standardization by ELISA. To check the accuracy of protein normalisation for the purified $MDM2^{WT}$, $MDM2^{K454A}$, $MDM2^{C464A}$ and $MDM2^{C478S}$ proteins (Standardization was performed for all the mutants shown in (**A**), whereas for the purpose of this chapter the shown mutants were sufficient). ELISA was performed in which a titration of MDM2 protein was coated onto the microtitre plate wells, following extensive washing. MDM2 protein levels were detected using 2A10 antibody.

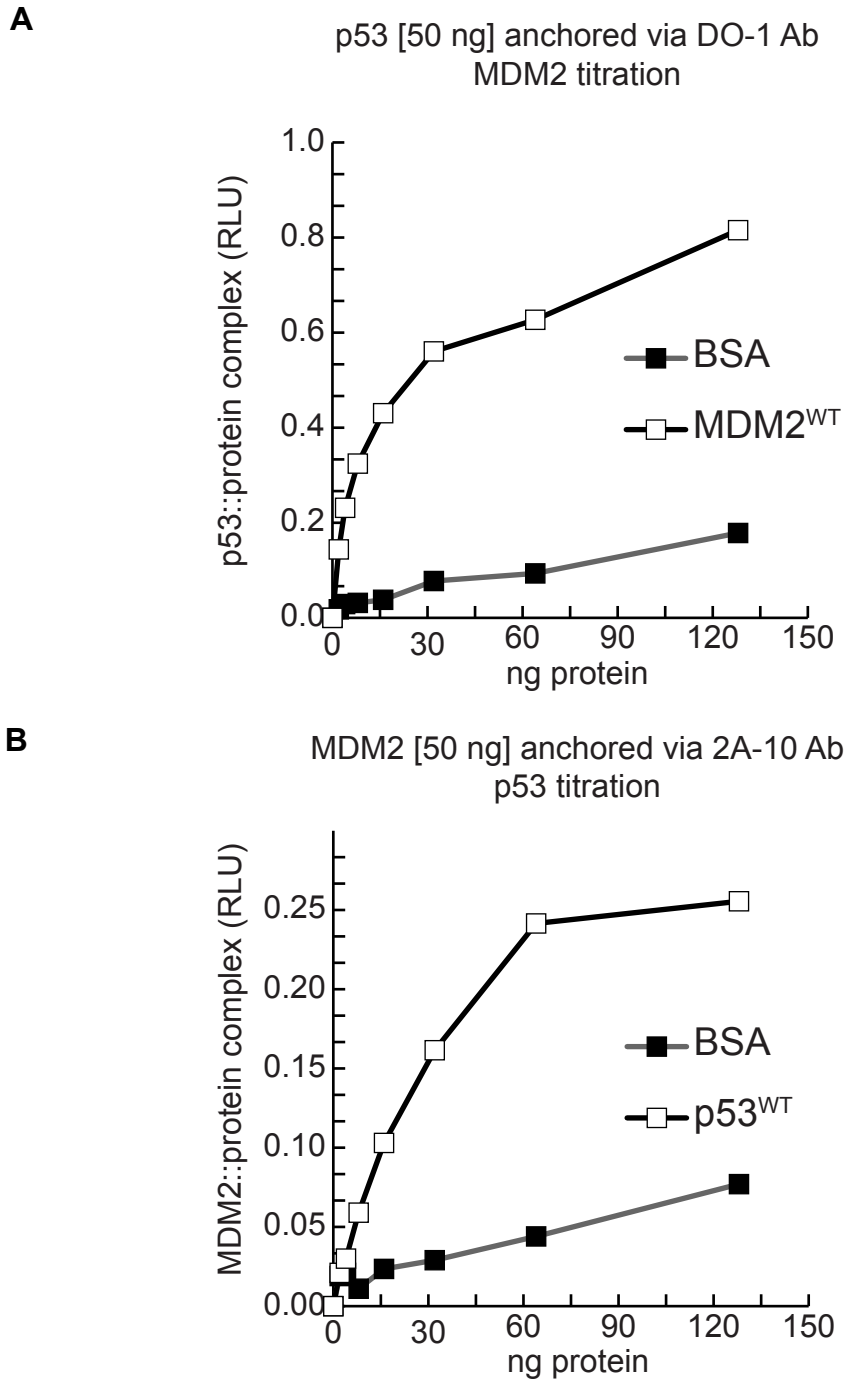

Figure 4.6 Initial quantitation of MDM2 p53 interaction

Purified untagged full-length human MDM2 was assayed for specific interaction with purified untagged human p53 protein by means of ELISA. Specific antibodies for both of the proteins were used to anchor one of the pair in the microtiter well.
(**A**) The anchoring DO1 Ab was attached to the microtiter well overnight by incubation in carbonate buffer (pH 9.2). BSA was used as a negative interaction control. The p53 protein was added in constant amount (100 ng) followed by titration of MDM2 protein, following extensive washing the MDM2::p53 complexes were detected with rabbit polyclonal anti MDM2 antibody (ab15471-Abcam).
(**B**) Procedure analogous to (**A**), with the anchoring antibody (2A10) specific for MDM2. The p53::MDM2 complexes were detected with rabbit polyclonal anti p53 antibody (CM1).

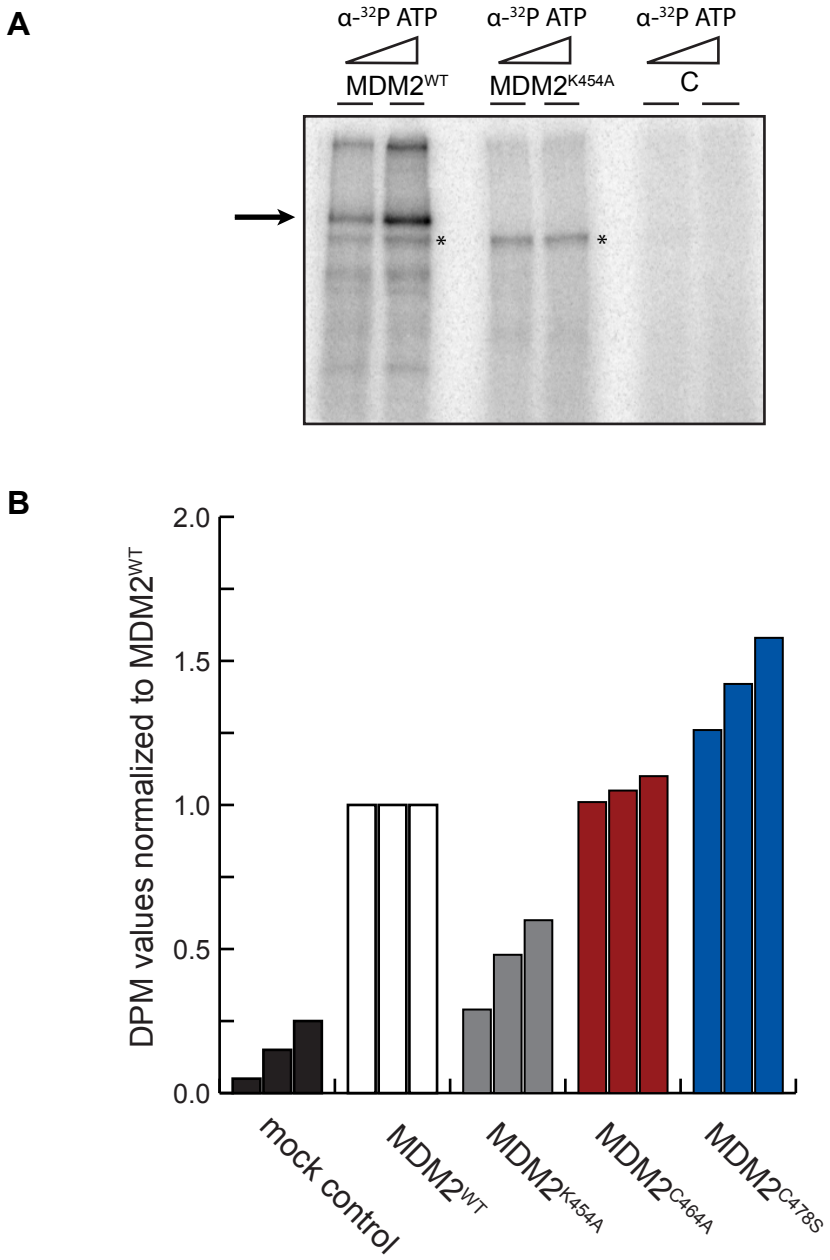

Figure 4.7 ATP binding by MDM2

Binding of ATP to purified MDM2 proteins. The basis for this experiment was provided by Poyurovsky, et al., 2003. The major difference though is the use of full length MDM2 proteins instead of just the GST-RING domain. Two methods were used to assay the ATP binding potential of MDM2.
(**A**) Constant amount of $MDM2^{WT}$ or $MDM2^{K454A}$ was incubated with increasing amounts of α-^{32}P ATP followed by UV crosslinking. The formed ATP-protein complexes were resolved by SDS-PAGE and an autoradiogram was obtained. C represents negative control where reaction buffer was used only. The arrow points at nucleotide bound MDM2.
(**B**) MDM2 protein species preincubated with constant amounts of α-^{32}P ATP and filtered through 0.44 µm nitrocelullose membrane. The bound protein-nucleotide complexes were analysed by means of a scintilation counter. ATP binding ability of specific mutant proteins was normalized to the ability for $MDM2^{WT}$. The data represents data sets from three independent experiments.

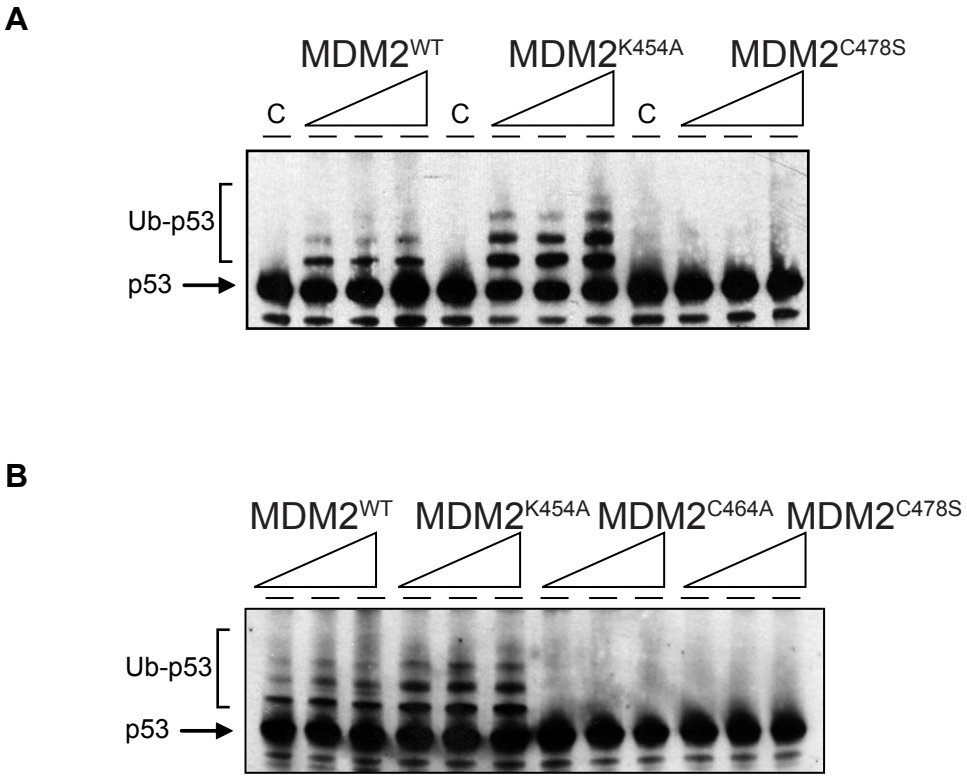

Figure 4.8 MDM2 E3 ubiquitin ligase activity *in vitro*

(**A**) (**B**) Ubiquitination reactions were assembled with constant p53, E1, E2 and increasing amounts of MDM2 wt or mutant proteins as indicated. The reactions were carried out at 37ºC for 15 min. Ubiquitination was analysed by immunoblot using a 4-12% gradient gel, p53 was detected using DO1. Unmodified (p53) and ubiquitinated p53 (Ub-p53) is shown. C - represents the control where all the mentioned components were added omitting the E3 ubiquitin ligase.The above data was obtained in cooperation with Erin Worrall.

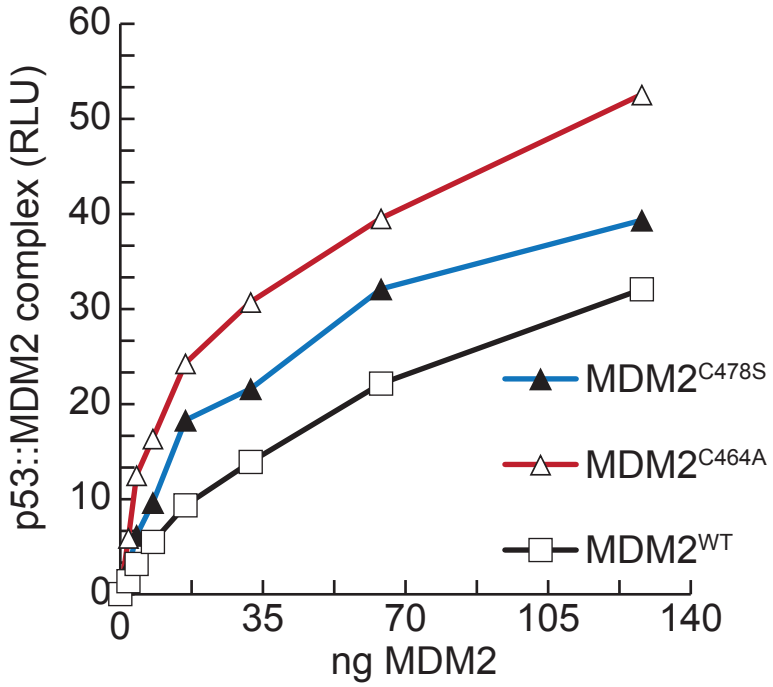

Figure 4.9 C2H2C4 mutants of MDM2 bind with a higher affinity to p53

p53 (100 ng/well) was coated onto microtitre wells and incubated with wt or mutant MDM2 as indicated. Following extensive washing the MDM2::p53 complexes were detected using 2A10 antibody. The experiment shown is representative of 4 independent experiments.

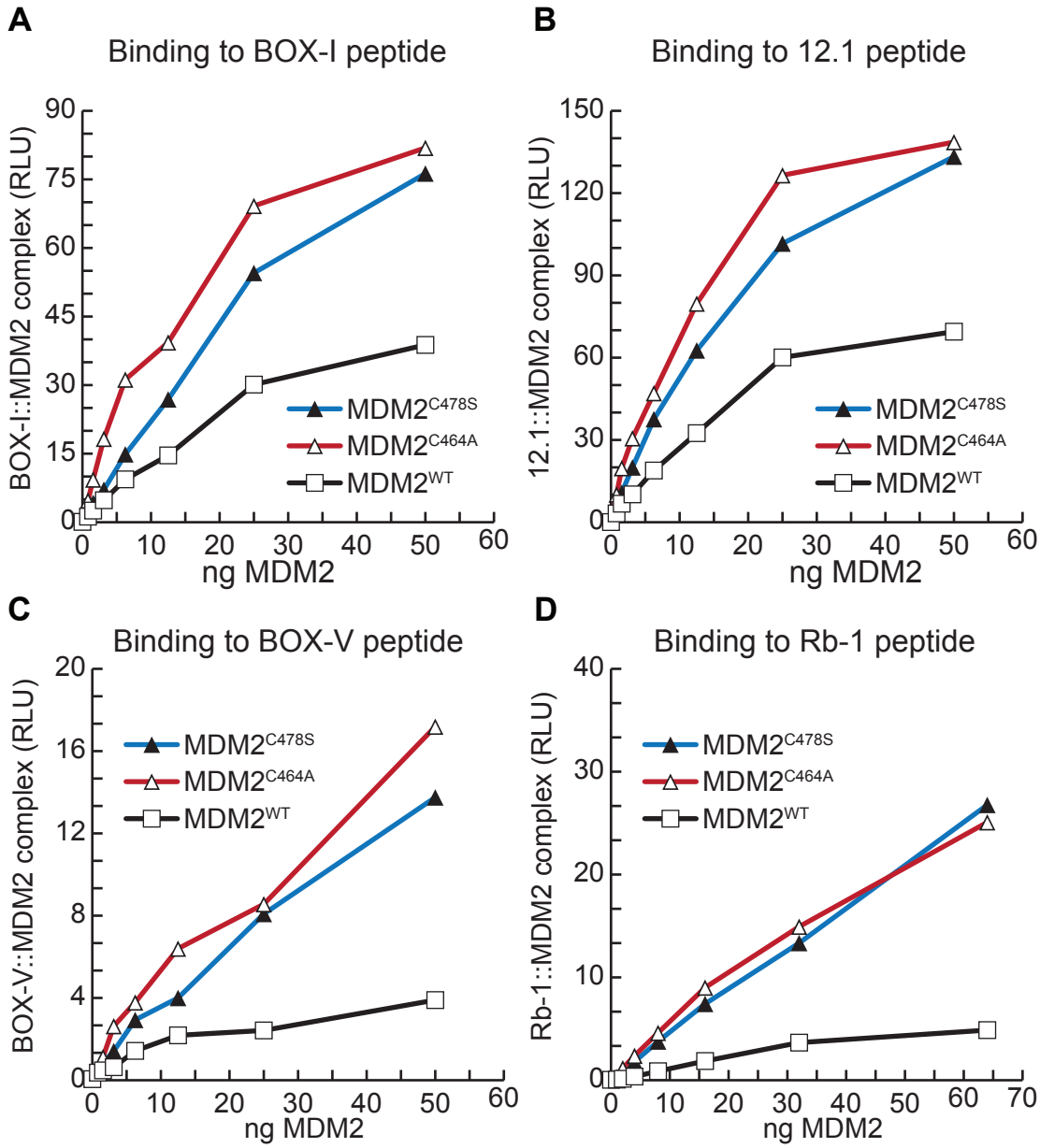

Figure 4.10 C2H2C4 mutants of MDM2 bind with a higher affinity to discrete domains of p53

(**A**) BOX-I domain peptide (5 μM) was captured onto streptavidin coated wells and MDM2 binding was detected using 2A10 and is expressed as relative light units (RLU) against MDM2 amount.
(**B**) 12.1 peptide (5 μM) was captured onto streptavidin coated wells and MDM2 binding was detected using 2A10 and is expressed as relative light units (RLU) against MDM2 amount and incubated with wt or mutant MDM2 as indicated.
(**C**) BOX-V domain peptide (5 μM) was captured onto streptavidin coated wells and MDM2 binding was detected using 2A10 and is expressed as relative light units (RLU) against MDM2 amount and incubated with wt or mutant MDM2 as indicated.
(**D**) Rb-1 peptide (5 μM) was captured onto streptavidin coated wells and MDM2 binding was detected using 2A10 and is expressed as relative light units (RLU) against MDM2 amount and incubated with wt or mutant MDM2 as indicated.
The experiments shown in (**A**) (**B**) (**C**) (**D**) are representative of 4 independent experiments.

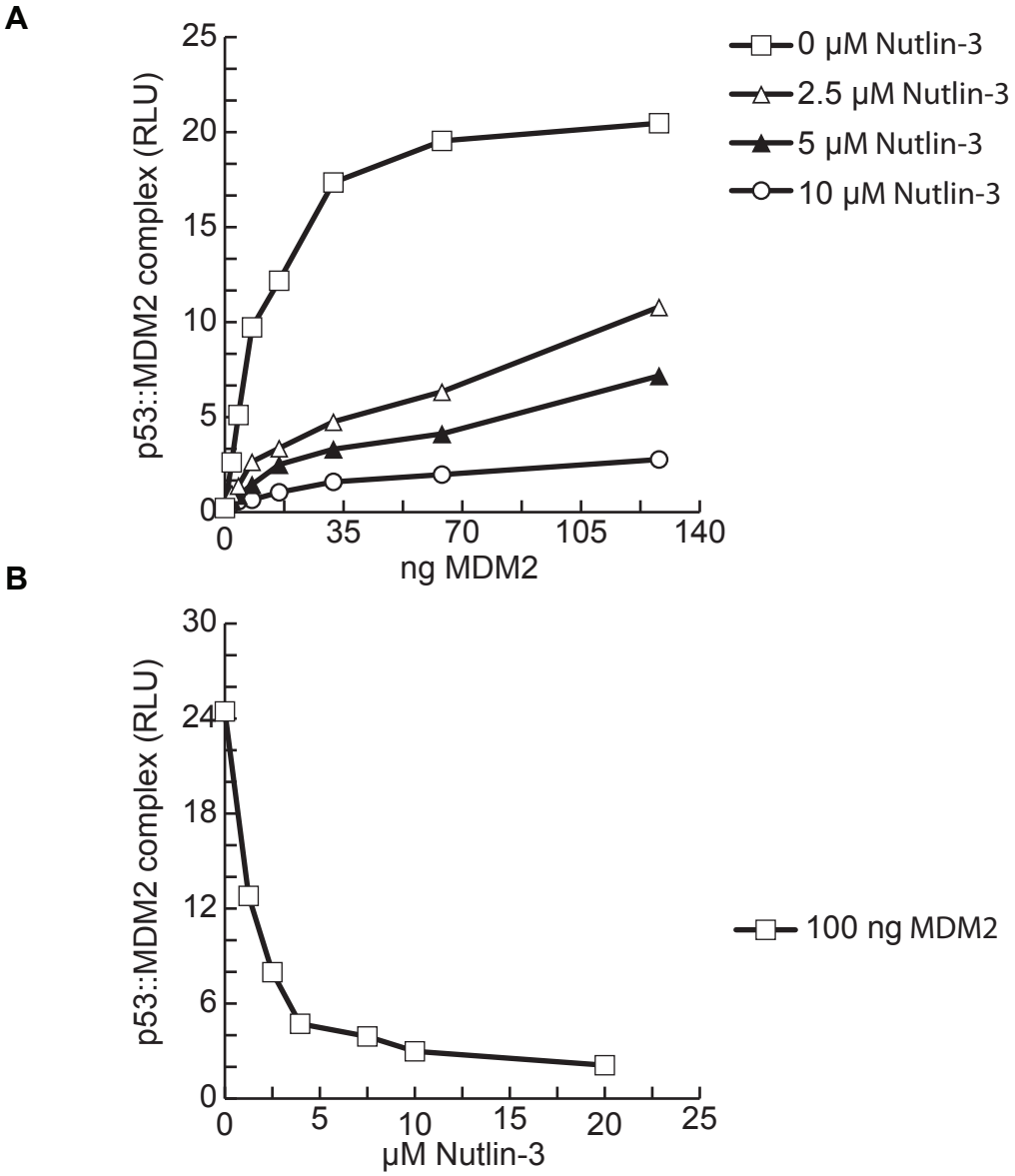

Figure 4.11 Nutlin-3 inhibits the formation of the p53::MDM2 complex in a dose dependent manner

(**A**) p53 (100 ng/well) was coated onto microtitre wells. The MDM2 protein before being titrated onto p53 was preincubated for 5 min with Nutlin-3 at amounts shown. MDM2 binding was detected using 2A10 and is expressed as relative light units (RLU) against MDM2 amount.
(**B**) p53 (100 ng/well) was coated onto microlitre wells. Constant amount of MDM2 was initially preincubated for 5 min with increasing amounts of Nutlin-3 inhibitor (0-20μM), then added onto p53. MDM2 binding was detected using 2A10 and is expressed as relative light units (RLU) against Nutlin-3 amount.
The experiment shown in (**A**) (**B**) are representative of 2 independent experiments.

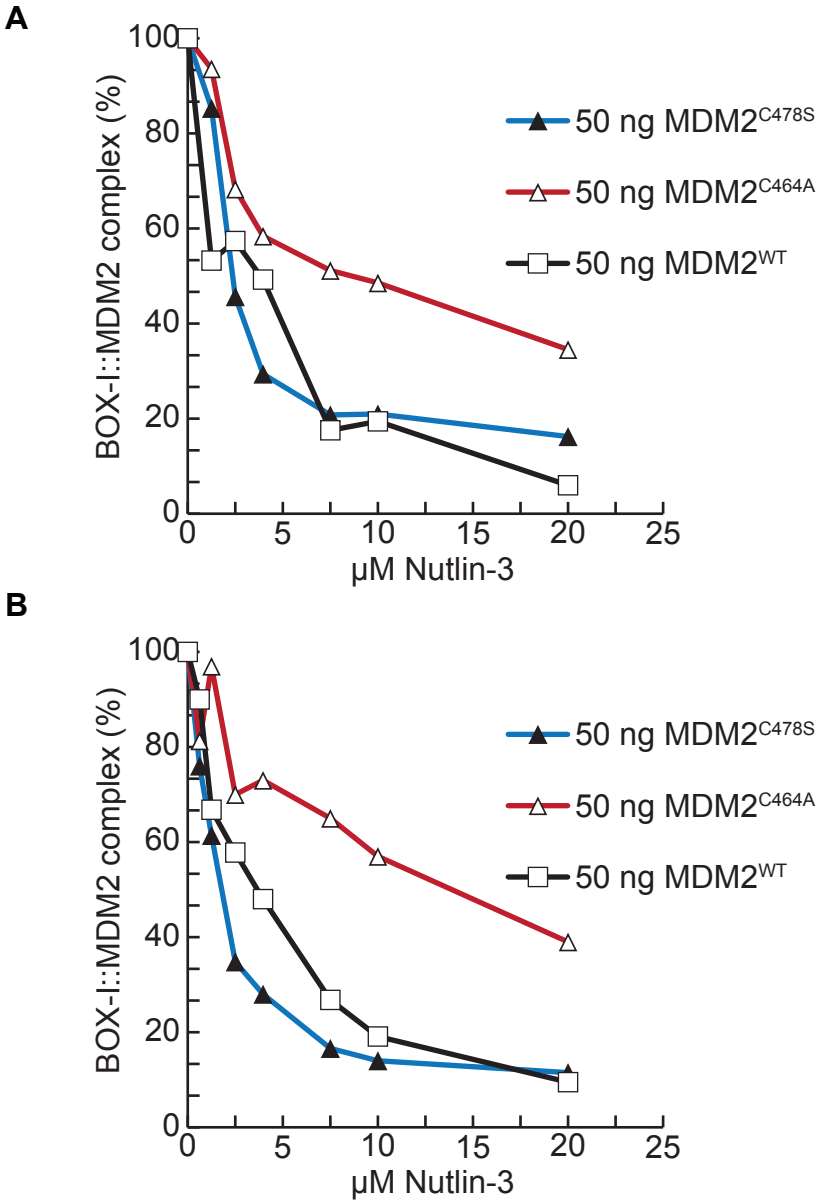

Figure 4.12 Nutlin-3 has a differential effect on the C2H2H4 MDM2 mutants

(**A**) (**B**) BOX-1 peptide (5 μM) was captured on streptavidin coated wells and incubated with the indicated form of MDM2 which had been preincubated (5 min) with a titration of Nutlin-3 (0-20 μM). MDM2 binding was detected using 2A10 and is given as relative binding expressed as a percentage, where 100% binding is that measured in the absence of Nutlin-3. The experiment shown in (**A**) (**B**) are representative of 2 independent experiments.

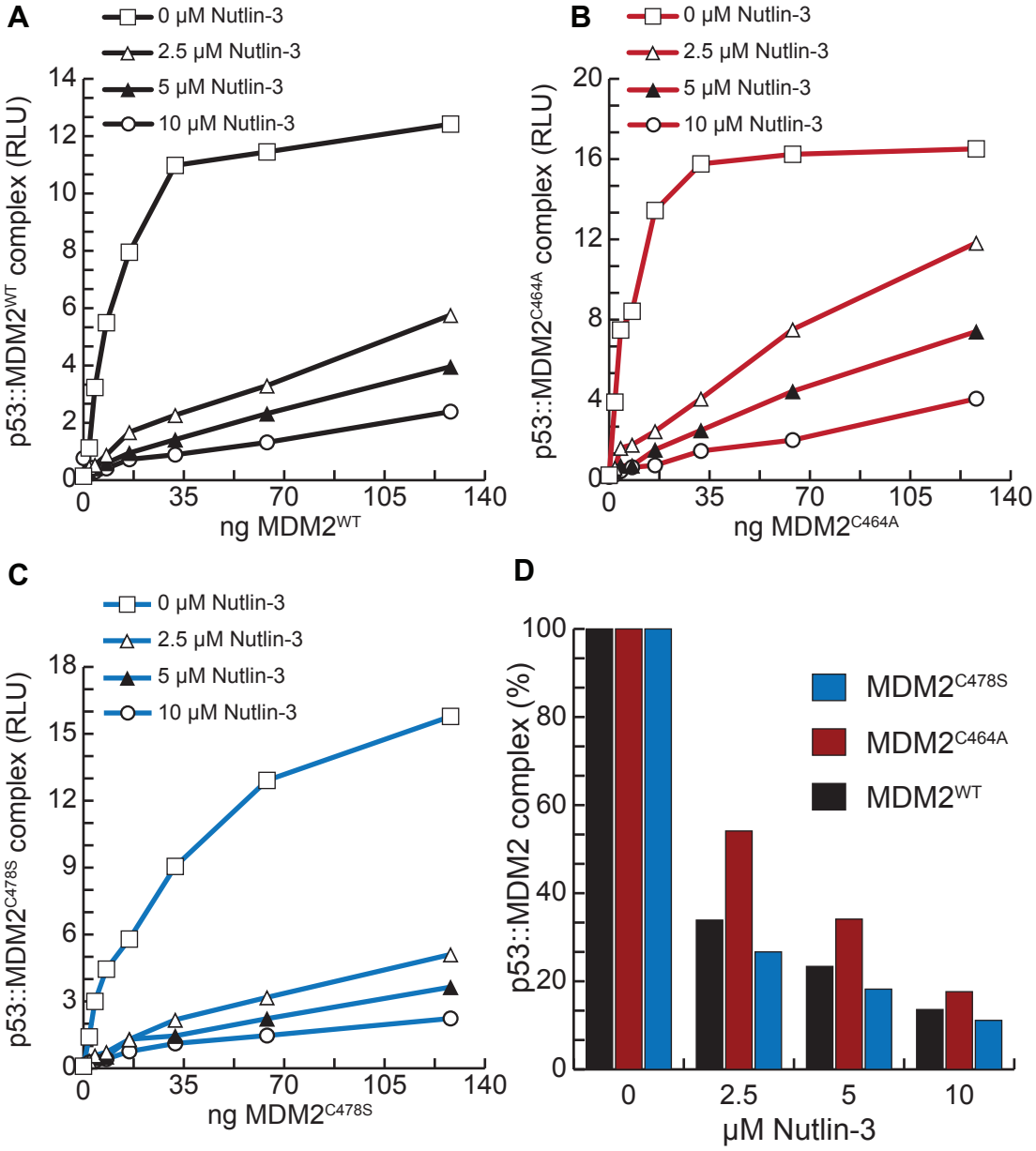

Figure 4.13 Nutlin-3 inhibition of the p53::MDM2 complex is dependant on the type of C2H2C4 RING mutation

(**A**) (**B**) (**C**) p53 (100 ng/well) was coated onto microtitre wells and incubated with the indicated form of MDM2 which had been preincubated (5 min) with Nutlin-3 (0-10 µM). MDM2 binding was detected using 2A10 and is given as MDM2::p53 complex formation in relative light units (RLU). The data presented is representative of three independent experiments.
(**D**) MDM2 p53 complex formation as a function of Nutlin-3 amount. Values for this panel were obtained by analyzing data sets from (**A**),(**B**) and (**C**), linear regression was performed within appropriate range, to obtain the rate of change of p53::MDM2 complex formation with respect to the concentration of Nutlin-3 present in the reaction mixture.

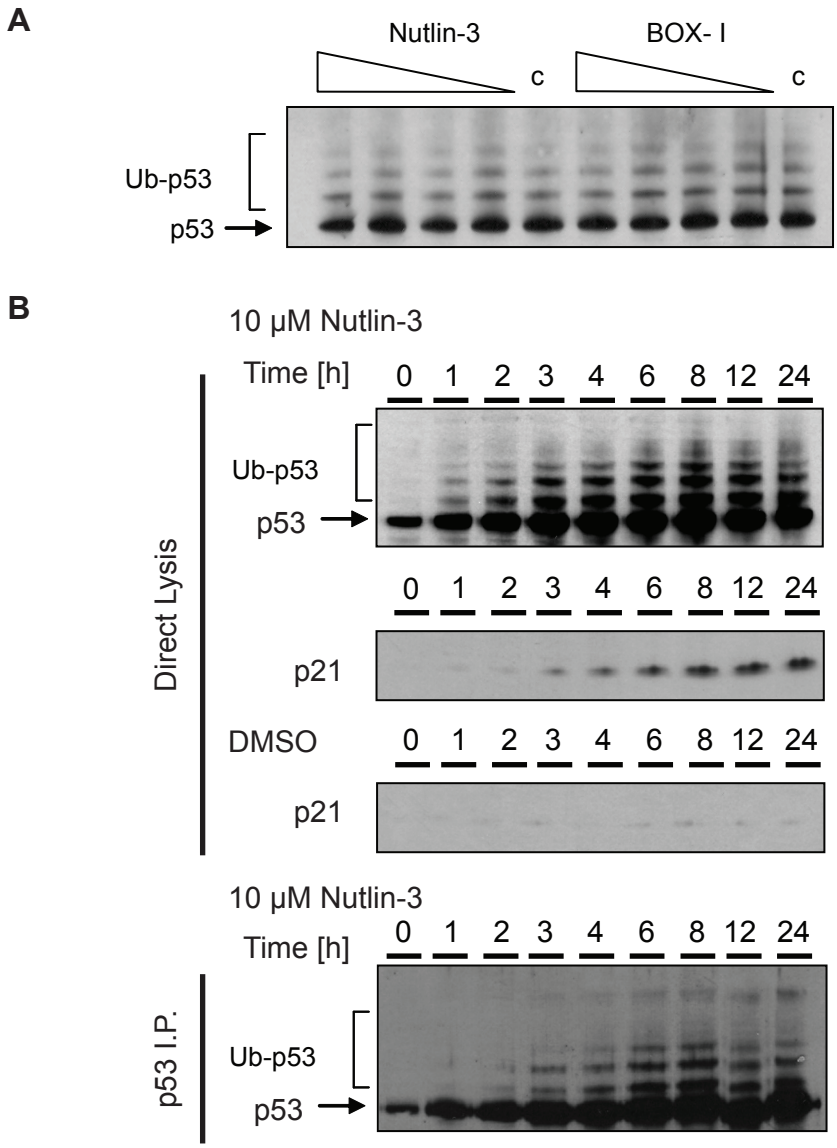

Figure 4.14 Nutlin-3 and BOX-I Mimetics do not inhibit MDM2 E3 ubiquitin ligase activity on p53

(**A**) In vitro ubiquitination reactions were assembled with p53, E1, E2 and MDM2 in the presence or absence (c) of either Nutlin-3 or BOX-I peptide (0, 10, 20, 40, 60 µM). Ubiquitination was analysed by immunoblot using a 4-12% gradient gel, p53 was detected using DO1. Unmodified (p53) and ubiquitinated p53 (Ub-p53) are shown. The data are representative of at least 4 separate experiments. Data for this panel was obtained in cooperation with Dr. Susanne Pettersson.
(**B**) Nutlin-3 (10 µM) was added to A375 cells and they were harvested over a 24 h time course (0, 1, 2, 3, 4, 6, 8, 12, 24). The lysates were analysed by immunoblot using either a 4-12% gradient gel (upper panel) or a 15% SDS PAGE gel p53 was detected using DO1 and p21 using AB-1 for direct lysis. DMSO was used as a control (carrier). The p53 protein was immunoprecipitated with DO-1 and probed with rabbit polyclonal CM1 anitbody. Modified forms of p53 are given as Ub-p53. The data are representative of 3 such experiments.

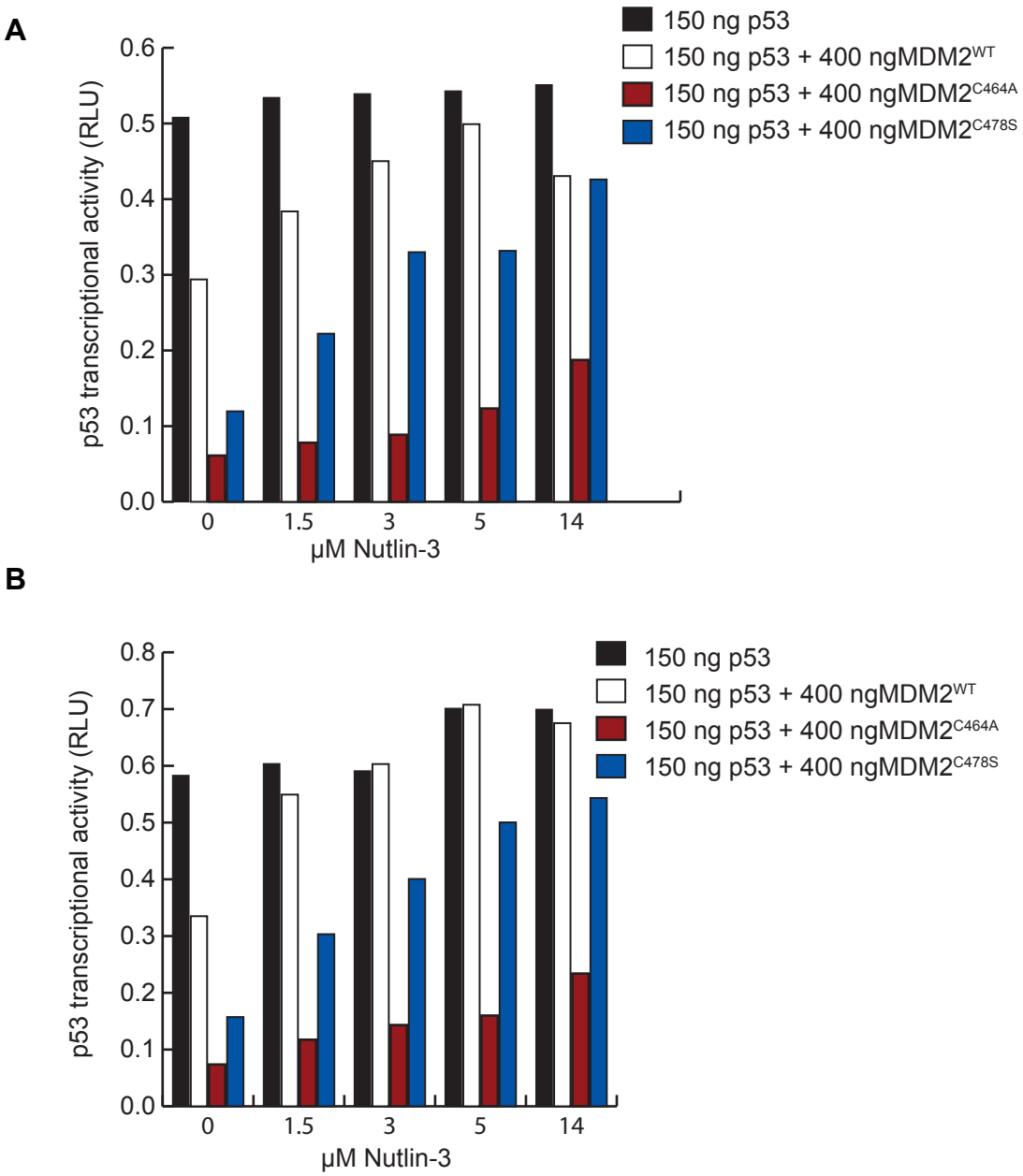

Figure 4.15 MDM2 mediated transrepression of p53 can be decreased with Nutlin-3

H1299 cells were transfected with p53 alone or together with MDM2. Total DNA was normalised using the vector control. After 24h Nutlin-3 was added in amounts shown above and the incubation continued for a further 6h. The cells were harvested and the Dual Luciferase Assay was performed. The results are normalised by expressing p21/consensus-Luciferase/Renilla activity in relative light units (RLU). Each of the bars represents a mean from three independent experiments.
(**A**) p21::luciferase reporter was used.
(**B**) Analogous to (**A**) but the TP53 consensus::reporter was used.

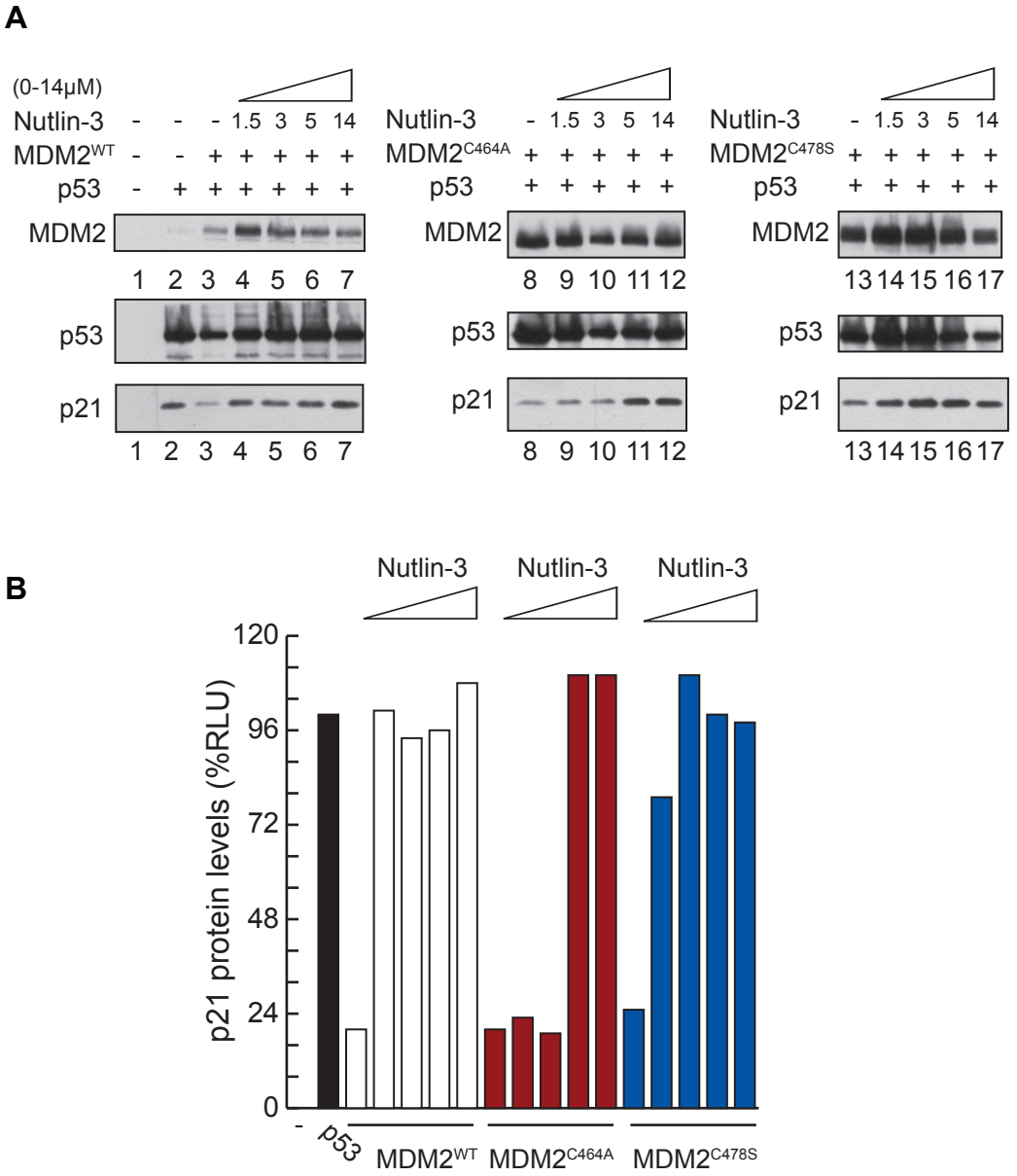

Figure 4.16 The efficacy of Nutlin-3 in cells is dependent on the C2H2H4 RING

(**A**) H1299 cells were transfected with p53 alone (150 ng) or in addition with (400 ng) of MDM2wt, MDM2^{C464A} or MDM2^{C478S}. Total DNA was normalised using the vector control. Post transfection (24 h) the cells were treated with Nutlin-3 (0, 1.5, 3, 5, 14 μM) for a further 6 h, after which lysis and immunoblot analysis followed, MDM2 (2A10), p53 (DO1) and p21 (Ab1) (**B**) Densitometry analysis of p21 immunoblot.

Chapter 5

The RING domain and MDM2 structure

Contents

5.1 Analytical tools used to measure protein conformational shift

5.1.1 Size exclusion chromatography

Cell culture based assays and end point kinetic measurements (ELISA) presented in the previous chapters highlighted an increase in affinity of the MDM2 protein to its major interacting target, p53. This is dependant on the integrity of the Zinc coordination with the RING domain of the oncoprotein. Key mutations within this domain (Cys^{464A}, Cys^{478S}) displayed preferential binding to the full length p53 tetramer in comparison to their wild–type counterpart. Moreover the mutations were later shown to be non-synonymous in terms of binding to the specific MDM2::p53 inhibitor Nutlin-3, where the $MDM2^{C478S}$ mutant displayed a considerably greater preference for the drug than the $MDM2^{C464A}$ protein. In order to further verify whether the mutations presented induce global conformational shifts involving intrinsic domain cross-talk within the protein as opposed to generating a non-specific aggregation-prone state the following techniques were employed.

Size exclusion chromatography, also referred to as gel filtration, is a technique of separating molecules according to their diffusion coefficient (a constant value prescribed to a macromolecule which is dependant on its size and shape). In contrast to ion exchange or affinity chromatography, molecules do not bind to the matrix hence buffer composition (increasing/decreasing ionic strength, nor pH fluctuations) does not directly affect resolution.

Separation of molecules by gel filtration chromatography is based on the porous nature of the matrix used and diffusion which applies to the solvent in the mobile phase and the macromolecules of interest alike. As the solute passes through the chromatographic bed its movement depends upon the bulk flow of the mobile phase and further upon the Brownian motion of the solute molecules which causes their diffusion both into and out of the stationary phase of the gel matrix. The separation in gel filtration depends on the different abilities of the various sample molecules to enter pores which are contained within the stationary phase. Assuming that the

biopolymers under investigation are properly folded and adopt a globular shape, very large molecules, which never enter the stationary phase, move through the chromatographic bed fastest. Smaller molecules, which have full or partial access to the gel pores, move more slowly through the column, since they spend a proportion of their time in the stationary phase. Molecules are, therefore, eluted in order of decreasing molecular size. Gel filtration is well suited for biomolecules that may be sensitive to changes in pH, concentration of metal ions or co-factors. Separations can be performed in the presence of essential ions or cofactors, ionic and non ionic detergents, at low or high ionic strength.

5.1.2 Intrinsic Fluorescence of Proteins

Among biopolymers, proteins are unique in displaying useful intrinsic fluorescence. Three aromatic amino acids; phenylalanine, tyrosine, and tryptophan all display fluorescent properties. These amino acids are relatively rare in proteins. Tryptophan which is the dominant intrinsic fluorophore is generally present at about 1 mol% in proteins. This minute number of tryptophan residues most probably results from the metabolic expense of its synthesis. A protein may carry as little as one tryptophan residue facilitating interpretation of the spectral data. Thus the intrinsic fluorescence of tryptophan residues in proteins has been widely used in the analysis of the dynamics and conformational perturbations in these macromolecules. Tryptophan residues, within proteins that are in their native fold, may occupy different locations where they can be influenced by distinct environment characterized by a particular set of physico-chemical conditions. Tryptophan fluorescence can be selectively excited at 295-305 nm. The emission spectrum of the residue occurs near 350 nm and, in contrast to tyrosine emission, is highly dependent on the polarity and/or local environment. Shifts in the emission spectrum of tryptophan occur in response to conformational transitions, subunit association, substrate binding and denaturation. Tryptophan is uniquely sensitive to collisional quenching, a contact phenomenon where the fluorophore (tryptophan residue) and the quencher present must come in direct contact with each other. Tryptophan can be quenched by externally added quenchers (acrylamide, KI, iodoacetamides) or by nearby amino acid groups within

the protein(s) (Lakowicz, 2000; Lakowicz and Maliwal, 1983; Lakowicz et al., 1983; Lakowicz and Weber, 1973). Tyrosine emission maximum is rather insensitive to its local environment when compared to the tryptophan. The reason for this difference lies in the structure of the residues, tryptophan is a uniquely complex fluorophore with two low-lying isoenergetic transitions. In contrast, emission from tyrosine appears to occur from a single electronic state.

The intrinsic tryptophan emission of proteins has proven quite valuable when studying protein folding. The sensitivity of tryptophan to its local environment usually results in changes in intensity or anisotropy during the folding process. The MDM2 oncoprotein contains 4 tryptophan residues (at positions 235, 303, 323 and 329) all within proximity to the acid domain. (Figure 5.4 Panel A)

5.1.3 Thermal Denaturation of Proteins

The denaturation of proteins, inducible by a variety of means, can be followed by any method sufficiently sensitive to detect conformational changes in a protein. Due to its simplicity and broad usage the thermal denaturation method can be used for a variety of purposes, such as the study of protein structure, folding and stability. For a vast majority of proteins, thermal denaturation is an irreversible process. Conformational instability of the protein is proportional to the temperature increase in the surrounding environment of the macromolecule/polypeptide. This change can be monitored by an increase in fluorescence emission. With the use of a specific marker/dye that has a higher quantum yield in a lower dielectric medium such as the one when protein unfolds exposing the hydrophobic region normally concealed within the folded conformation. However, after reaching a plateau, the fluorescence intensity starts to decrease, due to temperature induced aggregation of the denatured protein dye complexes. The true power of the assay comes forth when considering sensitivity, a vast group of proteins within the living cell (prokaryotic and eukaryotic alike) have a low margin of stability (Liberek et al., 2008) or rather are in a constant thermodynamic equilibrium between several favourable energy states across the energy landscape (Dobson, 2004).Thus employment of this method in a controlled

test tube environment can successfully show ligand induced disruption or stabilization of a preferred energy state.

5.1.4 Probing protein conformation using limited proteolysis

Antibodies, a corner stone of today's experimental molecular biology, are specific recognition markers provided by the immune system. They are extensively used to probe for endogenous changes of amount and localization of a protein molecule of interest. Their ability to bind with high affinity to a an epitope within the protein is employed in numerous variants of the immunoprecipitation assay, where multiple protein:antibody complexes can be selectively isolated from material of interest. They were shown in the previous chapters to be efficient anchoring agents immobilizing protein in a microtiter well and also shown to have competitive inhibitor properties inhibiting protein complex formation. In this chapter specific antibodies against the MDM2 oncoprotein will be used as regional markers. The epitope for an antibody may be a very short oligopeptide stretch. Bearing this in mind with lateral time-scaled proteolytic cleavage of the studied protein(s), the application of a diverse set of antibodies, may reveal valuable insights into exposed pockets of the protein structure. A specific advantage of limited proteolysis combined with molecular probes for elucidating protein structure and dynamics is that they can quickly provide valuable data, in contrast to other physiochemical techniques such as NMR or X-ray scattering that indeed provide an incomparable leap towards high resolution analysis, though are much more labour intensive and time consuming. An additional benefit of limited proteolysis is its modest requirements for the amount of protein sample required for investigation.(Fontana et al., 2004)

5.2 Experimental results

5.2.1 Point mutations within the RING domain of MDM2 do not cause high order oligomerization of the protein

It must be acknowledged that the isolated MDM2 protein species were initially overproduced in a heterogeneous, to the origin of the protein, prokaryotic system.
The state of a given protein that is populated under specific conditions will depend on the relative thermodynamic stabilities of the different states occupied with the protein folding energy field (Dobson, 2004). When one considers a case where within a relatively short period of time, a foreign polypeptide has a rapid influx within the host, the latter may react inducing the formation of large oligomeric structures i.e. protein aggregate composed of the foreign protein. In other words some eukaryotic proteins expressed in bacterial systems tend to aggregate upon over-expression. Moreover, isolated protein bearing single point mutations disrupting key structural motifs may be prone to aggregation *per se*. Considering the method of MDM2 isolation and the results presented in the previous chapter one may hypothesize that the observed increased affinity of the Cys^{464A} and Cys^{478S} mutants of MDM2 to p53 may be explained by disruption in their global fold leading to the formation of a protein aggregate, bearing numerous MDM2 specific epitopes thus recruiting numerous MDM2 specific antibodies used in the ELISA assays as detectors. To address this, two approaches were undertaken. Before any p53-MDM2, peptide- MDM2 binding assays were performed the proteins (MDM2 and all the single point mutants mentioned) were normalized for their sole affinity to the anti MDM2 antibody itself, as presented in Chapter 4. Secondly, the isolated proteins were subjected to size exclusion chromatography to investigate their apparent molecular mass hinting at their quaternary structure. In order to estimate the molecular mass from the elution profile, one must use specific protein standards of known molecular weight and globular shape. Figure 5.1 represents elution profiles obtained by gel filtration of commercially available standards. The chromatograms show the variation of concentration (in terms of UV absorbance at A_{280}nm) of sample components applied to the resin, as they elute from the column in order of decreasing

molecular size. Molecules that do not enter the matrix are eluted in the void volume, V_0 as they pass directly through the column at the same speed as the flow of buffer. The peak of Blue Dextran, a high molecular weight polysaccharide containing a blue chlorotriazine dye - Cibacron Blue; is a marker of the void volume (Figure 5.1). Having established the elution volumes for the individual protein standards (Figure 5.1 Panel A-C) and knowing the total volume of the column, the fraction of the stationary phase that is available for diffusion of a given protein species (K_{av}) was calculated (Figure 5.2). The partition coefficient was plotted over the logarithm of molecular weight, using linear regression an equation depicting partition coefficient (K_{av}) as a function of molecular weight was obtained.

Under the same conditions that the protein standards were applied and eluted from the column, wild-type and mutant MDM2 were investigated (Figure 5.3). The fractions collected were analysed by immunoblotting highlighting the peak fraction where the MDM2 was most prominent consistent with the elution peaks of the chromatograms (data not shown). The elution profile considering the data presented in Figure 5.3 is consistent with the purified MDM2 mutants compared to the wild-type protein. Single point mutations introduced into the RING domain of the protein do not induce spontaneous extensive oligomerization of the polypeptide. The mutations analyzed by size exclusion chromatography are equivalent, meaning that disruption of the zinc coordinating residues or the nucleotide binding pocket do not give rise to differential size species. Moreover the MDM2 peak fractions (14-16) estimate the protein to have a comparable mass to that seen when applied to SDS PAGE $\geq$ 90 kDa. Nevertheless one cannot conclude based on the data obtained, that the purified proteins are monomeric, dimeric, etc. This is because the variation of predicted molecular weight from sample 14 to 16 decreases from 264 to 94 kDa, (Figure 5.2) thus if one assumes that despite its actual molecular weight (55 kDa) the 94 kDa species is a monomer (based on migration on SDS-PAGE) then the 264 kDa species would be close to a trimeric state. This apparent migration issue for MDM2 is seen independent of the source material from which the protein in question is isolated, MDM2 purified from a prokaryotic expression system is synonymous in the SDS–PAGE migration pattern as the endogenous species from normal and tumourigenic mammalian cell lines. One may therefore assume, considering MDM2s

published propensity to dimerize that the SDS-PAGE solvent conditions (despite their denaturating character) are insufficient to break up the stable quaternary complex thus retaining the investigated protein in a dimeric form. This would explain its observed molecular size, when considering SDS PAGE. Moreover, the studied protein in a less stringent buffer composition (non-denaturating conditions) is likely to adopt structures of higher tetrameric order).

Full elucidation of this fascinating avenue lies beyond the scope of this thesis. Meric state analysis of the human MDM2 oncoprotein should be performed employing a sucrose/glycerol gradient centrifugation analysis technique.

In summary, one should be reminded that oligomeric state deciphering of MDM2 in essence was not the sole purpose of the size exclusion chromatography procedure. Interest was focused on whether various point mutations within the RING domain induce destructive (high order oligomers) aggregate-prone species, and whether the purification system to isolate the protein of interest may induce similar unwanted properties. Hence this assay provides satisfactory answers to both of these questions. All of the purified MDM2 species have access to the porous nature of the Superose 6 matrix and none of them elute within the void volume. Thus supporting the notion that increased affinity of MDM2 to p53 is dependent on the state (amino acid composition) of the RING domain.

5.2.2 Intrinsic Fluorescence profile of MDM2 is responsive to mutations within its RING domain

To investigate whether the Cys mutations within the RING may have a long range effect on the global conformation of the protein, yielding it more of an attractive binding partner to p53, the fluorescence properties of the isolated MDM2 species were investigated. Although all aromatic amino acids can contribute to protein fluorescence, tryptophan is the dominant intrinsic fluorophore. MDM2 contains a total of 4 tryptophan residues (Figure 5.4 Panel A) located in the central region of the protein in and around the central, acid domain. These residues will contribute unequally to the total emission spectrum, as emission reflects the average

environment surrounding a given tryptophan residue. For tryptophan in an apolar environment a blue-shifted (i.e. shorter value of λ_{max}) spectrum is observed. Under native conditions this occurs for a protein when its tryptophan residues are buried within the core structure thus being shielded, less mobile and less exposed to energy dissipating interactions with other residues of the protein or buffer. As the tryptophan residue becomes hydrogen bonded or exposed to buffer, the emission spectrum shifts to longer wavelengths (i.e. red-shift) and usually is accompanied by a decrease in the quantum yield, due to the above mentioned interactions. Hence the variations in tryptophan emission are due to the structure of the protein. The emission maximum and quantum yield of tryptophan can vary greatly between proteins. Denaturation of proteins results in similar emission spectra and quantum yields for the unfolded protein. One might expect that proteins that display blue-shifted emission spectrum will have higher quantum yields (Q) or lifetimes (τ). Such behaviour is expected from the usual increase in quantum yield when a fluorophore is placed in a less polar solvent (Lakowicz et al., 1992; Lakowicz and Weber, 1973)Lakowicz, 2004 #32489}(Gryczynski et al., 2003; Lakowicz, 2000).

There are several factors that determine the emission for tryptophan residues;

- Quenching by proton transfer by nearby charged amino groups
- Quenching by electron acceptors such as protonated carboxyl groups
- Electron transfer quenching by disulfides and amides
- Electron transfer quenching by peptide bonds in the protein backbone
- Resonance energy transfer among tryptophan residues
- Tryptophan dipole moment shielding by water molecules that form the first solvation layer surrounding the exposed amino acid moiety on the surface of the protein

For example, even a single hydrogen bond can eliminate the emission spectra of indole (i.e sensitivity to small changes in the local environment). The mentioned interactions are strongly dependent on distance especially the rate of electron transfer rate, which decreases exponentially with distance. The rates of electron transfer and resonance energy transfer can be large, so that some tryptophan residues may be essentially non-fluorescent. Trp-Trp resonance energy transfer can be expected in proteins, particularly if some of the residues display a blue shifted emission. Energy

resonance transfer is also possible among residues present on two monomer subunits building the quaternary holocomplex.

Initial experiments were carried out to set the optimum concentration of MDM2 showing a representative fluorescence emission spectrum within the sensitivity threshold of the spectrofluorometer used (Figure 5.4 Panel B). Panel C of Figure 5.4 represents all the MDM2 species investigated in this assay.

The following figure compares the emission fluorescence spectrum of MDM2 wt with the two Cys mutants (Figure 5.5 Panel A, B). For both of the mutant proteins we observe a red shift with λ_{max} at 349-349.5 nm in comparison to the emission spectrum of the wt protein of λ_{max} at 343 nm. Moreover the differential quenching of tryptophan fluorescence (difference in their quantum yield) for the two Cys mutants indicates that their conformation changes are not equivalent. This may not be attributed solely to the burial of tryptophan residues as it is also likely to reflect interactions with surrounding residues. In other words, changes in the fluorescence spectrum can arise as a result of subtle changes in the trypotophan's microenvironment. The data showing differences in conformation between wt and mutant forms of MDM2 demonstrate that the RING domain mutations do not produce an equal affect on MDM2 conformation. Moreover, they are consistent with differential binding affinity of the Cys^{464A} and Cys^{478S} mutants for BOX-I and Nutlin-3 (Chapter 4). Considering the Ile^{440A} mutation within MDM2 introduced initially in Chapter 3, one observes a strong correlation of its fluorescence emission spectrum to the wt counterpart, with an almost overlapping spectrum (Panel C Figure 5.5) with a negligible blue-shift. As presented before the $MDM2^{I440A}$ mutant shows an E3 ubiquitin ligase dead phenotype, most probably due to its lack of interaction with the E2 conjugating enzyme. Its zinc coordinating residues, within the RING domain, remain unaffected. This provides further evidence that disruption of the zinc coordination scheme within the C-terminus of MDM2 consistently affects its global perturbation in effect resulting in increased affinity of the N-terminal pocket of MDM2 towards p53 and analogous ligands. (As of writing this thesis the gel filtration profile of $MDM2^{I440A}$ was unavailable, yet performed later it showed the same elution profile as the wild type species).

The increased affinity towards the p53 BOX-I peptide by the Cys^{464} and Cys^{478} indicates a gain in conformational affinity of their hydrophobic cavity towards p53, this more efficient binding may allosterically induce both of the proteins in question to interact better through the secondary interaction site. Moreover the specific Cys mutations within the RING of MDM2 may 'transmit' their effect on the hydrophobic pocket in *cis* through the central region of MDM2 encompassing the acid domain which forms the molecular basis within MDM2 for interacting with p53 (Shimizu et al., 2002).

In summary, one can hypothesize whether RING generated conformational changes in MDM2 are transmitted to the hydrophobic pocket through the central domain. End point kinetic assays have shown (ELISA- presented in Chapter 4) that the two Cys mutations within the RING domain of MDM2 possess a higher affinity towards the secondary binding site represented in the form the p53 BOX-V domain peptide and Rb-1 peptide. As the p53 BOX-V motif itself lacks any tryptophan residues and as the fluorescence emission spectrum is not significant in contrast to BOX-I and its binding interface within MDM2 is closely located to the tryptophans of MDM2. The potential of the peptide was investigated in terms of a specific effect on the fluorescence emission spectrum of MDM2 and one of the Cys mutants (Initially the Cys^{464A} was investigated) presented in Figure 5.6. The peptide was preincubated with the protein as shown in the figure and spectral analysis was performed. In both cases ($MDM2^{WT}$ and $MDM2^{C464A}$ mutants alike) the addition of the peptide in a dose dependent manner induces a blue shift in the spectrum with an appropriate increase in the quantum yield indicating a BOX-V dependent specific effect on the microenvironment surrounding the tryptophans within the protein. A control was used in this experiment (data not shown) involving a non specific tryptophan free peptide moiety clearly highlighting the specific nature of the BOXV :MDM2 interaction. Comparing the spectral curves presented on Panel B, C (Figure 5.6) in more detail, one notices that the peptide induced blue-shift for the Cys^{464A} mutant spectrum is greater in terms of wavelength change than for the wild-type form. Considering the fluorescence emission spectrum for the Cys^{464A} mutant where the BOX-V peptide was added, one can notice a blue shift of λ_{max} to the region coinciding with the longest wavelength of the wild-type protein. Addition of the

peptide forces the MDM2 mutant to adopt a conformation, or at least the close surroundings of the tryptophan residues similar to that of wild type.

5.2.3 Thermal denaturation of MDM2 reveals further insights into inner domain cross-talk

Tryptophan based intrinsic fluorescence of the isolated MDM2 proteins, presented above, highlights their conformational differences dependent on the integrity of the zinc binding motif within the MDM2 RING domain. Moreover the two Cys mutants, which are inactive as E3 ubiquitin ligases and show a higher degree of affinity towards p53 in vitro and in cell based assays, are divergent when it comes to their fluorescence emission spectra hinting at the diverse structure of the two proteins. To further peruse this notion the extent of global unfolding for the studied MDM2 mutants was measured using a fluorescence based thermal shift/denaturation assay. The results presented in Figure 5.7 depict fluorescence intensity as a function of temperature. As mentioned in the introduction to this chapter a specific marker dye was used exhibiting a higher quantum yield in hydrophobic surroundings, hence as protein unfolding is driven by the increase in temperature, the recorded fluorescence will increase until reaching a plateau, following which the signal drops due to protein aggregation.

Considering Figure 5.7 Panel A and B alike, one striking feature can be noticed; the presence of nucleotide (ATP) in the protein mixture undergoing thermal denaturation has a strong positive correlation to the inflection of the curve recorded, highlighting strong exposition of hydrophobic patches within the assayed proteins. This occurrence was not recorded for the behaviour of fluorescence emission spectra presented earlier. This exciting data is reproducible within the concentration range of the protein used in the assay and although exciting should still be considered as preliminary due to the fact the fluorescence values recorded in the presented assays are low. Nevertheless this avenue is open for pursuit, as the scientific field lacks any conclusive data that addresses conformational change of MDM2 protein upon interaction with the ATP nucleotide.

Mutations within the P Walker motif of MDM2 hinder its ATP binding potential yet do not display any decrease in ubiquitin ligase activity, moreover they do not modulate the ability of MDM2 to interact with p53. The $MDM2^{K454A}$ which binds ATP with a much lower efficiency than the wild-type isoform (shown in Chapter 4), displays relatively small ATP dependent differences as its denaturation profile is investigated in the absence or presence of the nucleotide. A different picture is seen for the other protein species investigated. Figure 5.7 indicates that for $MDM2^{WT}$ and the $MDM2^{C464A}$ (Figure 5.7 Panel B), the presence of the nucleotide induces the formation of a sharp transition peak. As stated, the fluorescence intensity measured is proportional to the exposition of hydrophobic patches by the protein. Hence ATP binding by the MDM2 species induces a conformational shift within the protein, leading to a state where the marker dye binds with higher affinity. As it shall be shown later the melting temperature of all the proteins in question does not vary by a great deal, it appears that the presence of the nucleotide has a crucial role in reaching the transition point. Moreover, this transition is not equally comparable for the proteins. Yet again the Cys^{464A} mutant of MDM2 comes to the spotlight, showing a large increase of hydrophobic patch exposition, and once more the non-equivalent nature of the two Cys mutations is underlined (Figure 5.8 Panel A compared to Figure 5.7 Panel B). The $MDM2^{C478S}$ mutant shows a remarkably lower fluorescence signal in contrast to the Cys^{464A} mutant. This phenomenon is most likely sensitive to the state of the zinc binding residues as the $MDM2^{I440A}$ mutant (having all the key zinc coordinating residues intact), shows a nucleotide dependent peak (Figure 5.8 Panel B) that although higher in magnitude than the one for $MDM2^{WT}$, yet still drastically lower than the one for $MDM2^{C464A}$.

Considering the summarized data presented in Figure 5.9 one can observe that the single point mutations within MDM2 alter the melting temperature of appropriate proteins within the interval ΔT_m=1°C where $MDM2^{WT}$ was calculated to have the melting temperature of 55°C. With the Cys^{464A} having the melting temperature at 54°C and the Cys^{478S} at 56°C. The differences in melting temperature recorded for the mutant MDM2 species do not diverge greatly from each other, yet what is noticeable is the differential affinity to the solvatochromatic dye to the protein species investigated (Figure 5.9 Panel A), with the Cys^{464A} mutant in the lead. As all

of the proteins investigated were isolated from a prokaryotic expression system, one could argue that the samples may be differentially contaminated with an impurity leading to artefactual data. This most probably is not the case as the observed ATP 'switch' effect is specific for MDM2 proteins bearing active Walker P motif (with the negative control in the form of $MDM2^{K454A}$). Moreover the final concentration of protein used in this assay was quite low 1 μM, and the results presented were repeated with further dilutions giving similar results.

To fully capitalize and understand these results, one must analyze and consider the MDM2 polypeptide chain in terms of its hydrophobicity, which will be presented and discussed later in this chapter.

5.2.4 Proteolytic digestion of MDM2 reveals conformational changes

To further support the hypothesis that hydrophobic pocket affinity can be modulated by the RING domain, additional evidence of RING-dependent conformational change in full length MDM2 was sought. Partial proteolytic digestion of the protein combined with antibody reactivity may be useful to pinpoint regions within the protein that show a varying profile dependent on the mutation introduced. Limited proteolysis was used to probe for changes in the accessibility of trypsin cleavage sites in the MDM2 Cys mutants versus the wild-type protein. Trypsin (IntEnz Enzyme Nomenclature EC 3.4.21.4) is a serine protease that specifically cleaves at the carboxylic side of lysine and arginine. Restrictions to the specificity of trypsin occur when proline is at the carboxylic side of lysine or arginine; then the bond is almost completely resistant to lysis. Cleavage may also be considerably reduced when acidic residues are present on either side of a potentially susceptible bond (Bode et al., 1978; Bradshaw et al., 1970; Sanders et al., 1970).

Purified wt or mutant MDM2 was incubated with trypsin at a ratio of 100:1 (MDM2/trypsin) for up to 30 min, the reactions were stopped by addition of 1x SDS Sample buffer and the samples were then analysed by gradient SDS-PAGE/immunoblot and cleavage fragments identified using a cocktail of MDM2 monoclonal antibodies (Figure 5.10 Panel B). The results show that the wt protein

rapidly formed (within 5 min) a stable core comprising bands 1, 2 and 3 that was maintained throughout the course of the experiment. Although the $MDM2^{C464A}$ mutant initially formed a similar banding pattern to the wt protein, with bands 1, 2 and 3 being detected, it was then further processed so that by 15 minutes a new stable pattern had emerged comprising bands 2, 3, 4 and 5 with band 1 no longer being detected. Consistent with earlier results the $MDM2^{C478S}$ mutant appeared to be intermediate between wt and the Cys^{464A} protein as at 30 min all 5 bands were readily detected. These results suggest that the Cys^{464A} and Cys^{478S} mutants have a different conformation to the wt protein leading to the exposure of trypsin sensitive cleavage sites that are not accessible in wild-type MDM2.

The experiments presented above, using limited proteolysis and intrinsic fluorescence suggest that the introduction of point mutations in key RING domain Cys residues generates a measurable conformational change in full-length MDM2 protein. In order to establish whether these conformational changes have a direct impact on the structure of the hydrophobic pocket a monoclonal antibody (3G5) was employed which binds to an epitope in the centre of the hydrophobic pocket (Figure 5.11; Panel A (Bottger et al., 1997a)). With limited proteolysis and subsequent probing with the 3G5 antibody one can determine whether changes in the RING domain had an effect on the ability of mentioned antibody to bind to the hydrophobic pocket of MDM2. As a control for this experiment the 2A10 monoclonal antibody was used which has been mapped to two epitopes within the central and C-terminal domains of MDM2 (Figure 5.11; panel A). The results obtained with this antibody suggest that the core fragments identified in Figure 5.10 (in particular bands 2, 3 and 4) are comprised largely of the central domain of MDM2 together with C-terminal truncations. In contrast Figure 5.11 Panel B suggests that the hydrophobic pocket is rapidly cleaved from the core of MDM2 and that its removal generates a fast migrating 3G5 reactive product (band 6). The $MDM2^{C478S}$ mutant appears to be more sensitive to this type of cleavage as 3G5 positive full-length protein is lost more rapidly than it is for wt MDM2. Of particular interest in this assay is the $MDM2^{C464A}$ mutant, as incubation of this protein leads to a dramatic loss of the 3G5 epitope suggesting that the hydrophobic pocket in this protein is more ‘relaxed’ and therefore

more accessible to trypsin digestion during which the 3G5 binding site (amino acids 66-69) is cleaved leading to a loss of the epitope.

Together the data presented in this chapter support the conclusion that the RING domain of MDM2 can influence the activity of the N-terminal hydrophobic pocket by producing long range conformational changes that are transmitted through the central acid core of MDM2 and which in turn lead to varying degrees of relaxation in the hydrophobic pocket.

5.3 Discussion

The primary interaction site for p53 within MDM2 has been the focus of scientific attention for a number of years now, despite the plethora of crystallographic data showing the molecular basis of this interaction recent studies strongly suggest that the N-terminal hydrophobic groove is not a one state rigid entity (Espinoza-Fonseca and Garcia-Machorro, 2008; Espinoza-Fonseca and Trujillo-Ferrara, 2006a). Structural and computational analysis of the MDM2 hydrophobic pocket interaction with p53 has revealed that this domain has a high degree of plasticity and strongly suggests that the shape of the binding cleft can change significantly, underlying the dynamic nature of the p53::MDM2 interaction (Espinoza-Fonseca and Garcia-Machorro, 2008; Espinoza-Fonseca and Trujillo-Ferrara, 2006a). A mechanism has been proposed where binding to the BOX-I domain of p53 requires a progressive opening up of the binding cleft of MDM2 to reveal a hydrophobic interface. An intermediate step is involved in p53::MDM2 complex formation, where the MDM2 cleft gradually adopts a more open conformation eventually accommodating Thr^{18}-Asp^{29} of the p53 BOX-I domain. Based on this type of study it has been hypothesized that the cleft has enough plasticity to allow a range of low-energy states rather that a single 'open' or 'closed' conformation. As a result the pocket can accommodate a range of peptides and small molecules that might not have any obvious structural similarity (Bowman et al., 2007; Espinoza-Fonseca, 2005; Espinoza-Fonseca and Garcia-Machorro, 2008; Espinoza-Fonseca and Trujillo-Ferrara, 2006a; Stoll et al., 2001; Vassilev, 2004). It is likely therefore that the differential binding preferences of the two Cys mutants investigated are a result of different degrees of cavity accessibility. This hypothesis is supported by data showing that although the Cys^{464A}, Cys^{478S} mutant proteins both adopt a different stable conformation from the wild-type protein and that their conformation is not equivalent. The intrinsic fluorescence of tryptophan residues within the central domain of the Cys^{478S} mutant is quenched relative to the Cys^{464A} mutant suggesting that they are more solvent exposed and/or are involved in additional interactions with nearby residues. One can imagine that these two proteins can be in a slightly

different conformation that brings the residue closer or further from a quenching group such as other aromatic residues.

Another plausible notion, though in need of further investigation, is the possible resonance energy transfer between aromatic molecules present in two separate monomers of the protein holocomplex. The RING domain within MDM2 has been shown as the site of dimerization (Kostic et al., 2006; Linke et al., 2008; Maki, 1999). Resonance energy transfer is likely to occur due to the fact that a spectral overlap exists between absorption and emission spectra for all of the fluorescent amino acid residues; Phe, Tyr, Trp. Proteins exhibiting monomeric/dimeric transitions during their life cycle such as interferon-γ, display resonance energy transfer between residues within different subunits of the complex (Boteva et al., 1996). Furthermore site directed mutagenesis studies of proteins bearing several tryptophan residues highlights the fact that fluorescence resonance energy transfer can occur also within discreet subunits building the holocomplex of the protein (Meagher et al., 1998). Thus, the lower quantum yield in the fluorescence emission spectrum of $MDM2^{C478S}$ can be attributed to a divergence in its conformational state in comparison to the $MDM2^{WT}$ and the other Cys mutants $MDM2^{C464A}$. Size exclusion chromatography presented in this chapter indicates that all of the investigated proteins posses similar properties, hence a decrease in the quantum yield observed for the $MDM2^{C478S}$ mutant in comparison to the fluorescence emission spectra for all the other investigated MDM2 proteins cannot be easily explained by differences in the quaternary structure of this mutant. Moreover data presented in Chapter 3, focusing on cell based ubiquitination assays, suggest that the mutant is able to hetero-dimerize (with endogenous wild-type MDM2) giving rise to ubiquitinated p53 species in a cell based system.

To date no structural data is available regarding the full length MDM2 protein giving relative distances between the numerous domains within the macromolecule. The spectral data provided by the fluorescence emission spectra of the discussed Cys MDM2 mutants does not directly postulate that the substitution of cysteine physically affects the environment of the tryptophan molecules topologically located within the central part of the protein, thus affecting its spectral properties. What it does illuminate is the fact that structural cross talk between domains is possible. This

is strongly supported by the experimental data presented in Figure 5.6, where the addition of the p53 BOX-V domain peptide (representing the secondary interaction site within p53 binding to the acid domain of MDM2), shifts the spectrum of the $MDM2^{C464A}$ mutant to that of $MDM2^{WT}$. The BOX-V peptide::MDM2 Cys^{464A} interaction thus forces the protein to revert back to the conformation of the wild type species.

Experimental data from MDM2 thermal denaturation analysis further supports this notion. This assay measures protein unfolding as the propensity of a given protein to expose its hydrophobic surface dependent on environmental temperature influx. In light of the proposed hydrophobic collapse model for polypeptides, the process of protein folding leading to the native protein conformation consist of an early step which is the rearrangement of the nascent polypeptide to a compact collapsed structure (Brylinski et al., 2006; Dill et al., 1995). Hydrophobic collapse ensues the formation of a molten globule therefore constituting an early step in the folding pathway. The energy state of the molten globule is lower than that of the denatured state, yet higher than that of the native state - that is, within the energy landscape well of the folding funnel (Borgia et al., 2008) but not yet close to the energy minimum. This is believed to occur prior to the formation of secondary structures and native contacts present in the tertiary structure of the protein. Forced reversal of this process induced by energy increase to the system by means of temperature flux, gives rise to the to the exposition of the hydrophobic core consisting of nonpolar aromatic and aliphatic amino acid residues.

The hydrophobic profile of human MDM2 protein was investigated by means of readily available *in silico* algorithms, giving each amino acid within the primary structure of the protein a numerical value (score) directly proportional to its hydrophobic nature. Four independent sets of score matrices were used to obtain a synergy depicting hydrophobic hot spots within MDM2 (Figure 5.12). High scores were noted for residues building the N-terminal binding site for p53, a small central region, and the residues within the C-terminus topologically within the RING domain. Thus, the increase of hydrophobic exhibition by MDM2 induced by nucleotide (ATP) addition to the reaction can be explained not only by conformational changes in and around the site of nucleotide binding the RING

domain, but also by differential involvement of the other hydrophobic sites located further away within the protein. Currently it is unknown whether there is a preference for which hydrophobic patch to be exposed earlier than the other, hence all of them should be should be taken to account as contributors to the denaturation profile of MDM2. What one can conclude from the presented data is that mutations within key Cys residues of the RING alter the denaturation profile of the protein in comparison to the wild-type species. Again the mutations do not give an equivalent phenotype, where the Cys^{464A} mutant is seen to have a significantly larger exposition of hydrophobic residues over the wild-type protein and the Cys^{478S} mutant displays a decrease. This cannot be solely explained by a differential exposition of the residues within the N-terminal hydrophobic cavity of MDM2 as other parts of the protein have similar qualities, and as shown in the previous two chapters both of the mutants display a preferential affinity towards p53. What it does show is that substitutions within key residues of the RING domain perturb the polypeptide backbone in which they are present differentially. Moreover, this technique once again shows that discrete functions within the RING domain can be uncoupled. As the shape of the melting curves was dependent on the presence of ATP in the sample undergoing denaturation, and no such effect was observed for the $MDM2^{K454A}$ mutant with impaired nucleotide binding ability.

Limited proteolysis experiments can be successfully used to probe for conformational features of proteins. It has been demonstrated that the sites of limited digestion along the polypeptide chain of a protein are characterized by enhanced backbone flexibility, implying that proteolytic probes can pinpoint the local sites of conformational fluctuation in a protein chain (Fontana et al., 2004).

Further evidence for a difference in the conformation of the hydrophobic cleft dependent on the status of the RING domain comes from the use of the 3G5 monoloclonal antibody to probe for differences in conformation following limited tryptic digestion. This antibody recognises an epitope in the hydrophobic pocket of MDM2 where residues $^{66}LYDE^{69}$ are essential but not sufficient for binding i.e peptides containing the LYDE motif but not other surrounding residues are not sufficient for antibody recognition (Bottger et al., 1997a). The LYDE motif maps to

a loop structure in the hydrophobic pocket that lies between two of the α-helical structures that form the BOX-I binding cavity (Figure 5.13) and is flanked by lysines and arginine residues that provide tryptic cut sites when exposed (^{61}IMTKRLYDEKQQHIV^{75}). The data presented in this chapter hints that the cleft is more accessible in the Cys^{464A} mutant than in the wt or the Cys^{478S} protein, suggesting that the cleft is more relaxed and therefore more readily accommodate the p53 BOX-I peptide leading to increased affinity.

In conclusion, by generating mutations within the C2H2C4 RING domain of MDM2 an allosteric modulation of affinity and specificity of the hydrophobic pocket is observed. Thus indicating the importance of the mentioned domain in native cell surroundings for interactions with numerous protein binding partners and small molecule ligands (Zn^{2+}, ATP). The effect of which will be differential control of the transrepressor potential of the MDM2 oncoprotein, and efficiency of pocket binding drugs in tumour cells.

5.4 Figures

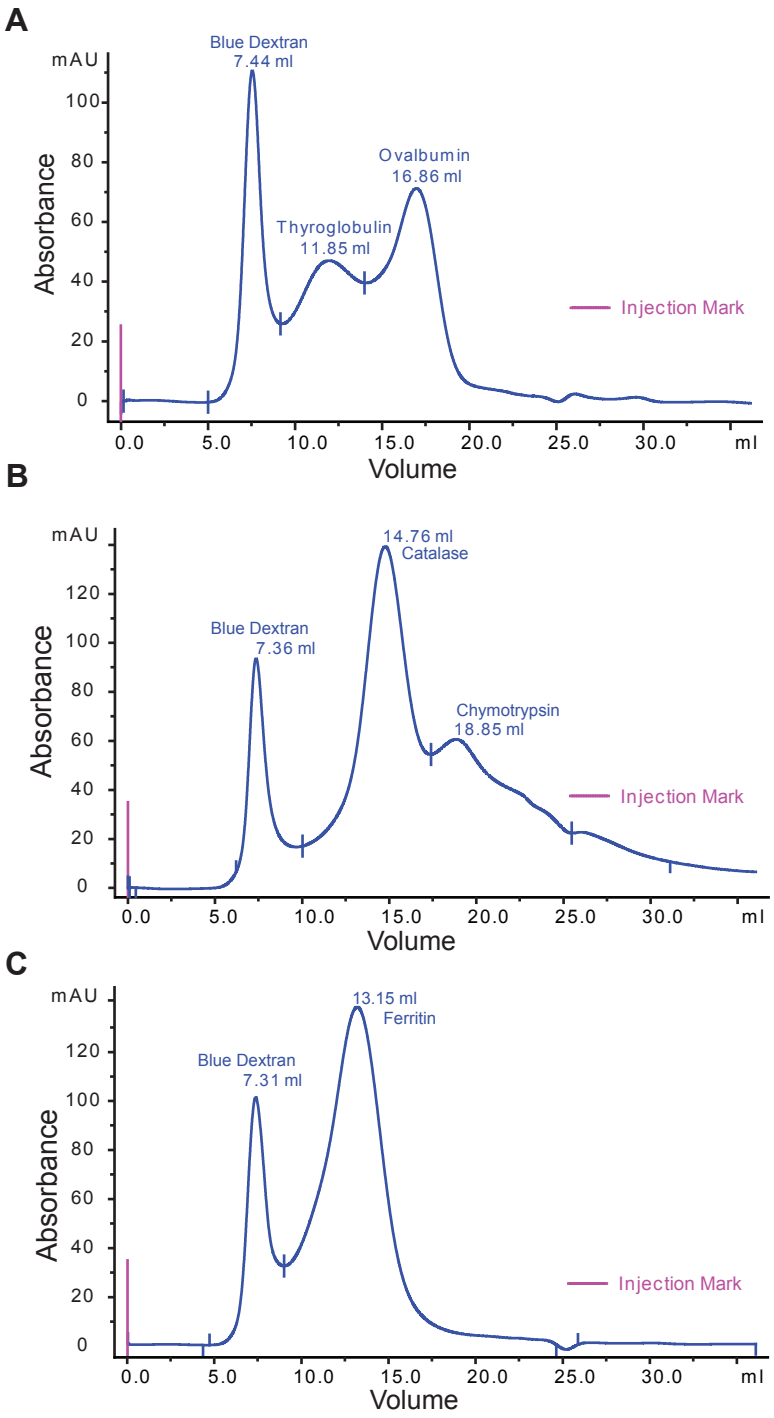

Figure 5.1 Elution profile of molecular weight standards applied to Superose® 6 10-300 GL column

Chromatograms presented above show the variation in concentration (UV Absorbance at A_{280}nm) of sample components as they elute from the column in order of their molecular size. Blue Dextran for all the chromatograms above was used to calculate the void volume - (V_0) of the column. The protein standards used with partial access partial access to the pores of the matrix elute from the column in order of decreasing molecular size. The molecular weight of the standards in a decreasing is as follows; M_W (Thyroglobulin) > M_W (Ferritin) > M_W (Catalase) > M_W (Ovalbumin) > M_W (Chymotrypsin). Elution volume in mililiters shown next to appropriate elution peak.

Blue Dextran	V_0 [ml]	Averaged-V_0 [ml]	V_t [ml]
	7.31	7.37	24
	7.36		
	7.43		

	M_w [kDa]	log M_w	V_e [ml]	K_{av}
Thyroglobulin	669	2.83	11.85	0.270
Ferritin	440	2.64	13.15	0.348
Catalase	232	2.37	14.76	0.444
Ovalbumin	44	1.64	16.86	0.571
Chymotrypsin	25	1.40	18.85	0.690

V_0 - void volume
V_t - total column volume
V_e - elution volume
K_{av} - distribution coefficient

$$K_{av} = \frac{V_e - V_0}{V_t - V_0}$$

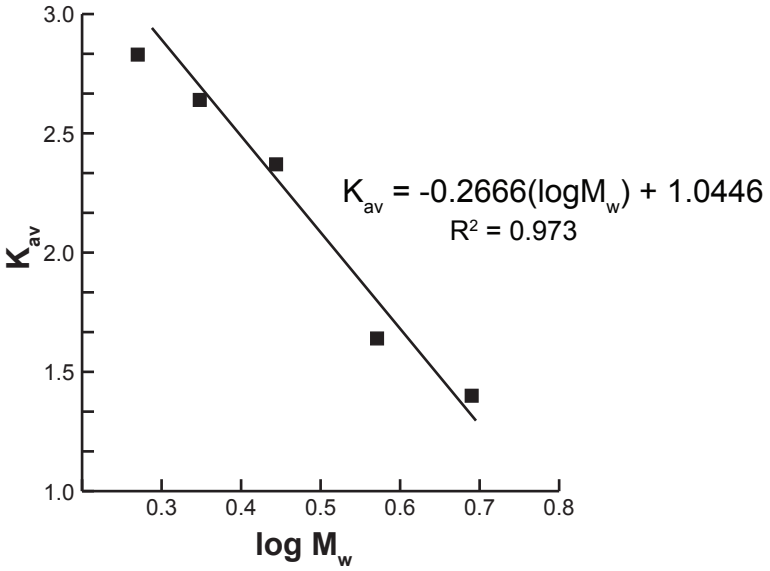

fractions	11	12	13	14	15	16	17	18
ml	11	12	13	14	15	16	17	18
K_{av}	0.218	0.279	0.339	0.399	0.459	0.519	0.579	0.639
Mw [kDa]	1256	747	445	264	157	94	56	33

Figure 5.2 Molecular weight determination for fractions collected

The relationship between molecular weight [M_w] of the protein standards, and their partition coefficient K_{av} was established. The equation obtained via linear regression depicts a linear relationship between K_{av} and M_W. Basing on this predicted molecular weight was calculated for the fractions collected upon passing through the Superose 6 column.

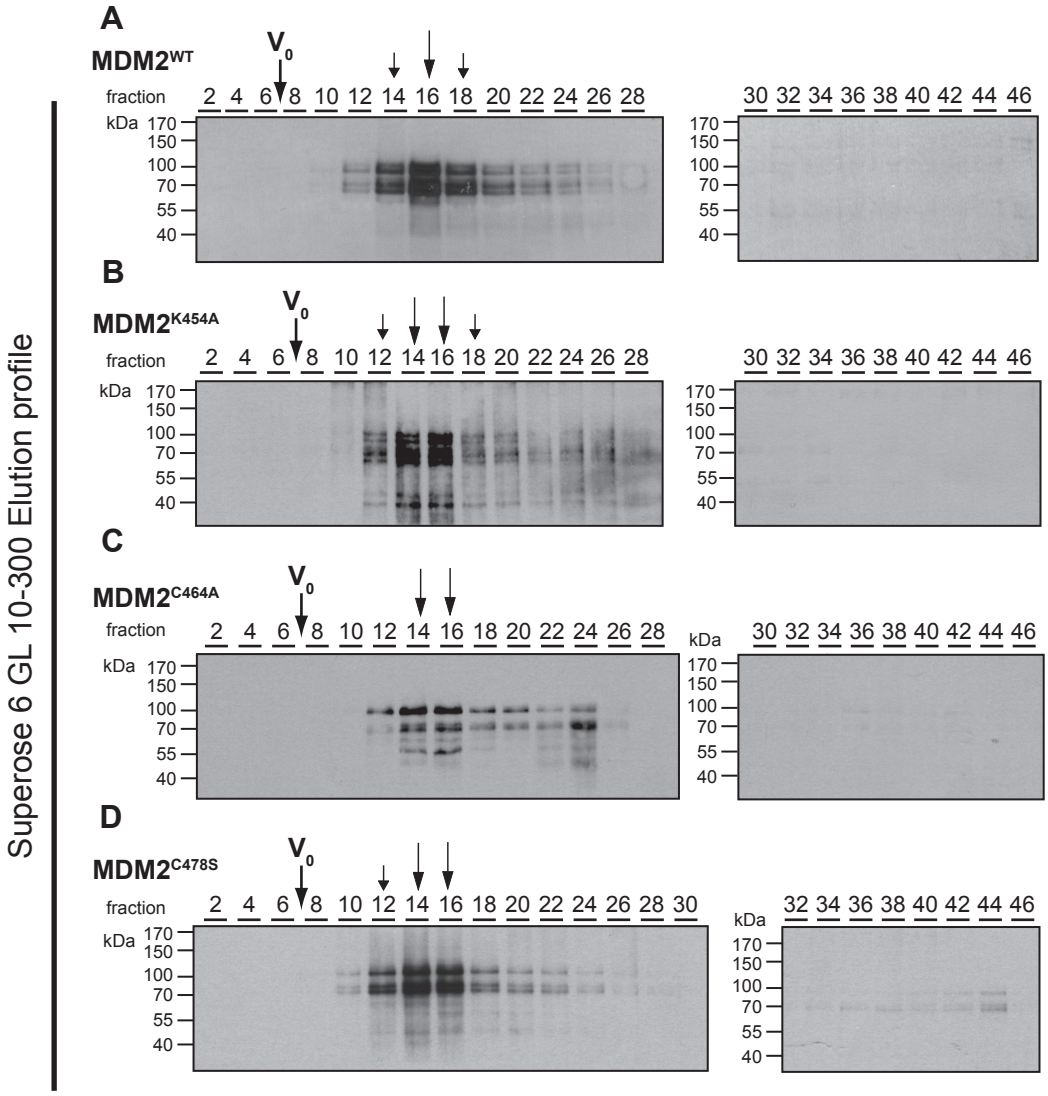

Figure 5.3 Mutations within the RING of MDM2 domain do not induce aggregation of the purified protein species.

Equal amounts of MDM2^{WT} (180 µmol) and all the studied RING domain mutants were subjected to size exclusion chromatography. The amount of buffer passed through the column was 1.5 column volume (25 mM Hepes pH 7.6 50 mM KCl 5% Glyc 10 µM $ZnSO_4$ 3 mM DTT), 1 ml fractions were collected, void volume (V_0) is indicated for each of the elution profiles above. Every second fraction from the elution was analyzed by means of 10% SDS PAGE (50 µl of sample loaded) and visualized by immunoblotting (2A10 Ab). Arrows indicate the peak fractions where MDM2 was most prominent.

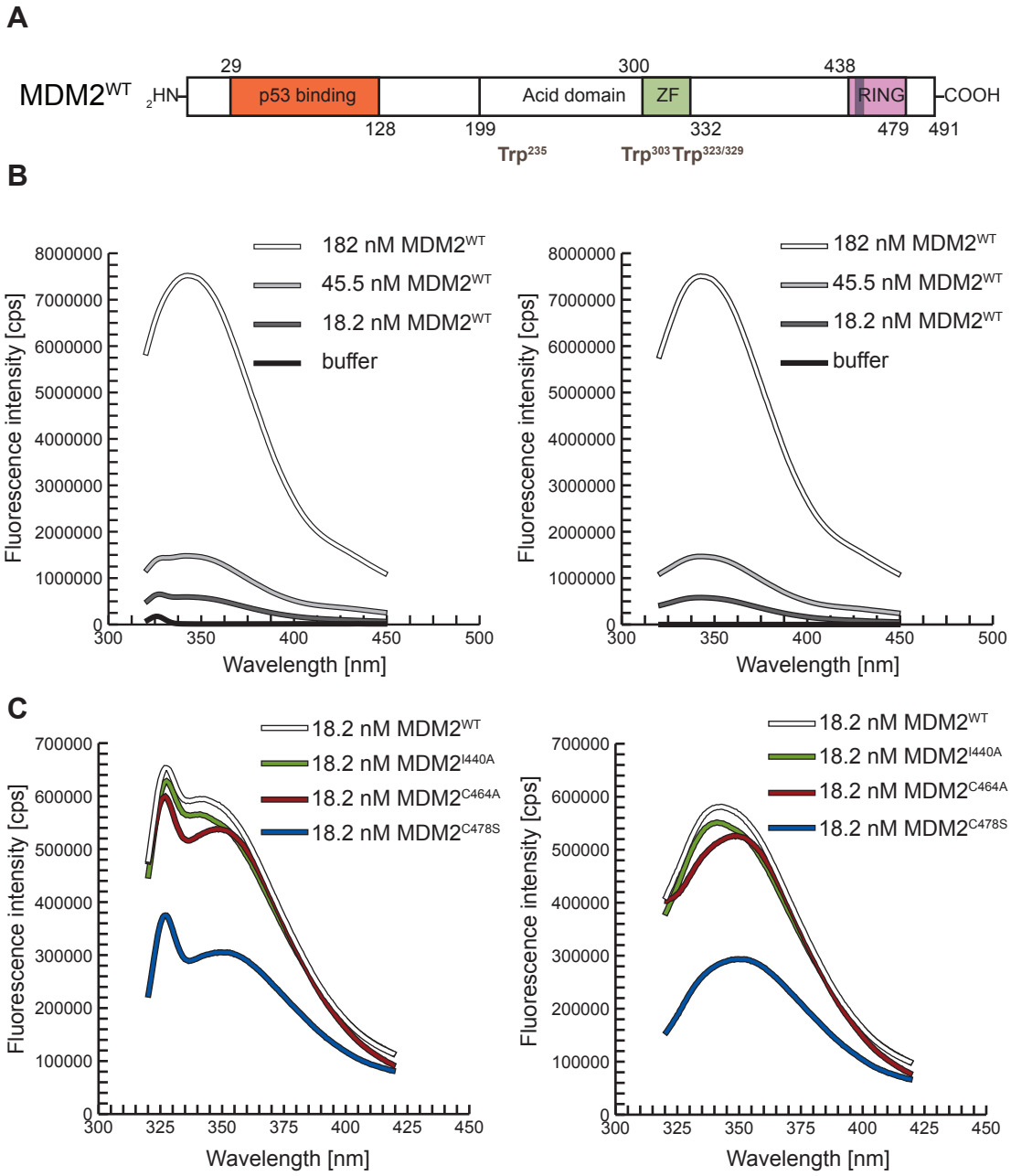

Figure 5.4 Fluorescence emission spectra of MDM2

Resolution of fluorescence emission spectra of MDM2. Intrinsic fluorescence measured with 295 nm excitation. For both of the graphs on the right of the figure, spectra were corrected for associated buffer background signals.
(**A**) Schematic representation of tryptophan residue localization within the primary structure of MDM2
(**B**) The quantum yield, of the emission spectrum is proportial to concentration of the investigated protein. Initial titration of MDM2 aimed at setting up the optimal window for experimentation. The spectrofluorometer used gives valid readings up to $3x10^6$ cps.
(**C**) The behaviour of the fluorescence emission spectra is dependent on key single point mutations within the C-terminal RING domain.
Graphs on the left represent spectra with background buffer dependent signal, the graph on the right represents values corrected for that. $MDM2^{WT}$ shown in white, $MDM2^{I440A}$ in green, $MDM2^{C464A}$ in brown and $MDM2^{C478S}$ is depicted in blue.

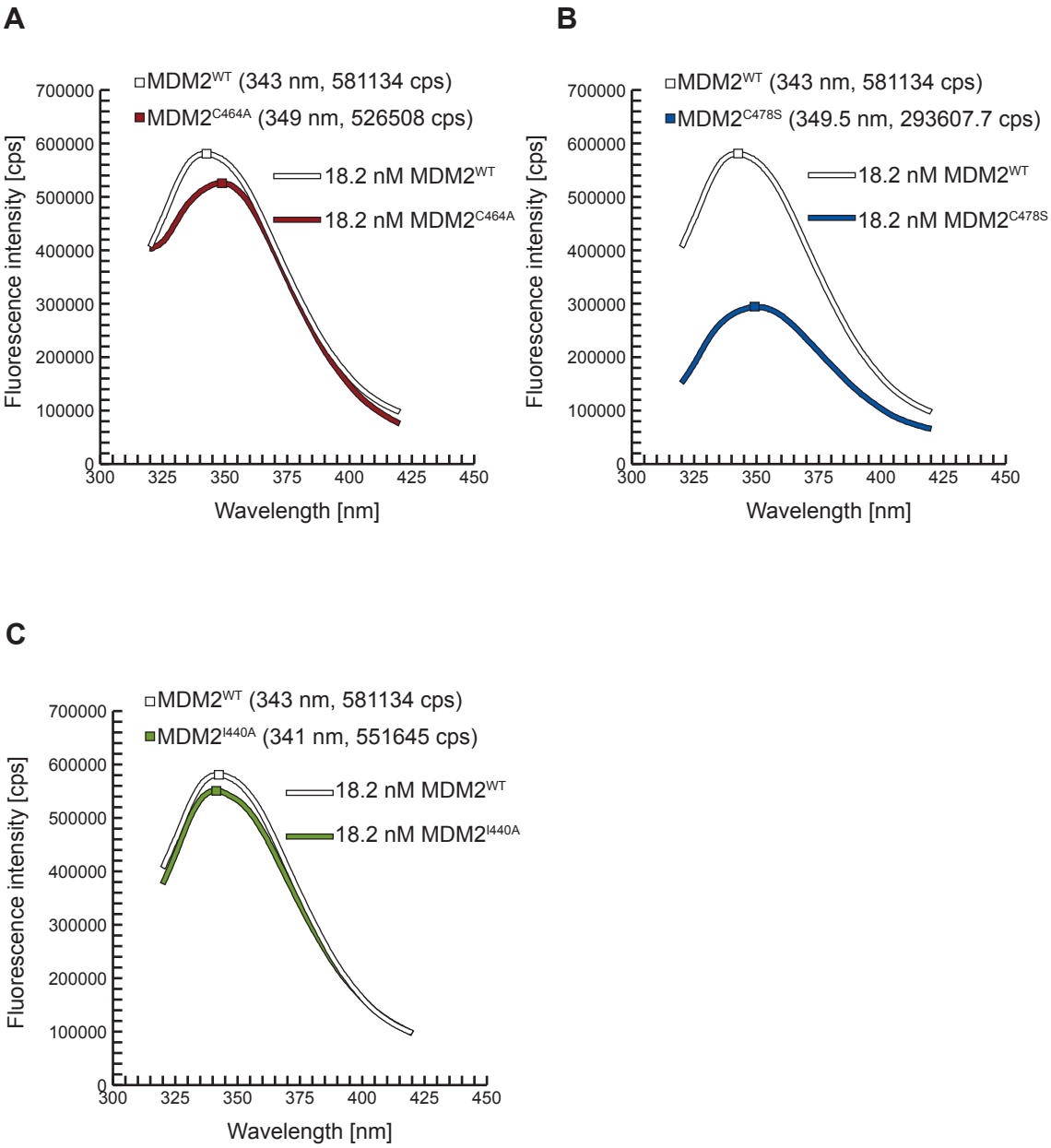

Figure 5.5 Resolution of fluorescence emission spectra of analysed MDM2 mutants with regards to wild-type MDM2.

(**A**) (**B**) (**C**) Intrinsic fluorescence measured with 295 nm excitation. Emisssion was recorded from 320 to 425 nm in 0.5 nm steps, with an integration time of 1 s. The spectra were corrected for associated buffer background signals. Maxima are indicated with shaded boxes on the spectra, with corresponding wavelength. The values were calculated with n-polynomial based algorithm, where R2≥0.999. $MDM2^{WT}$ shown in white, $MDM2^{I440A}$ in green, $MDM2^{C464A}$ in brown, and $MDM2^{C478S}$ is depicted in blue.

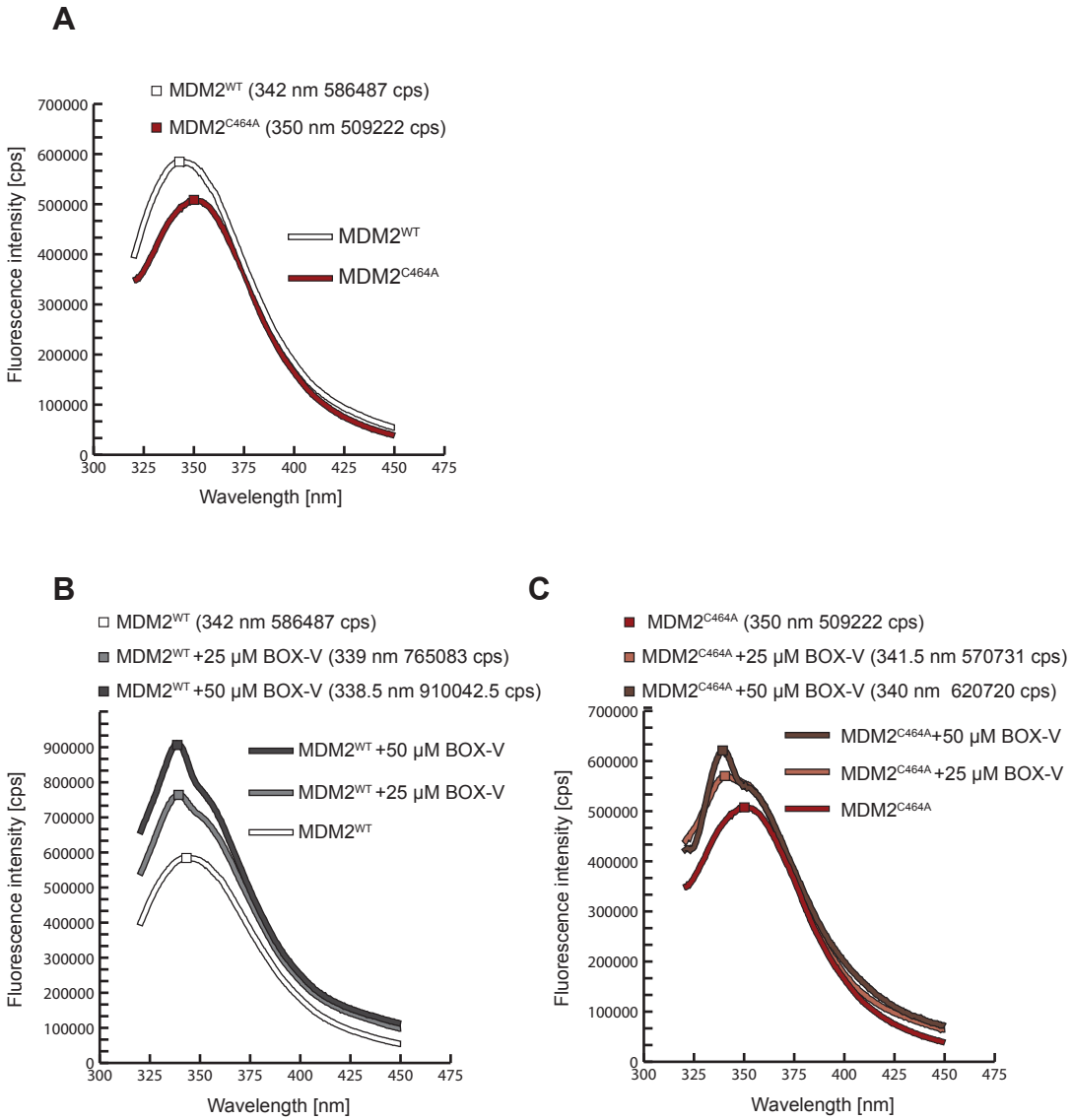

Figure 5.6 The contribution of the acid domain to MDM2 intrinsic fluorescence

(**A**) (**B**) (**C**) The protein samples analysed were preincubated without or with increasing amount of BOX V peptide. Intrinsic fluorescence measured with 295nm excitation. Emisssion was recorded from 320 to 475 nm in 0.5 nm steps, with an integration time of 1s. The spectra were corrected for associated protein buffer, peptide solvent background signals. Maxima are indicated with shaded boxes on the spectra, with corresponding wavelength. The values were calculated with n-polynomial based algorithm, where $R^2 \geq 0.999$. $MDM2^{WT}$ shown in white, $MDM2^{C464A}$ in brown. Data presented in this figure was obtained in cooperation with Dr. Susanne Pettersson.

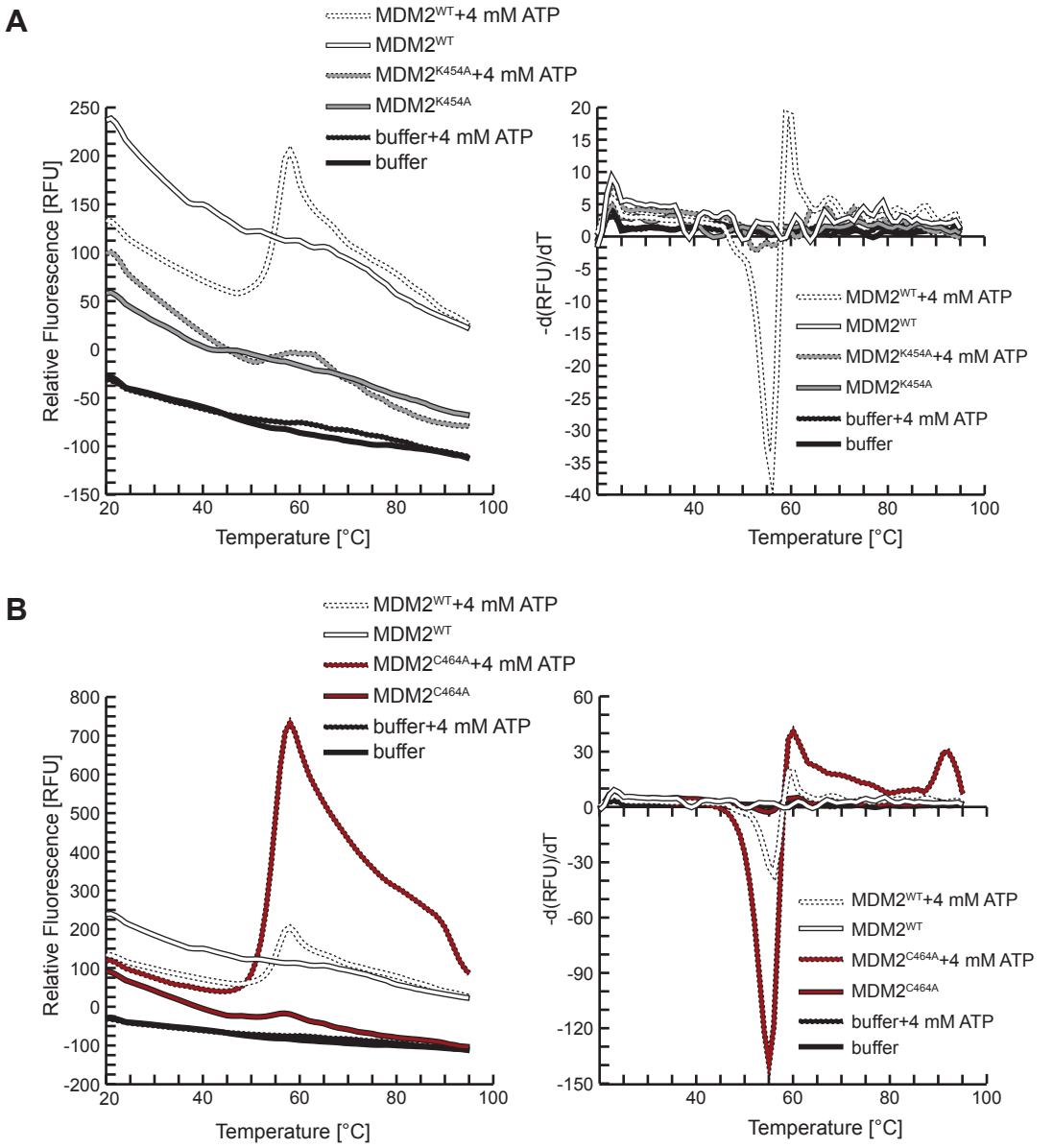

Figure 5.7 Thermal Denaturation of MDM2

Temperature driven MDM2 unfolding transition is ATP dependent. A stepwise temperature gradient was used from 20 °C to 95 °C (1 °C/min steps). A solvatochromatic dye was used as an indicator of protein unfolding that has a low-fluorescence quantum yield in buffer alone. Partitioning of the dye into melted protein results in a significant increase in fluorescence. Sypro Orange used as the protein dye was diluted to the final concentration of 5x.
(A) $MDM2^{WT}$ and $MDM2^{K454A}$ mutant protein (1 µM final concentration) were incubated either in the presence or absence of 4 mM ATP as indicated. $MDM2^{WT}$ shown in white, $MDM2^{K454A}$ depicted in grey, buffer alone in black.
(B) $MDM2^{WT}$ and $MDM2^{C464A}$ mutant protein (1 µM final concentration) were incubated either in the presence or absence of 4mM ATP as indicated. $MDM2^{WT}$ shown in white, $MDM2^{C464A}$ shown in brown.
Graphs for both Panels positioned on the left, represent fluorescence intensity measured as a function of temperature. Panels on the right represent the negative rate of change of fluorescence with respect to temperature. The minima of these functions are indicative of the point of inflection of the corresponding curves to the left, thus revealing the melting temperature of the protein sample.

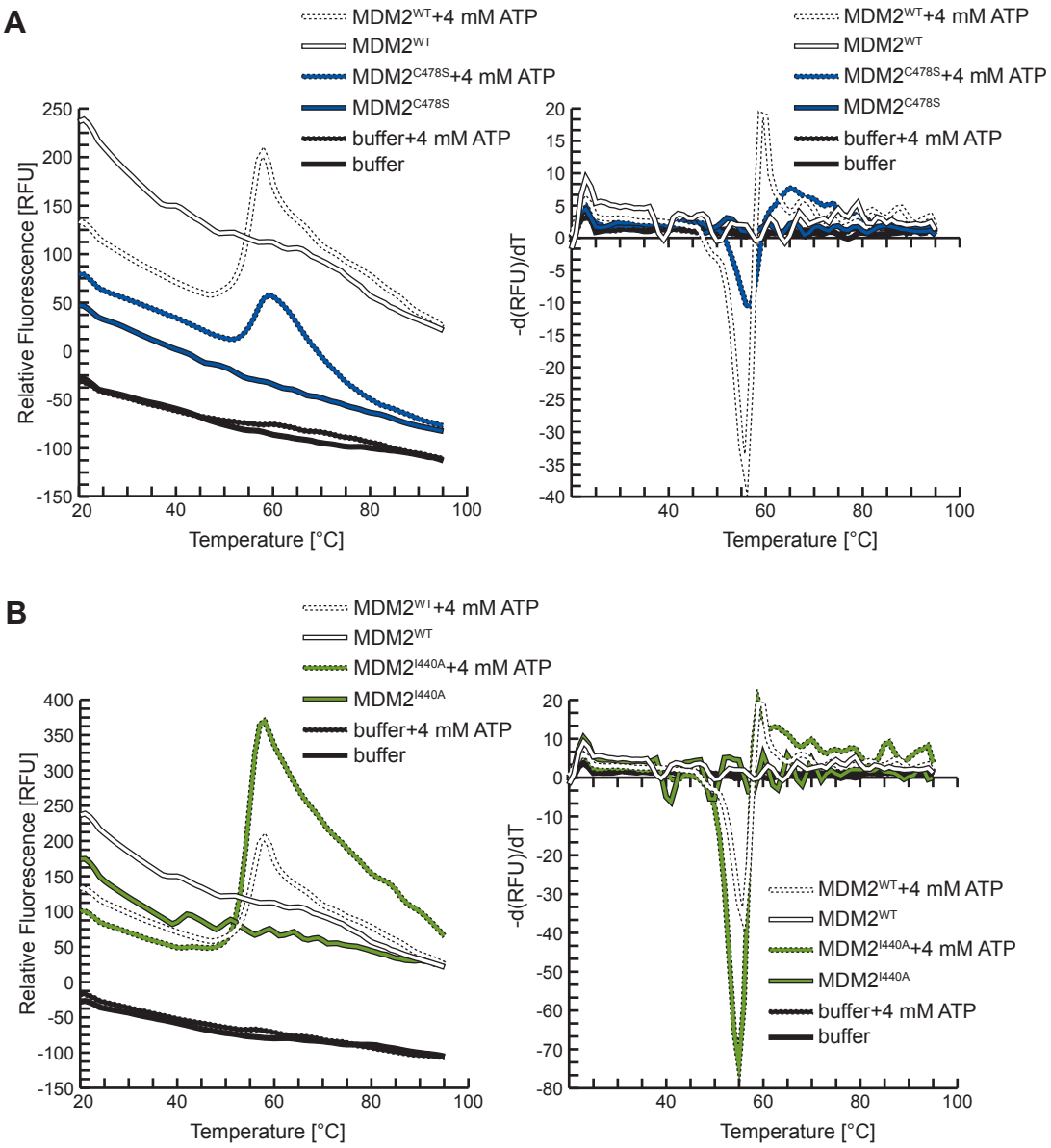

Figure 5.8 Thermal Denaturation of MDM2 continued

Temperature driven MDM2 unfolding transition is ATP dependent. A stepwise temperature gradient was used from 20 °C to 95 °C (1 °C/min steps). A solvatochromatic dye was used as an indicator of protein unfolding that has a low-fluorescence quantum yield in buffer alone. Partitioning of the dye into melted protein results in a significant increase in fluorescence. Sypro Orange used as the protein dye was diluted to the final concentration of 5x.
(A) $MDM2^{WT}$ and $MDM2^{C478S}$ mutant protein (1 µM final concentration) were incubated either in the presence or absence of 4mM ATP as indicated. $MDM2^{WT}$ shown in white, $MDM2^{C478S}$ depicted in blue, buffer alone in black.
(B) $MDM2^{WT}$ and $MDM2^{I440A}$ mutant protein (1 µM final concentration) were incubated either in the presence or absence of 4mM ATP as indicated. $MDM2^{WT}$ shown in white, $MDM2^{I440A}$ shown in green.
Graphs for both Panels positioned on the left, represent fluorescence intensity measured as a function of temperature. Panels on the right represent the negative rate of change of fluorescence with respect to temperature. The minima of these functions are indicative of the point of inflection of the corresponding curves to the left, thus revealing the melting temperature of the protein sample.

A

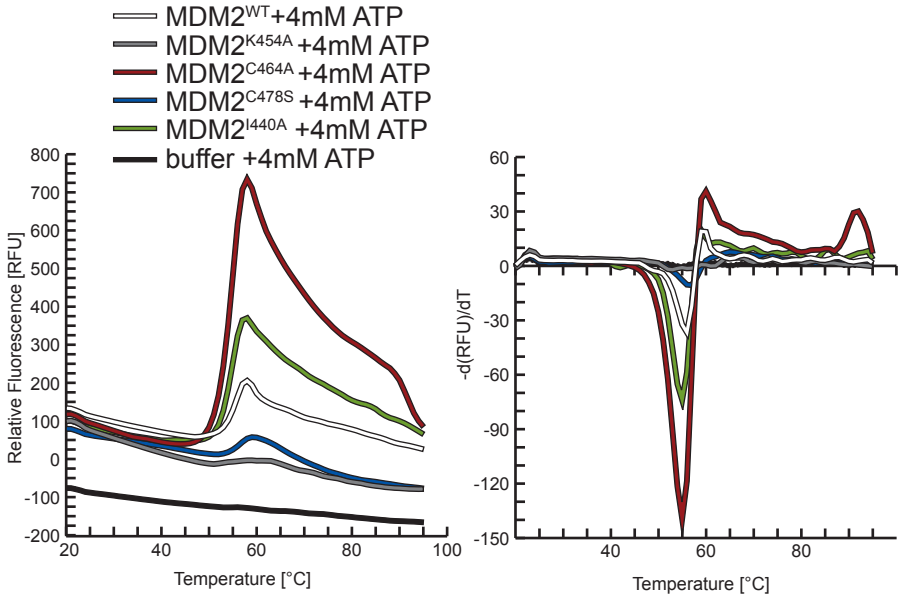

B

protein	Melting temperature T_m [°C]
MDM2^{WT}	**55**
MDM2^{K454A}	**54**
MDM2^{C464A}	**54**
MDM2^{C478S}	**56**
MDM2^{I440A}	**54**

Figure 5.9 Thermal Denaturation of MDM2 summarized

(A) Figures represent melting transitions for MDM2 proteins indicated in the presence of 4 mM ATP. Panels on the left represent fluorescence intensity measured as a function of temperature. Panels on the right represent the negative rate of change of fluorescence with respect to temperature. The minima of these functions are indicative of the melting temperature of the protein sample. MDM2^{WT} shown in white, MDM2^{C464A} in brown, MDM2^{C478S} in blue, MDM2^{I440A} in green and MDM2^{K454A} is depicted in grey.
(**B**) The calculated melting temperatures of MDM2 wild-type and all the mutants specified.

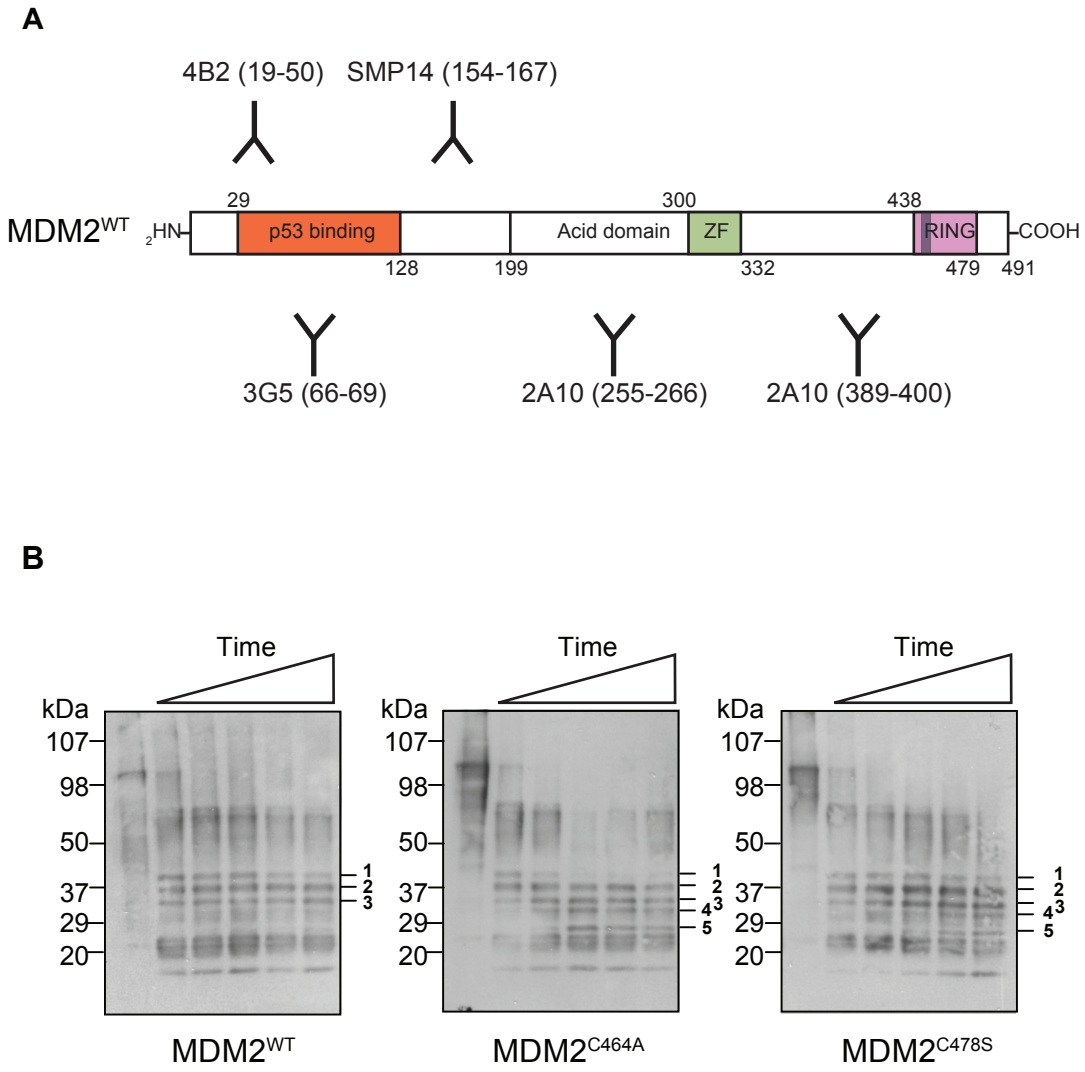

Figure 5.10 Partial proteolytic digestion of MDM2

(**A**) Schematic representation of MDM2 showing the epitopes for 3G5, 4B2, SMP14 and 2A10 antibodies in human MDM2 protein.
(**B**) Immunoblot showing wild-type or mutant forms of MDM2 following limited proteolysis with trypsin and SDS PAGE on a precast 4-12% gel. The blot was developed using a mixture of the MDM2 monoclonal antibodies 2A10, 4B2, 3G5 and SMP14. The numbers are used to label the banding pattern. The time points used were 0, 5, 10, 15, 20 and 30 min. Data presented in this figure was obtained in cooperation with Prof. Kathryn Ball.

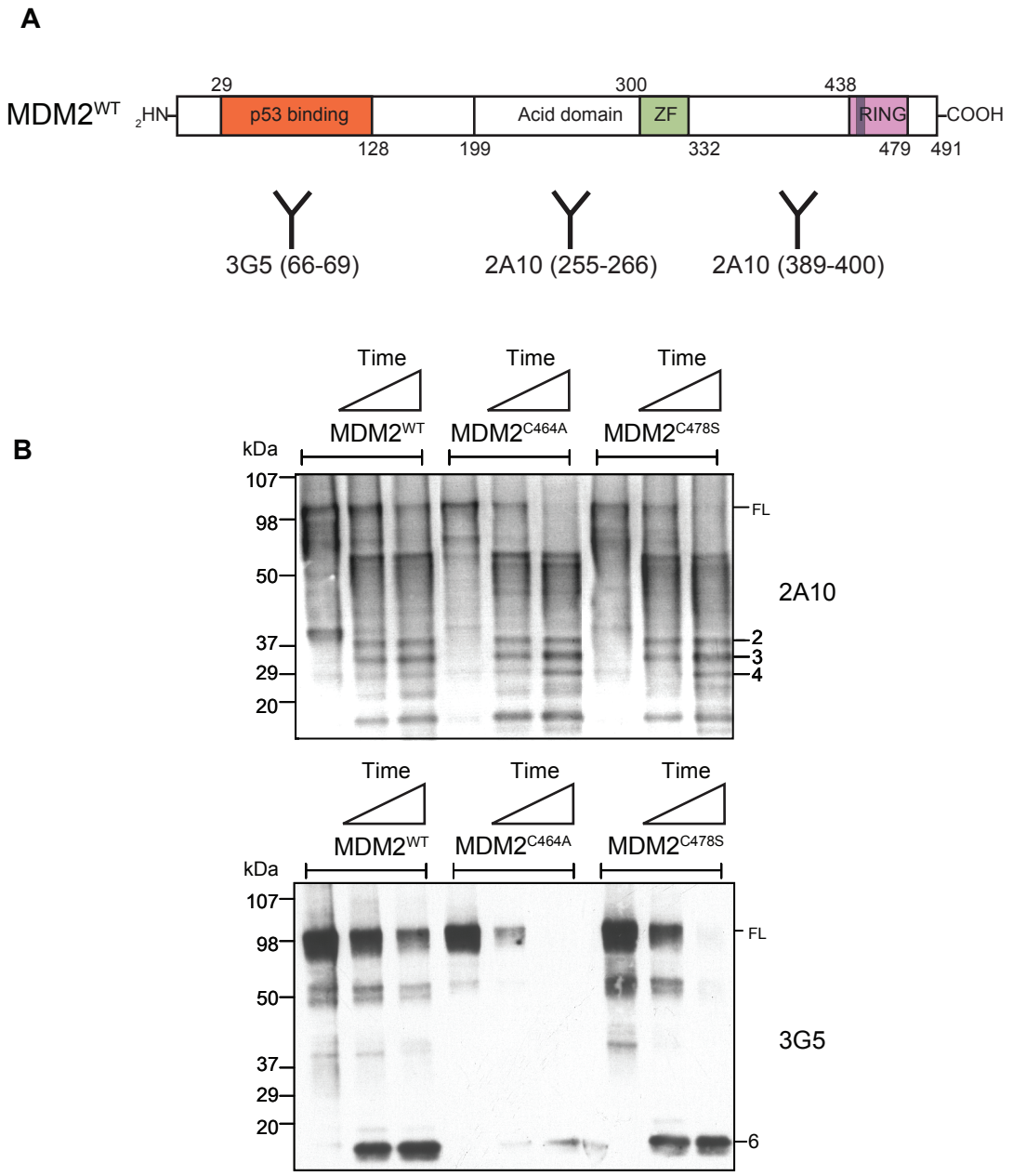

Figure 5.11 Partial proteolytic digestion of MDM2

(**A**) Schematic representation of MDM2 protein showing the epitopes for 3G5 and 2A10 in human MDM2.
(**B**) Immunoblot showing wild-type or mutant forms of MDM2 following limited proteolysis with trypsin. Following gradient SDS PAGE and western blot transfer. The blots were developed using 2A10 (upper panel) and 3G5 (lower panel). The numbers are used to label the banding pattern. The time points used were 0, 5, and 20 min. Data presented in this figure was obtained in cooperation with Prof. Kathryn Ball.

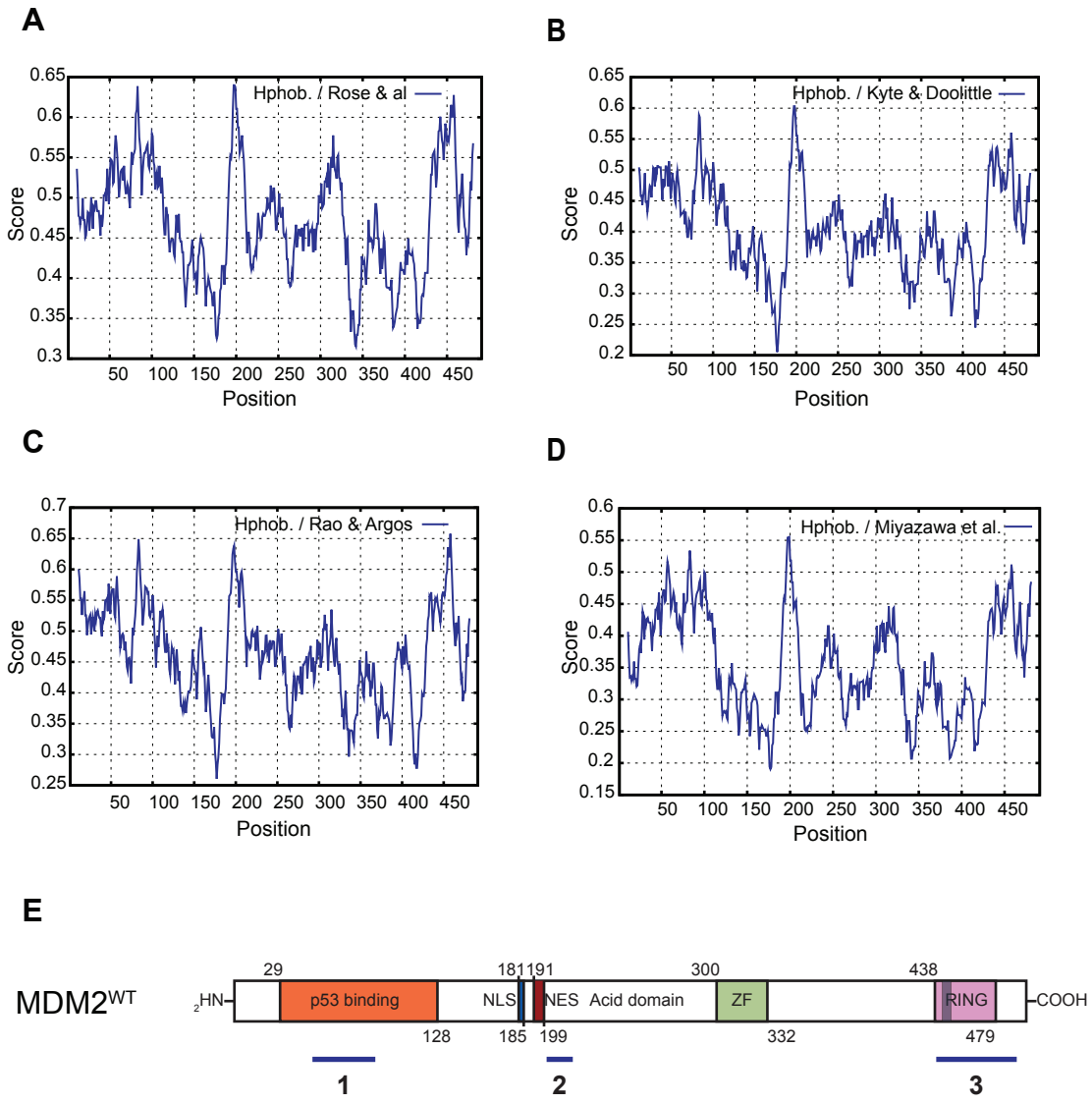

Figure 5.12 Hydrophobic profile of human MDM2

ProtScale (http://www.expasy.org/tools/protscale.html) computational analysis for MDM2 was used to represent this profile. The normalized hydrophobicity score is defined by a numerical value assigned to each type of amino acid,where 0 is the least and 1 is the most hydrophobic.
(**A**) - (**D**) Graphical representation of MDM2 hydrophobic profile where four independent sets of scores were used to characterize the primary structure of MDM2.
(**E**) Localization of major hydrophobic amino acid stretches within the multidomain organization of MDM2, representing convergence of data shown in (**A**) - (**D**).

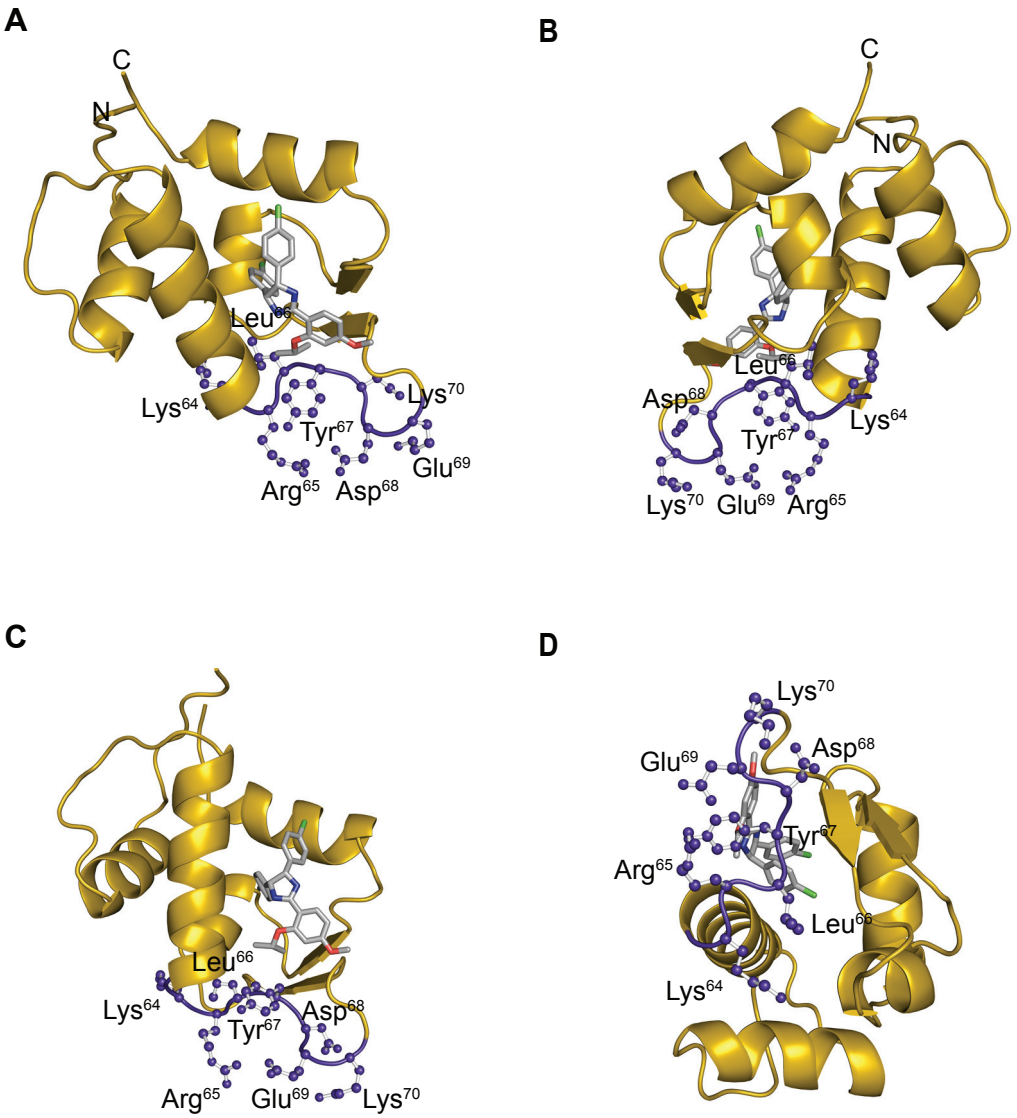

Figure 5.13 Localization of the 3G5 antibody epitope within the MDM2 hydrophobic pocket

Panels represent different stereoscopic views.
The MDM2 hydrophobic pocket shown in ribbon representation, coloured gold. Nutlin-3 bound to the pocket in stick representation (carbon-grey, nitrogen-blue and oxygen-red, chlorine-green). The epitope of 3G5 Ab consists of 4 amino acid residues; Leu^{66} Tyr^{67} Asp^{68} Glu^{69} highlighted in purple.
This figure was prepared using PyMOL [http://www.pymol.sourceforge.net/] and structural data from Fry et al., 2004 (file 1TTV RCSB PDB).

Chapter 6

Conclusions and future prospects

Contents

MDM2 is a multi-functional protein with numerous biochemical functions. The results presented in this thesis indicate that the functions of MDM2 oncoprotein in growth control and tumourigenesis are managed in part through the coordination, and intrinsic regulation of its discrete domains.

6.1 The RING finger domain – key intrinsic regulator of MDM2 function

The data in this thesis indicates that the MDM2 oncoprotein promotes p53 binding to responsive DNA sequences at physiological temperature. This seemingly contradictory role of the main p53 antagonist is supported by accumulating evidence indicating that degradation-independent mechanisms are crucial for both MDM2 and MDM4 in controlling p53 activity (Kruse and Gu, 2009). It was recently proposed that p53 activation *in vivo* requires not only stabilization and activation by post-translational modifications but also release from a repressed state. Considering genetic and *in vitro* data alike it was suggested that p53 is intrinsically active (Johnson et al., 2005; Ringshausen et al., 2006), yet is repressed by key negative regulators, MDM2 and MDM4 (Kruse and Gu, 2009).

Intriguingly, the ability of stress-induced, allosteric activation of unmodified p53 to bind sequence specific DNA (Hupp et al., 1992) was recently challenged. A considerable number of studies provide evidence that a significant portion of p53 is bound to DNA in unstressed cells (Cain et al., 2000; Kaeser and Iggo, 2002; Kim et al., 1999; Liu et al., 2004; Szak et al., 2001). Quantitative ChIP (chromatin immunoprecipitation) assays demonstrate that p53 is present at the promoters of *p21* and *MDM2* genes from wild-type unstressed cells. Lessons learned from cell culture based studies dictate that this is facilitated by an existing pool of basal post-translational modifications, which are significantly unregulated upon stress response (Appella and Anderson, 2001; Webley et al., 2000).

These numerous findings provide tangible support for a model in which p53 is capable of binding to DNA in unstressed cells but remains inactive probably due to repression by MDM2 and MDM4. Moreover MDM2 was shown to transiently localize with p53 at responsive elements and this recruitment of MDM2 to chromatin was postulated to keep p53 in latent form (Arva et al., 2005; Minsky and Oren, 2004; Ohkubo et al., 2006; White et al., 2006).

In light of this, association of the transcription factor with the promoter can occur without immediate activation of a given p53-responsive gene. The results presented in this thesis are coherent with this notion. They illuminate that MDM2 can elevate the amount of p53 bound to the promoter yet at the same time no increase of p53 transcriptional activity is observed.

The mode of action by which MDM2 facilitates efficient binding of p53 to the promoter is ATP dependent. Site directed mutagenesis studies and antibody mapping have confirmed the direct role of MDM2 in this process. The nucleotide is specifically bound by a motif located within the RING finger of MDM2, without interfering with the intrinsic E3 ubiquitin ligase activity of the domain.

It has been reported that nucleotide binding by the MDM2 oncoprotein induces a conformational change in its structure (Poyurovsky et al., 2003). Thermal denaturation studies shown in this thesis concur with these observations, moreover the shed additional light on the nature of the conformational flux. The ATP—bound form of MDM2 in contrast exhibits a characteristic denaturation profile. Indicating nucleotide driven conformational flux of the polypeptide. Moreover conformational changes driven by the ligand not only exhibit themselves in the oncoprotein, but additionally in the tumour suppressor. Monitoring p53 conformation in a mammalian cell lines by specific antibodies, displays a shift towards wild-type (DNA binding) structural arrangement of the protein driven by MDM2 species capable of ATP binding.

The discovery that MDM2, apart from its E3 ubiquitin ligase activity also possesses a function synonymous to that seen for molecular chaperones involved in protein folding and protection from aggregation raises an important question concerning the biological relevance of MDM2 chaperone activity toward p53 and other substrates.

The global *in vivo* situation of p53 is very complex. The results indicate that MDM2 promotes proper folding of p53, yet the same time MDM2 accelerates the degradation of the tumour suppressor. From the data presented a conclusion can be drawn that the activity of MDM2, in concert with a prominent p53 interacting molecular chaperone Hsp90 (Muller et al., 2004; Walerych et al., 2004), is required for shifting the conformation equilibrium of p53 to such a state where the transcription factor is potent to bind the promoter sequence. If such a state is not reached, the polypeptide is presented to the ubiquitination machinery and targeted for degradation (Sasaki et al., 2007). Furthermore, the results presented do not indicate that MDM2 is part of the complex once p53 is bound to its promoter sequence, indicating a transient mode of action. The fact that MDM2 can assist in correct non covalent assembly of the p53-promoter complex, where MDM2 is not a component of this assembled structure can be explained if one considers the following. The fact that the proteins used for the DNA binding experiments were isolated to high homogeneity from a prokaryotic expression system, rendering them devoid of any post-translational modifications, is a plausible answer. This would indicate that for a change from a transient interaction – ensuring efficient DNA binding, to stable complex on the promoter sequence – where MDM2 effectively represses p53 activity, is driven by reversible post-translational modifications of the two proteins in question. Of note are recent studies where purified proteins isolated form mammalian cells have confirmed the fact that MDM2 co-localizes with p53 on promoter sequences (Tang et al., 2008) in a fashion dependent on the acetylation state of p53.

Acetylation of p53 has recently been proposed to drive its specific target gene activation. This p53 modification involving the covalent linkage of an acetyl group to a lysine residue, was shown to be elevated in response to stress, and levels of acetylation correlate well with p53 activation and stabilization (Ito et al., 2001; Knights et al., 2006; Luo et al., 2001; Luo et al., 2000; Tang et al., 2008; Vaziri et al., 2001). The functional consequences of p53 acetylation imply that timing of acetylation of different p53 regions may be important for accurate p53 regulation and cell fate determination. In light of this several classes of genes are outlined in regards to when they are activated during the p53 response; modulators of excessive p53

activity, genes involved in growth arrest, and the last stringently controlled genes involved in programmed cell death.

The phenomena of biomolecular crowding present in living cells, (cytoplasm and nuceloplasm alike) renders it a hostile environment for proteins that display intrinsic conformational lability (Johansson et al., 2000; Tokuriki et al., 2004). This applies to p53, as it is known for its biophysical instability and is prone to conformational changes during its lifetime. Native conformation of p53 is essential for its biological activity executed in great part by its transcription factor potential. The MDM2 oncoprotein, along with other proteins interacting with p53, may constitute an additional level of p53 control.

It is known that molecular chaperones directly cooperate with ubiquitin/proteasome system during protein quality control in eukaryotic cells (Esser et al., 2004).

Among other E3 ubiquitin ligases specific for p53, CHIP (carboxyl terminus of Hsp70-interacting protein) was shown not only to target the tumour suppressor for proteasome mediated degradation (Esser et al., 2005a), but also aids in maintaining wild-type conformation capable of binding to DNA under physiological conditions (Tripathi et al., 2007). These published results show that CHIP mediates regulation of p53 conformation and abundance. The apparent redundancy of action carried out by CHIP and MDM2 should be considered as an evolutionary advantage, minimizing the pool of latent aggregate prone forms of the tumour suppressor.

Another intriguing open question, which remains to be fully elucidated, is whether p53 can be ubiquitinated by MDM2 while bound to DNA, and if so which post-translationalmodifications both on p53 and MDM2 regulate this process.

Although the fragment of the N-terminal transactivation domain of p53 was originally thought to be the predominant site of interaction with MDM2, both the DNA-binding domain (Kulikov et al., 2006; Shimizu et al., 2002; Wallace et al., 2006; Yu et al., 2006) and the C-terminal domain of p53 interact with MDM2 (Tang et al., 2008). The presence of multiple binding sites in both MDM2 and p53 leading to complex formation, may suggest that there is interplay between post-

translationalmodifications that activate p53 by stabilization and in effect release it form repression (Kruse and Gu, 2009).

This discovered activity of MDM2 could also in part explain the p53-independent oncogenic activity of MDM2. Further results in this thesis aim to illuminate the fact that MDM2 can function as a transrepressor independent of its ability to ubiquitinate p53.

The data presented in this thesis implies that the C-terminal C2H2C4 RING of MDM2 can allosterically modulate not only the affinity of the N-terminal hydrophobic pocket but also its specificity. This further suggests that in cells the binding of interacting proteins and/or ligands to the RING is likely to impact on both MDM2 transrepressor activity and on the efficacy of pocket binding drugs in tumour cells. This hypothesis is supported by data showing that binding of ligands such as Zinc and ATP to the RING finger domain of MDM2 generate discrete conformational changes in the protein (Poyurovsky et al., 2003; Shimizu et al., 2002). In fact, it was previously shown that Zinc binding can effect the interaction of MDM2 with the BOX-I domain of p53; in this case Zinc binding leads to a decrease in BOX-I binding (Poyurovsky et al., 2003; Shimizu et al., 2002). Together with the data presented in this thesis, it can be concluded that modulation of the RING domain has the potential to both negatively and positively regulate binding of BOX-I to the hydrophobic pocket. As the presented Cys mutants are E3-ligase dead thus it is not possible to determine if C2H2C4 RING interacting factors could also promote MDM2 E3-ligase activity. In a similar manner as increased binding to hydrophobic pocket binding ligands (Nutlin BOX-I mimetics) could potentially favour acid domain binding to the BOX-V domain of p53 signalling ubiquitination (Wallace et al., 2006). Thus, it will be interesting to determine whether RING domain interacting factors, or modifications, such as acetylation (Wang et al., 2004), within the RING domain, act in a concerted manner to promote both transrepression and ubiquitination of p53 or whether changes in RING conformation might act as a switch favouring one MDM2 activity over another.

Additionally the results in this thesis show that Nutlin does not inhibit MDM2 E3-ligase activity neither *in vitro* nor in cell models. However, despite its lack of E3-

ligase inhibitory activity Nutlin can function in cells and animal models of cancer to activate p53 and to elevate p53 protein levels (Vassilev, 2004; Vassilev et al., 2004). Evidence presented here showing that Nutlin can reverse transrepression imposed by both the wild-type and the Cys^{478S} mutated form of MDM2 suggests that it functions primarily by relieving MDM2-imposed transrepression allowing binding to coactivators such as p300. This conclusion is supported by the observation that Nutlin promotes rapid activation of p53-dependent transcription before changes in p53 protein level are recorded (White et al., 2006). The fact that Nutlin is proving to be an effective drug in some models of human cancer provides further evidence for the role of MDM2 transrepressor activity in tumour development.

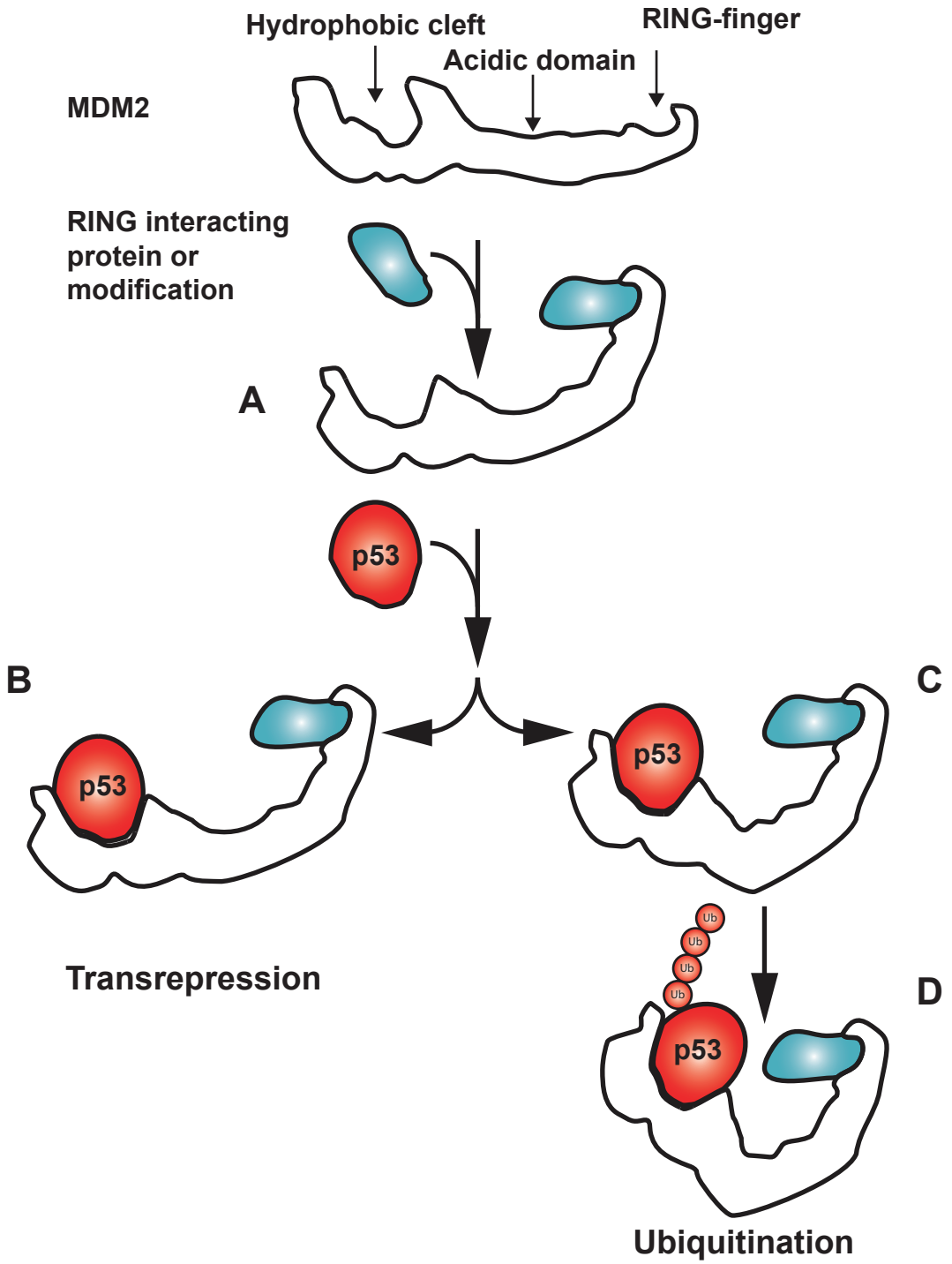

Figure 6.1 Model for Alosteric Regulation of MDM2

In summary the results presented in this thesis suggest that binding of interacting proteins and ligands or post-translational modification within the RING domain of MDM2 (**A**) which affect RING architecture will cause conformational modulation leading to changes in the affinity of the hydrophobic pocket for BOX-I domain of p53 and other ligands. This can result in formation of a transcriptionally inactive complex **(B)**, or based on previously published studies (Wallace et al., 2006), could result in a transition complex (**C**) where hydrophobic pocket binding leads the acid domain to bind to the core BOX-V site in p53 signalling p53 ubiquitination (**D**).

Bibliography

Adhikari, A., and Chen, Z.J. (2009). Diversity of polyubiquitin chains. Dev Cell *16*, 485-486.

Ambrosini, G., Sambol, E.B., Carvajal, D., Vassilev, L.T., Singer, S., and Schwartz, G.K. (2007). Mouse double minute antagonist Nutlin-3a enhances chemotherapy-induced apoptosis in cancer cells with mutant p53 by activating E2F1. Oncogene *26*, 3473-3481.

Anderson, M.E., Woelker, B., Reed, M., Wang, P., and Tegtmeyer, P. (1997). Reciprocal interference between the sequence-specific core and nonspecific C-terminal DNA binding domains of p53: implications for regulation. Mol Cell Biol *17*, 6255-6264.

Appella, E., and Anderson, C.W. (2001). Post-translational modifications and activation of p53 by genotoxic stresses. Eur J Biochem *268*, 2764-2772.

Arva, N.C., Gopen, T.R., Talbott, K.E., Campbell, L.E., Chicas, A., White, D.E., Bond, G.L., Levine, A.J., and Bargonetti, J. (2005). A chromatin associated and transcriptionally inactive p53-MDM2 complex occurs in MDM2 SNP 309 homozygous cells. J Biol Chem.

Ashcroft, M., Kubbutat, M.H., and Vousden, K.H. (1999). Regulation of p53 function and stability by phosphorylation. Mol Cell Biol *19*, 1751-1758.

Ashcroft, M., and Vousden, K.H. (1999). Regulation of p53 stability. Oncogene *18*, 7637-7643.

Balint, E.E., and Vousden, K.H. (2001). Activation and activities of the p53 tumour suppressor protein. Br J Cancer *85*, 1813-1823.

Bartel, F., Harris, L.C., Wurl, P., and Taubert, H. (2004). MDM2 and its splice variant messenger RNAs: expression in tumors and down-regulation using antisense oligonucleotides. Mol Cancer Res *2*, 29-35.

Bartel, F., Taubert, H., and Harris, L.C. (2002). Alternative and aberrant splicing of MDM2 mRNA in human cancer. Cancer Cell *2*, 9-15.

Bates, S., Phillips, A.C., Clark, P.A., Stott, F., Peters, G., Ludwig, R.L., and Vousden, K.H. (1998). p14ARF links the tumour suppressors RB and p53 [letter]. Nature *395*, 124-125.

Bates, S., Rowan, S., and Vousden, K.H. (1996). Characterisation of human cyclin G1 and G2: DNA damage inducible genes. Oncogene *13*, 1103-1109.

Baumeister, W., Walz, J., Zuhl, F., and Seemuller, E. (1998). The proteasome: paradigm of a self-compartmentalizing protease. Cell *92*, 367-380.

Bell, S., Klein, C., Muller, L., Hansen, S., and Buchner, J. (2002). p53 contains large unstructured regions in its native state. J Mol Biol *322*, 917-927.

Blattner, C., Hay, T., Meek, D.W., and Lane, D.P. (2002). Hypophosphorylation of Mdm2 augments p53 stability. Mol Cell Biol *22*, 6170-6182.

Blattner, C., Tobiasch, E., Litfen, M., Rahmsdorf, H.J., and Herrlich, P. (1999). DNA damage induced p53 stabilisation: no indication for an involvement of p53 phosphorylation. Oncogene *18*.

Boddy, M.N., Freemont, P.S., and Borden, K.L. (1994). The p53-associated protein MDM2 contains a newly characterized zinc-binding domain called the RING finger. Trends Biochem Sci *19*, 198-199.

Bode, A.M., and Dong, Z. (2004). Post-translational modification of p53 in tumorigenesis. Nat Rev Cancer *4*, 793-805.

Bode, W., Schwager, P., and Huber, R. (1978). The transition of bovine trypsinogen to a trypsin-like state upon strong ligand binding. The refined crystal structures of the bovine trypsinogen-pancreatic trypsin inhibitor complex and of its ternary complex with Ile-Val at 1.9 A resolution. J Mol Biol *118*, 99-112.

Bogan, A.A., and Thorn, K.S. (1998). Anatomy of hot spots in protein interfaces. J Mol Biol *280*, 1-9.

Bond, G.L., Hu, W., Bond, E.E., Robins, H., Lutzker, S.G., Arva, N.C., Bargonetti, J., Bartel, F., Taubert, H., Wuerl, P.*, et al.* (2004). A single nucleotide polymorphism in the MDM2 promoter attenuates the p53 tumor suppressor pathway and accelerates tumor formation in humans. Cell *119*, 591-602.

Bond, G.L., Hu, W., and Levine, A.J. (2005). MDM2 is a central node in the p53 pathway: 12 years and counting. Curr Cancer Drug Targets *5*, 3-8.

Borgia, A., Williams, P.M., and Clarke, J. (2008). Single-molecule studies of protein folding. Annu Rev Biochem *77*, 101-125.

Boteva, R., Zlateva, T., Dorovska-Taran, V., Visser, A.J., Tsanev, R., and Salvato, B. (1996). Dissociation equilibrium of human recombinant interferon gamma. Biochemistry *35*, 14825-14830.

Bottger, A., Bottger, V., Garcia-Echeverria, C., Chene, P., Hochkeppel, H.K., Sampson, W., Ang, K., Howard, S.F., Picksley, S.M., and Lane, D.P. (1997a). Molecular characterization of the hdm2-p53 interaction. J Mol Biol *269*, 744-756.

Bottger, A., Bottger, V., Sparks, A., Liu, W.L., Howard, S.F., and Lane, D.P. (1997b). Design of a synthetic Mdm2-binding mini protein that activates the p53 response in vivo. Curr Biol *7*, 860-869.

Bottger, V., Bottger, A., Howard, S.F., Picksley, S.M., Chene, P., Garcia-Echeverria, C., Hochkeppel, H.K., and Lane, D.P. (1996). Identification of novel mdm2 binding peptides by phage display. Oncogene *13*, 2141-2147.

Botuyan, M.V., Momand, J., and Chen, Y. (1997). Solution conformation of an essential region of the p53 transactivation domain. Fold Des *2*, 331-342.

Bourdon, J.C., Fernandes, K., Murray-Zmijewski, F., Liu, G., Diot, A., Xirodimas, D.P., Saville, M.K., and Lane, D.P. (2005). p53 isoforms can regulate p53 transcriptional activity. Genes Dev *19*, 2122-2137.

Bouska, A., and Eischen, C.M. (2009a). Mdm2 affects genome stability independent of p53. Cancer Res *69*, 1697-1701.

Bouska, A., and Eischen, C.M. (2009b). Murine double minute 2: p53-independent roads lead to genome instability or death. Trends Biochem Sci.

Bowman, A.L., Nikolovska-Coleska, Z., Zhong, H., Wang, S., and Carlson, H.A. (2007). Small molecule inhibitors of the MDM2-p53 interaction discovered by ensemble-based receptor models. J Am Chem Soc *129*, 12809-12814.

Boyd, S.D., Tsai, K.Y., and Jacks, T. (2000). An intact HDM2 RING-finger domain is required for nuclear exclusion of p53. Nat Cell Biol *2*, 563-568.

Bradshaw, R.A., Neurath, H., Tye, R.W., Walsh, K.A., and Winter, W.P. (1970). Comparison of the partial amino-acid sequence of dogfish trypsinogen with bovine trypsinogen. Nature *226*, 237-239.

Brenkman, A.B., de Keizer, P.L., van den Broek, N.J., Jochemsen, A.G., and Burgering, B.M. (2008). Mdm2 induces mono-ubiquitination of FOXO4. PLoS ONE *3*, e2819.

Brooks, C.L., and Gu, W. (2006). p53 ubiquitination: Mdm2 and beyond. Mol Cell *21*, 307-315.

Brooks, C.L., Li, M., and Gu, W. (2007a). Mechanistic studies of MDM2-mediated ubiquitination in p53 regulation. J Biol Chem *282*, 22804-22815.

Brooks, C.L., Li, M., Hu, M., Shi, Y., and Gu, W. (2007b). The p53-Mdm2-HAUSP complex is involved in p53 stabilization by HAUSP. Oncogene.

Brylinski, M., Konieczny, L., and Roterman, I. (2006). Hydrophobic collapse in (in silico) protein folding. Comput Biol Chem *30*, 255-267.

Brzovic, P.S., Rajagopal, P., Hoyt, D.W., King, M.C., and Klevit, R.E. (2001). Structure of a BRCA1-BARD1 heterodimeric RING-RING complex. Nat Struct Biol *8*, 833-837.

Buchwald, G., van der Stoop, P., Weichenrieder, O., Perrakis, A., van Lohuizen, M., and Sixma, T.K. (2006). Structure and E3-ligase activity of the Ring-Ring complex of polycomb proteins Bmi1 and Ring1b. Embo J *25*, 2465-2474.

Bullock, A.N., Henckel, J., and Fersht, A.R. (2000). Quantitative analysis of residual folding and DNA binding in mutant p53 core domain: definition of mutant states for rescue in cancer therapy. Oncogene *19*, 1245-1256.

Buschmann, T., Lerner, D., Lee, C.G., and Ronai, Z. (2001). The Mdm-2 amino terminus is required for Mdm2 binding and SUMO-1 conjugation by the E2 SUMO-1 conjugating enzyme Ubc9. J Biol Chem *276*, 40389-40395.

Butler, J.S., and Loh, S.N. (2006). Folding and misfolding mechanisms of the p53 DNA binding domain at physiological temperature. Protein Sci *15*, 2457-2465.

Bykov, V.J., Issaeva, N., Selivanova, G., and Wiman, K.G. (2002a). Mutant p53-dependent growth suppression distinguishes PRIMA-1 from known anticancer drugs: a statistical analysis of information in the National Cancer Institute database. Carcinogenesis *23*, 2011-2018.

Bykov, V.J., Issaeva, N., Shilov, A., Hultcrantz, M., Pugacheva, E., Chumakov, P., Bergman, J., Wiman, K.G., and Selivanova, G. (2002b). Restoration of the tumor suppressor function to mutant p53 by a low-molecular-weight compound. Nat Med *8*, 282-288.

Bykov, V.J., and Wiman, K.G. (2003). Novel cancer therapy by reactivation of the p53 apoptosis pathway. Ann Med *35*, 458-465.

Bykov, V.J., Zache, N., Stridh, H., Westman, J., Bergman, J., Selivanova, G., and Wiman, K.G. (2005). PRIMA-1(MET) synergizes with cisplatin to induce tumor cell apoptosis. Oncogene *24*, 3484-3491.

Cahilly-Snyder, L., Yang-Feng, T., Francke, U., and George, D.L. (1987). Molecular analysis and chromosomal mapping of amplified genes isolated from a transformed mouse 3T3 cell line. Somat Cell Mol Genet *13*, 235-244.

Cain, C., Miller, S., Ahn, J., and Prives, C. (2000). The N terminus of p53 regulates its dissociation from DNA. J Biol Chem *275*, 39944-39953.

Calabro, V., Mansueto, G., Parisi, T., Vivo, M., Calogero, R.A., and La Mantia, G. (2002). The human MDM2 oncoprotein increases the transcriptional activity and the protein level of the p53 homolog p63. J Biol Chem *277*, 2674-2681.

Canadillas, J.M., Tidow, H., Freund, S.M., Rutherford, T.J., Ang, H.C., and Fersht, A.R. (2006). Solution structure of p53 core domain: structural basis for its instability. Proc Natl Acad Sci U S A *103*, 2109-2114.

Candeias, M.M., Malbert-Colas, L., Powell, D.J., Daskalogianni, C., Maslon, M.M., Naski, N., Bourougaa, K., Calvo, F., and Fahraeus, R. (2008a). P53 mRNA controls p53 activity by managing Mdm2 functions. Nat Cell Biol *10*, 1098-1105.

Candeias, M.M., Malbert-Colas, L., Powell, D.J., Daskalogianni, C., Maslon, M.M., Naski, N., Bourougaa, K., Calvo, F., and Fahraeus, R. (2008b). p53 mRNA controls p53 activity by managing Mdm2 functions. Nat Cell Biol.

Carroll, P.E., Okuda, M., Horn, H.F., Biddinger, P., Stambrook, P.J., Gleich, L.L., Li, Y.Q., Tarapore, P., and Fukasawa, K. (1999). Centrosome hyperamplification in human cancer: chromosome instability induced by p53 mutation and/or Mdm2 overexpression. Oncogene *18*, 1935-1944.

Chan, W.M., Mak, M.C., Fung, T.K., Lau, A., Siu, W.Y., and Poon, R.Y. (2006). Ubiquitination of p53 at multiple sites in the DNA-binding domain. Mol Cancer Res *4*, 15-25.

Chang, L., Zhou, B., Hu, S., Guo, R., Liu, X., Jones, S.N., and Yen, Y. (2008). ATM-mediated serine 72 phosphorylation stabilizes ribonucleotide reductase small subunit p53R2 protein against MDM2 to DNA damage. Proc Natl Acad Sci U S A.

Chehab, N.H., Malikzay, A., Stavridi, E.S., and Halazonetis, T.D. (1999). Phosphorylation of Ser-20 mediates stabilization of human p53 in response to DNA damage. Proc Natl Acad Sci U S A *96*, 13777-13782.

Chen, D., Kon, N., Li, M., Zhang, W., Qin, J., and Gu, W. (2005a). ARF-BP1/Mule is a critical mediator of the ARF tumor suppressor. Cell *121*, 1071-1083.

Chen, J., Lin, J., and Levine, A.J. (1995). Regulation of transcription functions of the p53 tumor suppressor by the mdm-2 oncogene. Mol Med *1*, 142-152.

Chen, J., Marechal, V., and Levine, A.J. (1993). Mapping of the p53 and mdm-2 interaction domains. Mol Cell Biol *13*, 4107-4114.

Chen, L., Yin, H., Farooqi, B., Sebti, S., Hamilton, A.D., and Chen, J. (2005b). p53 alpha-Helix mimetics antagonize p53/MDM2 interaction and activate p53. Mol Cancer Ther *4*, 1019-1025.

Chen, Z.J., Parent, L., and Maniatis, T. (1996). Site-specific phosphorylation of IkappaBalpha by a novel ubiquitination-dependent protein kinase activity. Cell *84*, 853-862.

Cheney, M.D., McKenzie, P.P., Volk, E.L., Fan, L., and Harris, L.C. (2008). MDM2 displays differential activities dependent upon the activation status of NFkappaB. Cancer Biol Ther *7*, 38-44.

Chin, L., Pomerantz, J., and DePinho, R.A. (1998). The INK4a/ARF tumor suppressor: one gene--two products--two pathways. Trends Biochem Sci *23*, 291-296.

Chipuk, J.E., and Green, D.R. (2004). Cytoplasmic p53: bax and forward. Cell Cycle *3*, 429-431.

Chipuk, J.E., Kuwana, T., Bouchier-Hayes, L., Droin, N.M., Newmeyer, D.D., Schuler, M., and Green, D.R. (2004). Direct activation of Bax by p53 mediates mitochondrial membrane permeabilization and apoptosis. Science *303*, 1010-1014.

Chipuk, J.E., Maurer, U., Green, D.R., and Schuler, M. (2003). Pharmacologic activation of p53 elicits Bax-dependent apoptosis in the absence of transcription. Cancer Cell *4*, 371-381.

Cho, Y., Gorina, S., Jeffrey, P.D., and Pavletich, N.P. (1994). Crystal structure of a p53 tumor suppressor-DNA complex: understanding tumorigenic mutations [see comments]. Science *265*, 346-355.

Ciechanover, A., and Brundin, P. (2003). The ubiquitin proteasome system in neurodegenerative diseases: sometimes the chicken, sometimes the egg. Neuron *40*, 427-446.

Ciechanover, A., Heller, H., Elias, S., Haas, A.L., and Hershko, A. (1980). ATP-dependent conjugation of reticulocyte proteins with the polypeptide required for protein degradation. Proc Natl Acad Sci U S A *77*, 1365-1368.

Ciechanover, A., Orian, A., and Schwartz, A.L. (2000). Ubiquitin-mediated proteolysis: biological regulation via destruction. Bioessays *22*, 442-451.

Clackson, T., and Wells, J.A. (1995). A hot spot of binding energy in a hormone-receptor interface. Science *267*, 383-386.

Cordon-Cardo, C., Latres, E., Drobnjak, M., Oliva, M.R., Pollack, D., Woodruff, J.M., Marechal, V., Chen, J., Brennan, M.F., and Levine, A.J. (1994). Molecular abnormalities of mdm2 and p53 genes in adult soft tissue sarcomas. Cancer Res *54*, 794-799.

Corvi, R., Savelyeva, L., Breit, S., Wenzel, A., Handgretinger, R., Barak, J., Oren, M., Amler, L., and Schwab, M. (1995). Non-syntenic amplification of MDM2 and MYCN in human neuroblastoma. Oncogene *10*, 1081-1086.

Craig, A.L., Burch, L., Vojtesek, B., Mikutowska, J., Thompson, A., and Hupp, T.R. (1999). Novel phosphorylation sites of human tumour suppressor protein p53 at Ser20 and Thr18 that disrupt the binding of mdm2 (mouse double minute 2) protein are modified in human cancers. Biochem J *342 (Pt 1)*, 133-141.

Dai, M.S., Jin, Y., Gallegos, J.R., and Lu, H. (2006). Balance of Yin and Yang: ubiquitylation-mediated regulation of p53 and c-Myc. Neoplasia *8*, 630-644.

Dai, M.S., and Lu, H. (2004). Inhibition of MDM2-mediated p53 ubiquitination and degradation by ribosomal protein L5. J Biol Chem *279*, 44475-44482.

Dai, M.S., Zeng, S.X., Jin, Y., Sun, X.X., David, L., and Lu, H. (2004). Ribosomal protein L23 activates p53 by inhibiting MDM2 function in response to ribosomal perturbation but not to translation inhibition. Mol Cell Biol *24*, 7654-7668.

Damalas, A., Kahan, S., Shtutman, M., Ben-Ze'ev, A., and Oren, M. (2001). Deregulated beta-catenin induces a p53- and ARF-dependent growth arrest and cooperates with Ras in transformation. Embo J *20*, 4912-4922.

Daujat, S., Neel, H., and Piette, J. (2001a). MDM2: life without p53. Trends Genet *17*, 459-464.

Daujat, S., Neel, H., and Piette, J. (2001b). MDM2: life without p53. Trends Genet *17*, 459-464.

Dawson, R., Muller, L., Dehner, A., Klein, C., Kessler, H., and Buchner, J. (2003). The N-terminal domain of p53 is natively unfolded. J Mol Biol *332*, 1131-1141.

Dearth, L.R., Qian, H., Wang, T., Baroni, T.E., Zeng, J., Chen, S.W., Yi, S.Y., and Brachmann, R.K. (2007). Inactive full-length p53 mutants lacking dominant wild-type p53 inhibition highlight loss of heterozygosity as an important aspect of p53 status in human cancers. Carcinogenesis *28*, 289-298.

DeLano, W.L., Ultsch, M.H., de Vos, A.M., and Wells, J.A. (2000). Convergent solutions to binding at a protein-protein interface. Science *287*, 1279-1283.

DeLeo, A.B., Jay, G., Appella, E., Dubois, G.C., Law, L.W., and Old, L.J. (1979). Detection of a transformation-related antigen in chemically induced sarcomas and other transformed cells of the mouse. Proc Natl Acad Sci U S A *76*, 2420-2424.

Deng, L., Wang, C., Spencer, E., Yang, L., Braun, A., You, J., Slaughter, C., Pickart, C., and Chen, Z.J. (2000). Activation of the IkappaB kinase complex by TRAF6 requires a dimeric ubiquitin-conjugating enzyme complex and a unique polyubiquitin chain. Cell *103*, 351-361.

Dill, K.A., Bromberg, S., Yue, K., Fiebig, K.M., Yee, D.P., Thomas, P.D., and Chan, H.S. (1995). Principles of protein folding--a perspective from simple exact models. Protein Sci *4*, 561-602.

Dilla, T., Romero, J., Sanstisteban, P., and Velasco, J.A. (2002). The mdm2 proto-oncogene sensitizes human medullary thyroid carcinoma cells to ionizing radiation. Oncogene *21*, 2376-2386.

Ding, K., Lu, Y., Nikolovska-Coleska, Z., Qiu, S., Ding, Y., Gao, W., Stuckey, J., Krajewski, K., Roller, P.P., Tomita, Y.*, et al.* (2005). Structure-based design of potent non-peptide MDM2 inhibitors. J Am Chem Soc *127*, 10130-10131.

Ding, K., Lu, Y., Nikolovska-Coleska, Z., Wang, G., Qiu, S., Shangary, S., Gao, W., Qin, D., Stuckey, J., Krajewski, K.*, et al.* (2006). Structure-based design of spiro-oxindoles as potent, specific small-molecule inhibitors of the MDM2-p53 interaction. J Med Chem *49*, 3432-3435.

Dobson, C.M. (2004). Principles of protein folding, misfolding and aggregation. Semin Cell Dev Biol *15*, 3-16.

Dornan, D., Bheddah, S., Newton, K., Ince, W., Frantz, G.D., Dowd, P., Koeppen, H., Dixit, V.M., and French, D.M. (2004a). COP1, the negative regulator of p53, is overexpressed in breast and ovarian adenocarcinomas. Cancer Res *64*, 7226-7230.

Dornan, D., Shimizu, H., Perkins, N.D., and Hupp, T.R. (2003). DNA-dependent acetylation of p53 by the transcription coactivator p300. J Biol Chem *278*, 13431-13441.

Dornan, D., Wertz, I., Shimizu, H., Arnott, D., Frantz, G.D., Dowd, P., O'Rourke, K., Koeppen, H., and Dixit, V.M. (2004b). The ubiquitin ligase COP1 is a critical negative regulator of p53. Nature *429*, 86-92.

Drakos, E., Thomaides, A., Medeiros, L.J., Li, J., Leventaki, V., Konopleva, M., Andreeff, M., and Rassidakis, G.Z. (2007). Inhibition of p53-murine double minute 2 interaction by nutlin-3A stabilizes p53 and induces cell cycle arrest and apoptosis in Hodgkin lymphoma. Clin Cancer Res *13*, 3380-3387.

Dubs-Poterszman, M.C., Tocque, B., and Wasylyk, B. (1995). MDM2 transformation in the absence of p53 and abrogation of the p107 G1 cell-cycle arrest. Oncogene *11*, 2445-2449.

Dudkina, A.S., and Lindsley, C.W. (2007). Small molecule protein-protein inhibitors for the p53-MDM2 interaction. Curr Top Med Chem *7*, 952-960.

Dumaz, N., Milne, D.M., Jardine, L.J., and Meek, D.W. (2001). Critical roles for the serine 20, but not the serine 15, phosphorylation site and for the polyproline domain in regulating p53 turnover. Biochem J *359*, 459-464.

Dworakowska, D., Jassem, E., Jassem, J., Peters, B., Dziadziuszko, R., Zylicz, M., Jakobkiewicz-Banecka, J., Kobierska-Gulida, G., Szymanowska, A., Skokowski, J.*, et al.* (2004). MDM2 gene amplification: a new independent factor of adverse prognosis in non-small cell lung cancer (NSCLC). Lung Cancer *43*, 285-295.

Efeyan, A., and Serrano, M. (2007). p53: guardian of the genome and policeman of the oncogenes. Cell Cycle *6*, 1006-1010.

el-Deiry, W.S., Kern, S.E., Pietenpol, J.A., Kinzler, K.W., and Vogelstein, B. (1992). Definition of a consensus binding site for p53. Nat Genet *1*, 45-49.

Elenbaas, B., Dobbelstein, M., Roth, J., Shenk, T., and Levine, A.J. (1996). The MDM2 oncoprotein binds specifically to RNA through its RING finger domain. Mol Med *2*, 439-451.

Espinoza-Fonseca, L.M. (2005). Targeting MDM2 by the small molecule RITA: towards the development of new multi-target drugs against cancer. Theor Biol Med Model *2*, 38.

Espinoza-Fonseca, L.M., and Garcia-Machorro, J. (2008). Aromatic-aromatic interactions in the formation of the MDM2-p53 complex. Biochem Biophys Res Commun *370*, 547-551.

Espinoza-Fonseca, L.M., and Trujillo-Ferrara, J.G. (2006a). Conformational changes of the p53-binding cleft of MDM2 revealed by molecular dynamics simulations. Biopolymers *83*, 365-373.

Espinoza-Fonseca, L.M., and Trujillo-Ferrara, J.G. (2006b). Transient stability of the helical pattern of region F19-L22 of the N-terminal domain of p53: a molecular dynamics simulation study. Biochem Biophys Res Commun *343*, 110-116.

Esser, C., Alberti, S., and Hohfeld, J. (2004). Cooperation of molecular chaperones with the ubiquitin/proteasome system. Biochim Biophys Acta *1695*, 171-188.

Esser, C., Scheffner, M., and Hohfeld, J. (2005a). The chaperone associated ubiquitin ligase CHIP is able to target p53 for proteasomal degradation. J Biol Chem.

Esser, C., Scheffner, M., and Hohfeld, J. (2005b). The chaperone-associated ubiquitin ligase CHIP is able to target p53 for proteasomal degradation. J Biol Chem *280*, 27443-27448.

Evans, S.C., Viswanathan, M., Grier, J.D., Narayana, M., El-Naggar, A.K., and Lozano, G. (2001). An alternatively spliced HDM2 product increases p53 activity by inhibiting HDM2. Oncogene *20*, 4041-4049.

Fakharzadeh, S.S., Trusko, S.P., and George, D.L. (1991). Tumorigenic potential associated with enhanced expression of a gene that is amplified in a mouse tumor cell line. Embo J *10*, 1565-1569.

Fang, S., Jensen, J.P., Ludwig, R.L., Vousden, K.H., and Weissman, A.M. (2000). Mdm2 is a RING finger-dependent ubiquitin protein ligase for itself and p53. J Biol Chem *275*, 8945-8951.

Finch, R.A., Donoviel, D.B., Potter, D., Shi, M., Fan, A., Freed, D.D., Wang, C.Y., Zambrowicz, B.P., Ramirez-Solis, R., Sands, A.T.*, et al.* (2002). mdmx is a negative regulator of p53 activity in vivo. Cancer Res *62*, 3221-3225.

Fingerman, I.M., and Briggs, S.D. (2004). p53-mediated transcriptional activation: from test tube to cell. Cell *117*, 690-691.

Fiucci, G., Beaucourt, S., Duflaut, D., Lespagnol, A., Stumptner-Cuvelette, P., Geant, A., Buchwalter, G., Tuynder, M., Susini, L., Lassalle, J.M.*, et al.* (2004). Siah-1b is a direct transcriptional target of p53: identification of the functional p53 responsive element in the siah-1b promoter. Proc Natl Acad Sci U S A *101*, 3510-3515.

Fontana, A., de Laureto, P.P., Spolaore, B., Frare, E., Picotti, P., and Zambonin, M. (2004). Probing protein structure by limited proteolysis. Acta Biochim Pol *51*, 299-321.

Foster, B.A., Coffey, H.A., Morin, M.J., and Rastinejad, F. (1999). Pharmacological rescue of mutant p53 conformation and function. Science *286*, 2507-2510.

Fotouhi, N., and Graves, B. (2005). Small molecule inhibitors of p53/MDM2 interaction. Curr Top Med Chem *5*, 159-165.

Freedman, D.A., and Levine, A.J. (1998). Nuclear export is required for degradation of endogenous p53 by MDM2 and human papillomavirus E6. Mol Cell Biol *18*, 7288-7293.

Freemont, P.S., Hanson, I.M., and Trowsdale, J. (1991). A novel cysteine-rich sequence motif. Cell *64*, 483-484.

Fridman, J.S., Hernando, E., Hemann, M.T., de Stanchina, E., Cordon-Cardo, C., and Lowe, S.W. (2003). Tumor promotion by Mdm2 splice variants unable to bind p53. Cancer Res *63*, 5703-5706.

Fry, D.C., Graves, B., and Vassilev, L.T. (2005). Development of E3-substrate (MDM2-p53)-binding inhibitors: structural aspects. Methods Enzymol *399*, 622-633.

Fry, D.C., and Vassilev, L.T. (2005). Targeting protein-protein interactions for cancer therapy. J Mol Med *83*, 955-963.

Fuster, J.J., Sanz-Gonzalez, S.M., Moll, U.M., and Andres, V. (2007). Classic and novel roles of p53: prospects for anticancer therapy. Trends Mol Med *13*, 192-199.

Ganguli, G., and Wasylyk, B. (2003). p53-independent functions of MDM2. Mol Cancer Res *1*, 1027-1035.

Gannon, J.V., Greaves, R., Iggo, R., and Lane, D.P. (1990). Activating mutations in p53 produce a common conformational effect. A monoclonal antibody specific for the mutant form. Embo J *9*, 1595-1602.

Garcia-Echeverria, C., Chene, P., Blommers, M.J., and Furet, P. (2000). Discovery of potent antagonists of the interaction between human double minute 2 and tumor suppressor p53. J Med Chem *43*, 3205-3208.

Geyer, R.K., Yu, Z.K., and Maki, C.G. (2000). The MDM2 RING-finger domain is required to promote p53 nuclear export. Nat Cell Biol *2*, 569-573.

Goldberg, Z., Vogt Sionov, R., Berger, M., Zwang, Y., Perets, R., Van Etten, R.A., Oren, M., Taya, Y., and Haupt, Y. (2002). Tyrosine phosphorylation of Mdm2 by c-Abl: implications for p53 regulation. Embo J *21*, 3715-3727.

Gotz, C., Kartarius, S., Scholtes, P., Nastainczyk, W., and Montenarh, M. (1999). Identification of a CK2 phosphorylation site in mdm2. Eur J Biochem *266*, 493-501.

Grinkevich, V.V., Nikulenkov, F., Shi, Y., Enge, M., Bao, W., Maljukova, A., Gluch, A., Kel, A., Sangfelt, O., and Selivanova, G. (2009). Ablation of key oncogenic pathways by RITA-reactivated p53 is required for efficient apoptosis. Cancer Cell *15*, 441-453.

Grossman, S.R. (2001). p300/CBP/p53 interaction and regulation of the p53 response. Eur J Biochem *268*, 2773-2778.

Grossman, S.R., Deato, M.E., Brignone, C., Chan, H.M., Kung, A.L., Tagami, H., Nakatani, Y., and Livingston, D.M. (2003). Polyubiquitination of p53 by a ubiquitin ligase activity of p300. Science *300*, 342-344.

Grossman, S.R., Perez, M., Kung, A.L., Joseph, M., Mansur, C., Xiao, Z.X., Kumar, S., Howley, P.M., and Livingston, D.M. (1998). p300/MDM2 complexes participate in MDM2-mediated p53 degradation. Mol Cell *2*, 405-415.

Gryczynski, Z., Gryczynski, I., and Lakowicz, J.R. (2003). Fluorescence-sensing methods. Methods Enzymol *360*, 44-75.

Gu, J., Kawai, H., Nie, L., Kitao, H., Wiederschain, D., Jochemsen, A.G., Parant, J., Lozano, G., and Yuan, Z.M. (2002). Mutual dependence of MDM2 and MDMX in their functional inactivation of p53. J Biol Chem *277*, 19251-19254.

Guerra, B., Gotz, C., Wagner, P., Montenarh, M., and Issinger, O.G. (1997). The carboxy terminus of p53 mimics the polylysine effect of protein kinase CK2-catalyzed MDM2 phosphorylation. Oncogene *14*, 2683-2688.

Hansen, R.S., and Braithwaite, A.W. (1996). The growth-inhibitory function of p53 is separable from transactivation, apoptosis and suppression of transformation by E1a and Ras. Oncogene *13*, 995-1007.

Hansen, S., Hupp, T.R., and Lane, D.P. (1996). Allosteric regulation of the thermostability and DNA binding activity of human p53 by specific interacting proteins. CRC Cell Transformation Group. J Biol Chem *271*, 3917-3924.

Hardcastle, I.R., Ahmed, S.U., Atkins, H., Calvert, A.H., Curtin, N.J., Farnie, G., Golding, B.T., Griffin, R.J., Guyenne, S., Hutton, C*., et al.* (2005). Isoindolinone-based inhibitors of the MDM2-p53 protein-protein interaction. Bioorg Med Chem Lett *15*, 1515-1520.

Hardcastle, I.R., Ahmed, S.U., Atkins, H., Farnie, G., Golding, B.T., Griffin, R.J., Guyenne, S., Hutton, C., Kallblad, P., Kemp, S.J., *et al.* (2006). Small-molecule inhibitors of the MDM2-p53 protein-protein interaction based on an isoindolinone scaffold. J Med Chem *49*, 6209-6221.

Harris, L.C. (2005). MDM2 splice variants and their therapeutic implications. Curr Cancer Drug Targets *5*, 21-26.

Harris, S.L., and Levine, A.J. (2005). The p53 pathway: positive and negative feedback loops. Oncogene *24*, 2899-2908.

Haupt, Y., Maya, R., Kazaz, A., and Oren, M. (1997). Mdm2 promotes the rapid degradation of p53. Nature *387*, 296-299.

Hay, T.J., and Meek, D.W. (2000). Multiple sites of in vivo phosphorylation in the MDM2 oncoprotein cluster within two important functional domains. FEBS Lett *478*, 183-186.

Hershko, A., Ciechanover, A., Heller, H., Haas, A.L., and Rose, I.A. (1980). Proposed role of ATP in protein breakdown: conjugation of protein with multiple chains of the polypeptide of ATP-dependent proteolysis. Proc Natl Acad Sci U S A *77*, 1783-1786.

Hershko, A., Eytan, E., Ciechanover, A., and Haas, A.L. (1982). Immunochemical analysis of the turnover of ubiquitin-protein conjugates in intact cells. Relationship to the breakdown of abnormal proteins. J Biol Chem *257*, 13964-13970.

Hershko, A., Heller, H., Elias, S., and Ciechanover, A. (1983). Components of ubiquitin-protein ligase system. Resolution, affinity purification, and role in protein breakdown. J Biol Chem *258*, 8206-8214.

Hicke, L., Schubert, H.L., and Hill, C.P. (2005). Ubiquitin-binding domains. Nat Rev Mol Cell Biol *6*, 610-621.

Hochstrasser, M. (2009). Origin and function of ubiquitin-like proteins. Nature *458*, 422-429.

Hohfeld, J., Cyr, D.M., and Patterson, C. (2001). From the cradle to the grave: molecular chaperones that may choose between folding and degradation. EMBO Rep *2*, 885-890.

Hollstein, M., Hergenhahn, M., Yang, Q., Bartsch, H., Wang, Z.Q., and Hainaut, P. (1999). New approaches to understanding p53 gene tumor mutation spectra. Mutat Res *431*, 199-209.

Hollstein, M., Sidransky, D., Vogelstein, B., and Harris, C.C. (1991). p53 mutations in human cancers. Science *253*, 49-53.

Honda, R., Tanaka, H., and Yasuda, H. (1997). Oncoprotein MDM2 is a ubiquitin ligase E3 for tumor suppressor p53. FEBS Lett *420*, 25-27.

Honda, R., and Yasuda, H. (1999). Association of p19(ARF) with Mdm2 inhibits ubiquitin ligase activity of Mdm2 for tumor suppressor p53. Embo J *18*, 22-27.

Honda, R., and Yasuda, H. (2000). Activity of MDM2, a ubiquitin ligase, toward p53 or itself is dependent on the RING finger domain of the ligase. Oncogene *19*, 1473-1476.

Hupp, T.R., Meek, D.W., Midgley, C.A., and Lane, D.P. (1992). Regulation of the specific DNA binding function of p53. Cell *71*, 875-886.

Hupp, T.R., Sparks, A., and Lane, D.P. (1995). Small peptides activate the latent sequence-specific DNA binding function of p53. Cell *83*, 237-245.

Issaeva, N., Bozko, P., Enge, M., Protopopova, M., Verhoef, L.G., Masucci, M., Pramanik, A., and Selivanova, G. (2004). Small molecule RITA binds to p53, blocks p53-HDM-2 interaction and activates p53 function in tumors. Nat Med *10*, 1321-1328.

Itahana, K., Mao, H., Jin, A., Itahana, Y., Clegg, H.V., Lindstrom, M.S., Bhat, K.P., Godfrey, V.L., Evan, G.I., and Zhang, Y. (2007). Targeted inactivation of Mdm2 RING finger E3 ubiquitin ligase activity in the mouse reveals mechanistic insights into p53 regulation. Cancer Cell *12*, 355-366.

Ito, A., Lai, C.H., Zhao, X., Saito, S., Hamilton, M.H., Appella, E., and Yao, T.P. (2001). p300/CBP-mediated p53 acetylation is commonly induced by p53-activating agents and inhibited by MDM2. Embo J *20*, 1331-1340.

Iwai, A., Marusawa, H., Matsuzawa, S., Fukushima, T., Hijikata, M., Reed, J.C., Shimotohno, K., and Chiba, T. (2004). Siah-1L, a novel transcript variant belonging to the human Siah family of proteins, regulates beta-catenin activity in a p53-dependent manner. Oncogene *23*, 7593-7600.

Iwakuma, T., and Lozano, G. (2003). MDM2, an introduction. Mol Cancer Res *1*, 993-1000.

Jackson, M.W., and Berberich, S.J. (2000). MdmX protects p53 from Mdm2-mediated degradation. Mol Cell Biol *20*, 1001-1007.

Jin, A., Itahana, K., O'Keefe, K., and Zhang, Y. (2004). Inhibition of HDM2 and activation of p53 by ribosomal protein L23. Mol Cell Biol *24*, 7669-7680.

Jin, L., Williamson, A., Banerjee, S., Philipp, I., and Rape, M. (2008). Mechanism of ubiquitin-chain formation by the human anaphase-promoting complex. Cell *133*, 653-665.

Jin, Y., Lee, H., Zeng, S.X., Dai, M.S., and Lu, H. (2003). MDM2 promotes p21waf1/cip1 proteasomal turnover independently of ubiquitylation. Embo J *22*, 6365-6377.

Jin, Y., Zeng, S.X., Dai, M.S., Yang, X.J., and Lu, H. (2002). MDM2 inhibits PCAF (p300/CREB-binding protein-associated factor)-mediated p53 acetylation. J Biol Chem *277*, 30838-30843.

Johansson, H.O., Brooks, D.E., and Haynes, C.A. (2000). Macromolecular crowding and its consequences. Int Rev Cytol *192*, 155-170.

Johnson, T.M., Hammond, E.M., Giaccia, A., and Attardi, L.D. (2005). The p53QS transactivation-deficient mutant shows stress-specific apoptotic activity and induces embryonic lethality. Nat Genet *37*, 145-152.

Jones, S.N., Hancock, A.R., Vogel, H., Donehower, L.A., and Bradley, A. (1998). Overexpression of Mdm2 in mice reveals a p53-independent role for Mdm2 in tumorigenesis. Proc Natl Acad Sci U S A *95*, 15608-15612.

Jones, S.N., Roe, A.E., Donehower, L.A., and Bradley, A. (1995). Rescue of embryonic lethality in Mdm2-deficient mice by absence of p53. Nature *378*, 206-208.

Juven-Gershon, T., and Oren, M. (1999). Mdm2: the ups and downs. Mol Med *5*, 71-83.

Juven-Gershon, T., Shifman, O., Unger, T., Elkeles, A., Haupt, Y., and Oren, M. (1998). The Mdm2 oncoprotein interacts with the cell fate regulator Numb. Mol Cell Biol *18*, 3974-3982.

Kaeser, M.D., and Iggo, R.D. (2002). Chromatin immunoprecipitation analysis fails to support the latency model for regulation of p53 DNA binding activity in vivo. Proc Natl Acad Sci U S A *99*, 95-100.

Kaghad, M., Bonnet, H., Yang, A., Creancier, L., Biscan, J.C., Valent, A., Minty, A., Chalon, P., Lelias, J.M., Dumont, X.*, et al.* (1997). Monoallelically expressed gene related to p53 at 1p36, a region frequently deleted in neuroblastoma and other human cancers. Cell *90*, 809-819.

Kamijo, T., Weber, J.D., Zambetti, G., Zindy, F., Roussel, M.F., and Sherr, C.J. (1998). Functional and physical interactions of the ARF tumor suppressor with p53 and Mdm2. Proc Natl Acad Sci U S A *95*, 8292-8297.

Katoh, M., and Katoh, M. (2003). MGC9753 gene, located within PPP1R1B-STARD3-ERBB2-GRB7 amplicon on human chromosome 17q12, encodes the seven-transmembrane receptor with extracellular six-cystein domain. Int J Oncol *22*, 1369-1374.

Kawai, H., Lopez-Pajares, V., Kim, M.M., Wiederschain, D., and Yuan, Z.M. (2007). RING domain-mediated interaction is a requirement for MDM2's E3 ligase activity. Cancer Res *67*, 6026-6030.

Kawai, H., Wiederschain, D., and Yuan, Z.M. (2003). Critical contribution of the MDM2 acidic domain to p53 ubiquitination. Mol Cell Biol *23*, 4939-4947.

Khosravi, R., Maya, R., Gottlieb, T., Oren, M., Shiloh, Y., and Shkedy, D. (1999). Rapid ATM-dependent phosphorylation of MDM2 precedes p53 accumulation in response to DNA damage. PNAS *96*, 14973-14977.

Kim, E., Rohaly, G., Heinrichs, S., Gimnopoulos, D., Meissner, H., and Deppert, W. (1999). Influence of promoter DNA topology on sequence-specific DNA binding and transactivation by tumor suppressor p53. Oncogene *18*, 7310-7318.

Kim, H., Kwak, N.J., Lee, J.Y., Choi, B.H., Lim, Y., Ko, Y.J., Kim, Y.H., Huh, P.W., Lee, K.H., Rha, H.K.*, et al.* (2004). Merlin neutralizes the inhibitory effect of Mdm2 on p53. J Biol Chem *279*, 7812-7818.

King, F.W., Wawrzynow, A., Hohfeld, J., and Zylicz, M. (2001). Co-chaperones Bag-1, Hop and Hsp40 regulate Hsc70 and Hsp90 interactions with wild-type or mutant p53. Embo J *20*, 6297-6305.

Knights, C.D., Catania, J., Di Giovanni, S., Muratoglu, S., Perez, R., Swartzbeck, A., Quong, A.A., Zhang, X., Beerman, T., Pestell, R.G.*, et al.* (2006). Distinct p53 acetylation cassettes differentially influence gene-expression patterns and cell fate. J Cell Biol *173*, 533-544.

Kobet, E., Zeng, X., Zhu, Y., Keller, D., and Lu, H. (2000). MDM2 inhibits p300-mediated p53 acetylation and activation by forming a ternary complex with the two proteins. Proc Natl Acad Sci U S A *97*, 12547-12552.

Kostic, M., Matt, T., Martinez-Yamout, M.A., Dyson, H.J., and Wright, P.E. (2006). Solution structure of the Hdm2 C2H2C4 RING, a domain critical for ubiquitination of p53. J Mol Biol *363*, 433-450.

Kress, M., May, E., Cassingena, R., and May, P. (1979). Simian virus 40-transformed cells express new species of proteins precipitable by anti-simian virus 40 tumor serum. J Virol *31*, 472-483.

Krummel, K.A., Lee, C.J., Toledo, F., and Wahl, G.M. (2005). The C-terminal lysines fine-tune P53 stress responses in a mouse model but are not required for stability control or transactivation. Proc Natl Acad Sci U S A *102*, 10188-10193.

Kruse, J.P., and Gu, W. (2009). Modes of p53 regulation. Cell *137*, 609-622.

Kubbutat, M.H., Jones, S.N., and Vousden, K.H. (1997). Regulation of p53 stability by Mdm2. Nature *387*, 299-303.

Kulikov, R., Winter, M., and Blattner, C. (2006). Binding of p53 to the central domain of Mdm2 is regulated by phosphorylation. J Biol Chem *281*, 28575-28583.

Kurki, S., Peltonen, K., Latonen, L., Kiviharju, T.M., Ojala, P.M., Meek, D., and Laiho, M. (2004). Nucleolar protein NPM interacts with HDM2 and protects tumor suppressor protein p53 from HDM2-mediated degradation. Cancer Cell *5*, 465-475.

Kussie, P.H., Gorina, S., Marechal, V., Elenbaas, B., Moreau, J., Levine, A.J., and Pavletich, N.P. (1996a). Structure of the MDM2 oncoprotein bound to the p53 tumor suppressor transactivation domain. Science *274*, 948-953.

Kussie, P.H., Gorina, S., Marechal, V., Elenbaas, B., Moreau, J., Levine, A.J., and Pavletich, N.P. (1996b). Structure of the MDM2 oncoprotein bound to the p53 tumor suppressor transactivation domain. Science *274*, 948-953.

Kutzki, O., Park, H.S., Ernst, J.T., Orner, B.P., Yin, H., and Hamilton, A.D. (2002). Development of a potent Bcl-x(L) antagonist based on alpha-helix mimicry. J Am Chem Soc *124*, 11838-11839.

Lai, Z., Freedman, D.A., Levine, A.J., and McLendon, G.L. (1998). Metal and RNA binding properties of the hdm2 RING finger domain. Biochemistry *37*, 7005-7015.

Lai, Z., Yang, T., Kim, Y.B., Sielecki, T.M., Diamond, M.A., Strack, P., Rolfe, M., Caligiuri, M., Benfield, P.A., Auger, K.R.*, et al.* (2002). Differentiation of Hdm2-mediated p53 ubiquitination and Hdm2 auto-ubiquitination activity by small molecular weight inhibitors. Proc Natl Acad Sci U S A *99*, 14734-14739.

Lakowicz, J.R. (2000). On spectral relaxation in proteins. Photochem Photobiol *72*, 421-437.

Lakowicz, J.R., and Maliwal, B.P. (1983). Oxygen quenching and fluorescence depolarization of tyrosine residues in proteins. J Biol Chem *258*, 4794-4801.

Lakowicz, J.R., Maliwal, B.P., Cherek, H., and Balter, A. (1983). Rotational freedom of tryptophan residues in proteins and peptides. Biochemistry *22*, 1741-1752.

Lakowicz, J.R., Szmacinski, H., Nowaczyk, K., Berndt, K.W., and Johnson, M. (1992). Fluorescence lifetime imaging. Anal Biochem *202*, 316-330.

Lakowicz, J.R., and Weber, G. (1973). Quenching of protein fluorescence by oxygen. Detection of structural fluctuations in proteins on the nanosecond time scale. Biochemistry *12*, 4171-4179.

Lambert, J.M., Gorzov, P., Veprintsev, D.B., Soderqvist, M., Segerback, D., Bergman, J., Fersht, A.R., Hainaut, P., Wiman, K.G., and Bykov, V.J. (2009). PRIMA-1 reactivates mutant p53 by covalent binding to the core domain. Cancer Cell *15*, 376-388.

Landers, J.E., Cassel, S.L., and George, D.L. (1997). Translational enhancement of mdm2 oncogene expression in human tumor cells containing a stabilized wild-type p53 protein. Cancer Res *57*, 3562-3568.

Landers, J.E., Haines, D.S., Strauss, J.F., 3rd, and George, D.L. (1994). Enhanced translation: a novel mechanism of mdm2 oncogene overexpression identified in human tumor cells. Oncogene *9*, 2745-2750.

Lane, D.P., and Crawford, L.V. (1979). T antigen is bound to a host protein in SV40-transformed cells. Nature *278*, 261-263.

Lee, H., Mok, K.H., Muhandiram, R., Park, K.H., Suk, J.E., Kim, D.H., Chang, J., Sung, Y.C., Choi, K.Y., and Han, K.H. (2000). Local structural elements in the mostly unstructured transcriptional activation domain of human p53. J Biol Chem *275*, 29426-29432.

Leng, P., Brown, D.R., Shivakumar, C.V., Deb, S., and Deb, S.P. (1995). N-terminal 130 amino acids of MDM2 are sufficient to inhibit p53-mediated transcriptional activation. Oncogene *10*, 1275-1282.

Leng, R.P., Lin, Y., Ma, W., Wu, H., Lemmers, B., Chung, S., Parant, J.M., Lozano, G., Hakem, R., and Benchimol, S. (2003). Pirh2, a p53-induced ubiquitin-protein ligase, promotes p53 degradation. Cell *112*, 779-791.

Leveillard, T., Gorry, P., Niederreither, K., and Wasylyk, B. (1998). MDM2 expression during mouse embryogenesis and the requirement of p53. Mech Dev *74*, 189-193.

Leveillard, T., and Wasylyk, B. (1997). The MDM2 C-terminal region binds to TAFII250 and is required for MDM2 regulation of the cyclin A promoter. J Biol Chem *272*, 30651-30661.

Levine, A.J., Momand, J., and Finlay, C.A. (1991). The p53 tumour suppressor gene. Nature *351*, 453-456.

Li, M., Brooks, C.L., Wu-Baer, F., Chen, D., Baer, R., and Gu, W. (2003). Mono- versus polyubiquitination: differential control of p53 fate by Mdm2. Science *302*, 1972-1975.

Li, Y.B., and Jin, Z. (2007). [Effect of Qingdu Suppository-containing serum on cervical carcinoma SiHa cell MDM2 gene expression]. Zhongguo Zhong Xi Yi Jie He Za Zhi *27*, 147-150.

Liang, H., Atkins, H., Abdel-Fattah, R., Jones, S.N., and Lunec, J. (2004). Genomic organisation of the human MDM2 oncogene and relationship to its alternatively spliced mRNAs. Gene *338*, 217-223.

Liberek, K., Lewandowska, A., and Zietkiewicz, S. (2008). Chaperones in control of protein disaggregation. Embo J *27*, 328-335.

Lin, J., Chen, J., Elenbaas, B., and Levine, A.J. (1994). Several hydrophobic amino acids in the p53 amino-terminal domain are required for transcriptional activation, binding to mdm-2 and the adenovirus 5 E1B 55-kD protein. Genes Dev *8*, 1235-1246.

Linares, L.K., and Scheffner, M. (2003). The ubiquitin-protein ligase activity of Hdm2 is inhibited by nucleic acids. FEBS Lett *554*, 73-76.

Lindstrom, M.S., Jin, A., Deisenroth, C., White Wolf, G., and Zhang, Y. (2007). Cancer-associated mutations in the MDM2 zinc finger domain disrupt ribosomal protein interaction and attenuate MDM2-induced p53 degradation. Mol Cell Biol *27*, 1056-1068.

Linke, K., Mace, P.D., Smith, C.A., Vaux, D.L., Silke, J., and Day, C.L. (2008). Structure of the MDM2/MDMX RING domain heterodimer reveals dimerization is required for their ubiquitylation in trans. Cell Death Differ *15*, 841-848.

Linzer, D.I., and Levine, A.J. (1979). Characterization of a 54K dalton cellular SV40 tumor antigen present in SV40-transformed cells and uninfected embryonal carcinoma cells. Cell *17*, 43-52.

Linzer, D.I., Maltzman, W., and Levine, A.J. (1979). The SV40 A gene product is required for the production of a 54,000 MW cellular tumor antigen. Virology *98*, 308-318.

Liu, W.L., Midgley, C., Stephen, C., Saville, M., and Lane, D.P. (2001). Biological significance of a small highly conserved region in the N terminus of the p53 tumour suppressor protein. J Mol Biol *313*, 711-731.

Liu, X., Yue, P., Khuri, F.R., and Sun, S.Y. (2004). p53 upregulates death receptor 4 expression through an intronic p53 binding site. Cancer Res *64*, 5078-5083.

Lo Conte, L., Chothia, C., and Janin, J. (1999). The atomic structure of protein-protein recognition sites. J Mol Biol *285*, 2177-2198.

Lohrum, M.A., Ashcroft, M., Kubbutat, M.H., and Vousden, K.H. (2000). Identification of a cryptic nucleolar-localization signal in MDM2. Nat Cell Biol *2*, 179-181.

Lohrum, M.A., Ludwig, R.L., Kubbutat, M.H., Hanlon, M., and Vousden, K.H. (2003). Regulation of HDM2 activity by the ribosomal protein L11. Cancer Cell *3*, 577-587.

Lovering, R., Hanson, I.M., Borden, K.L., Martin, S., O'Reilly, N.J., Evan, G.I., Rahman, D., Pappin, D.J., Trowsdale, J., and Freemont, P.S. (1993). Identification and preliminary characterization of a protein motif related to the zinc finger. Proc Natl Acad Sci U S A *90*, 2112-2116.

Lu, Y., Nikolovska-Coleska, Z., Fang, X., Gao, W., Shangary, S., Qiu, S., Qin, D., and Wang, S. (2006). Discovery of a nanomolar inhibitor of the human murine double minute 2 (MDM2)-p53 interaction through an integrated, virtual database screening strategy. J Med Chem *49*, 3759-3762.

Lundgren, K., Montes de Oca Luna, R., McNeill, Y.B., Emerick, E.P., Spencer, B., Barfield, C.R., Lozano, G., Rosenberg, M.P., and Finlay, C.A. (1997). Targeted expression of MDM2 uncouples S phase from mitosis and inhibits mammary gland development independent of p53. Genes Dev *11*, 714-725.

Luo, J., Nikolaev, A.Y., Imai, S., Chen, D., Su, F., Shiloh, A., Guarente, L., and Gu, W. (2001). Negative control of p53 by Sir2alpha promotes cell survival under stress. Cell *107*, 137-148.

Luo, J., Su, F., Chen, D., Shiloh, A., and Gu, W. (2000). Deacetylation of p53 modulates its effect on cell growth and apoptosis. Nature *408*, 377-381.

Ma, L., and Pei, G. (2007). Beta-arrestin signaling and regulation of transcription. J Cell Sci *120*, 213-218.

MacPherson, D., Kim, J., Kim, T., Rhee, B.K., Van Oostrom, C.T., DiTullio, R.A., Venere, M., Halazonetis, T.D., Bronson, R., De Vries, A.*, et al.* (2004). Defective apoptosis and B-cell lymphomas in mice with p53 point mutation at Ser 23. Embo J *23*, 3689-3699.

Maki, C.G. (1999). Oligomerization is required for p53 to be efficiently ubiquitinated by MDM2. J Biol Chem *274*, 16531-16535.

Mandahl, N., Heim, S., Willen, H., Rydholm, A., Eneroth, M., Nilbert, M., Kreicbergs, A., and Mitelman, F. (1989). Characteristic karyotypic anomalies identify subtypes of malignant fibrous histiocytoma. Genes Chromosomes Cancer *1*, 9-14.

Marchenko, N.D., Wolff, S., Erster, S., Becker, K., and Moll, U.M. (2007). Monoubiquitylation promotes mitochondrial p53 translocation. Embo J *26*, 923-934.

Marechal, V., Elenbaas, B., Piette, J., Nicolas, J.C., and Levine, A.J. (1994). The ribosomal L5 protein is associated with mdm-2 and mdm-2-p53 complexes. Mol Cell Biol *14*, 7414-7420.

Marine, J.C., and Jochemsen, A.G. (2005). Mdmx as an essential regulator of p53 activity. Biochem Biophys Res Commun *331*, 750-760.

May, P., and May, E. (1999). Twenty years of p53 research: structural and functional aspects of the p53 protein. Oncogene *18*, 7651-7636.

Maya, R., Balass, M., Kim, S.T., Shkedy, D., Leal, J.F., Shifman, O., Moas, M., Buschmann, T., Ronai, Z., Shiloh, Y.*, et al.* (2001). ATM-dependent phosphorylation of Mdm2 on serine 395: role in p53 activation by DNA damage. Genes Dev *15*, 1067-1077.

Mayo, L.D., and Donner, D.B. (2001). A phosphatidylinositol 3-kinase/Akt pathway promotes translocation of Mdm2 from the cytoplasm to the nucleus. Proc Natl Acad Sci U S A *98*, 11598-11603.

Mayo, L.D., Turchi, J.J., and Berberich, S.J. (1997a). Mdm-2 phosphorylation by DNA-dependent protein kinase prevents interaction with p53. Cancer Res *57*, 5013-5016.

Mayo, L.D., Turchi, J.J., and Berberich, S.J. (1997b). Mdm-2 phosphorylation by DNA-dependent protein kinase prevents interaction with p53. Cancer Res *57*, 5013-5016.

McCoy, M.A., Gesell, J.J., Senior, M.M., and Wyss, D.F. (2003). Flexible lid to the p53-binding domain of human Mdm2: implications for p53 regulation. Proc Natl Acad Sci U S A *100*, 1645-1648.

McLure, K.G., and Lee, P.W. (1998). How p53 binds DNA as a tetramer. Embo J *17*, 3342-3350.

Meagher, J.L., Beechem, J.M., Olson, S.T., and Gettins, P.G. (1998). Deconvolution of the fluorescence emission spectrum of human antithrombin and identification of the tryptophan residues that are responsive to heparin binding. J Biol Chem *273*, 23283-23289.

Meek, D.W., and Knippschild, U. (2003). Post-translationalmodification of MDM2. Mol Cancer Res *1*, 1017-1026.

Melero, J.A., Stitt, D.T., Mangel, W.F., and Carroll, R.B. (1979). Identification of new polypeptide species (48-55K) immunoprecipitable by antiserum to purified large T antigen and present in SV40-infected and -transformed cells. Virology *93*, 466-480.

Meltzer, P.S., Jankowski, S.A., Dal Cin, P., Sandberg, A.A., Paz, I.B., and Coccia, M.A. (1991). Identification and cloning of a novel amplified DNA sequence in human malignant fibrous histiocytoma derived from a region of chromosome 12 frequently rearranged in soft tissue tumors. Cell Growth Differ *2*, 495-501.

Mendrysa, S.M., McElwee, M.K., Michalowski, J., O'Leary, K.A., Young, K.M., and Perry, M.E. (2003). mdm2 Is critical for inhibition of p53 during lymphopoiesis and the response to ionizing irradiation. Mol Cell Biol *23*, 462-472.

Mendrysa, S.M., O'Leary, K.A., McElwee, M.K., Michalowski, J., Eisenman, R.N., Powell, D.A., and Perry, M.E. (2006). Tumor suppression and normal aging in mice with constitutively high p53 activity. Genes Dev *20*, 16-21.

Mendrysa, S.M., and Perry, M.E. (2000). The p53 tumor suppressor protein does not regulate expression of its own inhibitor, MDM2, except under conditions of stress. Mol Cell Biol *20*, 2023-2030.

Michael, D., and Oren, M. (2003). The p53-Mdm2 module and the ubiquitin system. Semin Cancer Biol *13*, 49-58.

Midgley, C.A., Desterro, J.M., Saville, M.K., Howard, S., Sparks, A., Hay, R.T., and Lane, D.P. (2000). An N-terminal p14ARF peptide blocks Mdm2-dependent ubiquitination in vitro and can activate p53 in vivo. Oncogene *19*, 2312-2323.

Migliorini, D., Lazzerini Denchi, E., Danovi, D., Jochemsen, A., Capillo, M., Gobbi, A., Helin, K., Pelicci, P.G., and Marine, J.C. (2002). Mdm4 (Mdmx) regulates p53-induced growth arrest and neuronal cell death during early embryonic mouse development. Mol Cell Biol *22*, 5527-5538.

Mihara, M., Erster, S., Zaika, A., Petrenko, O., Chittenden, T., Pancoska, P., and Moll, U.M. (2003). p53 has a direct apoptogenic role at the mitochondria. Mol Cell *11*, 577-590.

Minsky, N., and Oren, M. (2004). The RING domain of Mdm2 mediates histone ubiquitylation and transcriptional repression. Mol Cell *16*, 631-639.

Mitchell, E.L., White, G.R., Santibanez-Koref, M.F., Varley, J.M., and Heighway, J. (1995). Mapping of gene loci in the Q13-Q15 region of chromosome 12. Chromosome Res *3*, 261-262.

Miyashita, T., and Reed, J.C. (1995). Tumor suppressor p53 is a direct transcriptional activator of the human bax gene. Cell *80*, 293-299.

Miyauchi, Y., Yogosawa, S., Honda, R., Nishida, T., and Yasuda, H. (2002). Sumoylation of Mdm2 by protein inhibitor of activated STAT (PIAS) and RanBP2 enzymes. J Biol Chem *277*, 50131-50136.

Moll, U.M., and Petrenko, O. (2003). The MDM2-p53 interaction. Mol Cancer Res *1*, 1001-1008.

Momand, J., Wu, H.H., and Dasgupta, G. (2000). MDM2--master regulator of the p53 tumor suppressor protein. Gene *242*, 15-29.

Momand, J., Zambetti, G.P., Olson, D.C., George, D., and Levine, A.J. (1992). The mdm-2 oncogene product forms a complex with the p53 protein and inhibits p53-mediated transactivation. Cell *69*, 1237-1245.

Montes de Oca Luna, R., Wagner, D.S., and Lozano, G. (1995). Rescue of early embryonic lethality in mdm2-deficient mice by deletion of p53. Nature *378*, 203-206.

Morrison, H., Sherman, L.S., Legg, J., Banine, F., Isacke, C., Haipek, C.A., Gutmann, D.H., Ponta, H., and Herrlich, P. (2001). The NF2 tumor suppressor gene product, merlin, mediates contact inhibition of growth through interactions with CD44. Genes Dev *15*, 968-980.

Muller, L., Schaupp, A., Walerych, D., Wegele, H., and Buchner, J. (2004). Hsp90 regulates the activity of wild type p53 under physiological and elevated temperatures. J Biol Chem *279*, 48846-48854.

Nakayama, K.I., and Nakayama, K. (2006). Ubiquitin ligases: cell-cycle control and cancer. Nat Rev Cancer *6*, 369-381.

Nalepa, G., Rolfe, M., and Harper, J.W. (2006). Drug discovery in the ubiquitin-proteasome system. Nat Rev Drug Discov *5*, 596-613.

Naski, N., Gajjar, M., Bourougaa, K., Malbert-Colas, L., Fahraeus, R., and Candeias, M.M. (2009). The p53 mRNA-Mdm2 interaction. Cell Cycle *8*, 31-34.

Nichols, N.M., and Matthews, K.S. (2002). Human p53 phosphorylation mimic, S392E, increases nonspecific DNA affinity and thermal stability. Biochemistry *41*, 170-178.

Ofir-Rosenfeld, Y., Boggs, K., Michael, D., Kastan, M.B., and Oren, M. (2008). Mdm2 regulates p53 mRNA translation through inhibitory interactions with ribosomal protein L26. Mol Cell *32*, 180-189.

Ohkubo, S., Tanaka, T., Taya, Y., Kitazato, K., and Prives, C. (2006). Excess HDM2 impacts cell cycle and apoptosis and has a selective effect on p53-dependent transcription. J Biol Chem *281*, 16943-16950.

Okamoto, K., and Beach, D. (1994). Cyclin G is a transcriptional target of the p53 tumor suppressor protein. Embo J *13*, 4816-4822.

Okamoto, K., Kashima, K., Pereg, Y., Ishida, M., Yamazaki, S., Nota, A., Teunisse, A., Migliorini, D., Kitabayashi, I., Marine, J.C.*, et al.* (2005). DNA damage-induced phosphorylation of MdmX at serine 367 activates p53 by targeting MdmX for Mdm2-dependent degradation. Mol Cell Biol *25*, 9608-9620.

Okamoto, K., Li, H., Jensen, M.R., Zhang, T., Taya, Y., Thorgeirsson, S.S., and Prives, C. (2002). Cyclin G recruits PP2A to dephosphorylate Mdm2. Mol Cell *9*, 761-771.

Okuda, M., Horn, H.F., Tarapore, P., Tokuyama, Y., Smulian, A.G., Chan, P.K., Knudsen, E.S., Hofmann, I.A., Snyder, J.D., Bove, K.E.*, et al.* (2000). Nucleophosmin/B23 is a target of CDK2/cyclin E in centrosome duplication. Cell *103*, 127-140.

Oliner, J.D., Kinzler, K.W., Meltzer, P.S., George, D.L., and Vogelstein, B. (1992). Amplification of a gene encoding a p53-associated protein in human sarcomas. Nature *358*, 80-83.

Oliner, J.D., Pietenpol, J.A., Thiagalingam, S., Gyuris, J., Kinzler, K.W., and Vogelstein, B. (1993). Oncoprotein MDM2 conceals the activation domain of tumour suppressor p53. Nature *362*, 857-860.

Olson, D.C., Marechal, V., Momand, J., Chen, J., Romocki, C., and Levine, A.J. (1993). Identification and characterization of multiple mdm-2 proteins and mdm- 2-p53 protein complexes. Oncogene *8*, 2353-2360.

Ongkeko, W.M., Wang, X.Q., Siu, W.Y., Lau, A.W., Yamashita, K., Harris, A.L., Cox, L.S., and Poon, R.Y. (1999). MDM2 and MDMX bind and stabilize the p53-related protein p73. Curr Biol *9*, 829-832.

Orner, B.P., Ernst, J.T., and Hamilton, A.D. (2001). Toward proteomimetics: terphenyl derivatives as structural and functional mimics of extended regions of an alpha-helix. J Am Chem Soc *123*, 5382-5383.

Orner, B.P., Salvatella, X., Sanchez Quesada, J., De Mendoza, J., Giralt, E., and Hamilton, A.D. (2002). De novo protein surface design: use of cation-pi interactions to enhance binding between an alpha-helical peptide and a cationic molecule in 50 % aqueous solution. Angew Chem Int Ed Engl *41*, 117-119.

Parant, J., Chavez-Reyes, A., Little, N.A., Yan, W., Reinke, V., Jochemsen, A.G., and Lozano, G. (2001). Rescue of embryonic lethality in Mdm4-null mice by loss of Trp53 suggests a nonoverlapping pathway with MDM2 to regulate p53. Nat Genet *29*, 92-95.

Parks, D.J., Lafrance, L.V., Calvo, R.R., Milkiewicz, K.L., Gupta, V., Lattanze, J., Ramachandren, K., Carver, T.E., Petrella, E.C., Cummings, M.D.*, et al.* (2005). 1,4-Benzodiazepine-2,5-diones as small molecule antagonists of the HDM2-p53 interaction: discovery and SAR. Bioorg Med Chem Lett *15*, 765-770.

Parsell, D.A., Kowal, A.S., Singer, M.A., and Lindquist, S. (1994). Protein disaggregation mediated by heat-shock protein Hsp104. Nature *372*, 475-478.

Perry, M.E., Piette, J., Zawadzki, J.A., Harvey, D., and Levine, A.J. (1993). The mdm-2 gene is induced in response to UV light in a p53-dependent manner. Proc Natl Acad Sci U S A *90*, 11623-11627.

Petitjean, A., Mathe, E., Kato, S., Ishioka, C., Tavtigian, S.V., Hainaut, P., and Olivier, M. (2007). Impact of mutant p53 functional properties on TP53 mutation patterns and tumor phenotype: lessons from recent developments in the IARC TP53 database. Hum Mutat *28*, 622-629.

Pettersson, S., Kelleher, M., Pion, E., Wallace, M., and Ball, K.L. (2009). Role of Mdm2 acid domain interactions in recognition and ubiquitination of the transcription factor IRF-2. Biochem J *418*, 575-585.

Pickart, C.M. (2000). Ubiquitin in chains. Trends Biochem Sci *25*, 544-548.

Pickart, C.M. (2001). Mechanisms underlying ubiquitination. Annu Rev Biochem *70*, 503-533.

Pickart, C.M. (2004). Back to the future with ubiquitin. Cell *116*, 181-190.

Picksley, S.M., Vojtesek, B., Sparks, A., and Lane, D.P. (1994). Immunochemical analysis of the interaction of p53 with MDM2;--fine mapping of the MDM2 binding site on p53 using synthetic peptides. Oncogene *9*, 2523-2529.

Pomerantz, J., Schreiber-Agus, N., Liegeios, N.J., Silverman, A., Alland, L., Chin, L., Potes, J., Chen, K., Orlow, I., Lee, H.-W.*, et al.* (1998a). The INK4a tumor suppressor gene product p19ARF interacts with MDM2 and neutralises MDM2's inhibition of p53. Cell *92*.

Pomerantz, J., Schreiber-Agus, N., Liegeois, N.J., Silverman, A., Alland, L., Chin, L., Potes, J., Chen, K., Orlow, I., Lee, H.W.*, et al.* (1998b). The Ink4a tumor suppressor gene product, p19Arf, interacts with MDM2 and neutralizes MDM2's inhibition of p53. Cell *92*, 713-723.

Poyurovsky, M.V., Jacq, X., Ma, C., Karni-Schmidt, O., Parker, P.J., Chalfie, M., Manley, J.L., and Prives, C. (2003). Nucleotide binding by the Mdm2 RING domain facilitates Arf-independent Mdm2 nucleolar localization. Mol Cell *12*, 875-887.

Poyurovsky, M.V., Priest, C., Kentsis, A., Borden, K.L., Pan, Z.Q., Pavletich, N., and Prives, C. (2007). The Mdm2 RING domain C-terminus is required for supramolecular assembly and ubiquitin ligase activity. Embo J *26*, 90-101.

Raboisson, P., Marugan, J.J., Schubert, C., Koblish, H.K., Lu, T., Zhao, S., Player, M.R., Maroney, A.C., Reed, R.L., Huebert, N.D.*, et al.* (2005). Structure-based design, synthesis, and biological evaluation of novel 1,4-diazepines as HDM2 antagonists. Bioorg Med Chem Lett *15*, 1857-1861.

Rajendra, R., Malegaonkar, D., Pungaliya, P., Marshall, H., Rasheed, Z., Brownell, J., Liu, L.F., Lutzker, S., Saleem, A., and Rubin, E.H. (2004). Topors functions as an E3 ubiquitin ligase with specific E2 enzymes and ubiquitinates p53. J Biol Chem *279*, 36440-36444.

Reifenberger, G., Liu, L., Ichimura, K., Schmidt, E.E., and Collins, V.P. (1993). Amplification and overexpression of the MDM2 gene in a subset of human malignant gliomas without p53 mutations. Cancer Res *53*, 2736-2739.

Reifenberger, G., Reifenberger, J., Ichimura, K., Meltzer, P.S., and Collins, V.P. (1994). Amplification of multiple genes from chromosomal region 12q13-14 in human malignant gliomas: preliminary mapping of the amplicons shows preferential involvement of CDK4, SAS, and MDM2. Cancer Res *54*, 4299-4303.

Ries, S., Biederer, C., Woods, D., Shifman, O., Shirasawa, S., Sasazuki, T., McMahon, M., Oren, M., and McCormick, F. (2000). Opposing effects of Ras on p53: transcriptional activation of mdm2 and induction of p19ARF. Cell *103*, 321-330.

Ringshausen, I., O'Shea, C.C., Finch, A.J., Swigart, L.B., and Evan, G.I. (2006). Mdm2 is critically and continuously required to suppress lethal p53 activity in vivo. Cancer Cell *10*, 501-514.

Rodriguez, M.S., Desterro, J.M., Lain, S., Lane, D.P., and Hay, R.T. (2000). Multiple C-terminal lysine residues target p53 for ubiquitin-proteasome-mediated degradation. Mol Cell Biol *20*, 8458-8467.

Romer, L., Klein, C., Dehner, A., Kessler, H., and Buchner, J. (2006). p53--a natural cancer killer: structural insights and therapeutic concepts. Angew Chem Int Ed Engl *45*, 6440-6460.

Rosser, M.F., Washburn, E., Muchowski, P.J., Patterson, C., and Cyr, D.M. (2007). Chaperone functions of the E3 ubiquitin ligase CHIP. J Biol Chem *282*, 22267-22277.

Roth, J., Dittmer, D., Rea, D., Tartaglia, J., Paoletti, E., and Levine, A.J. (1996). p53 as a target for cancer vaccines: recombinant canarypox virus vectors expressing p53 protect mice against lethal tumor cell challenge. Proc Natl Acad Sci U S A *93*, 4781-4786.

Roth, J., Dobbelstein, M., Freedman, D.A., Shenk, T., and Levine, A.J. (1998). Nucleo-cytoplasmic shuttling of the hdm2 oncoprotein regulates the levels of the p53 protein via a pathway used by the human immunodeficiency virus rev protein. Embo J *17*, 554-564.

Salcedo, A., Mayor, F., Jr., and Penela, P. (2006). Mdm2 is involved in the ubiquitination and degradation of G-protein-coupled receptor kinase 2. Embo J *25*, 4752-4762.

Sanders, M.M., Walsh, K.A., and Arnon, R. (1970). Immunological cross-reaction between trypsin and chymotrypsin as a guide to structural homology. Biochemistry *9*, 2356-2363.

Saporita, A.J., Maggi, L.B., Jr., Apicelli, A.J., and Weber, J.D. (2007). Therapeutic targets in the ARF tumor suppressor pathway. Curr Med Chem *14*, 1815-1827.

Sasaki, M., Nie, L., and Maki, C.G. (2007). MDM2 binding induces a conformational change in p53 that is opposed by heat-shock protein 90 and precedes p53 proteasomal degradation. J Biol Chem *282*, 14626-14634.

Saucedo, L.J., Myers, C.D., and Perry, M.E. (1999). Multiple murine double minute gene 2 (MDM2) proteins are induced by ultraviolet light. J Biol Chem *274*, 8161-8168.

Scheffner, M., Hubregtse, J.M., Vierstra, R.D., and Howley, P.M. (1993). The HPV-16 E6 and E6-AP complex functions as a ubiquitin protein ligase in the ubiquitination of p53. Cell *75*, 495-505.

Schon, O., Friedler, A., Bycroft, M., Freund, S.M., and Fersht, A.R. (2002). Molecular mechanism of the interaction between MDM2 and p53. J Mol Biol *323*, 491-501.

Schon, O., Friedler, A., Freund, S., and Fersht, A.R. (2004). Binding of p53-derived ligands to MDM2 induces a variety of long range conformational changes. J Mol Biol *336*, 197-202.

Sdek, P., Ying, H., Chang, D.L., Qiu, W., Zheng, H., Touitou, R., Allday, M.J., and Xiao, Z.X. (2005). MDM2 promotes proteasome-dependent ubiquitin-independent degradation of retinoblastoma protein. Mol Cell *20*, 699-708.

Sdek, P., Ying, H., Zheng, H., Margulis, A., Tang, X., Tian, K., and Xiao, Z.X. (2004). The central acidic domain of MDM2 is critical in inhibition of retinoblastoma-mediated suppression of E2F and cell growth. J Biol Chem *279*, 53317-53322.

Selivanova, G., and Wiman, K.G. (2007). Reactivation of mutant p53: molecular mechanisms and therapeutic potential. Oncogene *26*, 2243-2254.

Sharp, D.A., Kratowicz, S.A., Sank, M.J., and George, D.L. (1999). Stabilization of the MDM2 oncoprotein by interaction with the structurally related MDMX protein. J Biol Chem *274*, 38189-38196.

Sharpless, N.E., and DePinho, R.A. (2002). p53: good cop/bad cop. Cell *110*, 9-12.

Shenoy, S.K., and Lefkowitz, R.J. (2003). Trafficking patterns of beta-arrestin and G protein-coupled receptors determined by the kinetics of beta-arrestin deubiquitination. J Biol Chem *278*, 14498-14506.

Shenoy, S.K., McDonald, P.H., Kohout, T.A., and Lefkowitz, R.J. (2001). Regulation of receptor fate by ubiquitination of activated beta 2-adrenergic receptor and beta-arrestin. Science *294*, 1307-1313.

Sherr, C.J. (2006). Divorcing ARF and p53: an unsettled case. Nat Rev Cancer *6*, 663-673.

Shibagaki, I., Tanaka, H., Shimada, Y., Wagata, T., Ikenaga, M., Imamura, M., and Ishizaki, K. (1995). p53 mutation, murine double minute 2 amplification, and human papillomavirus infection are frequently involved but not associated with each other in esophageal squamous cell carcinoma. Clin Cancer Res *1*, 769-773.

Shieh, S.Y., Ikeda, M., Taya, Y., and Prives, C. (1997). DNA damage-induced phosphorylation of p53 alleviates inhibition by MDM2. Cell *91*, 325-334.

Shimizu, H., Burch, L.R., Smith, A.J., Dornan, D., Wallace, M., Ball, K.L., and Hupp, T.R. (2002). The conformationally flexible S9-S10 linker region in the core domain of p53 contains a novel MDM2 binding site whose mutation increases ubiquitination of p53 in vivo. J Biol Chem *277*, 28446-28458.

Shimizu, H., and Hupp, T.R. (2003). Intrasteric regulation of MDM2. Trends Biochem Sci *28*, 346-349.

Shimizu, H., Saliba, D., Wallace, M., Finlan, L., Langridge-Smith, P.R., and Hupp, T.R. (2006). Destabilizing missense mutations in the tumour suppressor protein p53 enhance its ubiquitination in vitro and in vivo. Biochem J *397*, 355-367.

Shirangi, T.R., Zaika, A., and Moll, U.M. (2002). Nuclear degradation of p53 occurs during down-regulation of the p53 response after DNA damage. Faseb J *16*, 420-422.

Shvarts, A., Steegenga, W.T., Riteco, N., van Laar, T., Dekker, P., Bazuine, M., van Ham, R.C., van der Houven van Oordt, W., Hateboer, G., van der Eb, A.J*., et al.* (1996a). MDMX: a novel p53-binding protein with some functional properties of MDM2. Embo J *15*, 5349-5357.

Shvarts, A., Steegenga, W.T., Riteco, N., van Laar, T., Dekker, P., bazuine, M., van Ham, R.C.A., van der Houven van Oordt, W., Hateboer, G., van der Eb, A.J*., et al.* (1996b). MDMX: a novel p53-binding protein with some functional properties of MDM2. EMBO J *15*, 5349-5357.

Sidhu, S.S., Fairbrother, W.J., and Deshayes, K. (2003). Exploring protein-protein interactions with phage display. Chembiochem *4*, 14-25.

Sigalas, I., Calvert, A.H., Anderson, J.J., Neal, D.E., and Lunec, J. (1996). Alternatively spliced mdm2 transcripts with loss of p53 binding domain sequences: transforming ability and frequent detection in human cancer. Nat Med *2*, 912-917.

Simpson, M.V. (1953). The release of labeled amino acids from the proteins of rat liver slices. J Biol Chem *201*, 143-154.

Skowyra, D., Georgopoulos, C., and Zylicz, M. (1990). The E. coli dnaK gene product, the hsp70 homolog, can reactivate heat-inactivated RNA polymerase in an ATP hydrolysis-dependent manner. Cell *62*, 939-944.

Spence, J., Sadis, S., Haas, A.L., and Finley, D. (1995). A ubiquitin mutant with specific defects in DNA repair and multiubiquitination. Mol Cell Biol *15*, 1265-1273.

Stad, R., Little, N.A., Xirodimas, D.P., Frenk, R., van der Eb, A.J., Lane, D.P., Saville, M.K., and Jochemsen, A.G. (2001). Mdmx stabilizes p53 and Mdm2 via two distinct mechanisms. EMBO Rep *2*, 1029-1034.

Steinman, H.A., Burstein, E., Lengner, C., Gosselin, J., Pihan, G., Duckett, C.S., and Jones, S.N. (2004). An alternative splice form of Mdm2 induces p53-independent cell growth and tumorigenesis. J Biol Chem *279*, 4877-4886.

Stoll, R., Renner, C., Hansen, S., Palme, S., Klein, C., Belling, A., Zeslawski, W., Kamionka, M., Rehm, T., Muhlhahn, P.*, et al.* (2001). Chalcone derivatives antagonize interactions between the human oncoprotein MDM2 and p53. Biochemistry *40*, 336-344.

Stoll, R., Renner, C., Muhlhahn, P., Hansen, S., Schumacher, R., Hesse, F., Kaluza, B., Engh, R.A., Voelter, W., and Holak, T.A. (2000). Sequence-specific 1H, 15N, and 13C assignment of the N-terminal domain of the human oncoprotein MDM2 that binds to p53. J Biomol NMR *17*, 91-92.

Stommel, J.M., Marchenko, N.D., Jimenez, G.S., Moll, U.M., Hope, T.J., and Wahl, G.M. (1999a). A leucine-rich nuclear export signal in the p53 tetramerization domain: regulation of subcellular localization and p53 activity by NES masking. Embo J *18*, 1660-1672.

Stommel, J.M., marchenko, N.D., Jimenez, G.S., Moll, U.M., Hope, T.J., and Wahl, G.M. (1999b). The leucine-rich nuclear export signal in the p53 tetramerisation domain: regulation of subcellular localization and p53 activity by NES masking. EMBO J *18*, 1660-1672.

Strano, S., Dell'Orso, S., Di Agostino, S., Fontemaggi, G., Sacchi, A., and Blandino, G. (2007). Mutant p53: an oncogenic transcription factor. Oncogene *26*, 2212-2219.

Strous, G.J., and Schantl, J.A. (2001). Beta-arrestin and Mdm2, unsuspected partners in signaling from the cell surface. Sci STKE *2001*, PE41.

Sun, Z.W., and Allis, C.D. (2002). Ubiquitination of histone H2B regulates H3 methylation and gene silencing in yeast. Nature *418*, 104-108.

Sykes, S.M., Mellert, H.S., Holbert, M.A., Li, K., Marmorstein, R., Lane, W.S., and McMahon, S.B. (2006). Acetylation of the p53 DNA-binding domain regulates apoptosis induction. Mol Cell *24*, 841-851.

Szak, S.T., Mays, D., and Pietenpol, J.A. (2001). Kinetics of p53 binding to promoter sites in vivo. Mol Cell Biol *21*, 3375-3386.

Tang, Y., Luo, J., Zhang, W., and Gu, W. (2006). Tip60-dependent acetylation of p53 modulates the decision between cell-cycle arrest and apoptosis. Mol Cell *24*, 827-839.

Tang, Y., Zhao, W., Chen, Y., Zhao, Y., and Gu, W. (2008). Acetylation is indispensable for p53 activation. Cell *133*, 612-626.

Tanimura, S., Ohtsuka, S., Mitsui, K., Shirouzu, K., Yoshimura, A., and Ohtsubo, M. (1999). MDM2 interacts with MDMX through their RING finger domains. FEBS Lett *447*, 5-9.

Tao, W., and Levine, A.J. (1999a). Nucleocytoplasmic shuttling of oncoprotein Hdm2 is required for Hdm2-mediated degradation of p53. Proc Natl Acad Sci U S A *96*, 3077-3080.

Tao, W., and Levine, A.J. (1999b). P19(ARF) stabilizes p53 by blocking nucleo-cytoplasmic shuttling of Mdm2. Proc Natl Acad Sci U S A *96*, 6937-6941.

Thomas, A., and White, E. (1998). Suppression of the p300-dependent mdm2 negative-feedback loop induces the p53 apoptotic function. Genes Dev *12*, 1975-1985.

Thrower, J.S., Hoffman, L., Rechsteiner, M., and Pickart, C.M. (2000). Recognition of the polyubiquitin proteolytic signal. Embo J *19*, 94-102.

Thut, C.J., Goodrich, J.A., and Tijan, R. (1997). repression of p53-mediated transcription by MDM2: a dual mechanism. Genes & Dev *11*, 1974-1986.

Tokuriki, N., Kinjo, M., Negi, S., Hoshino, M., Goto, Y., Urabe, I., and Yomo, T. (2004). Protein folding by the effects of macromolecular crowding. Protein Sci *13*, 125-133.

Toledo, F., and Wahl, G.M. (2006). Regulating the p53 pathway: in vitro hypotheses, in vivo veritas. Nat Rev Cancer *6*, 909-923.

Tortora, G., Caputo, R., Damiano, V., Bianco, R., Chen, J., Agrawal, S., Bianco, A.R., and Ciardiello, F. (2000). A novel MDM2 anti-sense oligonucleotide has anti-tumor activity and potentiates cytotoxic drugs acting by different mechanisms in human colon cancer. Int J Cancer *88*, 804-809.

Tovar, C., Rosinski, J., Filipovic, Z., Higgins, B., Kolinsky, K., Hilton, H., Zhao, X., Vu, B.T., Qing, W., Packman, K.*, et al.* (2006). Small-molecule MDM2 antagonists reveal aberrant p53 signaling in cancer: implications for therapy. Proc Natl Acad Sci U S A *103*, 1888-1893.

Treier, M., Staszewski, L.M., and Bohmann, D. (1994). Ubiquitin-dependent c-Jun degradation in vivo is mediated by the delta domain. Cell *78*, 787-798.

Tripathi, V., Ali, A., Bhat, R., and Pati, U. (2007). CHIP chaperones wild type p53 tumor suppressor protein. J Biol Chem *282*, 28441-28454.

Turc-Carel, C., Limon, J., Dal Cin, P., Rao, U., Karakousis, C., and Sandberg, A.A. (1986). Cytogenetic studies of adipose tissue tumors. II. Recurrent reciprocal translocation t(12;16)(q13;p11) in myxoid liposarcomas. Cancer Genet Cytogenet *23*, 291-299.

Uhrinova, S., Uhrin, D., Powers, H., Watt, K., Zheleva, D., Fischer, P., McInnes, C., and Barlow, P.N. (2005). Structure of free MDM2 N-terminal domain reveals conformational adjustments that accompany p53-binding. J Mol Biol *350*, 587-598.

Uldrijan, S., Pannekoek, W.J., and Vousden, K.H. (2007). An essential function of the extreme C-terminus of MDM2 can be provided by MDMX. Embo J *26*, 102-112.

van der Horst, A., and Burgering, B.M. (2007). Stressing the role of FoxO proteins in lifespan and disease. Nat Rev Mol Cell Biol *8*, 440-450.

Vander Kooi, C.W., Ohi, M.D., Rosenberg, J.A., Oldham, M.L., Newcomer, M.E., Gould, K.L., and Chazin, W.J. (2006). The Prp19 U-box crystal structure suggests a common dimeric architecture for a class of oligomeric E3 ubiquitin ligases. Biochemistry *45*, 121-130.

Vassilev, L.T. (2004). Small-molecule antagonists of p53-MDM2 binding: research tools and potential therapeutics. Cell Cycle *3*, 419-421.

Vassilev, L.T. (2005). p53 Activation by small molecules: application in oncology. J Med Chem *48*, 4491-4499.

Vassilev, L.T. (2007). MDM2 inhibitors for cancer therapy. Trends Mol Med *13*, 23-31.

Vassilev, L.T., Tovar, C., Chen, S., Knezevic, D., Zhao, X., Sun, H., Heimbrook, D.C., and Chen, L. (2006). Selective small-molecule inhibitor reveals critical mitotic functions of human CDK1. Proc Natl Acad Sci U S A *103*, 10660-10665.

Vassilev, L.T., Vu, B.T., Graves, B., Carvajal, D., Podlaski, F., Filipovic, Z., Kong, N., Kammlott, U., Lukacs, C., Klein, C.*, et al.* (2004). In vivo activation of the p53 pathway by small-molecule antagonists of MDM2. Science *303*, 844-848.

Vaziri, H., Dessain, S.K., Ng Eaton, E., Imai, S.I., Frye, R.A., Pandita, T.K., Guarente, L., and Weinberg, R.A. (2001). hSIR2(SIRT1) functions as an NAD-dependent p53 deacetylase. Cell *107*, 149-159.

Venot, C., Maratrat, M., Sierra, V., Conseiller, E., and Debussche, L. (1999). Definition of a p53 transactivation function-deficient mutant and characterization of two independent p53 transactivation subdomains. Oncogene *18*, 2405-2410.

Veprintsev, D.B., Freund, S.M., Andreeva, A., Rutledge, S.E., Tidow, H., Canadillas, J.M., Blair, C.M., and Fersht, A.R. (2006). Core domain interactions in full-length p53 in solution. Proc Natl Acad Sci U S A *103*, 2115-2119.

Vlatkovic, N., Guerrera, S., Li, Y., Linn, S., Haines, D.S., and Boyd, M.T. (2000). MDM2 interacts with the C-terminus of the catalytic subunit of DNA polymerase epsilon. Nucleic Acids Res *28*, 3581-3586.

Vogelstein, B., Lane, D., and Levine, A.J. (2000). Surfing the p53 network. Nature *408*, 307-310.

Wadhwa, R., Yaguchi, T., Hasan, M.K., Mitsui, Y., Reddel, R.R., and Kaul, S.C. (2002). Hsp70 family member, mot-2/mthsp70/GRP75, binds to the cytoplasmic sequestration domain of the p53 protein. Exp Cell Res *274*, 246-253.

Walerych, D., Kudla, G., Gutkowska, M., Wawrzynow, B., Muller, L., King, F.W., Helwak, A., Boros, J., Zylicz, A., and Zylicz, M. (2004). Hsp90 chaperones wild-type p53 tumor suppressor protein. J Biol Chem *279*, 48836-48845.

Walker, J.E., Saraste, M., Runswick, M.J., and Gay, N.J. (1982). Distantly related sequences in the alpha- and beta-subunits of ATP synthase, myosin, kinases and other ATP-requiring enzymes and a common nucleotide binding fold. Embo J *1*, 945-951.

Wallace, M., Worrall, E., Pettersson, S., Hupp, T.R., and Ball, K.L. (2006). Dual-site regulation of MDM2 E3-ubiquitin ligase activity. Mol Cell *23*, 251-263.

Wang, X., Taplick, J., Geva, N., and Oren, M. (2004). Inhibition of p53 degradation by Mdm2 acetylation. FEBS Lett *561*, 195-201.

Wang, Y., Blandino, G., Oren, M., and Givol, D. (1998). Induced p53 expression in lung cancer cell line promotes cell senescence and differentially modifies the cytotoxicity of anti-cancer drugs. Oncogene *17*, 1923-1930.

Wasylyk, C., Salvi, R., Argentini, M., Dureuil, C., Delumeau, I., Abecassis, J., Debussche, L., and Wasylyk, B. (1999). p53 mediated death of cells overexpressing MDM2 by an inhibitor of MDM2 interaction with p53. Oncogene *18*, 1921-1934.

Wawrzynow, A., Banecki, B., Wall, D., Liberek, K., Georgopoulos, C., and Zylicz, M. (1995a). ATP hydrolysis is required for the DnaJ-dependent activation of DnaK chaperone for binding to both native and denatured protein substrates. J Biol Chem *270*, 19307-19311.

Wawrzynow, A., Wojtkowiak, D., Marszalek, J., Banecki, B., Jonsen, M., Graves, B., Georgopoulos, C., and Zylicz, M. (1995b). The ClpX heat-shock protein of Escherichia coli, the ATP-dependent substrate specificity component of the ClpP-ClpX protease, is a novel molecular chaperone. Embo J *14*, 1867-1877.

Wawrzynow, B., Zylicz, A., Wallace, M., Hupp, T., and Zylicz, M. (2007a). MDM2 chaperones the p53 tumor suppressor. J Biol Chem.

Wawrzynow, B., Zylicz, A., Wallace, M., Hupp, T., and Zylicz, M. (2007b). MDM2 chaperones the p53 tumor suppressor. J Biol Chem *282*, 32603-32612.

Webley, K., Bond, J.A., Jones, C.J., Blaydes, J.P., Craig, A., Hupp, T., and Wynford-Thomas, D. (2000). Post-translationalmodifications of p53 in replicative senescence overlapping but distinct from those induced by DNA damage. Mol Cell Biol *20*, 2803-2808.

White, D.E., Talbott, K.E., Arva, N.C., and Bargonetti, J. (2006). Mouse double minute 2 associates with chromatin in the presence of p53 and is released to facilitate activation of transcription. Cancer Res *66*, 3463-3470.

Wickner, S., Gottesman, S., Skowyra, D., Hoskins, J., McKenney, K., and Maurizi, M.R. (1994). A molecular chaperone, ClpA, functions like DnaK and DnaJ. Proc Natl Acad Sci U S A *91*, 12218-12222.

Wolff, S., and Dillin, A. (2006). The trifecta of aging in Caenorhabditis elegans. Exp Gerontol *41*, 894-903.

Wolff, S., Ma, H., Burch, D., Maciel, G.A., Hunter, T., and Dillin, A. (2006). SMK-1, an essential regulator of DAF-16-mediated longevity. Cell *124*, 1039-1053.

Xiao, Z.X., Chen, J., Levine, A.J., Modjtahedi, N., Xing, J., Sellers, W.R., and Livingston, D.M. (1995). Interaction between the retinoblastoma protein and the oncoprotein MDM2. Nature *375*, 694-698.

Xirodimas, D., Saville, M.K., Edling, C., Lane, D.P., and Lain, S. (2001a). Different effects of p14ARF on the levels of ubiquitinated p53 and Mdm2 in vivo. Oncogene *20*, 4972-4983.

Xirodimas, D.P., Chisholm, J., Desterro, J.M., Lane, D.P., and Hay, R.T. (2002). P14ARF promotes accumulation of SUMO-1 conjugated (H)Mdm2. FEBS Lett *528*, 207-211.

Xirodimas, D.P., Stephen, C.W., and Lane, D.P. (2001b). Cocompartmentalization of p53 and Mdm2 is a major determinant for Mdm2-mediated degradation of p53. Exp Cell Res *270*, 66-77.

Xu, Y. (2003). Regulation of p53 responses by post-translational modifications. Cell Death Differ *10*, 400-403.

Xu, Z., Devlin, K.I., Ford, M.G., Nix, J.C., Qin, J., and Misra, S. (2006). Structure and interactions of the helical and U-box domains of CHIP, the C terminus of HSP70 interacting protein. Biochemistry *45*, 4749-4759.

Yang, A., Kaghad, M., Wang, Y., Gillett, E., Fleming, M.D., Dotsch, V., Andrews, N.C., Caput, D., and McKeon, F. (1998). p63, a p53 homolog at 3q27-29, encodes multiple products with transactivating, death-inducing, and dominant-negative activities. Mol Cell *2*, 305-316.

Yang, Y., Ludwig, R.L., Jensen, J.P., Pierre, S.A., Medaglia, M.V., Davydov, I.V., Safiran, Y.J., Oberoi, P., Kenten, J.H., Phillips, A.C.*, et al.* (2005). Small molecule inhibitors of HDM2 ubiquitin ligase activity stabilize and activate p53 in cells. Cancer Cell *7*, 547-559.

Yardley, G., Zauberman, A., Oren, M., and Jackson, P. (1998). Individual promoter and intron p53-binding motifs from the rat Cyclin G1 promoter region support transcriptional activation by p53 but do not show co-operative activation. FEBS Lett *430*, 171-175.

Yin, Y., Manoury, B., and Fahraeus, R. (2003). Self-inhibition of synthesis and antigen presentation by Epstein-Barr virus-encoded EBNA1. Science *301*, 1371-1374.

Yin, Y., Stephen, C.W., Luciani, M.G., and Fahraeus, R. (2002). p53 Stability and activity is regulated by Mdm2-mediated induction of alternative p53 translation products. Nat Cell Biol *4*, 462-467.

Yu, G.W., Rudiger, S., Veprintsev, D., Freund, S., Fernandez-Fernandez, M.R., and Fersht, A.R. (2006). The central region of HDM2 provides a second binding site for p53. Proc Natl Acad Sci U S A *103*, 1227-1232.

Zache, N., Lambert, J.M., Wiman, K.G., and Bykov, V.J. (2008). PRIMA-1MET inhibits growth of mouse tumors carrying mutant p53. Cell Oncol *30*, 411-418.

Zauberman, A., Flusberg, D., Haupt, Y., Barak, Y., and Oren, M. (1995a). A functional p53-responsive intronic promoter is contained within the human mdm2 gene. Nucleic Acids Res *23*, 2584-2592.

Zauberman, A., Lupo, A., and Oren, M. (1995b). Identification of p53 target genes through immune selection of genomic DNA: the cyclin G gene contains two distinct p53 binding sites. Oncogene *10*, 2361-2366.

Zhang, R., Mayhood, T., Lipari, P., Wang, Y., Durkin, J., Syto, R., Gesell, J., McNemar, C., and Windsor, W. (2004a). Fluorescence polarization assay and inhibitor design for MDM2/p53 interaction. Anal Biochem *331*, 138-146.

Zhang, R., Wang, H., and Agrawal, S. (2005a). Novel antisense anti-MDM2 mixed-backbone oligonucleotides: proof of principle, in vitro and in vivo activities, and mechanisms. Curr Cancer Drug Targets *5*, 43-49.

Zhang, T., and Prives, C. (2001). Cyclin a-CDK phosphorylation regulates MDM2 protein interactions. J Biol Chem *276*, 29702-29710.

Zhang, Y., Wolf, G.W., Bhat, K., Jin, A., Allio, T., Burkhart, W.A., and Xiong, Y. (2003). Ribosomal protein L11 negatively regulates oncoprotein MDM2 and mediates a p53-dependent ribosomal-stress checkpoint pathway. Mol Cell Biol *23*, 8902-8912.

Zhang, Y., and Xiong, Y. (2001). A p53 amino-terminal nuclear export signal inhibited by DNA damage-induced phosphorylation. Science *292*, 1910-1915.

Zhang, Y., Xiong, Y., and Yarbrough, W.G. (1998). ARF promotes MDM2 degradation and stabilizes p53: ARF-INK4a locus deletion impairs both the Rb and p53 tumor suppression pathways. Cell *92*, 725-734.

Zhang, Z., Wang, H., Li, M., Agrawal, S., Chen, X., and Zhang, R. (2004b). MDM2 is a negative regulator of p21WAF1/CIP1, independent of p53. J Biol Chem *279*, 16000-16006.

Zhang, Z., Wang, H., Li, M., Rayburn, E.R., Agrawal, S., and Zhang, R. (2005b). Stabilization of E2F1 protein by MDM2 through the E2F1 ubiquitination pathway. Oncogene *24*, 7238-7247.

Zhao, J., Wang, M., Chen, J., Luo, A., Wang, X., Wu, M., Yin, D., and Liu, Z. (2002). The initial evaluation of non-peptidic small-molecule HDM2 inhibitors based on p53-HDM2 complex structure. Cancer Lett *183*, 69-77.

Zheleva, D.I., Lane, D.P., and Fischer, P.M. (2003). The p53-Mdm2 pathway: targets for the development of new anticancer therapeutics. Mini Rev Med Chem *3*, 257-270.

Zhou, B.P., Liao, Y., Xia, W., Zou, Y., Spohn, B., and Hung, M.C. (2001). HER-2/neu induces p53 ubiquitination via Akt-mediated MDM2 phosphorylation. Nat Cell Biol *3*, 973-982.

Zhou, R., Frum, R., Deb, S., and Deb, S.P. (2005). The growth arrest function of the human oncoprotein mouse double minute-2 is disabled by downstream mutation in cancer cells. Cancer Res *65*, 1839-1848.

Zhu, J.W., DeRyckere, D., Li, F.X., Wan, Y.Y., and DeGregori, J. (1999). A role for E2F1 in the induction of ARF, p53, and apoptosis during thymic negative selection. Cell Growth Differ *10*, 829-838.

Ziemienowicz, A., Skowyra, D., Zeilstra-Ryalls, J., Fayet, O., Georgopoulos, C., and Zylicz, M. (1993). Both the Escherichia coli chaperone systems, GroEL/GroES and DnaK/DnaJ/GrpE, can reactivate heat-treated RNA polymerase. Different mechanisms for the same activity. J Biol Chem *268*, 25425-25431.

Ziemienowicz, A., Zylicz, M., Floth, C., and Hubscher, U. (1995). Calf thymus Hsc70 protein protects and reactivates prokaryotic and eukaryotic enzymes. J Biol Chem *270*, 15479-15484.

Zylicz, M., King, F.W., and Wawrzynow, A. (2001). Hsp70 interactions with the p53 tumour suppressor protein. Embo J *20*, 4634-4638.

Zylicz, M., and Wawrzynow, A. (2001). Insights into the function of Hsp70 chaperones. IUBMB Life *51*, 283-287.

Appendix

THE JOURNAL OF BIOLOGICAL CHEMISTRY VOL. 282, NO. 45, pp. 32603–32612, November 9, 2007

MDM2 Chaperones the p53 Tumor Suppressor*[S]

Received for publication, April 2, 2007, and in revised form, September 4, 2007 Published, JBC Papers in Press, September 11, 2007, DOI 10.1074/jbc.M702767200

Bartosz Wawrzynow[‡§], Alicja Zylicz[‡], Maura Wallace[¶], Ted Hupp[¶], and Maciej Zylicz[‡1]

From the [‡]International Institute of Molecular and Cell Biology in Warsaw, 02-109 Warsaw, Poland, [§]The Nencki Institute of Experimental Biology, PAS, 02-093 Warsaw, Poland, and the [¶]University of Edinburgh, Division of Oncology, Cancer Research UK Cell Signalling Unit, Edinburgh EH4 2XU, Scotland, United Kingdom

The murine double minute (*mdm2*) gene encodes an E3 ubiquitin ligase that plays a key role in the degradation of p53 tumor suppressor protein. Nevertheless recent data highlight other p53-independent functions of MDM2. Given that MDM2 protein binds ATP, can interact with the Hsp90 chaperone, plays a role in the modulation of transcription factors and protection and activation of DNA polymerases, and is involved in ribosome assembly and nascent p53 protein biosynthesis, we have evaluated and found MDM2 protein to possess an intrinsic molecular chaperone activity. MDM2 can substitute for the Hsp90 molecular chaperone in promoting binding of p53 to the *p21*-derived promoter sequence. This reaction is driven by recycling of MDM2 from the p53 complex, triggered by binding of ATP to MDM2. The ATP binding mutant MDM2 protein (K454A) lacks the chaperone activity both *in vivo* and *in vitro*. *Mdm2* cotransfected in the H1299 cell line with wild-type *p53* stimulates efficient p53 folding *in vivo* but at the same time accelerates the degradation of p53. MDM2 in which one of the Zn^{2+} coordinating residues is mutated (C478S or C464A) blocks degradation but enhances folding of p53. This is the first demonstration that MDM2 possesses an intrinsic molecular chaperone activity, indicating that the ATP binding function of MDM2 can mediate its chaperone function toward the p53 tumor suppressor.

The *p53* tumor suppressor gene encodes a sequence-specific transcription factor that is mutated in the vast majority of human cancers (1). Two other paralogs of p53, namely p63 and p73, have been identified, but the physiological functions of each member of the p53 family appear to be rather distinct (for review, see Refs. 2 and 3). One of the foremost characterized target genes of p53 is the *mdm2* gene. MDM2 protein possesses E3 ubiquitin ligase activity toward p53 that plays a role in the negative regulation of p53 and its degradation by the proteasome (for review, see Ref. 4).

Through its ability to ubiquitylate p53 and target it for proteasomal degradation, MDM2 plays a key role in maintaining p53 at very low levels under non-stress conditions. In such circumstances MDM2 and p53 form a negative feedback loop in which p53 induces *mdm2* transcription and MDM2 targets p53 for degradation (2). In stress situations, MDM2-dependent degradation of p53 is inhibited by a variety of mechanisms, including p14ARF binding to MDM2, phosphorylation of the C terminus of MDM2 by the ATM kinase, stress-induced phosphorylation of sites in the trans-activation domain of p53, subsequent binding of the p300 coactivator, and further acetylation of p53 in its C-terminal region (5), which results in an increase of the steady-state level of the p53 transcription factor and consequential flux in the expression of more than a hundred genes, including those involved in cell cycle arrest, senescence, and apoptosis (2).

Recent reports indicate that apart from its initially discovered RING finger-dependent enzymatic E3 ubiquitin ligase activity, MDM2 has other functions. A hydrophobic pocket in the N-terminal domain of MDM2 forms the basis for p53 transrepression. Small molecules that bind to this pocket can release p53 from MDM2-mediated transrepression (6). The MDM2 protein also possesses a nucleotide binding domain mediated by the consensus Walker P motif within the MDM2 RING domain that facilitates its nucleolar localization, but the ATP binding activity is not required for its E3 ubiquitin ligase activity (7). Allosteric effects within MDM2 protein involving its interaction with both the p53 transactivation motif and the p53 DNA binding domain can mediate p53 ubiquitylation (8). However, the collective roles of the RING domain, the ATP binding domain, and the hydrophobic pocket in the biological activity of MDM2 protein remain undefined.

MDM2 protein also interacts directly with the nascent p53 polypeptide (9), which suggests an unexpected role in protein biosynthesis. In the case of full-length p53, binding of MDM2 to an N-terminal sequence in p53 leads to its efficient proteasomal-dependent degradation. Surprisingly, it has been shown that the truncated version of p53, called p47, which lacks the p53 N-terminal MDM2 binding site, is expressed much more efficiently than full-length p53. It is proposed that this effect is not only due to decreased p47 degradation but also increased efficiency in the translation of p47 (9). A possible function in ribosomal biosynthesis or in translation regulation was suggested previously by specific interaction of MDM2 with the component of the large ribosomal subunit-L5 protein (10). MDM2 was also found to interact with several other ribosomal proteins like L11 and L23. Such binding that sequesters MDM2 inhibits p53 protein polyubiquitylation, resulting in its activation (11).

* This work was supported by Ministry of Education and Science Grant PBZ-KBN-107/P04/2004 and European Commission 5th Framework Programme Project Centre of Excellence in Molecular Bio-Medicine Contract QLK6-CT-2002-90363. The costs of publication of this article were defrayed in part by the payment of page charges. This article must therefore be hereby marked "*advertisement*" in accordance with 18 U.S.C. Section 1734 solely to indicate this fact.

[S] The on-line version of this article (available at http://www.jbc.org) contains supplemental material, Figs. 1 and 2, and additional references.

[1] To whom correspondence should be addressed: International Institute of Molecular and Cell Biology in Warsaw, 4 Trojdena St., 02-109 Warsaw, Poland. Tel.: 48-22-5970740; Fax: 48-22-5970743; E-mail: mzylicz@iimcb.gov.pl.

MDM2 oncoprotein also possesses numerous p53-independent activities, which contribute to the development of tumors where MDM2 is overexpressed, mostly by gene amplification possibly caused by polymorphism at the *mdm2* promoter sequence (Ref. 12; for review, see also Refs. 13–15). Human cancers with non-functional p53 and amplification of *mdm2* have poor prognosis (16). Transgenic mice with wild-type MDM2 genes are predisposed to spontaneous tumor formation in a $p53^{-/-}$ background and have a high incidence of lymphoma and sarcoma (17, 18). More than 40 MDM2 isoforms have been detected in human cancers (19). Interestingly, some of them, which do not possess a p53 binding domain, are associated with high grade and late-stage human cancer (20, 21).

The biochemical mechanism of oncogenic activity of MDM2 remains elusive. Indeed, although MDM2 interacts with proteins, fulfilling a variety of cellular functions (p300, pRb, Numb, MTBP (MDM2-binding protein), DNA polymerase ϵ, promyelocytic leukemia protein, Tip60, YY1, insulin-like growth factor 1 receptor, glucocorticoid receptor/estrogen receptor, androgen receptor, hypoxia-inducible factor 1, p73, NF-κB, PSD-95, ADP ribosylation factor, E2F1, TATA-binding protein, TAFII250, Sp1, ribosomal L5, TSG 101, Ras-GAP binding proteins), the biological significance of these multiple interactions remains to be explained (for review, see Refs. 15, 22). It should be stressed that not all MDM2 client proteins are targeted for proteasome-dependent degradation; hence, not all involvement of MDM2 protein can be explained by its E3 ubiquitin ligase activity (13, 15).

Several findings, namely binding to a nascent polypeptide chain (9), modulation of transcription factors (23–25), protection and activation of DNA polymerases (26), and involvement in ribosome assembly (10), indicate that the MDM2 protein possesses similar activities to those described for molecular chaperones (for review, see Ref. 27). Molecular chaperones are defined as a vast class of structurally unrelated proteins that assists in correct non-covalent assembly of other polypeptide-containing structures but which are not components of these assembled structures when they perform their normal biological functions (for review, see Ref. 28). Recently we have shown that the Hsp90 molecular chaperone, in an ATP-dependent reaction, retains p53 in a conformation that allows binding to a specific promoter sequence (29). Here we describe that, in the absence of polyubiquitylation machinery, MDM2 can work synergistically with Hsp90, thus enhancing the binding of p53 to the promoter-derived sequence. Surprisingly, MDM2 alone possesses ATP-dependent molecular chaperone activity involved in folding of the p53 tumor suppressor protein. This is the first biochemical function attributed to the ATP-dependent domain of MDM2. We suggest that this newly discovered activity of MDM2 could not only play a role in p53 protein biosynthesis but could also in part explain the p53-independent oncogenic activity of MDM2.

MATERIALS AND METHODS

Plasmid Preparation—Human untagged MDM2 open reading frame lacking the first five codons (amino acids 6–491) inserted into a PT7.7 vector was prepared as described previously (30–32). The pT7.7 MDM2 K454A plasmid was prepared by means of site-directed mutagenesis using the QuikChange™ XL site-directed mutagenesis kit from Stratagene. For mutagenesis the following primers were used: mdm2K454A, GCATTGTCCATGGCGCAACAGGACATC; mdm2K454Arev, GATGTCCTGTTGCGCCATGGACAATGC; mdm2C478S, GGAATAAGCCCTGCCCAGTAAGCAGACAACCAATTCAAATGATTGTG; mdm2C478Srev, CACAATCATTTGAATTGGTTGTCTGCTTACTGGGCAGGGCTTATTCC; mdm2C464A, GGACATCTTATGGCCTGCTTTACAGCGGCAAAGAAGCTAAAGAAAAGG; mdm2C464Arev, CCTTTTCTTTAGCTTCTTTGCCGCTGTAAAGCAGGCCATAAGATGTCC. The plasmids encoding MDM2 wt[2] and the K454A or C478S mutant were used for purification of MDM2 wild-type and mutant proteins from *Escherichia coli*. Analogous mutations were introduced into the MDM2 wt open reading frame subcloned into the pCDNA3.1 vector.

Expression and Purification of Recombinant Protein—Human MDM2 wt was overexpressed in *E. coli* BL-21 RIL DE3 strain at 20 °C for 3 h after induction with 0.5 mM isopropyl 1-thio-β-D-galactopyranoside. Cells were harvested by centrifugation at 8000 × *g* for 10 min and frozen in liquid nitrogen. Bacteria pellet was lysed in buffer A (100 mM Tris-HCl, pH 8.0, 200 mM KCl, 10% glycerol, 1 mM phenylmethylsulfonyl fluoride, 5 mM $Mg(CH_3COO)_2$, 5 mM DTT, 1 mM benzamidine, protease inhibitor mixture EDTA free (Roche Applied Science), 1 tablet/50 ml of buffer A) containing 1 mg/ml lysozyme for 1.5 h at 4 °C with frequent stirring followed by 2 min at 37 °C and an additional 15 min at 4 °C. Afterward the suspension was centrifuged at 100,000 × *g* for 1 h at 4 °C. Under these lysis conditions most of the desired protein was insoluble and localized within the pellet after centrifugation. Extraction of the MDM2 protein from the cell pellet was carried out overnight at 4 °C with constant shaking. The following extraction buffer (B) was used: 25 mM Tris-HCl, pH 7.6, 1.2 M KCl, 5 mM $Mg(CH_3COO)_2$, 1% Triton X-100, 5 mM DTT, 10% sucrose, 1 mM phenylmethylsulfonyl fluoride, 1 mM benzamidine, protease inhibitor tablets. After centrifugation (100,000 × *g* for 1 h at 4 °C) the supernatant was collected and dialyzed into buffer C (25 mM HEPES-KOH, pH 7.3, 1 M $(NH_4)_2SO_4$, 1 M KCl, 5% glycerol, 2 mM DTT, 1 mM phenylmethylsulfonyl fluoride). After two h dialysis the sample was loaded onto a butyl-Sepharose column (Amersham Biosciences) equilibrated with the same buffer. The protein that bound to the column was eluted via gradient of decreasing ionic strength and increasing glycerol concentration. The fractions containing MDM2 protein were pooled and loaded onto a Q-Sepharose column equilibrated with buffer D (25 mM HEPES, pH 7.6, 50 mM KCl, 10% glycerol, 2 mM DTT, 1 mM phenylmethylsulfonyl fluoride). The flow-through from the column was immediately loaded onto a SP-Sepharose column equilibrated with an analogous buffer as the Q-Sepharose. The bound proteins to the SP-column were eluted by means of ionic strength gradient (from 50 to 800 mM KCl in buffer D). Fraction containing MDM2 protein were pooled, frozen in liquid nitro-

[2] The abbreviations used are: wt, wild type; DTT, dithiothreitol; ELISA, enzyme-linked immunosorbent assay; BSA, bovine serum albumin; pAb, polyclonal antibody; EMSA, electrophoretic mobility shift assay.

gen, and kept at −80 °C for further experiments. An analogous method was used to purify MDM2 K454A and MDM2 C478S from *E. coli*. Human recombinant p53 was purified essentially as described by Nichols and Matthews (33). Hsp90 proteins were purified as described in Walerych *et al.* (29).

Enzyme-linked Immunosorbent Assay (ELISA)—Investigation of the p53-MDM2 interaction was carried out using an ELISA technique. The method was performed analogously to the one described in Walerych *et al.* (29). For anchoring and/or detection of MDM2, monoclonal 2A-10 and 4B2 antibodies and polyclonal H-221 (Santa Cruz Biotechnology) were used, and for p53, monoclonal DO-1 and polyclonal FL-393 (Santa Cruz Biotechnology) were chosen. Inactivation of wt p53 was carried out at 37 °C for 90 min. Subsequently, 200 ng of heat-inactivated or correctly folded p53 (an aliquot of p53, reactive with the pAb1620 antibody, which was kept at 4 °C during the mentioned 37 °C incubation step) was coated onto ELISA plate wells in the coating buffer (25 mM Hepes, pH 7.3, 150 mM KCl, 10 mM DTT, for 1 h at 17 °C). After washing and blocking procedure with blocking buffer (25 mM Hepes, pH 7.3, 100 mM KCl, 2 mg/ml BSA), the anchored p53 was titrated with increasing amounts of MDM2 (preincubated or not with 5 mM ATP for 90 min) in the reaction buffer (25 mM HEPES, pH 7.3, 100 mM KCl, 15 mM $MgCl_2$, 10 μM $ZnSO_4$, 5% glycerol, 5 mM DTT, 0.1% Triton X-100, 2 mg/ml BSA) at 17 °C for 60 min. The experiment was also performed without Zn^{2+} ions, and no significant differences were observed.

p53 DNA Binding Assay—The DNA binding activity of p53 was quantified by EMSA (gel-shift) assay. The procedure of the assay was carried out as described in Walerych *et al.* (29). Minor modifications were introduced; that is, extension of the incubation time at 37 °C to 1.5 h, and with experiments that were based on a temperature gradient, a Biometra T Gradient Thermoblock was used. The samples were also supplemented not only with Hsp90 (bovine brain or human recombinant αHsp90 isoform) but also with human recombinant MDM2 wt, MDM2 K454A, or MDM2 C478S. Activation of p53 was predominantly carried out by 100 ng of the antibody pAb421 (Ab-1; Oncogene). However, control experiments were done with CK2 activation of p53. The specific *p21* sequence was labeled, and the competitor unspecific DNA sequence was used as described in Walerych *et al.* (29).

In Vitro p53 Ubiquitylation Assay—100 ng of human recombinant p53 purified from *E. coli* was incubated in a 20-μl reaction volume containing 1× ubiquitination buffer (50 mM Tris pH 7.6, 100 mM KCl, 10 mM $MgCl_2$, 2 mM DTT, 0.07 units of creatine kinase, 10 mM creatine phosphate, 5 mM ATP, 6 μg ubiquitin (human recombinant purified from *E. coli* or from Boston Biochem), 50 nM E1 ubiquitin activating enzyme (rabbit/human recombinant), 1.5 μM E2-conjugating enzyme UbcH5a (mouse/human recombinant), 3–150 nM E3 human recombinant MDM2 wt, MDM2 K454A, or MDM2 C478S. The reactions were incubated at 37 °C for 2 h. Afterward they were terminated with SDS sample buffer with β-mercaptoethanol, and the reaction products were fractioned by SDS-PAGE (8–10%). Transfer to a nitrocellulose/polyvinylidene difluoride film followed, and standard Western blot detection was carried out using anti-p53 DO-1 antibody.

Tissue Culture Experiments—Human lung carcinoma H1299 cells were grown at 37 °C in RPMI with 10% (v/v) fetal bovine serum, 5% CO_2. Transient transfections were carried out as described in Dornan and Hupp (34). Cells were gently lysed on ice in Nonidet P-40 buffer (25 mM Hepes pH 7.5, 0.1% (v/v) Nonidet P-40, 150 mM KCl, 5 mM DTT, 50 mM NaF, protease inhibitor mixture by Roche Applied Science (1 tablet was added per 10 ml of lysis buffer)). The protein concentration of the cell lysates was quantified using the Bio-Rad Bradford assay kit. To estimate the amount of correctly folded p53 in H1299 $p53^{-/-}$ cell lines transfected with appropriate plasmids (pCDNA3.1 (EV)-mock, pCDNA3.1/p53wt, pCDNA3.1/MDM2wt, pCDNA3.1/MDM2K454A, pCDNA3.1/MDM2C464A, and pCDNA3.1/MDM2C478S in appropriate combinations), the ratio between the level of p53 captured by pAb1620 and DO-1 was calculated. The ELISA procedure was carried out as follows: the wells were coated with wt-p53 conformation-specific pAb1620 monoclonal antibody or DO-1 (both mouse origin, Moravian Biotechnology) at 200 ng per well in 100 mM carbonate buffer, pH 9.0, at 4 °C for 16 h. The wells were blocked for 1 h at 17 °C with blocking buffer (4 mg/ml BSA in phosphate-buffered saline). This was followed by titration of increasing amounts of appropriate cell lysate diluted with the reaction buffer (25 mM HEPES, pH 7.3, 150 mM KCl, 5 mM DTT, 10% glycerol, 0.1% Triton X-100, 4 mg/ml BSA, protease inhibitor mixture). The reaction was performed for 1 h at 17 °C. Detection of p53 protein was carried out using the FL-393 antibody (rabbit origin, Santa Cruz Biotechnology) for 1 h at 17 °C. This was followed by the addition of anti-rabbit IgG-horseradish peroxidase secondary antibodies (Santa Cruz Biotechnology). Analysis of bound antibodies was performed by colorimetric detection with the TMB peroxidase kit (Bio-Rad) followed by quenching the reaction with 1 M H_2SO_4 and by absorbance measurements at 450 nm. The results obtained were plotted as a function of absorbance with respect to the amount of protein in question. For each particular case within the linear range the first derivative was calculated. The final values presented on the graph in Fig. 7 represent the normalization fractions obtained by division of pAb1620 derivative values *versus* DO-1 derivative values. The data represent the mean from five independent experiments with a standard deviation.

RESULTS

Recently we have shown that the Hsp90 molecular chaperone in an ATP-dependent reaction retains p53 at 37 °C in a conformation that allows binding to a specific promoter sequence (29). As shown by previously published data, p53 incubated at 17 °C *in vitro* binds specifically to promoter sequences after activation by C-terminal-specific p53 antibody or phosphorylation by CK2 kinase (Refs. 35 and 29 and Fig. 1*A*, *lane 1*). The same reaction performed under more physiological temperatures, *i.e.* 37 °C, does not lead to the formation of a p53 consensus site DNA complex (Fig. 1*A*, *lane 2*). As published before, at 37 °C p53 loses its correct fold, which is required for efficient specific binding of p53 to the promoter sequence (29). However, the ability of p53 to bind to a promoter sequence at 37 °C is possible in the presence of the Hsp90 molecular chaperone and ATP both *in vivo* and *in vitro* (Fig. 1*A*, *lane 13*, and

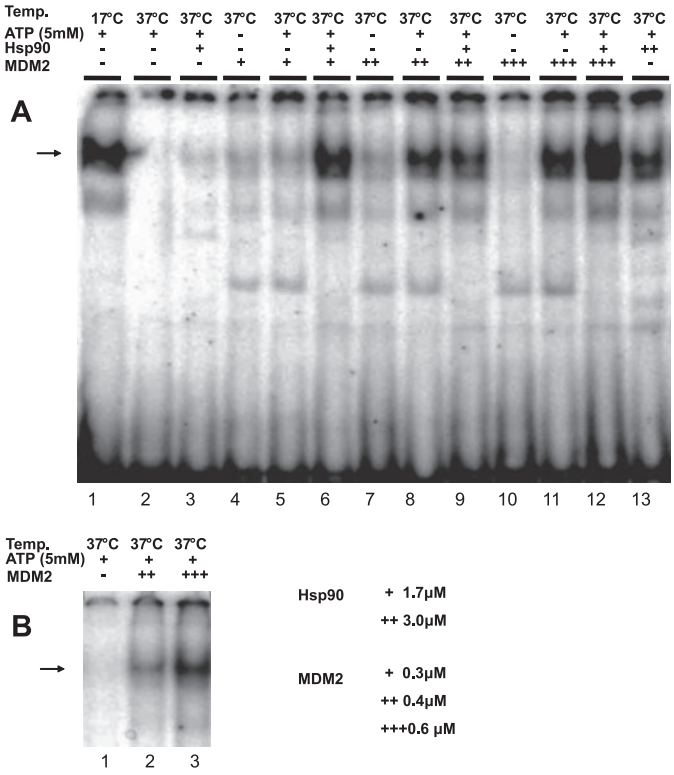

FIGURE 1. *A*, synergistic activity of MDM2 and Hsp90 in p53 binding to a specific DNA promoter-derived sequence at 37 °C. Reactions contained 0.05 μg of p53 (58.1 nM of the monomer) and were incubated for 1 h at 4 °C (*lane 1*) or 1.5 h at 37 °C (*lanes 2–13*) without or in the presence of a constant amount of Hsp90 (bovine brain) with or without 5 mM ATP and increasing amounts of MDM2 protein as indicated. To visualize the synergistic activity of Hsp90 and MDM2 protein, Hsp90 was added to the reaction mixture at 1.7 μM (of the monomer) final concentration, and under these conditions Hsp90 could only marginally restore the specific p53 binding to the promoter sequence (compare *lane 3* to control *lane 13* where the final concentration of Hsp90 was 1.7 and 3 μM, respectively). *B*, MDM2 restores p53-specific binding to the promoter sequence in a dose-dependent manner. The p53:MDM2 mass ratio for the reactions with increasing amounts of MDM2 (for *A* and *B* alike) is 1:8 to 1:12, which is still significantly less than the amount of Hsp90 needed to perform a similar task. At a 1:12 protein mass ratio, 0.05 μg of p53 (58.1 nM of the monomer) and 0.6 μg of MDM2 (0.6 μM of the monomer) of the proteins was used. All shown EMSA bands in this and subsequent figures correspond to the size of the p53 tetramer bound to the DNA, supershifted by the activating antibody pAb421.

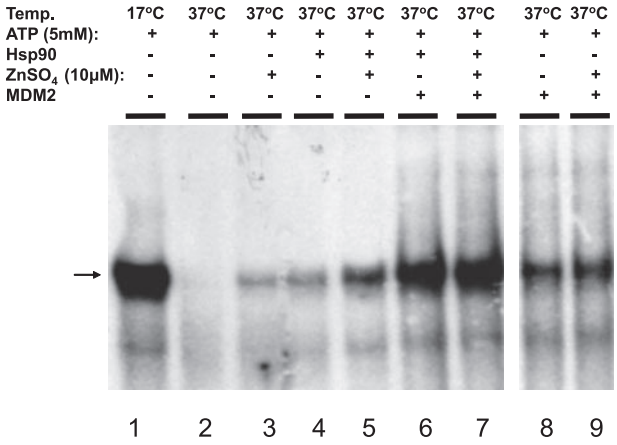

FIGURE 2. **The influence of zinc ions Zn^{2+}, Hsp90, and MDM2 on the binding of p53 to the *p21* promoter derived sequence.** Reactions containing 0.05 μg of p53 (58.1 nM of the monomer) were incubated for 1 h at 4 °C (*lane 1*) or for 1.5 h at 37 °C (*lanes 2–9*) without or in the presence of a constant amount of Hsp90 (bovine brain, 3 μM of the monomer), MDM2 (0.6 μM monomer), 10 μM $ZnSO_4$, and/or with 5 mM ATP. After activation of p53 by CK2, the DNA binding assay was performed. As seen in *lane 3* the presence of zinc alone slightly stabilizes p53 at 37 °C; the effect is pronounced when Hsp90 is added (*lane 5*), but dramatic evidence of stabilization can be monitored when all three components are present together during heat inactivation of p53 (*lane 7*). Although both proteins, namely Hsp90 and MDM2, stabilize the wild-type conformation of p53 separately (compare *lanes 2*, *4*, and *8*), the zinc effect is more visible for the stabilization of p53 by Hsp90 than by MDM2 (compare *lanes 4* and *5* and lanes *8* and *9*). It is worth noting the additive effect of both proteins on the stabilizing effect of p53 during protein inactivation (*lane 6*).

Refs. 29 and 36).[3] Surprisingly, the substitution of Hsp90 with MDM2 in this reaction leads to efficient binding of p53 to the promoter sequence (Fig. 1, *A*, *lanes 8* and *11*, and *B*, *lanes 2* and *3*). Moreover, the result presented in Fig. 1*A* (compare *lanes 5* and *6* with and *lanes 11* and *12*, respectively) suggests that Hsp90 and MDM2 may work synergistically.

The experiments described in Fig. 1, *A* and *B*, were performed in the absence of exogenous Zn^{2+}. Zn^{2+} ions are known to stabilize p53 and MDM2 structures, and the presence of Zn^{2+} is required for Hsp90-MDM2 complex formation (37). To test the effect of Zn^{2+}, we performed p53 DNA binding experiments in the presence or absence of 10 μM $ZnSO_4$. As shown in Fig. 2, the presence of 10 μM Zn^{2+} in the absence of any chaperones slightly stabilizes p53 at 37 °C, subsequently leading to binding to the *p21* promoter in the EMSA assay (Fig. 2, *lane 3*). In the presence of Hsp90 and Zn^{2+}, visibly more p53 is bound to the promoter sequence at 37 °C (Fig. 2, *lane 5*). The addition of MDM2 increases p53 DNA binding activity measured in the presence of Zn^{2+} and Hsp90 (Fig. 2, *lane 7*), but the effect of Zn^{2+} is less pronounced (compare *lanes 6* and *7* in Fig. 2). Zn^{2+} ions do not significantly change the ability of MDM2 to rescue p53 binding to the promoter sequence at 37 °C (Fig. 2, *lanes 8* and *9*).

The MDM2-dependent binding of p53 to the promoter sequence is limited to the physiological temperature of 37 °C (Fig. 3), suggesting that under heat shock conditions other chaperones could also be involved in these reactions. As shown in Figs. 1 and 2, the presence of MDM2 does not supershift the p53-promoter DNA complex, suggesting that MDM2 is only transiently required for p53 to adopt a DNA binding-competent conformation. To provide additional evidence that the interaction of MDM2 with p53 is indeed required for this effect, we used monoclonal antibodies that interfered with p53-MDM2 complex formation; 2A-10 binding to the central region of MDM2 and 4B2 antibody recognizing the epitope in the N terminus of MDM2. The presence of these antibodies during the preincubation of MDM2 with p53 at 37 °C severely, in the case of 2A-10, and partially, in the case of 4B2, reduced the ability of p53 to bind to the promoter sequence (Fig. 4, *lanes 4–6*). Additional controls showed that anti-MDM2 antibodies, 2A-10 and to some extent also 4B-2, directly interfere with MDM2-p53 complex formation, as judged by using the ELISA approach described under "Materials and Methods" (result not shown). These data support previous findings that multidomains of MDM2 (at least the N-terminal domain and acidic domain) are involved in the functional interactions with p53 (8). Interestingly, the addition of the mentioned antibodies after

[3] D. Walerych, unpublished results.

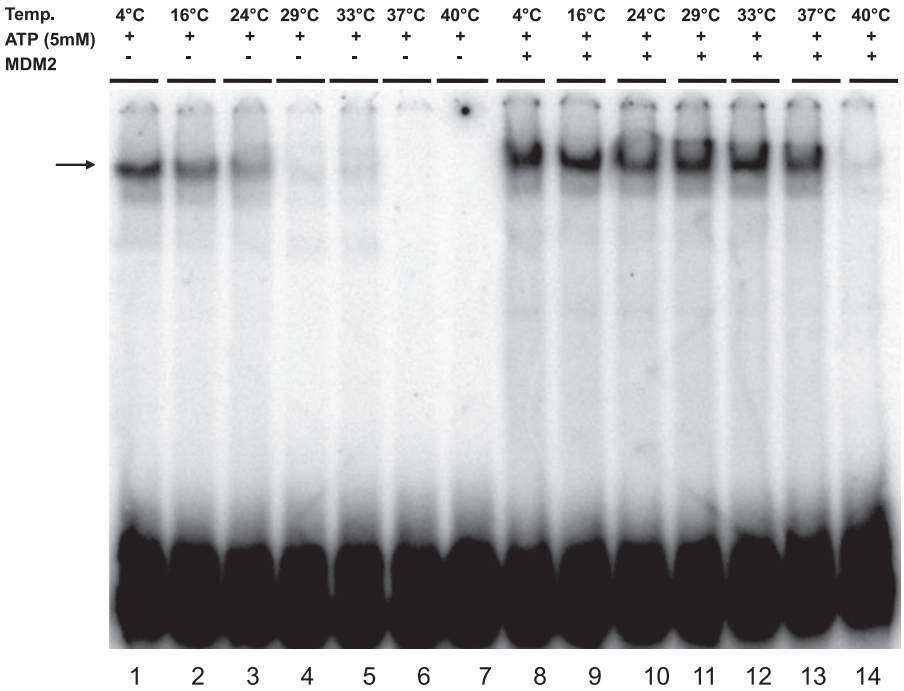

FIGURE 3. **p53 binding to a *p21* promoter-derived sequence is temperature-dependent in the presence and absence of MDM2.** Human recombinant MDM2 restores p53-specific DNA binding activity after 1 h of inactivation in a temperature gradient (4–40 °C). In all the lanes where MDM2 was added to p53, a constant 1:10 mass ratio of p53:MDM2 was used. At a 1:10 protein mass ratio, 0.05 μg of p53 was used (58.1 nM monomer) and 0.5 μg of MDM2 protein (0.45 μM of the monomer). To rule out unspecific protection effects, all reactions were supplemented with 1 μg/μl BSA.

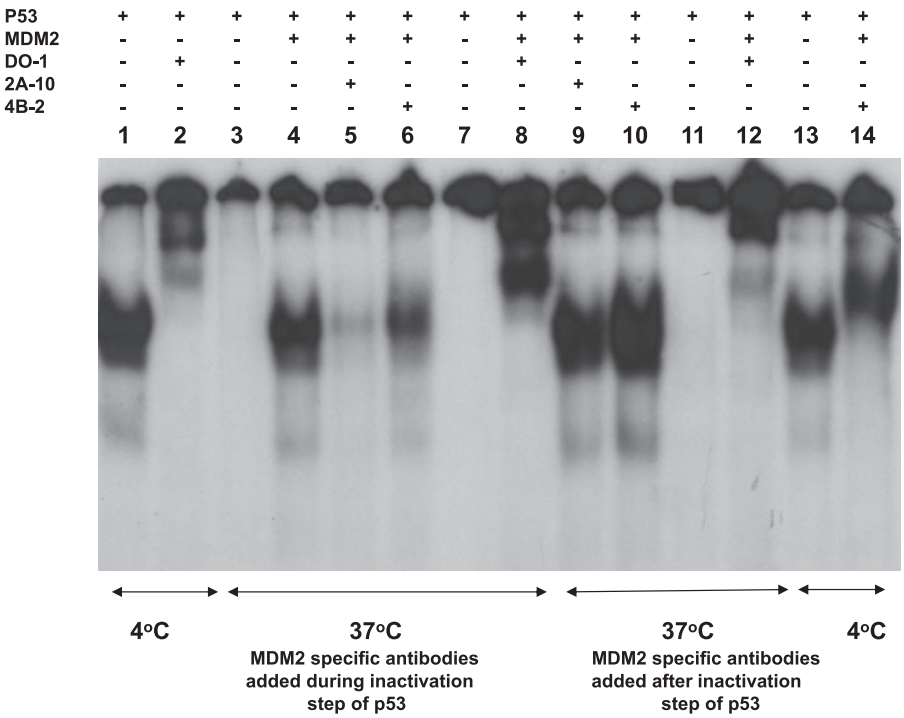

FIGURE 4. **MDM2 by transient interaction with p53 can assist in correct non-covalent assembly of the p53-promoter complex, but MDM2 is not a component of this assembled structure.** The DNA binding assay was performed as described in Fig. 1. The activation of p53 was performed either by CK2 or pAb421. The specific p53 antibody (*DO-1*) and MDM2 antibodies (*2A-10* or *4B-2*) were added during and after incubation of p53 with MDM2 and ATP at 37 °C. As *lanes 2*, *8*, and *12* demonstrate, the antibody DO-1 supershifts the DNA-p53 complex, whereas the MDM2-specific antibodies do not. It is highly probable that MDM2 is not a part of the p53-DNA complex. Moreover, these antibodies added during the incubation of p53 with MDM2/ATP at 37 °C interfere with p53-MDM2 complex formation, thus inhibiting binding of p53 to the DNA (*lanes 4–6*). This does not take place if the appropriate MDM2 antibodies are added after the 37 °C incubation step when the appropriate p53-MDM2 interactions has already occurred (compare *lanes 5* and *6* and *lanes 9* and *10*). *Lanes 3*, *7*, and *11* represent the controls of thermally denatured p53.

the activation step (activation by pAb421 (Fig. 4) or phosphorylation of p53 by CK2 kinase (result not shown)) do not inhibit the ability of p53 to bind to the promoter sequence (Fig. 4, *lane 9* and *10*), suggesting that on this stage MDM2 is no longer in the complex with p53. Moreover, the monoclonal MDM2-specific antibodies 4B-2 or 2A-10 do not change the mobility of p53-DNA complex which further supports the absence of MDM2 in the p53-DNA complex (Fig. 4, *lane 9* and *10*). However, if such a reaction is conducted at 4 °C, the monoclonal antibody 4B-2 supershifts the p53-DNA complex (Fig. 4, *lane 14*), suggesting that recycling of MDM2 from the p53 complex is caused by the diffusion accelerated by the temperature. The results presented in Fig. 4 suggest that the presence of MDM2 is required only when p53 is preincubated at 37 °C and that the p53-MDM2 complex dissociates after conversion of latent p53 to a transcriptionally active p53. In a control experiment (Fig. 4), we found that the addition of the p53-specific DO-1 antibody before (*lane 8*) and after preincubation of p53 at 37 °C (*lane 12*) leads to antibody-induced supershift, indicating that p53 is present in the complex with the promoter DNA sequence. In addition, using an ELISA approach, we have shown that DO-1 does not interfere with MDM2-p53 complex formation (see Fig. 6*A* and results not shown).

In the absence of ATP, MDM2 interacts with p53 independently of the conformational state in which p53 is, namely, a correct fold *i.e.* native-like or mutant-like fold (preincubation of p53 at 37 °C for 90 min, Fig. 5). This situation, however, is quite different in the presence of ATP. The nucleotide does not significantly influence the affinity of MDM2 to p53 with the correct wild-type conformation but has an effect when the wild-type conformation of p53 is abrogated. Here the presence of ATP leads to a reduction in the affinity of MDM2 toward p53 (Fig. 5*A*).

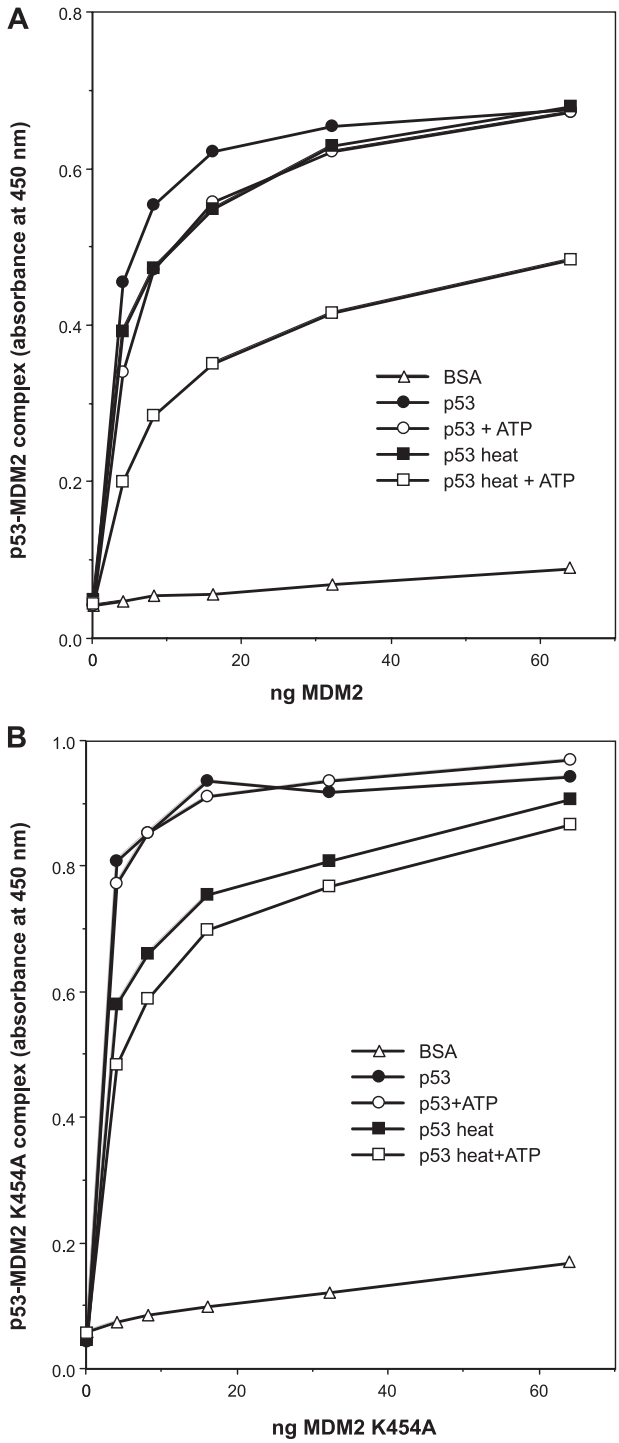

FIGURE 5. **The effect of ATP on MDM2-p53 complex formation.** Reactions containing 200 ng of wt p53 or heat-inactivated p53 (37 °C for 90 min) were coated onto each well of an ELISA plate. After a washing and blocking procedure, the reaction with MDM2 wt (*A*) or MDM2 K454A (*B*) in the presence of 5 mM ATP or without ATP was initiated. Visualization of the complex formation between two proteins was done using the MDM2 reactive antibody H-221 (described under "Materials and Methods").

As reported previously, MDM2 possesses a Walker motif allowing it to preferentially bind ATP with $K_D = 13.5\ \mu M$ (7). No ATPase activity of MDM2 was detected. Mutation of the *mdm2* gene in the K454A position inhibits ATP binding by the protein but does not interfere with its E3 ubiquitin ligase activity (7). As shown in Fig. 5*B* and 6*A*, the purified mutant MDM2 K454 tightly binds p53 regardless of the presence of ATP or the conformational status of p53. These experiments suggest that binding of ATP by MDM2 triggers the release of MDM2 from the MDM2-p53 complex only when the wild-type conformation of p53 is abrogated. At the same time the MDM2 K454A protein, which still possesses E3 ubiquitin ligase activity on a level comparable with wild-type MDM2 (Fig. 6*B*), is not able to rescue p53 binding to the promoter sequence at 37 °C (Fig. 6*C*). Because the MDM2 K454A mutation is within the RING finger domain of MDM2, we cannot exclude that this mutation not only affects the ability of MDM2 to bind ATP but in addition has another effect(s) on the overall structure of the RING finger domain. However, two experimental facts strongly suggest that this is not a case. First, the MDM2 K454A mutant possesses E3 ubiquitin ligase activity similar to MDM2 wt protein (Fig. 6*B*). Kinetic studies show that MDM2 K454A is slightly more active in ubiquitylation of p53.[4] Second, the point mutants MDM2 C464A and C478S in the zinc binding motif that are completely inactive in the p53 ubquitylation reaction still efficiently bind ATP and are able to rescue the ability of binding of p53 to the promoter DNA sequence at 37 °C (result not shown).

The data presented in Figs. 5 and 6 suggest that recycling of MDM2 from the p53 complex, triggered by binding of ATP to MDM2, is required for binding of p53 to the promoter sequence at 37 °C. One explanation of these results could be that the binding of MDM2 to latent p53 partially unfolds p53, and after activation of p53 and ATP-dependent dissociation of MDM2 from the p53-MDM2 complex, p53 spontaneously folds to the correct conformation, allowing its binding to the promoter DNA sequence.

To test the influence of MDM2 on correct folding of p53 within the cell, we used an immunochemical-based assay that measures p53 affinity to conformation-specific antibodies (38, 39). Human lung carcinoma H1299 $p53^{-/-}$ cells, which express a limited amount of MDM2 (result not shown), were cotransfected with a combination of plasmids encoding wild-type p53 and wild-type or mutant proteins, MDM2 K454A, MDM2 C464A, and MDM2 C478S. After gentle cell lysis, the ratio of wild-type correctly folded p53 (ELISA test with pAb1620) to total p53 (ELISA test with DO-1) in cell lysate was measured (Fig. 7). In the control experiments we show that binding of the DO-1 antibody does not interfere with the p53-MDM2 complex formation (Figs. 4 and 5 and result not shown). Transfection of H1299 cells with *p53* alone shows that less than 40% of p53 protein possesses a wild-type conformation (sensitive to pAb1620 monoclonal antibody). It is highly probable that in this case the correct folding of p53 is stimulated by the presence of other molecular chaperones, like the abundant Hsp90. Cotransfection of *p53* wt with *mdm2* wt substantially stimulates the folding of p53. More than 70% of p53 was found in a wild-type conformation. Cotransfection of p53 wt with

[4] C. Stevens, S. Petterson, M. Wallace, B. Wawrzynow, A. Zylicz, M. Zylicz, and T. Hupp, manuscript in preparation.

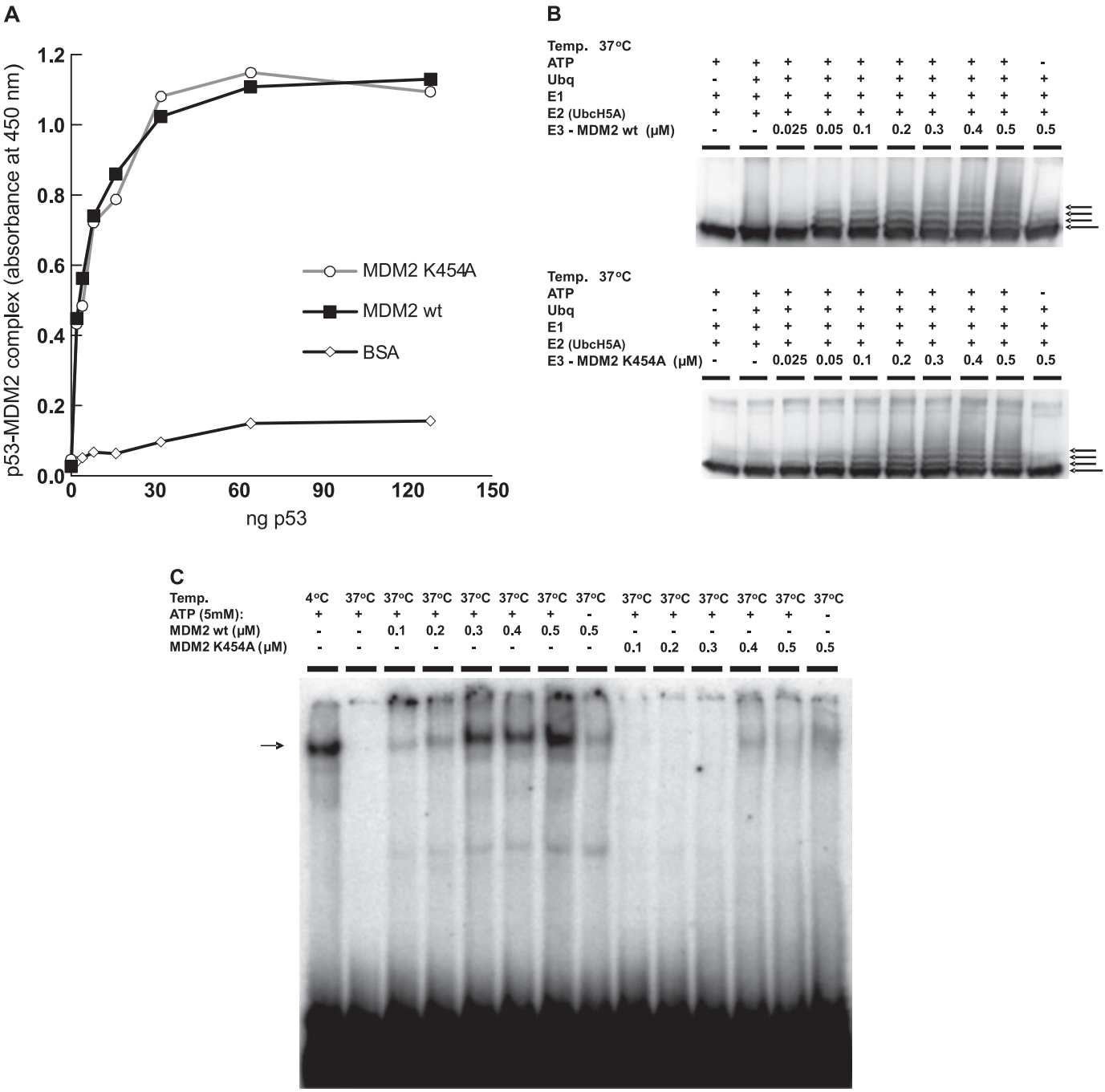

FIGURE 6. **The ATP binding mutant of MDM2, which is able to bind and ubiquitylate p53, is defective in promoting p53 binding to the *p21* promoter sequence.** *A*, purified MDM2 K454A, an ATP binding mutant, specifically interacts with human recombinant p53 similarly to wt-MDM2. An ELISA was used to verify binding, where constant amounts of MDM2 wt or MDM2 K454A (0.1 μg) were anchored onto the well via the 2A-10 monoclonal antibody, and increasing amounts of p53 protein were added. The secondary polyclonal antibody FL-393 was used to detect the complex formation. In a control experiment the p53 protein (0.1 μg) was anchored via the p53 antibody (DO-1) onto the well, and increasing amounts of MDM2 wt or MDM2 K454A proteins were added. The secondary polyclonal antibody H-221 was used to detect the complex formation. A BSA titration was used as a negative control of the interaction. *B*, MDM2 K454A possesses E3 ubiquitin ligase activity comparable with MDM2 wt in the *in vitro* ubiquitylation assay. The reaction was performed as indicated and visualized as described under "Materials and Methods." *C*, p53 protein binding to the specific DNA promoter at 37 °C, mediated by MDM2, is ATP-dependent. The MDM2 K454A mutant was not able to maintain p53 binding to the *p21* promoter sequence at restrictive temperature relative to wild-type MDM2. The EMSA assay was carried out as described under "Materials and Methods." As indicated, comparable amounts of the two proteins were used in the EMSA and polyubiquitylation assays.

MDM2 C478S or C464A mutants, which are deficient in E3 ubiquitin ligase activity, caused an even higher level of pAb1620-recognizable conformation of p53 (Fig. 7). It must be stressed that in the case when *mdm2* wt is used, we are dealing with at least three effects; that is, an increase of the degradation of p53 (result not shown), an increase of the chaperone-like activity of MDM2, and folding of wt p53 catalyzed by other chaperones like Hsp90. Cotransfection of cells with plasmid-encoding wt p53 and mutant MDM2 K454A substantially reduces the amount of p53 found in

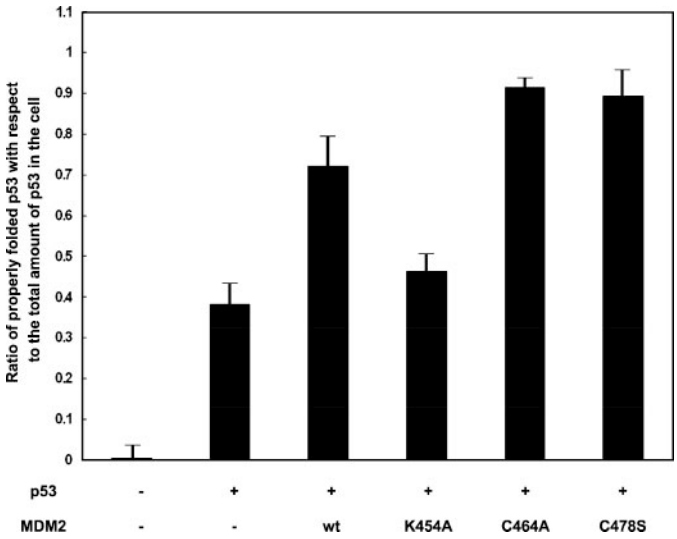

FIGURE 7. **The involvement of MDM2 in p53 folding.** The H1299 $p53^{-/-}$ cell line was transfected with pcDNA3.1 empty vector, pcDNA3.1/p53 (0.5 μg) alone, and combinations of pcDNA3.1/p53 (0.5 μg) with pcDNA3.1/MDM2 wt (1 μg), pcDNA3.1/MDM2 K454A (1 μg), pcDNA3.1/MDM2 C478S (1 μg), or pcDNA3.1/MDM2 C464A (1 μg). After cell lysis and the ELISA experiments described in detail under "Material and Methods" were carried out, the ratio of conformationally wild-type p53 (pAb1620 reactive) with respect to the total amount of p53 (DO-1 reactive) in the cell was calculated. MDM2 wt transfection stimulates the proper folding of p53, whereas the ATP binding mutant of MDM2 has no effect on p53 protein folding. Both mutant proteins deficient in E3 ubiquitin ligase activity stimulate the proper p53 folding much better than does MDM2 wt. The final values presented on the graph represent the normalization fractions obtained by division of pAb1620 derivative values *versus* DO-1 derivative values. The data represent mean from 5 independent experiments with *error bars* indicating a S.D.

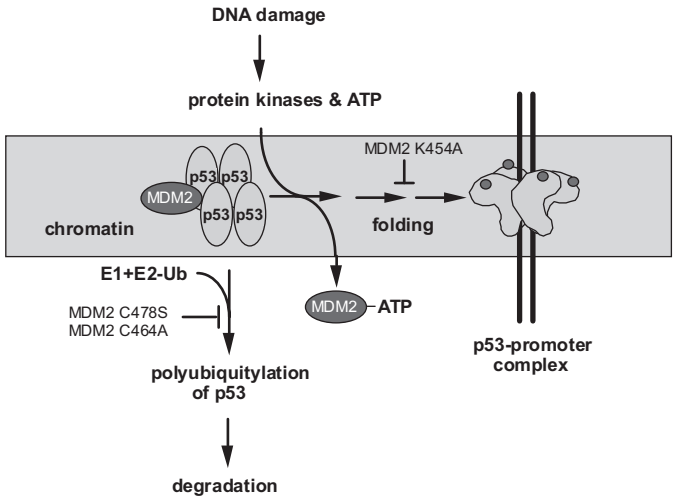

FIGURE 8. **The dual E3-ubiquitin ligase and chaperone-like activity of the MDM2 oncoprotein.** p53 protein assembles into a tetrameric form that can be degraded by an MDM2-dependent ubiquitylation pathway or assembled into a wild-type conformation by an MDM2 chaperone-dependent pathway. The factors that control the switch between these two pathways are undefined. However, a single point mutation in the *BOX-V* containing the ubiquitylation signal of p53 (8) can *in vitro* predispose p53 to hyperubiquitylation by MDM2 in a cell-free coupled translation system containing molecular chaperones (39). It means there are direct feedback sensors that can drive p53 into a wild-type conformation or into a hyperubiquitylated conformation. Most research in MDM2 has been centered on its E3 ubiquitin ligase function. In the molecular chaperone pathway, MDM2 binding to p53 induces a local conformational change in p53 in the flexible *BOX-V* motif (50). After activation by protein kinases (or by pAb421 *in vitro*), MDM2 dissociates from p53, thus allowing p53 to spontaneously fold to a conformation that has a high affinity toward binding to the promoter sequence. This chaperone-like reaction is ATP-dependent and can be uncoupled from the E3 ubiquitin ligase function of MDM2 (mutation C478S or C464A). The mutation within the *mdm2* gene, which encodes the MDM2 K454A protein with deficient binding of ATP, prevents the proper folding of p53 *in vitro* and *in vivo*. Activation of p53 after DNA damage and subsequent dissociation of MDM2 occurs on chromatin (53). Whether polyubiquitylation and subsequent degradation of p53 also occurs on chromatin remains still an open question (66).

wild-type conformation (Fig. 7), indicating that the observed effect of MDM2 on p53 folding is due to molecular chaperone activity of MDM2.

DISCUSSION

p53 is a protein of complex conformational flexibility, and it is in an equilibrium between different functional conformations. Strongly unfolded or misfolded forms of mutant p53 can function as gain-of-function oncogenes (40–42). Moreover, wild-type p53 tumor suppressor protein may adopt these different conformations either in response to various stress conditions (post-translational modifications or the direct effect of elevated temperature), binding to DNA, or the interacting proteins (for review, see Refs. 43 and 44). Some of these conformational states can be detected by p53 conformation-specific antibodies (pAb1620 and pAb240) (38, 45).

It has previously been proposed that wild-type p53 protein could be transiently associated with molecular chaperones (29, 43, 46, 47). *In vitro* wt p53 can interact with Hsp40 and Hsp70, but such a complex is dissociated in the presence of Hsp90 (46). Transient interaction of p53 with Hsp90 is required for p53 binding to its consensus promoter DNA sequence (29, 36). When p53 is in a complex with a promoter sequence, it is no longer in a complex with Hsp90. The presence of ATP is required for Hsp90-dependent binding of p53 to the promoter sequence at 37 °C. Whether Hsp90 can unfold p53 protein actively (analogy to the Hsp100 unfoldase activity as described in Ref. 48) or by transient binding to the conformationally flexible regions of p53 is still an open question. *In vivo* FRET experiments support the notion that the Hsp90 chaperone transiently interacts with wild-type p53.[3]

The presence of geldanamycin, a specific Hsp90 inhibitor, abrogates the binding of p53 to the *p21* promoter sequence as well as its transcriptional activity (29). Geldanamycin-mediated stimulation of degradation of both wt and 175H mutant of p53 in H1299 cells coexpressing CHIP (chaperone-associated E3 ubiquitin ligase) has been shown (47). Recently we reported that cooperation of Hsp90 with MDM2 and CHIP proteins stimulated unfolding of the native tetramer of p53 (37). At the same time the MDM2-dependent polyubiquitylation of mutant p53 is inhibited by Hsp90 (49).

In this paper we have shown that MDM2 alone, in an ATP-dependent reaction, can substitute for the Hsp90 molecular chaperone in promoting the binding of p53 to the *p21* promoter sequence at 37 °C. The results presented here and those published by others suggest a possible scenario depicted in Fig. 8. After binding to MDM2, p53 protein undergoes partial unfolding (50, 51). In a stress situation, after activation by protein kinases, like CK2, after UV radiation (52), MDM2 dissociates from partially unfolded p53, thus allowing p53 to spontaneously fold. Such repeated binding, unfolding, dissociation, and folding reaction could lead p53 to reach a conformation which has a high affinity toward its promoter sequence. Recently pub-

lished *in vivo* data strongly support the idea of dissociation of MDM2 after the activation of p53. Using a chromatin immunoprecipitation technique, White *et al.* (53) have shown that MDM2 localizes with latent p53 on the chromatin near *p21(waf1)* and *mdm2* genes before but not after DNA damage. We suggest that a transient complex of p53 with MDM2 and Hsp90 molecular chaperones may be important for the decision of whether to activate or degrade p53 by employing a series of post-translational modifications, like phosphorylation, acetylation, ubiquitylation, sumoylation, neddylation, and others. The situation where eukaryotic molecular chaperones are involved in folding and degradation of protein is similar to prokaryotic Hsp100/Clp family members, whereas an ATPase subunit of the appropriate protease at the same time is a molecular chaperone and the specificity factor for the protein substrates degradation (Refs. 54–56; for review, see Ref. 57). It is highly probable that in eukaryotes the quality control process starts upstream of the 19 S proteasome subunit, namely when the E3 ligases demonstrate their activities and the decision to repair or degrade the protein substrates occurs. This apparent contradictory mode of MDM2 as a component of the degradation machinery (E3 ubiquitin ligase activity) and as molecular chaperone-like activity resembles a dual function of CHIP, a cochaperone/ubiquitin ligase that targets a broad range of chaperone substrates for proteasomal degradation (58–60). Interestingly, while this paper was under revision, the Cyr and co-workers reported that CHIP alone possesses a molecular chaperone activity (61).

In addition to the fact that MDM2 can assist in correct noncovalent assembly of the p53-promoter complex, where MDM2 is not a component of this assembled structure, MDM2 fulfils other molecular chaperone criteria. The purified MDM2 protein, in an ATP-independent reaction, can function like the Hsp90 chaperone in protecting citrate synthase and firefly luciferase from aggregation (supplemental data). The discovery that MDM2, besides the E3 ubiquitin ligase activity, also possesses a molecular chaperone activity involved in protein folding and protection from aggregation raises an important question concerning the biological relevance of MDM2 chaperone activity toward p53 and other protein substrates. The *in vivo* situation of the p53 case is very complex. We observe that MDM2 promotes p53 folding but at the same time MDM2 accelerates the degradation of p53. We propose that molecular chaperone activities of MDM2 in concert with Hsp90 are required for shifting the equilibrium of p53 conformation toward such a state(s) where either p53 is potent to bind to the promoter sequence, thus being transcriptionally active, or to be recognized by the ubiquitylation machinery. If these and probably other chaperones are not able to shift the p53 conformational equilibrium, then p53 is directed by Hsp40 to a multichaperone complex, p53-Hsp40-Hsp70-HOP-Hsp90 (46). Such a stable complex inhibits not only p53 degradation but also p53 transcriptional activity. The overlapping chaperone activities (Hsp90, MDM2, and probably others) make verification of this hypothesis rather difficult. Nevertheless, recent findings from other laboratories indicate that ubiquitylation and proteasomal machinery are directly involved in transcriptional regulation. Zhu *et al.* (62) have shown that both ubiquitylation and proteasomal functions are required for efficient transcription mediated by p53. They postulate that among E3 ubiquitin ligases driving p53 toward ubiquitylation and degradation, MDM2 (besides TOPORS) cannot be excluded as a coactivator for p53 transcriptional activity. Emerging evidence indicates that MDM2 can modulate the activity of other transcription factors (23–25). We have found that MDM2, in an ATP-dependent reaction, stimulates unfolding of E2F1/DP1 transcription factor.[4] MDM2 has been proved to be a positive regulator of HIV transactivator Tat. MDM2 promotes ubiquitylation of Tat and enhances Tat-mediated transactivation (63). Furthermore, MDM2 has been shown to recruit to the estrogen receptor-α binding ps2 promoter (64) and modulate p63, p73, and E2F1 transcriptional activities and protein levels (3, 24, 65).

We postulate that molecular chaperone activity of MDM2 described here could not only help to explain the mechanism of involvement of ubiquitin-proteasome system in p53-mediated transcription (62) but also could shed new light on p53-independent activities of MDM2 as an oncogene (15). The findings reported in this paper that a single point mutation MDM2 K454A selectively inhibits a molecular chaperone activity of MDM2 should help in verifications of these hypotheses.

Acknowledgments—We thank Renata Filipek for sharing the protocols for polyubiquitylation assays and donating the E2-conjugating enzyme at the initial stage of this work. We are also grateful to Jakub Urbanski for experimental support with transfection of H1299 cells and to Dawid Walerych for fruitful discussions and for sharing the protocol for EMSA assay.

REFERENCES

1. Vogelstein, B., Lane, D., and Levine, A. J. (2000) *Nature* **408,** 307–310
2. Michael, D., and Oren, M. (2002) *Curr. Opin. Genet. Dev.* **12,** 53–59
3. Melino, G., Lu, X., Gasco, M., Crook, T., and Knight, R. (2003) *Trends Biochem. Sci.* **28,** 663–670
4. Michael, D., and Oren, M. (2003) *Semin. Cancer Biol.* **13,** 49–58
5. Shimizu, H., and Hupp, T. R. (2003) *Trends Biochem. Sci.* **28,** 346–349
6. Vassilev, L. T., Vu, B. T., Graves, B., Carvajal, D., Podlaski, F., Filipovic, Z., Kong, N., Kammlott, U., Lukacs, C., Klein, C., Fotouhi, N., and Liu, E. A. (2004) *Science* **303,** 844–848
7. Poyurovsky, M. V., Jacq, X., Ma, C., Karin-Schmidt, O., Parker, P. J., Chalfie, M., Manley, J. L., and Prives, C. (2003) *Mol. Cell* **12,** 875–887
8. Wallace, M., Worrall, E., Pettersson, S., Hupp, T., and Ball, K. (2006) *Mol. Cell* **23,** 251–263
9. Yin, Y., Stephen, C. W., Luciani, M. G., and Fahraeus, R. (2002) *Nat. Cell Biol.* **4,** 462–467
10. Marechal, V., Elenbaas, B., Piette, J., Nicolas, J. C., and Levine, A. J. (1994) *Mol. Cell. Biol.* **11,** 7414–7420
11. Dai, M. S., and Lu, H. (2004) *J. Biol. Chem.* **279,** 44475–44482
12. Bond, G. L., Hu, W., Bond, E. E., Robins, H., Lutzker, S. G., Arva, N.C., Bargonetti, J., Bartel, F., Taubert, H., Wuerl, P., Onel, K., Hwang, S. J., Strong, L. C., Lozano, G., and Levine, A. J. (2004) *Cell* **119,** 591–602
13. Daujat, S., Neel, H., and Piette, J. (2001) *Trends Genet.* **17,** 459–464
14. Ganguli, G., and Wasylyk, B. (2003) *Mol. Cancer Res.* **1,** 1027–1035
15. Zhang, Z., and Zhang, R. (2005) *Curr. Cancer Drug Targets* **5,** 9–20
16. Cordon-Cardo, C., Latres, E., Drobnjak, M., Oliva, M. R., Pollack, D., Woodruff, J. M., Marechal, V., Chen, J., Brennan, M. F., and Levine, A. J. (1994) *Cancer Res.* **54,** 794–799
17. Jones, S. N., Hancockm, A. R., Vogel, H., Donehower, L. A., and Bradley, A. (1998) *Proc. Natl. Acad. Sci. U. S. A.* **95,** 15608–15612
18. Vargas, D. A., Takahashi, S., and Ronai, Z. (2003) *Adv. Cancer Res.* **89,** 1–34

19. Bartel, F., Harris, L. C., Wurl, P., and Taubert, H. (2004) *Mol. Cancer Res.* **2,** 29–35
20. Liang, H., Atkins, H., Abdel-Fattah, R., Jones, S. N., and Lunec, J. (2004) *Gene* (*Amst.*) **338,** 217–223
21. Steinman, H. A., Burstein, E., Lengner, C., Gosselin, J., Pihan, G., Duckett, C. S., and Jones, S. N. (2004) *J. Biol. Chem.* **279,** 4877–4886
22. Kim, M. M., Wiederschain, D., Kennedy, D., Hansen, E., and Yuan, Z. M. (2007) *Oncogene* **26,** 4209–4215
23. Martin, K., Trouche, D., Hagemeier, C., Sorensen, T. S., La Thangue, N. B., and Kouzarides, T. (1995) *Nature* **375,** 691–694
24. Calabro, V., Mansueto, G., Parisi, T., Vivo, M., Calogero, R. A., and La Mantia, G. (2002) *J. Biol. Chem.* **277,** 2674–2681
25. Ongkeko, W. M., Wang, X. Q., Siu, W. Y., Law, A. W., Yamashita, K., Harris, A. L., Cox, L. S., and Poon, N. Y. (1999) *Curr. Biol.* **9,** 829–832
26. Asahara, H., Li, Y., Fuss, J., Haines, D. S., Vlatkovic, N., Boyd, M. T., and Linn, S. (2003) *Nucleic Acids Res.* **31,** 2451–2459
27. Hartl, F. U., and Hayer-Hartl, M. (2002) *Science* **295,** 1852–1858
28. Ellis, R. J. (1993) in *Molecular Chaperones* (Ellis, R. J., Laskey, R. A., and Lorimer, G. H., eds) pp. 1–5, Chapman & Hall, London
29. Walerych, D., Kudla, G., Gutkowska, M., Wawrzynow, B., Muller, L., King, F. W., Helwak, A., Boros, J., Zylicz, A., and Zylicz, M. (2004) *J. Biol. Chem.* **279,** 48836–48845
30. Burch, L. R., Midgley, C. A., Currie, R. A., Lane, D. P., and Hupp, T. R. (2000) *FEBS Lett.* **472,** 93–98
31. Midgley, C. A., Desterro, J. M., Saville, M. K., Howard, S., Sparks, A., Hay, R. T., and Lane, D. P. (2000) *Oncogene* **19,** 2312–2323
32. Shimizu, H., Burch, L. R., Smith, A. J., Dornan, D., Wallace, M., Ball, K. L., and Hupp, T. R. (2002) *J. Biol. Chem.* **32,** 28446–28458
33. Nichols, N. M., and Matthews, K. S. (2002) *Biochemistry* **41,** 170–178
34. Dornan, D., and Hupp, T. R. (2001) *EMBO Rep.* **2,** 139–144
35. Hupp, T. R., Sparks, A., and Lane, D. P. (1995) *Cell* **83,** 237–245
36. Muller, L., Schaupp, A., Walerych, D., Wegele, H., and Buchner, J. (2004) *J. Biol. Chem.* **279,** 48846–48854
37. Burch, L., Shimizu, H., Smith, A., Patterson, C., and Hupp, T. R. (2004) *J. Mol. Biol.* **337,** 129–145
38. Gannon, J. V., Greaves, R., Iggo, R., and Lane, D. P. (1990) *EMBO J.* **9,** 1595–1602
39. Shimizu, H., Saliba, D., Wallace, M., Finlan, L., Langridge-Smith, P. R., and Hupp, T. R. (2006) *Biochem. J.* **397,** 355–367
40. Blandin, G., Levine, A. J., and Oren, M. (1999) *Oncogene* **18,** 477–485
41. Song, H., Hollstein, M., and Hy, Y. (2007) *Nat. Cell Biol.* **9,** 573–580
42. Joerger, A. C., and Fersht, A. R. (2007) *Oncogene* **26,** 2226–2242
43. Zylicz, M., King, F. W., and Wawrzynow, A. (2001) *EMBO J.* **20,** 4634–4638
44. Kaustov, L., Yi, G.-S., Ayed, A., Bochkareva, E., Bochkarev, A., and Arrowsmith, C. H. (2006) *Cell Cycle* **5,** 489–494
45. Milner, J., and Medcalf, E. A. (1990) *J. Mol. Biol.* **216,** 481–484
46. King, F. W., Wawrzynow, A., Hohfeld, J., and Zylicz, M. (2001) *EMBO J.* **20,** 6297–6305
47. Esser, C., Scheffner, M., and Hohfeld, J. (2005) *J. Biol. Chem.* **280,** 27443–27448
48. Weber-Ban, E. U., Reid, B. G., Miranker, A. D., and Horwich, A. L. (1999) *Nature* **401,** 90–93
49. Peng, Y., Chen, L., Li, C., Lu, W., and Chen, J. (2001) *J. Biol. Chem.* **276,** 40583–40590
50. Yu, G. W., Rudiger, S., Veprintsev, D., Freund, S., Fernandez-Fernandez, M., and Fersht, A. R. (2006) *Proc. Natl. Acad. Sci. U. S. A.* **103,** 1227–1232
51. Sasaki, M., Nie, L., and Maki, C. G. (2007) *J. Biol. Chem.* **282,** 14626–14634
52. MacPherson, D., Kim, J., Kim, T., Rhee, B. K., Van Oostrom, C. T., DiTullio, R. A., Venere, M., Halazonetis, T. D., Bronson, R., De Vries, A., Fleming, M., and Jacks, T. (2004) *EMBO J.* **23,** 3689–3699
53. White, D. E., Talbott, K. E., Arva, N. C., and Bargonetti, J. (2006) *Cancer Res.* **66,** 3463–3470
54. Parsell, D. A., Kowal, A. S., Singer, M. A., and Lindquist, S. (1994) *Nature* **372,** 475–478
55. Wickner, S., Gottesman, S., Skowyra, D., Hoskins, J., McKenney, K., and Maurizi, M. R. (1994) *Proc. Natl. Acad. Sci. U. S. A.* **91,** 12218–12222
56. Wawrzynow, A., Wojtkowiak, D., Marszalek, J., Banecki, B., Jonsen, M., Graves, B., Georgopoulos, C., and Zylicz, M. (1995) *EMBO J.* **14,** 1867–1877
57. Wawrzynow, A., Banecki, B., and Zylicz, M. (1996) *Mol. Microbiol.* **21,** 895–899
58. Hohfeld, J., Cyr, D. M., and Patterson, C. (2001) *EMBO Rep.* **2,** 885–890
59. Cyr, D. M., Hohfeld, J., and Patterson, C. (2002) *Trends Biochem. Sci.* **27,** 368–375
60. Qian, S. B., McDonough, H., Boellmann, F., Cyr, D. M., and Patterson, C. (2006) *Nature* **440,** 551–555
61. Rosser, M. F. N., Washburn, E., Muchowski, P. J., Patterson, C., and Cyr, D. M. (2007) *J. Biol. Chem.* **282,** 22267–22277
62. Zhu, Q., Wani, G., Yao, J., Patnaik, S., Wang, Q.-E., El-Mahdy, M. A., Praetorius-Ibba, M., and Wani, A. A. (2007) *Oncogene* **26,** 4199–4208
63. Bres, V., Kiernan, R. E., Linares, L. K., Chable-Bessia, C., Plechakova, O., Treand, C., Peloponese, J. M., Jeang, K. T., Coux, O., Scheffner, M., and Benkirane, M. (2003) *Nat. Cell Biol.* **5,** 754–761
64. Reid, G., Hubner, M. R., Metivier, R., Brand, H., Denger, S., Manu, D., Beaudouin, J., Ellenberg, J., and Gannon, F. (2003) *Mol. Cell* **11,** 695–707
65. Zhang, Z., Wang, H., Li, M., Rayburn, E. R., Agrawal, S., and Zhang R. (2005) *Oncogene* **24,** 7238–7247
66. Hirano, Y., and Ronai, Z. (2006) *Cell* **127,** 675–677

the FEBS Journal

ATP stimulates MDM2-mediated inhibition of the DNA-binding function of E2F1

Craig Stevens[1,*], Susanne Pettersson[1,*], Bartosz Wawrzynow[1], Maura Wallace[2], Kathryn Ball[1], Alicja Zylicz[3] and Ted R. Hupp[1]

1 Cell Signaling Unit, University of Edinburgh, UK
2 Royal Dick School of Veterinary Studies, Easter Bush Veterinary Centre, Edinburgh, UK
3 International Institute of Molecular and Cell Biology in Warsaw, Poland

Keywords
ATP; chaperone; E2F; MDM2; p53

Correspondence
T. R. Hupp, Institute of Genetics and Molecular Medicine, Cell Signalling Unit, CRUK p53 Signal Transduction Group, University of Edinburgh, Edinburgh EH4 2XR, UK
Fax: +44 131 777 3542
Tel: +44 131 777 3583
E-mail: ted.hupp@ed.ac.uk

*These authors contributed equally to this paper

(Received 19 May 2008, revised 16 July 2008, accepted 4 August 2008)

doi:10.1111/j.1742-4658.2008.06627.x

Murine double minute 2 (MDM2) protein exhibits many diverse biochemical functions on the tumour suppressor protein p53, including transcriptional suppression and E3 ubiquitin ligase activity. However, more recent data have shown that MDM2 can exhibit ATP-dependent molecular chaperone activity and directly mediate folding of the p53 tetramer. Analysing the ATP-dependent function of MDM2 will provide novel insights into the evolution and function of the protein. We have established a system to analyse the molecular chaperone function of MDM2 on another of its target proteins, the transcription factor E2F1. In the absence of ATP, MDM2 was able to catalyse inhibition of the DNA-binding function of E2F1. However, the inhibition of E2F1 by MDM2 was stimulated by ATP, and mutation of the ATP-binding domain of MDM2 (K454A) prevented the ATP-stimulated inhibition of E2F1. Further, ATP stabilized the binding of E2F1 to MDM2 using conditions under which ATP destabilized the MDM2:p53 complex. However, the ATP-binding mutant of MDM2 was as active as an E3 ubiquitin ligase on E2F1 and p53, highlighting a specific function for the ATP-binding domain of MDM2 in altering substrate protein folding. Antibodies to three distinct domains of MDM2 neutralized its activity, showing that inhibition of E2F1 is MDM2-dependent and that multiple domains of MDM2 are involved in E2F1 inhibition. Dimethylsulfoxide, which reduces protein unfolding, also prevented E2F1 inhibition by MDM2. These data support a role for the ATP-binding domain in altering the protein–protein interaction function of MDM2.

One of the most evolutionarily conserved and widely recruited cellular defence pathways involves the heat-shock stress protein family. These polypeptides, now termed molecular chaperones, were originally classified based on differences in molecular weight, and comprise proteins of 25, 40, 60, 70, 90 and 110 kDa [1]. The biochemical function of molecular chaperones (including HSP70 and HSP90) is thought to revolve around the regulation of protein folding, unfolding, intracellular transport and protein degradation [2]. The biological consequences of molecular chaperone induction in many cell types involve not only repair of damaged polypeptides and cellular survival after injury, but acquisition of thermotolerance and protection of cells from normally lethal levels of damage [3]. In addition, molecular chaperones have also been shown to prevent drug- or radiation-dependent apoptosis in cells, highlighting the

Abbreviations
CHIP, carboxyl terminus of HSC70-interacting protein; E2F, E2A binding factor; GST, glutathione *S*-transferase; HSP, heat-shock protein; IPTG, isopropyl thio-β-D-galactoside; MDM2, murine double minute 2; pRB, retinoblastoma protein.

role that these proteins may play in tumour cell survival and drug resistance [4].

The molecular chaperones also form the nucleus of a large multi-protein complex or chaperone machine that coordinates protein folding or unfolding, protein ubiquitination, and protein degradation in cells. Defining the components of this molecular chaperone machine will facilitate understanding of how these proteins function as survival factors in normal tissue and cancer cells [5–7]. Of the molecular chaperones, HSP90 has elicited the most widespread interest as it is the target of the Ansamycin class of anti-cancer agent [2,8]. Small molecules named Geldanamycin and 17-allylamino demethoxygeldanamycin that target the nucleotide-binding site of HSP90 can alter the activity of the protein, change its conformation, and sensitize cells to death [9]. HSP90 inhibitors are currently undergoing clinical trials, although little is known about the mechanism of Ansamycin drug function at the proteome level or about the HSP90 holoenzyme protein complex in primary cancers. However, the core HSP90 multi-protein complex [comprising HSP90, HSP70, HSP40, HSP25 and Hsp70/Hsp90 organizing protein (Hop)] is known to be 're-arranged' in cancer cells into a distinct biochemical complex, compared to normal cells, suggesting a mechanism to explain the sensitivity of cancer cells to Ansamycins [6].

In addition to controlling the assembly or degradation rates of many cellular signalling proteins, most notably protein kinases, HSP90 can also control the conformation and function of the tumour suppressor protein p53. The first cellular protein shown to bind to p53 was a member of the HSP70 family of proteins [10], whose associations with p53 have since been extended to include the molecular chaperones HSP40 and HSP90 [11–13]. Interactions of wild-type and mutant p53 have been reconstituted *in vitro* and in cell culture with chaperone proteins, providing biochemical models enabling insights into the cell biology of HSP–p53 interactions [14–16]. The relevance of the interaction of mutant p53 with molecular chaperones in tumour cells has previously been unclear, but studies have indicated that one component of the anti-apoptotic function of molecular chaperones may be related to their ability to unfold and inactivate mutant p53 protein [12,13]. Novel anti-cancer drugs that target HSP90 chaperones promote reactivation of the specific DNA-binding function of mutant p53 in tumour cell lines by releasing the mutant p53 from the chaperone holoenzyme complexes [17,18]. In this situation, drugs such as Geldanamycin can reactivate the tumour suppressor function of p53 and have therapeutic value. However, more recent work has shown that HSP90 can also facilitate wild-type p53 assembly in a positive regulatory mode [14,19], and that HSP90, the E3 ubiquitin ligase MDM2 and denatured p53 form a trimeric complex in cancer cell lines [19,20]. The presence of MDM2 in this trimeric complex was the first clue that MDM2 could be linked to HSP function, at least in some tumour cells.

In an effort to expand on the potential protein interaction map of the anti-cancer drug target MDM2, we previously utilized peptide aptamer libraries to identify novel MDM2-binding proteins [21]. This biochemical approach for expansion of the 'interactome' of a target relies on the growing realization that many protein–protein interactions are driven by small linear motifs, sometimes as small as four amino acids. Of many peptide interaction motifs identified for MDM2, the one that is relevant for cancer biology is that for HSP90 [21]. MDM2 and HSP90 cooperate to unfold and inhibit the DNA-binding activity of the p53 protein [21]. We further found that HSP90:MDM2 and p53 form a complex in cancer cell lines, thus identifying a novel multi-protein complex with the two proto-oncogenes and p53 [21]. This complex between p53, MDM2 and HSP90 is now known to be common in cancer cell lines [19]. A striking discovery when analysing the folding of p53 protein based on validated chaperone assays [14–16] was that MDM2 possesses an ATP-dependent molecular chaperone function on p53 [22]. This is the first biochemical function attributed to the ATP-binding domain of MDM2, which was previously reported to play a role in controlling MDM2 intracellular localization [23]. In this paper, we extend and analyse the role of the ATP-binding domain of MDM2 with respect to its ability to function as a protein folding factor for another key target protein, E2F1, in order to determine whether the ATP-binding function of MDM2 can alter the protein conformation of other MDM2 substrates. In contrast to p53, which is positively folded by MDM2 in an ATP-dependent manner [22], MDM2 inhibits E2F1 DNA-binding activity in an ATP-stimulated manner. The results regarding p53 and E2F1 interactions with MDM2 provide biochemical insights into how polypeptide conformation can be regulated by the ATP-binding function of MDM2.

Results

Uncoupling the E3 ubiquitin ligase from the ATP-binding function of MDM2

Before examining whether MDM2 possesses any protein folding activity towards E2F1, we first characterized the interaction in an E3 ubiquitin ligase assay to

define the integrity of the E2F1 and MDM2 proteins used in this assay. MDM2 protein possesses an intrinsic RING finger-dependent E3 ubiquitin ligase function that is important for interaction with its client protein p53. The molecular mechanism of MDM2-mediated ubiquitination is not well defined, but at least two interfaces are required for MDM2 to drive ubiquitination of p53: a coordinated interaction of the N-terminus of MDM2 with the N-terminus of p53, and an interaction of the acid domain of MDM2 with the central domain of p53 [24]. Accordingly, ligands such as the NUTLIN and BOX1 peptides from p53 do not block p53 ubiquitination by MDM2 (Fig. 1A, lanes 2 and 4 versus lane 1), but peptide ligands such as RB1 that bind the acid domain can block MDM2 function towards p53 (Fig. 1A, lane 3 versus lane 1).

Using the assay described above for p53, the E2F1–MDM2 ubiquitination reaction was reconstituted using purified proteins. Titration of MDM2 and E2F1 (Fig. 1B,C) optimized the ubiquitination assay, in which multiple mono-ubiquitin adducts were apparently linked to E2F1 protein. Using this optimized assay, the RB1 peptide was able to inhibit MDM2-mediated ubiquitination of E2F1 (Fig. 1D, lane 3 versus lane 1), and this was also refractory to Nutlin (Fig. 1D, lanes 4-6 versus lane 1). Thus, MDM2-mediated ubiquitination of E2F1 operates by a similar two-site mechanism to that described for p53. The precise docking sites for MDM2 on E2F1 that drive the dual-site ubiquitination have not been defined.

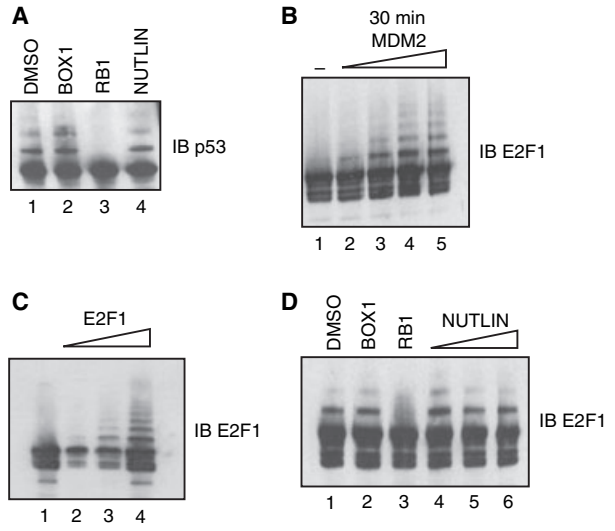

Fig. 1. The Rb1 peptide inhibits E2F1 ubiquitination by MDM2. Ubiquitination assays were performed as described in Experimental procedures. The following reactions were assembled and analysed for ubiquitination by immunoblotting: (A) p53 wild-type protein (30 ng) was incubated in the presence of dimethylsulfoxide (DMSO) (4.5%), BOX1 peptide (50 μM), RB1 peptide (50 μM) or NUTLIN (50μM). (B) GST–E2F1 protein (40 ng) was incubated with increasing concentrations of wild-type MDM2 protein for 30 min (30, 60, 120 and 180 ng, lanes 2–5). (C) Wild-type MDM2 protein (25 ng) was incubated with increasing concentrations of GST–E2F1 protein (10, 20 and 40 ng, lanes 2–4) for 30 min. (D) Wild-type MDM2 protein (120 ng) was incubated with GST–E2F1 protein (40 ng) in the presence of dimethylsulfoxide (4.5%), BOX1 peptide (50 μM), RB1 peptide (50 μM) or increasing amounts of NUTLIN (25, 50 and 100 μM).

A set of MDM2 mutants was next used to examine the role of the RING finger domain and the ATP-binding domain in substrate ubiquitination. As expected, mutation of the RING finger domain at codon 478 (MDM2-C478S) inhibited the E3 ubiquitin ligase function of MDM2 towards p53 (Fig. 2A, lanes 8–10 versus lanes 2–4). The codon 454 mutant of MDM2 (MDM2-K454A) that shows attenuated ATP-binding function was marginally more active as an E3 ubiquitin ligase towards p53 (Fig. 2A, lanes 5–7 versus 2–4; quantified in Fig. 2B). Similarly, mutation of the RING finger domain at codon 478 inhibited the E3 ubiquitin ligase function of MDM2 towards E2F1 (Fig. 2C, lanes 8–10 versus lanes 2–4), whilst MDM2-K454A showed enhanced E3 ubiquitin ligase activity towards E2F1 (Fig. 2B, lanes 5–7 versus 2–4; quantified in Fig. 2D). These latter data indicate that mutating the ATP-binding domain of MDM2 does not produce widespread conformational changes that disrupt its allosteric and multi-site E3 ubiquitin ligase function towards substrates.

MDM2-mediated inhibition of E2F1 DNA-binding function

Using the biochemically characterized forms of MDM2 described above, we evaluated whether E2F1 protein can be modified by the chaperonin function of MDM2, as described for p53 [22]. First, the specificity of glutathione *S*-transferase (GST)–E2F1 DNA binding in gel-retardation assays was confirmed using a mutant probe (Fig. 3A, lane 2 versus lane 1) and super-shifting with antibodies specific to E2F1 (Fig. 3A, lane 3 versus lane 1). p53 and E2F1 might be expected to be modified differently by MDM2: p53 is thermodynamically unstable at physiological temperatures [25] and is completely destabilized at 37 °C [22], while E2F1 is relatively thermostable at 37 °C and requires and elevated temperature to reduce its DNA-binding function (Fig. 3J, lanes 2 and 3 versus lane 1). In the absence of ATP, a titration of wild-type MDM2 destabilized the DNA-binding function of E2F1 (Fig. 3B, lanes 2–5 versus lane 1). Further, the MDM2-K454A (Fig. 3B, lanes 7–10) and MDM2-C478S (Fig. 3C, lanes 5 and 6) mutants were as active

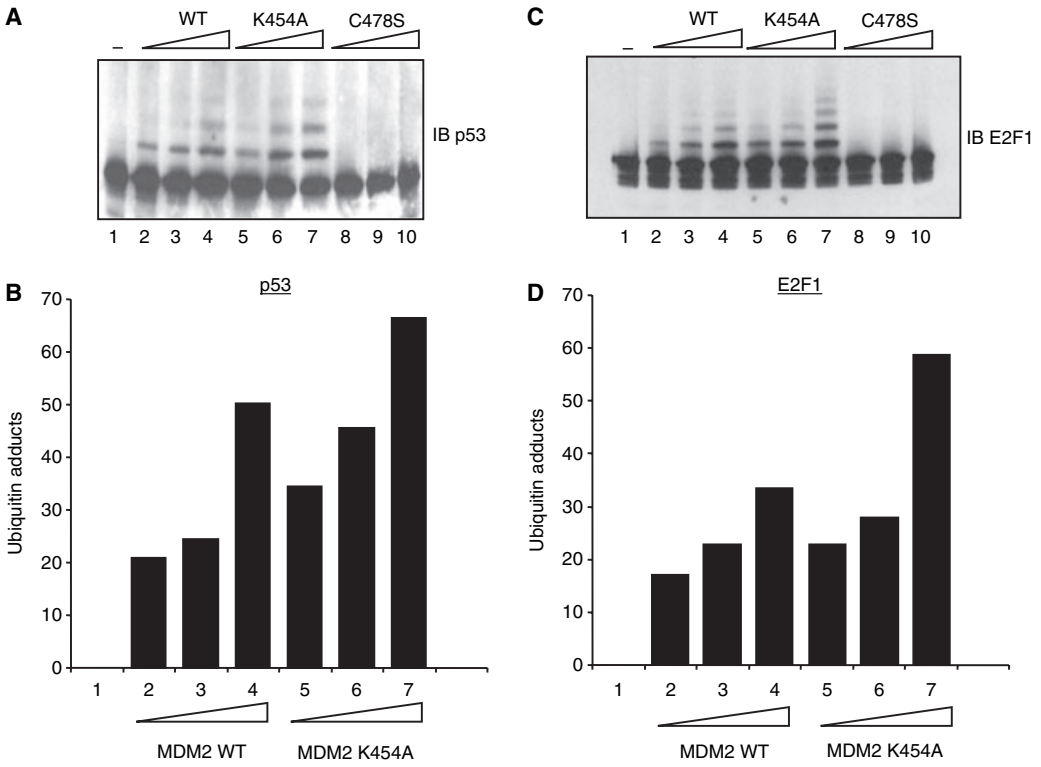

Fig. 2. An MDM2 mutant deficient for ATP binding does not have impaired E3 ubiquitin ligase function towards p53 or E2F1. Ubiquitination assays were performed as described in Experimental procedures. The following reactions were assembled and analysed for ubiquitination by immunoblotting. (A) p53 protein (30 ng) was incubated with increasing concentrations of wild-type MDM2 protein (6.25, 12.5 and 25 ng, lanes 2–4), MDM2-K454A (6.25, 12.5 and 25 ng, lanes 5–7) or MDM2-C478S (6.25, 12.5 and 25 ng, lanes 8–10). (B) Quantification of ubiquitin adducts. (C) GST–E2F1 protein (40 ng) was incubated with increasing concentrations of wild-type MDM2 protein (6.25, 12.5 and 25 ng, lanes 2–4), MDM2-K454A (6.25, 12.5 and 25 ng, lanes 5–7) or MDM2-C478S (6.25, 12.5 and 25 ng, lanes 8–10). (D) Quantification of ubiquitin adducts.

as wild-type MDM2 at inhibiting the DNA-binding function of E2F1. These data are similar to the previously reported inhibition of p53 function by the MDM2–HSP90 complex in the absence of ATP [21]. However, as ATP stimulates MDM2 folding of p53 into an active form [22], we evaluated whether ATP has any influence on E2F1 inhibition by MDM2. A titration of MDM2 in the presence of ATP stimulated the inhibitory activity of MDM2 towards E2F1 (Fig. 3D, lanes 7–10 versus lanes 2–5). This is in contrast to the stimulation of p53 DNA-binding function by MDM2 by ATP [22]. The ATP dependence of E2F1 inhibition was further confirmed using wild-type MDM2 (Fig. 3E, lanes 6–8 versus lanes 2–4; quantified in Fig. 3F) and MDM2-K454A: in the presence of ATP, wild-type MDM2 induces a more pronounced inhibition of E2F1 DNA-binding function compared with MDM2-K454A (Fig. 3G, lanes 7–10 versus lanes 2–5; quantified in Fig. 3H). As a control, preincubation of MDM2 with E2F1 does not alter E2F1 ubiquitination (Fig. 3I), indicating that the misfolding of E2F1 by MDM2 can be uncoupled from its ubiquitination. Together, these data confirm that the ATP-binding domain of MDM2 can modify its biochemical function, with distinct outcomes on the DNA-binding function of the p53 or E2F1 substrates.

Protein folding and/or unfolding functions operate through dynamic associations and dissociations. When ATP-binding proteins are involved in these processes, these transient interactions are in turn differentially stabilized by ATP. For example, the ATP-dependent stimulation of p53 DNA-binding function by MDM2 correlates with a destabilization of the MDM2–p53 complex by ATP [22] that presumably allows MDM2 to dissociate and p53 to bind to DNA. This is a classic example of an ATP-dependent chaperonin functioning as a 'catalyst'. We evaluated therefore whether the inhibition of E2F1 DNA-binding function by MDM2 correlated with its enhanced binding by MDM2 or destabilized binding by ATP addition. Unlike p53 [22],

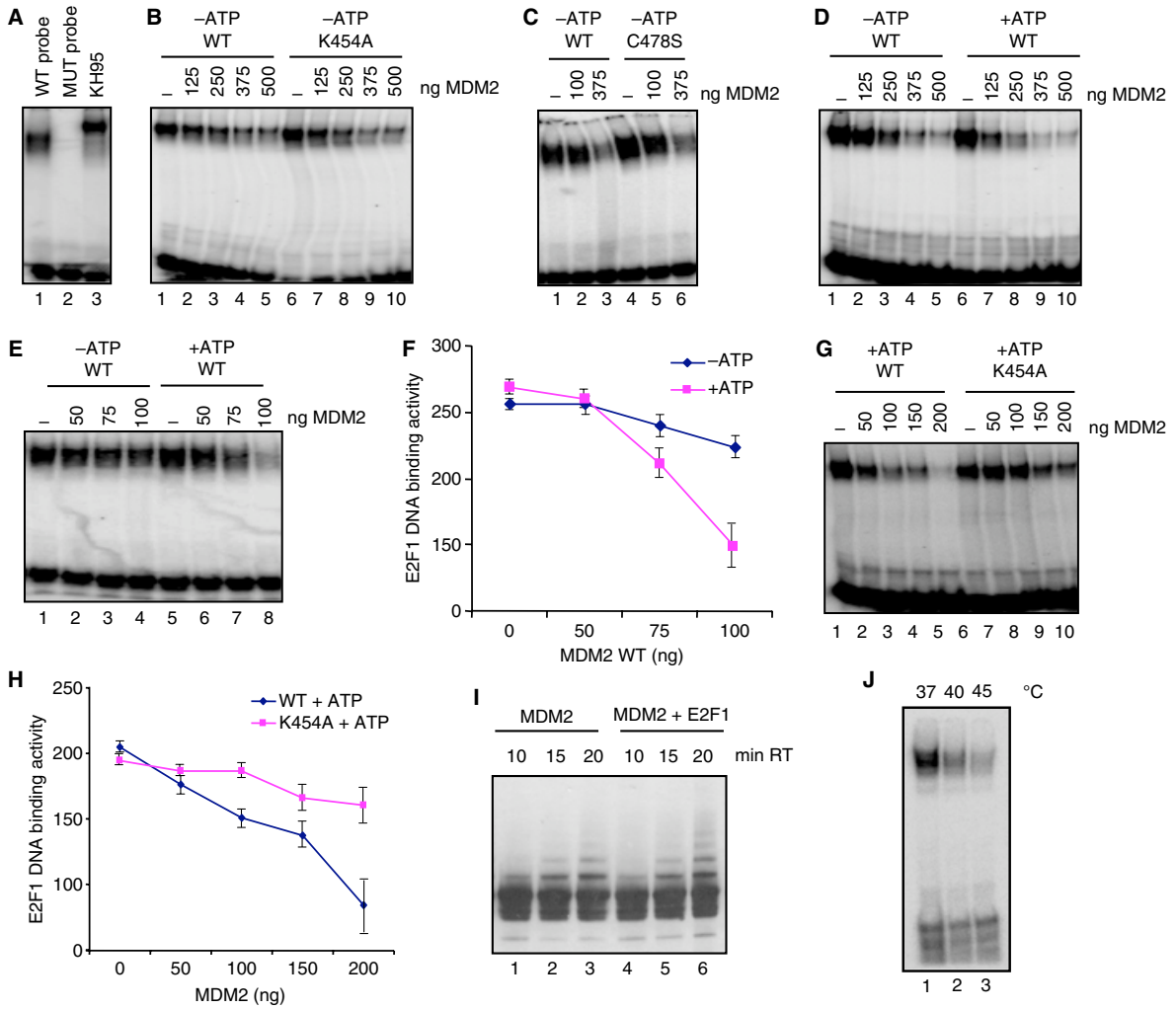

Fig. 3. MDM2 inhibition of E2F1 function is stimulated by ATP. DNA-binding assays were performed as described in Experimental procedures. The following reactions were assembled and analysed for E2F1 DNA-binding activity. (A) Specificity of E2F1 DNA binding. GST–E2F1 protein (100 ng) was incubated with wild-type probe (lanes 1 and 3) or mutant probe (lane 2). For super-shifting, GST–E2F1 protein (100 ng) was preincubated in the presence of E2F1 antibody KH95 (200 ng, lane 3), and DNA-binding reactions were analysed using native gel electrophoresis. (B) Analysis of E2F1 DNA binding using increasing concentrations of wild-type MDM2 or K454A-MDM2. GST–E2F1 protein (100 ng) was incubated in the presence of the indicated amounts of wild-type MDM2 protein (lanes 2–5) or MDM2-K454A protein (lanes 7–10) in the absence of ATP, and DNA-binding reactions were analysed using native gel electrophoresis. (C) Analysis of E2F1 DNA binding using wild-type MDM2 or MDM2-C478S. GST–E2F1 protein (100 ng) was incubated in the presence of the indicated amounts of wild-type MDM2 protein (lanes 2 and 3) or MDM2-C478S protein (lanes 5 and 6) in the absence of ATP, and DNA-binding reactions were analysed using native gel electrophoresis. (D) Analysis of E2F1 DNA binding using increasing concentrations of wild-type MDM2 and ATP. GST–E2F1 protein (100 ng) was incubated in the presence of the indicated amounts of wild-type MDM2 protein in the absence of ATP (lanes 2–5) or in the presence of ATP (1 mM, lanes 7–10), and DNA-binding reactions were analysed using native gel electrophoresis. (E,F) ATP stimulates wild-type MDM2 mediated inhibition of E2F1 DNA binding. GST–E2F1 protein (100 ng) was incubated with the indicated amounts of wild-type MDM2 protein in the absence (lanes 2–4) or presence (lanes 6–8) of ATP (1 mM), and DNA-binding reactions were analysed using native gel electrophoresis and quantified in (F) (error bars are SD of duplicate experiments). (G,H) Analysis of E2F1 DNA binding using increasing concentrations of wild-type MDM2 or MDM2-K454A and ATP. GST–E2F1 protein (100 ng) was incubated in the presence of the indicated amounts of wild-type MDM2 protein (lanes 2–5) or MDM2-K454A protein (lanes 7–10) in the presence of ATP (1 mM), and DNA-binding reactions were analysed using native gel electrophoresis and quantified in (H) (error bars are SD of duplicate experiments). (I) Preincubation of MDM2 with E2F1 does not alter E2F1 ubiquitination. Ubiquitination assays were performed without preincubation of MDM2 with E2F1 (lanes 1–3, as in Figs 1 and 2) or with preincubation with E2F1 using conditions under which MDM2 inhibits the DNA-binding function of E2F1 (lanes 4–6). Ubiquitination reactions were carried out for the indicated durations, and linearity was observed. (J) Temperature required to inhibit the DNA-binding function of E2F1. E2F1 was incubated at the indicated temperature, as performed for wild-type p53 [22], and analysed for DNA binding as described in Experimental procedures.

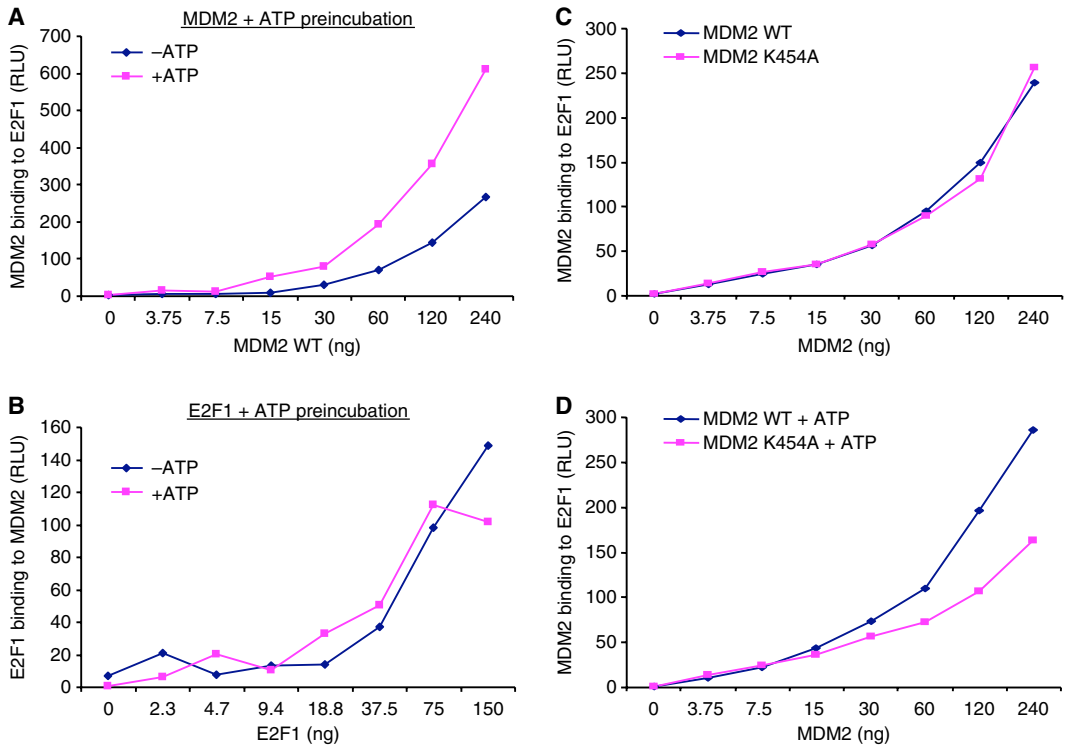

Fig. 4. ATP stabilizes MDM2 binding to E2F1. ELISA assays were performed as described in Experimental procedures to quantify the amount of MDM2 bound to E2F1 under various conditions. (A) MDM2 preincubation with ATP. Increasing amounts of MDM2 protein were preincubated in the presence or absence of ATP (1 mM) for 20 min at room temperature prior to incubation with GST–E2F1 protein (100 ng) adsorbed to the solid phase. The amount of MDM2 bound to E2F1 was quantified using monoclonal antibody 2A10 and expressed in relative light units. (B) E2F1 preincubation with ATP. Various amounts of GST–E2F1 protein were preincubated in the presence or absence of ATP (1 mM) for 20 min at room temperature prior to incubation with wild-type MDM2 protein (50 ng) adsorbed to the solid phase. The amount of E2F1 bound was quantified using monoclonal antibody KH95 and expressed in relative light units. (C) Comparison of E2F1 binding to wild-type MDM2 and MDM2-K454A. Increasing amounts of MDM2 protein were incubated with GST–E2F1 protein (100 ng) adsorbed to the solid phase. The amount of MDM2 bound to E2F1 was quantified using monoclonal antibody 2A10 and expressed in relative light units. (D) Preincubation of wild-type MDM2 and MDM2-K454A with ATP. Increasing amounts of MDM2 protein were preincubated in the presence of ATP (1 mM) for 20 min at room temperature prior to incubation with GST–E2F1 protein (100 ng) adsorbed to the solid phase. The amount of MDM2 bound to E2F1 was quantified using monoclonal antibody 2A10 and expressed in relative light units.

ATP preincubation with MDM2 actually stabilized MDM2–E2F1 complex formation as determined using a sandwich ELISA (Fig. 4A), and this presumably explains why the MDM2-mediated inhibition of E2F1 DNA-binding function is stimulated by ATP. By contrast, ATP preincubation with E2F1 has no effect on MDM2–E2F1 complex formation as determined using a sandwich ELISA (Fig. 4B). In the absence of ATP, wild-type MDM2 and MDM2-K454A exhibit a similar affinity for E2F1 (Fig. 4C); however, ATP stimulation of the MDM2–E2F1 complex is attenuated using the MDM2-K454A mutant (Fig. 4D). These data provide a correlation between ATP-stimulated MDM2 binding to E2F1 and ATP-stimulated destabilization of the E2F1–DNA complex by MDM2.

Further evidence for a stable interaction between E2F1 and MDM2 was evaluated by changes in partial proteolysis of E2F1. Increasing the duration of trypsinization resulted in a relatively rapid degradation of full-length E2F1 (Fig. 5A), with accumulation of a relatively stable set of trypsin-resistant fragments of lower molecular mass. Addition of MDM2 protected E2F1 from partial proteolysis, which is suggestive of a specific binding interaction between the two proteins (Fig. 5A bracket). Having established that MDM2 can inhibit E2F1 function in a DNA-binding assay, and that both the binding reaction and the inhibition reaction are ATP-stimulated, we developed assays to confirm MDM2 dependence in the assay, define which domain of MDM2 might be mediating the inhibition of E2F1, and determine whether classic protein misfolding is the mechanism by which E2F1 is inhibited by MDM2.

Deletion of any of three domains of MDM2 can inhibit the E3 ubiquitin ligase activity towards p53, as

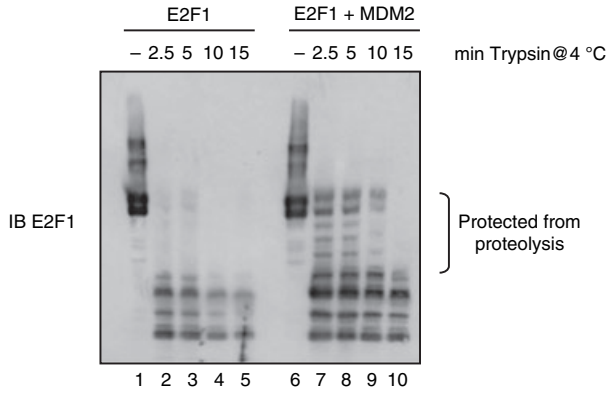

Fig. 5. MDM2 alters the tryptic digestion pattern of E2F1. Tryptic digestion assays were performed as described in Experimental procedures. (A) GST–E2F1 protein (100 ng) was incubated with trypsin (50 ng) at 4 °C for the indicated times in the absence of MDM2 (lanes 2–5) or in the presence of wild-type MDM2 protein (200 ng, lanes 7–10).

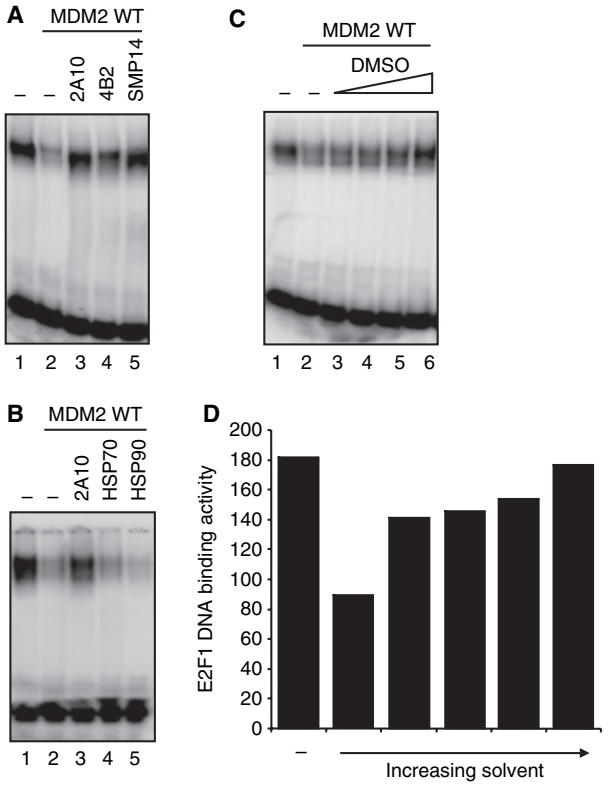

Fig. 6. E2F1 inhibition by MDM2 is attenuated by MDM2 antibodies and stabilizing solvents. DNA-binding assays were performed as described in Experimental procedures. (A) MDM2 monoclonal antibodies neutralize the ability of MDM2 to inhibit E2F1. GST–E2F1 protein (100 ng) was incubated with wild-type MDM2 protein (375 ng, lanes 2–5) in the presence of 200 ng of the MDM2 antibodies 2A10 (lane 3), 4B2 (lane 4) or SMP14 (lane 5). (B) HSP monoclonal antibodies do not neutralize the ability of MDM2 to inhibit E2F1. GST–E2F1 protein (100 ng) was incubated with wild-type MDM2 protein (375 ng, lanes 2–5) in the presence of 200 ng of MDM2 antibody 2A10 (lane 3), HSP70 antibody (lane 4) or HSP90 antibody (lane 5). (C) Dimethylsulfoxide (DMSO) prevents MDM2-mediated inhibition of E2F1. GST–E2F1 protein (100 ng) was incubated with wild-type MDM2 protein (375 ng, lanes 2–6) in the presence of increasing amounts of dimethylsulfoxide (1%, 2.5%, 5% and 10%, lanes 3–6). (D) Quantification of effects of solvents on E2F1 function in the presence of inhibitory levels of MDM2.

these domains are required for the interaction with multiple domains of p53 [24]. These deletion analyses do not provide mechanistic insight into the function of the full-length protein, and we therefore used monoclonal antibodies with defined binding sites on MDM2 to determine whether MDM2 could be neutralized as an inhibitor of E2F1. The addition of antibodies 2A10 and SMP14, which bind to the central region of MDM2, had the most pronounced effect on blocking MDM2 function (Fig. 6A, lanes 3 and 5 versus lane 2), whilst the 4B2 antibody, which binds to the N-terminal domain of MDM2, marginally attenuated MDM2 function (Fig. 6A, lane 4 versus lane 2). The ability of all three monoclonal antibodies to attenuate MDM2 function suggests that multiple domains of MDM2 play a mechanistic role in binding to E2F1 and altering its function in a DNA-binding assay. To ensure that the inhibition of E2F1 DNA-binding function is not a result of a contaminating chaperone from *Escherichia coli* in the recombinant MDM2 preparation, monoclonal antibodies for HSP70 and HSP90 were used as controls (Fig. 6B, lanes 4 and 5 versus lane 3). Together, these data show that MDM2 alone is responsible for inhibiting E2F1 function.

The study of p53 folding by factors including chaperones is greatly facilitated by the existence of monoclonal antibodies that discriminate between folded and unfolded p53. This has allowed the accumulation of direct evidence that p53 can be 'misfolded' or 'folded' by MDM2 and/or HSP90 [21,22]. Unfortunately no such reagents towards E2F1 are available to facilitate a mechanistic understanding. In order to determine whether MDM2 protein inhibits E2F1 by 'misfolding', we evaluated whether solvents that classically 'stabilize' protein conformation can reverse the MDM2-mediated effect on E2F1. Specifically, dimethylsulfoxide and glycerol have been shown to restore the proper folding and function of mutant p53 [26,27]. Titration of the stabilizing solvent dimethylsulfoxide (Fig. 6C,D) prevented the MDM2-mediated inhibition of E2F1 function, and almost completely restored E2F1 function, suggesting that E2F1 is in fact inhibited through conformational 'misfolding' of the protein by MDM2. Taken together, these data establish that the

ATP-binding domain of MDM2 plays a role in stabilizing the binding to E2F1, and that this induces a misfolded conformation in E2F1 that is incompatible with sequence-specific DNA binding.

Discussion

MDM2 is a multi-functional protein with biochemical functions in: (a) transcriptional suppression by direct contact of the activation domain of p53 and occlusion of the coactivator p300 [28], (b) p53 degradation through RING finger-dependent E3 ubiquitin ligase function [29], (c) p53 ubiquitination through MDM2 acid domain docking to a conformationally flexible region of p53 that is unfolded in human cancers [24,30,31], and (d) ATP-dependent folding of p53 mediated by the HSP90 chaperone [22]. It is interesting that the RING domain of MDM2 protein has an ATP-binding motif imbedded within it: this is unique for a RING finger domain-containing protein [23]. The presence of a nucleotide-binding domain in a signalling protein such as MDM2 is probably highly significant, and suggests that cells have evolved an energy-dependent stage that requires a stimulus for MDM2 function. The recent study [22] was the first to determine a molecular function for the ATP-binding domain of MDM2, and prompted the current study on E2F1 to determine how widespread the effects of the ATP-binding domain are and to provide novel insights into the evolution and function of MDM2.

The E2A binding factor (E2F) family of transcription factors plays a central role in regulating cellular proliferation by controlling the expression of genes that are involved in cell-cycle progression, particularly DNA synthesis, as well as genes that are involved in senescence and apoptosis [32]. Regulation of E2F activity is complex, and numerous studies have demonstrated the importance of protein–protein interactions as well as post-translational modifications such as phosphorylation, acetylation and ubiquitination. Retinoblastoma protein (pRB) is a major regulator of E2F1 transactivation [32], but MDM2 and MDMX proteins have also been reported to regulate E2F1 activity.

A positive role for MDM2 in the regulation of E2F1 was first reported by Martin *et al.* [33], who showed that MDM2 binds directly to the C-terminus of E2F1 and promotes its transcriptional activity. Additional studies have demonstrated that the central acidic domain of MDM2 binds to the C pocket of pRB, resulting in a reduction in the number of pRB–E2F1 complexes and subsequent stimulation of E2F1 transactivation [34]. Furthermore, E2F1 is reported to be stabilized by MDM2 through a mechanism that involves displacement of the F-box-containing protein $p45^{SKP2}$, which is the cell cycle-regulated component of the ubiquitin protein ligase SCF^{SKP2} [35].

In contrast to these studies, MDM2 has been shown to function as a negative regulator of E2F1 activity. For example, overexpression of MDM2 blocks E2F1-mediated accumulation of p53 and induction of apoptosis [36], and microinjection of neutralizing antibodies to MDM2 or MDM2 antisense oligonucleotides increases E2F1 protein levels [37]. Furthermore, Loughran and La Thangue [38] demonstrated that MDM2 promotes E2F1 degradation and antagonizes the apoptotic properties of E2F1 in a fashion that is dependent upon its heterodimeric partner DP1.

The opposing effects reported for MDM2 on E2F1 activity may be related to the status of p53. Treatment of tumour cells lacking functional p53 with the small molecule inhibitor of MDM2, Nutlin, results in E2F1 stabilization and activation. In these cells, Nutlin inhibits the binding of MDM2 to E2F1 [39]. However, in p53 wild-type cells, E2F1 levels and activity are downregulated by Nutlin treatment or depletion of MDM2 by siRNA [39]. Additionally, it has been demonstrated that MDM2 induction of E2F1 transactivation is p53-dependent. MDM2 was unable to enhance E2F1 transactivation in cells lacking p53 or the cdk inhibitor p21, suggesting that MDM2 activation of E2F1 occurs as a consequence of inhibition of p53 transactivation of p21 [40]. Upon overexpression of MDM2, p53 transactivation is blocked, leading to a reduction in p21 protein and a concomitant increase in hyperphosphorylated pRB and E2F1 activity [40]. At present, the relative affinities of p53 and E2F1 for MDM2 are not known, thus the interaction of p53 with MDM2 might affect the level of active MDM2 that can regulate E2F1. Furthermore, the regulation of E2F1 activity correlates with an MDM2-dependent regulation of DP1 [38]. Clearly, additional studies are required to elucidate the role that p53/MDM2 plays in the regulation of E2F1/DP1 *in vivo*.

By comparing the interactions of MDM2 with p53 and E2F1 *in vitro*, we have defined an important biochemical function for the ATP-binding domain of MDM2 that has implications for signalling *in vivo*. MDM2, as well as HSP90, is now known to play a positive role in p53 protein synthesis and mediate nuclear import of p53 protein [14,19]. Possibly, therefore, the ATP-binding domain can function to switch MDM2 from activity as an E3 ubiquitin ligase to activity as a 'foldase' that can function in cooperation with HSP90. This p53–MDM2–HSP90 pathway appears to be misregulated in some tumour cells, as

unfolded mutant p53, MDM2 and HSP90 form an inactive trimeric complex [19]. Further, MDM2–HSP90–carboxyl terminus of HSC70-interacting protein (CHIP) can cause misfolding of p53 *in vitro* [21], and CHIP can induce p53 ubiquitination in cells [41].

Binding of ATP to the ATP-binding domain of MDM2 can also alter its interaction with the E2F1 substrate, but with an outcome distinct from that for p53. One notable difference is the apparent misfolding of E2F1 by MDM2, which is stimulated by ATP. These data suggest that the ATP domain has evolved to manipulate MDM2 protein–protein interactions in a substrate-specific manner. Presumably, the documented MDM2-mediated regulation of E2F1 function in cells can be modified by ATP binding, which would control the specific activity of E2F1 in cells. Interestingly, the MDM2-related protein MDMX has also been shown to negatively regulate E2F1 function directly via inhibition of DNA-binding activity and repression of transactivation [42,43]. It is possible that an MDM2–MDMX complex might use the energy in ATP to misfold the E2F1 protein. Whether this misfolding is coupled to E2F1 ubiquitination remains to be determined, although we did not see any effects of mutating the ATP-binding site of MDM2 on E2F1 ubiquitination *in vitro* (Fig. 2).

In summary, this study and a recent report [22] describe a novel function for the ATP-binding domain of MDM2 in driving changes in protein–protein interactions with client proteins in classic molecular chaperone assays. This biochemical mechanism provides a foundation from which to begin to analyse the role of the ATP-binding domain as a modifier of transcription factors *in vivo*, with the prospect of developing drugs that either stabilize the ATP-bound conformation of MDM2 or inhibit the ATP-bound conformation of MDM2. Determination of how these ATP agonists or antagonists of MDM2 alter the chaperone functions of HSP90 with current anti-HSP90 small molecules has intriguing prospects for targeting the chaperone pathway in cancer.

Experimental procedures

In vitro ubiquitination assay

For the *in vitro* ubiquitination assay, reactions contained 25 mM Hepes pH 8.0, 10 mM $MgCl_2$, 4 mM ATP, 0.5 mM dithiothreitol, 0.05% v/v Triton X-100, 0.25 mM benzamidine, 10 mM creatine phosphate, 3.5 units·mL^{-1} creatine kinase, ubiquitin (1 mM), and E1 (50-200 nM), E2s (0.1–1 μM) and E2F1–GST purified from *E. coli* (40 ng). Reactions were initiated by the addition of purified MDM2 (120 ng). Following incubation at 30 °C, reactions were terminated by the addition of SDS sample buffer. The reactions were resolved by denaturing gel electrophoresis using 4–12% NuPAGE gels in a MOPS buffer system (Invitrogen, Carlsbad, CA, USA) and electro-transferred to Hybond-C Extra nitrocellulose membrane (Amersham, Little Chalfont, UK) followed by immunoblotting. Ubiquitin adducts were quantified using Scion Image (National Institutes of Health, Bethesda, MD, USA).

Gel retardation analysis

The E2F recognition site from the adenovirus E2A promoter (or a mutant site) was used in all gel retardation analyses. The following primers were used: wild-type, 5′-GATCTAGT TTTCGCGCTTAAATTTGA-3′ (forward) and 3′-ATCAA AAGCGCGAATTTAAACTCTAG-5′ (reverse); mutant, 5′-GATCTAGTTTTCGATATTAAATTTGA-3′ (forward) and 3′-ATCAAAAGCTATAATTTAAACTCTAG-5′ (reverse). The nucleotides changed in the mutant site are underlined.

For gel retardation using recombinant proteins, proteins were combined with binding buffer (10 mM HEPES pH 7.6, 100 mM KCl, 1 mM EDTA, 4% glycerol, 0.5 mM dithiothreitol), 2 μg of sheared salmon sperm DNA and 200 ng of mutant promoter oligonucleotide to reduce the non-specific DNA-binding activity. Antibodies for E2F1 (KH95, Santa Cruz Biotechnology, Santa Cruz, CA, USA), MDM2 (2A10, 4B2, SMP14 – gifts from B. Vojtesek, Masaryk Memorial Cancer Institute, Brno, Czech Republic), HSP70 (SPA-810, Stressgen, San Diego, CA, USA) and HSP90 (SPA-830, Stressgen) were added, and complexes were allowed to form at room temperature. After 15 min, 1 ng of a ^{32}P-labelled E2F oligomer was added for a further 20 min. Complexes were resolved on a 4% polyacrylamide gel in 0.5× Tris-borate EDTA (TBE) at 4 °C for 2 h (200 V), and visualized using a STORM 840 scanner and software (Amersham). E2F1 DNA-binding activity was quantified using Scion Image (National Institutes of Health).

Plasmid preparation

For expression in *E. coli*, the human untagged MDM2 ORF lacking the first five codons (amino acids 6–491) inserted into a PT7.7 vector was prepared as described previously [31]. pT7.7 MDM2-K454A and MDM2-C478S plasmids were prepared by means of site-directed mutagenesis using a QuickChange™ XL site-directed mutagenesis kit (Stratagene, San Diego, CA, USA). For expression in *E. coli*, pCMV HA-E2F1 WT was digested with *Bam*HI and *Sac*I and the resulting insert was cloned into the pGEX^{KG} vector (Amersham) at the same sites.

Purification of recombinant GST–E2F1 protein

Transformed BL21 bacteria (Invitrogen) were grown to mid-logarithmic phase in 500 mL of Luria–Bertani (LB)

broth containing the appropriate antibiotic at 37 °C. Then protein expression was induced by the addition of 0.5 mM (final concentration) of isopropyl thio-β-D-galactoside (IPTG) for 4 h at 30 °C.

For GST purification, bacterial pellets were resuspended in 10 mL NaCl/P_i, 1% Triton X-100 and 0.5 mM phenylmethanesulfonyl fluoride on ice, and then sonicated briefly (3 × 10 s) on ice. Bacterial debris was pelleted by centrifugation at 10 000 ***g*** for 20 min at 4 °C. A 500 μL suspension of glutathione–Sepharose beads (50% v/v) (Amersham) that had been pre-washed in NaCl/P_i, was added to the supernatant and mixed with constant rotation at 4 °C for 30 min. The suspension was washed three times with 50 mL NaCl/P_i by spinning in a bench-top centrifuge at 5000 ***g*** for 5 min at 4 °C. The GST proteins were eluted from the beads by incubating the bead pellet with an equal volume of 50 mM Tris pH 8, containing 10 mM of glutathione.

Expression and purification of recombinant MDM2 proteins

Human untagged wild-type MDM2, MDM2-K454A and MDM2-C478S were overexpressed in *E. coli* BL21 RIL (DE3) strain at 20 °C for 3 h after induction with 0.5 mM IPTG. Cells were harvested by centrifugation at 8000 ***g*** for 10 min. The bacterial pellet was lysed in buffer A [100 mM Tris/HCl pH 8.0, 200 mM KCl, 10% glycerol, 1 mM phenylmethanesulfonyl fluoride, 5 mM $Mg(CH_3COO)_2$, 5 mM dithiothreitol, 1 mM benzamidine, and protease inhibitor cocktail, EDTA-free (Roche, Basel, Switzerland), one tablet per 50 mL of buffer] containing 1 mg·mL^{-1} lysozyme for 1.5 h at 4 °C with frequent stirring, followed by 2 min at 37 °C and an additional 15 min at 4 °C. The suspension was then centrifuged at 100 000 ***g*** for 1 h at 4 °C. Under these lysis conditions, most of the desired protein was insoluble and located within the pellet after centrifugation. Extraction of the MDM2 protein from the pellet was carried out overnight at 4 °C with constant shaking. The following extraction buffer (B) was used: 25 mM Tris/HCl pH 7.6, 1.2 M KCl, 5 mM $Mg(CH_3COO)_2$, 1% Triton X-100, 5 mM dithiothreitol, 10% sucrose, 1 mM phenylmethanesulfonyl fluoride, 1 mM benzamidine, and protease inhibitor tablets. Following centrifugation (100 000 ***g*** for 1 h at 4 °C), the supernatant was collected, and dialysed into buffer C [25 mM Hepes-KOH pH 7.3, 1 M $(NH_4)_2SO_4$, 1 M KCl, 5% glycerol, 2 mM dithiothreitol, 1 mM phenylmethanesulfonyl fluoride]. After dialysis for 2 h, the sample was loaded onto a butyl-Sepharose column (Amersham) equilibrated with the same buffer. The protein that bound to the column was eluted via gradient of decreasing ionic strength and increasing glycerol concentration. The fractions containing MDM2 protein were pooled and loaded onto a Q-Sepharose column equilibrated with buffer D (25 mM Hepes pH 7.6, 50 mM KCl, 10% glycerol, 2 mM dithiothreitol, 1 mM phenylmethanesulfonyl fluoride). The flowthrough from the column was immediately loaded onto an SP-Sepharose column equilibrated with buffer D. The proteins bound to the SP column were eluted by means of an ionic strength gradient (50–800 mM KCl in buffer D). Fractions containing MDM2 protein were pooled, frozen in liquid nitrogen and stored at −80 °C.

Immunoblotting

Samples were resolved by denaturing gel electrophoresis using 4–12% NuPAGE gels in a MOPS buffer system (Invitrogen) and electro-transferred to Hybond-C Extra nitrocellulose membrane (Amersham), blocked in NaCl/P_i, 10% non-fat milk for 30 min, then incubated with primary antibody overnight at 4 °C in NaCl/P_i, 5% non-fat milk, 0.1% Tween-20. After washing (3 × 10 min) in NaCl/P_i, Tween-20, the blot was incubated with secondary horseradish peroxidase-conjugated anti-mouse IgG (DAKO, Glostrup, Denmark; 1 : 5000) for 1 h at room temperature in NaCl/P_i, 5% non-fat milk, 0.1% Tween-20. After washing (3 × 10 min) in NaCl/P_i, Tween-20, proteins were visualized by incubation with ECL reagent (Pierce, Rockford, IL, USA).

ELISA

For ELISA, a 96-well plate (Corning Incorporated, Schiphol-Rijk, Netherlands) was coated with purified E2F1 protein or wild-type MDM2 protein diluted in 0.1 M Na_2HCO_3 pH 8.0 and incubated overnight at 4 °C. Each well was washed six times with NaCl/P_i containing 0.1% Tween-20 (PBS-T), followed by incubation for 1 h at room temperature with gentle agitation in PBS-T supplemented with 3% BSA. The wells were then washed six times with PBS-T prior to incubation with purified E2F1 or MDM2 protein in the absence or presence of ATP, 10 mM creatine phosphate, 3.5 units·mL^{-1} creatine kinase, diluted in PBS-T/3% BSA for 1 h at room temperature. After 1 h incubation, the plate was washed again six times with PBS-T and incubated with antibody specific to E2F1 (KH95) or MDM2 (2A10) for 1 h at room temperature. After a further six washes with PBS-T, secondary horseradish peroxidase-conjugated anti-mouse IgG was added to wells, followed by further washing, and enhanced chemiluminescence assays were performed. The results were quantified using Fluoroskan Ascent FL equipment (Labsystems, Helsinki, Finland) and analysed with ASCENT software version 2.4.1 (Labsystems).

Tryptic digestion

Purified GST–E2F1 protein (100 ng) was incubated with or without purified MDM2 protein (200 ng) in the presence of trypsin (50 ng·reaction^{-1}) at 4 °C for 2.5, 5, 10 or 15 min

as indicated. For reactions with MDM2, proteins were mixed and incubated for 20 min at room temperature prior to the addition of trypsin. The reactions were resolved by denaturing gel electrophoresis using 4–12% NuPAGE gels in a MOPS buffer system (Invitrogen) and electro-transferred to Hybond-C Extra nitrocellulose membranes (Amersham) followed by immunoblotting.

Acknowledgements

This work was supported by a Cancer Research UK p53 Signal Transduction grant (to T. R. H.), a Cancer Research UK Cell Signaling and Interferon Responses grant (to L. K. B.), and Ministry of Science and Higher Education grant number N301 032534 (Poland).

References

1 Barral JM, Broadley SA, Schaffar G & Hartl FU (2004) Roles of molecular chaperones in protein misfolding diseases. *Semin Cell Dev Biol* **15**, 17–29.
2 Mosser DD & Morimoto RI (2004) Molecular chaperones and the stress of oncogenesis. *Oncogene* **23**, 2907–2918.
3 Westerheide SD and Morimoto RI (2005) Heat shock response modulators as therapeutic tools for diseases of protein conformation. *J Biol Chem* **280**, 33097–33100.
4 Bisht KS, Bradbury CM, Mattson D, Kaushal A, Sowers A, Markovina S, Ortiz KL, Sieck LK, Isaacs JS, Brechbiel MW *et al*. (2003) Geldanamycin and 17-allylamino-17-demethoxygeldanamycin potentiate the in vitro and in vivo radiation response of cervical tumor cells via the heat shock protein 90-mediated intracellular signaling and cytotoxicity. *Cancer Res* **63**, 8984–8995.
5 Kamal A, Boehm MF & Burrows FJ (2004) Therapeutic and diagnostic implications of Hsp90 activation. *Trends Mol Med* **10**, 283–290.
6 Kamal A, Thao L, Sensintaffar J, Zhang L, Boehm MF, Fritz LC & Burrows FJ (2003) A high-affinity conformation of Hsp90 confers tumour selectivity on Hsp90 inhibitors. *Nature* **425**, 407–410.
7 Ciocca DR & Calderwood SK (2005) Heat shock proteins in cancer: diagnostic, prognostic, predictive, and treatment implications. *Cell Stress Chaperones* **10**, 86–103.
8 Neckers L & Neckers K (2005) Heat-shock protein 90 inhibitors as novel cancer chemotherapeutics – an update. *Expert Opin Emerg Drugs* **10**, 137–149.
9 Pacey S, Banerji U, Judson I & Workman P (2006) Hsp90 inhibitors in the clinic. *Handb Exp Pharmacol* **172**, 331–358.
10 Pinhasi-Kimhi O, Michalovitz D, Ben-Zeev A & Oren M (1986) Specific interaction between the p53 cellular tumour antigen and major heat shock proteins. *Nature* **320**, 182–184.
11 Sepehrnia B, Paz IB, Dasgupta G & Momand J (1996) Heat shock protein 84 forms a complex with mutant p53 protein predominantly within a cytoplasmic compartment of the cell. *J Biol Chem* **271**, 15084–15090.
12 Whitesell L, Sutphin PD, Pulcini EJ, Martinez JD & Cook PH (1998) The physical association of multiple molecular chaperone proteins with mutant p53 is altered by geldanamycin, an hsp90-binding agent. *Mol Cell Biol* **18**, 1517–1524.
13 Whitesell L, Sutphin P, An WG, Schulte T, Blagosklonny MV & Neckers L (1997) Geldanamycin-stimulated destabilization of mutated p53 is mediated by the proteasome in vivo. *Oncogene* **14**, 2809–2816.
14 Walerych D, Kudla G, Gutkowska M, Wawrzynow B, Muller L, King FW, Helwak A, Boros J, Zylicz A & Zylicz M (2004) Hsp90 chaperones wild-type p53 tumor suppressor protein. *J Biol Chem* **279**, 48836–48845.
15 Zylicz M, King FW & Wawrzynow A (2001) Hsp70 interactions with the p53 tumour suppressor protein. *EMBO J* **20**, 4634–4638.
16 King FW, Wawrzynow A, Hohfeld J & Zylicz M (2001) Co-chaperones Bag-1, Hop and Hsp40 regulate Hsc70 and Hsp90 interactions with wild-type or mutant p53. *EMBO J* **20**, 6297–6305.
17 Blagosklonny MV (2002) p53: an ubiquitous target of anticancer drugs. *Int J Cancer* **98**, 161–166.
18 Blagosklonny MV, Toretsky J & Neckers L (1995) Geldanamycin selectively destabilizes and conformationally alters mutated p53. *Oncogene* **11**, 933–939.
19 Muller P, Ceskova P & Vojtesek B (2005) Hsp90 is essential for restoring cellular functions of temperature-sensitive p53 mutant protein but not for stabilization and activation of wild-type p53: implications for cancer therapy. *J Biol Chem* **280**, 6682–6691.
20 Peng Y, Chen L, Li C, Lu W & Chen J (2001) Inhibition of MDM2 by hsp90 contributes to mutant p53 stabilization. *J Biol Chem* **276**, 40583–40590.
21 Burch L, Shimizu H, Smith A, Patterson C & Hupp TR (2004) Expansion of protein interaction maps by phage peptide display using MDM2 as a prototypical conformationally flexible target protein. *J Mol Biol* **337**, 129–145.
22 Wawrzynow B, Zylicz A, Wallace M, Hupp T & Zylicz M (2007) MDM2 chaperones the p53 tumor suppressor. *J Biol Chem* **282**, 32603–32612.
23 Poyurovsky MV, Jacq X, Ma C, Karin-Schmidt O, Parker PJ, Chalfie M, Manley JL & Prives C (2003) Nucleotide binding by the Mdm2 RING domain facilitates Arf-independent Mdm2 nucleolar localization. *Mol Cell* **12**, 875–887.
24 Wallace M, Worrall E, Pettersson S, Hupp TR & Ball KL (2006) Dual-site regulation of MDM2 E3-ubiquitin ligase activity. *Mol Cell* **23**, 251–263.

25 Hansen S, Hupp TR & Lane DP (1996) Allosteric regulation of the thermostability and DNA binding activity of human p53 by specific interacting proteins. *J Biol Chem* **271**, 3917–3924.
26 Brown CR, Hong-Brown LQ & Welch WJ (1997) Correcting temperature-sensitive protein folding defects. *J Clin Invest* **99**, 1432–1444.
27 Brown CR, Hong-Brown LQ, Biwersi J, Verkman AS & Welch WJ (1996) Chemical chaperones correct the mutant phenotype of the delta F508 cystic fibrosis transmembrane conductance regulator protein. *Cell Stress Chaperones* **1**, 117–125.
28 Chen J, Marechal V & Levine AJ (1993) Mapping of the p53 and mdm-2 interaction domains. *Mol Cell Biol* **13**, 4107–4114.
29 Haupt Y, Maya R, Kazaz A & Oren M (1997) Mdm2 promotes the rapid degradation of p53. *Nature* **387**, 296–299.
30 Shimizu H, Saliba D, Wallace M, Finlan L, Langridge-Smith PR & Hupp TR (2006) Destabilizing missense mutations in the tumour suppressor protein p53 enhance its ubiquitination in vitro and in vivo. *Biochem J* **397**, 355–367.
31 Shimizu H, Burch LR, Smith AJ, Dornan D, Wallace M, Ball KL & Hupp TR (2002) The conformationally flexible S9–S10 linker region in the core domain of p53 contains a novel MDM2 binding site whose mutation increases ubiquitination of p53 in vivo. *J Biol Chem* **277**, 28446–28458.
32 Stevens C & La Thangue NB (2003) E2F and cell cycle control: a double-edged sword. *Arch Biochem Biophys* **412**, 157–169.
33 Martin K, Trouche D, Hagemeier C, Sorenson TS, La Thangue NB & Kouzarides T (1995) Stimulation of E2F1/DP1 transcriptional activity by MDM2 oncoprotein. *Nature* **375**, 691–694.
34 Sdek P, Ying H, Zheng H, Margulis A, Tang X, Tian K & Xiao Z-XJ (2004) The central acidic domain of MDM2 is critical in inhibition of retinoblastoma-mediated suppression of E2F and cell growth. *J Biol Chem* **279**, 53317–53322.
35 Zang Z, Wang H, Li M, Rayburn ER, Agrawal S & Zhang R (2005) Stabilization of E2F1 protein by MDM2 through the E2F1 ubiquitination pathway. *Oncogene* **24**, 7238–7247.
36 Kowalik TF, DeGregori J, Leone G, Jakoi L & Nevins JR (1998) E2F1-specific induction of apoptosis and p53 accumulation, which is blocked by Mdm2. *Cell Growth Differ* **9**, 113–118.
37 Blattner C, Sparks A & Lane D (1999) Transcription factor E2F-1 is upregulated in response to DNA damage in a manner analogous to that of p53. *Mol Cell Biol* **19**, 3704–3713.
38 Loughran O & La Thangue NB (2000) Apoptotic and growth-promoting activity of E2F modulated by MDM2. *Mol Cell Biol* **20**, 2186–2197.
39 Ambrosini G, Sambol EB, Carvajal D, Vassilev LT, Singer S & Schwartz GK (2006) Mouse double minute antagonist Nutlin-3a enhances chemotherapy-induced apoptosis in cancer cells with mutant p53 by activating E2F1. *Oncogene* **26**, 3473–3481.
40 Wunderlich M & Berberich SJ (2002) Mdm2 inhibition of p53 induces E2F1 transactivation via p21. *Oncogene* **21**, 4414–4421.
41 Esser C, Scheffner M & Hohfeld J (2005) The chaperone-associated ubiquitin ligase CHIP is able to target p53 for proteasomal degradation. *J Biol Chem* **280**, 27443–27448.
42 Strachan GD, Jordan-Sciutto KL, Rallapalli R, Tuan RS & Hall DJ (2003) The E2F-1 transcription factor is negatively regulated by its interaction with the MDMX protein. *J Cell Biochem* **88**, 557–568.
43 Wunderlich M, Ghosh M, Weghorst K & Berberich SJ (2004) MdmX represses E2F1 transactivation. *Cell Cycle* **3**, 472–478.

THE JOURNAL OF BIOLOGICAL CHEMISTRY VOL. 284, NO. 17, pp. 11517–11530, April 24, 2009

A Function for the RING Finger Domain in the Allosteric Control of MDM2 Conformation and Activity*

Received for publication, December 10, 2008, and in revised form, January 28, 2009 Published, JBC Papers in Press, February 2, 2009, DOI 10.1074/jbc.M809294200

Bartosz Wawrzynow[‡], Susanne Pettersson[‡], Alicja Zylicz[§1], Janice Bramham[¶], Erin Worrall[‖], Ted R. Hupp[‖2], and Kathryn L. Ball[‡3]

From the [‡]Cancer Research UK (CRUK) Interferon and Cell Signalling Group and [‖]CRUK p53 Signal Transduction Group, Cell Signalling Unit, Institute of Genetics and Molecular Medicine, University of Edinburgh, Crewe Road South, Edinburgh EH4 2SR, Scotland, United Kingdom, the [§]International Institute of Molecular and Cell Biology in Warsaw, 4 Trojdena Street, Warsaw, Poland, and the [¶]Center for Translation and Chemical Biology, University of Edinburgh, Michael Swann Building, Mayfield Road, Edinburgh EH9 3JR, Scotland, United Kingdom

The MDM2 oncoprotein plays multiple regulatory roles in the control of p53-dependent gene expression. A picture of MDM2 is emerging where structurally discrete but interdependent functional domains are linked through changes in conformation. The domain structure includes: (i) a hydrophobic pocket at the N terminus of MDM2 that is involved in both its transrepressor and E3-ubiqutin ligase functions, (ii) a central acid domain that recognizes a ubiquitination signal in the core DNA binding domain of p53, and (iii) a C-terminal C2H2C4 RING finger domain that is required for E2 enzyme-binding and ATP-dependent molecular chaperone activity. Here we show that the binding affinity of MDM2s hydrophobic pocket can be regulated through the RING finger domain and that increases in pocket affinity are reflected by a gain in MDM2 transrepressor activity. Thus, mutations within the RING domain that affect zinc coordination, but not one that inhibits ATP binding, produce MDM2 proteins that have a higher affinity for the BOX-I transactivation domain of p53 and a reduced $I_{0.5}$ for p53 transrepression. An allosteric model for regulation of the hydrophobic pocket is supported by differences in protein conformation and pocket accessibility between wild-type and the RING domain mutant MDM2 proteins. Additionally the data demonstrate that the complex relationship between different domains of MDM2 can impact on the efficacy of anticancer drugs directed toward its hydrophobic pocket.

The tumor suppressor protein p53 is a transcription factor that plays a key role in the control of pathways that protect cells from malignant transformation (1, 2). As such, p53 is the most frequently inactivated protein in human cancers (3). In response to cellular stress, p53 protein levels are elevated by a decrease in its rate of degradation, and this increase in levels is accompanied by changes in the status of p53 post-translational modifications. Together, elevated levels of p53 and activating post-translational modifications induce its sequence-specific DNA binding and transcriptional activity leading to changes in gene expression that classically result in either cell cycle arrest or apoptosis (4).

Under non-stressed conditions p53 is tightly controlled by the MDM2 oncoprotein through an autoregulatory feedback loop (5–8). MDM2 plays multiple regulatory roles in the control of p53-dependent gene expression. Originally identified as a transrepressor of p53-mediated transcription (5, 8), MDM2 was subsequently shown to control the steady-state levels of p53 in unstressed cells by acting as a RING finger domain E3[4]-ubiquitin ligase (9, 10). More recently MDM2 has also been implicated in the control of p53 translation (11) and in addition has been shown to possess an ATP-dependent molecular chaperone activity toward p53 (12, 13). MDM2 is a multidomain protein comprising: (i) A hydrophobic pocket at its N terminus that binds with a high affinity to the BOX-I transactivation domain of p53 (14). This interaction is required for both the E3-ligase and transrepressor functions of MDM2 (15). (ii) A central acid domain that recognizes and binds with a relatively low affinity to a ubiquitination signal in the core of p53 (16–18). (iii) A C-terminal C2H2C4 RING finger domain (19–21). This domain is essential for zinc coordination and is involved in E2-binding and the formation of RING domain dimers (22). In addition the RING domain houses a P-Walker motif that is required for MDM2 to act as an ATP-dependent molecular chaperone (12, 23).

Negative regulation of p53 transcription by MDM2 involves competition for binding to p53s N-terminal L*XX*LL transactivation domain (BOX-I domain), thus binding of MDM2 can occlude the binding of transcription components like the coactivator p300 preventing the formation of a pre-initiation complex (8, 24–27). Mutations in the p53 activation domain that prevent MDM2 binding can attenuate MDM2-catalyzed transrepression (15, 28), and peptide ligands mimicking the activation domain of p53 that bind to the N-terminal domain of MDM2 and disrupt the MDM2:p53 protein complex *in vitro* can stimulate p53-dependent gene expression in cells (27, 28). Together these data suggest that binding of the BOX-I activation domain of p53 to the hydrophobic pocket of MDM2 is

* This work was supported by Cancer Research UK (to S. P. and B. W.).
[1] Supported by the Polish Ministry of Science and Higher Education (Grant NN301 032534).
[2] Holds Programme Grant C483/A6354 from Cancer Research UK.
[3] Holds Programme Grant C377/A6355 from Cancer Research UK. To whom correspondence should be addressed. Tel.: 44-131-777-3560; Fax: 44-131-777-3520; E-mail: kathryn.ball@ed.ac.uk.

[4] The abbreviations used are: E3, ubiquitin-protein isopeptide ligase; CMV, cytomegalovirus; wt, wild type; E1, ubiquitin-activating enzyme; E2, ubiquitin carrier protein.

required for MDM2s oncogenic functions. Recent studies have identified a second MDM2 interaction site within the core domain (BOX-V) of p53 (16–18, 29). The BOX-V domain binds to the acid domain of MDM2, and, although this interaction has a relatively low affinity, it is key in determining the rate of p53 ubiquitination as it comprises part of the p53 ubiquitination signal (16).

The current study has used point mutations within critical C2H2C4 resides of the MDM2 RING domain to uncover cross-talk between the zinc coordinating structure and the hydrophobic pocket of MDM2. A gain in the ability of MDM2 to transrepress p53-dependent transcription is seen when zinc-coordinating residues are mutated, whereas mutation of a residue within the RING required for ATP binding has no effect on MDM2 mediated transrepression. Studies on purified MDM2 and p53 provide a mechanism for changes in transrepressor activity by demonstrating that the C2H2C4 RING mutants have a higher affinity for hydrophobic pocket interacting ligands and proteins. Thus, the RING finger domain of MDM2 is linked to the hydrophobic pocket through conformational changes that affect MDM2 transrepressor activity. In addition, the efficacy of small molecules, targeted to the hydrophobic pocket of MDM2, can be determined by the status of the C2H2C4 structure.

EXPERIMENTAL PROCEDURES

Reagents and Plasmids—Antibodies used were: DO-1 (p53) and 2A10/3G5/4B2/SMP14 (MDM2) produced in-house, p21 was detected using AB1 (Calbiochem). Peptides, N-terminal biotin-labeled plus an SGSG space (Chiron Mimotopes), were dissolved at 10 mg/ml in DMSO as previously described (16). The BOX-I and 12.1 sequences are PPLSQETFSDLWKLLP and MPRFMDYWEGLN, respectively. Nutlin-3 was from Alexis Biochemicals. Ubiquitin (U-100), UbcH5a (E2-616), and E1 (E-301) were from Boston Biochem. pcDNA3-p53 and His-ubiquitin were a gift from David Lane, pCMV-mycMDM2wt, pCMV-mycMDM2ΔN, and pCMV-MDM2ΔAc were provided by Aart Jochemsen. pcDNA3-MDM2 with the human MDM2 cDNA was used as a template to generate pcDNA3-MDM2C464A, pcDNA3-MDM2C478S, and pcDNA3-MDM2K454A using a QuikChange mutagenesis kit (Stratagene). The primers were as follows: K454A, GCATTGTCCATGGCGCAACAGGACATC; K454Arev, GATGTCCTGTTGCGCCATGGACAATGC; C464A, GGACATCTTATGGCCTGCTTTACAGCGGCAAAGAAGCTAAAGAAAAGG; C464Arev, CCTTTTCTTTAGCTTCTTTGCCGCTGTAAAGCAGGCCATAAGATGTCC; C478S, GGAATAAGCCCTGCCCAGTAAGCAGACAACCAATTCAAATGATTGTG; and C478Srev, CACAATCATTTGAATTGGTTGTCTGCTTACTGGGCAGGGCTTATTCC.

Cell Culture, Reporter Assays, and Immunoblots—H1299 cells were maintained in RPMI medium supplemented with 10% (v/v) fetal bovine serum and incubated at 37 °C with 5% CO_2. A375 cells were maintained in Dulbecco's modified Eagle's medium supplemented with 10% (v/v) fetal bovine serum and incubated at 37 °C with 10% CO_2. *MDM2*$^{-/-}$*p53*$^{-/-}$ cells were maintained in Dulbecco's modified Eagle's medium with 10% (v/v) fetal bovine serum and 10% CO_2. Upon reaching 80–90% confluency the cells were transfected using Lipofectamine 2000 (Invitrogen) with the total amount of DNA for all wells kept constant at 0.8 μg. A solution was formed with (30 ng) pGL4.10[*luc2*] bearing a 44-base stretch of the *p21* promoter and with 70 ng of the phRL-CMV plus p53 and MDM2 plasmids as detailed in the figure legends. Twenty-four hours post-transfection, the cells were washed once in ice-cold phosphate-buffered saline and lysed with 1× Passive Lysis Buffer (supplied with the Dual-Luciferase Reporter Assay System from Promega). Alternatively, Nutlin was added after 24 h (as detailed in the figure legends), and the incubation continued for a further 6 h. Afterward the Dual-Luciferase Reporter Assay was performed in accordance with the manufacturer's instructions. For immunoblot analysis transfected cells were lysed in Nonidet P-40 buffer (25 mM HEPES, pH 7.5, 0.1% (v/v) Nonidet P-40, 150 mM KCl, 5 mM dithiothreitol, 50 mM NaF), and lysates were separated on 4–12% NuPAGE (to detect p53 modification) or 10% SDS-PAGE and transferred to nitrocellulose (16).

Ubiquitination Assay—The *in vitro* assay was carried out as previously described (16). Reactions contained 25 mM HEPES, pH 8.0, 10 mM $MgCl_2$, 4 mM ATP, 0.5 mM dithiothreitol, 0.05% (v/v) Triton X-100, 0.25 mM benzamidine, 10 mM creatine phosphate, 3.5 units/ml creatine kinase, ubiquitin (2 μg), E1 (50–200 nM), E2s (0.1–1 μM), plus p53 purified from *Escherichia coli* (100 ng) and were initiated by the addition of purified human MDM2 (50 ng) in the presence or absence of either BOX-I or Nutlin as detailed in the figure legends. p53 ubiquitination in *p53*$^{-/-}$*MDM2*$^{-/-}$ mouse embryonic fibroblasts was determined using a previously described method (16).

Protein Binding Assays—Recombinant human full-length untagged MDM2 proteins and p53 protein were purified from *E. coli* as previously described (12, 30). For peptide and protein binding assays the microtiter wells were adsorbed with streptavidin overnight, washed 6× with phosphate-buffered saline-Tween with biotinylated peptides added for 1 h alternatively the wells were coated with purified p53 (150 ng) as previously described (16). Following extensive washing with phosphate-buffered saline-Tween increasing amounts of MDM2 were added either in the absence or presence of Nutlin (as detailed in the figure legends). Following washing (6× washes with phosphate-buffered saline-Tween) MDM2 was detected using the monoclonal antibody 2A10 and a secondary rabbit anti-mouse horseradish peroxidase antibody the wells were developed using ECL. The results were quantified using Fluoroskan Ascent FL equipment (Labsystems) and analyzed with Ascent Software.

Tryptic Digestion—wt or mutant MDM2 protein (1 μg) plus trypsin (10 ng) was incubated at 30 °C in 50 mM ammonium bicarbonate buffer for up to 30 min. Aliquots were removed, and the reaction was stopped by the addition of SDS sample buffer and heating at 80 °C for 4 min. The samples were analyzed by 4–12% gradient gels (Invitrogen) and immunoblotted.

Intrinsic Fluorescence Assay—Fluorescence emission spectra were recorded on a SPEX FLUOROMAX-3 (Jobin Yvon Horiba) spectrofluorometer. The bandwidths for excitation and emission were set at 5 nm, and an excitation wavelength of 295 nm was used. Fluorescence spectra were recorded from 320

to 450 nm in 0.5 nm steps, with an integration time of 1 s. All experiments were carried out at 4 °C in buffer containing: 25 mM HEPES (pH 7.5), 50 mM KCl, 5% (v/v) glycerol, 10 μM $ZnSO_4$, and 2 mM dithiothreitol. MDM2wt, MDM2C464A, and MDM2C478S used in this assay were initially preincubated on ice for 5 min at final concentrations raging from 20 nM to 1 μM (V_{total} = 0.5 ml). Each spectrum produced is the average of three emission scans minus the average of the three blanks (buffer) scans.

RESULTS

C2H2C4 MDM2 Mutant Proteins Have a Gain of Transrepressor Activity—We have recently shown that the E3-ligase activity of MDM2 requires interactions at both the hydrophobic pocket and the acid domain (16). These interactions are linked by an allosteric mechanism, with binding at the hydrophobic pocket favoring recognition of a p53 ubiquitination signal from its core DNA binding domain (BOX-V). This prompted us to ask whether similar mechanisms linked other MDM2 domains and how cooperation between domains impacted on the proteins multifunctional nature. The RING finger domain of MDM2 is required for both its E3-ligase and ATP-dependent chaperone activities through binding to an E2-ubiquitin conjugating enzyme and to ATP, respectively (12, 22). However, whether conformational changes in the RING domain are transmitted to other MDM2 functional domains affecting their activity remains unclear.

To study the RING domain in the context of full-length MDM2 we first generated a number of RING finger domain mutant constructs (Fig. 1*A*). Two of these, Cys^{464A} (MDM2C464A) and Cys^{478S} (MDM2C478S), introduced mutations into the C4 and H2C2 coordination sites of the C2H2C4 structure (21), respectively, and a third, Lys^{454A} (MDM2K454A), is a RING domain residue, which is not required for zinc coordination but is essential for MDM2 to bind ATP (12, 23). The Cys^{464A} mutant was chosen because it is the most widely studied E3-ligase-dead MDM2 RING mutant, in addition this cysteine lies within an α-helix, and structure predication using PyMOL suggests that mutation to Ala has little effect on the global structure of the RING or on the extent of solvent exposure. The Cys^{478S} mutant is similarly predicted to have a minimal effect on the local environment, because it lies within an irregular loop structure. To characterize these mutants we first determined the effect of introducing the RING mutations on E3-ligase activity using a cell-based assay. When $p53^{-/-}MDM2^{-/-}$ mouse fibroblasts were transfected with p53 and MDM2 together with His-tagged ubiquitin it was demonstrated that the Lys^{454A} mutant retained the ability to ubiquitinate p53, as determined by the isolation of His-ubiquitin-conjugated p53 protein (Fig. 1*B*), whereas, as expected, the C2H2C4 mutants were no longer able to mediate p53 modification by ubiquitin. Although the introduction of the Cys mutations is sufficient to inactivate MDM2 as an E3-ligase, they do not affect the overall integrity of the C terminus as we have shown that the Cys^{464A} and Cys^{478S} MDM2 mutants retain the ability to bind ATP, while ATP-binding activity is lost in the Lys^{454A} mutant (12). Thus, mutation of Cys residues in the RING appears to specifically inactivate RING function during ligation of ubiquitin to target substrates while leaving other RING domain functions intact.

The various MDM2 RING finger domain mutants were tested in a p53-dependent transcription assay to determine if inactivation of either its E3-ligase or ATP-binding activities affected the ability of MDM2 to repress p53-dependent transcription. The ability of p53 to activate transcription was determined using the p53-responsive region of the *p21*-promoter to drive luciferase expression. When human p53 was transfected into H1299 cells (human p53 null non-small cell lung carcinoma cells) along with the p21-reporter a characteristic activation of the promoter was detected (Fig. 1*C*), coexpression of wild-type MDM2 in a titrative manner led to a progressive decrease in reporter activity indicative of transrepression, with an $I_{0.5}$ in the region of 300 ng of MDM2 plasmid (150 ng of p53 plasmid (Fig. 1*C*)). All the RING mutants were expressed to a similar level and were able to inhibit p53-dependent transcription, however, both the Cys mutants displayed a gain of transrepressor function with an $I_{0.5}$ of <75 ng for MDM2C464A and <150 ng for MDM2C478S. In contrast, mutation of Lys^{454} did not enhance the repressor activity of MDM2, and like the wild-type protein, this mutant had an $I_{0.5}$ of around 300 ng. Similarly, although a titration of p53 could overcome transrepression imposed by a fixed amount of wild-type MDM2 and the Lys^{454A} mutant, there was a significant reduction in the ability of p53 to overcome the effects of the Cys^{464A} and Cys^{478S} mutants (Fig. 1*D*). To determine whether comparison of an Ala-substituted Cys to a Ser-substituted Cys underlined the apparent difference in potency of the MDM2C464A and MDM2C478S mutants we used a second mutant from within the C4 coordination (Fig. 1*E*; C461S) where we mutated Cys^{461} to Ser. Analysis of this mutant demonstrated that it was also more potent than the MDM2C478S mutant. These results suggest that the difference in activity of the RING mutants is unlikely to be due primarily to the choice of the substitution residue.

To determine if endogenous p53-responsive promoters respond to the MDM2 RING domain mutant proteins in a similar way to that observed using p53-responsive reporter constructs we used BAX protein expression as a measure of its promoter activity, because *BAX* is a well characterized target for p53 (31). For this assay we used MCF7 cells because they have a wild-type p53 pathway. Fig. 1*F* shows that BAX protein levels are unaffected by the expression of wt MDM2 at the concentrations used in the experiment (Fig. 1*F*, *lanes 2–4*), however under the same conditions the MDM2C464A mutant suppressed BAX protein expression even at the lowest amount used (*lanes 8–10*), and consistent with the reporter assays, the MDM2C478S mutant had intermediate activity, because it suppressed BAX protein expression when present at the highest amount (*lane 7*).

Together the data presented above suggest that mutation of residues within the RING finger domain that directly affect MDM2 E3-ligase activity facilitate transrepression of p53 transcriptional activity. In contrast, loss of MDM2 molecular chaperone activity in the ATP-binding mutant (Lys^{454A}) had no effect on transrepression of p53. Further, the data demonstrate

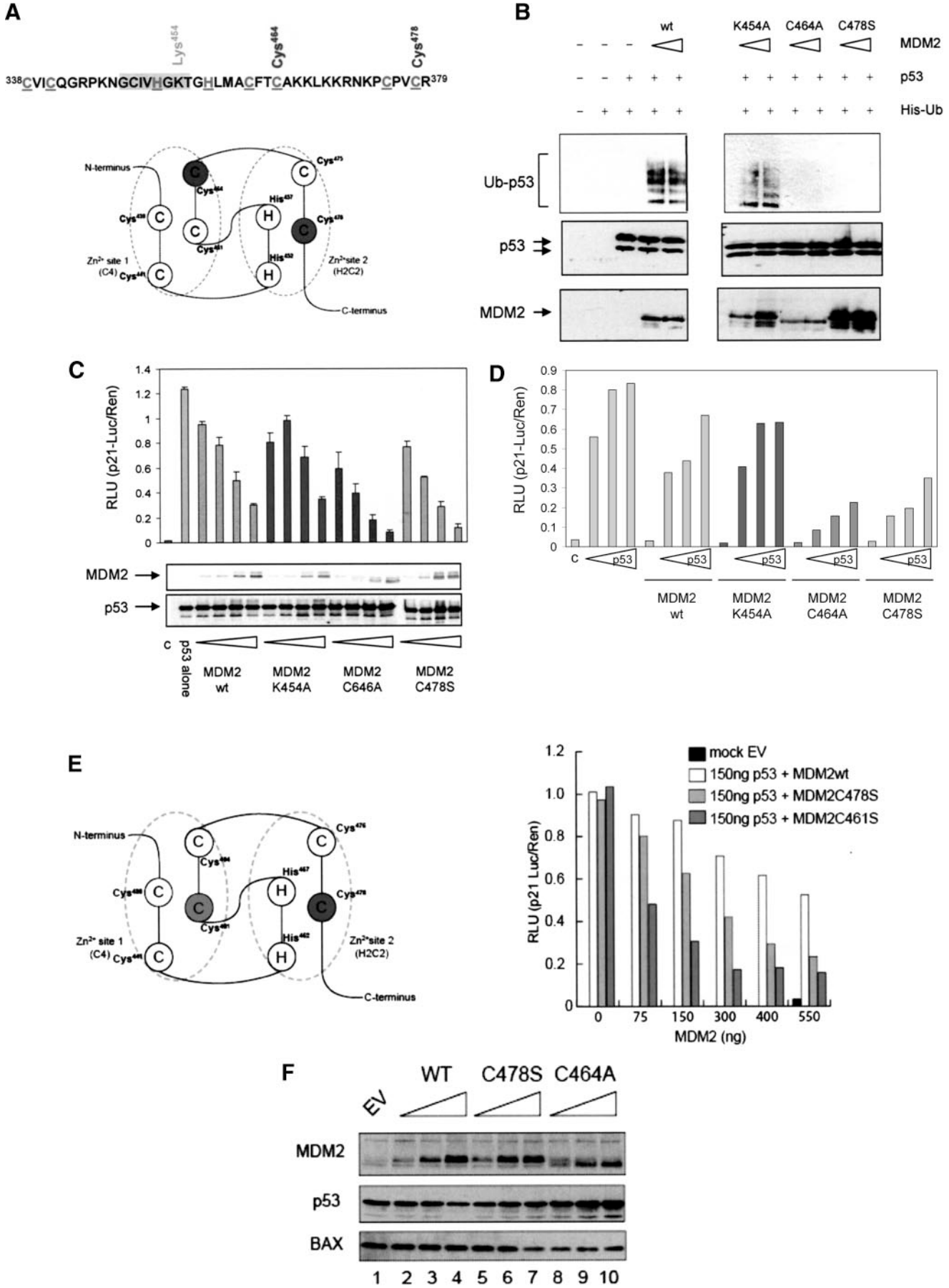

that MDM2 E3-ligase activity can be completely uncoupled from its ability to repress p53 transcription.

The MDM2 Hydrophobic Pocket but Not the Acid Domain Is Required for Efficient Transrepression of p53—Previous studies have suggested that the hydrophobic pocket of MDM2 is critical for its transrepressor activity (15, 28), however these studies were carried out before the complexity of the interaction between MDM2 and p53 was fully appreciated. Because the acid domain of MDM2 is now known to bind to the BOX-V domain of p53 (16, 18) we sought to use MDM2 deletion mutants to determine which interactions were salient for MDM2-mediated transrepression. To investigate the influence of MDM2 domain structure on p53 transrepression we used mutant forms of murine MDM2 where one or other of the two known p53 interacting domains had been deleted (Fig. 2*A*, *MDM2*Δ*N* and *MDM2*Δ*Ac*). MDM2ΔN prevents the interaction between the transactivation domain of p53 (BOX-I) and the hydrophobic pocket in the N terminus of MDM2 (14), whereas the MDM2ΔAc precludes binding of the core domain of p53 (BOX-V) and the acid domain of MDM2 that is essential for MDM2-mediated ubiquitination of p53 (16).

When the deletion mutants were analyzed in the p53-reporter assay (Fig. 2*B*) loss of the hydrophobic pocket essentially inactivated MDM2 as a transrepressor of p53-mediated transcription although expressed at a similar level to the wt protein (Fig. 2*C*), whereas deletion of the acid domain did not have a major impact on this activity of MDM2. The data suggest that the interaction between the acid domain of MDM2 and the BOX-V region of the p53 core domain is not essential for MDM2 mediated transrepression, whereas binding of the hydrophobic pocket to the BOX-I transactivation domain of p53 is absolutely required because the ΔN mutant is essentially dead in this assay. Together with data in the previous section our results suggest that RING domain mutants that loose the ability to ubiquitinate p53 but gain p53 repressor activity do so, most likely, through modulation of the MDM2-hydrophobic pocket: p53-BOX-I interaction.

RING Mutations Affect the Efficacy of Nutlin as an Inhibitor of MDM2-mediated Repression of p53—The data presented above establish that the hydrophobic pocket of MDM2 is essential for transrepression of p53 (Fig. 2*B*) and that the ability of MDM2 to transrepress p53-dependent transcription can be uncoupled from MDM2 E3-ligase activity (Fig. 1*C*). Furthermore, the C2H2C4 RING mutants have a gain of transrepressor activity when compared with the wt protein (Fig. 1*C*). To further investigate the link between hydrophobic pocket binding and RING domain function we used the cell-permeable MDM2 hydrophobic pocket binding molecule Nutlin as a tool (32, 33).

We have previously suggested that Nutlin most likely functions as an anticancer agent by affecting the ability of MDM2 to act as a transrepressor of p53 transcription rather than as an inhibitor of MDM2-dependent p53 ubiquitination (16). This hypothesis was based on observations, confirmed here, that Nutlin is not able to inhibit the ubiquitination of p53 *in vitro* using purified proteins (Fig. 3*A*) and that the addition of Nutlin to A375 cells does not decrease the number of modified p53 forms detected (Fig. 3*B*). In fact in the current experiments we show that an increase in p53 modification was proportionate to increases in total p53 protein levels (see Fig. 5*B*, *upper panel*) and to the activation of p53, as assessed by an increase in p21 protein levels (Fig. 3*B*, *lower panel*). Together these results suggest that modification of existing or newly synthesized p53 protein continues in the presence of Nutlin.

If the above hypothesis is correct we would predict that Nutlin binding to MDM2 would be sufficient to relieve transrepression imposed by both wt and E3-inactive MDM2 protein. Using the p53-reporter assay the ability of Nutlin to reverse transrepression imposed by a fixed amount of wt MDM2 was shown to be efficient (Fig. 3*C*). Furthermore, Nutlin had a striking effect on the transrepressor activity of the Cys^{478S} protein with p53 activity recovering to near the level seen in the absence of MDM2. This result lends strong support to the idea that Nutlin-dependent inhibition of MDM2 as a transrepressor occurs independently of MDM2 E3-ligase function and that this could be sufficient to explain the activating effect of Nutlin on p53.

Interestingly, although Nutlin was active against the Cys^{478S} MDM2 mutant protein it had only weak activity against the Cys^{464A} protein and even at 14 μM Nutlin did not inhibit this mutant. To confirm this result using a different assay system we looked at the ability of Nutlin to overcome wt and mutant MDM2-imposed transrepression of an endogenous p53 promoter using p21 protein levels as a downstream readout for transfected p53 (Fig. 3, *D* and *E*). An amount of transfected MDM2 wt and mutant constructs was chosen that gave maximal repression of endogenous p21

FIGURE 1. **Mutation of the C2H2C4 RING gives a gain of MDM2 transrepression.** *A*, schematic showing the RING finger domain of MDM2. The zinc conjugating residues are highlighted and *underlined*, the ATP binding site is *shaded gray*, and the residues picked out (*above*) are those that were mutated to generate the panel of mutants studied. *B*, immunoblot of p53 from $p53^{-/-}MDM2^{-/-}$ mouse embryonic fibroblasts transfected with p53 (150 ng) and MDM2 (wt and mutant constructs as indicated;150 and 250 ng) plus His-Ub (200 ng). His-conjugated proteins were isolated using nickel-agarose and analyzed on a 4–12% gradient gel. p53 was detected using DO-1. The data are representative of two independent experiments. In *C*: *upper panel*, H1299 cells were transfected with p53 alone (150 ng) or with a titration (75, 150, 300, 400, and 550 ng) of MDM2wt, MDM2K454A, MDM2C464A, or MDM2C478S plus the reporter plasmids. Total DNA was normalized using the vector control, and *c* is a vector only control. Post transfection (24 h) the Dual Luciferase Assay was performed. The results are normalized by expressing p21-Luciferase/*Renilla* activity in relative light units (*RLU*) and are the mean ± S.D. (*lower panel*). Immunoblot showing the levels of p53 with MDM2wt and mutant proteins, p53 was detected using DO-1 and MDM2 using 2A10. *D*, as above except that the cells were transfected with a p53 titration (75, 150, and 300 ng) alone or in the presence of a fixed concentration of wt and mutant MDM2 as indicated (400 ng). The vector-only control is shown as *c*, and total DNA was normalized as above the data are representative of two individual experiments. *E*, schematic depicting zinc coordination scheme of MDM2 (*left panel*). The key residues that were mutated are *highlighted*. The *histogram* represents data obtained from Dual Luciferase Assay carried out as described above, with MDM2wt MDM2C478S and MDM2C461S. *F*, MCF7 cells were transfected with plasmids encoding MDM2WT, MDM2C464A, and MDM2C478S (0–4 μg). Total DNA amount was normalized using vector control. Twenty-four hours post transfection immunoblot analysis was carried out, p53, MDM2, and BAX were detected using DO-1, 2A10, and anti-BAX, respectively. The results are representative of at least three independent experiments.

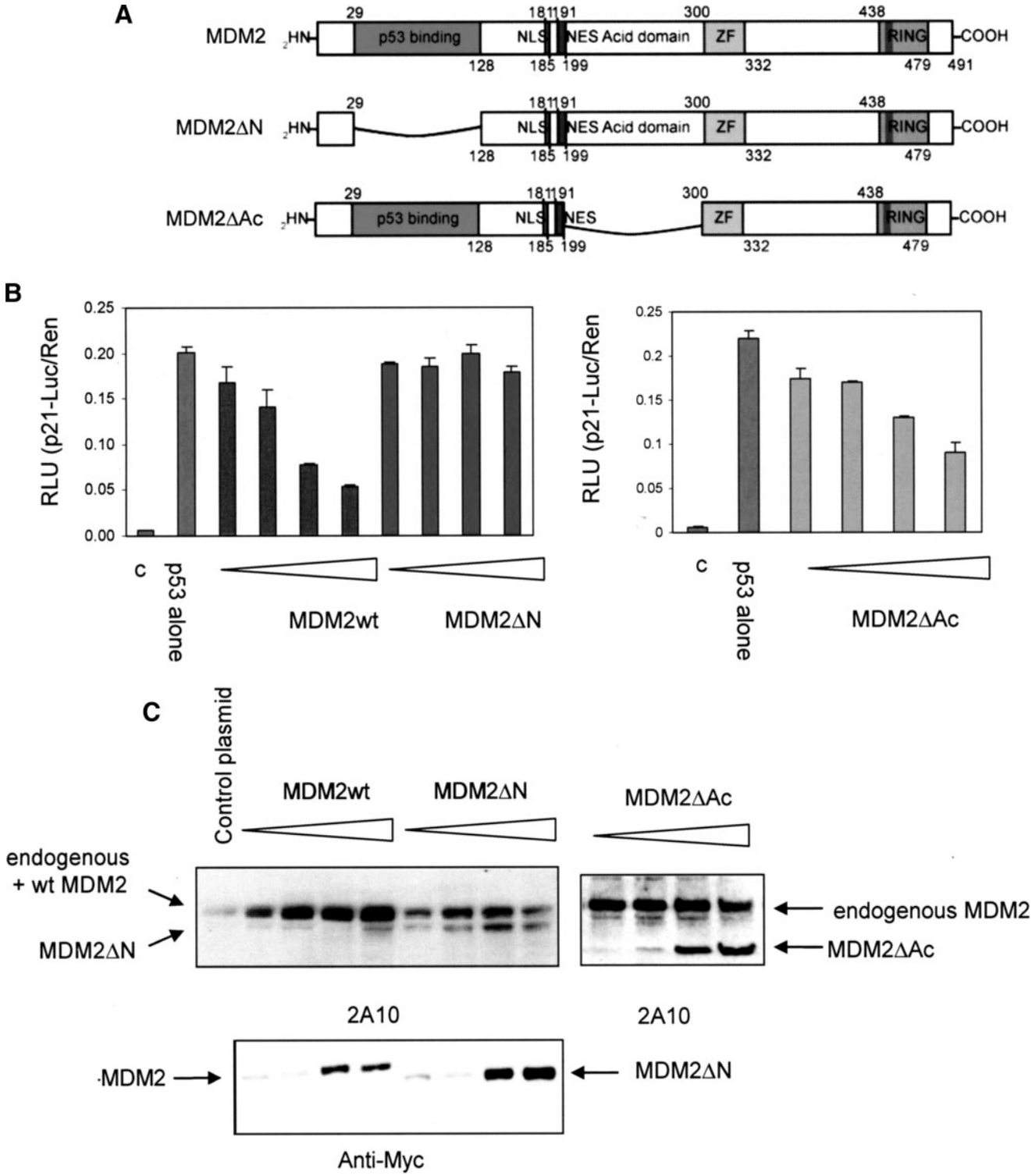

FIGURE 2. **The hydrophobic pocket of MDM2 is essential for transrepression of p53.** *A*, a schematic showing murine MDM2 deletion constructs. MDM2 ΔN is missing the MDM2 hydrophobic pocket, which binds the BOX-I domain of p53, and MDM2 ΔAc does not have the acid domain, which binds the BOX-V domain of p53. *B*, H1299 cells were transfected with p53 alone (150 ng) or with a titration (75, 150, 300, and 550 ng) of MDM2wt, MDM2ΔN, or MDM2ΔAc plus the reporter plasmids. Total DNA was normalized using the vector control. Post transfection (24 h) the Dual Luciferase Assay was performed. The results are normalized by expressing p21-Luciferase/*Renilla* activity in relative light units (*RLU*), are the mean ± S.D., and *c* is the vector-only control. *C*, immunoblot showing the levels of mycMDM2wt and mycMDM2ΔN detected using 2A10 (*top panel*) and anti-myc antibody (*bottom panel*), and MDM2ΔAc detected using 2A10 (*top right panel*).

protein expression in H1299 cells (p21 levels decreased by ~80%), Nutlin was then added to the cells in a titrative manner, and the effect on p21 levels was determined. Quantitation of the data generated in Fig. 3*D* shows that Nutlin can relieve transrepression imposed by both the wt and Cys^{478S} mutant forms of MDM2 at the lowest concentration used

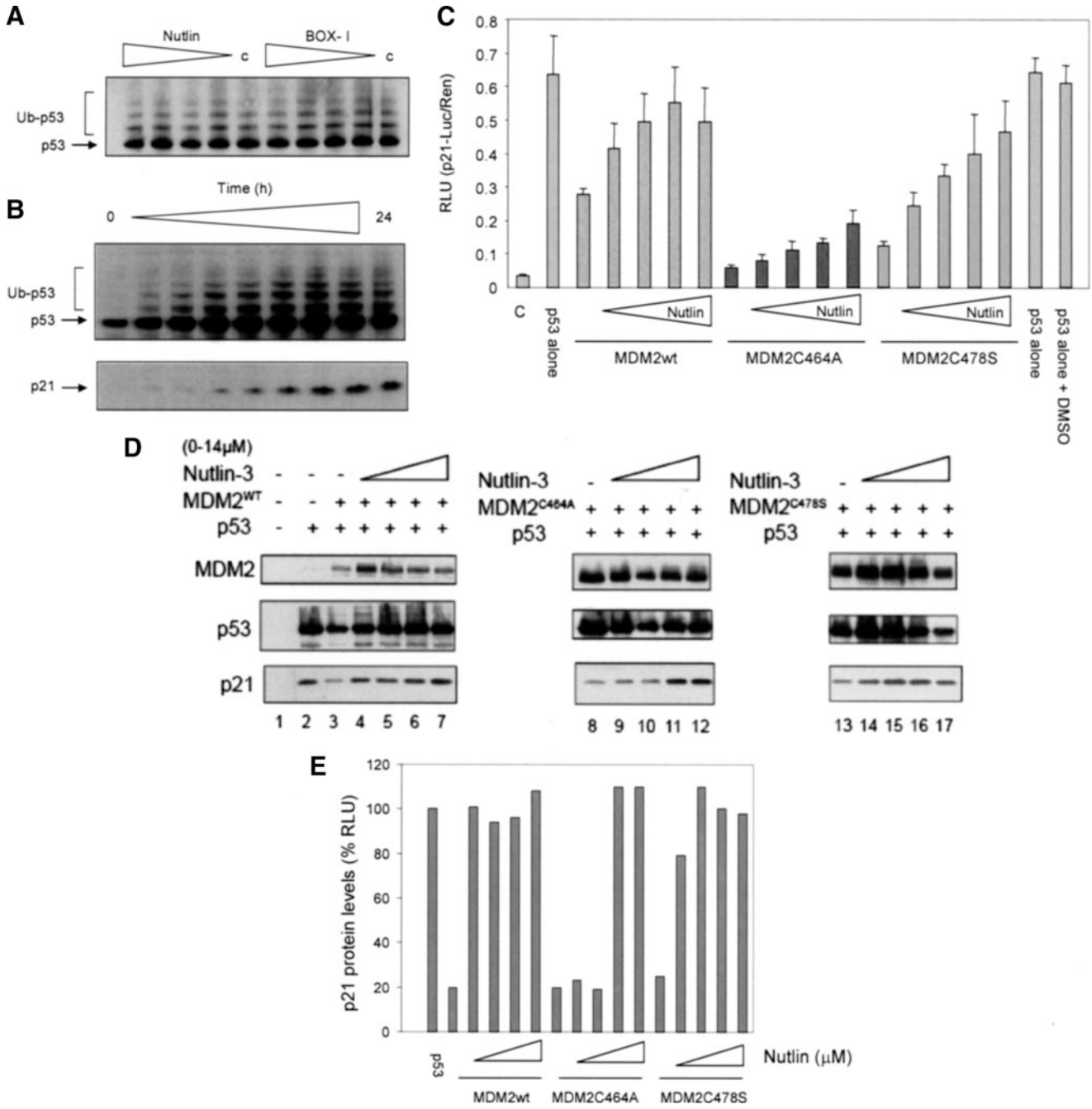

FIGURE 3. **The efficacy of Nutlin in cells is dependent on the C2H2H4 RING.** *A*, ubiquitination reactions were assembled with p53, E1, E2, and MDM2 in the presence or absence (*c*) of either Nutlin or BOX-I peptide (0, 10, 20, 40, and 60 μM). Ubiquitination was analyzed by immunoblot using a 4–12% gradient gel, p53 was detected using DO-1. Unmodified (*p53*) and ubiquitinated p53 (*Ub-p53*) are shown. The data are representative of at least four separate experiments. *B*, Nutlin (10 μM) was added to A375 cells, and they were harvested over a 24-h time course (0, 1, 2, 3, 4, 6, 8, 12, and 24 h). The lysates were analyzed by immunoblot using either a 4–12% gradient gel (*upper panel*) or a 15% SDS-PAGE gel (*lower panel*) p53 was detected using DO-1 and p21 using AB-1. Modified forms of p53 are given as Ub-p53. The data are representative of three such experiments. *C*, H1299 cells were transfected with p53 alone (150 ng) or together with MDM2 (400 ng) after 24 h Nutlin (0, 1.5, 3, 5, and 14 μM) was added, and the incubation continued for a further 6 h. Total DNA was normalized using the vector control. The cells were harvested and the Dual Luciferase Assay was performed. The results are normalized by expressing p21-Luciferase/*Renilla* activity in relative light units (*RLU*) and are the mean ± S.D., and *c* is the vector-only control. A DMSO control is included for the Nutlin carrier. *D*, H1299 cells were transfected with p53 alone (150 ng) or together with (300 ng) of MDM2wt, MDM2C464A, or MDM2C478S. Total DNA was normalized using the vector control (*c*). Post transfection (24 h) cells were treated with Nutlin (0, 1.5, 3, 5, and 14 μM) for a further 6 h. Immunoblot analysis of MDM2, p53, and p21 was carried out using 2A10, DO-1, and Ab-1, respectively. *E*, densitometry analysis of the p21 immunoblot; p21 levels are given as a percentage of protein detected in the presence of p53 alone.

(1.5 μM). However at 1.5 μM, Nutlin had no measurable effect on the levels of p21 protein in the presence of MDM2C464A, in fact it required 7 μM Nutlin to relief transrepression by the Cys^{464A} protein on p21 protein expression.

The differential effect of Nutlin, dependent on the status of the C2H2C4 RING structure, suggests that the introduction of mutations that directly impact on RING structure can differentially impact on the affinity or availability of MDM2's hydrophobic pocket for p53 BOX-I binding.

MDM2 Cys RING Finger Mutant Proteins Bind with a Higher Affinity to the Transactivation Domain of p53—The cell-based experiments described above show that (i) C2H2C4 RING mutants have a gain of transrepressor activity and (ii) the hydrophobic pocket, but not the acid domain, is essential for MDM2 repressor activity. These results suggested to us that the affinity of the hydrophobic pocket for the BOX-I domain of p53 might be sufficient to dictate the potency of MDM2 as a transrepressor and may also determine the efficacy of hydrophobic pocket binding drugs such as Nutlin.

If the above hypothesis is correct we would expect the C2H2C4 RING domain MDM2 mutant proteins to bind BOX-I with a higher affinity than the wild-type protein. To address this we first purified full-length untagged human MDM2, as well as the Cys^{464A} and Cys^{478S} mutant MDM2 proteins from an *E. coli* expression system. The protein concentrations were normalized and the quantitation was confirmed using an enzyme-linked immunosorbent assay (Fig. 4*A*). E3-ligase activity was assayed using a purified assay system (16) and as expected (based on the results presented in Fig. 1*B*), whereas the wt protein was an active E3-ligase, neither the Cys^{464A} nor the Cys^{478S} mutant were able to mediate ubiquitination of p53 (Fig. 4*B*). Next the ability of the proteins to bind to full-length purified p53 was determined (Fig. 4*C*). In this assay a constant amount of full-length untagged p53, purified form *E. coli*, was captured onto microtiter wells and incubated with a titration of wt or mutant MDM2 protein. Following extensive washing bound MDM2 was detected using a monoclonal antibody (2A10). This showed that both of the MDM2 C2H2C4 mutant proteins bound with a higher affinity to full-length p53 than did wt MDM2, however, consistent with its lower $I_{0.5}$ in the transrepressor assay (Fig. 1*C*), the Cys^{464A} mutant bound better to p53 than the Cys^{478S} mutant protein.

Although the interaction between the acid domain of MDM2 and the BOX-V domain of p53 is not essential for MDM2 mediated transrepression (Fig. 2*B*) it is likely to play a role in binding of MDM2 to full-length p53 protein (16). Binding to the isolated BOX-I domain was therefore used to determine whether the increase in affinity of the Cys^{464A} and Cys^{478S} mutants for full-length p53 reflected a change in affinity for the p53 BOX-I domain. Binding of wt and the C2H2C4 mutant MDM2 proteins to a peptide based on the BOX-I domain of p53, or to an optimized hydrophobic pocket binding peptide, 12.1 (34), was determined. Biotinylated BOX-I domain or 12.1 peptide were immobilized on streptavidin-coated wells and incubated with a titration of wt MDM2 or the two C2H2C4 mutant proteins. Consistent with the data presented above, showing that the mutants bind better to full-length p53, both the Cys^{464A} and Cys^{478S} proteins bound with a higher affinity to BOX-I and 12.1 than wt MDM2 protein. Mirroring its decreased $I_{0.5}$ for transrepression and increased affinity for full-length p53 the Cys^{464A} mutant consistently bound better to BOX-I or the BOX-I mimetic (12.1) than the Cys^{478} mutant protein. The data presented above suggest that the increased transrepressor activity of the MDM2 C2H2C4 RING mutants is dictated by an increase in the affinity of their hydrophobic pockets for the BOX-I transactivation domain of p53.

The MDM2 RING Mutant Proteins Differ in Their Sensitivity to the Hydrophobic Pocket Binding Drug Nutlin—To determine whether the differential effect of Nutlin on the C2H2C4 MDM2 mutants observed in a cellular environment represented a quantitative difference in the affinity of the mutants for Nutlin binding, we determined the ability of Nutlin to compete with BOX-I for binding to MDM2. In this assay equal amounts of biotinylated BOX-I peptide were captured onto streptavidin-coated microtiter wells and incubated with a fixed amount of wt or mutant MDM2 in the presence of increasing Nutlin concentrations (Fig. 5*A*). Consistent with the results observed in cells (Fig. 3*C*) this assay demonstrated an apparent difference in the ability of the RING mutants to bind Nutlin, suggesting that mutations within the C2H2C4 structure have a direct influence on Nutlin binding that is not mediated by other cellular proteins. Thus, Nutlin is a weak inhibitor of BOX-I binding to the Cys^{464A} mutant, relative to wild-type MDM2 protein, with an $I_{0.5}$ 4× higher than wt MDM2. This suggests that the Cys^{464A} protein has a lower affinity for Nutlin than the wild-type protein and binds with a higher affinity to BOX-I resulting in preferential BOX-I binding. Conversely, the Cys^{478S} mutant appears to bind Nutlin with a higher affinity than the wt and Cys^{464A} proteins. Thus, in this case Nutlin competes more easily with BOX-I for binding to the hydrophobic pocket. To determine if the differences observed in Nutlin binding are reflected in the ability of Nutlin to disrupt the interaction between full-length p53 and MDM2 the following experiment was performed. Full-length p53 was coated onto the microtiter well and incubated with a titration of MDM2 in the presence of various fixed concentrations of Nutlin (Fig. 5*B*; 2.5, 5, and 10 μM). Again there was a clear difference in Nutlin-dependent disruption of full-length p53 binding to the MDM2 proteins, with the p53-Cys^{478S} mutant complex showing increased Nutlin sensitivity compared with the p53-Cys^{464A} and the p53-MDM2wt interactions. Once again this suggests that the Cys^{478S} mutant has a higher affinity for Nutlin than does the Cys^{464A} protein.

In conclusion, although both the Cys^{464A} and Cys^{478S} proteins bind with a higher affinity to hydrophobic pocket interacting ligands than the wt protein, resulting in a gain of transrepressor activity (Fig. 2*C*), they do so differentially. Thus, whereas the Cys^{478S} protein binds preferentially to Nutlin, the Cys^{464A} protein binds with a higher affinity to BOX-I (Fig. 5) resulting in differential Nutlin sensitivity in cells (Fig. 2*C*). Moreover, mutations within the zinc coordinating structure of the RING are not synonymous.

RING-generated Conformational Changes in MDM2 Are Transmitted to the Hydrophobic Pocket through the Central Domain—To support our hypothesis that hydrophobic pocket affinity can be modulated by the RING domain, evidence of a RING-dependent conformational change in full-length MDM2 was sought. Firstly, limited proteolysis was used to probe for changes in the accessibility of trypsin cleavage sites in the MDM2 Cys mutants *verses* the wt protein. Purified wt or mutant MDM2 was incubated with trypsin at a ratio of 1:100 (protein) for up to 30 min, the samples were then analyzed by gradient SDS-PAGE/immunoblot and cleavage fragments identified using a mixture of MDM2 monoclonal antibodies

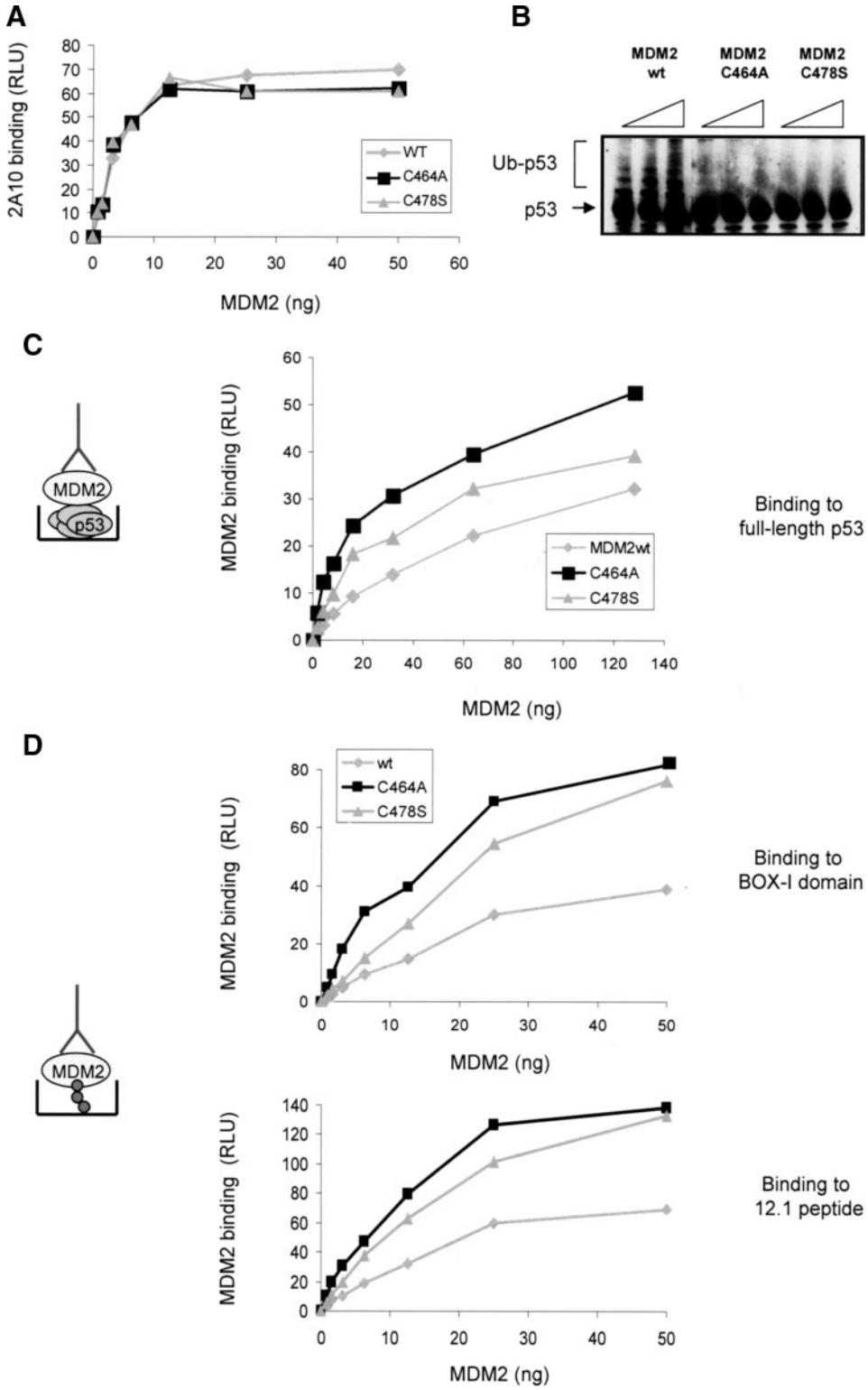

FIGURE 4. **C2H2C4 mutant MDM2 binds with a higher affinity to p53.** *A*, to check the accuracy of protein normalization for the purified MDM2wt, MDM2C464A, and MDM2C478S proteins an enzyme-linked immunosorbent assay was performed in which a titration of MDM2 protein was coated onto the microtiter plate wells, following extensive washing, and MDM2wt and mutant protein levels were detected using 2A10. *B*, ubiquitination reactions were assembled with p53, E1, E2, and MDM2 wt or mutant proteins as indicated. Ubiquitination was analyzed by immunoblot using a 4–12% gradient gel, p53 was detected using DO-1. Unmodified (*p53*) and ubiquitinated p53 (*Ub-p53*) is shown. *C*, p53 (100 ng/well) was coated onto microtiter wells and incubated with wt or mutant MDM2 as indicated. MDM2 binding was detected using 2A10 and is expressed as relative light units (*RLU*) against the MDM2 amount. The experiment is representative of three independent experiments where each condition was carried out in duplicate. In the *schematic* the detecting antibody 2A10 is depicted. *D*, BOX-I (*upper panel*) or 12.1 (*lower panel*) peptides (5 μM) were captured onto streptavidin-coated wells, and MDM2 binding was determined as described in *C*. In the *schematic* BOX-I/12.1 are depicted and the detecting antibody is 2A10.

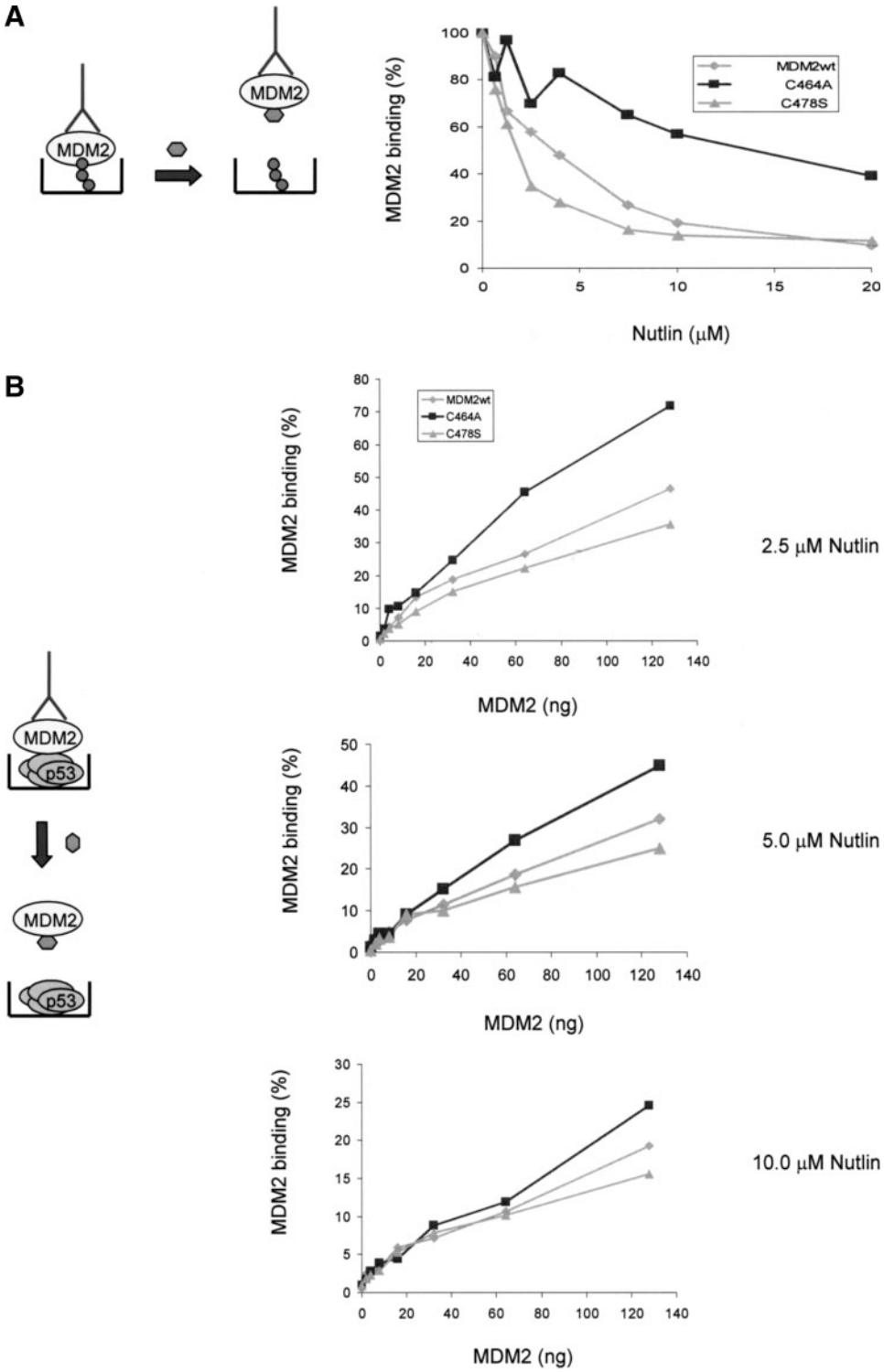

FIGURE 5. **Nutlin has a differential effect on the C2H2H4 MDM2 mutants.** *A*, a *schematic* (*left panel*) shows the assay format with BOX-I peptide Nutlin and the detecting antibody in *blue*. *Right panel*, BOX-1 peptide (5 μM) was captured on streptavidin-coated wells and incubated with the indicated form of MDM2 (50 ng), which had been preincubated (5 min) with a titration of Nutlin (μM). MDM2 binding was detected using 2A10 and is given as relative binding expressed as a percentage where 100% binding is that measured in the absence of Nutlin. *B*, p53 protein (100 ng/well) was coated onto microtiter wells and incubated with a titration of wt and mutant MDM2 as indicated. The MDM2 had been preincubated with Nutlin (2.5, 5, and 10 μM as indicated). MDM2 binding was detected using 2A10 and is normalized to maximal binding to p53 in the presence of saturating amounts of each mutant in %. The experiment is representative of at least three independent experiments where each condition was carried out in duplicate. In the *schematic* the detecting antibody 2A10 and Nutlin are depicted.

(Fig. 6*B*). The results show that the wt protein rapidly formed (within 5 min) a stable core comprising bands 1, 2, and 3, which was maintained throughout the course of the experiment. Although the MDM2C464A mutant initially formed a similar banding pattern to the wt protein, with bands 1, 2, and 3 being detected, it was then further processed so that by 15 min a new stable pattern had emerged comprising bands 2, 3, 4, and 5 with band 1 no longer being detected. Consistent with earlier results the MDM2C478S mutant appeared to be intermediate between wt and the Cys^{464A} protein as at 30 min all five bands were readily detected. These results suggest that the Cys^{464A} and Cys^{478S} mutants have a different conformation to the wt protein leading to the exposure of trypsin-sensitive cleavage sites that are not accessible in wt MDM2.

Further support for a difference in conformation between the RING mutants and wt MDM2 was provided by investigating the intrinsic fluorescence properties of the protein (Fig. 6, *C* and *D*). Although all aromatic amino acids can contribute to protein fluorescence, tryptophan is the dominant intrinsic fluorophore. MDM2 contains a total of four tryptophan residues (Fig. 6*A*) located in the central region of the protein, in and around the acid domain. Because the emission observed reflects the average environment surrounding each individual tryptophan and the tryptophans within MDM2 are not in identical local environments, each of these residues will contribute unequally to the emission spectrum. The λ_{max} of the emission spectrum of a tryptophan will be shifted to longer wavelengths (*i.e.* red-shift) if it is involved in hydrogen bonding and/or is exposed to buffer relative to the lower wavelength λ_{max} (blue shift) of a tryptophan buried within the hydrophobic core of the protein. Fig. 6*C* compares the emission fluorescence spectra of MDM2 wt and the two Cys mutants. For both of the mutant proteins we observe a red

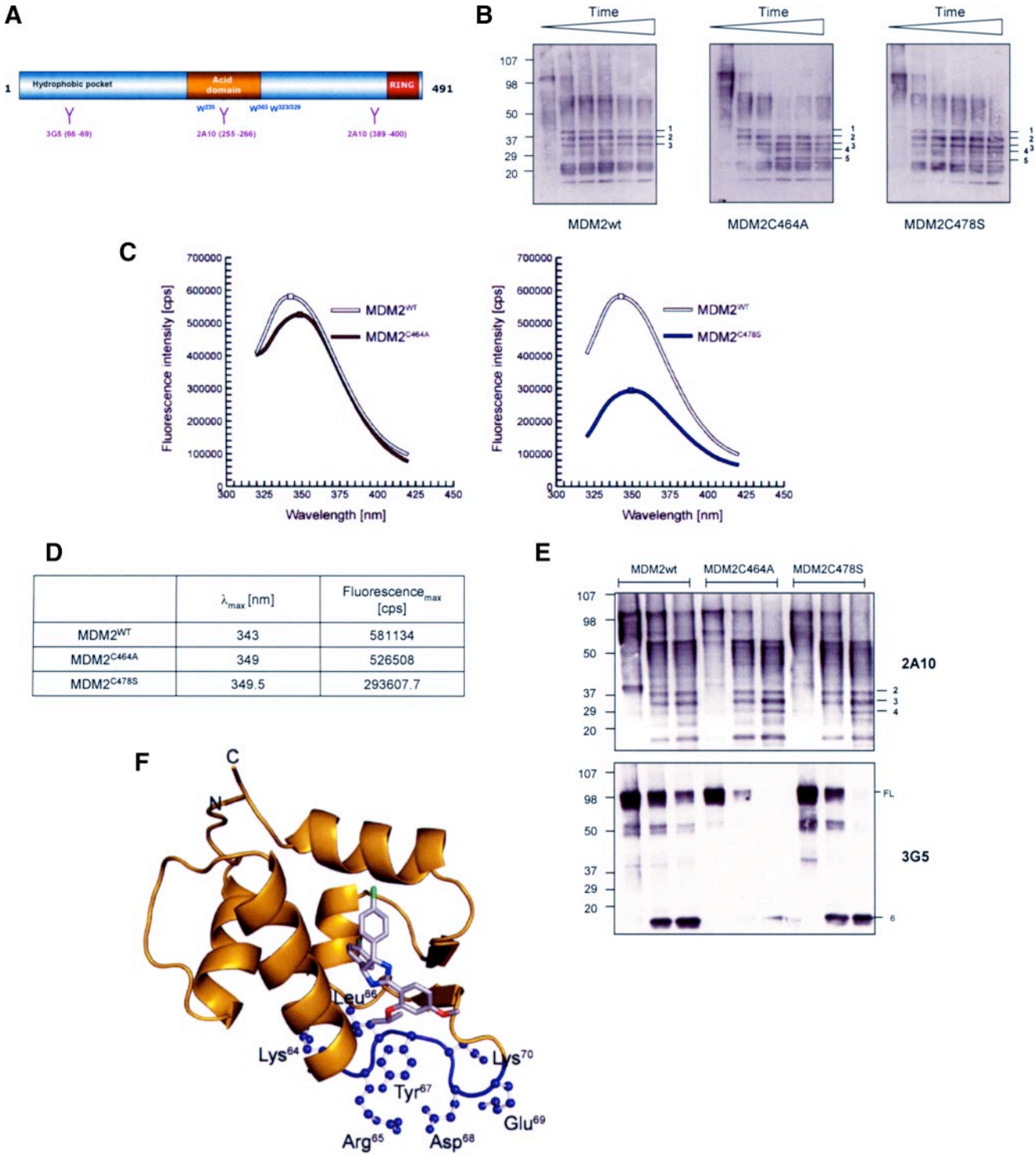

	λ_{max} [nm]	Fluorescence$_{max}$ [cps]
MDM2^{WT}	343	581134
MDM2^{C464A}	349	526508
MDM2^{C478S}	349.5	293607.7

FIGURE 6. **Conformational differences between wt and RING domain mutants of MDM2.** *A*, a *schematic* representation of MDM2 showing the epitopes for 3G5 and 2A10; the position of the 4 tryptophan residues in MDM2 is marked. *B*, immunoblot showing wt or mutant forms of MDM2 following limited proteolysis with trypsin. The blot was developed using a mixture of the MDM2 monoclonal antibodies 2A10, 4B2, 3G5, and SMP14. The numbers are used to label the banding pattern; time points used were 0, 5, 10, 15, 20, and 30 min. The data are representative of three separate experiments. *C*, resolution of fluorescence emission spectra of MDM2wt (*white*) and the MDM2C464A (*brown*) and MDM2C478S (*blue*) RING mutants. The spectra were corrected for associated buffer background signals. *D*, maxima with corresponding wavelength of MDM2 fluorescence emission spectra. The values were calculated with mathematical *n*-polynomial based algorithm, where $R^2 \geq 0.999$. *E*, as in *B* except the time course was 0, 5, and 20 min. The blots were developed using 2A10 (*upper panel*) and 3G5 (*lower panel*). *F*, localization of the 3G5 antibody epitope within the MDM2 hydrophobic pocket (pocket shown in *ribbon representation*, colored *gold*). Nutlin-3 bound to the pocket in *stick representation* (chlorine in *green*, carbon in *gray*, nitrogen in *blue*, and oxygen in *red*). The epitope of 3G5 antibody consists of four critical residues; Leu^{66}, Tyr^{67}, Asp^{68}, and Glu^{69}, surrounded by trypsin cleavable Lys and Arg residues (highlighted in *purple*). This figure was prepared using PyMOL (W. L. DeLano (2002) PyMOL, DeLano Scientific, San Carlos, CA), and structural data were from file 1TTV-RCSB PDB.

shift with λ_{max} at 349–349.5 nm in contrast to that of the wt protein of λ_{max} at 343 nm (Fig. 6*D*). Moreover the differential quenching of the emission spectrum (Fig. 6*C*) for the two mutants indicates that their conformation changes are not equivalent. Thus, the data show differences in conformation between wt and mutant forms of MDM2 and between the two mutants. The intrinsic fluorescence measurements are therefore consistent with the partial proteolytic digestion data (Fig. 6*B*) and with the differential binding affinity of the Cys^{464A} and Cys^{478S} mutants for BOX-I and Nutlin (Figs. 4 and 5).

The experiments presented above using limited proteolysis (Fig. 6*B*) and intrinsic fluorescence (Fig. 6*C*) suggest that the introduction of point mutations in key RING domain Cys residues generates a measurable conformational change in full-length MDM2 protein. To establish whether these conformational changes have a direct impact on the structure of the hydrophobic pocket we employed a monoclonal antibody (3G5), which binds to an epitope in the center of the hydrophobic pocket (Fig. 6*A*) (35). Using limited proteolysis we determined whether changes in the RING domain had an effect on the ability of 3G5 to bind to the hydrophobic pocket of MDM2. As a control for this experiment we used the monoclonal antibody 2A10, which has been mapped to two epitopes within the central and C-terminal domains of MDM2 (Fig. 6*A*). The 2A10 data (Fig. 6*E*, *upper panel*) suggests that the core fragments identified in Fig. 6*B* (in particular *bands 2–4*) are comprised largely of the central domain of MDM2 together with C-terminal truncations. In contrast 3G5 (Fig. 6*E*, *lower panel*) suggests that the hydrophobic pocket is rapidly cleaved from the core of MDM2 and that its removal generates a fast migrating 3G5 reactive product (*band 6*). The MDM2C478S mutant appears to be more sensitive to this type of cleavage, because 3G5-positive full-length protein is lost more rapidly than it is for wt MDM2. Of particular interest in this assay is the MDM2C464A mutant, as incubation of this protein leads to a dramatic loss of the 3G5 epitope suggesting that the hydrophobic pocket in this protein is more "relaxed" and therefore more accessible to trypsin digestion during which the 3G5 epitope is cleaved leading to a loss of antibody binding.

Together the data presented in this section support the conclusion that the RING domain of MDM2 can influence the activity of the N-terminal hydrophobic pocket by producing long range conformational changes that are transmitted through the central acid core of MDM2 and which lead to varying degrees of relaxation in the hydrophobic pocket.

DISCUSSION

Studies addressing how MDM2 structure supports its functional diversity have begun to provide insight into the proteins conformational flexibility. Thus, a picture is immerging of interdependent functional domains linked through changes in conformation, emphasizing the need to study the domain structure of MDM2 within the context of the whole protein. In the current study we have used point mutations within the RING finger domain to uncover cross-talk between the C terminus and interactions taking place at the N-terminal hydrophobic pocket of MDM2. Our results show that RING-mediated allosteric modulation of the hydrophobic pocket has implications for both MDM2 transrepressor activity and for the efficacy of MDM2-targeted therapy (Fig. 7).

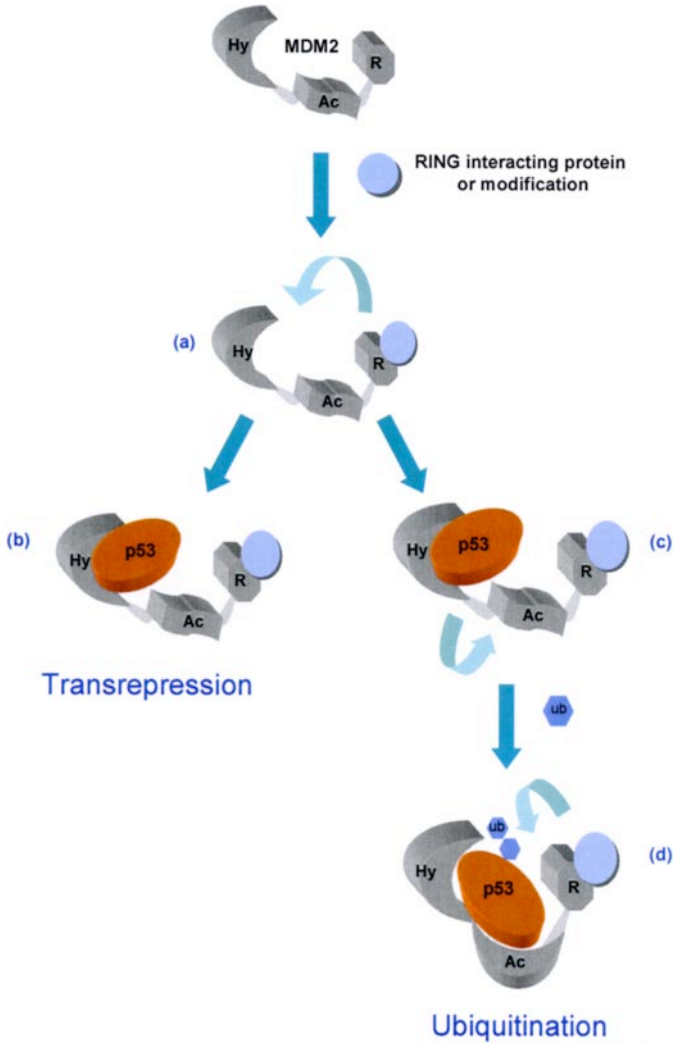

FIGURE 7. **Model for the allosteric regulation of MDM2.** Our data suggest the binding of interacting proteins and ligands or post-translational modification within the RING domain of MDM2 (*a*), which affect RING architecture, will cause conformational changes leading to changes in the affinity of the hydrophobic pocket for BOX-I domain of p53 and other ligands. This can result in formation of a transcriptionally inactive complex (*b*), or, based on our previous studies (16), could result in a transition complex (*c*) where hydrophobic pocket binding leads the acid domain to bind to the core BOX-V site in p53-signaling p53 ubiquitination (*d*).

We previously described a link between the hydrophobic pocket of MDM2 and its acid domain (16). In this case occupation of the hydrophobic pocket promoted conformational changes in MDM2 that favored acid domain binding to a ubiquitination signal in the core DNA binding domain of p53. This allosteric mechanism promotes MDM2 function as an E3-ubiquitin ligase by stabilizing a low affinity interaction between the BOX-V domain of p53 and the acid domain of MDM2. The current data add to this model for the regulation of one MDM2 domain through modulation of a second by demonstrating that the RING finger domain, and more specifically residues required to form the C2H2C4 RING structure, can allosterically modulate hydrophobic pocket interactions. In this case the result is an increase in the affinity of the hydrophobic pocket, which produces a gain in transrepressor function in

cells. Interestingly, mutations of Cys^{464} and Cys^{478} residues are not equivalent in terms of their effect on the hydrophobic pocket. Thus, although both mutants display increased binding to the BOX-I domain of p53 (Fig. 4), the Cys^{478S} mutant binds Nutlin in preference to BOX-I, whereas the Cys^{464A} protein preferentially binds to BOX-I (Fig. 5).

Structural and computational analysis of the MDM2 hydrophobic pocket interaction with p53 has revealed that this domain has a high degree of plasticity and has suggested that the shape of the binding cleft can change significantly (36, 37). A mechanism has been proposed where binding to the BOX-I domain of p53 requires a progressive opening up of the binding cleft to reveal a hydrophobic interface. p53 binding then proceeds through an intermediate complex where the cleft gradually adopts a more open conformation eventually accommodating Thr^{18}–Asp^{29} of BOX-I. Based on this type of study it has been hypothesized that the cleft has enough plasticity to allow a range of low energy states rather than a single "open" or "closed" conformation. As a result the pocket can accommodate a range of peptides and small molecules that might not have any obvious structural similarity (32, 36–39). It is likely therefore that the differential binding preferences of our two Cys mutants are a result of different degrees of cleft accessibility. This hypothesis is supported by data showing that, although the Cys^{464A} and Cys^{478S} mutant proteins both adopt a different stable conformation from the wt protein (Fig. 6), their conformation is not equivalent. The intrinsic fluorescence of tryptophan residues within the central domain of the Cys^{478S} mutant is quenched relative to those in the Cys^{464A} mutant, suggesting that they are more solvent-exposed or are involved in additional interactions with nearby residues. Further evidence for a difference in the conformation of the hydrophobic cleft dependent on the status of the RING domain comes from the use of the monoclonal antibody 3G5 to probe for differences in conformation following limited tryptic digestion (Fig. 6*E*). This antibody recognizes an epitope in the hydrophobic pocket of MDM2, where residues ^{66}LYDE^{69} are essential but not sufficient for binding, *i.e.* peptides containing the LYDE motif but not other surrounding residues are not sufficient for antibody recognition (35). The LYDE motif maps to a loop structure in the hydrophobic pocket that lies between two of the α-helical structures that form the BOX-I binding cleft (Fig. 6*F*) and is flanked by lysine and arginine residues that provide tryptic cut sites when exposed (^{61}IMTKRLYDEKQQHIV^{75}). Our data show that the LYDE motif is more accessible in the Cys^{464A} mutant than in the wt or the Cys^{478S} protein (Fig. 6*F*), suggesting that the cleft is more relaxed and therefore more readily able to accommodate the BOX-I peptide leading to an increase in BOX-I affinity.

Our data, showing that mutations in the C-terminal C2H2C4 RING of MDM2 can allosterically modulate not only the affinity of the hydrophobic pocket but also its specificity (Fig. 5), suggest that in cells the binding of interacting proteins and/or ligands to the RING is likely to impact on both MDM2 transrepressor activity and on the efficacy of pocket binding drugs in tumor cells (Fig. 6). This hypothesis is supported by data showing that binding of ligands such as zinc and ATP to the RING finger domain of MDM2 generate conformational changes (17, 23). In fact, we have previously shown that zinc binding can affect the interaction of MDM2 with the BOX-I domain of p53; in this case zinc binding leads to a decrease in BOX-I binding (17, 23). Together with our current data this suggests that modulation of the RING domain has the potential to both negatively and positively regulate binding of BOX-I to the hydrophobic pocket. As the Cys mutants used in the current study are E3-ligase dead, it is not possible to determine if C2H2C4 RING interacting factors could also promote MDM2 E3-ligase activity, because increased binding to hydrophobic pocket binding ligands could potentially favor acid domain binding to the BOX-V domain of p53 signaling ubiquitination (16). Thus, it will be interesting to determine whether RING domain-interacting factors, or modifications, such as acetylation (40), within the RING domain act in a concerted manner to promote both transrepression and ubiquitination of p53 or whether changes in RING conformation might act as a switch favoring one MDM2 activity over another.

Recent genetic studies have suggested that the primary physiological role of MDM2 is the regulation of p53 protein levels mediated by its E3-ligase activity (41, 42). These experiments were largely carried out in mouse embryonic fibroblasts and developing mouse embryos where MDM2 activity has been lost or reduced and is therefore rate-limiting. However, this situation is unlikely to reflect the environment encountered in most tumor cells. In fact current estimates suggest that MDM2 levels are elevated in ~10% of all human tumors (43) due for example to enhanced translation or transcription in addition to amplification of the MDM2 gene (44). In contrast to the studies in non-transformed mouse cell models mentioned above work in tumor cells endogenously overexpressing MDM2 protein suggests that its ability to act as a transrepressor contributes significantly to the impaired p53-response seen in these cells. Thus, in cells that are homozygous for a polymorphism (SNP309) that enhances SP1-dependent *MDM2* transcription the MDM2 protein is found in association with p53 resulting in transcriptionally inactive complexes (25, 45). Depletion of MDM2 by siRNA in these cells results in activation of p53-dependent transcription in the absence of increase p53 protein levels supporting the idea that, at least in some tumor cells, MDM2 acts predominantly as a transrepressor of p53 function (25). Furthermore, it has been demonstrated that tumor cells that do not have increased MDM2 levels also operate an MDM2-dependent mechanism for controlling p53 transcription in the absence of changes in p53 protein levels (46). Thus, the data presented here, showing that C2H2C4 RING mutants that loose E3-ubiquitin ligase activity preferentially bind to p53 inhibiting its transactivation activity, may be pertinent to the physiological environment of a tumor cell where MDM2 is controlling p53 activity primarily through transrepression.

We have shown that Nutlin does not inhibit MDM2 E3-ligase activity neither *in vitro* nor in cell models (Fig. 3; 16). However, despite its lack of E3-ligase inhibitory activity Nutlin can function in cells and animal models of cancer to activate p53 and to elevate p53 protein levels (32, 33). Evidence presented here showing that Nutlin can reverse transrepression imposed by both the wild-type and the Cys^{478S} mutated form of MDM2 suggests that it functions primarily by relieving MDM2-im-

posed transrepression allowing binding to coactivators such as p300. This conclusion is supported by the observation that Nutlin promotes rapid activation of p53-dependent transcription before changes in p53 protein level are recorded (46). The fact that Nutlin is proving to be an effective drug in some models of human cancer provides further evidence for the role of MDM2 transrepressor activity in tumor development.

Acknowledgments—We thank Malcolm Walkinshaw for stimulating discussion and advice and Martin Wear (Center for Translation and Chemical Biology) for his expertise and helpful discussions on the biophysics of MDM2.

REFERENCES

1. Vogelstein, B., Lane, D., and Levine, A. J. (2000) *Nature* **408,** 307–310
2. Levine, A. J. (1997) *Cell* **88,** 323–331
3. Hollstein, M., Rice, K., Greenblatt, M. S., Soussi, T., Fuchs, R., Sorlie, T., Hovig, E., Smith-Sorensen, B., Montesano, R., and Harris, C. C. (1994) *Nucleic Acids Res.* **22,** 3551–3555
4. Vousden, K. H. (2006) *J. Cell Sci.* **119**, 5015–5020
5. Oliner, J. D., Pietenpol, J. A., Thiagalingam, S., Gyuris, J., Kinzler, K. W., and Vogelstein, B. (1993) *Nature* **362,** 857–860
6. Wu, X., Bayle, J. H., Olson, D., and Levine, A. J. (1993) *Genes Dev.* **7,** 1126–1132
7. Brooks, C. L., and Gu, W. (2004) *Cell Cycle* **3,** 895–899
8. Momand, J., Zambetti, G. P., Olson, D. C., George, D., and Levine, A. J. (1992) *Cell* **69,** 1237–1245
9. Honda, R., Tanaka, H., and Yasuda, H. (1997) *FEBS Lett.* **420,** 25–27
10. Kubbutat, M. H., Jones, S. N., and Vousden, K. H. (1997) *Nature* **387,** 299–303
11. Yin, Y., Stephen, C. W., Luciani, M. G., and Fahraeus, R. (2002) *Nat. Cell Biol.* **4,** 462–467
12. Wawrzynow, B., Zylicz, A., Wallace, M., Hupp, T., and Zylicz, M. (2007) *J. Biol. Chem.* **282,** 32603–32612
13. Burch, L., Shimizu, H., Smith, A., Patterson, C., and Hupp, T. R. (2004) *J. Mol. Biol.* **337,** 129–145
14. Kussie, P. H., Gorina, S., Marechal, V., Elenbaas, B., Moreau, J., Levine, A. J., and Pavletich, N. P. (1996) *Science* **274,** 948–953
15. Lin, J., Chen, J., Elenbaas, B., and Levine, A. J. (1994) *Genes Dev.* **8,** 1235–1246
16. Wallace, M., Worrall, E., Pettersson, S., Hupp, T. R., and Ball, K. L. (2006) *Mol. Cell* **23,** 251–263
17. Shimizu, H., Burch, L. R., Smith, A. J., Dornan, D., Wallace, M., Ball, K. L., and Hupp, T. R. (2002) *J. Biol. Chem.* **277,** 28446–28458
18. Yu, G. W., Rudiger, S., Veprintsev, D., Freund, S., Fernandez-Fernandez, M. R., and Fersht, A. R. (2006) *Proc. Natl. Acad. Sci. U. S. A.* **103,** 1227–1232
19. Fang, S., Jensen, J. P., Ludwig, R. L., Vousden, K. H., and Weissman, A. M. (2000) *J. Biol. Chem.* **275,** 8945–8951
20. Boddy, M. N., Freemont, P. S., and Borden, K. L. (1994) *Trends Biochem. Sci.* **19,** 198–199
21. Kostic, M., Matt, T., Martinez-Yamout, M. A., Dyson, H. J., and Wright, P. E. (2006) *J. Mol. Biol.* **363,** 433–450
22. Linke, K., Mace, P. D., Smith, C. A., Vaux, D. L., Silke, J., and Day, C. L. (2008) *Cell Death Differ.* **15,** 841–848
23. Poyurovsky, M. V., Jacq, X., Ma, C., Karni-Schmidt, O., Parker, P. J., Chalfie, M., Manley, J. L., and Prives, C. (2003) *Mol. Cell* **12,** 875–887
24. Knights, C. D., Liu, Y., Appella, E., and Kulesz-Martin, M. (2003) *J. Biol. Chem.* **278,** 52890–52900
25. Arva, N. C., Gopen, T. R., Talbott, K. E., Campbell, L. E., Chicas, A., White, D. E., Bond, G. L., Levine, A. J., and Bargonetti, J. (2005) *J. Biol. Chem.* **280,** 26776–26787
26. Thut, C. J., Goodrich, J. A., and Tijan, R. (1997) *Genes Dev.* **11,** 1974–1986
27. Dornan, D., and Hupp, T. R. (2001) *EMBO Rep.* **2,** 139–144
28. Liu, W. L., Midgley, C., Stephen, C., Saville, M., and Lane, D. P. (2001) *J. Mol. Biol.* **313,** 711–731
29. Yu, D., Jing, T., Liu, B., Yao, J., Tan, M., McDonnell, T. J., and Hung, M. C. (1998) *Mol Cell* **2,** 581–591
30. Hupp, T. R., Meek, D. W., Midgley, C. A., and Lane, D. P. (1992) *Cell* **71,** 875–886
31. Miyashita, T., and Reed, J. C. (1995) *Cell* **80,** 293–299
32. Vassilev, L. T., Vu, B. T., Graves, B., Carvajal, D., Podlaski, F., Filipovic, Z., Kong, N., Kammlott, U., Lukacs, C., Klein, C., Fotouhi, N., and Liu, E. A. (2004) *Science* **303,** 844–848
33. Vassilev, L. T. (2004) *Cell Cycle* **3,** 419–421
34. Bottger, V., Bottger, A., Howard, S. F., Picksley, S. M., Chene, P., Garcia-Echeverria, C., Hochkeppel, H. K., and Lane, D. P. (1996) *Oncogene* **13,** 2141–2147
35. Bottger, A., Bottger, V., Garcia-Echeverria, C., Chene, P., Hochkeppel, H. K., Sampson, W., Ang, K., Howard, S. F., Picksley, S. M., and Lane, D. P. (1997) *J. Mol. Biol.* **269,** 744–756
36. Espinoza-Fonseca, L. M., and Garcia-Machorro, J. (2008) *Biochem. Biophys. Res. Commun.* **370,** 547–551
37. Espinoza-Fonseca, L. M., and Trujillo-Ferrara, J. G. (2006) *Biopolymers* **83,** 365–373
38. Bowman, A. L., Nikolovska-Coleska, Z., Zhong, H., Wang, S., and Carlson, H. A. (2007) *J. Am. Chem. Soc.* **129,** 12809–12814
39. Stoll, R., Renner, C., Hansen, S., Palme, S., Klein, C., Belling, A., Zeslawski, W., Kamionka, M., Rehm, T., Muhlhahn, P., Schumacher, R., Hesse, F., Kaluza, B., Voelter, W., Engh, R. A., and Holak, T. A. (2001) *Biochemistry* **40,** 336–344
40. Wang, X., Taplick, J., Geva, N., and Oren, M. (2004) *FEBS Lett.* **561,** 195–201
41. Itahana, K., Mao, H., Jin, A., Itahana, Y., Clegg, H. V., Lindstrom, M. S., Bhat, K. P., Godfrey, V. L., Evan, G. I., and Zhang, Y. (2007) *Cancer Cell* **12,** 355–366
42. Toledo, F., Krummel, K. A., Lee, C. J., Liu, C. W., Rodewald, L. W., Tang, M., and Wahl, G. M. (2006) *Cancer Cell* **9,** 273–285
43. Toledo, F., and Wahl, G. M. (2006) *Nat. Rev. Cancer* **6,** 909–923
44. Ganguli, G., and Wasylyk, B. (2003) *Mol. Cancer Res.* **1,** 1027–1035
45. Bond, G. L., Hu, W., Bond, E. E., Robins, H., Lutzker, S. G., Arva, N. C., Bargonetti, J., Bartel, F., Taubert, H., Wuerl, P., Onel, K., Yip, L., Hwang, S. J., Strong, L. C., Lozano, G., and Levine, A. J. (2004) *Cell* **119,** 591–602
46. White, D. E., Talbott, K. E., Arva, N. C., and Bargonetti, J. (2006) *Cancer Res.* **66,** 3463–3470

J Chem Biol (2009) 2:113–129
DOI 10.1007/s12154-009-0019-5

ORIGINAL ARTICLE

Regulation of the E3 ubiquitin ligase activity of MDM2 by an N-terminal pseudo-substrate motif

Erin G. Worrall · Bartosz Wawrzynow · Liam Worrall · Malcolm Walkinshaw · Kathryn L. Ball · Ted R. Hupp

Received: 10 February 2009 / Accepted: 25 March 2009 / Published online: 16 May 2009

Abstract The tumor suppressor p53 has evolved a MDM2-dependent feedback loop that promotes p53 protein degradation through the ubiquitin–proteasome system. MDM2 is an E3-RING containing ubiquitin ligase that catalyzes p53 ubiquitination by a dual-site mechanism requiring ligand occupation of its N-terminal hydrophobic pocket, which then stabilizes MDM2 binding to the ubiquitination signal in the DNA-binding domain of p53. A unique pseudo-substrate motif or "lid" in MDM2 is adjacent to its N-terminal hydrophobic pocket, and we have evaluated the effects of the flexible lid on the dual-site ubiquitination reaction mechanism catalyzed by MDM2. Deletion of this pseudo-substrate motif promotes MDM2 protein thermoinstability, indicating that the site can function as a positive regulatory element. Phospho-mimetic mutation in the pseudo-substrate motif at codon 17 ($MDM2^{S17D}$) stabilizes the binding of MDM2 towards two distinct peptide docking sites within the p53 tetramer and enhances p53 ubiquitination. Molecular modeling orientates the phospho-mimetic pseudo-substrate motif in equilibrium over a charged surface patch on the MDM2 at Arg^{97}/Lys^{98}, and mutation of these residues to the MDM4 equivalent reverses the activating effect of the phospho-mimetic mutation on MDM2 function. These data highlight the ability of the pseudo-substrate motif to regulate the allosteric interaction between the N-terminal hydrophobic pocket of MDM2 and its central acidic domain, which stimulates the E3 ubiquitin ligase function of MDM2. This model of MDM2 regulation implicates an as yet undefined lid-kinase as a component of pro-oncogenic pathways that stimulate the E3 ubiquitin ligase function of MDM2 in cells.

Keywords MDM2 · p53 · Allostery · Kinase · Ubiquitination

E. G. Worrall · T. R. Hupp
CRUK p53 Signal Transduction Group, University of Edinburgh, Edinburgh, Scotland, UK, EH4 2XR

B. Wawrzynow · K. L. Ball
CRUK Interferon and Cell Signaling Group, University of Edinburgh, Edinburgh, Scotland, UK, EH4 2XR

E. G. Worrall · B. Wawrzynow · K. L. Ball · T. R. Hupp (✉)
Institute of Genetics and Molecular Medicine, University of Edinburgh, Edinburgh, Scotland, UK, EH4 2XR
e-mail: ted.hupp@ed.ac.uk

L. Worrall
Institute for Translational and Chemical Biology, University of Edinburgh, Edinburgh, Scotland, UK, EH4 2XR

M. Walkinshaw
Institute for Translational and Chemical Biology, University of Edinburgh, Edinburgh, Scotland, UK, EH9 3JR

Present Address:
L. Worrall
Biochemistry and Molecular Biology and the Center for Blood Research, University of British Columbia, Vancouver, British Columbia, Canada, V6T 1Z3

Introduction

Reconstitution of a multicomponent ubiquitin–enzyme reaction mechanism, including the role of E1, E2, and E3 subcomponents as well as the substrate, is a fundamental goal in understanding the molecular events that regulate the ubiquitin–proteasome pathway [32]. The proteins within the E3 class of ubiquitination catalysts include among others the HECT domain and the RING domains. Unlike

the HECT domain containing ubiquitin ligases, the E3-RING domain containing proteins do not form a covalent bond with ubiquitin, but catalyze the transfer of ubiquitin from the activated E2 to the substrate by as yet undefined mechanisms. How E3-RING domain containing ubiquitin ligases alter substrate conformation and drive E2 recognition of substrate are critical mechanistic goals. The pro-oncogenic protein MDM2 is such a RING domain containing E3 ubiquitin ligase that can promote the ubiquitination of the p53 tumor suppressor protein [44, 49], and MDM2 represents a model E3 ubiquitin ligase to evaluate the dynamics of a multiprotein ubiquitination system.

The E3-RING domain containing ubiquitin ligase MDM2 itself has been dissected into multiple domains with specific biochemical functions. The C-terminal RING domain in MDM2 co-ordinates the activity of MDM2 in E2-mediated ubiquitin transfer [22] and contains a C-terminal peptide tail that maintains RING-domain conformation [36, 46]. The RING domain also promotes MDM2-dependent stimulation of p53 protein synthesis through interactions with p53 mRNA during translation [7], and RNA itself can stimulate MDM2:p53 interactions and substrate ubiquitination [5, 6, 33]. There also is an ATP-binding motif imbedded within the RING domain that regulates the molecular chaperone functions of MDM2 [41, 51]. Thus, the RING domain of MDM2 mediates biochemical functions, including E2 binding, ATP binding, and RNA binding.

In addition to the C-terminal RING domain, MDM2 also contains an N-terminal allosteric hydrophobic pocket, which interacts with a specific linear peptide motif in proteins such as p53 and interferon-responsive transcription factors [20, 33]. This hydrophobic pocket was the first region on MDM2 that was shown to bind directly to p53 [8]. Adjacent to this N-terminal domain is an "acidic" domain that interacts at a second binding site within a flexible motif in the DNA binding domain of p53 [38]. The N-terminal hydrophobic binding pocket has been targeted by small molecules like Nutlins that can interact with MDM2 and activate p53 function by releasing p53 from MDM2-mediated transrepression [47]. However, such ligands do not block p53 ubiquitination [50] as ligand occupation of this N-terminal hydrophobic pocket forms a positive role in MDM2 function as an E3 ubiquitin ligase. MDM2 hydrophobic pocket occupation promotes a more stable interaction between the internal acidic domain of MDM2 and a ubiquitination signal in the DNA-binding domain of p53 [50].

These data have formed a "dual-site" model of MDM2-mediated ubiquitination of p53. Accordingly, small peptides derived from the *BOX-I* domain of p53 (containing the primary MDM2 binding site) or small molecules like Nutlin do not block p53 ubiquitination. By contrast, peptides derived from the *BOX-V* domain of p53 (containing the ubiquitination signal in the DNA-binding domain of p53) do inhibit MDM2 ubiquitination of p53 [50]. Allosteric interactions within full-length MDM2 protein has been recently examined through structure-function studies demonstrating that mutation of selected amino acids in the RING domain promotes a conformation change both in the N-terminal domain of MDM2 as defined by proteolytic cleavage susceptibility and in the acidic domain as defined by elevated intrinsic tryptophan fluorescence [52]. These latter data provided the first biophysical evidence for allosteric interactions among the various sub-domains in full-length MDM2 protein.

This dual-site model for MDM2-mediated ubiquitination of p53 presumably operates due to the striking flexibility of the N-terminal p53-binding domain in the presence of distinct peptide ligands [37, 40, 45]. A predominant feature of this ubiquitination reaction mechanism is that there is an induced stabilization of the acidic domain of MDM2 to the conformationally flexible region in the DNA-binding domain of p53 [38, 55] when the MDM2 hydrophobic pocket is occupied by substrate [50]. This linear peptide motif in the DNA-binding domain of p53 (named *BOX-V* motif) is normally cryptic in the folded p53 tetramer, but it is exposed on mutant p53 in human cancers as defined using a monoclonal antibody that binds to this peptide-epitope on denatured p53 protein [13, 48].

This flexible *BOX-V* motif in the DNA-binding domain of p53 is also a multiprotein docking site; many protein kinases, including CHK1/2, DAPK, and CK1, interact with this region on p53 to catalyze phosphorylation of the transactivation domain of p53 at Ser20 [9, 23]. Destabilizing mutations in p53 that "unfold" p53 protein at the conformationally flexible region of p53 in the *BOX-V* domain enhance mutant p53 protein ubiquitination in cell systems [39] and can induce mutant p53 degradation via MDM2 function in murine transgenes [42]. The enhanced degradation of mutant p53 protein by an MDM2-dependent pathway has important implications for regulating the pro-oncogenic functions of mutant p53 in human cancers; indeed, most human cancers appear to have a form of mutant p53 protein with enhanced steady-state levels [30] and therefore has presumably evaded the normal mutant protein degradation machinery.

In order to define further the nature of the allosteric regulation of MDM2, we have examined the function of a flexible and unstructured N-terminal peptide motif adjacent to the hydrophobic pocket of MDM2. Such small flexible peptide motifs have been postulated to be important in a wide range of signaling proteins [27–29]. This flexible motif in MDM2 has been called a pseudo-substrate motif or lid. Pseudo-substrate motifs operate in a range of allosterically regulated enzymes, including protein kinases and metabolic enzymes, and have been termed intrasteric

regulatory motifs [1, 16, 17]. The pseudo-substrate motif of MDM2 harbors a phosphorylation site whose phospho-mimetic mutation can alter the conformation of the N-terminal domain of MDM2 protein as defined by NMR studies [25, 40]. This phospho-mimetic mutation was proposed to stabilize the pseudo-substrate motif over the hydrophobic pocket and occlude p53 binding. However, this has not been tested experimentally. As ligands that fill the hydrophobic pocket like Nutlin can prime MDM2 and stimulate the MDM2 E3 ubiquitin ligase function toward p53 [50], the role of the unphosphorylated or phosphorylated lid is not necessarily evident—would it function as a positive or negative cofactor in regulating the stability of the MDM2:p53 complex, and therefore, would it ultimately stimulate or attenuate p53 protein ubiquitination?

In this report, we show that the flexible lid is a positive regulatory motif that maintains the thermostability of MDM2 and that a phospho-mimetic mutation in the MDM2 lid stabilizes the MDM2:p53 complex. We propose a *cis*-acting intrasteric mechanism to explain how phospho-mimetic mutation of the MDM2 lid might open the hydrophobic pocket. This results in enhanced binding of MDM2 to the first site on p53, which in turn enhances the allosteric interaction between the acidic domain of MDM2 and the ubiquitination signal in the DNA-binding domain of p53. These data also highlight the growing realization that flexible and unstructured linear peptide motifs play critical roles in controlling protein function in signal transduction pathways [29] and provide a biochemical foundation to study how changes in the rates of MDM2 phosphorylation at this flexible motif regulates the E3 ubiquitin ligase function of MDM2.

Results

A phospho-mimetic mutation in the pseudo-substrate motif stimulates the E3 ubiquitin ligase function of MDM2

MDM2 is composed of distinct ligand binding domains that regulate its multiple functions (Fig. 1). The integration of our current study on the MDM2 pseudo-substrate motif to

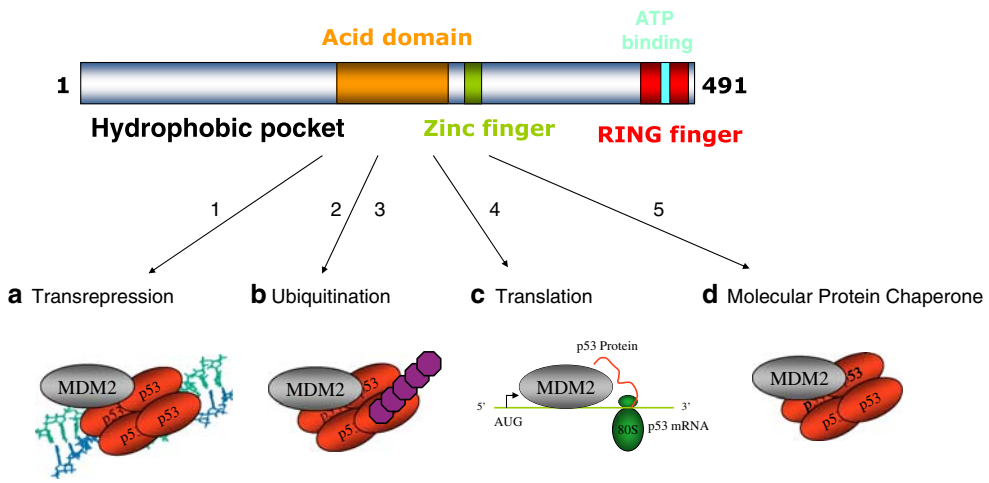

Fig. 1 Four distinct modes of MDM2 function. The *top panel* highlights the domain structure of MDM2, including the hydrophobic pocket in the N-terminus [20], the acidic central domain [55], a zinc-binding motif [56], the RING domain [18], and ATP-binding site imbedded within the RING domain [35]. MDM2 was identified as a protein that regulates the p53 tumor suppressor via (*1*) inhibition of p53-dependent transcription [26, 43]. Germline mutations in the *mdm2* promoter that result in MDM2 over-production result in enhanced MDM2 protein in chromatin fractions, which mediates suppression of p53 function as a transcription factor [2, 52]. The second function identified for MDM2 involved its ability to (*2*, *3*) catalyze p53 degradation through a ubiquitin-dependent pathway [19] [15]. This ubiquitination function of MDM2 also involves ubiquitination and degradation of ribosomal proteins that can normally function to stimulate p53 protein synthesis [31]. According to the dual-site mechanism of MDM2-mediated ubiquitination of p53 [50], two structural changes can enhance p53 ubiquitination by MDM2: one structural change involves (*2*) destabilizing missense mutations in p53 that unfolds the p53 tetramer and that can expose the ubiquitination signal in the DNA-binding domain [38], thus enhancing p53 ubiquitination in cells [39]; the second structural change involves (*3*) the lid of MDM2 whose phospho-mimetic mutation increases MDM2-mediated ubiquitination of p53 tetramers by stabilizing the MDM2:p53 complex (this study). Small molecules that bind to the N-terminal hydrophobic pocket of MDM2 (Nutlins) can activate p53 [47] presumably by inhibiting the chromatin-bound pool of MDM2 since Nutlins cannot inhibit MDM2 function as an E3 ubiquitin ligase [50]. Rather, to date, peptide mimetics that bind to the MDM2 acidic domain provide a lead for inhibiting MDM2 function as a E3 ubiquitin ligase [50]. Additional research has highlighted novel molecular functions of MDM2. A cellular function was assigned to the RNA-binding activity of MDM2 [12, 21, 24], which involves (*4*) an interaction of MDM2 with p53 mRNA at ribosomes to stimulate p53 protein synthesis [7]. A function was also assigned to the ATP-binding motif of MDM2 [35], which involves (*5*) the ability of MDM2 to exhibit the property of a molecular chaperone by catalyzing the ATP-dependent folding of the p53 tetramer to enhance p53 function as a transcription factor [41, 51]

the known biochemical functions of MDM2 is also summarized in Fig. 1. The MDM2 oncoprotein is known to have diverse molecular functions in (1) transcriptional repression of p53, (2) ubiquitination and degradation of p53, (3) synthesis of p53 protein, and (4) ATP-dependent molecular chaperone functions on p53 protein (Fig. 1). It is not known if these four functions are integrated, function in parallel, or are coordinately switched on or off. However, human and mouse genetic studies have established a specific role for the RING domain and hydrophobic pocket in the control of MDM2 function as a transrepressor and as an E3 ubiquitin ligase [2, 44].

In order to dissect further the dual-site model of MDM2-mediated ubiquitination of p53, we focused our analysis on the effects of the pseudo-substrate motif (Fig. 2a) on the in vitro E3 ubiquitin ligase function of MDM2. An NMR study of the unliganded *apo*-form of the N-terminal domain of MDM2 revealed the pseudo-substrate motif to be largely unstructured and in a dynamic equilibrium (Fig. 2b). Further, ligands that occupy the hydrophobic pocket can alter the conformation of MDM2 [25, 37, 40, 45], highlighting the conformational flexibility of MDM2. However, ligands such as Nultin or a p53 peptide (*BOX-I* domain peptide) do not inhibit MDM2-mediated ubiquitination (Fig. 2c and d), while peptides that bind to the acidic domain of MDM2 (*BOX-V* domain homology peptides) can inhibit MDM2 function (Fig. 2e; as in [33, 50, 52]). As the conformational flexibility of this N-terminal pseudo-substrate motif of MDM2 could have significant regulatory effects on MDM2 conformation, this motif also provides a novel tool with which to evaluate how perturbation of the hydrophobic pocket of MDM2 might regulate allosterically the E3 ubiquitin ligase function of MDM2.

To define a role for this flexible pseudo-substrate motif or lid, purified untagged wild-type MDM2 and MDM2 mutants were generated, including one with an N-terminal flexible pseudo-substrate motif deletion ($MDM2^{\Delta LID}$; Fig. 3a). A titration of MDM2 (Fig. 3b, lanes 1–5) or $MDM2^{\Delta LID}$ (Fig. 3b, lanes 6–10) in ubiquitination reactions demonstrated that $MDM2^{\Delta LID}$ has a lower specific activity, although it can still catalyze ubiquitination. The lowered specific activity of $MDM2^{\Delta LID}$ suggests the pseudo-substrate motif normally has an intrinsic positive regulatory effect on MDM2 function.

The pseudo-substrate motif also has a SQ phospho-acceptor site whose phospho-mimetic mutation (S to D) induces a conformational change in the N-terminal domain of MDM2 as defined using NMR [25] (Fig. 2a and b). This mutation was predicted to stabilize the lid equilibrium into a position that partially occludes ligands like p53 and that this mutation might therefore block the MDM2:p53 complex. However, the biochemical effects of this mutation on MDM2 function in vitro and in vivo have not actually been defined experimentally. As such, we also evaluated the effect of the phospho-mimetic pseudo-substrate motif mutant ($MDM2^{S17D}$; Fig. 3a) on MDM2:p53 interactions. Three possibilities include (1) that the phospho-mimetic motif could act like a lid and partially cover the hydrophobic pocket, thus destabilizing the MDM2–p53 interaction [25]; (2) the phospho-mimetic motif could act like a lid and partially cover the hydrophobic pocket, thus stabilizing MDM2 acid domain interactions with p53 via the dual site allosteric model [50]; and (3) the phospho-mimetic mutation might stabilize the lid in equilibrium in a distinct conformation and "open" the hydrophobic pocket (Fig. 2b). The phospho-mimetic mutation in MDM2 in fact did not inhibit the ubiquitination function of MDM2; rather, the Asp^{17} mutation increased the specific activity of MDM2 as an E3 ubiquitin ligase (Fig. 3c, lanes 5–7 vs 2–4 and d).

These data are consistent with the lid functioning as a positive rather than as a negative regulatory motif. Regulatory motifs often alter the thermostability of an enzyme or protein [11], and we evaluated whether the pseudo-substrate motif deletion alters thermostability of MDM2. The preincubation of $MDM2^{\Delta LID}$ at the indicated temperatures completely inactivated the E3 ubiquitin ligase function of the protein (Fig. 3e, lanes 8–12 vs 7). $MDM2^{S17D}$ was not thermosensitive when preincubated at elevated temperatures compared to $MDM2^{\Delta LID}$ (Fig. 3f). These data suggest that the pseudo-substrate motif contributes positively to maintaining the thermostability of MDM2 protein. Consistent with this, transfection of the plasmid encoding $MDM2^{\Delta LID}$ into cells destabilizes the protein and accordingly reduces its specific activity as an E3 ubiquitin ligase toward p53 (Fig. 3g, lanes 6–8 vs 3–5).

A phospho-mimetic mutation in the pseudo-substrate motif stabilizes MDM2:p53 interactions

We next analyzed whether the elevated specific activity of $MDM2^{S17D}$ as a E3 ubiquitin ligase could be attributed to enhanced binding of MDM2 to p53 protein resulting in a more stable MDM2:p53 protein complex. This enhanced stability of the MDM2:p53 complex would in turn translate to enhanced p53 ubiquitination. A titration of $MDM2^{S17D}$, wt-MDM2, or $MDM2^{\Delta LID}$ provided a correlation between specific activity of an E3 ubiquitin ligase and enhanced stability of the MDM2:p53 protein complex (Fig. 4b). Although $MDM2^{\Delta LID}$ was essentially unable to form a stable contact with the p53 tetramer presumably as a result of pseudo-substrate motif deletion, $MDM2^{S17D}$ exhibited a striking increase in its binding for p53 protein as defined by the stability of the MDM2:p53 complex (Fig. 4b). The preincubation of $MDM2^{S17D}$, wt-MDM2, or $MDM2^{\Delta LID}$ at distinct temperatures had no effect in altering wt-MDM2

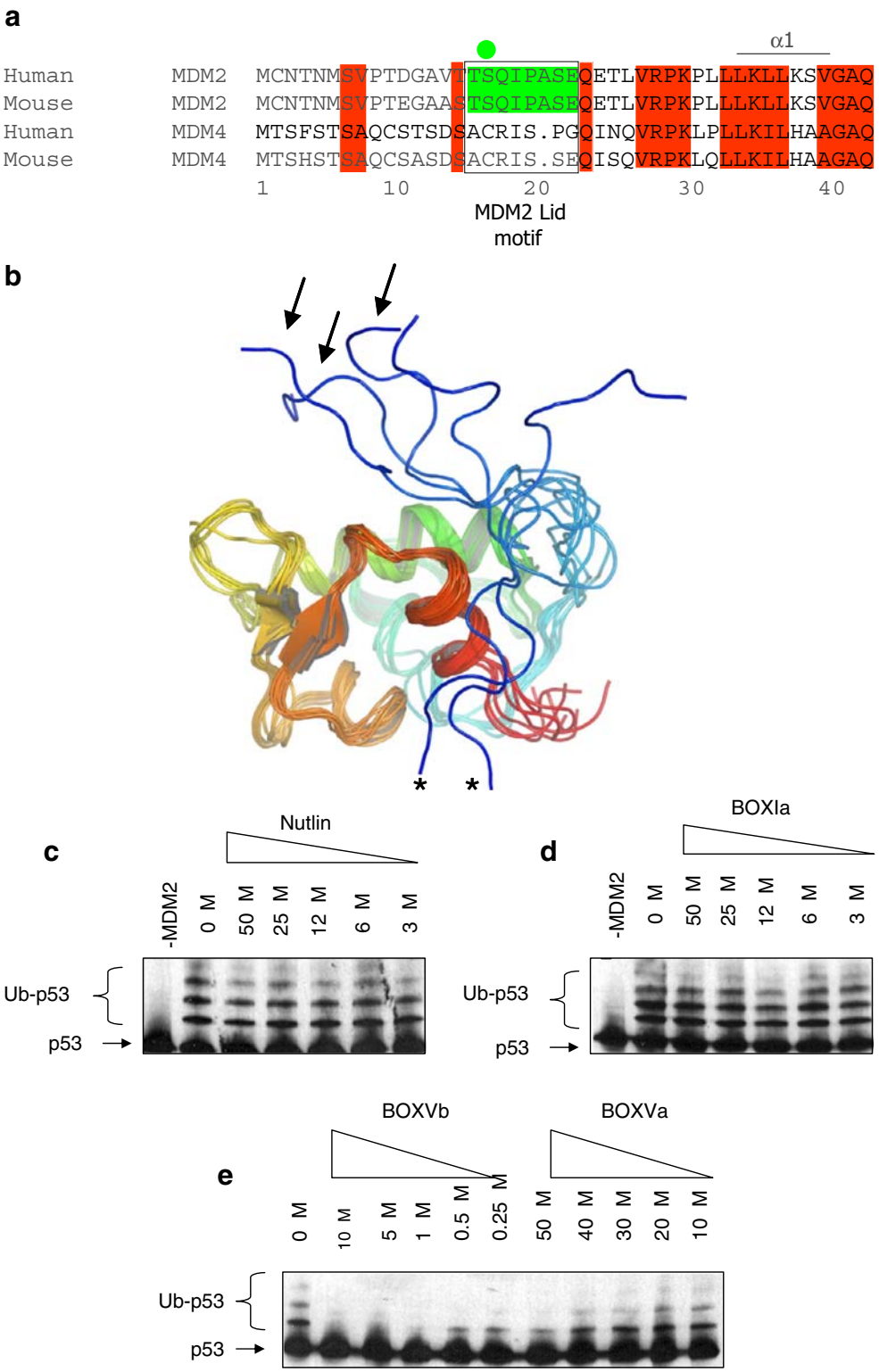

Fig. 2 The N-terminal pseudo-substrate motif of MDM2. **a** Conservation of amino acids 1–44, including the pseudo-substrate motif (aka, the lid) within MDM2 homologues and absence of the pseudo-substrate motif in the orthologue MDM4. The pseudo-substrate motif is surrounded by a *box*, and the phosphorylation site at Ser^{17} is highlighted with a *green circle*. **b** The NMR structure of the non-liganded N-terminal p53 binding domain of MDM2 (PDB ID 1Z1M, residues 10–109; *apo*-MDM2 [45]) reveals a large degree of conformational heterogeneity in the N-terminal 20 residues (colored from *blue* (N-terminal) to *red* (C-terminal)). Pseudo-substrate motif conformations acting like a lid to cover the MDM2 hydrophobic pocket are highlighted with *arrows*, and conformations with the pseudo-substrate motif interacting with the MDM2 surface are highlighted with *asterisks*. **c**–**e** The effects of small ligands on MDM2 function as an E3 ubiquitin ligase. A ubiquitination assay was assembled with purified E1, E2, MDM2, and p53 proteins without or with increasing concentrations of **c** Nutlin, **d** *BOX-I* peptide derived from the N-terminus of p53, or **e** *BOX-V* homology peptides derived from Rb (BOX-Vb) and p53 DNA binding domain (BOX-Va). Ubiquitination was assayed as indicated in the "Materials and methods". The position of the un-ubiquitinated p53 substrate is highlighted with *arrows* and p53-ubiquitin adducts with *brackets*

protein or $MDM2^{S17D}$ interactions with p53 (Fig. 4c). This elevated stability of the MDM2:p53 complex as a result of the Asp^{17} mutation in MDM2 is consistent with the enhanced E3 ubiquitin ligase activity of $MDM2^{S17D}$ (Fig. 3). However, these data are not compatible with the hypothesis that this phospho-mimetic substitution would destabilize the MDM2:p53 interactions [25].

The data presented above showing that the phospho-mimetic S17D substitution of MDM2 stabilizes the MDM2:p53 interaction could be explained by two models consistent

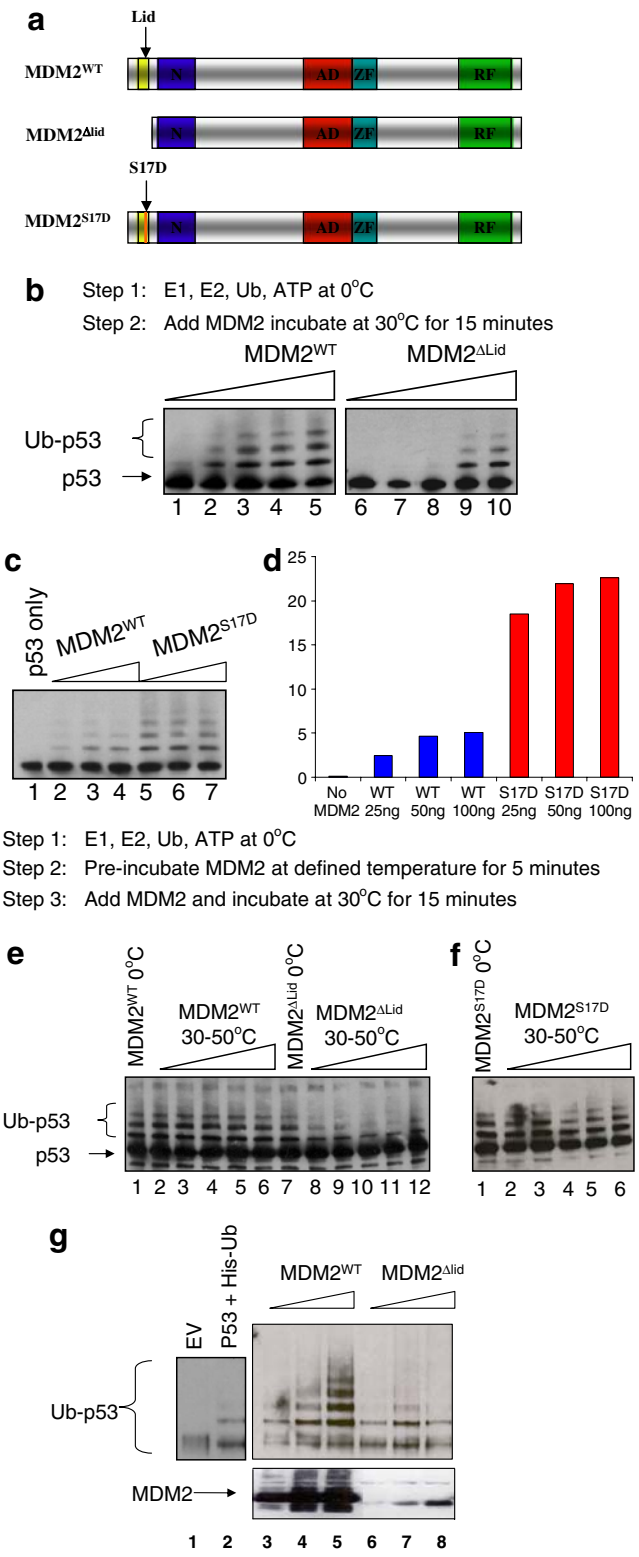

Fig. 3 A phospho-mimetic substitution in the MDM2 lid stimulates the E3 ubiquitin ligase function of MDM2. **a** Diagram of the functional domains of MDM2, including (1) wt-MDM2; (2) MDM2$^{\Delta LID}$, which has a deletion of the flexible motif; and (3) MDM2^{S17D}, which has a phospho-mimetic aspartate mutation at Ser17 (S17D). **b** MDM2-pseudo-substrate motif deletion reduces the specific activity of MDM2. Purified wt-MDM2 or MDM2$^{\Delta LID}$ was titrated directly into ubiquitination reactions using p53 as a substrate. After 10 min, the reactions were stopped and processed for immunoblotting to measure extents of p53 ubiquitination. **c** The S17D mutation in the MDM2 pseudo-substrate motif stimulates its E3 ubiquitin ligase function. Purified wt-MDM2 (*lanes 2–4*) or MDM2^{S17D} (*lanes 5–7*) were titrated directly into ubiquitination reactions using p53 as a substrate. After 10 min, the reactions were stopped and processed for immunoblotting to measure extents of p53 ubiquitination, which is quantified in **d**. **e** MDM2-pseudo-substrate motif deletion promotes thermoinstability in MDM2. Purified wt-MDM2 or MDM2$^{\Delta LID}$ was added directly to ubiquitination reactions (*lanes 1* and *7*) or was preincubated at increasing temperatures (0–50 °C) in ubiquitination buffer (*lanes 2–6* and *8–12*) followed by titration in ubiquitination reactions using p53 as a substrate. After 10 min, the reactions were stopped and processed for immunoblotting to measure extents of p53 ubiquitination. **f** S17D mutation in the MDM2 pseudo-substrate motif does not destabilize MDM2. Purified MDM2^{S17D} was preincubated at increasing temperatures (0–50 °C) in ubiquitination buffer followed by titration in ubiquitination reactions using p53 as a substrate. After 10 min, the reactions were stopped and processed for immunoblotting to measure extents of p53 ubiquitination. **g** MDM2-pseudo-substrate motif deletion promotes MDM2 instability in cells. P53 was co-transfected into cells with his-tagged ubiquitin and vector control (*lane 2*) or increasing amounts of MDM2 (*lanes 3–5*) or MDM2$^{\Delta LID}$ (*lanes 6–8*). The reactions were processed to measure p53 ubiquitination as indicated [39]

with the dual site docking model of MDM2 function [50]; (1) the phospho-mimicking pseudo-substrate motif is indeed partially occluding the hydrophobic binding pocket [25], but is acting in a positive auto-allosteric manner (i.e., like Nutlin [50]), or (2) the S17D mutation orientates the pseudo-substrate motif in a position that stabilizes the N-terminal domain of MDM2 in an open conformation with the pseudo-substrate motif in equilibrium at a position outwith the hydrophobic pocket (Fig. 2b, asterisks). The striking conformational flexibility of MDM2 when peptide ligands of differing length occupy the pocket [37] or when the lid is in distinct conformations [40] is consistent with either of these two models. We carried out further biochemical characterization of MDM2^{S17D} in order to distinguish between these two models.

One method to examine whether the Asp^{17} mutation stabilizes the pseudo-substrate motif over the hydrophobic pocket of MDM2 or whether the mutation opens the hydrophobic pocket by shifting lid equilibrium would be to determine whether MDM2^{S17D} is sensitive or resistant to Nutlin. It could be predicted that MDM2^{S17D} cannot interact with Nutlin (or the *BOX-I* domain of p53) if the Asp^{17} modified pseudo-substrate motif is stabilized over the hydrophobic pocket. However, Nutlin destabilizes the MDM2^{S17D}:p53 complex as well as the wt-MDM2:p53 complex (Fig. 5b and c). Although these data might not be compatible with the model that the Asp^{17} substituted pseudo-substrate motif is partially stabilized over the

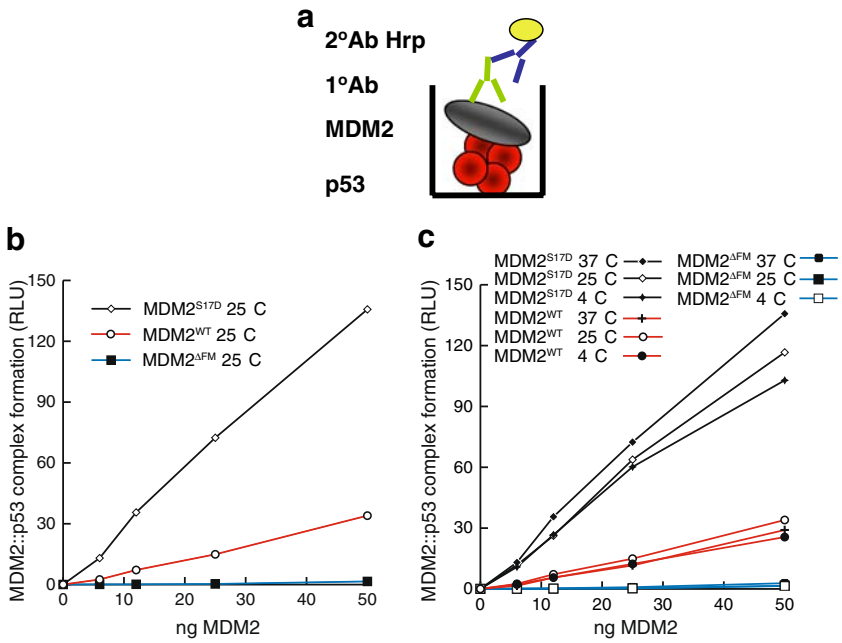

Fig. 4 A phospho-mimetic substitution in the MDM2 lid stabilizes MDM2:p53 tetramer complex formation. **a** Strategy for measuring the stability of the MDM2:p53 complex. Tetrameric forms of p53 protein were adsorbed onto the solid phase (in *red*) followed by MDM2 titration (*gray*). The stability of MDM2 bound to p53 tetramers was measured using a monoclonal antibody specific for MDM2 by chemiluminescence. **b** The S17D mutation in the MDM2 pseudo-substrate motif stabilizes the MDM2:p53 tetrameric complex. Increasing amounts of the indicated MDM2 protein (wt-MDM2, $MDM2^{\Delta LID}$, or $MDM2^{S17D}$) were titrated into reactions where fixed amounts of tetrameric p53 were on solid phase as described previously [38]. The extent of MDM2 binding was quantified using an anti-MDM2 monoclonal antibody and binding stability depicted using enhanced chemiluminescence in relative light units (*RLU*). **c** Elevated temperature does not alter the activating effect of S17D mutation on MDM2:p53 complex stability. MDM2 was preincubated at distinct temperatures, as indicated, and binding activity to the p53 tetramer was measured as described above in RLU

hydrophobic pocket of MDM2, modeling data have shown that if the phospho-mimetic lid does occlude the hydrophobic pocket, it does so only in the entry region of the N-terminal p53 peptide [40]. Thus, we evaluated whether the $MDM2^{S17D}$ has a higher or lower binding activity for the p53 peptide itself derived from the *BOX-I* domain.

As seen with the full-length p53 tetramers, $MDM2^{S17D}$ also binds more stably to the *BOX-I* peptides, relative to wt-MDM2 (Fig. 6c and d). The *BOX-I* peptide "a" is the naturally occurring peptide from p53, while *BOX-I p*eptide "b" is the optimized higher affinity peptide named 12.1 identified using combinatorial peptide libraries [4]. This enhanced binding of $MDM2^{S17D}$ to the *BOX-I* peptide from p53 again is not compatible with the model that the Asp^{17} pseudo-substrate motif is stabilized over the hydrophobic pocket, and if this were the case, then $MDM2^{S17D}$ should have a lower binding activity for the p53 *BOX-I* peptide. As a control, $MDM2^{\Delta LID}$ cannot form a stable complex with the *BOX-I* peptide (Fig. 6c and d), although $MDM2^{\Delta LID}$ can form a stable complex with the ubiquitination signal within the *BOX-V* peptide from p53 (Fig. 6f and g). These latter data indicate that the integrity of the acidic domain of MDM2 is maintained to a significant degree in $MDM2^{\Delta LID}$. Furthermore, the $MDM2^{S17D}$ is also more active in binding to the *BOX-V* peptide that wt-MDM2 (Fig. 6f and g), which together explains in part why $MDM2^{S17D}$ binds better to the p53 tetramer (Fig. 4b and c). These data also suggest that conformational changes in the N-terminal hydrophobic pocket of MDM2 as a result of the phospho-mimetic lid mutation are transferred to the acidic domain of MDM2, which is consistent with the dual-site model of MDM2-mediated ubiquitination of p53.

A single missense mutation of the RING domain of MDM2 changes the conformation of both the hydrophobic pocket and the acidic domain [52]. We evaluated further this intra/interdomain allosteric interaction in $MDM2^{S17D}$ protein by examining its binding activity for *BOX-I*- and *BOX-V*-derived p53 peptides in the absence and presence of Nutlin. A Nutlin titration into reactions containing wt-MDM2 or $MDM2^{S17D}$ indicated that Nutlin is able to compete with MDM2 binding to the *BOX-I*-derived peptide (Fig. 7b and c), as expected. However, quantitative differences are observed in this reaction. $MDM2^{S17D}$ protein is more sensitive in its binding to the *BOX-I* peptide in the

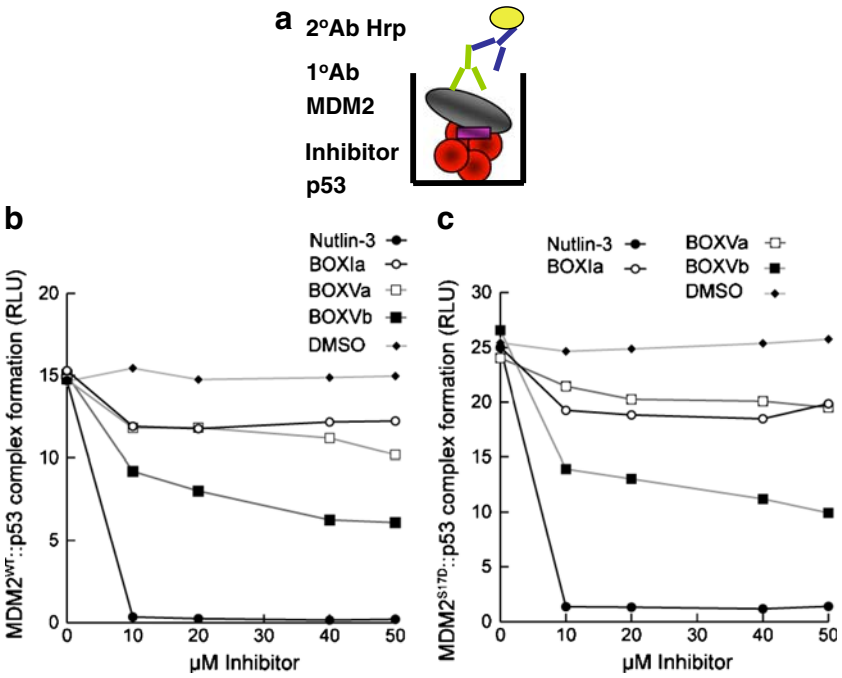

Fig. 5 Nutlin destabilizes the MDM2^{S17D}:p53 tetramer complex. **a** Strategy for measuring the stability of the MDM2:p53 complex in the presence of small ligands. Tetrameric forms of p53 protein were adsorbed onto the solid phase (in *red*) followed by MDM2 titration (*gray*) in the absence or presence of the indicated inhibitors, including (1) Nutlin-3, (2) *BOX-Ia* peptides, (3) *BOX-Va* or *BOX-Vb* peptides, and (4) DMSO carrier. The stability of MDM2 bound to p53 tetramers was measured using a monoclonal antibody specific for MDM2 by chemiluminescence. **b** and **c** MDM2^{S17D} binding to p53 is not inhibited by Nutlin. MDM2 (**b**) or MDM2^{S17D} (**c**) was assembled into reactions containing the indicated ligand: *BOX-I* peptide, *BOX-V* peptides, or Nutlin. The mixture was added to tetrameric p53 protein on the solid phase, and the amount of MDM2 bound stably to p53 was quantified using an MDM2 monoclonal antibody. The stability of the MDM2:p53 complex is depicted in relative light units

presence of Nutlin relative to wt-MDM2, consistent with the model that the phospho-mimetic mutation opens the hydrophobic pocket. Another prediction of this allosteric model would be that Nutlin would alter the binding activity of MDM2^{S17D} to the *BOX-V*-domain-derived peptides. This is observed experimentally; although the *BOX-I* peptide can partially destabilize MDM2^{S17D}:*BOX-V* peptide complexes (Fig. 7e), Nutlin completely destabilizes this interaction (Fig. 7f). The acute sensitivity of the MDM2:p53 tetrameric complex to Nutlin (Fig. 5) can therefore be explained because not only does Nutlin destabilize the MDM2:*BOX-I* peptide complex by direct competition but it can also destabilize the MDM2:*BOX-V* peptide complex by allosteric effects as suggested previously [52].

Mutation of basic residues in the hydrophobic domain is dominant over Asp17 and inactivates MDM2^{S17D}

Together, the data allow the formation of a model, whereby the Asp^{17} substitution does change the conformation of MDM2 [25], but it does so by "opening" the hydrophobic pocket. One model to explain why the phospho-mimetic mutation in the MDM2 lid stabilizes MDM2:p53 interactions is that the phospho-amino acid is stabilized by interactions with a second binding site on MDM2 (as in Fig. 2b, asterisks). NMR analysis shows that, in comparison to the peptide bound form, the N-terminal domain of *apo*-MDM2 is more unstructured and flexible, especially the regions surrounding the peptide binding cleft [45]. The unliganded structure shows a narrow, shallow binding groove as a result of the closer association of the two subdomains. As suggested previously [25], some conformers show MDM2 residues 18–24 can have helical character and partially occlude the shallow end of the p53 binding cleft (Fig. 8b). The remainder of the binding pocket, however, is not occupied by the remainder of the pseudo-substrate motif [25], and further, conformers show this region unwound and more displaced from the binding pocket (Fig. 2b, asterisks). This conformational heterogeneity of the pseudo-substrate motif eludes to a dynamic equilibrium between more structured conformations occupying part of the binding groove and less ordered states removed from binding pocket. The mutual occupancy of the p53 peptide and the pseudo-substrate domain is excluded (Fig. 8b), and

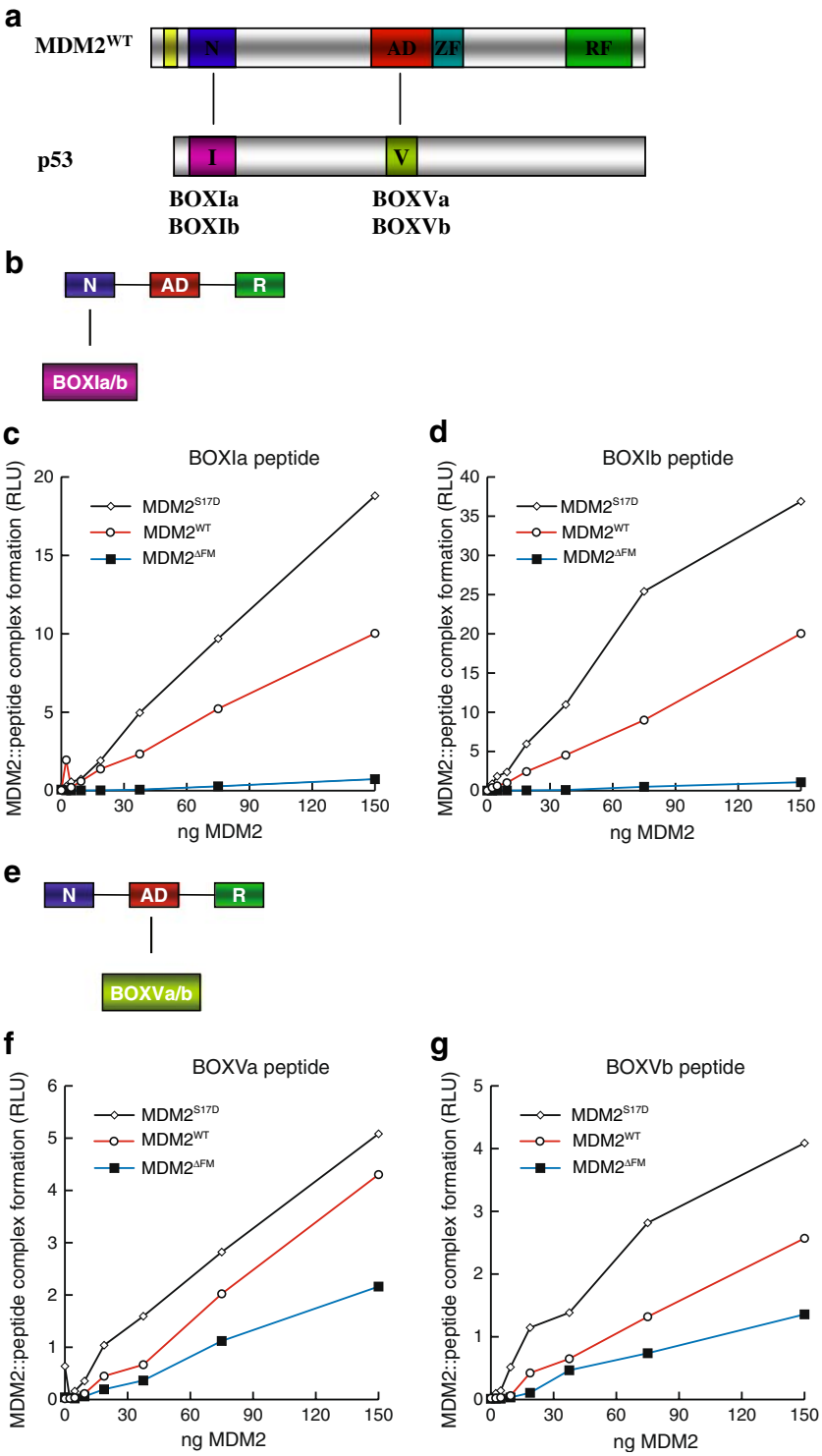

Fig. 6 Phospho-mimetic substitution in the MDM2 lid motif enhances MDM2 binding activity for *BOX-I* and *BOX-V* peptide ligands. **a** The domain structure of MDM2 minidomains, relative to p53 minidomains containing the BOX-I and BOX-V docking regions is *highlighted*. The panel highlights (*a*) an interaction between the N-terminal MDM2 domain (*N*) and the p53 *BOX-I* motif (*I*) and (*b*) an interaction between the acid domain of MDM2 (*AD*) and the *BOX-V* motif of p53 (*V*). **b** The assay was designed to measure the interaction between the N-terminal domain of full-length MDM2 and the *BOX-I*-derived p53 peptide. **c** and **d** $MDM2^{S17D}$ has an enhanced binding activity for the BOX-I domain of p53. wt-MDM2, $MDM2^{\Delta LID}$, or $MDM2^{S17D}$ proteins were titrated into reaction buffer and incubated onto the solid phase containing *BOX-I* a peptide (*left panel*) and *BOX-I* b peptide (*right panel*). The amount of MDM2 bound stably to the p53 peptides was quantified using an MDM2 monoclonal antibody. The stability of the MDM2:p53 complex is depicted in relative light units. **e** The assay was designed to measure the interaction between the central acidic domain of full-length MDM2 and the *BOX-V*-derived peptides. **f** and **g** $MDM2^{S17D}$ has an enhanced binding activity for the BOX-V domain of p53. wt-MDM2, $MDM2^{\Delta LID}$, or $MDM2^{S17D}$ proteins were titrated into reaction buffer and incubated onto the solid phase containing *BOX-V* a peptide (*left panel*) and *BOX-V* b peptide (*right panel*). The amount of MDM2 bound stably to the p53 peptides was quantified using an MDM2 monoclonal antibody. The stability of the MDM2:p53 complex is depicted in relative light units

p53 would preferentially bind to the N-terminal domain of MDM2 when the D17-pseudo-substrate domain was displaced from the binding site (Fig. 8c and d).

The increased ligand binding activity of $MDM2^{S17D}$ could thus be explained by the mutation causing a shift in equilibrium toward a more open conformation primed for peptide binding. In fact, the phospho-pseudo-substrate motif peptide of $MDM2^{S17D}$ has a higher binding activity for MDM2 compared to wild-type peptide [25], and the phospho-mimetic mutation may preferentially bind to a cationic region on the MDM2 surface. Inspection of the MDM2 *apo*-structure NMR ensemble reveals that the

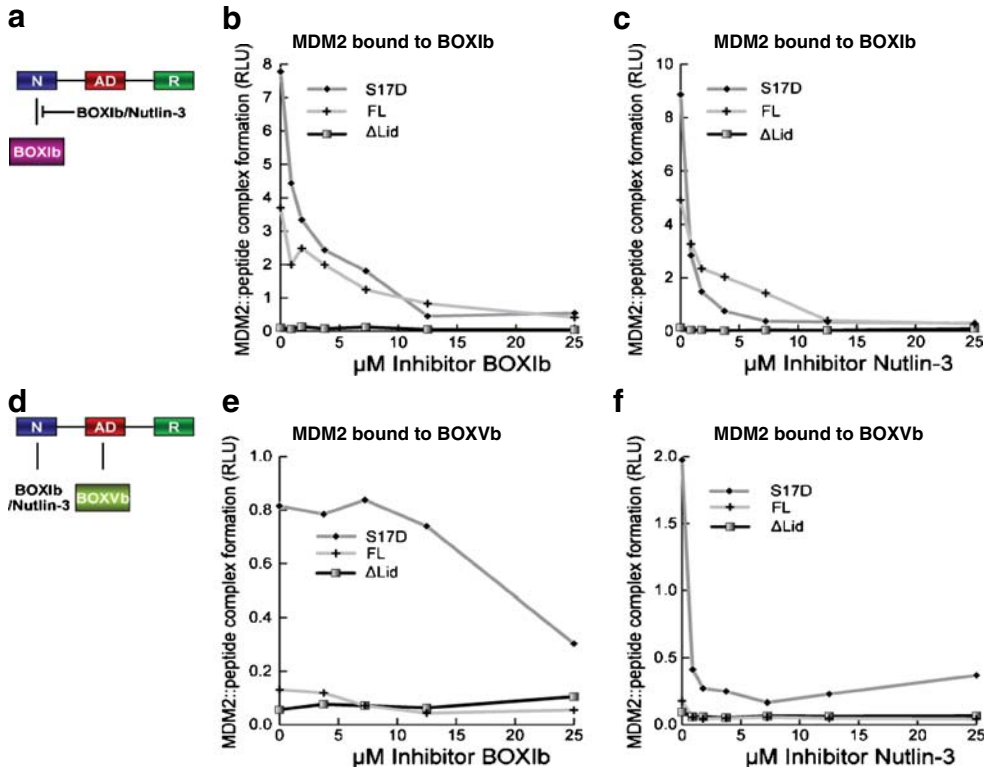

Fig. 7 Nutlin destabilizes the MDM2:p53 *BOX-I* and *BOX-V* peptide complex. **a** Strategy for measuring the stability of the MDM2:p53 BOX-I peptide complex in the presence of small ligands. The biotinylated BOX-Ib peptide was adsorbed onto the streptavidin-coated solid phase followed by wt-MDM2, $MDM2^{\Delta LID}$, or $MDM2^{S17D}$ proteins titration in the absence or presence of the indicated inhibitors, including **b** the *BOX-Ib* peptide and **c** Nutlin-3. The stability of MDM2 bound to the *BOX-I* peptide was measured using a monoclonal antibody specific for MDM2 by chemiluminescence and is depicted in relative light units. **d** Strategy for measuring the stability of the MDM2:p53 BOX-V peptide complex in the presence of small ligands. The biotinylated BOX-Vb peptide was adsorbed onto the streptavidin-coated solid phase followed by wt-MDM2, $MDM2^{\Delta LID}$, or $MDM2^{S17D}$ proteins titration in the absence or presence of the indicated inhibitors, including **e** the *BOX-Ib* peptide and **f** Nutlin-3. The stability of MDM2 bound to the *BOX-V* peptide was measured using a monoclonal antibody specific for MDM2 by chemiluminescence and is depicted in relative light units

conformationally heterogeneous pseudo-substrate motif can be in proximity to a positively charged region at the N-terminal part of helix α2′ composed of His^{96}, Arg^{97}, and Lys^{98}, which could complex acidic residues (Fig. 8c and d). Binding of Asp^{17} to this positively charged region may help stabilize the pseudo-substrate motif away from the binding groove and shift the equilibrium toward a conformation favorable for peptide binding by MDM2.

In regard to this equilibrium model, it is interesting to note that the His^{96}, Arg^{97}, and Lys^{98} equivalent residues of MDM4 are altered, thus removing a potentially cationic interface (Fig. 9a). This might give clues to residues that have co-evolved with the MDM2 pseudo-substrate motif, which is also absent in MDM4. To disrupt this positively charged patch (Fig. 9a), we created an MDM2 mutant which contains the $Arg^{97}Lys^{98}$ mutated to the MDM4 equivalent of $Ser^{97}Pro^{98}$ (Fig. 8a). MDM4 has been shown to have a conserved structure with MDM2 and bind p53 peptides in the same manner and with comparable affinities [34]. A titration of the wt-MDM2 and $MDM2^{R97S:K98P}$ demonstrated that the basic substitutions maintain an equivalent ability of MDM2 to bind to tetrameric p53 (Fig. 8e), reduced interactions with the p53 *BOX-I* peptide (Fig. 8f), and maintain equivalent binding activity of MDM2 for the p53 *BOX-V* peptide (Fig. 8g). These data indicate that the $Ser^{97}Pro^{98}$ substitutions do not disrupt fundamentally the core folding of the hydrophobic domain, not the allosteric interactions with the acidic domain of MDM2.

By contrast, the enhanced binding of $MDM2^{S17D}$ to the p53 tetramer is completely eliminated in the $MDM2^{S17D:R97S:K98P}$ triple mutant (Fig. 9c). Further, the $MDM2^{S17D:R97S:K98P}$ triple mutant is unable to form a stable complex with the p53 *BOX-I* peptide (Fig. 9d), but can still bind to the *BOX-V* peptide (Fig. 9e). Thus, the R97S:K98P double mutations can convert $MDM2^{S17D}$ protein from an activated to an inhibited form, under conditions where the MDM2 R97S:K98P double mutant remains active. This inactivated triple mutant is consistent with the model that mutation of the basic patch stabilizes the phospho-mimetic lid over the hydrophobic pocket, which is not compatible with p53 binding (Fig. 9b).

Discussion

MDM2 is a multidomain E3 RING-finger ubiquitin ligase and represents a model protein with which to define mechanisms of substrate ubiquitination. The recent dual-site model for MDM2-mediated ubiquitination of p53 suggested an allosteric component to the E3 ubiquitin ligase function, which invokes MDM2 docking to two distinct sites on p53: the *BOX-I* transactivation domain and a conformationally flexible motif in the *BOX-V* domain of p53. The allostery in the N-terminal domain that operates toward the acidic domain [50] can be propagated presumably via the striking conformational flexibility of the N-terminal domain of MDM2 as defined by NMR [25, 37, 45]. The unexpected feature of the dual site model was that the N-terminal hydrophobic pocket of MDM2 can act as an allosteric ligand binding site and that ligands like Nutlin can prime MDM2 and "activate" the E3 ubiquitin ligase function of MDM2 [50]. The allosteric interactions have been further linked to the RING domain, as certain mutation in the RING can induce conformational changes in both the hydrophobic pocket and the central acidic domain [52].

A novel model can be developed that incorporates the various biochemical and biophysical studies of the flexible N-terminal domain of MDM2 and which supports an equilibrium model for pseudo-substrate motif function. As originally suggested [25] and later confirmed in the NMR structure of *apo*-MDM2 [40, 45], the N-terminal segment of MDM2 can partially occlude the shallow end of the p53-binding cleft (Fig. 8b); however, this motif is not well structured, and the remainder of the binding pocket remains empty, at least in the non-phosphorylated state. In this conformation, Ile^{19} occupies much of the space taken up by Pro^{27} of the p53 peptide chain [20] and as such excludes the mutual occupancy of the pseudo-substrate motif and p53. Interestingly, Ile^{19} is the only residue in the N-terminal region that exhibits any significant interaction with the rest of *apo*-MDM2 [45], forming hydrophobic contacts with His^{96}, Arg^{97}, and Tyr^{100} in the N-terminal part of $\alpha 2'$. In some NMR conformers, Ile^{19} is displaced from the site occupied by Pro^{27}, forming a more intimate association with the N-terminal region of helix $\alpha 2'$. Based on this, we have proposed that the pseudo-substrate motif exists in dynamic equilibrium between states that are incompatible with or compatible with p53 peptide binding; p53 can only bind when the pseudo-substrate motif has dissociated from the hydrophobic binding site. In favor of this equilibrium, both NMR studies indicated several residues within the pseudo-substrate domain and the region surrounding helix $\alpha 2'$ that behaved as though in slow conformational exchange [25, 45]. Furthermore, it is interesting to note that the shorter p53 peptide, lacking residues 27–29, which share an overlapping binding site with the pseudo-substrate motif, binds to MDM2 with a ten-fold higher affinity [37].

Thus, in order for p53 to bind to MDM2, the following events need to occur possibly in a concerted fashion; residues 19–25 forming the pseudo-substrate motif must dissociate from one end of the groove and be replaced by segments 27–29 of the incoming p53; the two MDM2 subdomains swing apart from one another by 3–4 Å; during the process of binding, strand $\beta 3'$ is formed, completing the terminal ($\beta 1$, $\beta 2$, $\beta 3'$) sheet that caps one end of the groove and helps to hold the two subdomains in their new more rigid conformation. However, deletion of the flexible lid destabilizes the N-terminal domain of MDM2 (this study), so this motif also has a positive role to play in the MDM2-p53 interaction. In addition to these ordered and sequential changes in MDM2-substrate binding, our current study suggests an activating model for the function of the flexible pseudo-substrate motif upon phosphorylation, which enhances displacement of the pseudo-substrate domain by altering its equilibrium, thus opening the groove to stabilize p53-peptide binding to MDM2 (Fig. 10). This conformational change upon hydrophobic pocket occupation by its ligand then appears to be propagated to the central acidic domain of MDM2 that results in enhanced MDM2 interactions with p53 (Fig. 10).

MDM2 regulation in *cis* by a pseudo-substrate peptide motif highlights the growing realization that many signal transduction events are modulated by relatively small and unstructured polypeptide motifs [27–29]. Although there are many well-defined globular protein domains that form folded independent compact structures, these globular domains represent only a fraction of the cellular polypeptide sequence repertoire. The remaining peptide sequences are intrinsically disordered and comprise linear motifs with weaker binding kinetics. Thus, signal transduction among many components interacting via linear peptide motifs with weaker binding kinetics can provide specific and sensitive regulation of cellular signal transduction processes. The regulation of MDM2 by such a flexible motif highlights how these motifs can impact signal transduction. Further perturbations in these linear interaction motifs, for example by covalent modifications like phosphorylation, have the potential to drive signaling changes that mediate changes in the protein–protein interaction dynamics central to signal transduction. The ability of MDM2 to be modulated by a flexible peptide motif opens the door to identify the physiological signals that regulate this conformational switch in MDM2 as well as potentially novel pathways that respond to such an activated MDM2 conformation. For example, if the MDM2-lid kinase were to be identified, it is possible that this would promote p53 protein ubiquitination and degradation in cells, and this lid-kinase pathway would therefore function as a pro-oncogenic signal in cancers. By contrast, protein phosphatases that antagonize this kinase would be predicted to function as co-tumor suppressor of

p53 function by attenuating MDM2-mediated ubiquitination of p53.

Conclusions: perspectives on potential drug leads in the MDM2 pathway based on protein–protein interactions in the ubiquitination system

The molecular and structural mechanisms of MDM3 E3-RING domain-E2-mediated ubiquitination of p53 are only beginning to be defined. Complex and dynamic protein–protein interactions can be anticipated a priori. These include firstly the allosteric intradomain interactions in MDM2 itself, for example, highlighted by the fact that the RING domain plays a role in regulating the conformation of the N-terminal hydrophobic domain and the acidic domain [52]. It is striking that specific mutations in the RING domain appear to open the conformation of the acidic domain of MDM2 based on elevated intrinsic tryptophan fluorescence. This suggests that ligands that bind to the RING domain (like RNA, ATP, and E2 ubiquitin–conjugating protein) would regulate the interconversion between open and closed conformations of MDM2 within the acidic domain. This might in turn modify the type of small molecules acquired in screens for ligands that bind to the acidic domain of MDM2 and inhibit p53 ubiquitination, i.e., reconstitution of the complete E2–E3–p53 tetramer ubiquitination reaction using highly purified proteins and with specific RING-domain co-factors will likely affect the dynamics of the acidic domain conformation. The ability of the phospho-mimetic MDM2 lid to stabilize the MDM2:*BOX-V* peptide interaction (Fig. 10) further puts focus on the acidic domain as a key site for developing small ligands that disrupt MDM2 ubiquitination of p53.

The second protein–protein interaction to consider is the undefined effect of E3-RING domain on the E2-mediated enzymatic transfer of ubiquitin to the p53 substrate. Small molecule first generation leads have already been identified that disrupt substrate ubiquitination possibly by effecting E2 activity as well as E3 functions [54]. We do not know how E2 protein conformation is altered by E3-RING domain binding and in turn how ligand binding at the RING domain of MDM2 would alter the catalytic function of the E2 proteins. The definition of E2–E3 interfaces using purified minidomains and then using the reconstituted ubiquitination system would likely shed light on novel allosteric stages in this multicomponent ubiquitination reaction. The third protein–protein dynamic is the fact that the p53 protein is tetrameric, and although it has at least two main binding sites for MDM2, it is not clear how quaternary structure of p53 contributes to the valency of the MDM2:p53 interaction and in turn what changes occur in p53 tetramers that allow E2-dependent ubiquitination transfer to p53.

Fig. 8 A model of lid function through stabilization of the phospho-mimetic motif on the surface of MDM2. **a** Multiple sequence alignment of MDM2 and MDM4 highlighting the evolutionary divergence between MDM2 and MDM4 at the potential pseudo-substrate motif basic docking site for acidic residues (i.e., Asp, phosphate) at amino acid residues 97–98. **b** The C-terminal region of the pseudo-substrate domain (residues 18–24; colored *yellow*) can have helical character and occupy the shallow end of the hydrophobic binding pocket as reported previously [25]. The p53 peptide from PDB structure 1YCR [20] is shown for comparison (colored *orange*). The N-terminal p53 peptide sequence and the lid cannot occupy the hydrophobic pocket simultaneously. **c** The pseudo-substrate motif can also exist displaced from the binding pocket with Ser^{17} (S17D mutation shown for illustration) in proximity to a basic region (see **d**) at the N-terminal of helix $\alpha2'$ composed of Arg^{97}/Lys^{98}. Based on this, it is postulated that the S17D (mimicking phosphorylation of Ser^{17}) mutation could stabilize the N-terminal domain of MDM2 in a conformation primed for p53 binding by forming electrostatic interactions with residues Arg^{97}/Lys^{98}. **e**–**g** Effects of Arg^{97}/Lys^{98} mutation on wild-type MDM2 activity. **e** MDM2 codon 97–98 residue mutation to the MDM4 equivalent does not destabilize the MDM2:p53 tetramer complex. Increasing amounts of the indicated MDM2 protein (wt-MDM2 or $MDM2^{R97S:K98P}$) were titrated into reactions where fixed amounts of tetrameric p53 were on solid phase as described previously above. The extent of MDM2 binding was quantified using an anti-MDM2 monoclonal antibody and binding stability depicted using enhanced chemiluminescence in relative light units (*RLU*). **f** The effects of MDM2 codon 97–98 residue mutation to the MDM4 equivalent on MDM2:BOX-I peptide complex stability. Increasing amounts of MDM2 protein (wt-MDM2 or the double mutant $MDM2^{R97S:K98P}$) were titrated into reactions with fixed amounts of the BOX-I peptide on solid phase, as described previously above. The extent of MDM2 binding was quantified using an anti-MDM2 monoclonal antibody and binding stability depicted using enhanced chemiluminescence in relative light units (*RLU*). **g** The effects of MDM2 codon 97–98 residue mutation to the MDM4 equivalent on MDM2:BOX-V peptide complex stability. Increasing amounts of MDM2 protein (wt-MDM2 or the double mutant $MDM2^{R97S:K98P}$) were titrated into reactions with fixed amounts of the *BOX-V* peptide on solid phase, as described previously above. The extent of MDM2 binding was quantified using an anti-MDM2 monoclonal antibody and binding stability depicted using enhanced chemiluminescence in relative light units (*RLU*)

Although the N-terminal hydrophobic pocket of MDM2 is a drug binding site, drug occupation at this site does not inhibit p53 ubiquitination due to the allosteric nature of the E3 ubiquitin ligase function of MDM2. However, the three scenarios reviewed above provide biochemical approaches with which to develop peptide-mimetic leads for disrupting protein–protein interactions in the p53 substrate–E3–E2 enzymatic ubiquitination system. Additionally, if phosphorylation in vivo of the MDM2 lid will be proven to stabilize the interaction between the acidic domain of MDM2 and the *BOX-V* peptide in the p53 DNA-binding domain, this would drive p53 protein ubiquitination and degradation in cells. The lid-kinase pathway itself would in turn provide a novel approach for developing drug leads that attenuate MDM2-mediated ubiquitination and degradation of p53 protein.

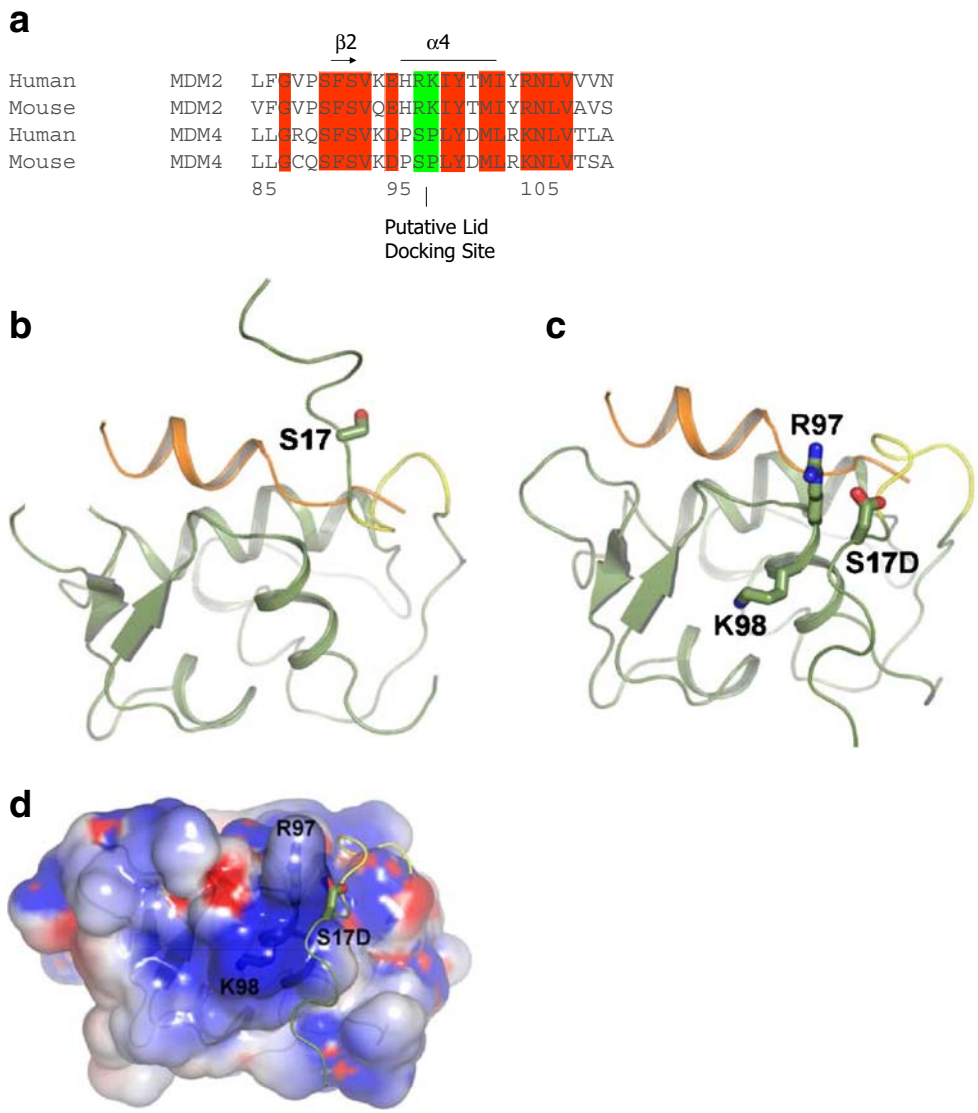

Materials and methods

Plasmids and site-directed mutagenesis

MDM2^{WT} and MDM2$^{\Delta Lid}$ were cloned into the *Invitrogen* Gateway system entry vector pDONR221 (Invitrogen) using the following primers: full-length MDM2 Fwd 5′-GGGGACAAGTTTGTACAAAAAAGCAGGCTTCGAAGGAGATAGAACCAT GTGCAATACCAACATGTCTGTACCTACT-3′ and Rev 5′-GGGGACCACTTTGTACAAGAAAGCTGGGTCCTAGGGGAAATAAGTTAGCACAATCAT-3′: lid deletion MDM2 Fwd 5′- GGGGACAAGTTTGTACAAAAAAGCAGGCTTCGAAGGAGATAGAACCATGACCCTGGTTAGACCAAAGCCATTGCTT-3′ and Rev—same as full length MDM2. This vector was used as a template to perform site-directed mutagenesis using the in vitro mutagenesis system QuikChange (Stratagene) as directed by the manufacturer. MDM2 serine 17 was mutated to an aspartic acid using the following primers (bases which introduce amino acid change are in bold): amino acid 17 S>D Fwd 5′-GGTGCTGTAACCACC**GAC**CAGATTCCAGCTTCG-3′ and Rev 5′CGAAGCTGGA ATCTG**GTC**GGTGGTTA-CAGCACC-3′. For native expression of protein in *Escherichia coli*, pDONR221-MDM2 vectors were recombined with the pDEST14 vector (Invitrogen) as recommended by the manufacturer. For expression in mammalian cells, the pDONR-MDM2 vectors were recombined with the pDEST3.2 vector (Invitrogen). pDONR221-MDM2 was used as a template to PCR clone MDM2$^{\Delta Lid}$ into pCDNA3.1 with

Fig. 8 (continued)

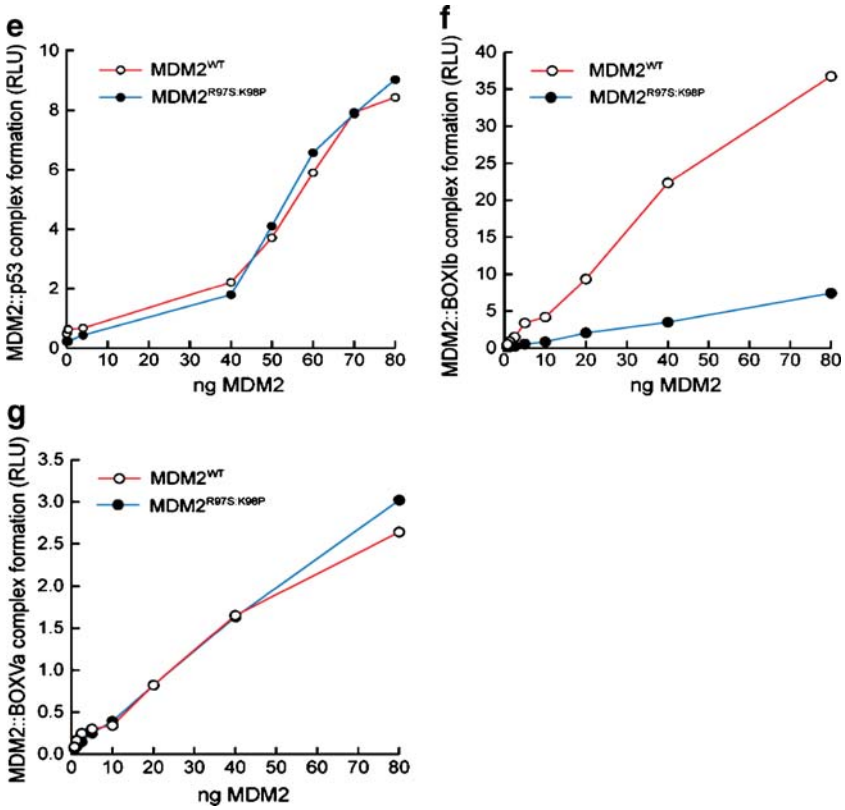

*Eco*R1 and *Xho*1 restriction sites. *Eco*R1 Fwd primer 5′-GCCTCGAATTCATGACCCTGGTTAGAC CAAAGC-CATTGCTT-3′ and *Xho*1 Rev 5′- GCCTCGA GCTCCTAGGGGAAATAAGTTAGCACAATCAT-3′. pCDNA3.1 full length MDM2 was subjected to site-directed mutagenesis as described before to introduce mutation at serine 17 (S>D).

Protein expression and purification

pDEST14-MDM2 constructs were overexpressed in BL-21 arabinose-inducible *E. coli* for 3 h at room temperature. Cells were harvested by centrifugation at 6,000×*g* for 10 min and frozen in liquid nitrogen. Bacterial pellet was lysed in 10% sucrose, 50 mM Tris–HCl (pH8), 150 mM NaCl, and 150 μg/ml lysozyme and left on ice for 45 min before sonication. After sonication, 2 mM Pefabloc, 5 mM DTT, and 1 mM benzamidine was added to lysate before centrifugation at 30,000×*g* for 20 min. Lysate was loaded onto a fast flow SP column (GE Healthcare) equilibrated with buffer A (25 mM Hepes, pH7.5, 10% glycerol, 1 mM benzamidine, 5 mM DTT, 50 mM KCl, and 2 mM Pefabloc). Bound protein was eluted with increasing salt concentration using buffer B (same as buffer A but 1M KCl) and MDM2 function measured in E3 ubiquitin ligase assays.

MDM2-peptide and p53 protein binding activity assays

Recombinant human MDM2 protein, ubiquitination assays, and p53 protein binding assays were developed as described previously [38, 50]. For p53-peptide binding assays, the plate was adsorbed with streptavidin overnight and washed six times with PBS-T, and biotinylated peptides were added for 1 h followed by titrating increasing amounts of MDM2 (from 3 to 200 ng). Following further washes for six times with PBS-T, wells were incubated with secondary rabbit anti-mouse horseradish peroxidase antibodies followed by further washing and ECL. The results were quantified using Fluoroskan Ascent FL equipment (Labsystems) and analyzed with Ascent Software version 2.4.1 (Labsystems). Peptides BOXIa, BOXIb, BOXVa, and BOXVb were from Chiron Mimetopes and Nutlin3a from Alexis Biochemicals. Peptide sequences are as follows: BOXIa - Biotin-SGSGPPLSQETFSDLWKLLP; BOXIb-Biotin-SGSGMPRFMDYWEGLN; BOXVa-Biotin-SGS GRNSFEVRVCACPGRD; BOXVb-Biotin-SGSGDQIM MCSMYGICKVKNIDLK.

In vitro ubiquitination assay

Reactions contained 25 mM HEPES (pH8.0), 10 mM $MgCl_2$, 4 mM ATP, 0.5 mM DTT, 0.05% (*v*/*v*) Triton X-

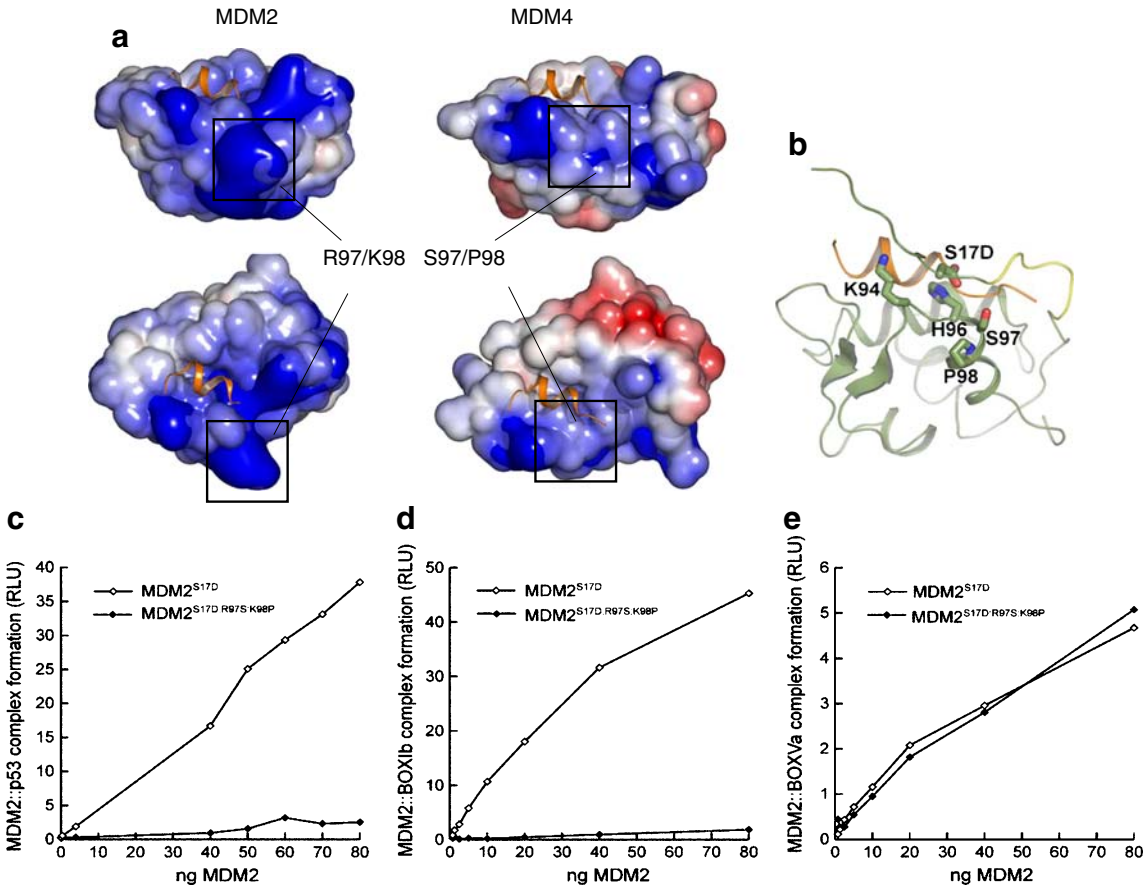

Fig. 9 Inactivation of MDM2^{S17D} by mutation of surface basic residues of MDM2. **a** Electrostatic potential mapped onto the solvent accessible surface. Positive- and negative-charged regions colored *blue* and *red*, respectively. Alignment figure generated with ESPript [14]. Structural figures generated with PyMol (www.pymol.org). The electrostatic calculations were performed with APBS [3] and highlighted is (*left*) wild-type MDM2 and (*right*) MDM2 with R97/K98 residues substituted with the S97/P98 MDM4 residues. **b** When the basic patch on MDM2 is mutated to Ser97/Pro98, the phospho-mimetic pseudo-substrate motif may bind other basic regions of the MDM2 surface such as Lys^{94}/His^{96}, which line the hydrophobic binding pocket and explain why the MDM2 triple mutant (MDM2$^{S17D:R97S:K98P}$) binds p53 with a substantially lower activity than does the MDM2 double mutant (MDM2$^{R97S:K98P}$; see **c**–**e**). **c** MDM2 codon 97–98 residue mutation to the MDM4 equivalent inactivates MDM2^{S17D} as a p53 binding protein. Increasing amounts of the indicated MDM2 protein (MDM2^{S17D} or the triple mutant MDM2$^{S17D:R97S:K98P}$) were titrated into reactions where fixed amounts of tetrameric p53 were on solid phase as described previously above. The extent of MDM2 binding was quantified using an anti-MDM2 monoclonal antibody and binding stability depicted using enhanced chemiluminescence in relative light units (*RLU*). **d** The effects of MDM2 codon 97–98 residue mutation to the MDM4 equivalent on MDM2^{S17D}:BOX-I peptide complex stability. Increasing amounts of MDM2 protein (MDM2^{S17D} or the triple mutant MDM2$^{S17D:R97S:K98P}$) were titrated into reactions with fixed amounts of the *BOX-I* peptide on solid phase, as described previously above. The extent of MDM2 binding was quantified using an anti-MDM2 monoclonal antibody and binding stability depicted using enhanced chemiluminescence in relative light units (*RLU*). **e** The effects of MDM2 codon 97–98 residue mutation to the MDM4 equivalent on MDM2^{S17D}:BOX-V peptide complex stability. Increasing amounts of MDM2 protein (MDM2^{S17D} or the triple mutant MDM2$^{S17D:R97S:K98P}$) were titrated into reactions with fixed amounts of the *BOX-V* peptide on solid phase, as described previously above. The extent of MDM2 binding was quantified using an anti-MDM2 monoclonal antibody and binding stability depicted using enhanced chemiluminescence in relative light units (*RLU*)

100, 0.25 mM benzamidine, 10 mM creatine phosphate, 3.5 units/ml creatine kinase, ubiquitin (2 μg), E1 (100 nM), E2 (1 μM), and p53 (0.5 μg). Reactions were assembled on ice by adding, last, purified MDM2, MDM2$^{\Delta lid}$, or MDM2^{S17D} at various concentrations (3–200 ng), followed by incubations for 15 min at 30 °C, and analyzed with 4–12% NuPAGE gels in a MOPS buffer system (Invitrogen) followed by immunoblot. For temperature gradient, MDM2 was subjected to heat treatment for 5 min prior to addition to ubiquitination reaction.

Cell culture and purification of his-ubiquitin conjugates

H1299 cells were grown at 37 °C in RPMI with 10% FBS and 5% CO_2. p53$^{-/-}$MDM2$^{-/-}$ mouse embryonic fibroblasts were grown in DMEM with 10% (*v*/*v*) FBS and 10% CO_2.

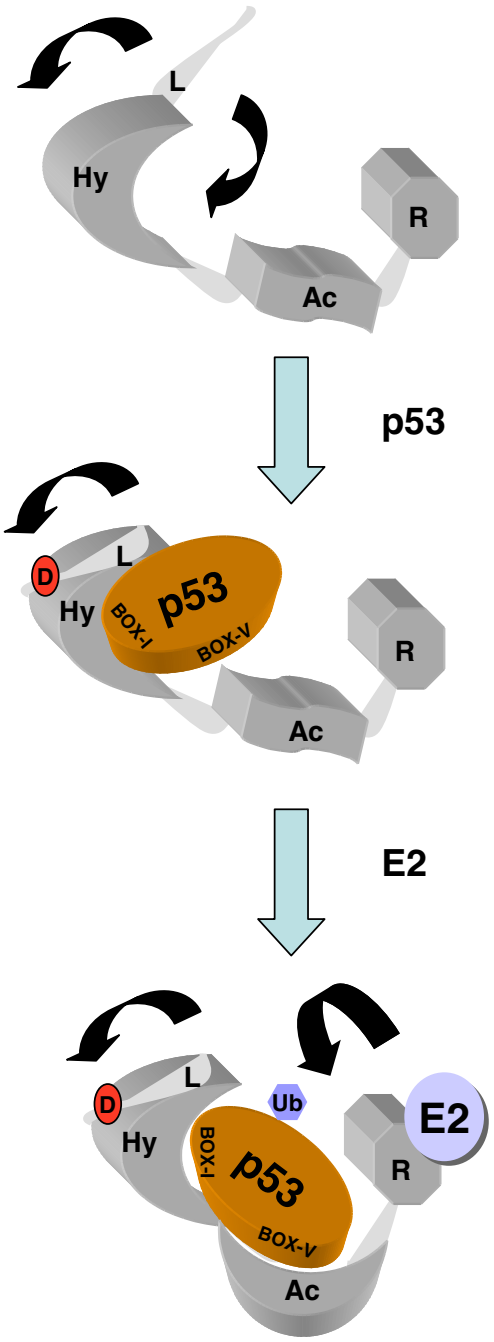

◀ **Fig. 10** Effects of the MDM2 lid on allosteric regulation of its E3 ubiquitin ligase function. (*a*) MDM2 is composed of three key functional domains, including the hydrophobic pocket in the N-terminus (*Hy*), the acidic domain in the central portion of MDM2 (*Ac*), and the C-terminal RING domain (*R*). The N-terminus also has a flexible and unstructured pseudo-substrate motif (*L*), which is in equilibrium over the hydrophobic pocket (like a lid) or outwith the pocket (*arrows*). (*b*) Upon generation of the phospho-mimetic mutation in the pseudo-substrate motif, the flexible lid chain is stabilized in an equilibrium outwith the hydrophobic pocket, allowing enhanced binding to p53 at the *BOX-I* motif. (*c*) A conformational change ensues, which stabilizes the interaction between the Ac domain of MDM2 and the *BOX-V* motif in the DNA-binding domain of p53. This allows the E2-mediated ubiquitin transfer to the p53 substrate. The mechanisms whereby the E3:E2 interaction drives p53 substrate recognition and ubiquitin transfer is not defined nor is it known whether interactions between MDM2 and p53 occur intra or intermolecularly within the p53 tetramer. The model does not incorporate the p53 tetrameric structure since it is not known if MDM2 docking to p53 tetramers is an intra- or intermolecular mechanism

Transient transfections were carried out as described [10]. Cells were lysed in NP40 buffer (25 mM HEPES, pH7.5, 0.1% NP40, 150 mM KCl, 5 mM DTT, and 50 mM NaF) and analyzed by 4–12% NuPAGE/immunoblot. His-ubiquitin conjugates were purified as previously described [53].

Acknowledgments This work was supported by Programme Grants to KLB (C377/A6355) and TRH (C483/A6354) from the Cancer Research UK. EW is funded by a Cancer Research UK PhD studentship (C483/A5547).

References

1. Adams J, Chen ZP, Van Denderen BJ, Morton CJ, Parker MW, Witters LA, Stapleton D, Kemp BE (2004) Protein Sci 13:155
2. Arva NC, Gopen TR, Talbot KE, Campbell LE, Chicas A, White DE, Bond GL, Levine AJ, Bargonetti J (2005) J Biol Chem 280:26776
3. Baker NA, Sept D, Joseph S, Holst MJ, McCammon JA (2001) Proc Natl Acad Sci U S A 98:10037
4. Bottger V, Bottger A, Howard SF, Picksley SM, Chene P, Garcia-Echeverria C, Hochkeppel HK, Lane DP (1996) Oncogene 13:2141
5. Burch LR, Midgley CA, Currie RA, Lane DP, Hupp TR (2000) FEBS Lett 472:93
6. Burch L, Shimizu H, Smith A, Patterson C, Hupp TR (2004) J Mol Biol 337:129
7. Candeias MM, Malbert-Colas L, Powell DJ, Daskalogianni C, Maslon MM, Naski N, Bourougaa K, Calvo F, Fahraeus R (2008) Nat Cell Biol 10:1098
8. Chen J, Marechal V, Levine AJ (1993) Mol Cell Biol 13:4107
9. Craig AL, Chrystal JA, Fraser JA, Sphyris N, Lin Y, Harrison BJ, Scott MT, Dornreiter I, Hupp TR (2007) Mol Cell Biol 27:3542
10. Dornan D, Hupp TR (2001) EMBO Rep 2:139
11. Dyson HJ, Wright PE (2002) Curr Opin Struct Biol 12:54
12. Elenbaas B, Dobbelstein M, Roth J, Shenk T, Levine AJ (1996) Mol Med 2:439
13. Gannon JV, Greaves R, Iggo R, Lane DP (1990) EMBO J 9:1595
14. Gouet P, Courcelle E, Stuart DI, Metoz F (1999) Bioinformatics 15:305
15. Haupt Y, Maya R, Kazaz A, Oren M (1997) Nature 387:296
16. Kobe B, Kemp BE (1999) Nature 402:373
17. Kobe B, Heierhorst J, Kemp BE (1997) Adv Second Messenger Phosphoprotein Res 31:29

18. Kostic M, Matt T, Martinez-Yamout MA, Dyson HJ, Wright PE (2006) J Mol Biol 363:433
19. Kubbutat MH, Jones SN, Vousden KH (1997) Nature 387:299
20. Kussie PH, Gorina S, Marechal V, Elenbaas B, Moreau J, Levine AJ, Pavletich NP (1996) Science 274:948
21. Lai Z, Freedman DA, Levine AJ, McLendon GL (1998) Biochemistry 37:17005
22. Linke K, Mace PD, Smith CA, Vaux DL, Silke J, Day CL (2008) Cell Death Differ 15:841
23. Maclaine NJ, Oster B, Bundgaard B, Fraser JA, Buckner C, Lazo PA, Meek DW, Hollsberg P, Hupp TR (2008) J Biol Chem 283:28563
24. Marechal V, Elenbaas B, Piette J, Nicolas JC, Levine AJ (1994) Mol Cell Biol 14:7414
25. McCoy MA, Gesell JJ, Senior MM, Wyss DF (2003) Proc Natl Acad Sci U S A 100:1645
26. Momand J, Zambetti GP, Olson DC, George D, Levine AJ (1992) Cell 69:1237
27. Neduva V, Russell RB (2005) FEBS Lett 579:3342
28. Neduva V, Russell RB (2006) Nucleic Acids Res 34:W350
29. Neduva V, Russell RB (2006) Curr Opin Biotechnol 17:465
30. Nenutil R, Smardova J, Pavlova S, Hanzelkova Z, Muller P, Fabian P, Hrstka R, Janotova P, Radina M, Lane D, Coates P, Vojtesek B (2005) J Pathol 207:251
31. Ofir-Rosenfeld Y, Boggs K, Michael D, Kastan MB, Oren M (2008) Mol Cell 32:180
32. Passmore LA, Barford D (2004) Biochem J 379:513–525
33. Pettersson S, Kelleher M, Pion E, Wallace M, Ball KL (2009) Role of MDM2 acid domain interactions in recognition and ubiquitination of the transcription factor IRF-2. Biochem J 418:575–585
34. Popowicz GM, Czarna A, Rothweiler U, Sszwagierczak A, Krajewski M, Weber L, Holak TA (2007) Cell Cycle 6:2386
35. Poyurovsky MV, Jacq X, Ma C, Karni-Schmidt O, Parker PJ, Chalfie M, Manley JL, Prives C (2003) Mol Cell 12:875
36. Poyurovsky MV, Priest C, Kentsis A, Borden KL, Pan ZQ, Pavletich N, Prives C (2007) EMBO J 26:90
37. Schon O, Friedler A, Freund S, Fersht AR (2004) J Mol Biol 336:197
38. Shimizu H, Burch LR, Smith AJ, Dornan D, Wallace M, Ball KL, Hupp TR (2002) J Biol Chem 277:28446
39. Shimizu H, Saliba D, Wallace M, Finlan L, Langridge-Smith PR, Hupp TR (2006) Biochem J 397:355
40. Showalter SA, Bruschweiler-Li L, Johnson E, Zhang F, Bruschweiler R (2008) J Am Chem Soc 130:6472
41. Stevens C, Pettersson S, Wawrzynow B, Wallace M, Ball K, Zylicz A, Hupp TR (2008) FEBS J 275:4875
42. Terzian T, Suh YA, Iwakuma T, Post SM, Neumann M, Lang GA, Van Pelt CS, Lozano G (2008) Genes Dev 22:1337–1344
43. Thut CJ, Goodrich JA, Tjian R (1997) Genes Dev 11:1974
44. Toledo F, Wahl GM (2007) MDM2 and MDM4: p53 regulators as targets in anticancer therapy. Int J Biochem Cell Biol 39:1476
45. Uhrinova S, Uhrin D, Powers H, Watt K, Zheleva D, Fischer P, McInnes C, Barlow PN (2005) J Mol Biol 350:587
46. Uldrijan S, Pannekoek WJ, Vousden KH (2007) EMBO J 26:102
47. Vassilev LT, Vu BT, Graves B, Carvajal D, Podlaski F, Filipovic Z, Kong N, Kammlott U, Lukacs C, Klein C, Fotouhi N, Liu EA (2004) Science 303:844
48. Vojtesek B, Dolezalova H, Lauerova L, Svitakova M, Havlis P, Kovarik J, Midgley CA, Lane DP (1995) Oncogene 10:389
49. Vousden KH, Lane DP (2007) Nat Rev Mol Cell Biol 8:275
50. Wallace M, Worrall E, Pettersson S, Hupp TR, Ball KL (2006) Mol Cell 23:251
51. Wawrzynow B, Zylicz A, Wallace M, Hupp T, Zylicz M (2007) J Biol Chem 282:32603
52. Wawrzynow B, Pettersson S, Zylicz A, Bramham J, Worrall E, Hupp TR, Ball KL (2009) J Biol Chem 284:11517–11530
53. Xirodimas D, Saville MK, Edling C, Lane DP, Lain S (2001) Oncogene 20:4972
54. Yang Y, Ludwig RL, Jensen JP, Pierre SA, Medaglia MV, Davydov IV, Safiran YJ, Oberoi P, Kenten JH, Phillips AC, Weissman AM, Vousden KH (2005) Cancer Cell 7:547
55. Yu GW, Rudiger S, Veprintsev D, Freund S, Fernandez-Fernandez MR, Fersht AR (2006) Proc Natl Acad Sci U S A 103:1227
56. Yu GW, Allen MD, Andreeva A, Fersht AR, Bycroft M (2006) Protein Sci 15:384